4

CONTENTS

1. LIST OF PARTICIPANTS

AUSTRALIA

G	Boughton	Curtin University of Techn., Perth
R H	Leicester	CSIRO, Highett, Victoria

CANADA

J D	Barrett	University of British Columbia, Vancouver
R	Fouquet	Council of For. Ind. of B.C., Vancouver
Y H	Chui	University of New Brunswick
C	Lum	Forintek Canada Corp., Vancouver
B	Madsen	University of British Columbia, Vancouver
D J	Masse	Eng. and Statist. Res. Centre, Ottawa
D	Onysko	Forintek Canada Corp., Ottawa
J J	Salinas	Carleton University, Ottawa
I	Smith	University of New Brunswick
C K A	Stieda	Forintek Canada Corp., Vancouver
E	Varoglu	Forintek Canada Corp., Vancouver

DENMARK

T	Feldborg	Danish Building Research Institute, Horsholm
H J	Larsen	Danish Building Research Institute, Horsholm
H	Riberholt	Technical University of Denmark, Lyngby

FEDERAL REPUBLIC OF GERMANY

H J	Blass	University of Karlsruhe
J	Ehlbeck	University of Karlsruhe
P	Glos	University of München

FINLAND

M	Fonselius	Technical Research Centre of Finland, Espoo
T	Poutanen	Tampere Technical University
A	Ranta-Maunus	Technical Research Centre of Finland, Espoo
K	Riipola	Technical Research Centre of Finland, Espoo
U	Saarelainen	Technical Research Centre of Finland, Espoo

GERMAN DEMOCRATIC REPUBLIC

W	Rug	Bauakademie der DDR, Berlin

IRELAND

P R	Colclough	Institute for Ind. Res. + Stand., Dublin

ISRAEL

U	Korin	Building Research Station, Technion, Haifa

ITALY

A	Ceccotti	University of Florence

JAPAN

Y	Hirashima	Shizuoka University, Shizuoka
K	Komatsu	Forestry and For. Prod. Res., Ibaraki
T	Nakai	Forestry and For. Prod. Res., Ibaraki
M	Yasumura	Building Research Institute, Tsukuba

NETHERLANDS

J	Kuipers	Technical University, Delft
A J M	Leijten	Technical University, Delft

NEW ZEALAND

A H	Buchanan	University of Canterbury, Christchurch
G B	Walford	Forest Research Institute, Rotorua

NORWAY

E	Aasheim	Norwegian Build. Res. Inst., Oslo
P	Aune	Techn. University of Norway, Trondheim
T	Ramstad	Norwegian Build. Res. Inst., Oslo

SWEDEN

L	Bostrom	Lund University, Lund
A	Girhammar	RSFA-Research Department, Masta
P J	Gustafsson	Lund University, Lund

G	Johansson	Chalmers University of Techn., Goteborg
B	Källsner	Swedish Inst. for Wood Techn. Res., Stockholm
J	König	Swedish Inst. for Wood Techn. Res., Stockholm
S	Mohager	Department of Building Materials, Stockholm
S	Ohlsson	Chalmers University of Techn., Goteborg
S	Thelandersson	Lund University, Lund
B	Thunell	Royal Inst. of Techn., Stockholm

SWITZERLAND

U A	Meierhofer	EMPA, Dübendorf

UNITED KINGDOM

A R	Abbott	TRADA, High Wycombe
H J	Burgess	TRADA, High Wycombe
A R	Fewell	Building Research Establishment, Watford
R	Marsh	Ove Arup, London
R C	Mitzner	APA, London
J G	Sunley	Monks Risborough
L R J	Whale	Brighton Polytechnic, Brighton

UNITED STATES OF AMERICA

E G	Elias	American Plywood Association, Tacoma
D W	Green	USDA Forest Products Laboratory, Madison
J	Johnson	University of Washington, Seattle
E G	Stern	Virginia Polytechnic Inst. + State University, Blacksburg

2. CHAIRMAN'S INTRODUCTION

DR. STIEDA welcomed the participants, mentioning the positions of MR. SUNLEY, DR. LEICESTER, DR. CECCOTTI and DR. NAKAI in international discussions and also DR. VAROGLU and DR. DANGERFIELD in the FORINTEK organisation.

3. COOPERATION WITH OTHER ORGANISATIONS

ISO/TC 165: MR. LARSEN explained the relationship of ISO and CEN standards, saying the latter would replace international standards and by 1992 would become part of national building regulations via the Eurocodes.

Standards had been completed on the testing of panel products, nail plates, density requirements and strength and density classifications, and the work was continuing with the testing of nails and staples. Work on a grading standard had been stopped as a strength classification was felt to be needed rather than a grading standard.

Answering MR. BUCHANAN, he said the CIB Code was important as a basis for the European work but work on the corresponding ISO standard had been suspended for the present.

RILEM: DR. CECCOTTI described the objectives of his group. Four topics were to be studied: seismic behaviour with PROFESSOR NIELSEN as Chairman, long-term behaviour of composite construction including timber with himself as Chairman, fracture mechanics under PROFESSOR RANTA-MAUNUS and creep under PROFESSOR MOLIER, University of Bordeaux.

Answering MR. ABBOTT, PROFESSOR RANTA-MAUNUS said the fracture mechanics work would summarize the present state of knowledge and determine how to apply it in practice.

Following a remark by PROFESSOR KUIPERS, it was agreed that the cooperation between RILEM and CIB-W18A would continue in the work of the four committees.

EUROCODE: MR. SUNLEY said MR. LARSEN was Chairman of the drafting panel dealing with EC5, which would be applied in the twelve Common Market countries and perhaps also the EFTA countries. National comments on EC5 by the end of 1989 would lead to a finished document in 1991. MR. LARSEN emphasised the importance of the ongoing CIB work for the Eurocode.

CEN/TC 124: MR. SUNLEY described the work of CEN committees on adhesives and wood-based panel products. Answering PROFESSOR GLOS, MR. LARSEN said a chapter on fire was being drafted by a group representing all materials. DR. LEICESTER enquired about input from non-European workers; MR. LARSEN replied that EC5 was sent to all ISO members and ISO had been asked to supply information to countries not involved in CEN work.

MR. SUNLEY said he had written a paper on CEN Committees for the United Kingdom, and could make it available to CIB-W18A. MR. LARSEN said he could prepare a CIB-W18A paper. The CEN 124 Bulletin was mentioned, and it was agreed to circulate this with the advance report of the meeting, together with MR. SUNLEY's paper.

IABSE: MR. JOHANSSON said this organisation was dominated by steel and concrete, and timber should play a greater part. At the last meeting in Helsinki, 6-10 June 1988, a number of people from Sweden had represented timber. DR. GREEN said a new US bridge manual would soon be available, and MR. MARSH said there had been papers at the Seattle Conference on the transverse stressing of bridge decks.

IUFRO S5.02: Speaking as former Chairman, PROFESSOR MADSEN said W18 dealt with Code matters, RILEM with testing and IUFRO with basic research. S5.02 met every two years, most recently in Finland in June 1988 where the attendance had been smaller than usual; the Proceedings were ready to print and could be obtained from him for US$25. The next meeting would be in early August 1990 in conjunction with the IUFRO Congress in New Brunswick. PROFESSOR HOFFMEYER was now Chairman and PROFESSOR GLOS the vice-Chairman.

OTTAWA SYMPOSIUM: DR. CHUI said the May 1988 symposium on serviceability of buildings had been jointly organized by the University of Ottawa and the National Research Council of Canada. An informal meeting on floor vibration had been held, and DR. OHLSSON said he had initiated this to try and harmonize work by different groups. DR. SMITH said a discussion document would be obtainable from DR. DAVE ALLEN of the National Research Council, Ottawa. MR. ONYSKO said the related CIB group had also met in Ottawa.

SEATTLE CONFERENCE: The Chairman said many of those present had attended the Conference. DR. BUCHANAN added that a conference would be held in New Zealand in a year's time and perhaps one in Japan at a later stage. MR. SUNLEY thought the frequency of such conferences might be better regulated. MR. RIBERHOLT introduced a discussion of the need for participation by practising engineers to encourage the wider use of structural timber, concluding with a remark by MR. MARSH that a conference should have an aim, as in the case of CIB-W18A meetings.

BAUAKADEMIE der DDR: DR. RUG said arrangements were in hand for a CIB-W18A meeting on 25-28 September 1989, and an announcement would appear shortly. He said representatives of CMEA countries would also be invited, and DR. STIEDA said the meeting would follow the normal W18 procedure for the submission and distribution of papers.

CIB-W18A: Introducing his paper 21-150-1, 'Tropical and hardwood timber structures', DR. LEICESTER said it gave project proposals developed at a meeting in Singapore in October 1987, and a further meeting in Seattle had discussed their implementation. His discussion of the work concluded that funding would be needed to fulfil the proposals.

He added that a meeting might be held in 1989 in South America in conjunction with UNIDO and there would be one at the time of the next PATEC. A future conference on tropical and hardwood structures was also being considered.

4. TRUSSED RAFTER SUB-GROUP

As Chairman of the working group, MR. RIBERHOLT said simplified design had been sought but this was very difficult. After a discussion of design methods he concluded that guidelines had been produced and the work would continue by comparing the results for frame models with those of more scientific analyses.

MR. BURGESS expressed the feeling that the Annex already produced should be incorporated in EC5 for consideration along with the rest of the Eurocode.

At a later stage, further discussion concluded that MR. RIBERHOLT would contact the industry for design recommendations and that the sub-group would continue its work to establish a calcuation method, reviewing progress after a year.

5. SUB-GROUP ON DERIVATION OF CHARACTERISTIC VALUES

PROFESSOR GLOS said a paper had been produced for the meeting (paper 21-6-2 under STRESSES FOR SOLID TIMBER below).

6. VIBRATION

Paper 21-8-1 `Floor vibration : addendum to paper 20-8-1` by Y.H. Chui and I.Smith was presented by DR. CHUI and discussed by the authors with MESSRS. ONYSKO, LARSEN, OHLSSON and KONIG.

After presenting his paper 21-8-2 `Floor vibration serviceability and the CIB model code`, DR. OHLSSON expressed the view that the proposal by Chui and Smith was not acceptable. If the Code was to give any guidance on vibration it would be better to limit it to static point-load deflection pending further study.

The results of an additional discussion were reported by MR. ONYSKO, who said the problem would receive further consideration in the coming months, and it was concluded that progress would be reported at the next meeting. DR. OHLSSON mentioned that CIB-W85 would also be continuing their work on the subject.

7. MECHANICAL JOINTS

Paper 21-7-1 `Nails under long-term withdrawal loading` by T. Feldborg and M. Johansen was introduced by MR. FELDBORG, saying that the project arose from the collapse of a ceiling fixed with annularly-threaded nails after long service. In response to a suggestion by PROFESSOR EHLBECK, he agreed that the tests did not demonstrate how the failure occurred. PROFESSOR STERN said the fibres in the grooves tend to shear when the wood changes size, and he would prefer helically-threaded nails.

PROFESSOR KUIPERS reiterated his research findings that there was no latent `damage` after long-term loading.

MR. RIBERHOLT reviewed his paper 21-7-2 `Glued bolts in glulam - proposals for CIB Code`.

MR. LEIJTEN said that in fatigue testing for modern windmills in Holland, the different properties of wood and steel had caused cracks to propagate but the problem had been overcome by suitable dimensioning. MR. RIBERHOLT said that in Denmark this had arisen only with GRP blades and not with wood; fatigue strength had been thoroughly investigated.

PROFESSOR EHLBECK felt the material was acceptable for the Code. He suggested bringing the embedment formula to the same form as the one now in the Code if possible, and defining the roughness required for the bolts.

MR. POUTANEN introduced his paper 21-7-3 `Nail plate joint under shear loading`, extolling the merits of elastic design and decrying the `ugliness` of plastic theory. MR. LARSEN countered that plasticity was nature's gift to bad designers while elasticity was ugly, leading to failures unless plasticity gave a reserve of strength.

In the subsequent discussion MR. LUM emphasised that tests had shown joints behave linearly up to design load and in a non-linear way thereafter. DR. MEIERHOFER said knowledge of plasticity effects was still limited, especially for long-term loading; however MR. RIBERHOLT pointed out that abandoning plasticity would require a new test method together with calculations allowing for moments.

Paper 21-7-4 `Design of joints with laterally loaded dowels - proposals for improving the design rules in the CIB Code and the draft Eurocode 5` by J. Ehlbeck and H. Werner was presented by PROFESSOR EHLBECK.

There followed a discussion of the difficulty of measuring the effect of tension perpendicular to grain and allowing for it in design, including a description by DR. LEICESTER of new proposals for the Australian code AS 1720: 1988.

Introducing paper 21-7-5 `Axially loaded nails - proposals for a supplement to the CIB Code` by J. Ehlbeck and W. Siebert, PROFESSOR EHLBECK said it derived formulae from many test on nails of different kinds.

PROFESSOR STERN described differing proposals made in the USA for an ISO standard on pallets. The subsequent discussion concluded by PROFESSOR EHLBECK suggesting that withdrawal values should be included in the section of EC5 referring to nails, while allowing for higher values to be obtained by testing under an approval system.

Paper 21-13-1 `Design values for nailed chipboard-timber joints` by A.R.Abbott was presented by the author who said the tests were made in conjunction with the Princes Risborough Laboratory starting in 1982 and involving some 7000 tests. He said embedment tests had also been done but the results had not yet been analysed.

A number of questions were asked regarding the test method, the influence of edge distance and thickness and the applications envisaged for the results, and the Chairman concluded that further results would be awaited with great interest.

8. STRESSES FOR SOLID TIMBER

Presenting his paper 21-6-1 `Draft Australian Standard : methods for evaluation of strength and stiffness of graded timber`, DR. LEICESTER said test configurations in conformity with practical use had been selected.

Questions were answered regarding sampling, the use of a confidence limit and continuous assessment of mill quality. Answering DR. BARRETT, DR. LEICESTER said no further length effect was taken for the occurrence of defects throughout a truss, and the same system was applied for all types of structures with provision for redundancy in the code rather than the grading system.

The description of paper 21-6-2 `The determination of characteristic strength values for stress grades of structural timber` by A.R.Fewell and P. Glos was started by PROFESSOR GLOS and continued by MR. FEWELL with a further contribution by DR. GREEN.

Answering PROFESSOR MADSEN, MR. FEWELL said not all tests were made with the same depth-to-span ratio, but some were adjusted for length effect. A depth effect was in line with European data and was needed. After a display of data by DR. GREEN which will be available in the proceedings of the IUFRO meeting in Finland, PROFESSOR GLOS said there was a possibility of harmonizing the proposals by himself and MR. FEWELL with those by DR. GREEN, and urged taking this course worldwide.

DR. KORIN presented his paper 21-6-3 `Shear strength in bending of timber`. MS. RIPOLA said a similar paper by Dr. Murphy had appeared and suggested that stress concentrations would influence the results. The point was taken up by other speakers who suggested that a wider slot would be preferable for the test specimen. Following questions by DR. LEICESTER and DR. BARRETT it was confirmed by MR. LARSEN and MR. SUNLEY that a shear test was needed.

9. STRESS GRADING

Paper 21-5-1 `Non-destructive test by frequency of full size timber for grading` by T. Nakai and T. Tanaka was presented by DR. NAKAI. PROFESSOR GLOS said the dynamic MoE was usually greater than the static value, but DR. OHLSSON said his results from a small test range using impact-induced compression waves gave support to DR. NAKAI. MR. BOUGHTON asked if the effect of moisture content had been examined, and DR. NAKAI stated that only a density correction was needed.

10. STRUCTURAL CODES

MR. LARSEN introduced his paper 21-100-1 `CIB Structural Timber Design Code-proposed changes of sections on lateral instability, columns and nails`, saying it followed decisions made at the Dublin meeting. The format for columns introduced a relative slenderness ratio of the same form as in a later paper by DR. LEICESTER (paper 21-2-1 below) and proposals by DR. BLASS and DR. BUCHANAN had also been adopted. Information for the nail spacing rules had been supplied by DR. KONIG, and the nailed joint design formulae followed proposals in paper 20-7-1 with supplementary comments by DRS. WHALE and SMITH.

The Chairman said the report was the result of a great deal of technical study, and MR. LARSEN confirmed that the work would be incorporated in the next edition of the CIB Code.

Paper 21-103-1 `Concept of a complete set of standards` by R. H. Leicester was presented by the author. He also showed slides of cyclone damage, suggesting this was often due to shortcomings in the construction of buildings when the designer's intentions were not put into effect. The Chairman thought a suitable system of control was applied in many countries although perhaps not formally laid down. Failures were referred to builders and eventually came to the attention of code authorities, but it was preferable to have a formal control system.

After presenting paper 21-102-1 ` Research activities towards a new GDR Timber Design Code based on limit states design` by W. Rug and M. Badstube, DR.RUG showed slides of impressive building interiors in Berlin and said he looked forward to the next CIB-W18A meeting in his country next year.

MR. MARSH asked if a code concerned with historical timber structures was available, saying his organization had just reconstructed one of the 13th century. DR. RUG replied that fundamental work towards such a code was being undertaken and a draft was expected in 1991.

11. SPECIAL TOPICS

An address concerning the application of reliability principles in the Canadian code was given by PROFESSOR FOSCHI, who said reports were being produced and would be made available.

MR. KARACABEYLI gave details of load-duration tests in progress at FORINTEK, and preliminary findings for timber in tension and compression.

A discussion of strength classes took place, led by MR. SUNLEY. The Chairman concluded by expressing the hope that the dialogue between Europe, North America and Australia would continue.

12. TIMBER BEAMS

Paper 21-10-1 `A study of strength of notched beams` by P.J. Gustafsson was presented by the author. MS. RIPOLA said this was an excellent demonstration of the need for fracture mechanics and went on to explain the nature of this subject.

The succeeding discussion with contributions by PROFESSOR GLOS and DR. LEICESTER concluded with a suggestion by MR. RIBERHOLT that test reports for larger beams might be sent to MR. GUSTAFSSON for comparison with the theory.

Having introduced paper 21-12-1 `Modulus of rupture of glulam beam composed of arbitrary laminae` by K. Komatsu and N. Kawamoto, DR. KOMATSU showed slides including tension proof-testing and bending tests of laminations, and strain-gauging and fracture in tested glue-laminated beams. No further discussion arose and the Chairman suggested that any queries might be sent to DR. KOMATSU.

Paper 21-12-2 `An appraisal of the Young's modulus values specified for glulam in draft Eurocode 5` by L.R.J.Whale, B.O.Hilson and P.D. Rodd was presented by DR. WHALE, who said it was hoped to continue the work with more extensive data sets.

MR. LARSEN said more time was needed to consider the paper. He questioned whether the boards used were representative of glulam material and suggested repeating the simulations with data more representative of the material used in practice.

Paper 21-12-3 `The strength of glued laminated timber (GLULAM): influence of lamination qualities and strength of finger joints` by J. Ehlbeck and F. Colling was presented by DR. BLASS. He confirmed that for the present the

bending strength of glulam should be taken as 0.8 times the flatwise bending strength of finger joints, so that the characteristics value for finger joints in highly stressed zones needed to be 25% higher than the characteristic bending strength of the glulam strength class.

DR. KORIN said he had found similar results in tests of standard glulam beams from Germany. MR. WALFORD thought proof testing was needed for outer laminations but MR. LARSEN said high finger-joint strength could be guaranteed by quality control as applied in Europe.

Replying to PROFESSOR GLOS, PROFESSOR EHLBECK said the work provided background to values in EC5 and continued work could lead to changes.

MR. RIBERHOLT introduced his paper 21-12-4 `Comparison of a shear strength design method in Eurocode 5 and a more traditional one`. PROFESSOR RANTA-MAUNUS supported the proposed approach as more conventional. MR. LARSEN said almost the same results were obtained by the simpler method and discussed with MR. RIBERHOLT whether this was reflected adequately in EC5.

DR. SMITH was unsure whether the EC5 formula gave a correct basis for the comparison, and suggested adding a comparison with test results.

13. STRUCTURAL STABILITY

Paper 21-2-1 `Format for buckling strength` by R.H.Leicester was presented by the author. MR. LARSEN said the same basic idea woul be incorporated in the CIB code following his paper at the present meeting (21-100-1 above). He agreed that simple approximations were possible but did not think of these as `empirical`. He thought design curves could be drawn for world-wide acceptance, although local values could be used if desired.

DR. LEICESTER continued with his paper 21-2-2 `Beam-column formulae for design codes`, saying that extension from a column to a beam-column introduced still more unknowns, leading to a very complicated solution which was undesirable.

MR. WALFORD supported the equation used in the New Zealand code as given by DR. LEICESTER, mentioning that DR. BUCHANAN was Chairman of the code committee, and PROFESSOR FOSCHI said he was using the same equation.

The following papers were reviewed by their author: 21-15-1 `Rectangular section deep beam-columns with continuous lateral restraint`, 21-15-2 `Buckling modes and permissible axial loads for continuously braced columns`, 21-15-3 `Simple approaches for column bracing calculations`, 21-15-4 `Calculations for discrete column restraints` - all by H.J. Burgess.

In relation to the last of these, MR. BURGESS said that it was an initial exploratory study and was only presented to show the type of approach that he felt might replace present proposals for the CIB code and EC5.

DR. LEICESTER said the initial crookedness adopted to cater for a number of effects in unbraced buckling members might be found by tests to be inappropriate, but MR. BURGESS felt that the established structural model should not be changed when restraint was added.

Paper 21-15-5 `Behaviour factor of timber structures in seismic zones (Part two) by A. Ceccotti and A. Vignoli was introduced by DR. CECCOTTI. He said previous work had not allowed for slip in joints but this was taken into account in the current paper. The object of the work was to convince the Eurocode 8 drafting panel that structures could be treated more favourably than at present in EC8.

MR. RIBERHOLT thought this should be demonstrated for a wider range of timber structures, and MR. WALFORD said New Zealand were considering plywood shear walls, portal frames and glued joints. DR. YASUMURA gave information on related work in Japan, and the Chairman hoped the discussion would continue in future meetings.

14. SHEET MATERIALS

DR. HIRASHIMA presented his paper 21-4-1 `Modelling for prediction of strength of veneer having knots`, and answered questions by MR. LEIJTEN and DR. MEIERHOFER concerning measurements of grain slope.

MR. RIBERHOLT and MR. MITZNER said higher stress values would be obtained in veneers reinforced by crossbands, and DR. HIRASHIMA replied that consideration was being given to such questions. MR. ELIAS said a knot was not the weakest link but was also reinforced. He added that related studies for solid timber had been undertaken using finite elements and fluid mechanics at Colorado State University.

15. DURABILITY

Introducing paper 21-11-1 `Durability classifications: a proposed format for engineering purposes` by R.H.Leicester and J.E.Barnacle, DR. LEICESTER said that in the tropics durability might be more important than strength.

DR. MEIERHOFER suggested the CIB code should introduce similar material but MR. SUNLEY said construction codes do not usually extend to numerical assessments for durability and MR. RIBERHOLT questioned the development of some magnitudes. MR. ABBOTT asked if the scheme could be extended to board materials, mixed species and gluelines. DR. LEICESTER replied that this was desirable but said it only allowed for solid timber at present.

16. OTHER BUSINESS

PROFESSOR EHLBECK said papers for CIB-W18A should be of a kind assisting the development of the CIB Code, and the subsequent discussion concluded with a proposal by MR. MARSH that an author should start by relating his paper to the objectives of W18.

PROFESSOR EHLBECK said there had been many papers since the Code was published in 1983 and a second edition was desirable in a year or two. The Europeans were heavily pre-occupied with the Eurocode and CEN standards, and he wondered if an editorial group should be set up as done for the present edition. The Chairman said he would consider this question and report next year.

Topics mentioned for emphasis at the next meeting were perpendicular-to-grain stress in joints, seismic effects, methods of test (e.g. shear), draft CEN standards, size effects in the general sense and a follow-up of the topic of durability.

FUTURE MEETINGS: It was agreed that the next meeting would be held on the 25-28 September 1989 in East Berlin. Invitations had been received from Portugal for 1990 and from the United Kingdom for 1991.

MR. SUNLEY asked what dates would be best for a 1991 meeting combined with a timber engineering conference. It was concluded that the first week of September was best, with a single UK venue for both meetings.

The Chairman expressed the thanks of members to PROFESSOR EHLBECK and DR. BLASS for the continued preparation and distribution of the Proceedings, and to MS. LORI KELLER for her background work in organizing facilities for the Vancouver meeting, assisting individual participants and generally achieving a successful meeting. He also expressed appreciation to MR. BURGESS who had acted as Secretary of the seven meetings from Karlsruhe 1982 to Vancouver 1988 and would now hand over to MR. ANDREW ABBOTT who would take responsibility for the next meeting.

DR. STEIDA then closed the 21st meeting of CIB-W18A, hoping to see a good attendance in Berlin next year, and MR. SUNLEY thanked him for his able conduct of the Vancouver meeting, involving all the extra work of acting for the host country.

17. List of CIB-W18A Papers
Parksville, Vancouver Island 1988

17. LIST OF CIB-W18A PAPERS
PARKSVILLE, VANCOUVER ISLAND 1988

21-2-1 Format for Buckling Strength -
R H Leicester

21-2-2 Beam-Column Formulae for Design Codes -
R H Leicester

21-4-1 Modelling for Prediction of Strength of Veneer
Having Knots - Y Hirashima

21-5-1 Non-Destructive Test by Frequency of Full Size Timber
for Grading - T Nakai

21-6-1 Draft Australian Standard: Methods for Evaluation of
Strength and Stiffness of Graded Timber - R H Leicester

21-6-2 The Determination of Characteristic Strength Values for
Stress Grades of Structural Timber. Part 1 - A R Fewell
and P Glos

21-6-3 Shear Strength in Bending of Timber -
U Korin

21-7-1 Nails under Long-Term Withdrawal Loading - T Feldborg
and M Johansen

21-7-2 Glued Bolts in Glulam-Proposals for CIB Code -
H Riberholt

21-7-3 Nail Plate Joint Behaviour under Shear Loading -
T Poutanen

21-7-4 Design of Joints with Laterally Loaded Dowels. Proposals for
Improving the Design Rules in the CIB Code and the Draft
Eurocode 5 - J Ehlbeck and H Werner

21-7-5 Axially Loaded Nails: Proposals for a Supplement to the
CIB Code - J Ehlbeck and W Siebert

21-8-1 An Addendum to Paper 20-8-1 Proposed Code Requirements for
Vibrational Serviceability of Timber Floors - Y H Chui and
I Smith

21-8-2 Floor Vibrational Serviceability and the CIB Model Code -
S Ohlsson

21-10-1 A Study of Strength of Notched Beams-
P J Gustafsson

21-11-1 Durability Classifications. A Proposed Format for
Engineering Purposes - R H Leicester and J E Barnacle

21-12-1 Modulus of Rupture of Glulam Beam Composed of Arbitrary
Laminae - K Komatsu and N Kawamoto

21-12-2 An Appraisal of the Young's Modulus Values Specified for Glulam in Eurocode 5 - L R J Whale, B O Hilson and P D Rodd

21-12-3 The Strength of Glued Laminated Timber (Glulam): Influence of Lamination Qualities and Strength of Finger Joints - J Ehlbeck and F Colling

21-12-4 Comparison of a Shear Strength Design Method in Eurocode 5 and a More Traditional One - H Riberholt

21-13-1 Design Values for Nailed Chipboard - Timber Joints - A R Abbott

21-15-1 Rectangular Section Deep Beam-Columns with Continuous Lateral Restraint - H J Burgess

21-15-2 Buckling Modes and Permissible Axial Loads for Continuously Braced Columns - H J Burgess

21-15-3 Simple Approaches for Column Bracing Calculations - H J Burgess

21-15-4 Calculations for Discrete Column Restraints - H J Burgess

21-15-5 Behaviour Factor of Timber Structures in Seismic Zones (Part Two) - A Ceccotti and A Vignoli

21-100-1 CIB Structural Timber Design Code. Proposed Changes of Sections on Lateral Instability, Columns and Nails - H J Larsen

21-102-1 Research Activities Towards a New GDR Timber Design Code Based on Limit States Design - W Rug and M Badstube

21-103-1 Concept of a Complete Set of Standards - R H Leicester

21-105-1 First Conference of CIB-W18B, Tropical and Hardwood Timber Structures Singapore, 26 - 28 October 1987 - R H Leicester

18. Current List of CIB-W18A Papers

18. CURRENT LIST OF CIB-W18A PAPERS

Technical papers presented to CIB-W18A are identified by a code CIB-W18A/a-b-c, where:

a denotes the meeting at which the paper was presented. Meetings are classified in chronological order:

1 Princes Risborough, England; March 1973
2 Copenhagen, Denmark; October 1973
3 Delft, Netherlands; June 1974
4 Paris, France; February 1975
5 Karlsruhe, Federal Republic of Germany; October 1975
6 Aalborg, Denmark; June 1976
7 Stockholm, Sweden; February/March 1977
8 Brussels, Belgium; October 1977
9 Perth, Scotland; June 1978
10 Vancouver, Canada; August 1978
11 Vienna, Austria; March 1979
12 Bordeaux, France; October 1979
13 Otaniemi, Finland; June 1980
14 Warsaw, Poland; May 1981
15 Karlsruhe, Federal Republic of Germany; June 1982
16 Lillehammer, Norway; May/June 1983
17 Rapperswil, Switzerland; May 1984
18 Beit Oren, Israel; June 1985
19 Florence, Italy; September 1986
20 Dublin, Ireland; September 1987
21 Parksville, Canada; September 1988

b denotes the subject:

1 Limit State Design
2 Timber Columns
3 Symbols
4 Plywood
5 Stress Grading
6 Stresses for Solid Timber
7 Timber Joints and Fasteners
8 Load Sharing
9 Duration of Load
10 Timber Beams
11 Environmental Conditions
12 Laminated Members
13 Particle and Fibre Building Boards
14 Trussed Rafters
15 Structural Stability
16 Fire
17 Statistics and Data Analysis
18 Glued Joints
100 CIB Timber Code
101 Loading Codes
102 Structural Design Codes
103 International Standards Organisation
104 Joint Committee on Structural Safety
105 CIB Programme, Policy and Meetings
106 International Union of Forestry Research Organisations

c is simply a number given to the papers in the order in which they appear:

Example: CIB-W18/4-102-5 refers to paper 5 on subject 102 presented at the fourth meeting of W18.

Listed below, by subjects, are all papers that have to date been presented to W18. When appropriate some papers are listed under more than one subject heading.

LIMIT STATE DESIGN

1-1-1 Limit State Design - H J Larsen

1-1-2 The Use of Partial Safety Factors in the New Norwegian Design Code for Timber Structures - O Brynildsen

1-1-3 Swedish Code Revision Concerning Timber Structures - B Norén

1-1-4 Working Stresses Report to British Standards Institution Committee BLCP/17/2

6-1-1 On the Application of the Uncertainty Theoretical Methods for the Definition of the Fundamental Concepts of Structural Safety - K Skov and O Ditlevsen

11-1-1 Safety Design of Timber Structures - H J Larsen

18-1-1 Notes on the Development of a UK Limit States Design Code for Timber - A R Fewell and C B Pierce

18-1-2 Eurocode 5, Timber Structures - H J Larsen

19-1-1 Duration of Load Effects and Reliability Based Design (Single Member) - R O Foschi and Z C Yao

21-102-1 Research Activities Towards a New GDR Timber Design Code Based on Limit States Design - W Rug and M Badstube

TIMBER COLUMNS

2-2-1 The Design of Solid Timber Columns - H J Larsen

3-2-1 The Design of Built-Up Timber Columns - H J Larsen

4-2-1 Tests with Centrally Loaded Timber Columns - H J Larsen and S S Pedersen

4-2-2 Lateral-Torsional Buckling of Eccentrically Loaded Timber Columns - B Johansson

5-9-1 Strength of a Wood Column in Combined Compression and Bending with Respect to Creep - B Källsner and B Norén

5-100-1 Design of Solid Timber Columns (First Draft) - H J Larsen

6-100-1 Comments on Document 5-100-1, Design of Solid Timber Columns - H J Larsen and E Theilgaard

6-2-1	Lattice Columns - H J Larsen
6-2-2	A Mathematical Basis for Design Aids for Timber Columns - H J Burgess
6-2-3	Comparison of Larsen and Perry Formulas for Solid Timber Columns - H J Burgess
7-2-1	Lateral Bracing of Timber Struts - J A Simon
8-15-1	Laterally Loaded Timber Columns: Tests and Theory - H J Larsen
17-2-1	Model for Timber Strength under Axial Load and Moment - T Poutanen
18-2-1	Column Design Methods for Timber Engineering - A H Buchanan, K C Johns, B Madsen
19-2-1	Creep Buckling Strength of Timber Beams and Columns - R H Leicester
19-12-2	Strength Model for Glulam Columns - H J Blaß
20-2-1	Lateral Buckling Theory for Rectangular Section Deep Beam-Columns - H J Burgess
20-2-2	Design of Timber Columns - H J Blaß
21-2-1	Format for Buckling Strength - R H Leicester
21-2-2	Beam-Column Formulae for Design Codes - R H Leicester
21-15-1	Rectangular Section Deep Beam - Columns with Continuous Lateral Restraint - H J Burgess
21-15-2	Buckling Modes and Permissible Axial Loads for Continuously Braced Columns - H J Burgess
21-15-3	Simple Approaches for Column Bracing Calculations - H J Burgess
21-15-4	Calculations for Discrete Column Restraints - H J Burgess
SYMBOLS	
3-3-1	Symbols for Structural Timber Design - J Kuipers and B Norén
4-3-1	Symbols for Timber Structure Design - J Kuipers and B Norén
1	Symbols for Use in Structural Timber Design

PLYWOOD

2-4-1 The Presentation of Structural Design Data for Plywood - L G Booth

3-4-1 Standard Methods of Testing for the Determination of Mechanical Properties of Plywood - J Kuipers

3-4-2 Bending Strength and Stiffness of Multiple Species Plywood - C K A Stieda

4-4-4 Standard Methods of Testing for the Determination of Mechanical Properties of Plywood - Council of Forest Industries, B.C.

5-4-1 The Determination of Design Stresses for Plywood in the Revision of CP 112 - L G Booth

5-4-2 Veneer Plywood for Construction - Quality Specifications - ISO/TC 139. Plywood, Working Group 6

6-4-1 The Determination of the Mechanical Properties of Plywood Containing Defects - L G Booth

6-4-2 Comparsion of the Size and Type of Specimen and Type of Test on Plywood Bending Strength and Stiffness - C R Wilson and P Eng

6-4-3 Buckling Strength of Plywood: Results of Tests and Recommendations for Calculations - J Kuipers and H Ploos van Amstel

7-4-1 Methods of Test for the Determination of Mechanical Properties of Plywood - L G Booth, J Kuipers, B Norén, C R Wilson

7-4-2 Comments Received on Paper 7-4-1

7-4-3 The Effect of Rate of Testing Speed on the Ultimate Tensile Stress of Plywood - C R Wilson and A V Parasin

7-4-4 Comparison of the Effect of Specimen Size on the Flexural Properties of Plywood Using the Pure Moment Test - C R Wilson and A V Parasin

8-4-1 Sampling Plywood and the Evaluation of Test Results - B Norén

9-4-1 Shear and Torsional Rigidity of Plywood - H J Larsen

9-4-2 The Evaluation of Test Data on the Strength Properties of Plywood - L G Booth

9-4-3 The Sampling of Plywood and the Derivation of Strength Values (Second Draft) - B Norén

9-4-4 On the Use of the CIB/RILEM Plywood Plate Twisting Test: a progress report - L G Booth

10-4-1 Buckling Strength of Plywood - J Dekker, J Kuipers and H Ploos van Amstel

11-4-1 Analysis of Plywood Stressed Skin Panels with Rigid or Semi-Rigid Connections - I Smith

11-4-2 A Comparison of Plywood Modulus of Rigidity Determined by the ASTM and RILEM CIB/3-TT Test Methods - C R Wilson and A V Parasin

11-4-3 Sampling of Plywood for Testing Strength - B Norén

12-4-1 Procedures for Analysis of Plywood Test Data and Determination of Characteristic Values Suitable for Code Presentation - C R Wilson

14-4-1 An Introduction to Performance Standards for Wood-base Panel Products - D H Brown

14-4-2 Proposal for Presenting Data on the Properties of Structural Panels - T Schmidt

16-4-1 Planar Shear Capacity of Plywood in Bending - C K A Stieda

17-4-1 Determination of Panel Shear Strength and Panel Shear Modulus of Beech-Plywood in Structural Sizes - J Ehlbeck and F Colling

17-4-2 Ultimate Strength of Plywood Webs - R H Leicester and L Pham

20-4-1 Considerations of Reliability - Based Design for Structural Composite Products
- M R O'Halloran, J A Johnson, E G Elias and T P Cunningham

21-4-1 Modelling for Prediction of Strength of Veneer Having Knots - Y Hirashima

STRESS GRADING

1-5-1 Quality Specifications for Sawn Timber and Precision Timber - Norwegian Standard NS 3080

1-5-2 Specification for Timber Grades for Structural Use - British Standard BS 4978

4-5-1 Draft Proposal for an International Standard for Stress Grading Coniferous Sawn Softwood - ECE Timber Committee

16-5-1 Grading Errors in Practice - B Thunell

16-5-2 On the Effect of Measurement Errors when Grading Structural Timber - L Nordberg and B Thunell

19-5-1 Stress-Grading by ECE Standards of Italian-Grown Douglas-Fir Dimension Lumber from Young Thinnings - L Uzielli

19-5-2 Structural Softwood from Afforestation Regions in Western Norway - R Lackner

21-5-1 Non-Destructive Test by Frequency of Full Size Timber for Grading - T Nakai

STRESSES FOR SOLID TIMBER

4-6-1 Derivation of Grade Stresses for Timber in the UK - W T Curry

5-6-1 Standard Methods of Test for Determining some Physical and Mechanical Properties of Timber in Structural Sizes - W T Curry

5-6-2 The Description of Timber Strength Data - J R Tory

5-6-3 Stresses for EC1 and EC2 Stress Grades - J R Tory

6-6-1 Standard Methods of Test for the Determination of some Physical and Mechanical Properties of Timber in Structural Sizes (third draft) - W T Curry

7-6-1 Strength and Long-term Behaviour of Lumber and Glued Laminated Timber under Torsion Loads - K Möhler

9-6-1 Classification of Structural Timber - H J Larsen

9-6-2 Code Rules for Tension Perpendicular to Grain - H J Larsen

9-6-3 Tension at an Angle to the Grain - K Möhler

9-6-4 Consideration of Combined Stresses for Lumber and Glued Laminated Timber - K Möhler

11-6-1 Evaluation of Lumber Properties in the United States - W L Galligan and J H Haskell

11-6-2 Stresses Perpendicular to Grain - K Möhler

11-6-3 Consideration of Combined Stresses for Lumber and Glued Laminated Timber (addition to Paper CIB-W18/9-6-4) - K Möhler

12-6-1 Strength Classifications for Timber Engineering Codes - R H Leicester and W G Keating

12-6-2 Strength Classes for British Standard BS 5268 - J R Tory

13-6-1 Strength Classes for the CIB Code - J R Tory

13-6-2 Consideration of Size Effects and Longitudinal Shear Strength for Uncracked Beams - R O Foschi and J D Barrett

13-6-3 Consideration of Shear Strength on End-Cracked Beams - J D Barrett and R O Foschi

15-6-1 Characteristic Strength Values for the ECE Standard for Timber - J G Sunley

16-6-1 Size Factors for Timber Bending and Tension Stresses - A R Fewell

16-6-2 Strength Classes for International Codes - A R Fewell and J G Sunley

17-6-1 The Determination of Grade Stresses from Characteristic Stresses for BS 5268: Part 2 - A R Fewell

17-6-2 The Determination of Softwood Strength Properties for Grades, Strength Classes and Laminated Timber for BS 5268: Part 2 - A R Fewell

18-6-1 Comment on Papers: 18-6-2 and 18-6-3 - R H Leicester

18-6-2 Configuration Factors for the Bending Strength of Timber - R H Leicester

18-6-3 Notes on Sampling Factors for Characteristic Values - R H Leicester

18-6-4 Size Effects in Timber Explained by a Modified Weakest Link Theory - B Madsen and A H Buchanan

18-6-5 Placement and Selection of Growth Defects in Test Specimens - H Riberholt

18-6-6 Partial Safety-Coefficients for the Load-Carrying Capacity of Timber Structures - B Norén and J-O Nylander

19-6-1 Effect of Age and/or Load on Timber Strength - J Kuipers

19-6-2 Confidence in Estimates of Characteristic Values - R H Leicester

19-6-3 Fracture Toughness of Wood - Mode I - K Wright and M Fonselius

19-6-4 Fracture Toughness of Pine - Mode II - K Wright

19-6-5 Drying Stresses in Round Timber - A Ranta-Maunus

19-6-6 A Dynamic Method for Determining Elastic Properties of Wood - R Görlacher

20-6-1 A Comparative Investigation of the Engineering Properties of "Whitewoods" Imported to Israel from Various Origins - U Korin

20-6-2 Effects of Yield Class, Tree Section, Forest and Size on Strength of Home Grown Sitka Spruce - V Picardo

20-6-3 Determination of Shear Strength and Strength Perpendicular to Grain - H J Larsen

21-6-1 Draft Australian Standard: Methods for Evaluation of Strength and Stiffness of Graded Timber - R H Leicester

21-6-2 The Determination of Characteristic Strength Values for Stress Grades of Structural Timber. Part 1 - A R Fewell and P Glos

21-6-3 Shear Strength in Bending of Timber - U Korin

TIMBER JOINTS AND FASTENERS

1-7-1 Mechanical Fasteners and Fastenings in Timber Structures - E G Stern

4-7-1 Proposal for a Basic Test Method for the Evaluation of Structural Timber Joints with Mechanical Fasteners and Connectors - RILEM 3TT Committee

4-7-2 Test Methods for Wood Fasteners - K Möhler

5-7-1 Influence of Loading Procedure on Strength and Slip-Behaviour in Testing Timber Joints - K Möhler

5-7-2 Recommendations for Testing Methods for Joints with Mechanical Fasteners and Connectors in Load-Bearing Timber Structures - RILEM 3 TT Committee

5-7-3 CIB-Recommendations for the Evaluation of Results of Tests on Joints with Mechanical Fasteners and Connectors used in Load-Bearing Timber Structures - J Kuipers

6-7-1 Recommendations for Testing Methods for Joints with Mechanical Fasteners and Connectors in Load-Bearing Timber Structures (seventh draft) - RILEM 3 TT Committee

6-7-2 Proposal for Testing Integral Nail Plates as Timber Joints - K Möhler

6-7-3 Rules for Evaluation of Values of Strength and Deformation from Test Results - Mechanical Timber Joints - M Johansen, J Kuipers, B Norén

6-7-4 Comments to Rules for Testing Timber Joints and Derivation of Characteristic Values for Rigidity and Strength - B Norén

7-7-1 Testing of Integral Nail Plates as Timber Joints - K Möhler

7-7-2 Long Duration Tests on Timber Joints - J Kuipers

7-7-3 Tests with Mechanically Jointed Beams with a Varying Spacing of Fasteners - K Möhler

7-100-1 CIB-Timber Code Chapter 5.3 Mechanical Fasteners; CIB-Timber Standard 06 and 07 - H J Larsen

9-7-1 Design of Truss Plate Joints - F J Keenan

9-7-2 Staples - K Möhler

11-7-1 A Draft Proposal for International Standard: ISO Document ISO/TC 165N 38E

12-7-1 Load-Carrying Capacity and Deformation Characteristics of Nailed Joints - J Ehlbeck

12-7-2 Design of Bolted Joints - H J Larsen

12-7-3 Design of Joints with Nail Plates - B Norén

13-7-1 Polish Standard BN-80/7159-04: Parts 00-01-02-03-04-05. "Structures from Wood and Wood-based Materials. Methods of Test and Strength Criteria for Joints with Mechanical Fasteners"

13-7-2 Investigation of the Effect of Number of Nails in a Joint on its Load Carrying Ability - W Nozynski

13-7-3 International Acceptance of Manufacture, Marking and Control of Finger-jointed Structural Timber - B Norén

13-7-4 Design of Joints with Nail Plates - Calculation of Slip - B Norén

13-7-5 Design of Joints with Nail Plates - The Heel Joint - B Källsner

13-7-6 Nail Deflection Data for Design - H J Burgess

13-7-7 Test on Bolted Joints - P Vermeyden

13-7-8 Comments to paper CIB-W18/12-7-3 "Design of Joints with Nail Plates" - B Norén

13-7-9 Strength of Finger Joints - H J Larsen

13-100-4 CIB Structural Timber Design Code. Proposal for Section 6.1.5 Nail Plates - N I Bovim

14-7-1 Design of Joints with Nail Plates (second edition) - B Norén

14-7-2 Method of Testing Nails in Wood (second draft, August 1980) - B Norén

14-7-3 Load-Slip Relationship of Nailed Joints - J Ehlbeck and H J Larsen

14-7-4 Wood Failure in Joints with Nail Plates - B Norén

14-7-5 The Effect of Support Eccentricity on the Design of W- and WW-Trussed with Nail Plate Connectors - B Källsner

14-7-6 Derivation of the Allowable Load in Case of Nail Plate Joints Perpendicular to Grain - K Möhler

14-7-7 Comments on CIB-W18/14-7-1 - T A C M van der Put

15-7-1 Final Recommendation TT-1A: Testing Methods for Joints with Mechanical Fasteners in Load-Bearing Timber Structures. Annex A Punched Metal Plate Fasteners - Joint Committee RILEM/CIB-3TT

16-7-1 Load Carrying Capacity of Dowels - E Gehri

16-7-2 Bolted Timber Joints: a Literature Survey - N Harding

16-7-3 Bolted Timber Joints: Practical Aspects of Construction and Design; a Survey - N Harding

16-7-4 Bolted Timber Joints: Draft Experimental Work Plan - Building Research Association of New Zealand

17-7-1 Mechanical Properties of Nails and their Influence on Mechanical Properties of Nailed Timber Joints Subjected to Lateral Loads - I Smith, L R J Whale, C Anderson and L Held

17-7-2 Notes on the Effective Number of Dowels and Nails in Timber Joints - G Steck

18-7-1 Model Specification for Driven Fasteners for Assembly of Pallets and Related Structures - E G Stern and W B Wallin

18-7-2 The Influence of the Orientation of Mechanical Joints on their Mechanical Properties - I Smith and L R J Whale

18-7-3 Influence of Number of Rows of Fasteners or Connectors upon the Ultimate Capacity of Axially Loaded Timber Joints - I Smith and G Steck

18-7-4 A Detailed Testing Method for Nailplate Joints - J Kangas

18-7-5 Principles for Design Values of Nailplates in Finland - J Kangas

18-7-6 The Strength of Nailplates - N I Bovim and E Aasheim

19-7-1 Behaviour of Nailed and Bolted Joints under Short-Term Lateral Load - Conslusions from Some Recent Research - L R J Whale, I Smith B O Hilson

19-7-2 Glued Bolts in Glulam - H Riberholt

19-7-3 Effectiveness of Multiple Fastener Joints According to National Codes and Eurocode 5 (Draft) - G Steck

19-7-4 The Prediction of the Long-Term Load Carrying Capacity of Joints in Wood Structures - Y M Ivanov and Y Y Slavic

19-7-5 Slip in Joints under Long-Term Loading - T Feldborg and M Johansen

19-7-6 The Derivation of Design Clauses for Nailed and Bolted Joints in Eurocode 5 - L R J Whale and I Smith

19-7-7 Design of Joints with Nail Plates - Principles - B Norén

19-7-8 Shear Tests for Nail Plates - B Norén

19-7-9 Advances in Technology of Joints for Laminated Timber - Analyses of the Structural Behaviour - M Piazza and G Turrini

19-15-1 Connections Deformability in Timber Structures: a Theoretical Evaluation of its Influence on Seismic Effects - A Ceccotti and A Vignoli

20-7-1 Design of Nailed and Bolted Joints-Proposals for the Revision of Existing Formulae in Draft Eurocode 5 and the CIB Code - L R J Whale, I Smith and H J Larsen

20-7-2 Slip in Joints under Long Term Loading - T Feldborg and M Johansen

20-7-3 Ultimate Properties of Bolted Joints in Glued-Laminated Timber - M Yasumura, T Murota and H Sakai

20-7-4 Modelling the Load-Deformation Behaviour of Connections with Pin-Type Fasteners under Combined Moment, Thrust and Shear Forces - I Smith

21-7-1 Nails under Long-Term Withdrawal Loading - T Feldborg and M Johansen

21-7-2 Glued Bolts in Glulam-Proposals for CIB Code - H Riberholt

21-7-3 Nail Plate Joint Behaviour under Shear Loading - T Poutanen

21-7-4 Design of Joints with Laterally Loaded Dowels. Proposals for Improving the Design Rules in the CIB Code and the Draft Eurocode 5 - J Ehlbeck and H Werner

21-7-5 Axially Loaded Nails: Proposals for a Supplement to the CIB Code - J Ehlbeck and W Siebert

LOAD SHARING

3-8-1 Load Sharing - An Investigation on the State of Research and Development of Design Criteria - E Levin

4-8-1 A Review of Load-Sharing in Theory and Practice - E Levin

4-8-2 Load Sharing - B Norén

19-8-1 Predicting the Natural Frequencies of Light-Weight Wooden Floors - I Smith and Y H Chui

20-8-1 Proposed Code Requirements for Vibrational Serviceability of Timber Floors - Y H Chui and I Smith

21-8-1 An Addendum to Paper 20-8-1 - Proposed Code Requirements for Vibrational Serviceability of Timber Floors - Y H Chui and I Smith

21-8-2 Floor Vibrational Serviceability and the CIB Model Code - S Ohlsson

DURATION OF LOAD

3-9-1 Definitions of Long Term Loading for the Code of Practice - B Norén

4-9-1 Long Term Loading of Trussed Rafters with Different Connection Systems - T Feldborg and M Johansen

5-9-1 Strength of a Wood Column in Combined Compression and Bending with Respect to Creep - B Källsner and B Norén

6-9-1 Long Term Loading for the Code of Practice (Part 2) - B Norén

6-9-2 Long Term Loading - K Möhler

6-9-3 Deflection of Trussed Rafters under Alternating Loading during a Year - T Feldobrg and M Johansen

7-6-1 Strength and Long Term Behaviour of Lumnber and Glued-Laminated Timber under Torsion Loads - K Möhler

7-9-1 Code Rules Concerning Strength and Loading Time - H J Larsen and E Theilgaard

17-9-1 On the Long-Term Carrying Capacity of Wood Structures - Y M Ivanov and Y Y Slavic

18-9-1 Prediction of Creep Deformations of Joints - J Kuipers

19-9-1 Another Look at Three Duration of Load Models - R O Foschi and Z C Yao

19-9-2 Duration of Load Effects for Spruce Timber with Special Reference to Moisture Influence - A Status Report - P Hoffmeyer

19-9-3 A Model of Deformation and Damage Processes Based on the Reaction Kinetics of Bond Exchange - T A C M van der Put

19-9-4 Non-Linear Creep Superposition - U Korin

19-9-5 Determination of Creep Data for the Component Parts of Stressed-Skin Panels - R Kliger

19-9-6 Creep an Lifetime of Timber Loaded in Tension and Compression - P Glos

19-1-1 Duration of Load Effects and Reliability Based Design (Single Member) - R O Foschi and Z C Yao

19-6-1 Effect of Age and/or Load on Timber Strength - J Kuipers

19-7-4 The Prediction of the Long-Term Load Carrying Capacity of Joints in Wood Structures - Y M Ivanov and Y Y Slavic

19-7-5 Slip in Joints under Long-Term Loading - T Feldborg and M Johansen

20-7-2 Slip in Joints under Long-Term Loading - T Feldborg and M Johansen

TIMBER BEAMS

4-10-1 The Design of Simple Beams - H J Burgess

4-10-2 Calculation of Timber Beams Subjected to Bending and Normal Force - H J Larsen

5-10-1 The Design of Timber Beams - H J Larsen

9-10-1 The Distribution of Shear Stresses in Timber Beams - F J Keenan

9-10-2 Beams Notched at the Ends - K Möhler

11-10-1 Tapered Timber Beams - H Riberholt

13-6-2 Consideration of Size Effects in Longitudinal Shear Strength for Uncracked Beams - R O Foschi and J D Barrett

13-6-3 Consideration of Shear Strength on End-Cracked Beams - J D Barrett and R O Foschi

18-10-1 Submission to the CIB-W18 Committee on the Design of Ply Web Beams by Consideration of the Type of Stress in the Flanges - J A Baird

18-10-2 Longitudinal Shear Design of Glued Laminated Beams - R O Foschi

19-10-1 Possible Code Approaches to Lateral Buckling in Beams - H J Burgess

19-2-1 Creep Buckling Strength of Timber Beams and Columns - R H Leicester

20-2-1 Lateral Buckling Theory for Rectangular Section Deep Beam-Columns - H J Burgess

20-10-1 Draft Clause for CIB Code for Beams with Initial Imperfections - H J Burgess

20-10-2 Space Joists in Irish Timber - W J Robinson

20-10-3 Composite Structure of Timber Joists and Concrete Slab - T Poutanen

21-10-1 A Study of Strength of Notched Beams - P J Gustafsson

ENVIRONMENTAL CONDITIONS

5-11-1 Climate Grading for the Code of Practice - B Norén

6-11-1 Climate Grading (2) - B Norén

9-11-1 Climate Classes for Timber Design - F J Keenan

19-11-1 Experimental Analysis on Ancient Downgraded Timber Structures - B Leggeri and L Paolini

19-6-5 Drying Stresses in Round Timber - A Ranta-Maunus

LAMINATED MEMBERS

6-12-1 Directives for the Fabrication of Load-Bearing Structures of Glued Timber - A van der Velden and J Kuipers

8-12-1 Testing of Big Glulam Timber Beams - H Kolb and P Frech

8-12-2 Instruction for the Reinforcement of Apertures in Glulam Beams - H Kolb and P Frech

8-12-3 Glulam Standard Part 1: Glued Timber Structures; Requirements for Timber (Second Draft)

9-12-1 Experiments to Provide for Elevated Forces at the Supports of Wooden Beams with Particular Regard to Shearing Stresses and Long-Term Loadings - F Wassipaul and R Lackner

9-12-2 Two Laminated Timber Arch Railway Bridges Built in Perth in 1849 - L G Booth

9-6-4 Consideration of Combined Stresses for Lumber and Glued Laminated Timber - K Möhler

11-6-3 Consideration of Combined Stresses for Lumber and Glued Laminated Timber (addition to Paper CIB-W18/9-6-4) - K Möhler

12-12-1 Glulam Standard Part 2: Glued Timber Structures; Rating (3rd draft)

12-12-2 Glulam Standard Part 3: Glued Timber Structures; Performance (3 rd draft)

13-12-1 Glulam Standard Part 3: Glued Timber Structures; Performance (4th draft)

14-12-1 Proposals for CEI-Bois/CIB-W18 Glulam Standards - H J Larsen

14-12-2 Guidelines for the Manufacturing of Glued Load-Bearing Timber Structures - Stevin Laboratory

14-12-3 Double Tapered Curved Glulam Beams - H Riberholt

14-12-4 Comment on CIB-W18/14-12-3 - E Gehri

18-12-1 Report on European Glulam Control and Production Standard - H Riberholt

18-10-2 Longitudinal Shear Design of Glued Laminated Beams - R O Foschi

19-12-1 Strength of Glued Laminated Timber - J Ehlbeck and F Colling

19-12-2 Strength Model for Glulam Columns - H J Blaß

19-12-3 Influence of Volume and Stress Distribution on the Shear Strength and Tensile Strength Perpendicular to Grain - F Colling

19-12-4 Time-Dependent Behaviour of Glued-Laminated Beams - F Zaupa

21-12-1 Modulus of Rupture of Glulam Beam Composed of Arbitrary Laminae - K Komatsu and N Kawamoto

21-12-2 An Appraisal of the Young's Modulus Values Specified for Glulam in Eurocode 5 - L R J Whale, B O Hilson and P D Rodd

21-12-3 The Strength of Glued Laminated Timber (Glulam): Influence of Lamination Qualities and Strength of Finger Joints - J Ehlbeck and F Colling

21-12-4 Comparison of a Shear Strength Design Method in Eurocode 5 and a More Traditional One - H Riberholt

PARTICLE AND FIBRE BUILDING BOARDS

7-13-1 Fibre Building Boards for CIB Timber Code (First Draft) - O Brynildsen

9-13-1 Determination of the Bearing Strength and the Load-Deformation Characteristics of Particleboard - K Möhler, T Budianto and J Ehlbeck

9-13-2 The Structural Use of Tempered Hardboard - W W L Chan

11-13-1 Tests on Laminated Beams from Hardboard under Short- and Longterm Load - W Nozynski

11-13-2 Determination of Deformation of Special Densified Hardboard under Long-term Load and Varying Temperature and Humidity Conditions - W Halfar

11-13-3 Determination of Deformation of Hardboard under Long-term Load in Changing Climate - W Halfar

14-4-1 An Introduction to Performance Standards for Wood-Base Panel Products - D H Brown

14-4-2 Proposal for Presenting Data on the Properties of Structural Panels - T Schmidt

16-13-1 Effect of Test Piece Size on Panel Bending Properties - P W Post

20-4-1 Cousiderations of Reliability - Based Design for Structural Composite Products - M R O'Halloran, J A Johnson, E G Elias and T P Cunningham

20-13-1 Classification Systems for Structural Wood-Based Sheet Materials - V C Kearley and A R Abbott

21-13-1 Design Values for Nailed Chipboard - Timber Joints - A R Abbott

TRUSSED RAFTERS

4-9-1 Long-term Loading of Trussed Rafters with Different Connection Systems - T Feldobrg and M Johansen

6-9-3 Deflection of Trussed Rafters under Alternating Loading During a Year - T Feldborg and M Johansen

7-2-1 Lateral Bracing of Timber Struts - J A Simon

9-14-1 Timber Trusses - Code Related Problems - T F Williams

9-7-1 Design of Truss Plate Joints - F J Keenan

10-14-1 Design of Roof Bracing - The State of the Art in South Africa - P A V Bryant and J A Simon

11-14-1 Design of Metal Plate Connected Wood Trusses - A R Egerup

12-14-1 A Simple Design Method for Standard Trusses - A R Egerup

13-14-1 Truss Design Method for CIB Timber Code- A R Egerup

13-14-2 Trussed Rafters, Static Models - H Riberholt

13-14-3 Comparison of 3 Truss Models Designed by Different Assumptions for Slip and E-Modulus - K Möhler

14-14-1	Wood Trussed Rafter Design - T Feldborg and M Johansen
14-14-2	Truss-Plate Modelling in the Analysis of Trusses - R O Foschi
14-14-3	Cantilevered Timber Trusses - A R Egerup
14-7-5	The Effect of Support Eccentricity on the Design of W- and WW-Trusses with Nail Plate Connectors - B Källsner
15-14-1	Guidelines for Static Models of Trussed Rafters - H Riberholt
15-14-2	The Influence of Various Factors on the Accuracy of the Structural Analysis of Timber Roof Trusses - F R P Pienaar
15-14-3	Bracing Calculations for Trussed Rafter Roofs - H J Burgess
15-14-4	The Design of Continuous Members in Timber Trussed Rafters with Punched Metal Connector Plates - P O Reece
15-14-5	A Rafter Design Method Matching U.K. Test Results for Trussed Rafters - H J Burgess
16-14-1	Full-Scale Tests on Timber Fink Trusses Made from Irish Grown Sitka Spruce - V Picardo
17-14-1	Data from Full Scale Tests on Prefabricated Trussed Rafters - V Picardo
17-14-2	Simplified Static Analysis and Dimensioning of Trussed Rafters - H Riberholt
17-14-3	Simplified Calculation Method for W-Trusses - B Källsner
18-14-1	Simplified Calculation Method for W-Trusses (Part 2) - B Källsner
18-14-2	Model for Trussed Rafter Design - T Poutanen
19-14-1	Annex on Simplified Design of W-Trusses - H J Larsen
19-14-2	Simplified Static Analysis and Dimensioning of Trussed Rafters - Part 2 - H Riberholt
19-14-3	Joint Eccentricity in Trussed Rafters - T Poutanen
20-14-1	Some Notes about Testing Nail Plates Subjected to Moment Load - T Poutanen
20-14-2	Moment Distribution in Trussed Rafters - T Poutanen
20-14-3	Practical Design Methods for Trussed Rafters - A R Egerup

STRUCTURAL STABILITY

8-15-1 Laterally Loaded Timber Columns: Tests and Theory - H J Larsen

13-15-1 Timber and Wood-Based Products Structures. Panels for Roof Coverings. Methods of Testing and Strength Assessment Criteria. Polish Standard BN-78/7159-03

16-15-1 Determination of Bracing Structures for Compression Members and Beams - H Brüninghoff

17-15-1 Proposal for Chapter 7.4 Bracing - H Brüninghoff

17-15-2 Seismic Design of Small Wood Framed Houses - K F Hansen

18-15-1 Full-Scale Structures in Glued Laminated Timber, Dynamic Tests: Theoretical and Experimental Studies - A Ceccotti and A Vignoli

18-15-2 Stabilizing Bracings - H Brüninghoff

19-15-1 Connections Deformability in Timber Structures: a Theoretical Evaluation of its Influence on Seismic Effects - A Ceccotti and A Vignoli

19-15-2 The Bracing of Trussed Beams - M H Kessel and J Natterer

19-15-3 Racking Resistance of Wooden Frame Walls with Various Openings - M Yasumura

19-15-4 Some Experiences of Restoration of Timber Structures for Country Buildings - G Cardinale and P Spinelli

19-15-5 Non-Destructive Vibration Tests on Existing Wooden Dwellings - Y Hirashima

20-15-1 Behaviour Factor of Timber Structures in Seismic Zones A Ceccotti and A Vignoli

21-15-1 Rectangular Section Deep Beam - Columns with Continuous Lateral Restraint - H J Burgess

21-15-2 Buckling Modes and Permissible Axial Loads for Continuously Braced Columns - H J Burgess

21-15-3 Simple Approaches for Column Bracing Calculations - H J Burgess

21-15-4 Calculations for Discrete Column Restraints - H J Burgess

21-15-5 Behaviour Factor of Timber Structures in Seismic Zones (Part Two) - A Ceccotti and A Vignoli

FIRE

12-16-1 British Standard BS 5268 the Structural Use of Timber: Part 4 Fire Resistance of Timber Structures

13-100-2 CIB Structural Timber Design Code. Chapter 9. Performance in Fire

19-16-1 Simulation of Fire in Tests of Axially Loaded Wood Wall Studs - J König

STATISTICS AND DATA ANALYSIS

13-17-1 On Testing Whether a Prescribed Exclusion Limit is Attained - W G Warren

16-17-1 Notes on Sampling and Strength Prediction of Stress Graded Structural Timber - P Glos

16-17-2 Sampling to Predict by Testing the Capacity of Joints, Components and Structures - B Norén

16-17-3 Discussion of Sampling and Analysis Procedures - P W Post

17-17-1 Sampling of Wood for Joint Tests on the Basis of Density - I Smith, L R J Whale

17-17-2 Sampling Strategy for Physical and Mechanical Properties of Irish Grown Sitka Spruce - V Picardo

18-17-1 Sampling of Timber in Structural Sizes - P Glos

18-6-3 Notes on Sampling Factors for Characteristic Values - R H Leicester

19-17-1 Load Factors for Proof and Prototype Testing - R H Leicester

19-6-2 Confidence in Estimates of Characteristic Values - R H Leicester

21-6-1 Draft Australian Standard: Methods for Evaluation of Strength and Stiffness of Graded Timber - R H Leicester

21-6-2 The Determination of Characteristic Strength Values for Stress Grades of Structural Timber. Part 1 - A R Fewell and P Glos

GLUED JOINTS

20-18-1 Wood Materials under Combined Mechanical and Hygral Loading - A Martensson and S Thelandersson

20-18-2 Analysis of Generalized Volkersen - Joints in Terms of Non-Linear Fracture Mechanics - P J Gustafsson

20-18-3 The Complete Stress-Slip Curve of Wood-Adhesives in Pure Shear - H Wernersson and P J Gustafsson

CIB TIMBER CODE

2-100-1 A Framework for the Production of an International Code of Practice for the Structural Use of Timber - W T Curry

5-100-1 Design of Solid Timber Columns (First Draft) - H J Larsen

5-100-2 A Draft Outline of a Code for Timber Structures - L G Booth

6-100-1 Comments on Document 5-100-1; Design of Solid Timber Columns - H J Larsen and E Theilgaard

6-100-2 CIB Timber Code: CIB Timber Standards - H J Larsen and E Theilgaard

7-100-1 CIB Timber Code Chapter 5.3 Mechanical Fasteners; CIB Timber Standard 06 and 07 - H J Larsen

8-100-1 CIB Timber Code - List of Contents (Second Draft) - H J Larsen

9-100-1 The CIB Timber Code (Second Draft)

11-100-1 CIB Structural Timber Design Code (Third Draft)

11-100-2 Comments Received on the CIB Code

a U Saarelainen
b Y M Ivanov
c R H Leicester
d W Nozynski
e W R A Meyer
f P Beckmann; R Marsh
g W R A Meyer
h W R A Meyer

11-100-3 CIB Structural Timber Design Code; Chapter 3 - H J Larsen

12-100-1 Comment on the CIB Code - Sous-Commission Glulam

12-100-2 Comment on the CIB Code - R H Leicester

12-100-3 CIB Structural Timber Design Code (Fourth Draft)

13-100-1 Agreed Changes to CIB Structural Timber Design Code

13-100-2 CIB Structural Timber Design Code. Chapter 9: Performance in Fire

13-100-3a Comments on CIB Structural Timber Design Code

13-100-3b Comments on CIB Structural Timber Design Code - W R A Meyer

13-100-3c Comments on CIB Structural Timber Design Code - British Standards Institution

13-100-4 CIB Structural Timber Design Code. Proposal for Section 6.1.5 Nail Plates - N I Bovim

14-103-2 Comments on the CIB Structural Timber Design Code - R H Leicester

15-103-1 Resolutions of TC 165-meeting in Athens 1981-10-12/13

21-100-1 CIB Structural Timber Design Code. Proposed Changes of Sections on Lateral Instability, Columns and Nails - H J Larsen

LOADING CODES

4-101-1 Loading Regulations - Nordic Committee for Building Regulations

4-101-2 Comments on the Loading Regulations - Nordic Committee for Building Regulations

STRUCTURAL DESIGN CODES

1-102-1 Survey of Status of Building Codes, Specifications etc., in USA - E G Stern

1-102-2 Australian Codes for Use of Timber in Structures - R H Leicester

1-102-3 Contemporary Concepts for Structural Timber Codes - R H Leicester

1-102-4 Revision of CP 112 - First Draft, July 1972 - British Standards Institution

4-102-1 Comparsion of Codes and Safety Requirements for Timber Structures in EEC Countries - Timber Research and Development Association

4-102-2 Nordic Proposals for Safety Code for Structures and Loading Code for Design of Structures - O A Brynildsen

4-102-3 Proposal for Safety Codes for Load-Carrying Structures - Nordic Committee for Building Regulations

4-102-4 Comments to Proposal for Safety Codes for Load-Carrying Structures - Nordic Committee for Building Regulations

4-102-5 Extract from Norwegian Standard NS 3470 "Timber Structures"

4-102-6 Draft for Revision of CP 112 "The Structural Use of Timber" - W T Curry

8-102-1 Polish Standard PN-73/B-03150: Timber Structures; Statistical Calculations and Designing

8-102-2 The Russian Timber Code: Summary of Contents

9-102-1 Svensk Byggnorm 1975 (2nd Edition); Chapter 27: Timber Construction

11-102-1 Eurocodes - H J Larsen

13-102-1 Program of Standardisation Work Involving Timber Structures and Wood-Based Products in Poland

17-102-1 Safety Principles - H J Larsen and H Riberholt

17-102-2 Partial Coefficients Limit States Design Codes for Structural Timberwork - I Smith

18-102-1 Antiseismic Rules for Timber Structures: an Italian Proposal - G Augusti and A Ceccotti

18-1-2 Eurocode 5, Timber Structures - H J Larsen

19-102-1 Eurocode 5 - Requirements to Timber - Drafting Panel Eurocode 5

19-102-2 Eurocode 5 and CIB Structural Timber Design Code - H J Larsen

19-102-3 Comments on the Format of Eurocode 5 - A R Fewell

19-102-4 New Developments of Limit States Design for the New GDR Timber Design Code - W Rug and M Badstube

19-7-3 Effectiveness of Multiple Fastener Joints According to National Codes and Eurocode 5 (Draft) - G Steck

19-7-6 The Derivation of Design Clauses for Nailed and Bolted Joints in Eurocode 5 - L R J Whale and I Smith

19-14-1 Annex on Simplified Design of W-Trusses - H J Larsen

20-102-1 Development of a GDR Limit States Design Code for Timber Structures - W Rug and M Badstube

21-102-1 Research Activities Towards a New GDR Timber Design Code Based on Limit States Design - W Rug and M Badstube

INTERNATIONAL STANDARDS ORGANISATION

3-103-1 Method for the Preparation of Standards Concerning the Safety of Structures (ISO/DIS 3250) - International Standards Organisation ISO/TC98

4-103-1 A Proposal for Undertaking the Preparation of an International Standard on Timber Structures - International Standards Organisation

5-103-1 Comments on the Report of the Consultion with Member Bodies Concerning ISO/TC/P129 - Timber Structures - Dansk Ingeniorforening

7-103-1 ISO Technical Committees and Membership of ISO/TC 165

8-103-1 Draft Resolutions of ISO/TC 165

12-103-1 ISO/TC 165 Ottawa, September 1979

13-103-1 Report from ISO/TC 165 - A Sorensen

14-103-1 Comments on ISO/TC 165 N52 "Timber Structures; Solid Timber in Structural Sizes; Determination of Some Physical and Mechanical Properties"

14-103-2 Comments on the CIB Structural Timber Design Code - R H Leicester

21-103-1 Concept of a Complete Set of Standards - R H Leicester

JOINT COMMITTEE ON STRUCTURAL SAFETY

3-104-1 International System on Unified Standard Codes of Practice for Structures - Comité Européen du Béton (CEB)

7-104-1 Volume 1: Common Unified Rules for Different Types of Construction and Material - CEB

CIB PROGRAMME, POLICY AND MEETINGS

1-105-1 A Note on International Organisations Active in the Field of Utilisation of Timber - P Sonnemans

5-105-1 The Work and Objectives of CIB-W18-Timber Structures - J G Sunley

10-105-1 The Work of CIB-W18 Timber Structures - J G Sunley

15-105-1 Terms of Reference for Timber - Framed Housing Sub-Group of CIB-W18

19-105-1 Tropical and Hardwood Timbers Structures - R H Leicester

21-105-1 First Conference of CIB-W18B, Tropical and Hardwood Timber Structures Singapore, 26 - 28 October 1987 - R H Leicester

INTERNATIONAL UNION OF FORESTRY RESEARCH ORGANISATIONS

7-106-1 Time and Moisture Effects - CIB W18/IUFRO 55.02-03 Working Party

5

INTERNATIONAL COUNCIL FOR BUILDING RESEARCH STUDIES AND DOCUMENTATION

WORKING COMMISSION W18A - TIMBER STRUCTURES

FORMAT FOR BUCKLING STRENGTH

by

R H Leicester
CSIRO
Australia

MEETING TWENTY-ONE
PARKSVILLE, VANCOUVER ISLAND
CANADA
SEPTEMBER 1988

FORMAT.RHL/210688

FORMAT FOR BUCKLING STRENGTH

by

R.H. Leicester
(CSIRO, Melbourne, Australia)

1. INTRODUCTION

Buckling strength is a complex function of many parameters including the following,

- material properties (strength stiffness, failure criterion, defect dispersion, crookedness),
- climate (as it affects material properties, creep),
- member cross-section (area, section modulus, plywood and glulam layup, structure of built-up members), and
- structural geometry (member length, end fixity conditions, method of load application).

Because of these complexities, a systematic and consistent approach should be used in the presentation of equations for buckling strength in a design code; if this is not done, the code users are likely to be confused and unclear as to the type of structure being analysed and whether the results obtained are reasonable.

The following is a proposal for a code format to be applied uniformly for all types of buckling strength specifications. In so doing, it is well to bear in mind that to strive for a high degree of accuracy is inappropriate; many of the critical parameters that affect buckling strength are either unknown or vary significantly from one member to another; examples of such parameters are crookedness, defect dispersion and failure criteria.

2. PROPOSAL

2.1 Format

The ultimate load capacity, P_{ult}, for a slender member will be given by

$$P_{ult} = K_{inst} P_{squash} \quad (1)$$

where P_{squash} is the 'squash load', i.e. the load capacity if there are no out-of-plane buckling deformations, and K_{inst} is the instability factor; note that by definition $K_{inst} \leqslant 1.00$.

The instability factor will be described in terms of a slenderness coefficient λ defined by

$$\lambda = (P_{squash}/P_{crit})^{1/2} \quad (2)$$

where P_{crit} is the critical elastic buckling load. The instability factor is then given by

$$K_{inst} = g(\lambda) \quad (3)$$

where g (λ) is some function of λ.

An example of this function is given in Rule 5.1.6 of Eurocode 5 (Larsen *et al.* 1986) for the buckling strength of beams, and is shown in Figure 1.

2.2 Considerations

The definition of slenderness coefficient in equation (2) is awkward to use as it includes both material and geometry parameters. However it has general applicability, and it does include all the essential parameters that are specified in an engineering design. P_{squash} is a function of strength and cross-section parameters; P_{crit} is a function of stiffness, cross-section and structural geometry parameters. All other parameters are obtained indirectly, by fitting g (λ) to experimental data, i.e. in practice g (λ) is really an empirical and not an analytical function.

The function g (λ) should be specified for one common case. For other cases it should be possible to specify a good approximation by using an 'effective slenderness coefficient' λ_{eff}, where

$$\lambda_{eff} = \alpha_1 \alpha_2 \alpha_3 \ldots \alpha_n \lambda \quad (4)$$

in which α_1, α_2 ... are modification factors to account for different end fixity conditions, creep, crookedness etc.

3. EXAMPLES FOR SHORT DURATION STRENGTH

3.1 Beams and Columns

Examples for beam and columns have been given in a previous paper (Leicester, 1986). For beams, subjected to a uniform moment M and with the assumption of a linear failure criterion as shown in Figure 2, the ultimate moment capacity M_{ult} is given by

$$M_{ult} = K_{inst} M_{squash} \tag{5}$$

for which

$$M_{squash} = Z_x f_b \tag{6}$$

$$M_{crit} = (\pi/L) (EI_y GJ)^{1/2} \tag{7}$$

$$\lambda = (M_{squash}/M_{crit})^{1/2} \tag{8}$$

$$K_{inst} = 1/2 \{\psi - [\psi^2 - (4/\lambda^2)]^{1/2}\} \tag{9}$$

where

$$\psi = (1/\lambda^2)[1 + \Delta_{\phi o} (Z_x/Z_y)] \tag{10}$$

in which Z_x, Z_y are section moduli, EI_y and GJ are lateral and torsional stiffness L is the length of the beam $\Delta_{\phi o}$ is the initial twist at the centre of the beam, and f_b is the modulus of rupture.

Hence provided the term $\Delta_{\phi o} (Z_x/Z_y)$ can be written as a function of the slenderness coefficient λ, then the instability factor will also be a function of the slenderness coefficient λ. A similar result can be shown for the case of a column.

3.2 Point Load on a I-beam with a Plywood Web

For the case of a point load P acting on the flange of an I-beam as shown in Figure 3, the ultimate load capacity P_{ult} is given by (Leicester and Pham, 1984)

$$P_{ult} = K_{inst} P_{squash}$$

for which

$$P_{squash} = B_{eff} t_w f_{c,ply,y} \tag{11}$$

$$P_{crit} = \pi^2 \, a_{eff} \, D_y / d_w^2 \tag{12}$$

$$\lambda = (P_{squash}/P_{crit})^{1/2} \tag{13}$$

$$K_{inst} = 1.0 - 0.25 \, \lambda \tag{14}$$

where

$$B_{eff} = B + 3.0 \, t_f \tag{15}$$

$$a_{eff} = 2.0 \, B_{eff} + 2.5 \, d_w \, (D_x/D_y)^{0.25} \tag{16}$$

in which B is the bearing width of the load, d_w and t_w are the depth and thickness of the plywood web, t_f is the thickness of the flange, D_x and D_y are the bending stiffness per unit length in the x and y directions, and $f_{c,ply,y}$ is the compression strength per unit area of cross-section of the plywood in the y direction.

For practical purposes the plywood parameters should be written $f_{c,ply,y} = \alpha_1 \, f_c$, $D_x = \alpha_2 \, E_L \, t_w^3/12$ and $D_y = \alpha_3 \, E_L \, t_w^3/12$ where E_L and f_c are the modulus of elasticity and compression strength of the wood in the grain direction; the parameters α_1, α_2 and α_3 can be tabulated for various plywood lay-ups.

3.3 Shear Capacity of Stiffened Plywood Webs

For the case of a shear force V acting on a plywood web as shown in Figure 4, the ultimate load capacity V_{ult} is given by (Leicester and Pham, 1984)

$$V_{ult} = K_{inst} \, V_{squash} \tag{17}$$

for which

$$V_{squash} = d_w \, t_w \, f_{s,ply,} \tag{18}$$

$$V_{crit} = d_w \, t_w \, f_{s,crit} \tag{19}$$

$$\lambda = (V_{squash}/V_{crit})^{1/2} \tag{20}$$

$$K_{inst} = 1.00 \tag{21a}$$

$$K_{inst} = 0.64 + (0.79/\lambda^2) \tag{21b}$$

where K_{inst} is taken to be the lesser of the two values given in equations (21a) and (21b) and $f_{s,crit}$ is taken to be the lesser of the two following values,

$$f_{s,crit} = 1.8\ (\pi/d_w)^2\ .\ (D_x\ D_y^3)^{0.25}\ (3.66 + 2.0\ \beta) \qquad (22)$$

$$f_{s,crit} = 1.8\ (\pi/a_w)^2\ .\ (D_x^3\ D_y)^{0.25}\ (3.66 + 2.0\ \beta). \qquad (23)$$

In the above a_w is the panel length as shown in Figure 4, $f_{s,ply}$ is the in-plane shear strength per unit length of the plywood, and $\beta = (D_{xy} + \alpha)/(D_x\ D_y)^{0.5}$ where $D_{xy} = G_{LT}\ t_w^3/6$, $\alpha = E_L\ \mu_{TL}\ t_w^3/(12\ \gamma)$, $\gamma = 1 - \mu_{TL}\ \mu_{LT}$ and μ denotes a Poisson ratio.

It would be convenient to tabulate the parameter β for various plywood lay-ups, and to tabulate D_x and D_y as suggested in Section 3.2.

It is of interest to note that the 0.64 in equation (21b) arises not from buckling, but from the development of membrane tension stresses in the shear panels.

4. EXAMPLE FOR LONG DURATION STRENGTH

As an example of long duration strength, a numerical study from a previous paper (Leicester, 1986) will be used. For a pin-ended column, buckling through bending about the x-axis, the ultimate load capacity P_{ult} will be given by

$$P_{ult} = K_{inst}\ P_{squash} \qquad (24)$$

for which K_{inst} is a function of the slenderness coefficient λ computed from

$$P_{squash} = A\ f_c \qquad (25)$$

$$P_{crit} = \pi^2\ (EI)_x/L_x^2 \qquad (26)$$

$$\lambda = (P_{squash}/P_{crit}) \qquad (27)$$

where A is the cross-section area, L_x is the column length, and EI_x is the stiffness about the major axis.

In the study (Leicester 1986) the instability factor was computed numerically on the assumption of a bilinear failure criterion as shown in Figure 2, applied to the centre of a pin-ended column with initial crookedness $\Delta_{vo} = 0.0035\ L_x$. The results are shown in Figure 5 for the case of an instantaneous load ($\xi = 0$) and for a long duration load ($\xi = 2$). The creep factor $\xi = 2$ means that the climate of the column environment is such that a beam in the same environment would in the long term increase its initial deflection by 200 percent due to mechano-sorptive effects.

The first step is to obtain a simple empirical equation to fit the short term strength curve ($\xi = 0$). A suitable equation is the following;

For $\lambda \leqslant 1.28$,

$$K_{inst} = 1 - 0.306\ \lambda^2 \tag{28a}$$

and for $\lambda \geqslant 1.28$,

$$K_{inst} = 0.818/\lambda^2. \tag{28b}$$

To obtain an equation for the long duration load ($\xi = 2$) an 'effective slenderness coefficient' λ_{eff} is used in equation (28). To do this the two curves shown in Figure 5 are matched at the value $K_{inst} = 0.5$. This leads to

$$\lambda_{eff} = 1.28\ \lambda. \tag{29}$$

Replacing λ by λ_{eff} in equation (28) leads to the following instability factors;

for $\lambda \leqslant 1.00$,

$$K_{inst} = 1 - 0.5\ \lambda^2 \tag{30a}$$

and for $\lambda \geqslant 1.00$,

$$K_{inst} = 0.5/\lambda^2. \tag{30b}$$

The excellent fit of equations (28) and (30) to the numerical solution can be seen in Figure 5.

The influence of end fixity can be covered in a similar manner. For example if the column has fully fixed ends then the critical elastic load P_{crit} will be increased by a factor of 4.0, and thus from equation

(27) it is seen that for a short term load the effective slenderness coefficient to be used is $\lambda_{eff} = 0.5\ \lambda$.

5. CONCLUSIONS

The proposed format for buckling strength described by equations (1) to (4) in Section 2, would appear to be applicable to define the buckling strengths of a wide range of structural members.

6. REFERENCES

Larsen, H.J., Crubile, P., Elhbeck, J., Bruninghoff, H. and Sunley, J. (1986). Eurocode 5. Common Unified Rules for Timber Structures.

Leicester, R.H. and Pham, L. (1984). Ultimate Strength of Plywood Webs. *Proceedings of Pacific Timber Conference*, IPENZ. Auckland, New Zealand, 21-25 May, pp.604-615.

Leicester, R.H. (1986). Creep Buckling Strength of Timber Beams and Columns. *Proceedings of 19th Conference of CIB-W18B*, Firenze, Italy, September.

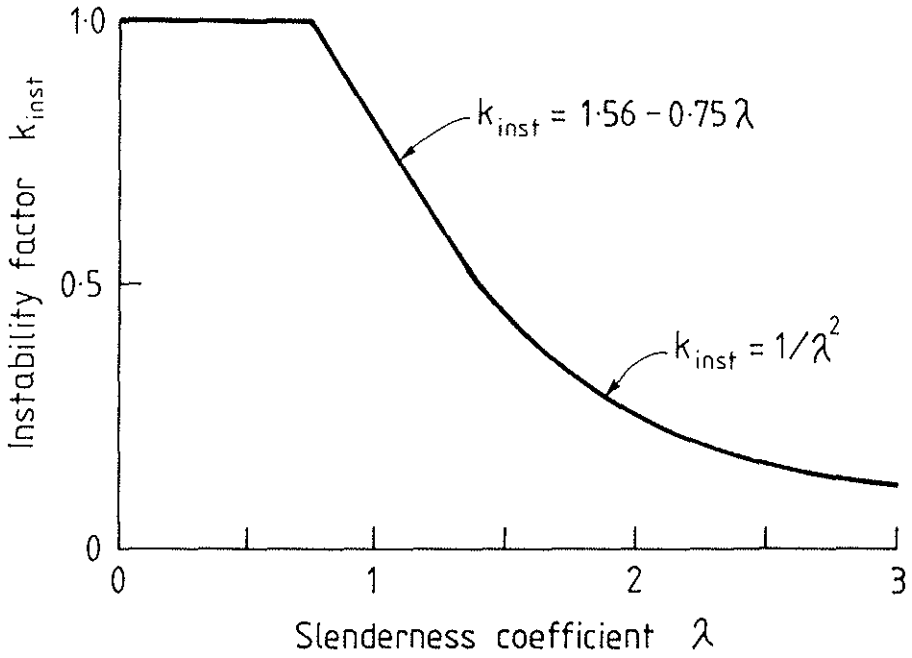

Figure 1. Instability factor from Eurocode 5 for strength of beams.

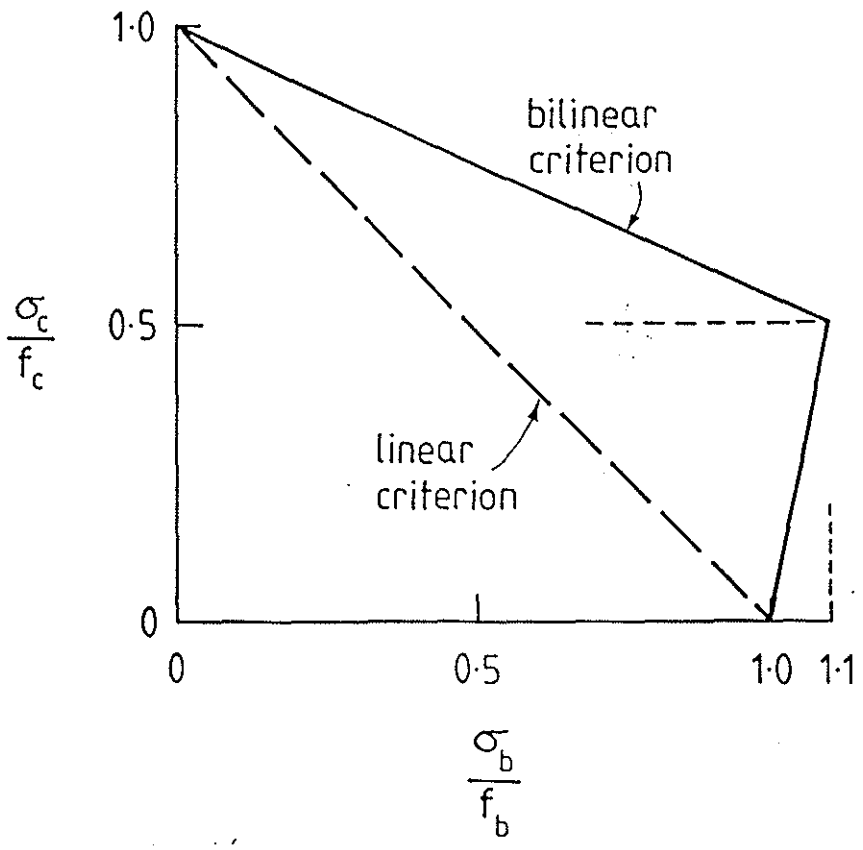

Figure 2. Failure criteria for solid timber.

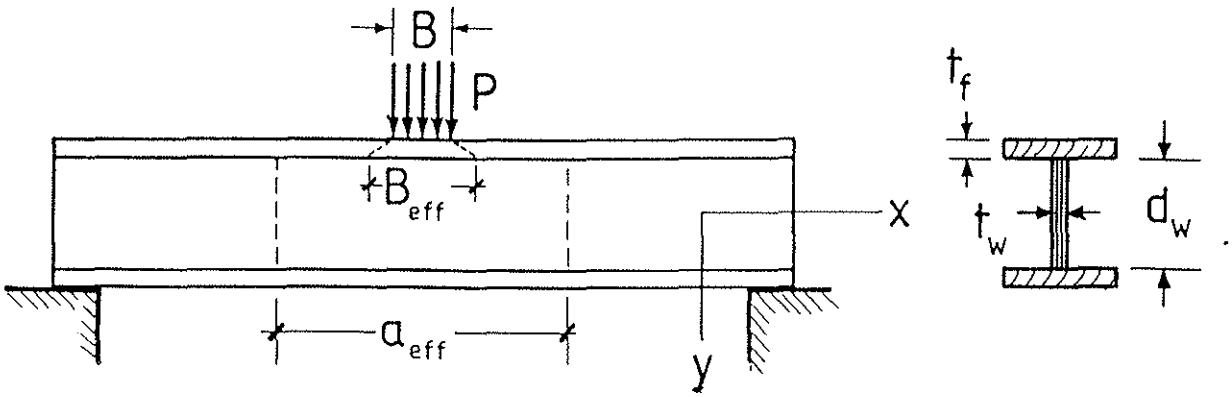

Figure 3. Concentrated load on flange of an I-beam.

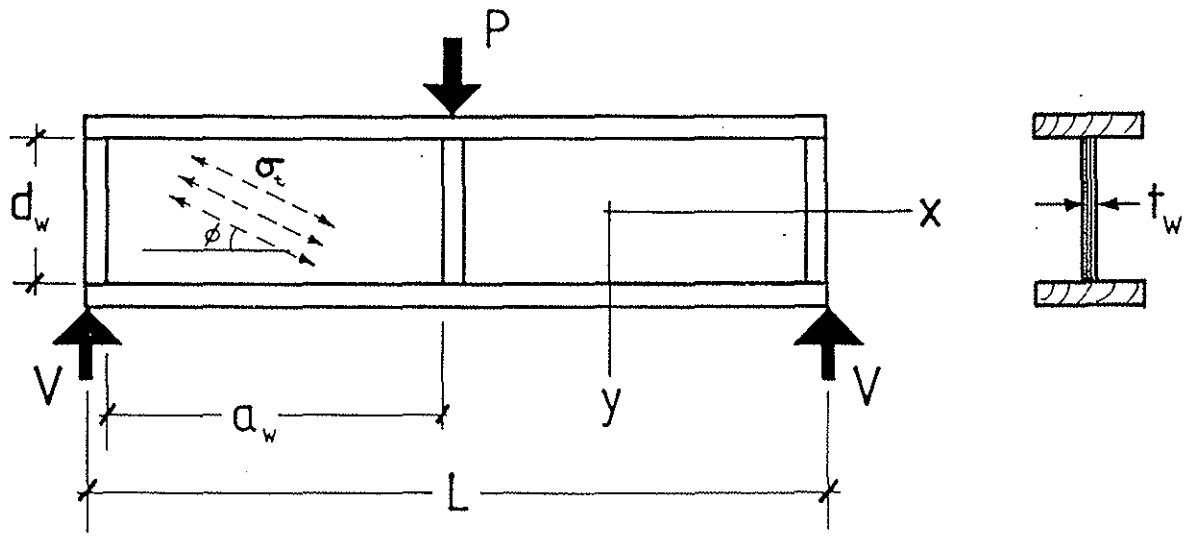

Figure 4. I-beam with stiffened plywood web subjected to shear forces.

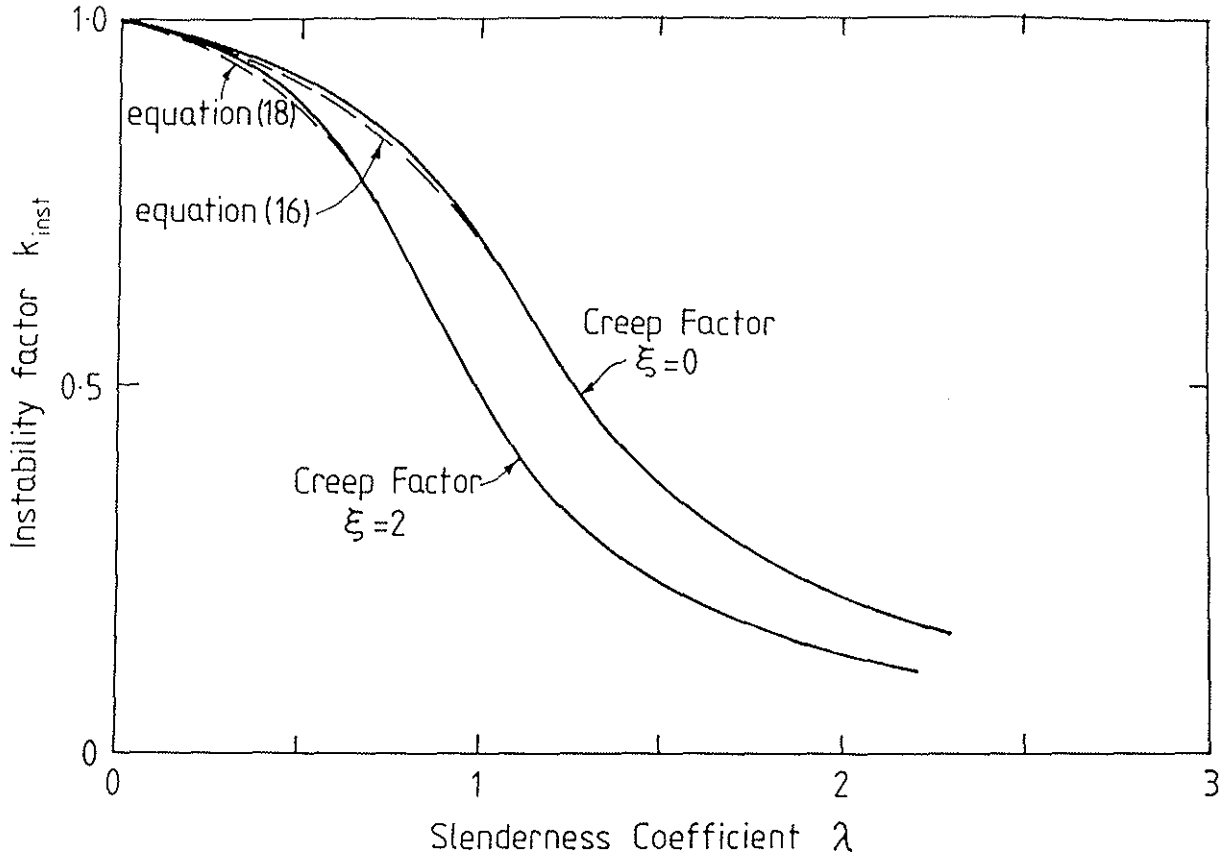

Figure 5. Instability factor for column subjected to short and long duration loads.

6

CIB-W18A/21-2-2

INTERNATIONAL COUNCIL FOR BUILDING RESEARCH STUDIES AND DOCUMENTATION

WORKING COMMISSION W18A - TIMBER STRUCTURES

BEAM-COLUMN FORMULAE FOR DESIGN CODES

by

R H Leicester
CSIRO
Australia

MEETING TWENTY-ONE
PARKSVILLE, VANCOUVER ISLAND
CANADA
SEPTEMBER 1988

BEAMCOL.RHL/210688

BEAM-COLUMN FORMULAE FOR DESIGN CODES

by

R.H. Leicester

(CSIRO, Melbourne, Australia)

1. INTRODUCTION

Analytical solutions of beam-column formulae can be extremely complex and are not very suitable for use in design codes. The complexities of these formulae are confusing to the designer and imply an accuracy that is not in line with the available knowledge for any specific real structural situation.

Usually data on the buckling strength of beams and columns can be obtained without too much difficulty through direct measurement on a specific grade of a particular species of timber. From this data, the five-percentile value is extracted for design purposes. However data on the interaction between bending and axial compression strength is difficult to obtain and hence it is appropriate to use some simple empirical estimate of this interaction for design purposes.

In the following a simple interaction equation is proposed, and checked where feasible against analytical solutions and experimental data.

2. PROPOSED INTERACTION EQUATION

For a beam-column, such as that shown in Figure 1, the ultimate load capacity is taken to be the lesser of the two following criteria,

$$M/M_{ult} + N/N_{ult,x} = 1 \quad (1)$$

$$(M/M_{ult})^2 + N/N_{ult,y} = 1 \quad (2)$$

where M is the applied bending moment about the x-axis, M_{ult} is the ultimate value of M (including buckling effects), N is the applied axial load, $N_{ult,x}$ is the ultimate value of N if the column is constrained so that it can bend only about the x-axis, and $N_{ult,y}$ is the ultimate value of N if the column is constrained so that it can bend only about the y-axis.

The failure criteria of equations (1) and (2) are illustrated in Figure 2.

The following will provide checks for the case of $N_{ult,x} > N_{ult,y}$ and $N_{ult,x} < N_{ult,y}$. The checks will be made for the case of short intermediate and slender beam-columns. In the diagrams the terms N_o will be taken to be the axial load capacity if there were no bending moment, and M_o is the ultimate bending movement in the absence of an axial load, i.e. $M_o = M_{ult}$.

3. COMPARISON WITH ANALYTICAL SOLUTIONS

3.1 General

The analytical solution will be based on an analysis of the beam-column shown in Figure 1, with a bilinear failure criterion as indicated in Figure 3. The analysis for this case has been given in a previous paper (Leicester, 1986). The cross-section is 150 x 40 mm, and the material properties are bending strength f_b = 30 MPa, compression strength f_c = 27 MPa, modulus of elasticity E = 7500 MPa and modulus of rigidity G = 500 MPa. The initial crookedness is given by $v_o = 0.0035\ L_x$ in the x-direction, $u_o = 0.0035\ L_y$ in the y-direction and twist $\phi_o = 0.05$ b/d.

3.2 Short Columns

For columns, that are sufficiently short that buckling does not affect stgrength, the critical failure criterion, equation (1), is quite conservative in comparison with the bilinear failure criterion as shown in Figure 4.

3.3 Intermediate and Long Columns

Comparison between analytical solutions, and the empirical equations (1) and (2) are shown in Figures 5-8. Figures 5 and 6 are cases where $N_{x,ult} < N_{y,ult}$, and Figures 7 and 8 are cases where $N_{x,ult} > N_{y,ult}$. In all cases the comparison between analytical and empircal equations are quite good.

3.4 Very Long Columns, $N_{x,ult} << N_{y,ult}$

For very long columns that can buckle only about the x-axis, the stress due to the axial load is negligible and hence the failure criterion can be written

$$M/[1 - (N/N_{crit,x})] = Z_x f_b \qquad (3)$$

where Z_x is the section modulus, f_b is the modulus of rupture, and $N_{crit,x}$ is the critical elastic load for buckling about the x-axis, i.e. $N_{crit,x} = \pi^2 EI_x/L_x^2$.

When there is no axial load $M = M_o$, i.e. $M_o = Z_x f_b$ and when there is no bending moment $N = N_o$, i.e. $N_o = N_{crit,x}$. Substituting these values into equation (3) leads to

$$(M/M_o) + (N/N_o) = 1 \qquad (4)$$

which is identical to the failure criterior of equation (1).

3.5 Very Long Columns, $N_{x,ult} >> N_{y,ult}$

The case of lateral buckling for a bisymmetrical beam subjected to a uniform end moment $M = Ne$ as shown in Figure 9 has been analysed by Bleich (1952). Equation (313) in Bleich's monograph can be written

$$1 - N/N_{crit,y} = M^2/[M_{crit}^2 (1-N/N_{crit,\phi})] \qquad (5)$$

where $N_{crit,y}$ is the critical axial load for lateral buckling about the

y-axis, $N_{crit,\phi}$ is the critical axial load for torsional buckling and M_{crit} is the critical buckling moment.

$$N_{crit,y} = \pi^2 \, EI_y/L^2 \tag{6}$$

$$N_{crit,\phi} = [E \, (\pi/L)^2 + GJ]/(I_p/A) \tag{7}$$

$$M_{crit} = (\pi/L) \, (EI_y \, GJ)^{\frac{1}{2}} \, [1 + (\pi^2 \, E\Gamma/L^2 \, GJ)]^{\frac{1}{2}} \tag{8}$$

where EI_y and GJ are the bending and torsional stiffnesses, A is the cross-section area, and I_p is the polar moment of inertia.

For practical cases $N/N_{crit,\phi} << 1$, and hence equation (5) may be written

$$N/N_o + (M/M_o)^2 = 1 \tag{9}$$

where $N_o = N_{crit,y}$ and $M_o = M_{crit}$.

Equation (9) is identical to the failure criterion given by equation (2).

4. COMPARISON WITH EXPERIMENTAL DATA

Experiments were undertaken by Buchanan (1984) to measure beam-column strengths of 100 x 50 mm Canadian SPF timber constrained to bend only about the x-axis.

The five-percentile value of the test results are shown for a short and intermediate length column in figures 10 and 11. It is seen that the empirical equation (1) is conservative for the case of short columns and about correct for intermediate columns, as was the case in the previous comparison with the analytical solution.

5. DISCUSSION

It is seen that the analyses with the bilinear criterion tend to match the test data available for short and intermediate columns, and of course tend to the 'exact' solutions given by equations (3) and (9) as the beam-columns become very slender. Hence the analyses based on the bilinear criterion provide a reasonably realistic prediction of beam-column strength.

Nothwithstanding the above, it should be noted that the bilinear analysis is slightly liberal in that the applied bending moment was assumed to be given by $M = Ne$, rather than the more correct relationship of $M = N(e+v)$, where e is the eccentricity of the applied load, and v is the deflection in the y-direction at the mid-height (Leicester, 1986). This matter has been discussed by Hill and Clarke (1951). The analysis is also liberal in the sense that the possibility of failure due to tension stresses was not considered.

The failure criteria given by equations (1) and (2) fit the bilinear analysis quite well except for the case of a very short column, when equation (1) leads to conservative predictions.

To assess the capacity of a beam-column subjected to an axial load N and bending moments M_x and M_y about the x and y axis respectively the following failure criteria are suggested;

$$M_x/M_{x,ult} + (M_y/M_{y,ult})^2 + N/N_{ult,x} = 1 \quad (10)$$

$$(M_x/M_{x,ult})^2 + M_y/M_{ult,y} + N/N_{ult,y} = 1 \quad (11)$$

where $M_{ult,x}$ and $M_{ult,y}$ denote the ultimate values of M_x and M_y respectively (including buckling effects) if the moments are applied alone.

No checks have been made on the accuracy of these criteria, but comparison with equations (1) and (2) indicates that the result should be conservative.

6. CONCLUSIONS

The beam-column interaction equations (1) and (2) appear to be satisfactory for use in design codes.

7. REFERENCES

1. Bleich, F. (1952). *Buckling Strength of Metal Structures*. McGraw-Hill Book Co. Inc., pp. 153-160.

2. Buchanan, A. (1984). Design of sawn timber members for combined bending and axial loading. Proc. of Pacific Timber Engineering Conference. Auckland, New Zealand, pp. 588-595.

3. Hill, H.N. and Clarke, J.W. (1951). Lateral buckling of eccentrically loaded I- and H-Section columns. Proceedings of Firest National Congress of Applied Mechanics, ASME. pp. 407-413.

4. Leciester, R.H. (1986). Creep buckling strength of timber beams and columns. Proc. of 19th Conference of CIB-W18, Firenze, Italy.

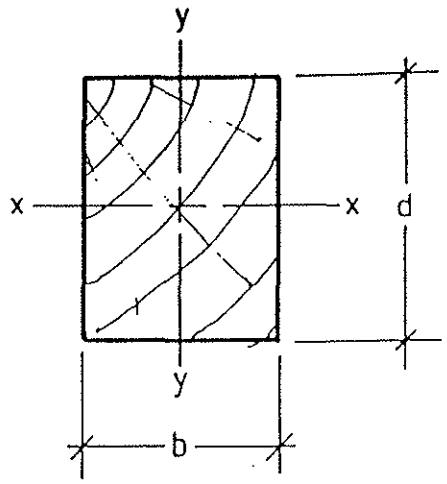

b = 40 mm
d = 150 mm

(a) Member cross section

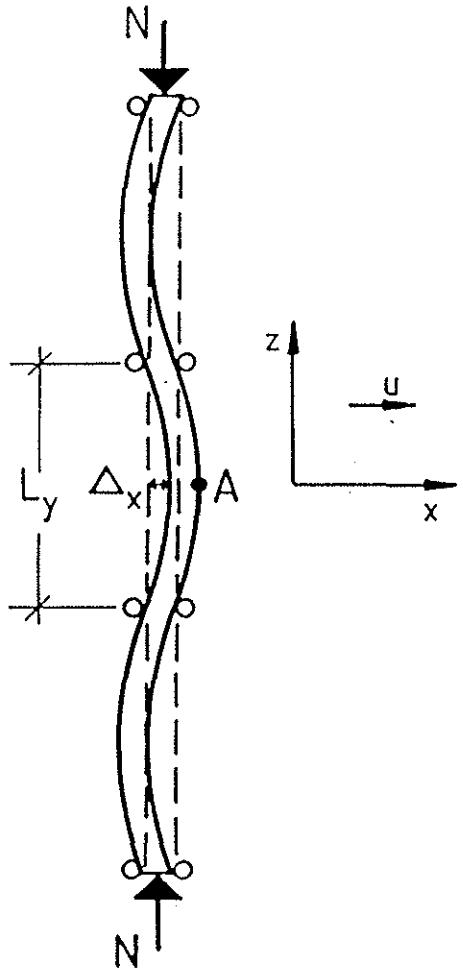

(b) Front Elevation

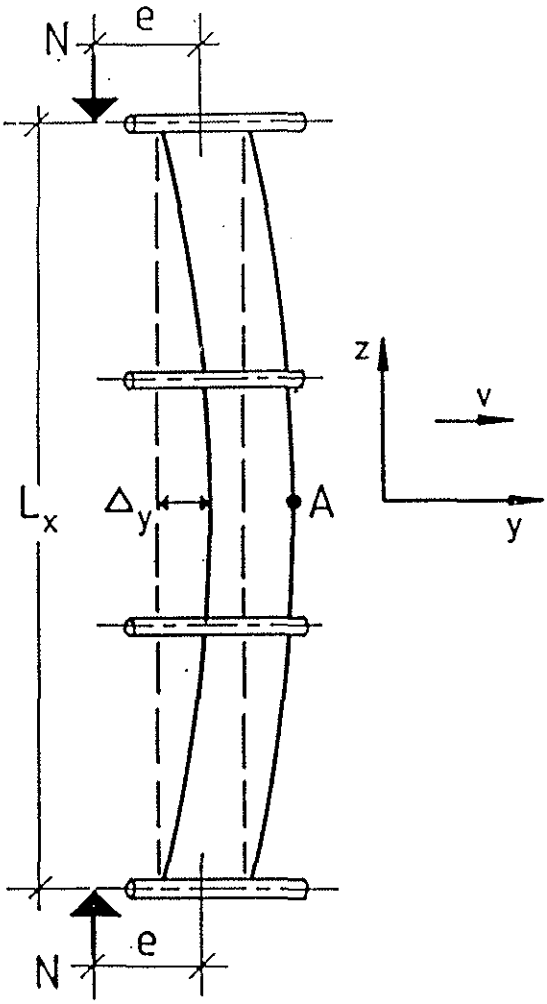

(c) Side Elevation

Figure 1. Beam-Column and Notation.

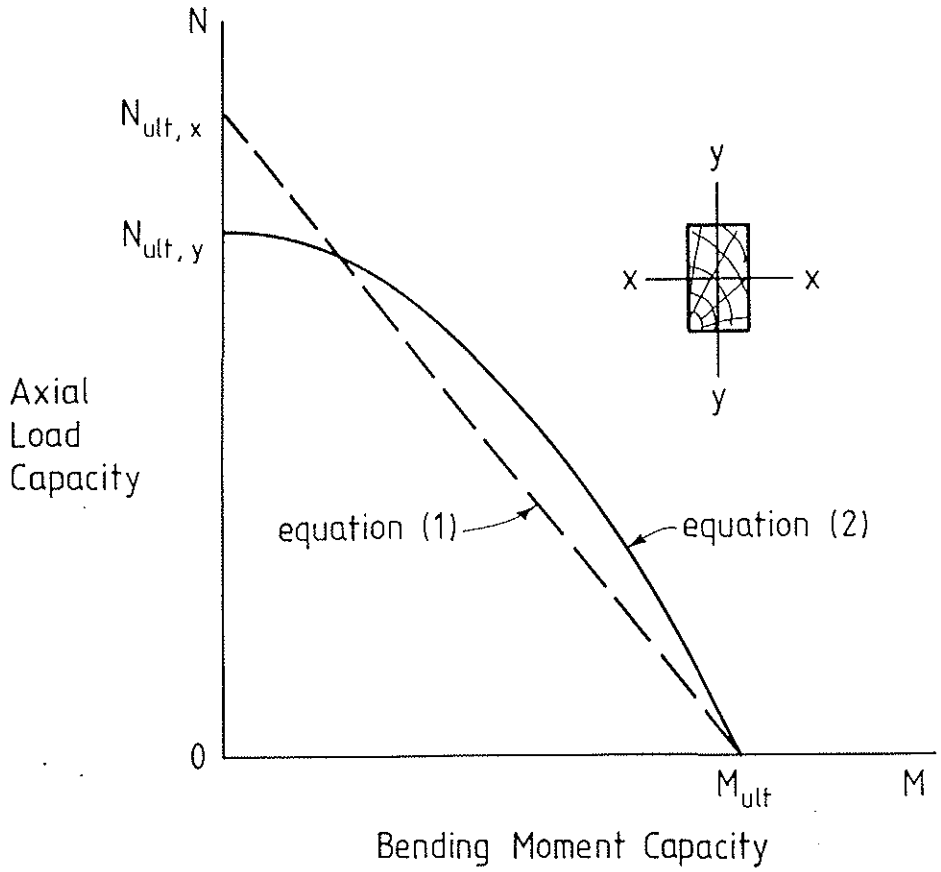

Figure 2. Interaction criteria for beam-columns.

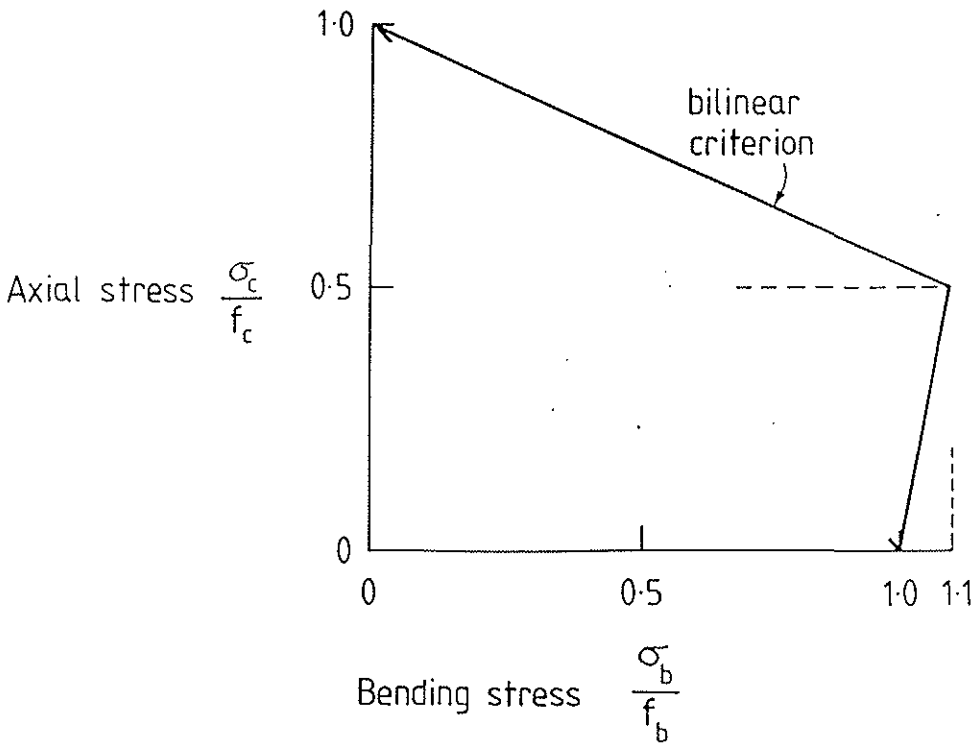

Figure 3. Bilinear failure criterion.

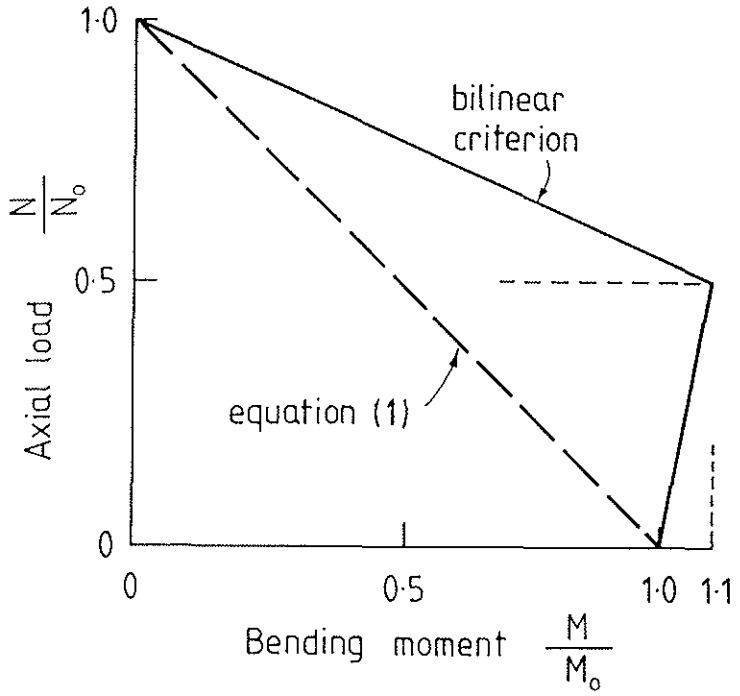

Figure 4. Failure envelope for short beam-columns.

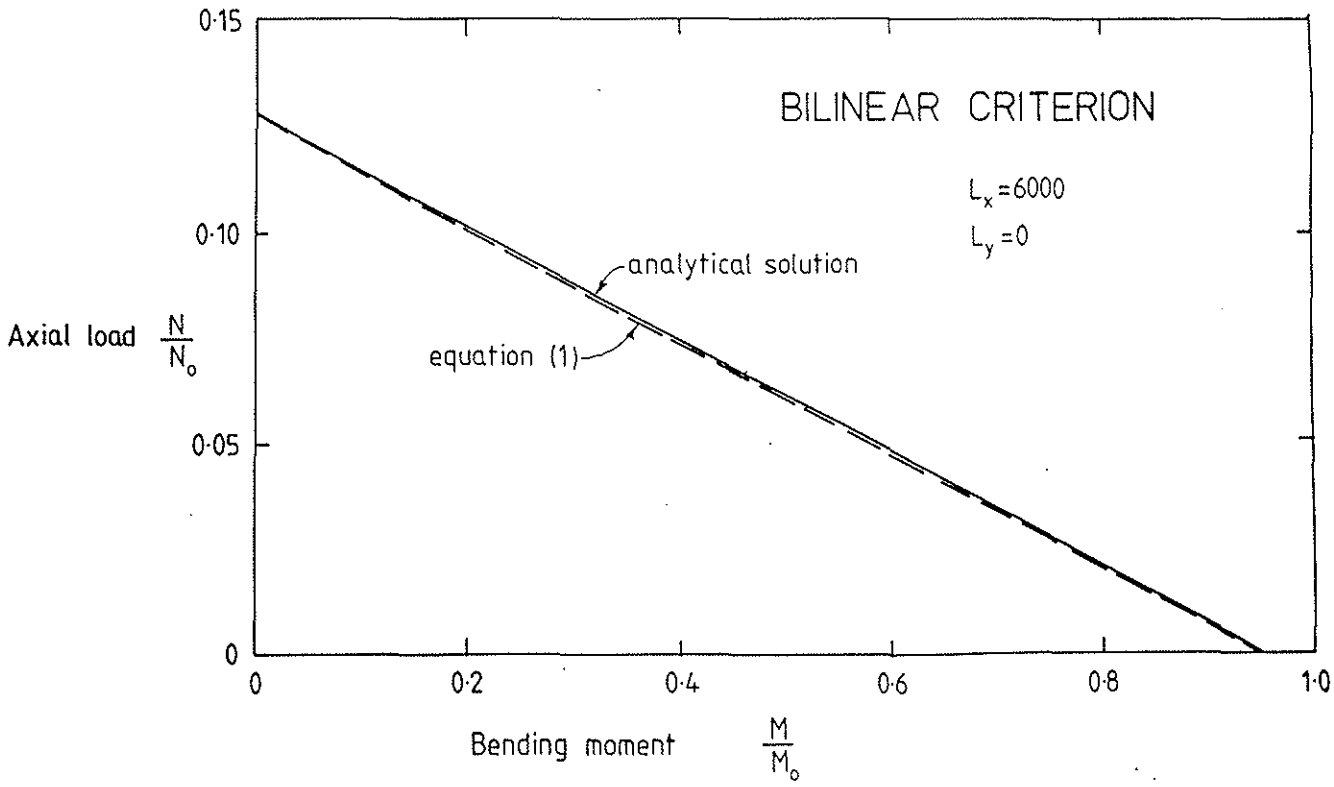

Figure 5. Failure envelope for beam-columns buckling about major axis ($L_x/d=20$, $L_y/b=0$).

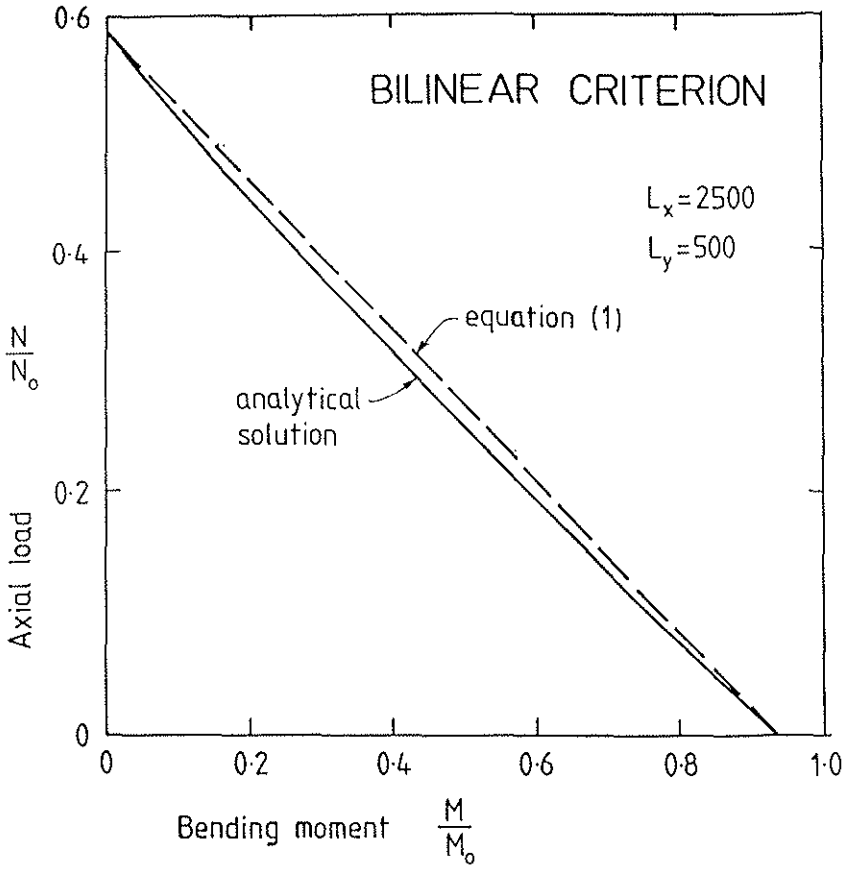

Figure 6. Failure envelope for beam-column buckling primarily about the major axis ($L_x/d=16.7$, $L_y/b=12.5$).

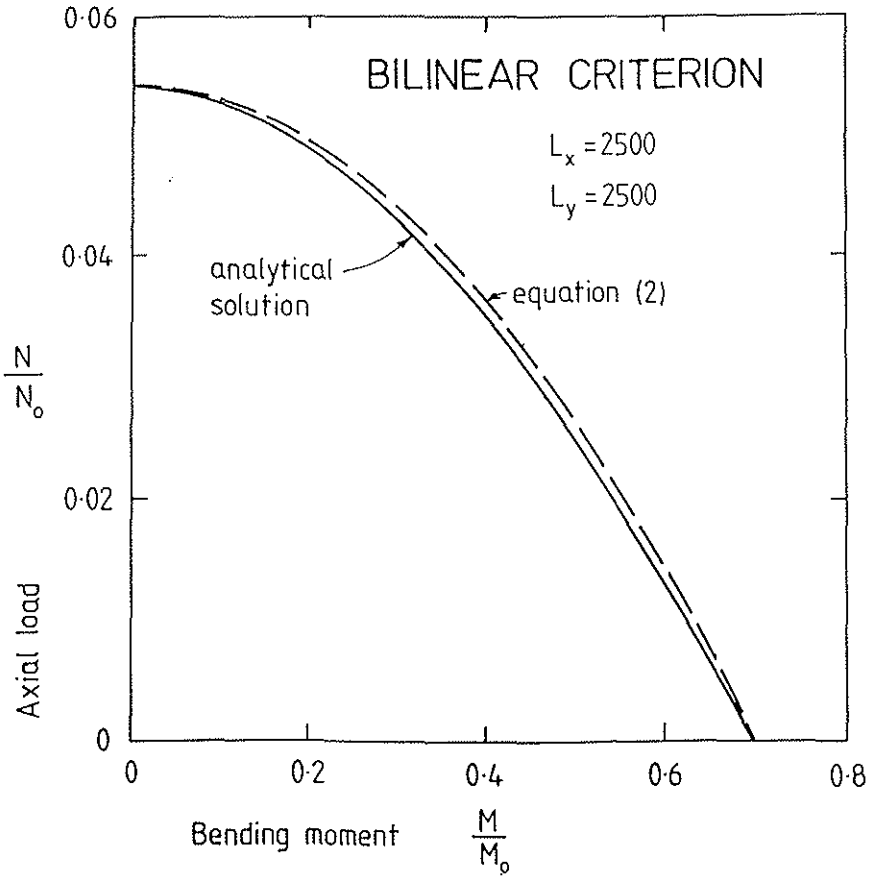

Figure 7. Failure envelope for beam-column buckling primarily about the minor axis ($L_x/d=16.7$, $L_y/b = 62.5$).

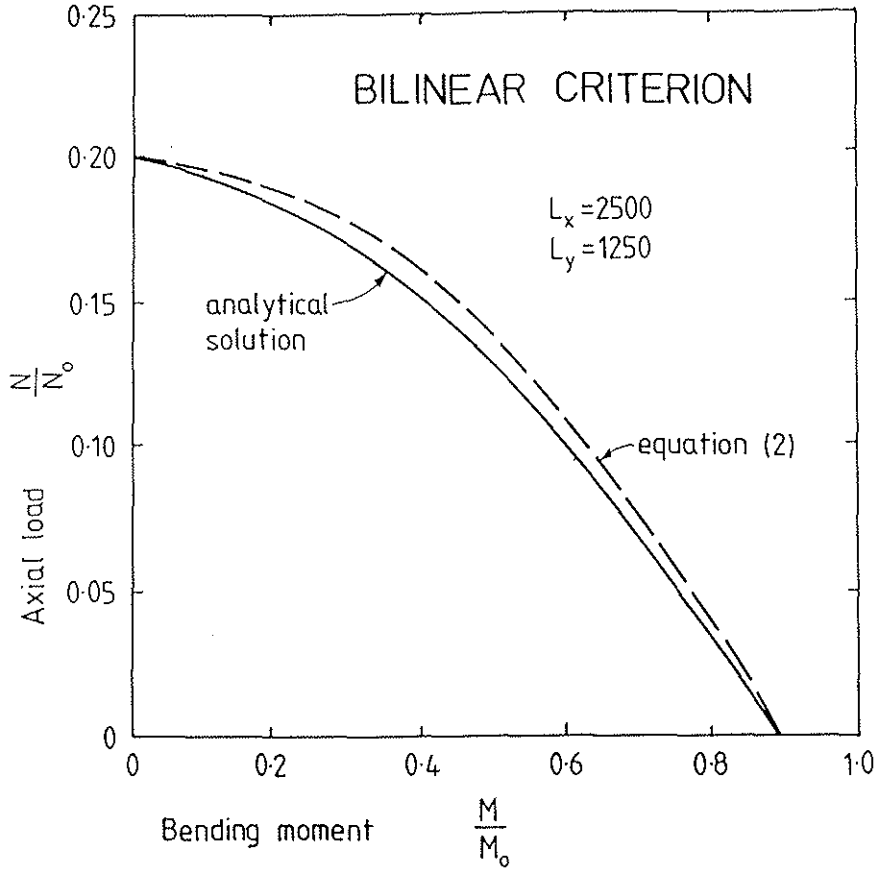

Figure 8. Failure envelope for beam-column buckling primarily about the minor axis (L_x/d=16.7, L_y/b=31.3).

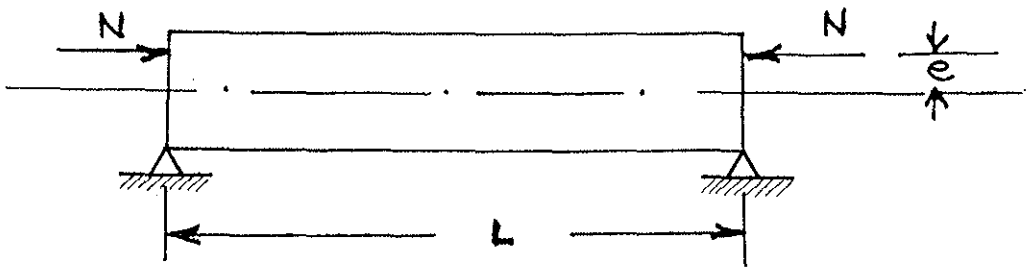

Figure 9 Notation for beam-column

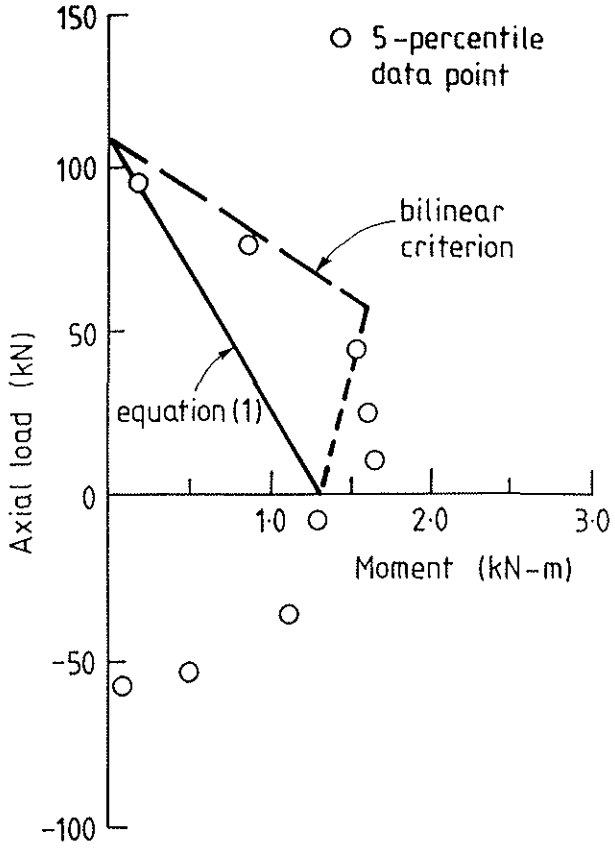

Figure 10. Measured failure envelope for short column.

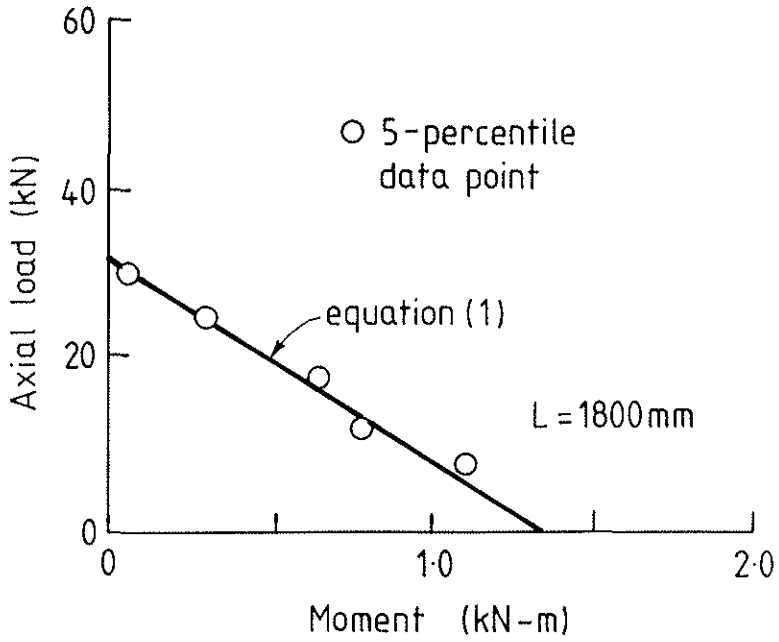

Figure 11. Measured failure envelope for beam-column buckling about major axis (L_x/d = 18.0, L_y/b = 0.0).

7

CIB-W18A/21-4-1

INTERNATIONAL COUNCIL FOR BUILDING RESEARCH STUDIES AND DOCUMENTATION

WORKING COMMISSION W18A - TIMBER STRUCTURES

MODELING FOR PREDICTION OF STRENGTH OF VENEER HAVING KNOTS

by

Y Hirashima
Shizuoka University
Japan

MEETING TWENTY-ONE
PARKSVILLE, VANCOUVER ISLAND
CANADA
SEPTEMBER 1988

MODELING FOR PREDICTION OF STRENGTH OF VENEER HAVING KNOTS

Y.Hirashima
Shizuoka University

Introduction

Plywood has a long history of successful use in structures including highly stressed aircraft, concrete formwork and house sheathing. Most structural plywood contains defects and its strength is predicted by a theory that is largely empirical, i.e. the measured strength of clear plywood is adjusted by grade factors to account for the presence of defects.

Most past work employed statistical methods to define a strength distribution from mean values, exclusion limits, standard deviations, etc. These methods are valid for specific test configurations, but if the test conditions like lay up of the plywood, veneer species and knot distribution are changed, their results need to be modified. The existing methods using grade factors have not considered the effects of knots in detail.

Therefore, it is considered desirable to derive a theory to predict the strength of plywood of any construction containing defects in order to provide a more rigorous basis for stress grading rules.

It is well known that the fibres deviate around knots in wood, and consequently the strength and stiffness of wood veneers containing knots are adversely affected. Thus, it is desirable to determine the strength distribution around the knots to predict the strength properties of veneer. For this reason tensile tests were made on strips of veneer taken from the vicinity of knots and on veneer or plywood containing knot(s). (Results of tensile tests on plywood are not reported in this paper.)

Previous work

Early work on plywood as a construction material began early in the twentieth century, and for the most part was done on clear plywood. Theory to evaluate the strength of knotty plywood cannot be obtained from these works.

Recently a testing machine to bend full size panels has been developed and many in-grade tests have been conducted in the USA, Canada and Japan.

Using these in-grade test data, the strength and the allowable stresses of plywood have been derived statistically for plywood conforming to the relevant products standards(1).

Hirashima(2) conducted full size pure bending tests on softwood plywood as well as Lauan plywood by using such a testing machine and reported on the relationship between strength ratio and knot ratio. McGowan(3) conducted tensile tests on strips of Douglas-fir veneer and plywood containing single knots. He reports a reduction in strength for knotty plywood strips five inches wide but his results are of only limited use because he has not proposed a method to apply them to panels of different widths.

Yline(4) and Sasaki(5) conducted tensile tests on Scots pine and Hinoki strips containing single knots, and measured the apparent ultimate strength and strain distribution around the knot. But they did not determine the distribution of strength near the knot which is required if a general theory is to be developed.

Recently, Bier(6) reported the study of bending properties of radiata pine plywood having knots. His work analysed the effect of knots on veneer using a theory to predict the effects of associated grain deviation. He reported the good agreement between the experimental and the theoretical value of the regression line for knot ratio versus MOR of plywood. The effectiveness of the theory, however, still unknown because of the lack of the application of the theory to the individual plywood.

Hatayama(7) conducted tensile tests on a number of test slices cut from around knots in lumber. He investigated the slope of grain of the test piece, and derived an empirical formula expressed by the knot size and the distance from knot. He made a model to predict the strength of lumber using the hypothetical strip element, and reported the good predictions of strength of lumber having a knot.

This methodology appears to be useful to analyse the effect of grain deviation on veneer. So, the same method as Hatayama's was employed in this paper to predict the strength of knotty veneer.

Test Materials

Eight peeler bolts of radiata pine were selected to give a range of knot

sizes and cut to 1.3m length. They were spray painted on one end marking a 60 sector. Discs were cut off the other end of each bolt in order to measure shrinkage and density.

Bolts were peeled to produce 3 mm or 1.5 mm thick veneer without using the scriber on one end to leave the paint markings.

Peeling was done with the centre of rotation at the pith. Peeled veneer was clipped to 130 cm lengths providing square sheets, numbered consecutively in order of production. The veneers were dried to about 7 percent moisture content at a plywood manufacturing factory.

Experimental

Veneer sampling

Matched specimens of veneer were fabricated from the numbered ribbons of rotary peeled veneer. Four specimens of veneer containing a knot from the same branch were selected as shown Figure 1.

No differentiation was made between a tight knot, loose knot, or knot hole; that is, the effect of a given size of knot on strength was assumed to the same regardless of its type.

Knot dimensions were measured across the grain.

Two specimens became the face and back of 3 ply plywood, one became the

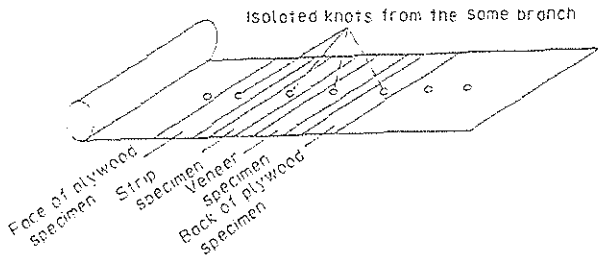

Figure 1. Matching of veneer.

tension veneer specimen, and fourth was cut into tensile strips. There were a total about 1400 such strip test specimens, 8 mm wide and 300 mm long, cut parallel to the grain from both edges of knot up to a distance of four times of knot size.

A line across grain was drawn through the centre of the knot at the centre of the veneer before cutting. Another line at 45 to this, was drawn from the edge of the knot. The distance between these lines on the cut strips accurately located the distance from the knot, without concern over kerf width.

Strips were cut using a 14 inch band saw. When the distance between knots was not enough to obtain clear strips four knot widths away from the knot edge, the strips required to obtain clear properties were cut from end-matched veneer. Test strips were taken from veneer for thirty-five knot

Table 1. Particulars of bolt and veneer used in this test.

Test veneer designation[1]	Bolt No.	Ring[2] width (mm)	Rate of[2] latewood	Number of[2] rings from pith	Distance[3] from pith (mm)	Specific[4] gravity
A	1	1.8- 5.0	0.13-0.60	32-40	310	0.514
B	1	2.0- 5.9	0.07-0.31	24-26	271	0.491
C	1	10.7-15.0	0.13-0.21	11-12	154	0.461
D	2	2.6- 5.1	0.23-0.39	30-40	308	0.500
E	2	0.9- 4.0	0.17-0.25	37-43	281	0.500
F	3	3.0- 3.6	0.27-0.28	32-34	241	0.520
G	4	1.8- 6.0	0.15-0.17	17-23	150	0.504
H	4	2.6- 6.2	0.13-0.23	16-20	145	0.504
I	5	2.1- 2.4	0.17-0.30	26-34	158	0.608
J	5	4.8- 5.4	0.22-0.41	14-15	108	0.608
K	6	4.0- 5.1	0.16-0.20	27-34	262	0.577
L	7	3.2- 6.0	0.19-0.30	22-28	221	0.503
M	7	4.8- 5.8	0.21-0.23	14-15	174	0.503
N	7	7.5- 9.1	0.13-0.16	10-10	148	0.441
O	8	4.0- 4.0	0.13-0.25	17-18	132	0.572
P	8	3.8- 4.0	0.18-0.26	14-16	119	0.572

1) Thickness of veneer is 3mm for A-K, 1.5mm for L-P.
2) These values were obtained from blocks cut from one end of the bolt.
3) This value was obtained from the length of sector painted at the end of bolt adjusting shrinkage.
4) Air-dryweight/air-dry volume at moisture content 11 %.

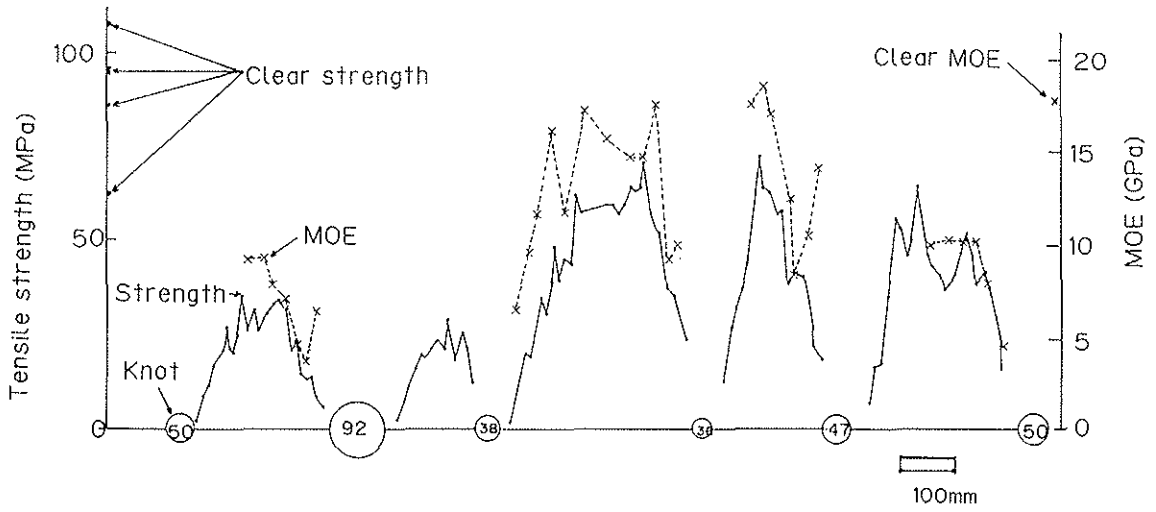

Figure 2. Distribution diagram of tesile strength and MOE around knot.

sizes ranging from 6 mm to 100 mm.

Since the knots in each set of four veneers (Figure 1) were produced by the same branch, the knots and knot-free materials adjacent to the knots were closely side matched.

Table 1 shows the particulars of the bolts and veneer used in this study obtained by investigation of the blocks cut from one end of each bolt.

Test methods

Veneer Strips:

The test specimens were kept in a temperature-humidity control room for at least 2 weeks (20 C, 65% RH) prior to test. Moisture content at test was about ten percent.

To measure Modulus of Elasticity, some strips were selected and a strain gauge glued on side (paper-based wire strain gauge, gauge length 5 mm).

The load was applied to the test specimen in tension at rate of 1 mm/min. A load-strain curve was drawn by an X-Y recorder.

Strips closest to the knot had the greatest grain deviation. These were tested first, followed in succession by strips further from the knot. When failure occurred near the grip of the testing machine, the remaining specimens were reshaped to dumbbell shape with a width of 3 mm at centre and curvature of 200 mm.

The inclination of fibres was measured at the failed section in the plane of the face of the veneer and in the plane through the thickness of the veneer by means of a graduator. This was done only for the 3 mm thick specimens, because there existed some

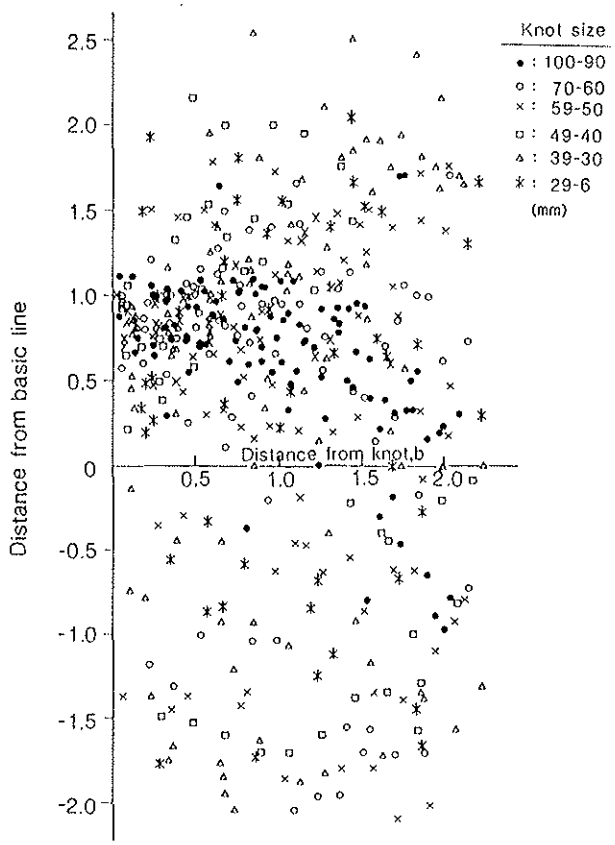

Figure 3. Position of failure section.

difficulties in the 1.5 mm veneer to measure the inclination of fibre in the plane through the thickness.

The position of failure was also determined using the origin at edge of the knot.

Veneer sheets and plywood;

Tensile tests on veneer containing knots were conducted for test pieces of various widths up to 240 mm by using the laboratory's in-grade tension testing machine developed for lumber.

The test specimen was held between steel plates coated with polyurethane plastic high friction contact surface. Side pressure of 55 K^{-2} over the whole contact area was applied by hydraulic jacks. The load was applied by another hydraulic jack so that each test lasted about four minutes.

The extension of the test specimen was measured using a displacement transducer on each side of the specimen over the knot.

Load and deformation data were collected by a data logger controlled by a Digital PDP 1123 computer.

Results and Discussions

Distribution of strength around knot

An example of distribution of tensile strength and MOE in a sheet of veneer is shown in Figure 2 including clear data. The strength properties increase as distance increases from the edge of the knot up to a distance of about twice the knot width.

Figures 3 and 4 show the position where failure occurred in the veneer, using a normalised distance; that is the distance from the knot divided by prescribed knot size.

The basic line, appeared in the figures, is that perpendicular to non-disturved fibre direction passing through the center of the knot.

In these figures, it is evident that the weakest position in the longitudinal direction is about 0.9 knot widths above the knot within the breadth of about twice the knot width perpendicular to fibre from the knot edge. In the region at distances greater than 2 knot widths fractures are widely scattered.

Generally speaking, a branch forms a cone at the interface between branch and trunk. This cone has a steeper slope in the upper side than on the lower. This shows the annual ring

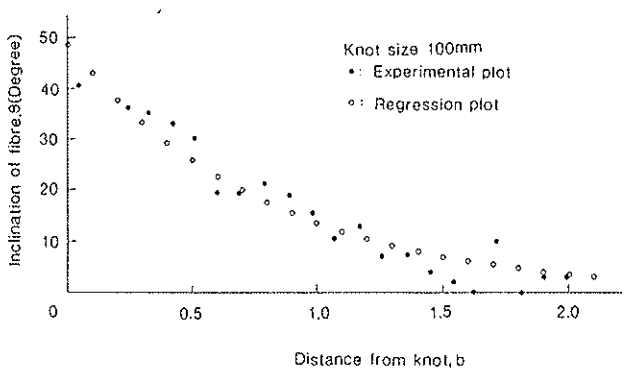

Figure 5. Relationship between inclination of fibre and non-dimensional distance from knot.

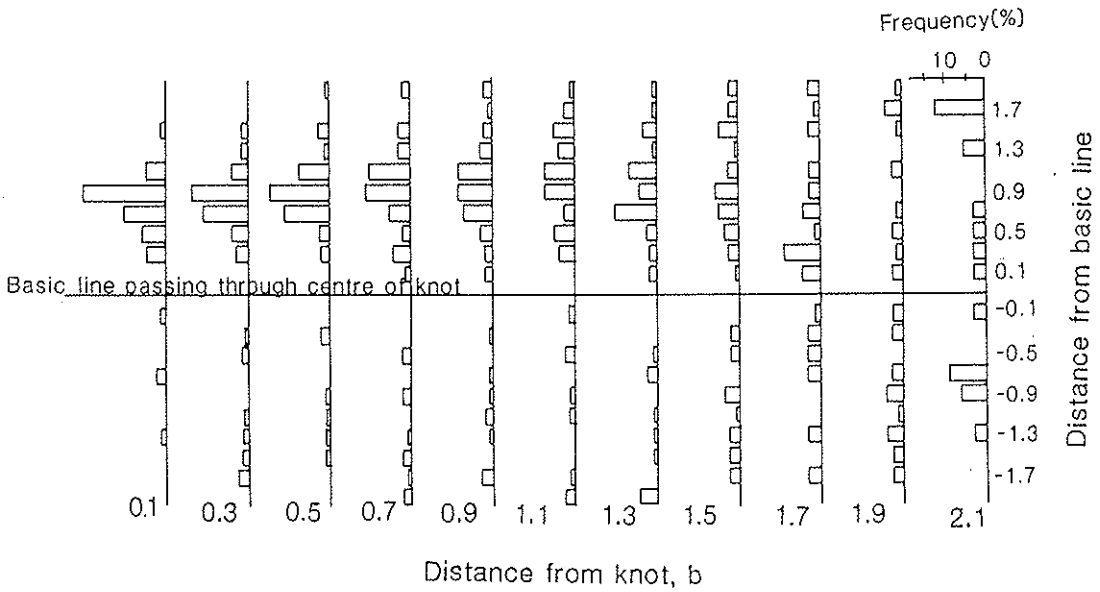

Figure 4. Frequancy histogram of position of failure section.

pattern on peeled veneer surface around the knot. The annual rings are closer together on the upper portion around the knot, and this causes adverse inclination of grain. This effect seems to extend to about twice the knot width. Strength and MOE will therefore vary both parallel and perpendicular to the face grain on the veneer surface.

Clear strength characteristics were determined by averaging data obtained from tests for more than two knot sizes and from end-matched clear data.

Almost all the specimens taken from the vicinity of the knots ruptured at earlywood. Therefore, the clear data obtained from test pieces with latewood at the failure portion were excluded.

Fibre angle θ, has two components, component in plane of veneer, A, component in plane through the thickness, B, and may be expressed as:

$$\theta = \tan^{-1} (\tan^2 A + \tan^2 B)^{1/2} \quad (1)$$

Figure 5 shows the fibre inclination at failure portion of one of the specimens.

There is a decreasing inclination as the distance from the knot increases.

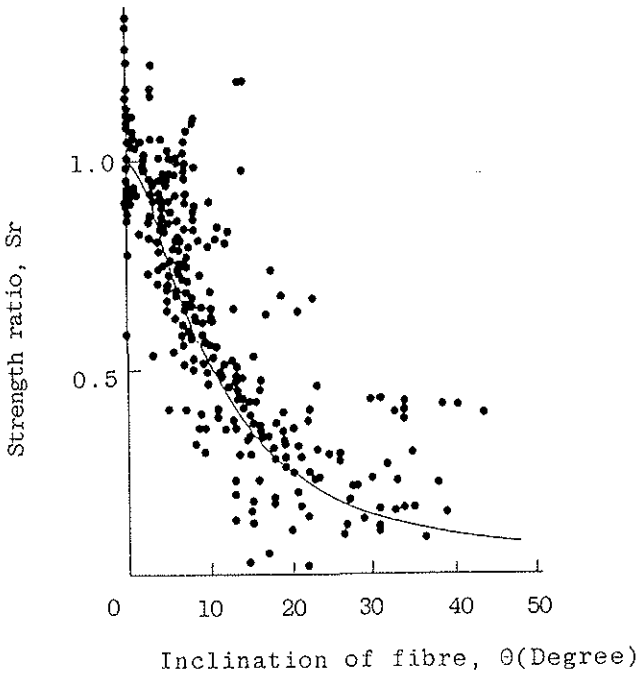

Figure 6. Relationship between strength ratio and inclination of fibre, and their regression curve.

Mathematical model for strength characteristics

Strength or MOE from fibre angle

A model was made for strength and stiffness using Hankinson's formula;

$$S_r \text{ or } E_r = \frac{a}{\sin^n \theta + a \cos^n \theta} \quad (2)$$

where Sr, Er are strength ratio or stiffness ratio, respectively and θ is the inclination of the fibres or fibre angle.

Previous works have suggested that the ratio of the property perpendicular to that parallel could be used for parameter 'a' in this equation. In this study an optimization method was used to determine a and because of the lack of data about that ratio. Thus, for strength

$$a = 0.050 \quad n = 1.690$$

and for MOE

$$a = 0.184 \quad n = 1.585$$

with the coefficients of determination of 0.720 and 0.768 respectively.

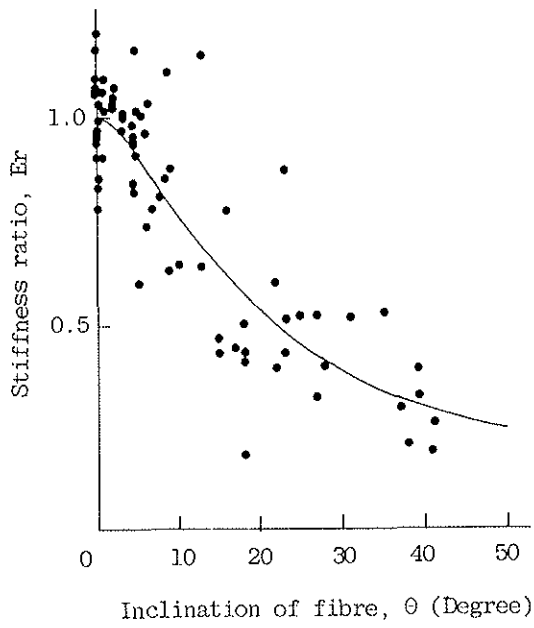

Figure 7. Relationship between stiffness ratio and inclination of fibre, and their regression curve.

In the regression analysis for MOE, the only data used were those from test pieces where the strain gauges were at the failure point on the adjacent annual ring.

Figures 6 and 7 show that measured data fit the models well.

Figure 8 is an example of the strength ratio calculated from Eq. (2) using the measured inclination of fibre compared with experimental results. It can be said that calculated plots agree well with experimental ones. The same good agreement was obtained for stiffness (Figure 9).

Thus it is clear that the strength or MOE of the veneer strips can be predicted from the fibre angle.

Fibre angle from knot size and distance from knot

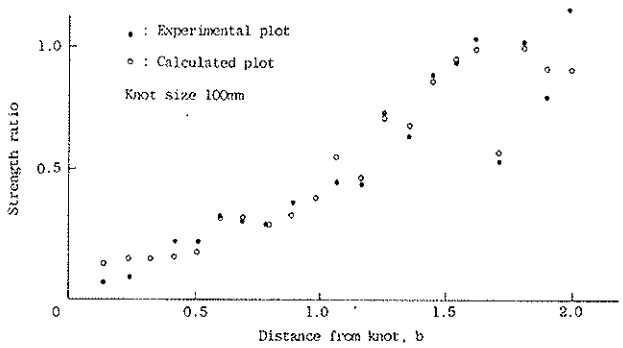

Figure 8. Comparison of strength ratio calculated from Hankinson's formula with that of experimental result.

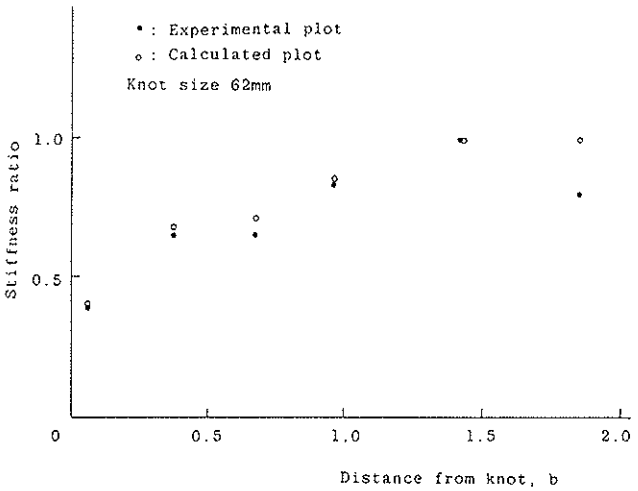

Figure 9. Comparison of stiffness ratio calculated from Hankinson's formula with that of experimental result.

Data for fibre angle was divided into seven groups depending on knot size and fitted to an exponential curve

$$\theta = B \cdot R^{b} \qquad (3)$$

using an optimisation method; where θ is fibre in degrees, b is a non-dimensional distance from knot, B,R are parameters determined by regression for each group.

Figure 5 shows the experimental and regression plots derived in 100 mm diameter knot.

Each parameter from the seven data sets was plotted by knot size in Figure 10 and a regression relationship between each parameter and knot size was obtained. It follows that the fibre angle can be calculated from:

$$\theta = (29.30 + 0.1659d)(0.1926 + 0.001082d)^{b} \qquad (4)$$

where d is knot size in mm.

Estimation of strength by model

A numerical experiment was done to estimate the strength of veneer having knots using the formulae derived in this study. The veneer was divided into individual virtual strips and steadily increasing stress was applied. This computation was based on the following assumptions:

(a) the stress-strain curve remains linear until ultimate strength (this was shown clearly by the experiments).

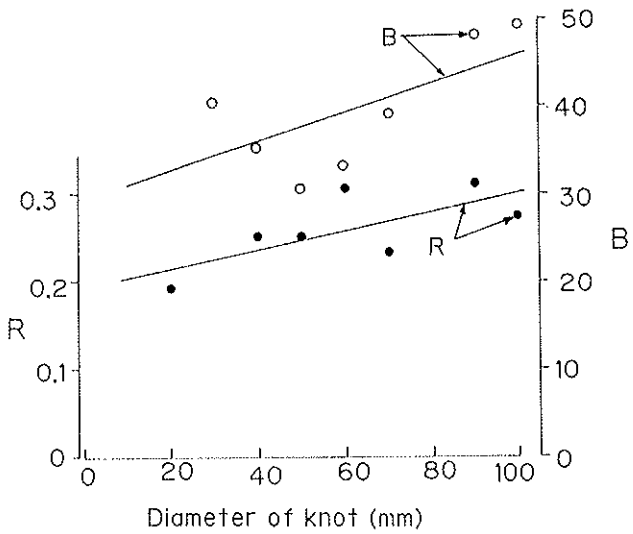

Figure10. Regression for coefficients B and R.

(b) Stress distributions are elastic until failures under uniform strain expressed by Hooke's Law (follows by (a)).

(c) Effect of stress concentration around the knot is negligible. Experiments showed that the weakest point is about 0.9 times the knot size from the edge of the knot (Figure 4).

(d) The failure in a hypothetical narrow strip occurs when the stress reaches the ultimate strength of that strip obtained previously from experiment.

(e) Individual failure of a strip does not interact with any other strip with the proviso that the failed strip reduces the stressed area and thereby increases the stress on remaining strips.

This last assumption is based on the nature of the tensile test apparatus which has many parts where the strain energy can be stored, (e.g. the hydraulic jack, H-shaped steel frame and especially the contact surface made of rubber). This machine is considered flexible enough to supply the constant load to test specimen immediately after partial failure occurred in any section of veneer.

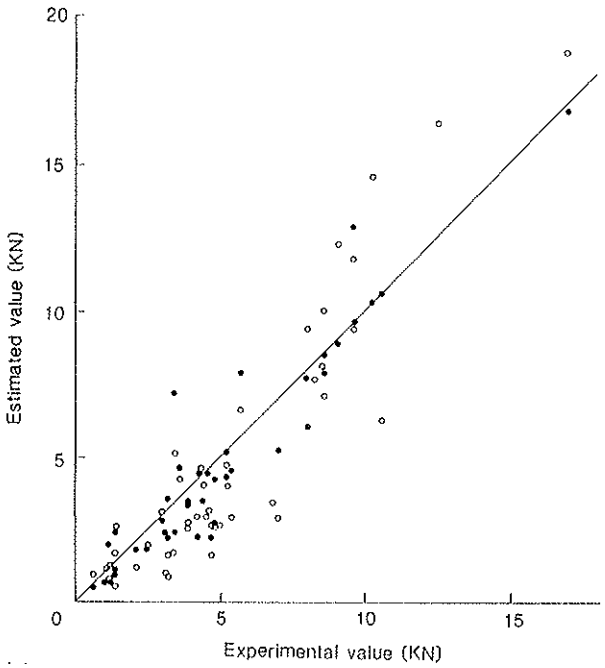

∘ : Estimated value by using stress distribution obtained from experiment on strip

•: Estimated value obtained from generalized estimation formula

Figure 11. Comparison of experimental value of strength of veneer having knot with two kinds of estimated value.

The calculation of the ultimate strength of veneer having knots was done as follows:

1. The distribution of strength and MOE around knot was determined using either the results of the strip tensile tests or calculation from equations (2) and (4).

2. Test specimen was divided into virtual narrow strips. In this case, 500 strips having a range of width 0.02 mm - 0.4 mm.

3. An external force was applied so that a uniform initial elastic stress did not exceed the ultimate strength in any virtual strips.

4. The external load was increased with very small increments until failure occured in a strip.

5. At failure of a strip the stress in the remaining strips was increased, to maintain the external load. If this increment of stress caused any other failure, this procedure was repeated until equilibrium.

6. Procedures 4 and 5 were repeated.

The ultimate strength of veneer was considered to be the final state of stress at equilibrium just before all the strips fractured.

Figure 11 shows the result of these calculation compared with the results of the tests on sheets of veneer.

One of the difficulties in estimating veneer strength is the variability in the strength of clear veneer. It is considered that this is partly due to the random distribution of latewood and earlywood. Other defects such as cross grain in clear veneer, and/or the effect of peeling on the deviated fibres around the knot, also contribute to variation.

Considering these factors, it can be said that the estimated values agree well with the experimental results.

Figure 12 illustrates the incremental stress distribution around the knot and the spread of failure for one specimen. The first failure occurred at the right hand side of the knot when the stress reached the ultimate strip strength of 3 MPa. Then, the failure spread gradually on both sides. This was similar to the spread of failure observed in the experiment.

When the stress in outermost strip reached about 39 MPa, failure spread over all the remaining strips, giving final stage of equilibrium. The sum of this stress distribution gave the ultimate strength of this veneer specimen.

Figure 13 shows the load-strain curve, comparing a theoretical plot with the experimental curve from the same test specimen as Figure 12.

The experimental apparent MOE is obtained from slope of the curve at lower load, i.e. before any failure. At higher load level, the experimental plot indicates wider spread of failure with equilibrium which causes slight increase of load. This is probably caused by supplying the strain energy transferred to the test specimen by the testing machine. The theoretical plot does not follow this phenomenon. To do so, the model should include the stiffness of the testing machine and calculate the strain energy supplied to the test specimen. Such a model was not the objective of this study.

The model developed in this study expresses well the non-linear relationship of the load-strain curve.

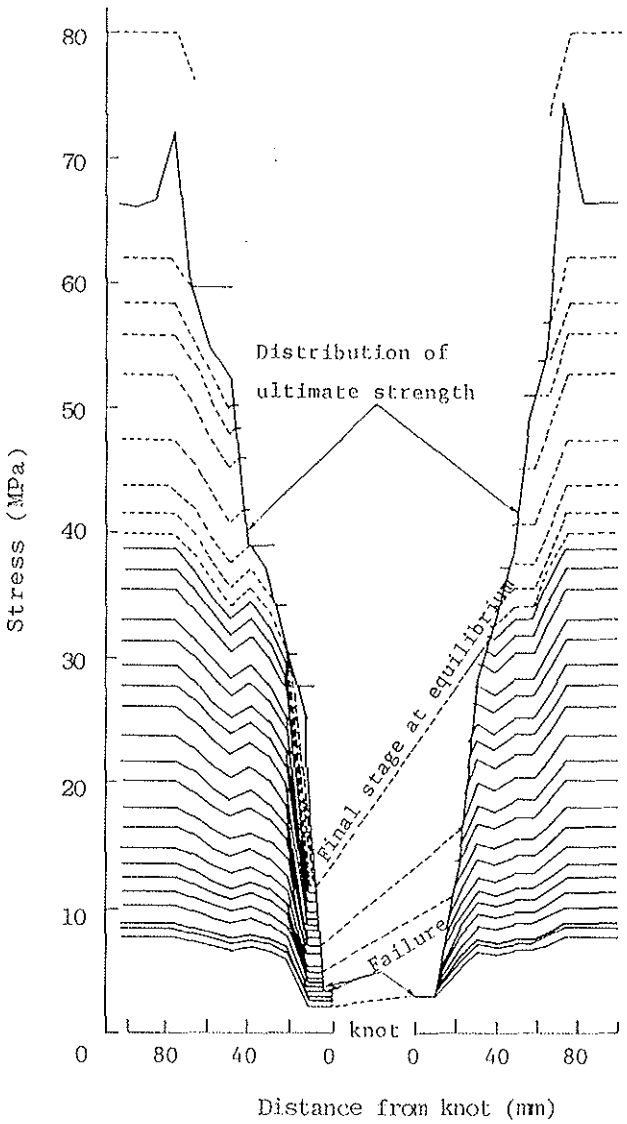

Figure 12. Diagram of spread of failure.

Conclusion

From the tensile tests on strips from around knots and on veneer, strength and stiffness distributions were investigated.

Using these distributions, a model which can predict the strength of veneer having knots has been made. Comparison of estimated values with experimental results showed good agreement, and feasible to apply the model to plywood.

Results obtained are summarised as follows:

1. In the vicinity of knot, the weakest points are located at the position of 0.9 times the knot size from centre of knot.

2. Inclination of fibre at failure point can calculated from an exponential function containing knot size and distance from knot.

3. Strength and stiffness of strips have a close relation with inclination of fibre at failure point and they can be expressed well by Hankinson's formula.

4. The model predicts the strength of veneer well and it can also represent the non-linear load-strain relation caused by partial failure.

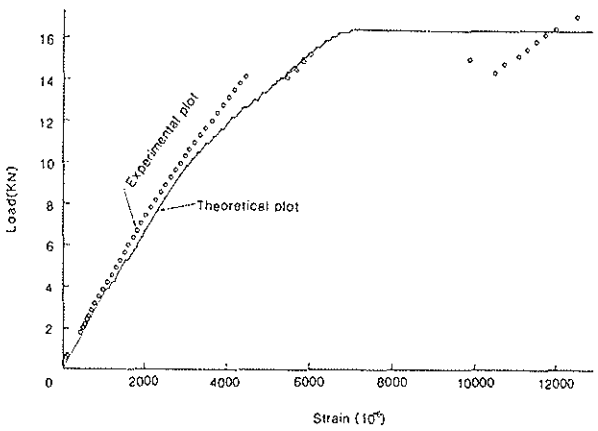

Figure 13. Load-strain curve in tension of knotty veneer.

Acknowledgements

The main part of this research was done during the author's stay at Forest Research Institute of New Zealand as a research fellow.

The author wishes to thank Dr G.B. Walford, Leader of Timber Engineering Group at FRI, for his advice for this study. Also, the author would like to express his appreciation to Messrs H. Bier, J. Parker and Miss K. Prichard for their valuable suggestions and execution of experiments, and to Dr S.O. Hong for his aid in statistical handling of data.

References

1. C. R. Wilson et al : Engineering Properties for Unsanded COFI Exterior Douglas Fir plywood, (1978).

2. Y. Hirashima et al : Strength Tests on Softwood Plywood II. Full-size panel Bending Test on American Softwood Plywood and Japanese Lauan Plywood, Jour. of the Japan Wood Research Society, Vol. 30, No.4 (1984).

3. W. M. McGowan : Effect of Prescribed Defects on Tensile Properties of Douglas Fir Plywood Strips. F.P.J. Vol. 24, No.5 (1974).

4. A. Ylinen : Extension Measurements in Neighbourhood Knots in Scots Pine, Holz als Roh-U.W. 5 (1942).

5. H. Sasaki et al : On the Strain Distribution and Failure of Wood Plates with a Round knot under Tensile Load, Wood Research No.28 (1962).

6. H. Bier : Radiata Pine Plywood : A Theoretical Prediction of the Bending Properties of Structural Plywood, FRI Bulletin No.54 (1983).

7. Y. Hatayama : A New Estimation of structural lumber considering the slope of grain around knots, Bulletin of the Forestry and Forest Products Research Institute, No. 326 (1984).

8

CIB-W18A/21-5-1

INTERNATIONAL COUNCIL FOR BUILDING RESEARCH STUDIES AND DOCUMENTATION

WORKING COMMISSION W18A - TIMBER STRUCTURES

NON-DESTRUCTIVE TEST BY FREQUENCY OF FULL SIZE TIMBER FOR GRADING

by

T Nakai and T Tanaka
Forestry and Forest Products Research Institute
Japan

MEETING TWENTY-ONE
PARKSVILLE, VANCOUVER ISLAND
CANADA
SEPTEMBER 1988

[Paper for the Meeting of CIB-W18A, 24-27 September, 1988]

NON-DESTRUCTIVE TEST BY FREQUENCY OF FULL SIZE TIMBER FOR GRADING

by
Takashi Nakai and Toshinari Tanaka
(FFPRI, Tsukuba, Japan)

1. INTRODUCTION

The main purpose of this experimental work is to tap the possibility of using the frequency measurement on full size timber for grading. There are many ways for estimating strength of timber through non-destructive parameters. One of the most usuful parameters is modulus of elasticity, which could be also obtained by various methods,too.

In searching of the more feasible method of measuring modulus of elasticity at saw mill or lumber yard, the method to measure the fundamental vibration frequency of timber was investigated. It was concerned about the effect of moistur content on density, which is one of the essential items to apply this method.

At the same time, another three methods to obtain the static modulus of elasticity and dynamic one were selected for comparison. These methods were deflection, ultra sonic propagation time and stress wave propagation time measurings.

The frequency measurement has merit of easy handling, because non-contact measuring is possible using relatively reasonable price equipment.

The reason why this work has conducted reflects the current Japanese timber construction tendancy, which is directing to large scale building. Supply of well stress graded timber with reliable strength is the key to keep and promote this trend. Mainly due to the larger cross section of Japanese timber than that of dimension lumber which is used world wide, it is impossible to use today's commercial grading machine, that has normally the limitation of the maximum height of timber to 75 mm.

The results shown in this paper is excerpted from the project which is now underway at FFPRI.

2. EXPERIMENTS

2.1 Materials

Species used in this experiment were sugi(*Cryptomeria japonica*) and akamatsu (*Pinus densiflora*).. The cross sections of timber were scantlings, squares and flat squares, all of which were the most popular structural member used for the current Japanese wooden houses and the nominal sizes were 45mm X 105mm X4000mm, 105mm X 105mm X 4000mm, 120mm X (240-270)mm X 4000mm, respectively.

The sample size were 195 each for sugi scantling and square, 150 for akamatsu scantling and 55 for akamatsu flat square. In the latter case, the frequency measurment was also conducted at saw-mill on akamatsu logs before sawing.

Except akamatsu flat square, measurement of moduli of elasticity was conducted at green moisture condition and at kiln-dried moisture condition of about 15%. In the case of akamatsu flat square, data were obtained only at green moisture condition.

2.2 Methods

The four methods used to obtain modulus of elasticity for comparison were described as below.

2.2.1. Deflection measurement

Adopting concentrated loading system, dead weight was put manually on specimen and deflection at mid-span was measured by a digital dial gauge, monitoring the linear relationship between load and deflection. The total span was 3600mm.

The calculated modulus of elasticity by this method (Edw) was a static one and taken as a control value.

2.2.2. Stress wave propagation time measurement

The two wave types were used, namely ultrasonic and impact-induced compressional waves. Specimen was put on the soft formed polyurethane pillows to be able to measure the free vibration of timber.

a) Ultrasonic wave propergation time measurement

With a 6 KHz transmit transducer, the propagation time of transveres wave from one end of timber to the other end was measured. An ultrasonic modulus of elasticity (Euw) was calculated by the equation (1).

Diagram of an ultrasonic wave propagation time measuring method is shown in Figure 1.

$$\frac{1}{tuw} = \sqrt{\frac{Euw \cdot g}{\rho}} \qquad \text{---(1)}$$

where tuw: propagation time per unit length(e.g. one centimeter) of specimen
Euw: ultrasonic modulus of elasticity
g : gravitational accelaration constant
ρ : average density of specimen at test

b) Impact-induced stress wave propagation time measurement

As shown in Figure 2, an impact-induced stress wave propargation time was measured by an electric counter. Two accelerate transducer were used for starting and stopping the counter. A stress wave modulus of elasticity (Esw) was caluculated by the equation (1), except tuw and Euw were replaced tsw and Esw respectively.

2.2.3. Fundamental vibration frequency measurement

A specimen was put on the same polyurethane pillows. Immediately after a small steel hammer hit the one end of specimen, the sound at another end of specimen was catched by a microphone. Then this signal was put into a Fast Fourier Transformation (FFT) spectrum analyzer and the fundamental vibration frequency was detected. (Figure 3)

Using the equation (2), a frequency modulus of elasticity (Efr) was calculated.

$$f = \frac{1}{21}\sqrt{\frac{Efr \cdot g}{\rho}} \qquad \text{---(2)}$$

where f : fundamental vibration frequency
l : length of specimen
Efr: frequency modulus of elasticity
g : gravitational acceleration constant
ρ : average density of specimen at test

In the case of the measurement on akamatsu log, a log was hung up by a small crane with two slings at saw mill's lumber yard. Weight of log was obtained directly by a load cell. Then, fundamental vibration frequency was detected. Apparent density was calclated by the weight and the volume with the diameter at center and length of log.

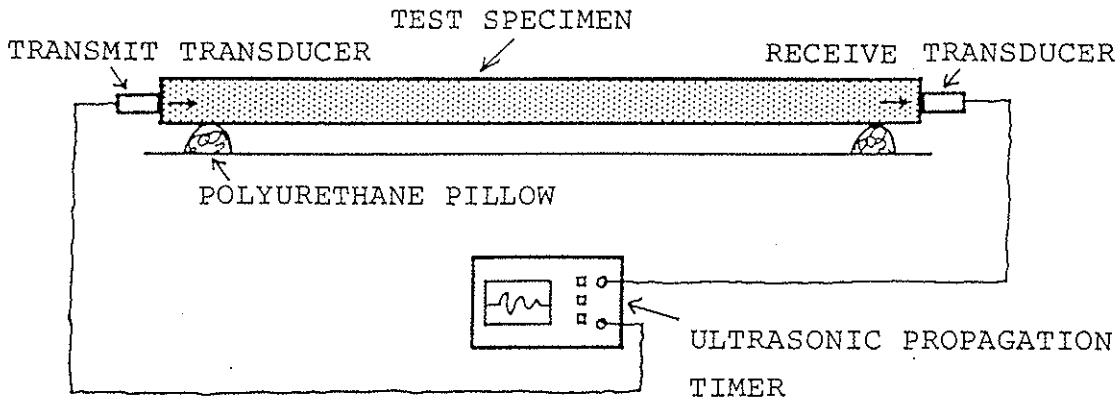

Figure 1. Diagram of an ultrasonic wave propagation time measuring method.

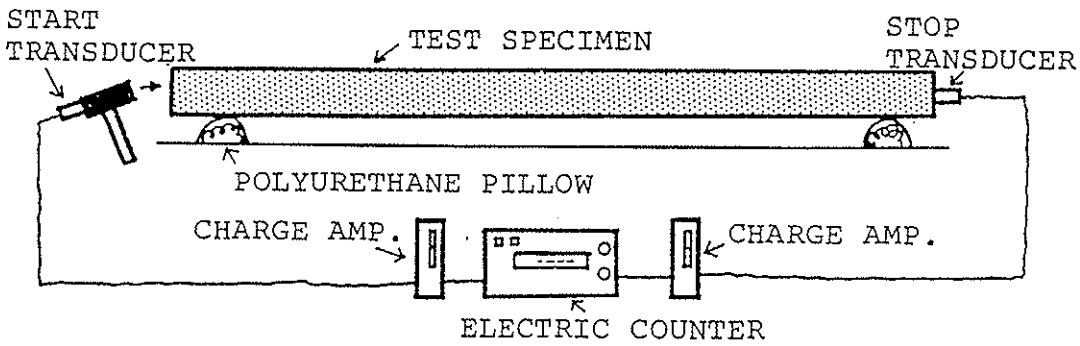

Figure 2. Diagram of an impact-induced stress wave propagation time measuring method.

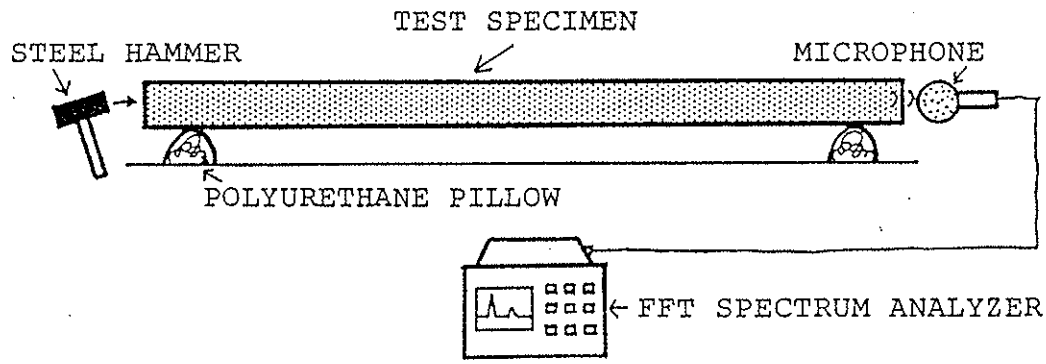

Figure 3. Diagram of a fundamental vibration frequency measuring method.

In Figure 4, typical spectra of akamatsu scantling was shown.

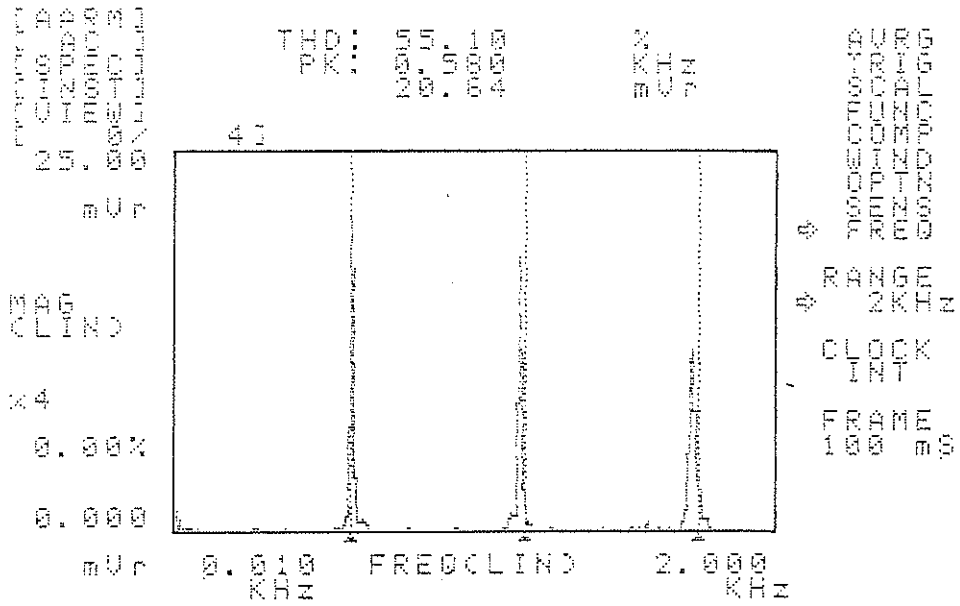

Figure 4. Typical spectra of akamatsu scantling.

3. RESULTS AND DISCUSSION

The comparison of various E values in green and air-dried moisture condition were shown in Figures 5-7. It was concluded that among the four moduli of elasticity measured by different method, we could not find any large difference for the purpose of grading timber. The value of correlation coefficient was the biggest between Efr and Edw compared with another cases.

Also, when timber is green or air-dried conditions, it was shown that using the value of apparent density at measuring, we could obtain the dynamic modulus of elasticity such as ultrasonic, stress wave and frequency modulus of elasticity.

The frequency modulus of elasticity seemed to have very high possibility in commercial usage. Because, it is the most easiest way to measure the modulus of elasticity at saw mill or lumber yard. The deflection measurement has the most higest accuracy, but it takes rather long time to operate without suitable machine. The ultrasonic stress wave propagation time measuring might be impossible in the case of large volume of timber, due to severe damping or with some limitation of energy at transmit transducer. Impact-induced stress wave measuring has the same disadvantage as ultrasonic case has, because receive transducer should be firmly contacted on the surface of timber while measuring. This simple work is practically quite difficult

to conduct.

On the other hand, to hit a timber and detect sound spectra through a microphone is easy as it is a non-contact method. Adding to this fact, there would be no limitation of size of timber for measuring. Even for log or large scale glue-laminated timber, this method can be used. Although we have only seven observations for large scale glue laminated timber, which cross sections were 170mm in width, from 300mm to 570mm in height and 6000mm or 11000mm in length, the results obtained showed good agreement with the static modulus of elasticity.

In Figure 8, it was shown the relationship of frequency modulus of elasticity between log and flat squares of akamatsu. We could estimate modulus of elasticity of a log and sawn timbers from the log. This could be useful especially for round timbers grading in pole construction.

Finally, in Figure 9, relationship between modulus of rupture and two types of modulus of elasticity were shown. Although the value of correlation coefficient between Efr and MOR showed a little bit smaller value then that between MOE-L and MOR, measuring frequency modulus of elasticity could be used practically for timber grading.

4. CONCLUSION

It was concluded that the fundamental vibration frequency measurement had high possibility to obtain modulus of elasticity, which could be used for stress grading, at saw mill or lumber yard.

Frequency modulus of elasticity could be obtained in green or air-dried moisture condition with the apparent density at test and the fundamental vibration frequency.

Frequency modulus of elasticity could be measured on log and large scale glue-laminated timber, for which it is usually hard to measure.

Among the four moduli of elasticity measured by deflection, ultrasonic propagation time, stress wave propagation time and fundamental vibration frequency, little difference was observed for the purpose of grading timber.

note

Edw: ststic modulus of elasticity
Euw: ultrasonic modulus of elasticity
Esw: stress wave modulus of elasticity
Efr: frequency modulus of elsticity
r : correlation coefficient
n : number of specimens
Gr: green moisture condition
AD: air-dried moisture condition

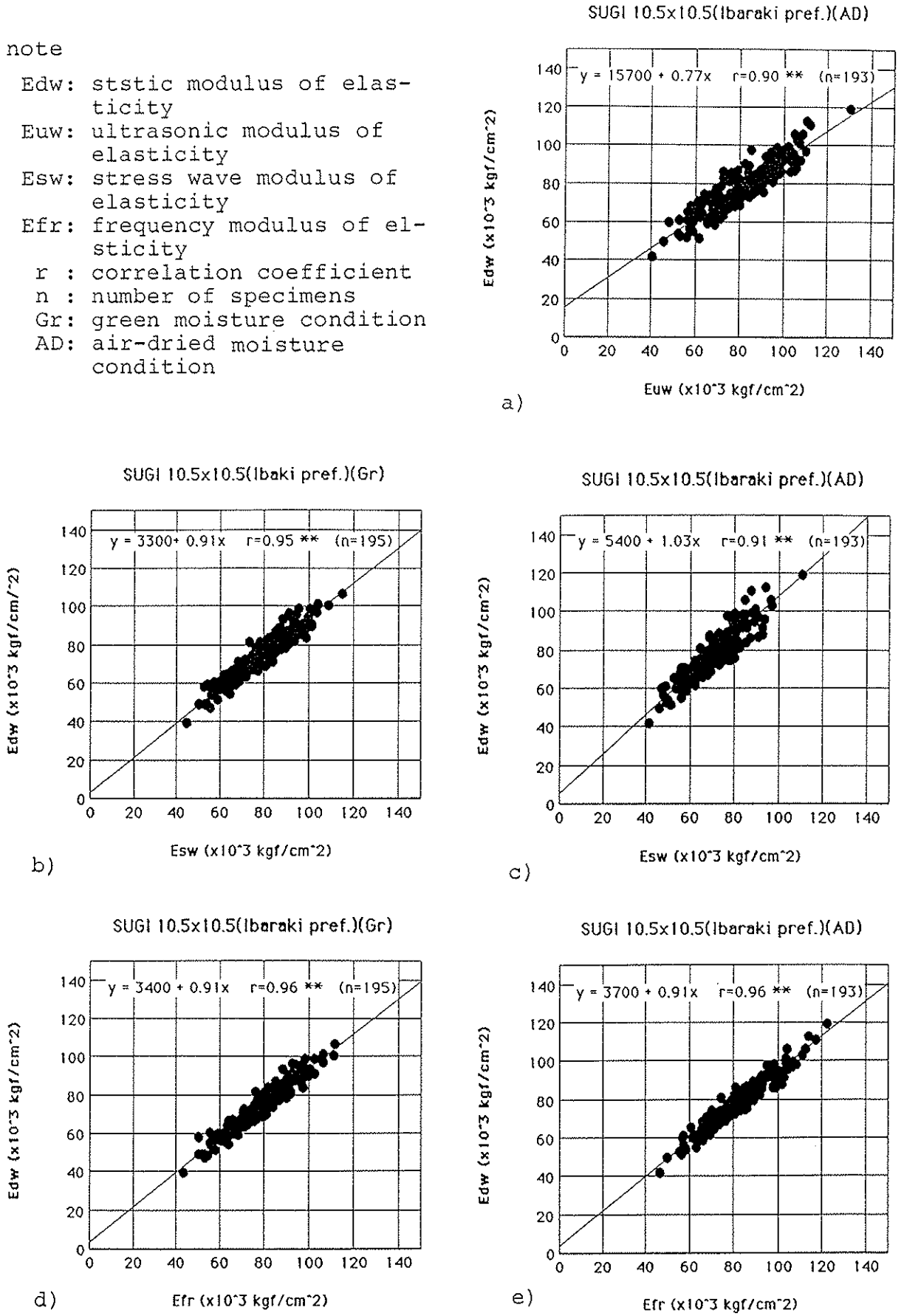

Figure 5. The comparison of four moduli of elasticity on sugi squares.

note: see Figure 5.

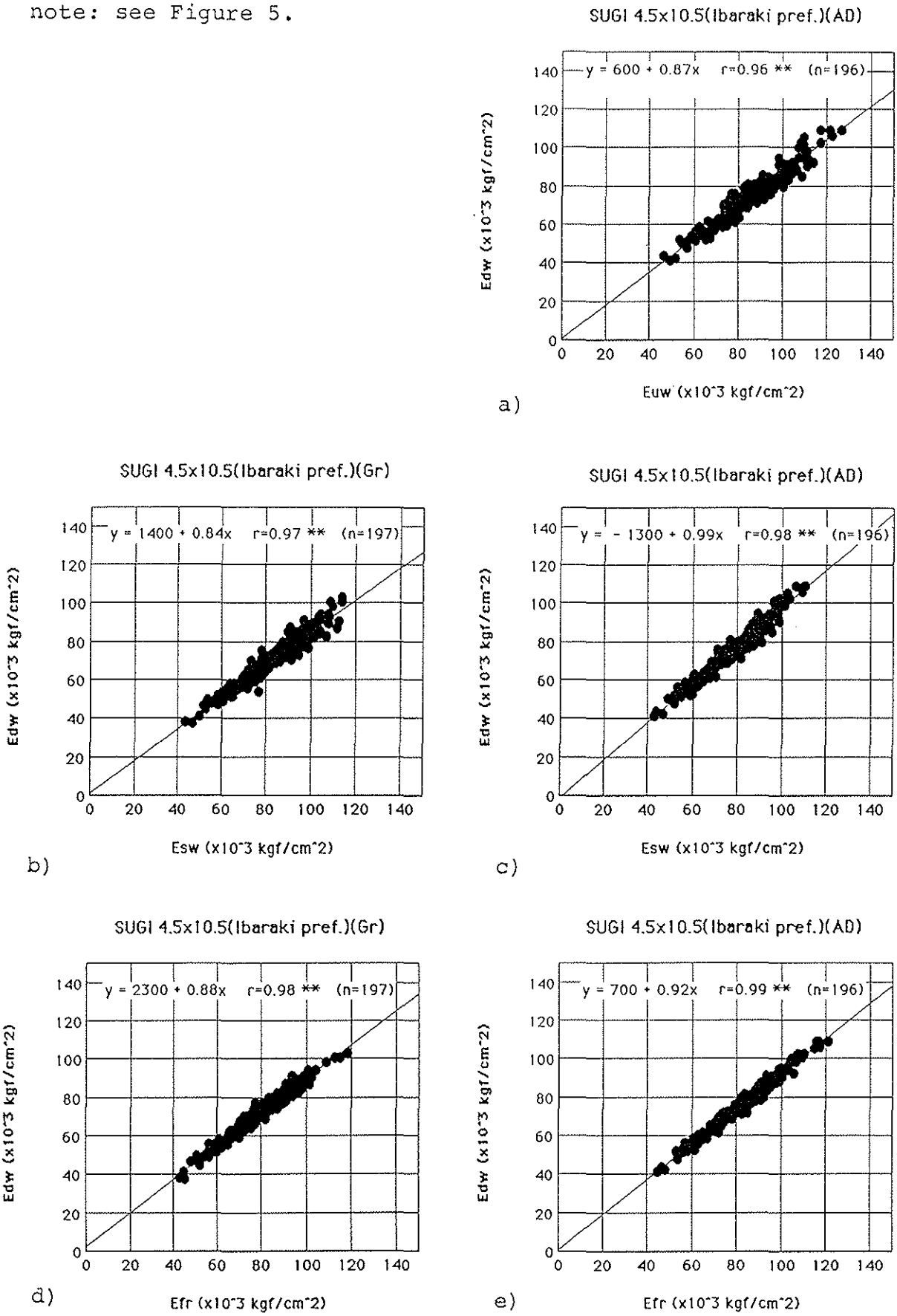

Figure 6. The comparison of four moduli of elasticity on sugi scantlings.

note: see Figure 5.

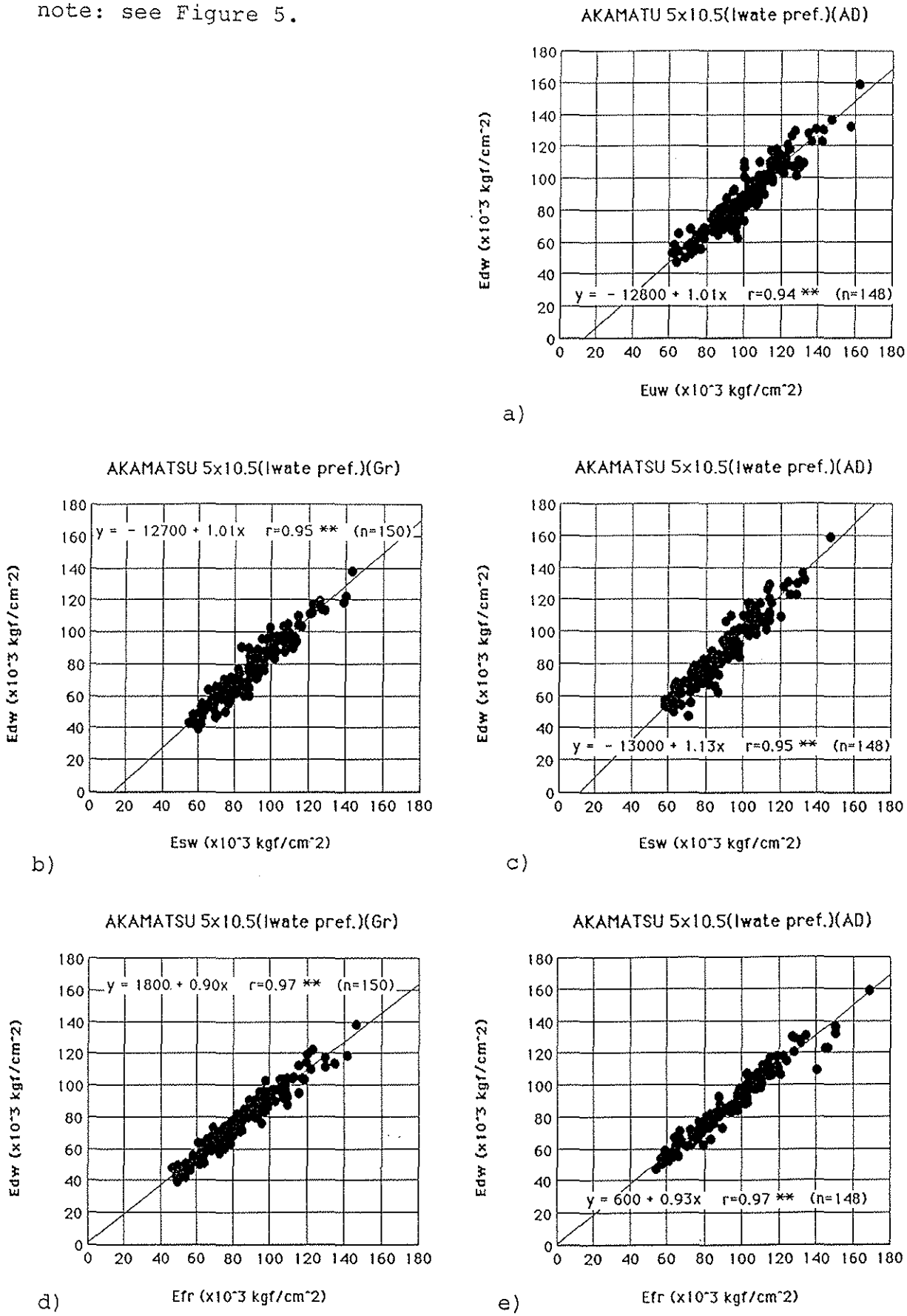

Figure 7. The comparison of four moduli of elasticity on akamatsu scantlings.

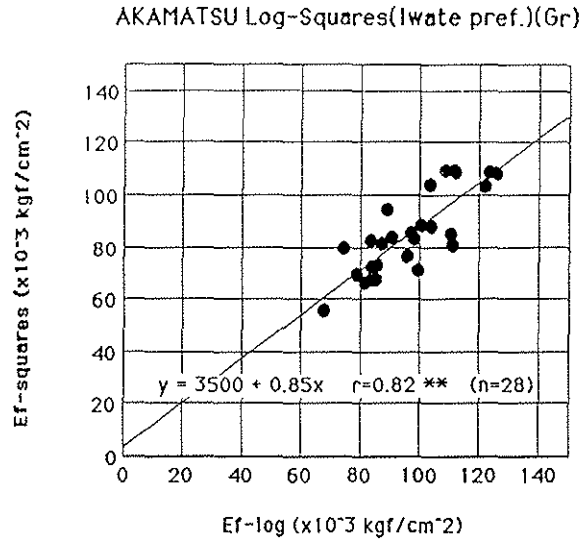

note

$E_{f\text{-}log}$: frequency modulus of elasticity in log

$E_{f\text{-}squares}$: frequency modulus of elasticity in squares

Figure 8. Relationship of frequency modulus of elasticity between log and flat squares of akamatsu.

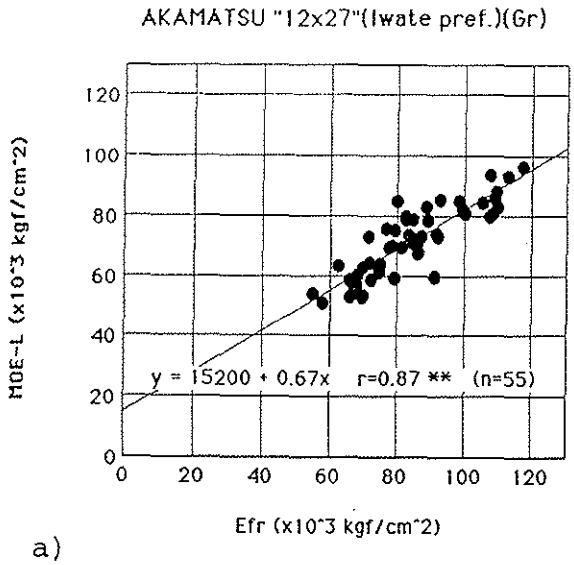

a)

note

MOE-L : static modulus of elasticity at rupture test

MOR : modulus of rupture

E_{fr} : frequency modulus of elasticity in square

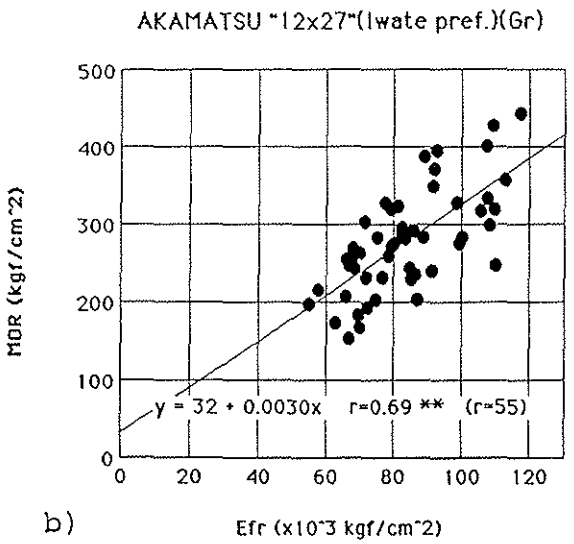

b)

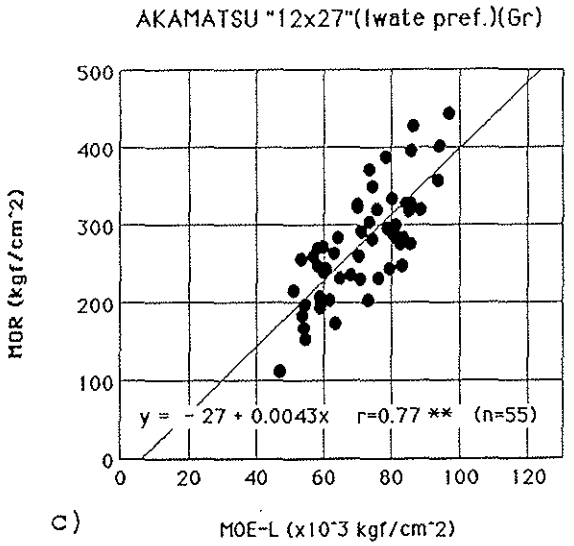

c)

Figure 9. Relationship among frequency modulus of elasticity, static modulus of elasticity at test and modulus of rupture.

CIB-W18A/21-6-1

INTERNATIONAL COUNCIL FOR BUILDING RESEARCH STUDIES AND DOCUMENTATION

WORKING COMMISSION W18A - TIMBER STRUCTURES

DRAFT AUSTRALIAN STANDARD: METHODS FOR EVALUATION OF STRENGTH AND STIFFNESS OF GRADED TIMBER

by

R H Leicester
CSIRO
Australia

MEETING TWENTY-ONE
PARKSVILLE, VANCOUVER ISLAND
CANADA
SEPTEMBER 1988

TM102.RHL/210688

INTERNATIONAL COUNCIL FOR BUILDING RESEARCH STUDIES AND DOCUMENTATION

WORKING COMMISSION W18A - TIMBER STRUCTURES

DRAFT AUSTRALIAN STANDARD: METHODS FOR EVALUATION OF STRENGTH AND STIFFNESS OF GRADED TIMBER

by

R. H. Leicester

(CSIRO, Melbourne, Australia)

PREFACE

The following is based on a draft Australian Standard, but modified in terms of presentation and with the emphasis on the assessment of characteristic values for limit states codes. Over the past five years the draft Standard has been used to evaluate the design properties of a variety of timber products including sawn timber (both hardwoods and softwoods), laminated veneer lumber, plywood and Scrimber. In all cases the results obtained have been considered by the timber industry to be reasonable and acceptable.

Vancouver September 1988

CONTENTS

APPENDICES

SECTION 1. DEFINITIONS AND NOTATION

1.1 Definitions

Characteristic Value. Basic material parameter defined in statistical terms.

Reference Population. This is a population of graded structural timber for which the design properties are being evaluated. The reference population is defined in terms of the source of timber, the moisture content (whether seasoned or unseasoned) and size of sticks, the stress grade, and the method of grading used.

Stick. Piece of sawn timber of rectangular or square cross-section.

Standard Test Configuration. The test configuration specified for the standard evaluation procedure.

1.2 Notation

E = modulus of elasticity

E_{av} = nominal average stiffness

E_k = characteristic value of E

E_{mean} = mean value of E of the data

$E_{0.05}$ = five percentile value of E of the data

F = lateral load

$F_R(x)$ = cumulative distribution function of R at the value x

h = depth of test specimen, Figures 5.1-5.4

k_b = modification factor to bending strength to account for bias in defect location, Table A.1

k_g = modification factor for lengths of graded timber, equation

(A.2)

l_{gs} = normal length of graded sticks

l_{gn} = unusual length of graded sticks

k_l = modification factor for test specimen length, equation (A.1)

k_s = modification factor for sample size, equations (7.1) and (7.2)

l = standard span

l_o = non-standard span

n = sample size

N = axial load

R = strength

R_k = characteristic value of R

R_{basic} = basic working stress

$R_{0.05}$ = five-percentile value of R of the data

V_R, V_E = coefficient of variation of R and E of the data

α = bias factor for location of defects, Appendix A.4

SECTION 2. SCOPE AND METHOD

2.1 Scope

This Standard describes methods for evaluating structural properties of graded timber. The method may be used for verifying the accuracy of specific grading techniques; it may also be used to resolve doubts concerning the specified design properties of particular populations of graded timber. This is a quality assurance and not a quality control document.

Specifically, this Standard is concerned with the evaluation of characteristic values of strength and stiffness for use with limit states codes; it is also concerned with the evaluation of basic working stresses and specified stiffness for use in working stress codes. These evaluated properties apply to a given reference population.

2.2 Method

The procedures of this standard are based on assessing (with 75 percent confidence) the characteristic values of the structural properties of timber as they occur under service conditions. However the use of other procedures that provide an equivalent assessment are not precluded.

The evaluations are based notionally on a set of standard tests. These tests are described in terms of standard sampling procedures and testing configurations. Methods of using data obtained from non-standard evaluation procedures are discussed in Appendix A.

NOTE. The standard test configurations to be specified have been chosen to simulate in-service conditions. Thus typical sizes, spans and loading arrangements are recommended, and the test specimens are cut from locations selected at random from within the sticks of timber samples.

NOTE. It may be desirable to use non-standard tests for various reasons. For example, it may be desired to test pieces of timber that are shorter than the specified standard length, because of difficulties in obtaining long lengths of timber.

Sometimes it may be useful to bias the test procedure in order to reduce the necessary sample size for a given degree of accuracy. A typical method of producing a bias would be that of selecting test specimens so that they include the worst defect in the piece of timber from which they are cut; another method is to select specimens from pieces that are assessed visually or otherwise to comprise the weakest 10% of the population of a specific grade of timber. In order to use biased sampling procedures it is first necessary to determine the statistical relationships between biased and unbiased population properties, and then to use special statistical techniques.

SECTION 3. EVALUATION EQUATIONS

3.1 Evaluation Equations for Limit State Codes

The characteristics strength R_K is given by

$$R_K = [1 - (2.7\ V_R/\sqrt{n})]\ R_{0.05} \quad (1)$$

where $R_{0.05}$ and V_R are the five percentile value and coefficient of variation of the measured data, and n is the sample size.

The characteristic stiffness E_K is given by

$$E_K = [1 - (2.7\ V_E/\sqrt{n})]\ E_{0.05} \quad (2)$$

where $E_{0.05}$ and V_E are the five percentile and coefficient of variation of the measured data.

The nominal average stiffness E_{av} is given by the minimum of the two following values,

$$E_{av} = [1 - (0.7\ V_E/\sqrt{n})]\ E_{mean} \quad (3)$$

$$E_{av} = 1.4\ E_K \quad (4)$$

where E_{mean} is the average value of the data.

NOTE. From the above it follows that values of R_K and E_K apply to populations of timber and not to single sticks.

NOTE. The terms $[1 - (2.7\ V_R/\sqrt{n})]$, $[1 - (2.7\ V_E/\sqrt{n})]$ and $[1 - (0.7\ V_E/\sqrt{n})]$ are to provide a 75 per cent confidence in the derived characteristic values. The use of other methods that provide an equivalent assessment may also be used.

NOTE. V_{data} is computed as follows:

$$V_{data} = \frac{1}{x_{mean}} \sqrt{\frac{\sum (x_i - x_{mean})^2}{n}}$$

where

$$x_{mean} = \frac{1}{n} \sum x_i$$

in which x_i denotes the sample values

NOTE. The use of equation (4) is to cover the case of a species mixture, or an unusual species that has a coefficient of variation greater than 25 percent in its modulus of elasticity.

3.2 Evaluation equations for working stress codes

The basic working stress R_{basic} shall be given by

$$R_{basic} = R_k/[1.75(1.3 + 0.7\ V_R)] \qquad (5)$$

However, if the timber is of a species, moisture content, grade and size such as to be prone to checking in service, the value given in equation (5) shall be reduced by a factor of 1.5 when evaluating the basic working stress in shear.

For working stress codes, the specified stiffness shall be taken to be the nominal stiffness given by the equations (3) and (4).

NOTE. In equation (5) The factor 1.75 is the value of modifier K_1 given in Table 2.5 of AS 1720: Part 1. It is used to define the relationship between the three minute design strength and the long term strength associated with the basic working

stress. The true factor of safety is $(1.3 + 0.7\ V_R)$.

NOTE. In the absence of other guidance, the criterion for tendency to split may be based on the parameter α defined by

$$\alpha = \varepsilon^2/\gamma$$

where

ε = tangential shrinkage (%),

γ = tangential cleavage strength of unseasoned timber (N/mm), as measured by BS373(1957) or ASTM D143 (1952).

Species for which $\alpha > 0.8$ often have a high tendency to split, particularly in exposed locations; species for which $\alpha < 0.55$ may be considered to have a negligible tendency to split.

Information on shrinkage can be obtained from 'Shrinkage and density of Australian and other woods' by R.S.T. Kingston and C.J.E. Risdon. Division of Forest Products Technological Paper No. 13, CSIRO 1961. Information on cleavage strength can be obtained from 'The mechanical properties of 174 Australian timbers' by E. Bolza and N.H. Kloot. Division of Forest Products Technological Paper No. 25, CSIRO 1963.

SECTION 4. REFERENCE POPULATION

The reference population must be clearly defined since it is only to this population that the derived design properties apply. It is the population that is supplied commercially as a specific grade of timber obtained from a specific source. A reference population may be graded from a single species or a defined mixture of species. The results of an evaluation apply only to the reference population.

NOTE. From the above it follows that if the reference population changes, then the structural properties may also change and hence should be reassessed.

Note. The reference population depends on the accuracy of the grading. Thus the reference population of commercial and laboratory graded timber may differ.

SECTION 5. SAMPLING

The sample to be tested must be chosen so as to be representative of the reference population. Considerable care must be taken to ensure that all structural characteristics which affect or concievably might affect strength or stiffness, are distributed within the sample in much the same frequency as they are to be found within the reference population.

In order to simulate in-service conditions, test specimens must be cut from random locations within the sticks of the timber sample. A suitable method for doing this is given in Appendix B.

The minimum sample size used shall be not less than 20 for stiffness and not less than 30 for strength.

> NOTE. Before choosing a sample size reference should be made to Section (7.1) which gives the penalty for using samples that are too small. Consideration should also be given as to whether the sample size is sufficiently large to reflect all the characteristics of the parent population.

SECTION 6. STANDARD TEST CONDITIONS

The standard test configurations for evaluating basic working stresses and modulus of elasticity are shown in Figures 6.1 to 6.4. For the tests to evaluate bending and shear strengths, the choice of the edge to be stressed in tension shall be selected at random. The specimens shall be conditioned to a temperature of 20°±3°C; specimens to be tested unseasoned shall be conditioned in an environment having a relative humidity of 100%; specimens to be tested seasoned shall be conditioned in an environment having a relative humidity of 65%±5%.

Testing shall be undertaken in accordance with good laboratory practice. Examples of good laboratory practice are given in .....

Conditioning shall continue until the moisture content is uniform within each stick.

NOTE. Methods of conditioning timber to a relative humidity of 100% include wrapping in plastic, placing under water sprays, submerging in a pond or use of a conditioning room.

NOTE. The selection of a random edge for bending tests is intended to simulate in-service conditions.

NOTE. The configuration required for the compression test shown in Figure 6.3 is awkward to achieve because of the requirement of lateral restraints. However, this test may be simulated with sufficient accuracy as follows. First a test specimen of the standard test length is selected at random from

a piece of timber. Then a smaller test specimen is cut from the original test specimen in such a way that it includes the worst visual defect at its mid length. A value of eight would be suitable for the length to thickness ratio used in this test.

NOTE. The conditioning regime specified may be modified provided at the time of test moisture contents are measured and appropriate corrections made for deviations from the expected values for conditioning under standard conditions. The appropriate corrections for moisture content are available for the modulus of elasticity, but may be quite difficult to obtain in the case of strength.

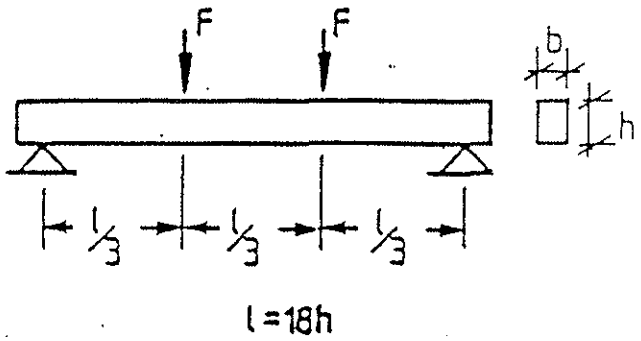

Figure 6.1 Standard test configuration for measurement of bending strength and modulus of elasticity

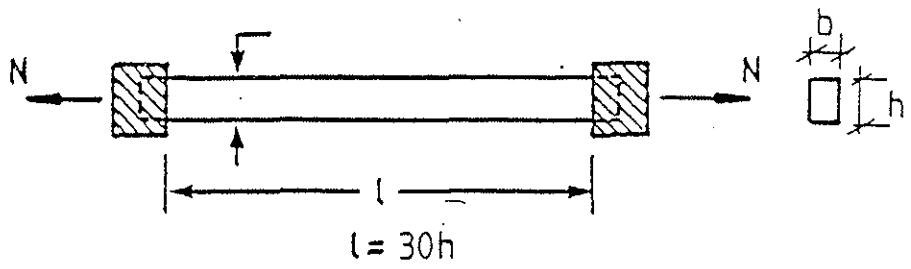

Figure 6.2 Standard test configuration for measurement of tension strength

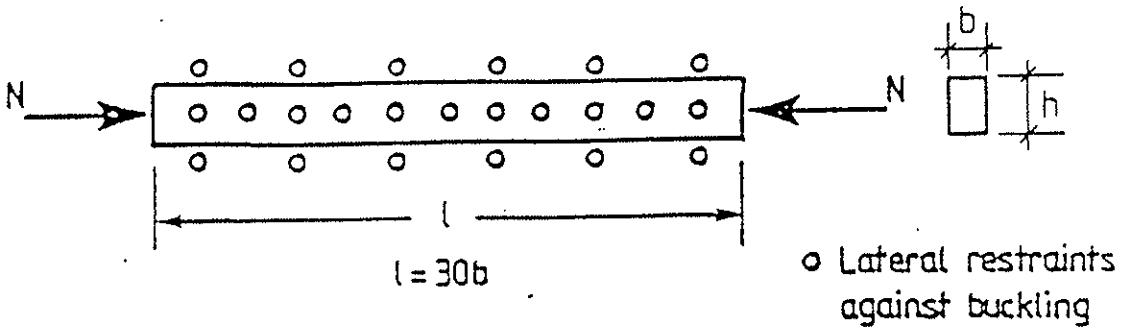

Figure 6.3 Standard test configuration for measurement of compression strength

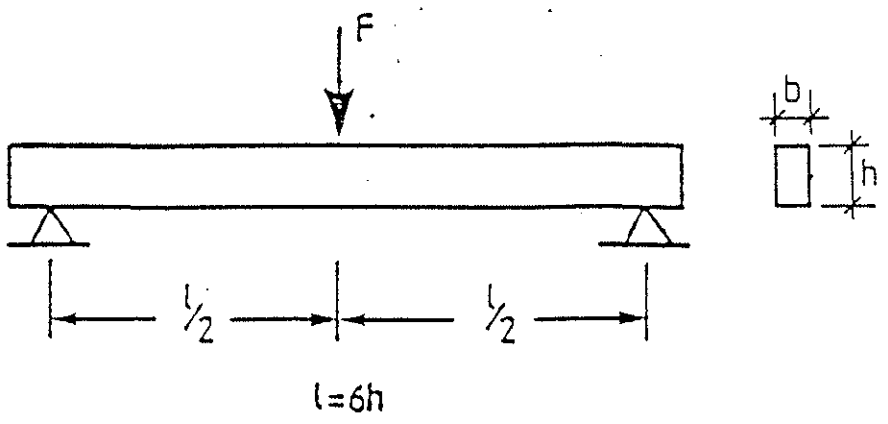

Figure 6.4 Standard test configuration for measurement of shear strength

SECTION 7. STRESS GRADE

In addition to the derivation of characteristic or nominal values for each structural property, it may be desired to classify a timber into a stress grade.

In order to classify the reference population into a stress grade, preliminary classifications are first made for each of the individual properties. On the basis of these preliminary classifications, the final classification for the reference population is made according to the rules shown in Table 10.1.

TABLE 10.1

RULES FOR STRESS GRADE CLASSIFICATION

OF THE REFERENCE POPULATION

Preliminary classification			Resultant stress grade for reference population
Bending strength	Tension strength	Modulus of elasticity	
F	F	F	F
F	F+1	F-1	F
F	F-1	F+2	F
F-1	F+1	F+2	F

Note: Stress grade F+1 is one grade higher than the stress grade F

SECTION 8. ASSESSMENT REPORTS

Reports of assessments of structural properties shall include the following information:

(a) Name of laboratory carrying out the tests

(b) Date

(c) Definition of the reference population. (These may include the source of timber, species, age of tree, method of sampling, moisture content, dimension of pieces of timber from which the test specimens were cut, and method of grading).

(d) Test configurations, including dimensions of test specimens.

(e) Data obtained.

(f) Estimates of means, coefficients of variation and five percentile values.

(g) Derived values of strength and modulus of elasticity.

APPENDIX A

MODIFICATION FACTORS FOR NON-STANDARD CONDITIONS

A.1 GENERAL

When non-standard conditions are used for the structural evaluation of characteristic values, it is necessary to make a translation of the data to estimate the characteristic value that would be obtained under standard conditions. The following describes modification factors that may be applied when the method of evaluation is close to that recommended as standard.

A.2 TEST SPECIMEN LENGTH

A.2.1 Effect on Basic Working Stress

If the length of the test specimen is shorter than the standard length, then the measured strength values will be increased. For this case, a conservative correction will be obtained if the measured five percentile value $R_{0.05}$ is multiplied by a factor k_1 given by

$$k_1 = (l_o/l_s)^{V_R} \qquad (A.1)$$

l_s = span in standard test

l_o = span in actual test.

NOTE. This correction need not be applied to the test data for compression tests when shortened specimens are used as

described in the note to Section 5.

Editors Note. The modification given by equation (A.3) is derived on the assumption that the strengths of segments of timber cut from the same stick are perfectly uncorrelated.

A.2.2 Effect on Modulus of Elasticity

The modification to the modulus of elasticity measured with non-standard spans shall be given by

$$E_s = (E_o/1.04)\ [1 + 14\ (h/l_o)^2] \qquad (A.2)$$

where

E_s = the value for a standard span

E_o = the value measured on the non-standard span

h = member depth

l_o =length of non-standard span.

NOTE. The design modulus of elasticity specified in Table 2.3 of AS 1720: Part 1 contains an allowance for the deformation due to shear. This allowance is based on the value for a standard span-to-depth ratio. Equation (A.2) provides a compensation for the fact that shear deformations form a greater proportion of the total deflection as the span-to-depth ratio is reduced.

A.3 GRADED LENGTH

If the graded length of timber is longer than the normal value marketed, then the measured strength values will be increased. For this case, a conservative correction will be obtained if the five percentile value of strength $R_{0.05}$ is multiplied by a factor k_g given by

$$k_g = (l_{gs}/l_{gn})^{V_R} \qquad (A.3)$$

NOTE. There is no effect of graded length on the modulus of elasticity.

A.4 DEFECT LOCATION

A.4.1 General

In a standard test the locations of defects are assumed to occur at random locations. If the selection of test specimens is biased in some way with regard to the location of defects then an appropriate modification factor should be applied.

In the case of radiata pine for which the bending test specimens have been selected in such a way that the worst defect in each stick is located at the centre of the tension edge of the test specimens, the five percentile value of bending strength may be increased by the factor k_b given in Table A.1.

TABLE A.1

FACTOR k_b FOR RADIATA PINE

Stress grade	Grade designation	k_b
F14	Str. No. 1	1.00
F11	Str. No. 2	1.05
F8	Str. No. 3	1.10
F7	Str. No. 4	1.15
F5	Str. No. 5	1.20

APPENDIX B

METHOD FOR SELECTION OF RANDOM SPECIMEN LOCATION

In order to choose a random location for a specimen of length l_s in a stick of length L, the end of the specimen should be located at a length l_e from the end of the stick, where l_e is given by

$$l_e = r(L - l_s) \qquad (B.1)$$

in which r is a number selected at random from a uniform distribution in the range 0 to 1. the end from which the length l_e is measured is to be chosen at random, possibly by the toss of a coin. The notation is illustrated in Figure B.1. A set of values for the random number r is given in Table B.1.

NOTE. Frequently, because of the random method of cutting sticks, the complexity involved in using the above procedure for selecting specimen locations may not be warranted. In this case, adequate accuracy is obtained if the specimens are cut either from the centre or from a randomly chosen end.

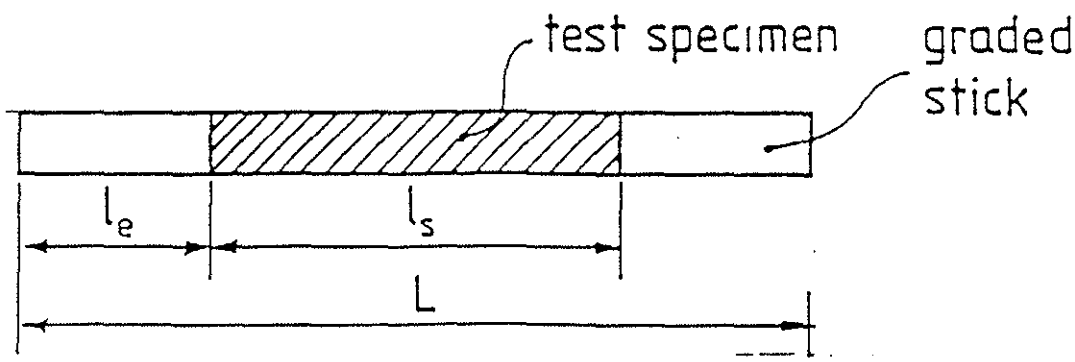

Fig. B.1 Notation for specimen selection procedure

TABLE B1

SET OF RANDOM NUMBERS

.6552	.9653	.3023	.8391	.5647	.8457
.8455	.5821	.2266	.5335	.0392	.1335
.2716	.4624	.3739	.3425	.2724	.4361
.3765	.0603	.5101	.5559	.9617	.5400
.9670	.9690	.9851	.4161	.8156	.6281
.3560	.2120	.8765	.4320	.9084	.0100
.0720	.8838	.2850	.1285	.8310	.3289
.1954	.4314	.6273	.4286	.0244	.8013
.4826	.7587	.0616	.0048	.2176	.9445
.5738	.4955	.8756	.4298	.2094	.7737
.2276	.7676	.1506	.4785	.0604	.7551
.6633	.2742	.2830	.9473	.6115	.0743
.1094	.8607	.4183	.8184	.1189	.4631
.5890	.0988	.3927	.9395	.5753	.7954
.1263	.4118	.0961	.4103	.5539	.8751
.6093	.2108	.1549	.1307	.5897	.3126
.6211	.0915	.7378	.7573	.4032	.7064
.2044	.1828	.8447	.6671	.7673	.6207
.2969	.1433	.3433	.2806	.2102	.8894
.2329	.9965	.9982	.5173	.2436	.2460
.5620	.3815	.7170	.9310	.4422	.2426
.7593	.9406	.9197	.7243	.9760	.9864
.5897	.3764	.4235	.2650	.7975	.4118
.8833	.8564	.9030	.8493	.4542	.1829
.2968	.4435	.6071	.4064	.4372	.7323
.6708	.0726	.4570	.8166	.2767	.8481
.1127	.6242	.7380	.5319	.3118	.8770
.5370	.2849	.0477	.4740	.1601	.2950
.8709	.8003	.4833	.6597	.4927	.9074
.3209	.6881	.8612	.6899	.5489	.7451
.6537	.3184	.7832	.5218	.0230	.4614
.5401	.9465	.6185	.3581	.2461	.5252
.2777	.9851	.6035	.1981	.3152	.0453
.3259	.7580	.5475	.9152	.0308	.1467
.2827	.4562	.6902	.6083	.0780	.8552
.3168	.5857	.2572	.4833	.9441	.8480
.6212	.7987	.3670	.1059	.4448	.1049
.3345	.6598	.6201	.7179	.5649	.0995
.3556	.7070	.4567	.4643	.9176	.3109

.6583	.7293	.0192	.7320	.4936	.0730
.4129	.7985	.6803	.2599	.8019	.6041
.9366	.1807	.8368	.7746	.2809	.7528
.1691	.2580	.0581	.8070	.2254	.1076
.7389	.1630	.3763	.3556	.0464	.1651
.8938	.1896	.7194	.2653	.8179	.9808
.5045	.4712	.4341	.7452	.6425	.4740
.9049	.0321	.0077	.3888	.2895	.9499
.2226	.5067	.7834	.2055	.1777	.7217
.7328	.3060	.4523	.0625	.9730	.6023
.0085	.2390	.3483	.0911	.4563	.8880
.2533	.2353	.5364	.8004	.9884	.3325
.9366	.1677	.1894	.1842	.2583	.1604
.8023	.3619	.6483	.2663	.5265	.1822
.0554	.5805	.8025	.8501	.4288	.3994
.8591	.6419	.3367	.5172	.6855	.9144
.9178	.2199	.3252	.3753	.6071	.2065
.0961	.4389	.5472	.1600	.2081	.4960
.6550	.4775	.4735	.1336	.3545	.2607
.5510	.3233	.1016	.0486	.3943	.3916
.9750	.5392	.3383	.0181	.8760	.6744
.5990	.8499	.0390	.4312	.5626	.3667
.3298	.9218	.8005	.6153	.2982	.2766
.6685	.8055	.2066	.7217	.9740	.5561
.8810	.3153	.8037	.4309	.3444	.0904
.0581	.5218	.4853	.7063	.5926	.8229
.7407	.8934	.2625	.9445	.1705	.0070
.3757	.4258	.3193	.3065	.8339	.3297
.4800	.9766	.2934	.4429	.7838	.0251
.2478	.2177	.7408	.5452	.4289	.5950
.6067	.2099	.5936	.6970	.9324	.9296
.5903	.7321	.5761	.8450	.4583	.1708
.5918	.2968	.9824	.1686	.5767	.1073
.1154	.3333	.8555	.2925	.7706	.0753
.9793	.2011	.7329	.5837	.1399	.8496
.0374	.8322	.5780	.6948	.2156	.5033
.4849	.2411	.8175	.2761	.7998	.6970
.9913	.7989	.5063	.9731	.8774	.8564
.5299	.9261	.3035	.2648	.7396	.4548
.4112	.0527	.6185	.5700	.8938	.6499
.1056	.4715	.0600	.7560	.9854	.6740

APPENDIX C

EXAMPLE

C.1 DATA

The following is an example of the method for processing data obtained for the derivation of a basic working stress in bending.

The measured bending strength R of randomly selected pieces of radiata pine graded as F8 structural grade is given in Table B.1. The sample size used is 109. The derived coefficient of variation V_{data} is 0.37. The cross-section is 100 x 35 mm, and the test span used was 1500 mm. The test specimens were selected and biased so that the worst visual defect of each sample was located in the maximum tension zone of the test specimen cut therefrom.

C.2 DERIVATION

The cumulative distribution function of R is computed as shown in Table C.1 and graphed in Figure C.1.

The required five percentile value is read off this graph and is seen to be -

$$R_{0.05} = 28.2 \text{ MPa}$$

Because the span for a standard test as shown in Figure 5.1 is 1800 mm, the correction factor for using a non-standard span is

$$k_1 = (1500/1800)^{0.37}$$
$$= 0.93$$

Because the defect locations are biased, a modification factor k_b given in Table A.1 is used. For the case of F8 structural grade this is

$$k_b = 1.10$$

Using equation (1), the characteristic value of bending strength R_K correlated for non-standard span and defect-bias factors is

$$R_K = K_1 K_b [1 - (2.7 V_R/\sqrt{n})] R_{0.05}$$

$$= (0.93)(1.10) [1 - (2.7 \times 0.37/\sqrt{109})] (28.2)$$
$$= 26.1 \text{ MPa}$$

From equation (5) the basic working stress in bending R_{basic} is given by

$$R_{basic} = R_K/[1.75 (1.3 + 0.7 V_R)]$$
$$= 26.1/[1.75 (1.3 + 0.7 \times 0.37)]$$

$$= 9.6 \text{ MPa}.$$

TABLE B.1

BENDING STRENGTH DATA

Strength ranking i	Bending strength x (MPa)	Cumulative distribution function $F_R(x)$
1	15.7	0.0046
2	19.5	0.0138
3	24.0	0.0229
4	24.2	0.0321
5	27,1	0.0413
6	28.3	0.0505
7	28.6	0.0596
8	29.4	0.0688
9	30.4	0.0780
10	30.6	0.0872
11	31.8	0.0963
12	32.3	0.1055
108	126.9	0.9862
109	138.3	0.9954

$n = 109$

$F_R(x_i) = [i - 0.5]/n$

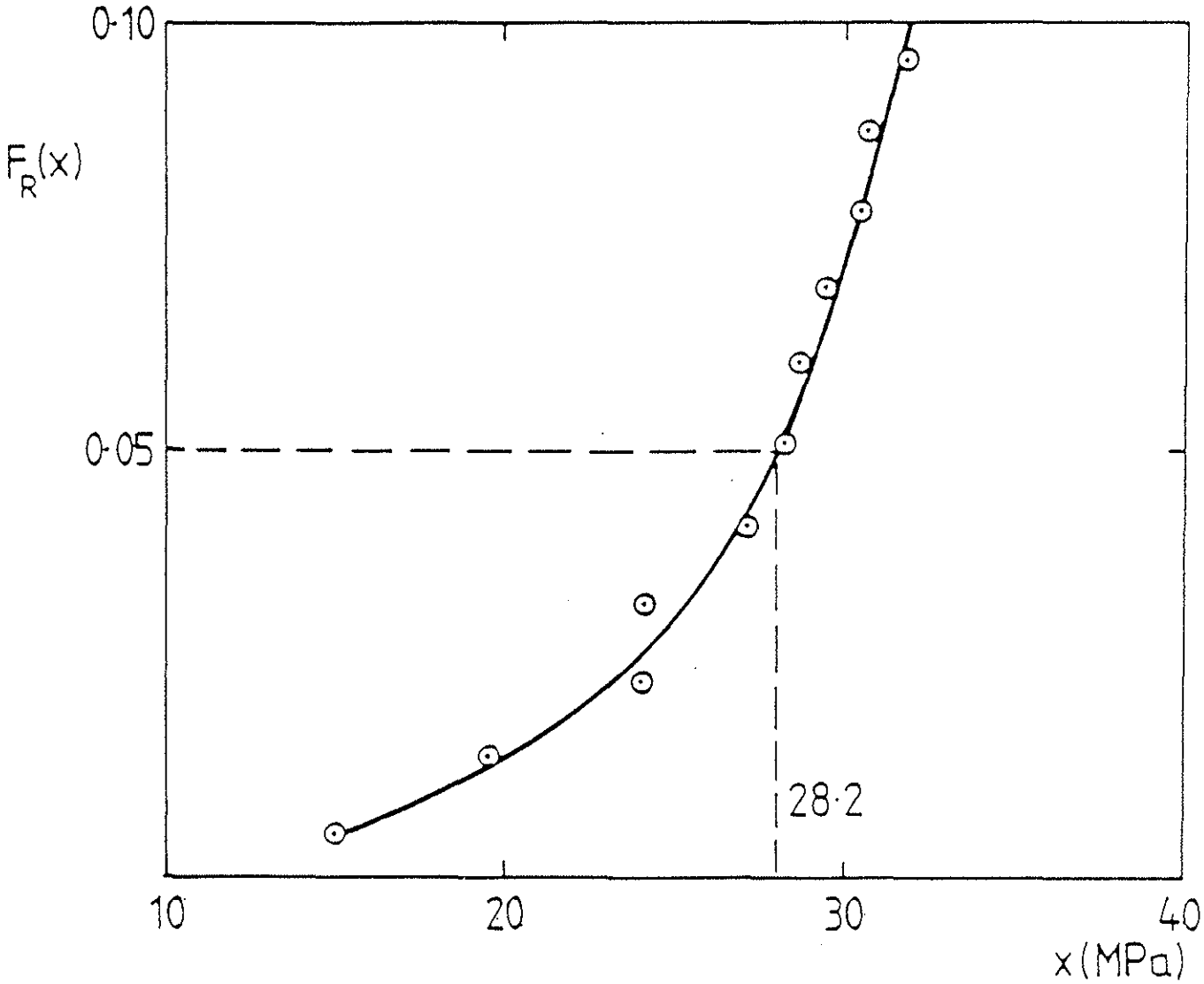

Figure C.1 Cumulative distribution function of measured bending strength

CIB-W18A/21-6-2

INTERNATIONAL COUNCIL FOR BUILDING RESEARCH STUDIES AND DOCUMENTATION

WORKING COMMISSION W18A - TIMBER STRUCTURES

THE DETERMINATION OF CHARACTERISTIC STRENGTH VALUES FOR STRESS GRADES OF STRUCTURAL TIMBER. PART 1

by

A R Fewell
Princes Risborough Laboratory
United Kingdom

P Glos
University of München
Federal Republic of Germany

MEETING TWENTY-ONE
PARKSVILLE, VANCOUVER ISLAND
CANADA
SEPTEMBER 1988

THE DETERMINATION OF CHARACTERISTIC STRENGTH VALUES FOR STRESS GRADES OF STRUCTURAL TIMBER. PART 1

By A R Fewell and P Glos

1 INTRODUCTION

1.1 Background

With the introduction of the timber design code EC5(1), which will have authority throughout the European Economic Community and is aimed at reducing barriers to trade, it is important that international agreement can be reached on a standardised method for determining characteristic strength values for stress graded timber. Indeed the authors would argue that it is more important than producing an international standard on methods of stress grading; something which CEN is already seeking to ensure. The reason for the authors view is that EC5 uses a strength class system which could incorporate any number of national grades. Different countries have developed their own grading systems which suit their species, market conditions and structural demands and it is unlikely that one grading system would find favour with all of them. The aim should therefore be to assign the various grading systems to the strength classes, and for this a standardised method for deriving characteristic values and a standard for quality control of graded timber are essential.

A characteristic strength value is defined in the Eurocode as a population fifth percentile value. These values are dependent on sampling, test methods and analytical procedures.

This paper is in two parts. Part 1 discusses the necessary procedural steps and points out some of the effects resulting from the various decisions that can be reached. Part 2 proposes a set of rules that could form the basis of a standard.

The authors have endeavoured to ensure that as much existing test data as possible will be acceptable and that minor species are not neglected by the need for large and expensive test programmes. It is also important that timber is not made less

competitive as a structural material by adopting conservative approaches at each step in the procedure that would accumulate to an unacceptable degree.

Whilst various grade/species combinations with different strength properties can be incorporated in a strength class system without complicating the code, other values given by the code such as factors for moisture content adjustments, size effects and duration of load need to remain constant for grades and species to enable interchangeability within a strength class.

1.2 Special considerations with respect to machine graded timber.

It is well known that machine graded timber has higher yields and lower variability between the fifth percentile values for different samples, than visually graded timber. This last effect gives rise to the lower bending stress characteristic values and partial factor for machine grades in EC5 and is illustrated in Figure 1 which is taken from Fewell(2). The figure shows the distributions of sample fifth percentiles for 20 sub-samples of 100, 200 and 300 pieces randomly selected from a parent sample of 652 pieces of European redwood/whitewood. The distributions are shown for both visual grading and machine grading with the modulus of elasticity limit selected to give approximately the same yield as the visual grade.

In addition there is a fundamental difference between the two grading systems that affects the approach for deriving characteristic values. For a visual grade you can sample the graded timber, follow procedures for testing and analysis and determine a characteristic stress. For machine grades (in a 'machine controlled' system such as used in Europe) you start with a characteristic stress, (and it makes sense to use the strength class values) and determine the appropriate machine settings. This is necessary because the settings need to vary for grade, species and size and so a mathematical model relating all these variables to strength

needs to be determined. The test samples therefore need to be larger and ungraded. Where the North American 'output controlled' machine grading system is used, the test samples can be smaller and the model simpler because the settings are refined during production. That system is more appropriate for sawmills operating long production runs for a very limited number of grades and sizes. You can of course test samples of machine graded timber to verify the settings in a 'machine controlled' system. Whilst this paper gives guidance on the requirements of a machine grading system it is intended that the topics of the approval, control and setting of grading machines should be the subject of another paper, owing to the size of the subject.

2 EVALUATING CHARACTERISTIC STRENGTH VALUES FROM FULL SIZE TEST DATA

2.1 Sampling

2.1.1 Population

The first step must be to identify the population for which the strength properties are to be applicable. Practical considerations will determine whether a particular population should include one species or a combination of species, the extent of the source of the timber and the manufacturing process. For example a population could be for Swedish whitewood or for redwood/whitewood from the whole of Europe or some intermediate size region such as the Nordic countries. One important practical consideration that determines the extent of the population is whether the timber can be identified at all stages of production, supply and on the construction site. The manufacturing process may also affect the population. For example some sawmills only use certain size logs which produce timber with different strength properties. However these differences are probably too difficult to cope with on a Europe-wide scale, although could be taken into account where the source can be identified.

It may be that all three of the above example populations would be tested and assigned to the strength class system.

Whether these populations are combined or treated separately will depend on the difference in their characteristic values, i.e. whether the higher values merit inclusion in higher strength classes.

> Note: The strength class boundary values will therefore become a major point of discussion, because they will affect the commercial advantages of the various populations and may therefore be influenced by other arguments than simply just to give maximum advantage to the major grade/species/source combinations, as can be done for a national strength class system. Machine grading overcomes this because the machine settings can be determined to suit the strength class boundaries.

Ideally a population will be for one stress grade but there are instances where the population may include a number of grades. For example some timber is imported into the UK ungraded and is then graded by the timber supplier. It has been found that by testing ungraded samples, the sampling is made easier and cheaper and subsequent grading in the laboratory enables additional information on grade yields to be obtained which is useful when comparing the merits of proposals for changes to the grading rules. The same ungraded samples can be used for determining settings for machine grading. The disadvantage with this approach is that until the test sample is graded you do not know if sufficient pieces are present in each grade to enable analysis to proceed.

It must be remembered that the test samples will reflect the strength of the timber available at the time of sampling and that changes in forestry practices etc may bring significant changes. There is therefore a need for the strength properties to be reviewed at intervals which will reflect any known changes to the forestry or production practices.

2.1.2 Sampling method

Having defined the population in terms of species, source, grade etc the next step is to obtain samples for testing.

It is possible to take one sample or combine a number of samples to determine the characteristic values, but the preferred approach is to test a number of samples of different cross section sizes, calculate the lower fifth percentile for each sample, adjust to a common size (eg 200 mm depth for bending strength) and then take the weighted mean of the fifth percentiles as the characteristic value. Because the number and size of samples is always likely to be limited, taking the mean value reduces the effect on the characteristic values, of a sample with extremely low or high values, thus making values for different populations more comparable. The analysis needs to take the number of samples into account and give some benefit to populations for which there are more data.

The samples should be selected on the basis of the stratified cluster technique described by Glos(3). This means that any known or suspected differences in the population due to regions, sawmills, loading areas, tree size, method of conversion etc are used to divide the population into groups, or strata. Specimens are then taken from each of the strata in the same proportion as represented by that stratum in the population.

2.1.3 Sample size

The effect of sample size is illustrated in Figures 1 and 2. From these can be gauged the significance of increasing the sample size which should be reflected in the procedures for deriving characteristic values. This can be done by multiplying the mean of the fifth percentiles by a factor k_s which is based on both the number of samples and their size. A value for k_s can be obtained from Figure 3, which has been deduced from a logical and experienced interpretation of Figure 2. The uncertainties of lower fifth percentile estimates for small samples dictate that samples with less than 40 specimens should not be used.

2.2 TESTING

Testing should be carried out in accordance with ISO 8375(5). A critical section must be selected in each piece of timber. This section is the position at which failure is expected, based on a visual examination and any other information such as measurements from a grading machine. The critical section must be in a position that can be tested, eg not outside the inner load points in a bending strength test or in close proximity to the jaws in a tension test.

For a bending test the tension edge should be selected at random.

Existing data from different test methods or moisture conditions is acceptable provided sufficient information exists to adjust the results to the requirements mentioned above. These differences might be in moisture content, test spans, orientation of test piece etc. Recommendations for adjustments are given in 2.3.2.

ISO 8375 does not give test methods for shear, tension perpendicular to grain and compression perpendicular to grain strengths. For these a procedure is required, but as an interim measure they can be assessed from other properties (see section 4). For the determination of settings for most of the grading machines currently in production in Europe, a modulus of elasticity measured as a plank over a 900 mm span with a centre point load is used.

2.3 ANALYSIS

2.3.1 Statistical model

Numerous investigations have been carried out comparing the various statistical methods of calculating lower fifth percentiles. Many of these are summarized by Glos(4) from which Figure 4 is taken. This illustrates the effectiveness of various distributions and a non-parametric method for calculating lower fifth percentiles for populations of different

distributions. It can be seen that the upper and lower bounds of the fifth percentile estimates using a 3 parameter Weibull are generally closer to the parent population value than for the other methods, particularly the upper bound which of course reflects the degree of safety in using any particular method.

Based on these investigations and taking account of the need for different levels of sophistication, the following three alternative procedures a, b and c are proposed. In accordance with the procedure adopted by the Eurocodes for other materials, no lower confidence bound is included because this uncertainty is considered to be part of the partial coefficient γ_M.

a) The lower fifth percentile of each sample($f_{0.05}$) is calculated using the 3 parameter Weibull distribution and the maximum likelihood method.

   Note: Computer programs are available, e.g. from Princes Risborough Laboratory

b) The lower fifth percentile of each sample($f_{0.05}$) is calculated using the following non-parametric approach. The lower fifth percentile ranked test value is multiplied by a factor k_c to allow for the higher variation of this method evident in Figure 4.

$$k_c = 0.95 + (N-50)/7000 \quad \text{for sample size} < 400$$

$$k_c = 1 \quad \text{for sample size} \geq 400$$

c) The lower fifth percentile of each sample ($f_{0.05}$) is calculated using the Gaussian distribution modified to reduce the level of conservatism inherent in this model.

$$f_{0.05} = \bar{x} - 1.6\ s$$

where $\bar{x}$ and s are the mean and standard deviation of the test values respectively.

2.3.2 Adjustment factors

Before the lower fifth percentile values for different samples of the same population can be combined to determine the characteristic value, they must be adjusted to the standard conditions of moisture content, size and test method. In line with Eurocode 5 these standard conditions are 20°C, 65 r.h. which results in a moisture content of around 12%, a depth for bending members and width for tension members of 200 mm and test methods according to ISO 8375.

Where there are no experimental data available to adjust the $f_{0.05}$ values for a particular population, then the following factors should be used.

Due to uncertainties in the moisture effect on the strength properties, caused by the method of drying, the authors are not in favour of adjusting fifth percentiles from high moisture content samples to the standard conditions of 12%. However, where samples are tested at a moisture content equal to or below 18% then adjustment to 12% should be made. The following factors are based on information from Hoffmeyer(9).

Bending and tension stress, 1% change in lower fifth percentile for every 1 percentage point change in moisture content.

Compression stress, 4% change in lower fifth percentile for every 1 percentage point change in moisture content.

Modulus of elasticity, 2% change for every 1 percentage point change in moisture content.

No adjustment should be made for shear stress. This statement does not come from Hoffmeyer but from the knowledge that the shear adjustment for small clear specimens is less

than for bending stress and that shear strength is greatly influenced by fissures which will increase in dryer timber.

In all cases the above factors are applied so that the stresses and modulus of elasticity increase for lower moisture contents.

Results from the test data bank at PRL are shown in Figures 5 and 6 to indicate the size effects for bending and tension strength respectively. The datum size is 300 mm instead of 200 mm to relate to UK design stresses. The data include various species graded to the UK BS 4978 grades (same as ECE grades) and the Canadian NLGA grades. From Figures 5 and 6 it is recommended that to adjust to the standard size of 200 mm, the lower fifth percentile values should be multiplied by k_h, where

$$\left.\begin{aligned} k_h &= (200/h)^{0.3} \text{ for bending} \\ \text{and} \quad k_h &= (200/h)^{0.2} \text{ for tension} \end{aligned}\right\} \text{ where } 60 < h < 400$$

where h is the depth of a bending member or width of a tension member.

Where the bending test set-up is not as in the ISO standard (ie span = 18 h and distance between inner load points = 6h) then the bending stress f_m is obtained following Madsen(10) by dividing the lower fifth percentile stress f_{m5} by k_t,

$$\text{ie } f_m = f_{m5}/k_t$$

where $k_t = (L_{es}/L_{et})^{0.286}$ and L_{es} and L_{et} are respectively the effective lengths for the standard and test sample set ups calculated as follows:

$$L_{es} \text{ or } L_{et} = [(1 + 3.5a/L)/(1 + 3.5)]L$$

where 'L' is the span and 'a' is the distance between the inner loading points.

2.3.3 Determination of characteristic values

The characteristic value is calculated as the mean of the adjusted sample lower fifth percentiles, weighted according to the number of pieces in each sample, and multiplied by the factor k_s given earlier to adjust for the number of samples and their size.

> Note: The analytical procedures for calculating settings for grading machines is complicated and should be the subject of another paper. The method used in the UK is given in the revised edition of BS 4978(11) to be published in 1988 and a note by Fewell(12) which gives explanations. To bring the UK approach into line with the proposals here and in the EC5, certain changes would need to be made, eg for size factors.

3 DETERMINING CHARACTERISTIC VALUES FOR BENDING STRENGTH AND MODULUS OF ELASTICITY FROM SMALL CLEAR TEST DATA

Some countries may use too many different combinations of grade and species to enable all of them to be comprehensively tested in structural sizes. For example the number of grade and species combinations in the UK code is around 150, and for each of these there are 6 different strength properties. Although an international standard would enable data to become more readily available for more of these, a solution has to be found for the interim period. The following approach which is used in the UK and described more fully by Fewell(6) is recommended here.

Where no structural size test data exist for a given species then mean values of bending strength and modulus of elasti-

city from small clear specimen tests are multiplied by 0.34 and 1.14 to obtain respectively the characteristic bending strength and the mean modulus of elasticity values for the SS grade. The SS grade is a BS 4978(7) grade which is almost identical to the EEC S8 grade (8) referred to in Eurocode 5. The mean small clear bending strength is used rather than a lower percentile, to minimise sampling variability. These factors were established from grade/species combinations where both small clear and structural size test data are available, and similar factors can be established for other grading systems. It is of course important to note that these factors relate to particular test standards. Similar factors can be determined for other grades.

Using these characteristic bending stresses the characteristic values for the other properties can be determined from section 4.

4 DETERMINING CHARACTERISTIC VALUES OF OTHER PROPERTIES FROM CHARACTERISTIC VALUES OF BENDING STRENGTH AND DENSITY

The following factors are applicable to softwoods only and are for use where no experimental data are available.

The characteristic tension parallel to grain stress at 200 mm width can be taken as 0.6 times the characteristic bending stress.

The characteristic compression parallel to grain stress can be taken as 0.9 times the characteristic bending stress.

The characteristic shear stress can be taken as 0.1 times the characteristic bending stress.

The characteristic tension perpendicular to grain stress in N/mm^2 can be given the same numerical value as the characteristic density in g/cm^3.

The characteristic compression perpendicular to grain stress in N/mm^2 can be taken as 15 times the characteristic density in g/cm^3.

5 QUALITY CONTROL

It is imperative that all stress grading, particularly machine grading, is covered by some form of independent quality control. Stress grading standards should cover this aspect, for example see reference 11. However from time to time it may be necessary to check a sample of graded timber against its assigned characteristic stress or check a stated characteristic value for a given grade. The same procedures outlined above can be used except that because a characteristic value is a point estimate, any sample fifth percentile has a 50% chance of being below the characteristic value.

It is suggested by the authors that for a single sample lower fifth percentile to be in agreement with the characteristic value, it should not be below the characteristic value multiplied by a factor k_q given in Figure 7. This figure has been deduced from Figures 1 and 2 and is of course suitable for checking both visual and machine graded samples or characteristic values.

6 CONCLUSIONS

With a strength class system, as in Eurocode 5, in which many grading systems can be incorporated, it is more important to have a standard method of deriving characteristic values than to have an international standard for stress grading.

This paper discusses the criteria and conditions that affect the determination of characteristic values. Proposals are made for procedures which are intended to serve as the basis for an international standard.

REFERENCES

1 Eurocode No 5: Common unified rules for timber structures. Draft report EUR 9887 EN. 1988.

2 FEWELL, A. R. Notes on the determination of characteristic stress values for timber. IUFRO S5.02 Meeting Boras 1982.

3 GLOS, P. Sampling timber in structural sizes. CIB.W18 Meeting Beit Oren 1985.

4 GLOS, P. Notes on sampling and strength prediction of stress graded structural timber. CIB.W18 Meeting Lillehammer 1983.

5 ISO 8375 - 1985 (E). Solid timber in structural sizes - Determination of some physical and mechanical properties. ISO. 1985.

6 FEWELL, A. R. The determination of softwood strength properties for grades, strength classes and laminated timber for BS 5268:Part 2. BRE Report 1984.

7 BS 4978:1973. Timber grades for structural use. BSI 1973.

8 U.N. ECE Recommended standard for stress grading of coniferous sawn timber. 1982.

9 HOFFMEYER, P. The moisture-mechanical property relationship as dependent on wood quality. IUFRO, Oxford 1980.

10 MADSEN, B. Size effects in timber explained by a modified weakest link theory. CIB.W18 Beit Oren. 1985.

11 BS 4978:1988. Specification for softwood grades for structural use. BSI (Unpublished at time of writing this paper).

12 FEWELL, A. R. Derivation of settings for stress grading machines. BRE report 1986.

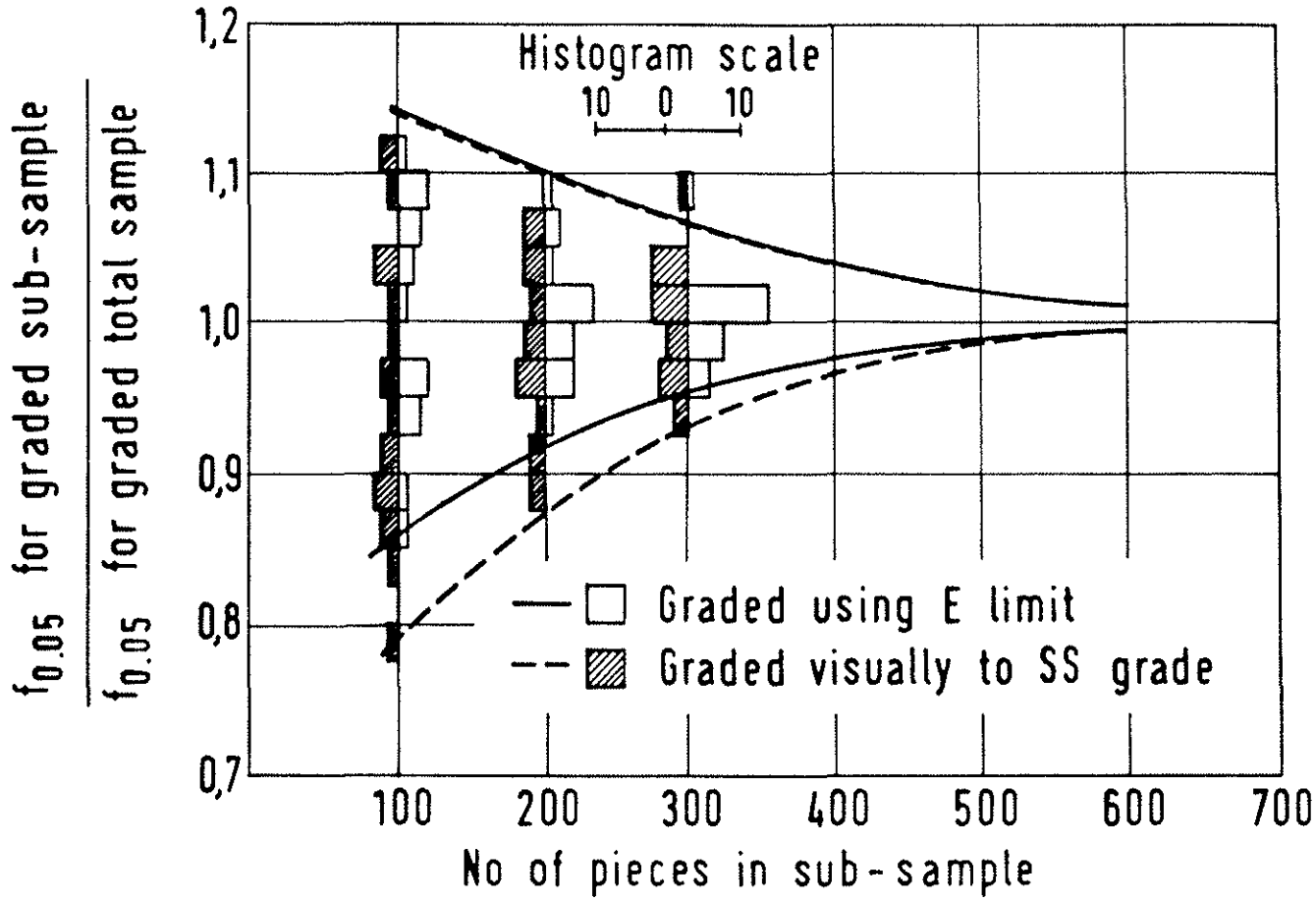

Fig. 1: Ratios of lower 5% bending strength values of randomly selected sub-samples from a parent sample of 652 pieces

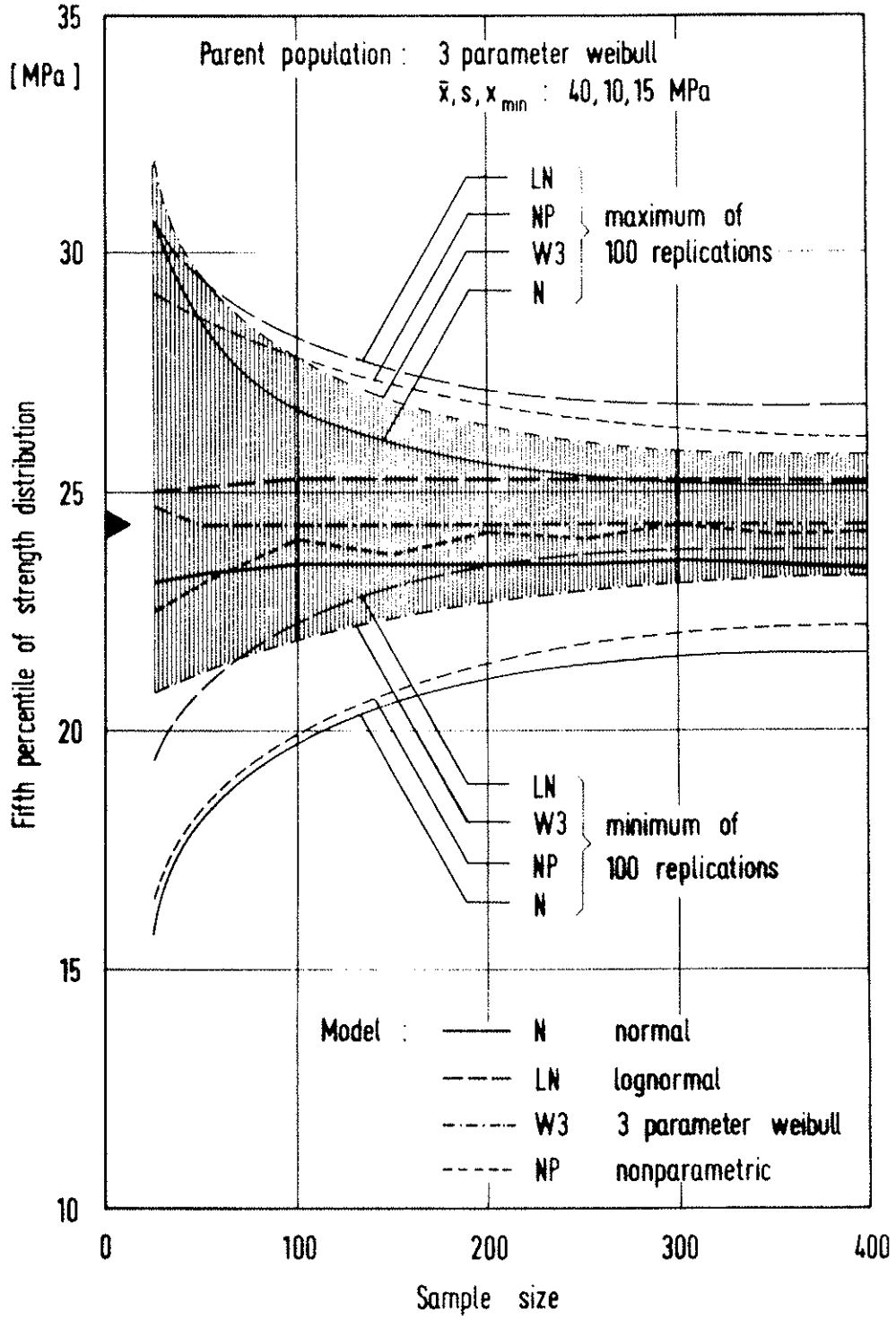

Fig. 2: Point estimate of 5% exclusion limit as dependent on sample size and statistical model used. Simulation results. Minimum, maximum value and mean of 100 replications. Population: 3 parameter Weibull

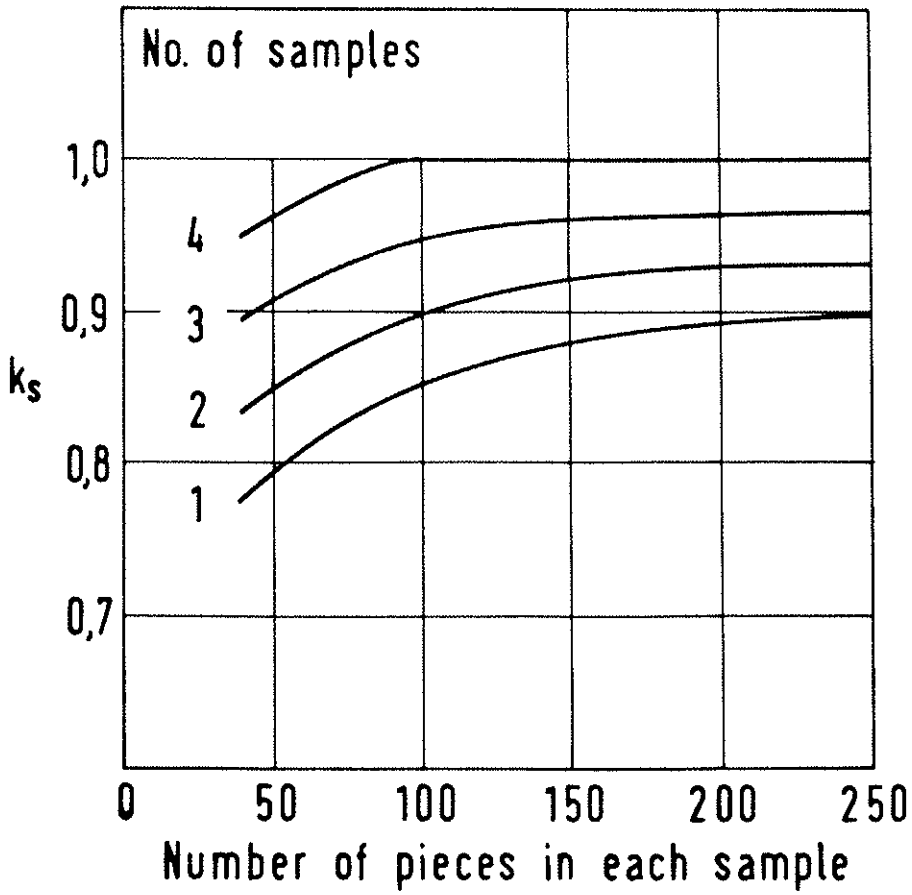

Fig. 3: The effects of the number of samples and their size on the factor k_s

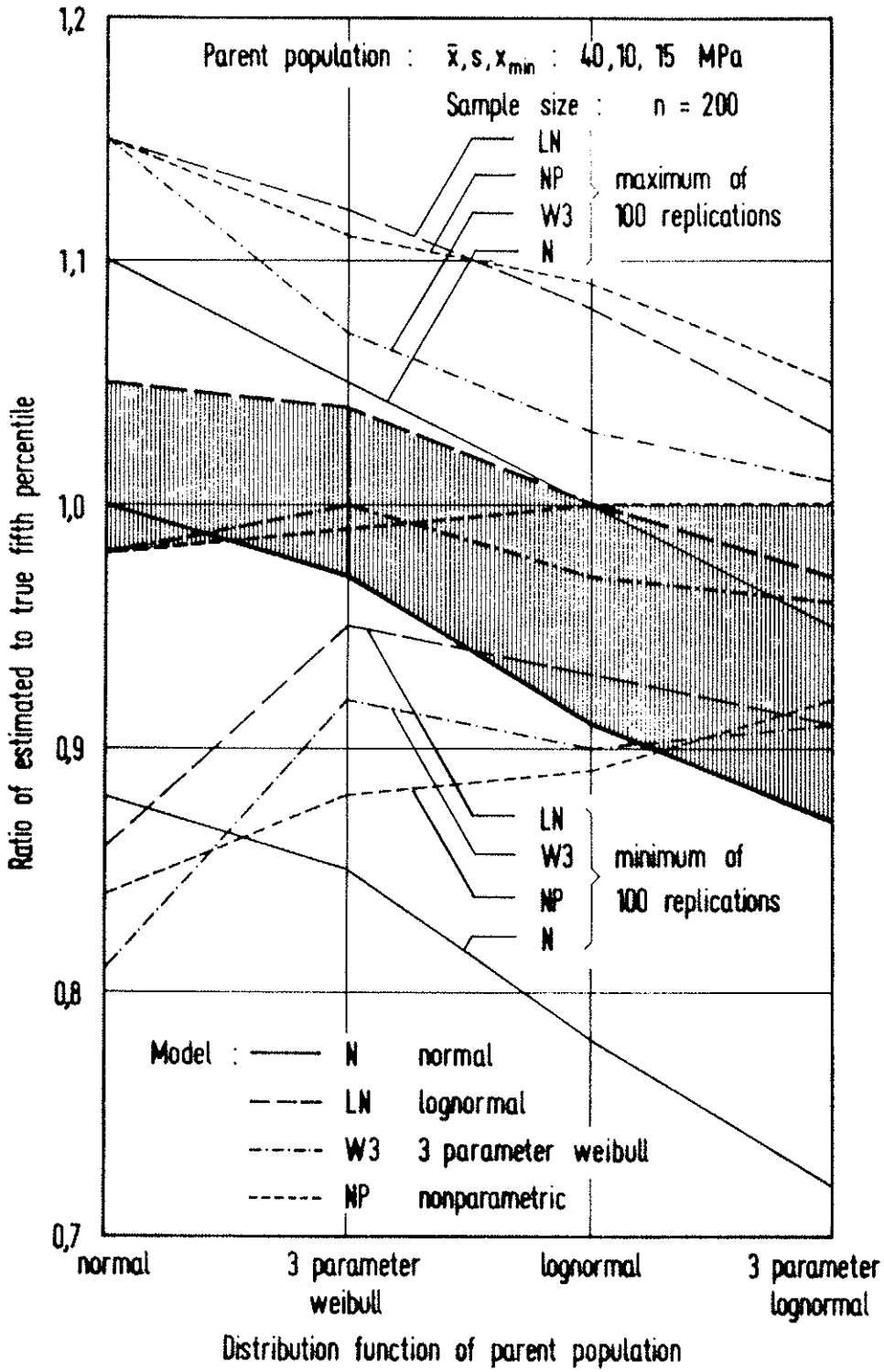

Fig. 4: Ratio between estimated and true 5% exclusion limit (point estimate) as dependent on statistical model used. Simulation results, sample size n = 200. Minimum, maximum value and mean of 100 replications

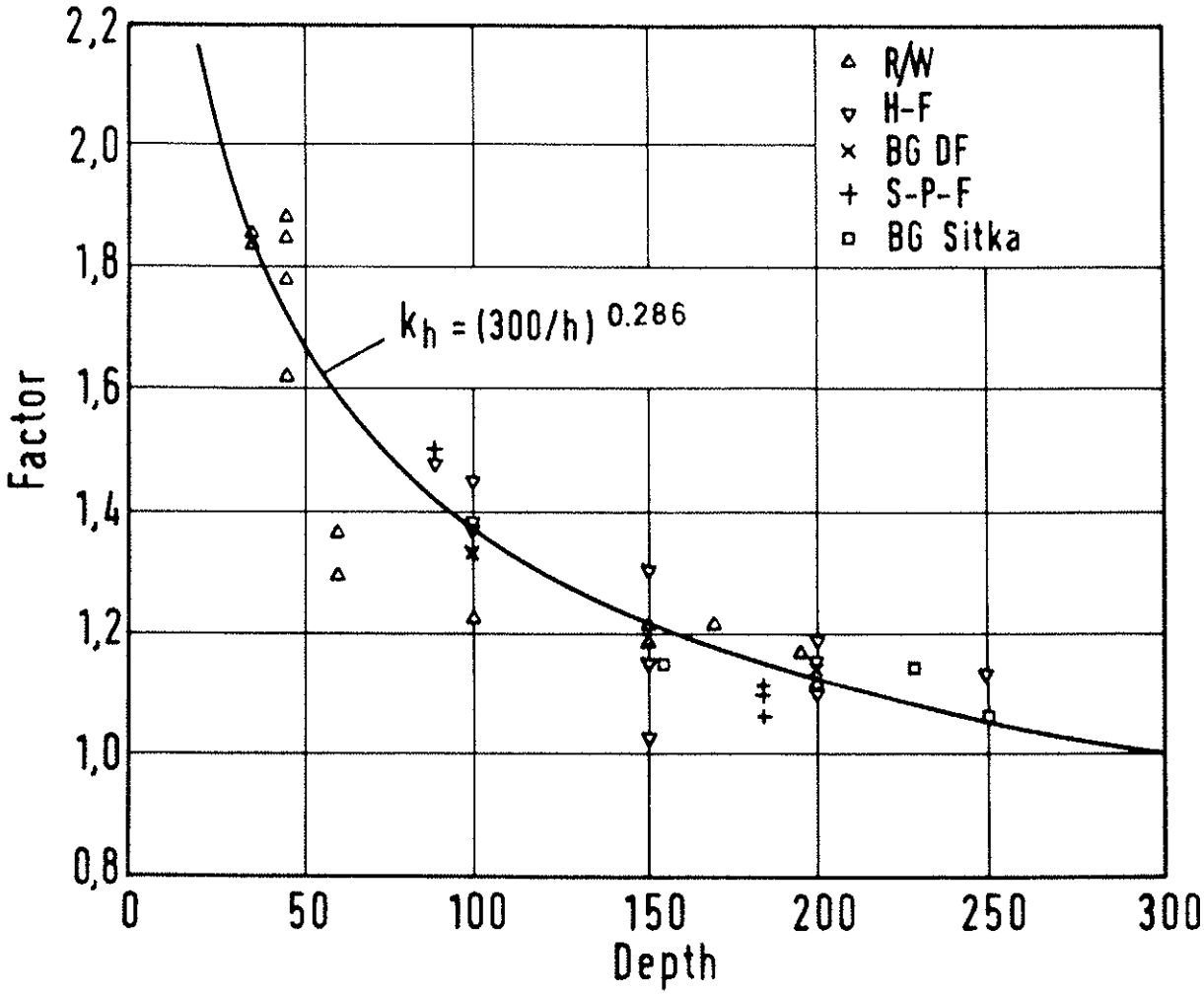

Fig. 5: Size factor for bending stress according to data from Princes Risborough Laboratory

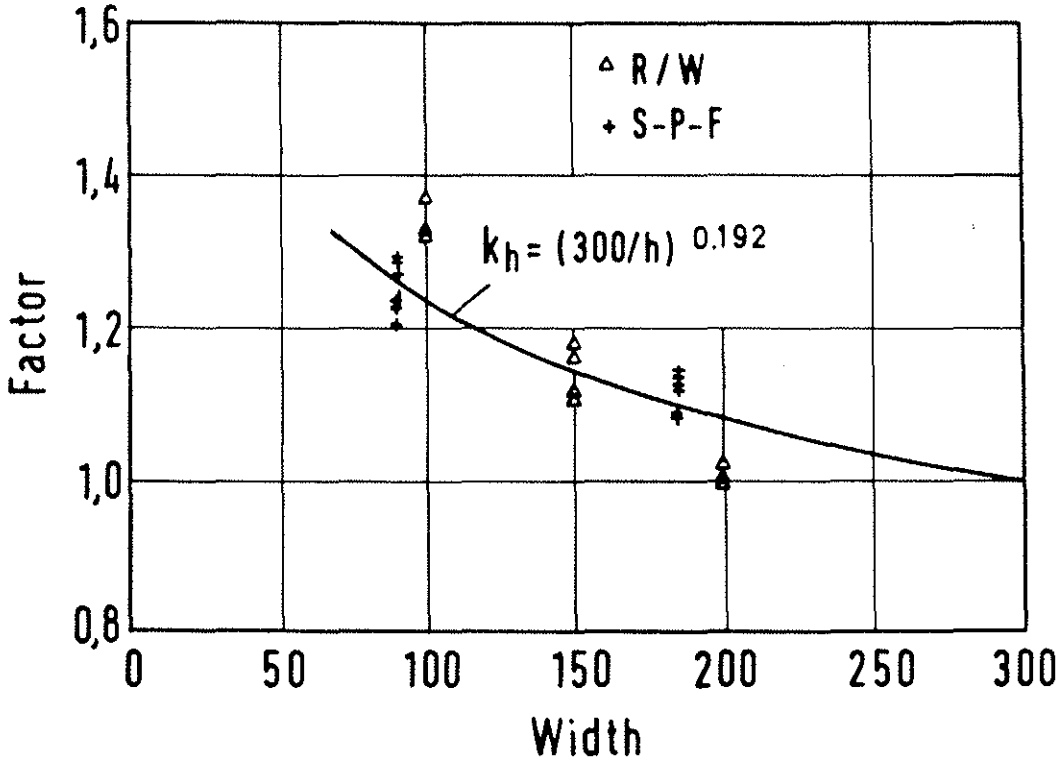

Fig. 6: Size factor for tension stress according to data from Princes Risborough Laboratory

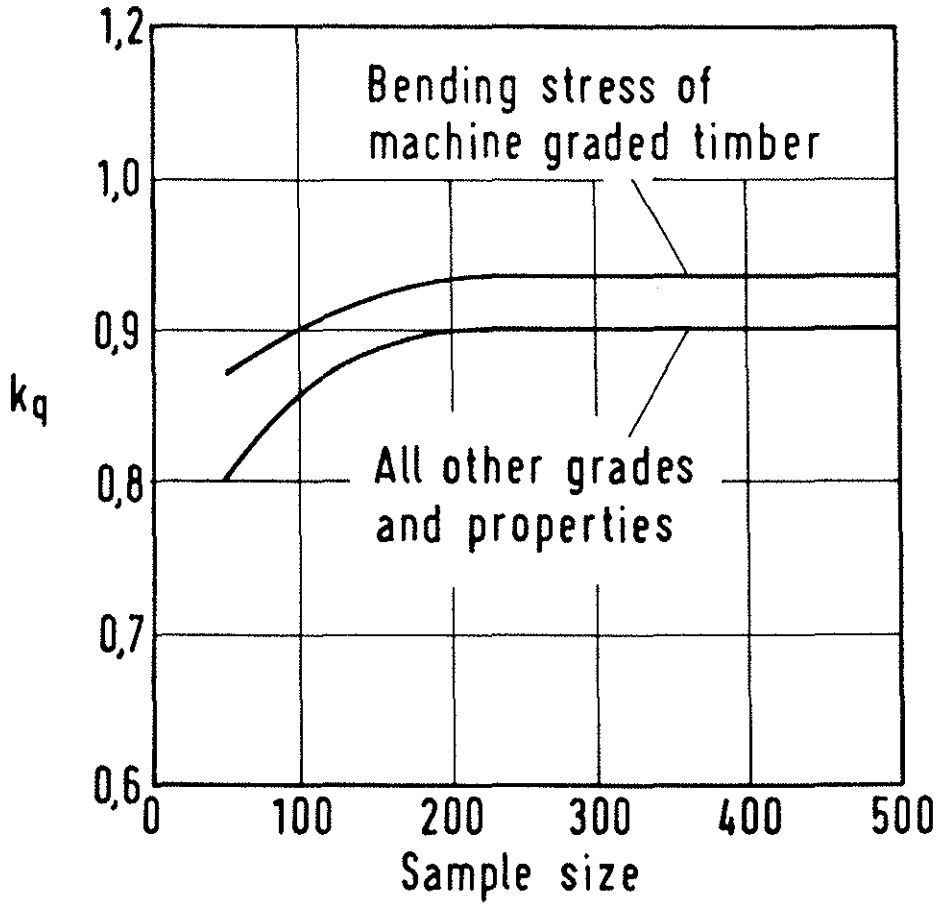

Fig. 7: Values of factor k_q for quality control

CIB-W18A/21-6-3

INTERNATIONAL COUNCIL FOR BUILDING RESEARCH STUDIES AND DOCUMENTATION

WORKING COMMISSION W18A - TIMBER STRUCTURES

SHEAR STRENGTH IN BENDING OF TIMBER

by

U Korin
Technion, Israel Institute of Technology
Israel

MEETING TWENTY-ONE
PARKSVILLE, VANCOUVER ISLAND
CANADA
SEPTEMBER 1988

SHEAR STRENGTH IN BENDING OF TIMBER

Dr. U. Korin

SUMMARY

The paper discusses the behavior in shear of timber beams. It reports the process of development of a test method for determining the shear strength in bending. Some test results of shear strength in bending (BSS) are submitted and are compared with the MOR and direct shear strength (DSS) of timber.

A "Tentative Recommendation for a Testing Method of Shear Strength in Bending of Timber" is submitted in the appendix to the paper.

SYMBOL LIST

A - cross section
b - beam width
d - support, loading length (along x direction)
F - ultimate strength
h - beam hight
I - second moment of inertia
m - bending
M - bending moment
N - axial load
NP - neutral plane
P - concentrated transvers load
q - distributed load; $Q - \int q_{dx}$
Q_x - first static moment of the sheared section around the neutral plane
R - reaction
t - groove thickness
V - shear force
x - beam in plane axial direction
y - beam in plane transvers (vertical) direction
σ - stress

1. PREFACE

Shear failure of timber beams is very rare. Nevertheless, as shear stresses in beams are a very important design feature, knowing the shear strength is very important for assessment of the safety of structures. So far, there is no established method to study this mechanical property of timber.

The purpose of this investigation was to develope a testing method which will promote the shear failure of a beam before other modes of failure take place and thus enable to determine the shear strength of stuctural timber.

2. ACTION AND REACTIONS IN A LOADED BEAM

On a beam subjected to external plane loads and maintaining a static equilibrium with the external loads, we can find according to the classic mechanics theory the following load components(1):

a) External loads and bending moments (q, P_x, M, R_x), and their resulting internal bending moments and shear forces:
b) bending moments M_x.
c) Shear force V_x.

The relations between external loads, bending moments and shear forces (fig. 1) are presented in the following equations system. The static equilibrium conditions for a beam element, dx long, yield:

$$\Sigma Y = +V - qdx - (V+d\,V) = 0 \tag{1}$$

$$dV = qdx \tag{2}$$

$$M + V.\tfrac{1}{2}dx - (M+dM) - (V+a,V).\ \tfrac{1}{2}dx = 0 \tag{3}$$

$$dM = Vdx - \tfrac{1}{2}q(dx)^2 \simeq Vdx \tag{4}$$

hence:

$$V = dM/dx \tag{5}$$

$$q = -dV/dx = d^2M/dx^2 \tag{6}$$

and after integration

$$\Delta V = V_2 - V_1 = \int_{x_1}^{x_2} q\,dx \tag{7}$$

$$\Delta M = M_2 - M_1 = \int_{x_1}^{x_2} V\,dx \tag{8}$$

These equations are valid also for the case of concentrated forces, which are actually distributed loads acting along a very short length dx of the beam (fig. 2).

From equations 5,6,7 and 8 we may conclude:

- The distributed load q is equal to the slope of the shear forces curve V;
- When q = constant (evenly distributed load), the curve V will be a sloping streight line;
- When q=0 (along an unloaded section of the beam) the curve V will be a straight horizontal line;
- A concentrated external force will result in a sudden change in the slope of V curve (actually this will be a very steap gradual change of the slope);
- The shear force V is equal to the slope of M curve.

Thus, M reaches extreme values in section of the beam with V=0.

- In the points of change in the slope of V curve (kinks in the shear curve), a common tangent characterises the various sections of M curve (fig. 3), and in point of a sudden change of the value of V (a jump in the shear curve) there is a kink in M curce.

3. STRESSES IN A LOADED BEAN

It is common to assume that on a horizontal beam loaded by external loads in one plane, the main stresses acting simultaneously are:

a. Stresses in the vertical direction σ_2 in the points of action of loads and reaction of the supports.
b. Longitudinal stresses, σ_1 required to form an internal bending moment to balance the external moments acting on the beam.

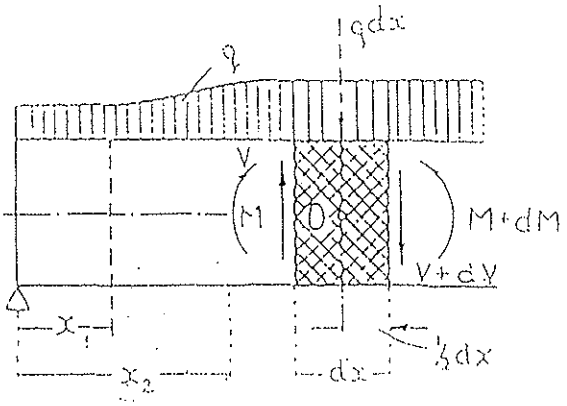

Fig 1 - Equiberlium of a free body

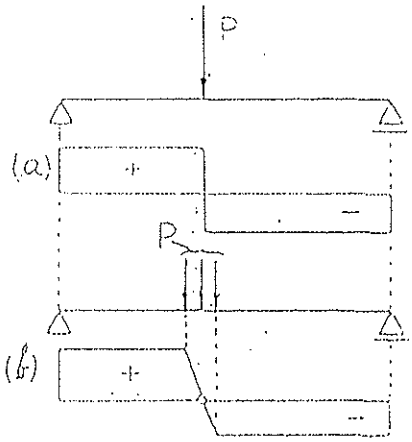

Fig 2 - The distributed load equivalent of a concentrated force

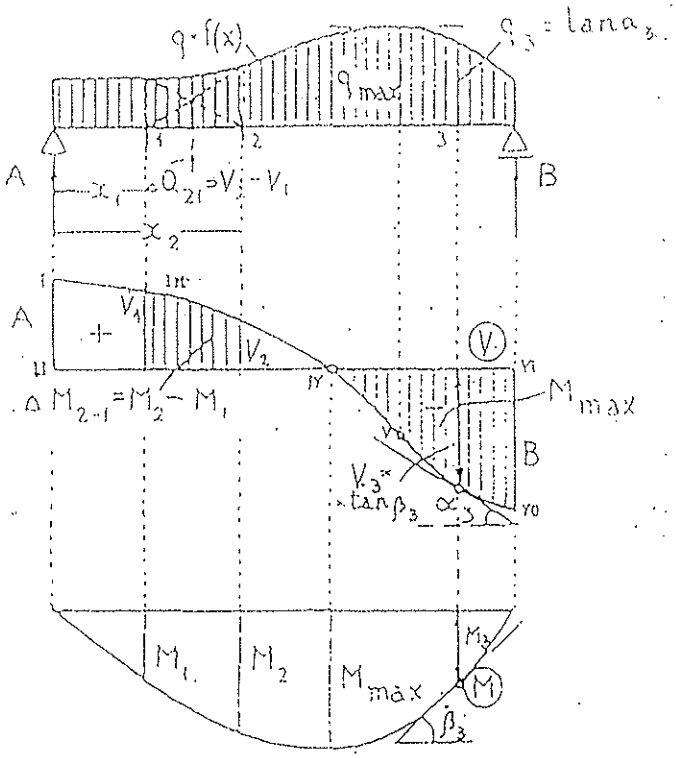

Fig 3 - Load, shear force and bending moments

c. Shear stresses σ_{21} and σ_{12} required to balance the shear forces acting on the beam.

The megnitude and the distribution of the stresses σ_2 are affected by the particular details of the contact points between the external loads and the beam. In the case of a timber beam having a large strain compliance to perpendicular stresses and a loading plate of a sufficient thickness made of metal or hard wood, the perpendicular stresses σ_2 are:

$$\sigma_2 = (-q-P/d)/b \qquad (9)$$

were q - distributed external load, P - concentrated load.

d - the length of contact between the concentrated load and the beam.

The longitudinal stresses σ_1 are calculated according to the equations of reaction to axial stresses and bending. The stress at any point at a distance y from the neutral axis of a beam with a cross section A and second order moment of inertia I_X, loaded by an axial load P_X and a bending moment M_X is:

$$\sigma_1 = \pm M_X.y/I_X - P_X/A \qquad (10)$$

The shear stresses $\sigma_{21} = \sigma_{12}$ in any section of a beam (fig. 4)[2] are calculated according to the equation:

$$\sigma_{21} = V\ Q_X/I\ b \qquad (11)$$

where V - the shear force acting on the beam.

Q_X - the static moment of the sheared area A' around the neutral axis.

I - the second moment of Inertia of the beam.

b - the width of the loaded section at the examined point.

In a rectangular beam (fig. 5),[2] having an area A equation 11 may be reduced to:

$$\sigma_{21} = 1.5\ V/A \qquad (12)$$

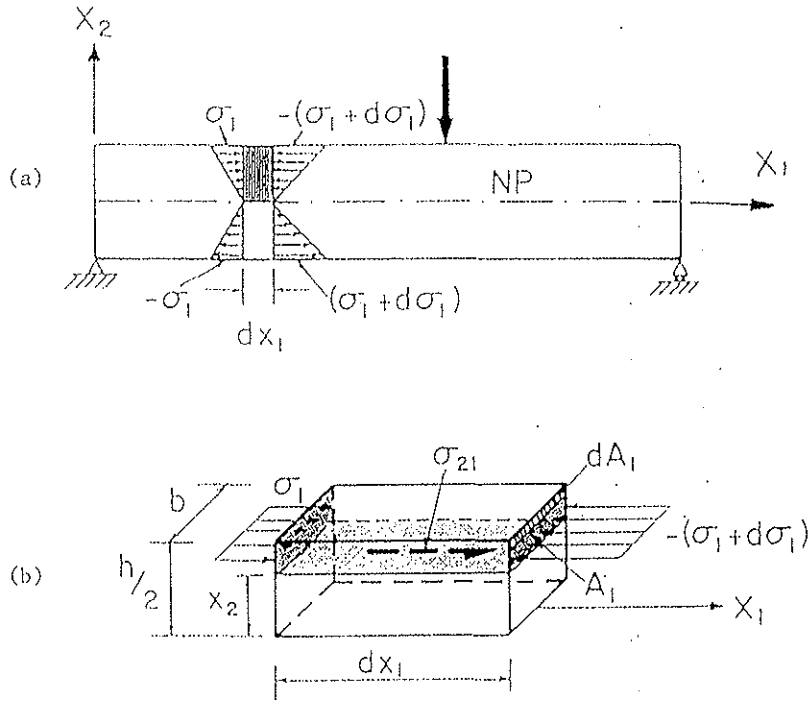

Fig 4 - Shear stress in an engineering beam: (a) differential bending stress, (b) horizontal stress equilibrium

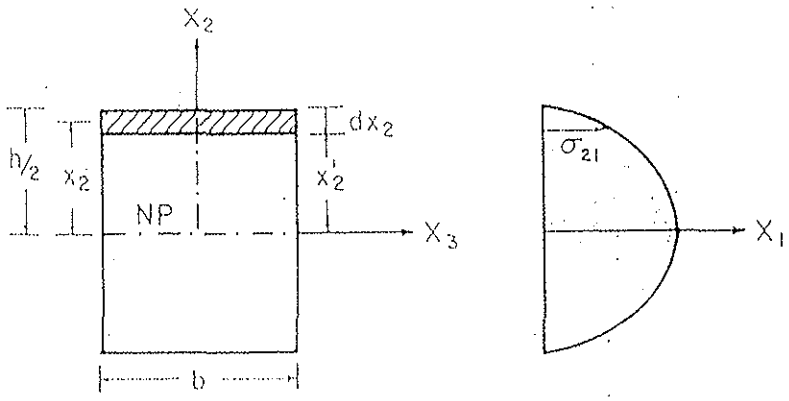

Fig 5 - Computation of the area moment for a rectangular cross section with the resulting shear stress distribution

4. DETERMINATION OF THE SHEAR STRENGTH OF TIMBER

The shear stress required to separate between layers paralles to the growth axis of the wood is related to as the shear strength of the wood.

One way to determine this strength is the direct shear strength (ASTM D 143) (3).

The direct shear strength of the wood is calculated according to:

$$F_v = Palt/A \qquad (13)$$

where Palt is the shear force required to separate the wood layers and A is the cross section of the sheared area (nominal cross section of 50x50 mm) (fig. 6).

We may meet this type of loading, for example, in composite timber beams where the shear forces between the layers are transfered through hard wood blocks inserted in suitable groves. However, this is not the shear action of timber in a bended beam.

During the direct shear experiment, we iqnore the other stresses acting simultaneously on the loaded test piece. We may do so because we know that the other stresses such as the longitudonal contact pressure required to prevent the test piece from overturning are small in comparison with the relevant strengths.

When we try to load a simple rectangular wooden beam in bending even a very short span, a mode of shear failure is hardly obtained. It is more likly that the beam will fail through bending or through crushing at the loading points or at the beam supports.

In planning an experiment intended to determine the shear strength in bending of timber, we have to consider the bending stresses and the normal pressure stresses, and to avoid bending failure and crushing failure. The bending stress in the beam (σ_1) should not approach the

bending strength (F_m) :

$$\frac{\sigma_1}{F_m} < 1 \qquad (14)$$

and the strsses in y direction σ_2 should not approach the perpendicular to grain compressive strength $F_{c,y}$

$$\frac{\sigma_2}{F_{c,y}} < 1 \qquad (15)$$

The beam zones where a shear failure is expected for a simple supported bean loaded by simetrical controlled forces are the lengths of the beam located between the supports and the first acting force where the shear force has its maximum magnitude.

The simplest form of loading which may answere this condition is a short beam loaded by a single concentrated force in its mid-span.

Choosing a rectangular cross section for the testing piece arises some difficulties:

- When the span of the beam is reduced, the beam fails by crushing at the supports and at the loading point.
- When the span is slightly increased - the result is a bending failure.

Some initial experiments on very short rectangular beams during the study yielded such results, and thus, the use of a rectangular cross section as a testing specimen to determine the shear strength in bending of timber was ruled out.

5. TEST SPECIMENS FOR SHEAR IN BENDING STRENGTH

Examining the static characteristics of some engineering cross sections, it was decided to choose an I cross section as testing specimen for the shear in bending strength experiment.

The I section is characterised by three features important for the shear experiment case:

- The bending resistance of the section is high, due to the wide flanges of the I beam.
- The concentrated load resistance is high due to the same reason.
- The shear resistance of the I section is small due to the small width of the web of the I beam.

Thus, there was a good chance that failure in shear will be obtained.

I sections of timber were prepared by grooving timber prisms from two sides along their neutral axis to certain depths.

Shear failure mode was obtained when the depth of the grooves from each side was about 0.3 of the prism width b. The grooves were formed by passing the prism flatwise over a disc sow with carbide tips 2.5 mm thick.

The shear stress distribution in the cross section may be calculated by equation 11 ($\sigma_{21} = VQ_x/Ib$). For a prism (hxb) groved evenly from both sides by a tool having a thickness t and resulting in a web of b' width (fig.7) the moment of inertia, I, of the cross section is:

$$I = [b\text{-}h^3 - (b\text{-}b')t^3]/12 \qquad (16)$$

The static moment of half section around the neutral axis, Q_x is:

$$Q_x = [bh^2 - (b\text{-}b')t^2]/8 \qquad (17)$$

Thus, equation 11 may be writen:

$$\sigma_{12} = 1.5\ V\ \ [bh^2\text{-}(b\text{-}b')t^2]/[bh^3 - (b\text{-}b')t^3]b' \qquad (18)$$

but due to the very small ratio between the width of the groove t and the height of section h it is possible to write:

$$\sigma_{21} = 1.5\ V/hb' \qquad (19)$$

or

$$\sigma_{21} = 0.75\ P_{alt}/hb' \qquad (20)$$

where P_{alt} is the ultimate load for shear failure and σ_{21} the shear in bending strength of the tested prism.

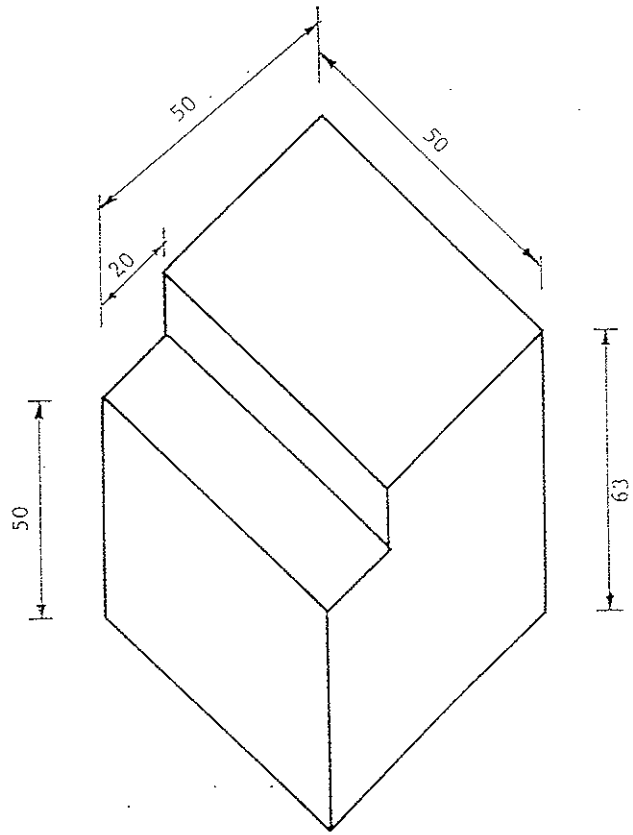

Fig 6 - Shear Parallel to Grain Test Specimen

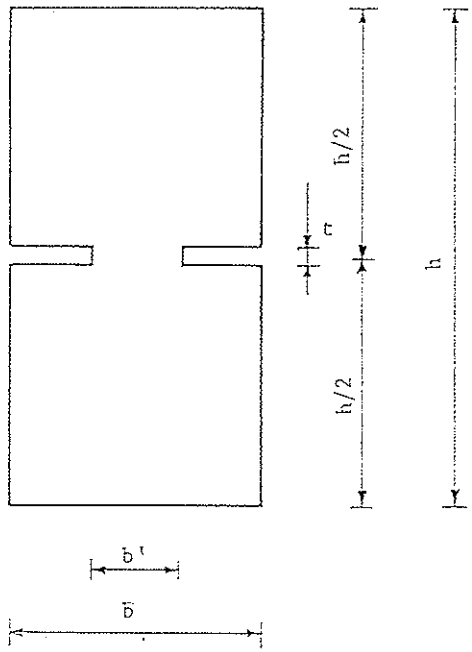

Fig 7 - Cross section of the bending shear strength specimen

6. THE EXPERIMENTAL INVESTIGATION

An experimental study for practical assessment of the proposed testing method was undertaken. Timber from various species and origins used for a parallel study investigating their engineering properties were subjected to direct shear test and to shear in bending tests according to the proposed procedure.

The test specimen prepared had a nominal cross section of 45 mm x 95 mm and a nominal length of 500 mm with grooves cut from both sides to a nominal depth of 13 mm (the actual dimensions of each specimen were taken prior the shear test).

The beams were loaded over a span of 450 mm long. 50 mm long plates were laid between the beam and the roller bearings and 100 mm long plate was inserted between the loading head and the beam.

The beams were gradually loaded until failure which was usually a shear failure along the groves from the center of the beam to one of the ends of the beam, was attained.
The shear bending strength for each one of the tested specimens was calculated according to equation (20).

The samples of timber tested were:

- 25 specimens of imported softwood (5 timber groups x 5 specimens for each group).
- 5 specimens of hard wood (2 specimens of European beech and 3 specimens of locally grown eucalyptus.

The specimens selected for the test were sections of boards containing all the natural defects of the timber such as knots of various sizes and sloppy grain etc. Other sections of the same loads were used for other investigations (modulus of rupture and modul of elasticity in bending, compression strength and modulus of elasticity in compression).

7. TEST RESULTS

Tables 1-6 submit the test results:
(1) Modulus of rapture (MOR); (2) Bending shear strength (BSS); and (3) Direct shear strength (DSS). In addition, the ratio between the bending shear strength and the modulus of rupture ((2)/(1)) and the ratio between the direct shear strength and the modulus of rupture ((3)/(1)) are presented.

Ignoring some deviations in the modulus of rupture of the timber due to severe local defects, the average values of (2)/(1) and (3)/(1) were calculated.For the softwoods, the average ratios between BSS and MOR ((2)/(1)) were in the range of 0.185-0.21 with a total average of 0.193.
The ratios between DSS and MOR ((3)/(1)) were in the range of 0.14-0.17 with a total average of 0.153.
Similar values were obtained for the eucalyptus timber but for the beech, much higher ratio of BSS to MOR was obtained. However, the number of hardwood specimen tested was very small and no conclusion may be taken.

In some of the tests, in addition to the shear failure, there were substential crushing effect of the timber due to transvers stresses at the supports and the loading head.

8. DISCUSSION AND CONCLUSIONS

The purpose of the investigation was to develop a testing method for determining of the bending shear strength of structural timber.

According to the results of the experimental investigation, the proposed method successfully fulfils the function of a test method:

- The test specimens are in dimensions and quality of structural timber;
- The mode of failure mainly obtained is a shear in bending failure;
- There were no indications of sideway buckling of the specimens during the tests;

- The test specimen is easy to produce;
- The test specimen may be selected from any desirable portion of an examined board, thus, edge effects on the shear strength of the timber may be studied.
- The test method may be used to study the shear strength of glue line as well as the shear strength of the boards in glue laminated beams, by locating the groove at any desirable position along the height of a beam and trimming the specimen to symmetry around the cut groove.
- For timber having particularly low bending strength and/or low transvers compression strength, deeper grooves may be produced in order to minimize the bending and transvers compression stresses while maintaining high shear in bending stress.

In line of the work of the Joint committee RILEM/CIB-3TT, "Testing methods for timber in structural sizes"(4), a proposal of a testing method for shear strength in bending is submitted in an appendix to this work.

REFERENCES

(1) S.G. Ettingen - "Engineering Handbook", Vol. 1, "Massadah", Tel-Aviv (in Hebrew), pp. 314-315.

(2) J. Bodig and B.A. Jayne, "Mechanics of Wood and Wood Composites", Van Norstrand Reinhold, 1982, pp. 146-147.

(3) ASTM D143 - Standard methods of testing small clear specimens of timber.

(4) Joint Committee RILEM/CB-3TT, "Testing methods for timber in structural sizes", Materials and Structures, Vol. 11 - No. 66, pp. 445-452.

Table 1 - Test results for group 1 - Pine (Sweden).

Specimen	MOR (1) (Mpa)	BSS (2) (Mpa)	DSS (3) (Mpa)	(2)/(1)	(3)/(1)
1	50.0	10.0	6.5	0.20	0.13
** 2	29.5	9.8	9.0	0.33	0.31
3	43.8	8.5	7.0	0.19	0.16
4	52.5	9.0	8.1	0.17	0.15
5	51.4	9.3	7.5	0.18	0.14
X	49.4	9.2	7.3	0.185	0.145
S	3.9	0.6	0.7	0.014	0.013
V	0.08	0.07	0.09	0.07	0.09

** excluded from the average

Table 2 - Test results for group 2 - Lodge pole Pine (Canada).

Specimen	MOR (1) (Mpa)	BSS (2) (Mpa)	DSS (3) (Mpa)	(2)/(1)	(3)/(1)
1	51.4	10.2	7.8	0.20	0.15
2	41.6	10.5	7.6	0.25	0.18
3	50.7	10.5	7.8	0.21	0.15
** 4	18.2	9.0	6.6	0.49	0.36
5	47.8	8.6	5.2	0.18	0.11
X	47.9	10.0	7.1	0.21	0.15
S	4.5	0.9	1.3	0.029	0.029
V	0.09	0.09	0.18	0.14	0.20

** excluded from the average

Table 3 - Test results for group 3 - SPF (Canada), mill a).

Specimen	MOR (1) (Mpa)	BSS (2) (Mpa)	DSS (3) (Mpa)	(2)/(1)	(3)/(1)
1	56.8	9.3	7.9	0.16	0.14
2	58.1	12.0	8.7	0.21	0.15
3	53.6	9.7	8.2	0.18	0.15
4	34.5	* 6.9	5.7	0.20	0.17
5	32.1	* 6.8	6.3	0.21	0.20
$\bar{X}$	47.0	8.9	7.4	0.19	0.16
s	12.7	2.2	1.3	0.022	0.024
v	0.029	0.412	0.175	0.11	0.15

* simulteanous failure of the timber in transvers compresion.

Table 4 - Test results for group 4 - SPF (Canada,mill b).

Specimen	MOR (1) (Mpa)	BSS (2) (Mpa)	DSS (3) (Mpa)	(2)/(1)	(3)/(1)
1	37.2	* 8.6	7.6	0.23	0.20
2	55.4	* 8.0	5.9	0.14	0.11
3	67.8	12.2	8.5	0.18	0.13
4	48.1	10.1	6.8	0.21	0.14
5	37.5	6.4	9.9	0.17	0.26
$\bar{X}$	49.2	9.1	7.7	0.185	0.17
s	12.9	2.2	1.5	0.035	0.061
v	0.26	0.24	0.20	0.19	0.37

* simultaneous failure of the timber in transvers compresion.

Table 5 - Test results for group 5 - Spruce (Yugoslavia).

Specimen	MOR (1) (Mpa)	BSS (2) (Mpa)	DSS (3) (Mpa)	(2)/(1)	(3)/(1)
1	54.0	7.5	4.9	0.14	0.09
2	30.8	8.6	6.4	0.28	0.21
3	55.8	8.6	5.5	0.15	0.10
4	35.6	7.8	5.6	0.22	0.16
** 5	22.9	4.4	4.8	0.19	0.21
$\bar{X}$	44.1	8.1	5.6	0.195	0.14
s	12.7	0.56	0.62	0.066	0.056
v	0.29	0.07	0.11	0.33	0.40

** excluded from the average.

Table 6 - Test results for group 6 - Hard wood.

Specimen	MOR (1) (Mpa)	BSS (2) (Mpa)	DSS (3) (Mpa)	(2)/(1)	(3)/(1)
beech					
1	71.4	18.0	14.5	0.25	0.20
2	64.2	18.2	10.0	0.28	0.16
eucalyptus					
1	115.7	21.7	16.4	0.19	0.14
2	86.5	18.2	15.8	0.21	0.18
3	92.1	15.1	14.0	0.16	0.15

APPENDIX

Shear Strength in Bending

1. Test specimen

The test specimen shall have a length of 5.5±0.5 times the nominal depth of the section (b).

A groove 2.5±0.5 mm width with depth equal to 0.3±0.03 the width (b) of the specimen should be cut at each side of the specimen at mid height, all along the specimen as shown in fig. 1.

2. Test procedure

The test specimen shall be loaded in mid - span bending over a span of 5 times the nominal depth as shown in fig. 2. If the test equipment does not permit these conditions to be achieved exactly then the span and the specimen length may be increased or descreased or decreased by an amount not greater than 1.5 time the nominal depth, while maintaining the symmetry of the test.

The specimen shall be supported on rollers and a fixed knife edge reaction, or by other devices which achieve an acceptable free support condition. Small plates of a length equal to one-half the nominal depth should be inserted between the specimen and the supports and of a length equal to the nominal depth should be inserted between the specimen and the loading head.

If the depth to width ratio of the specimen exceeds four lateral restraint shall be provided to prevent buckling. This restraint shall permit the specimen to deflect without significant frictional resistance.

The loading equipment used shall be capable of measuring load to an accuracy of 1% or better.

Load shall be applied at a continuous rate so adjusted that maximum load is reached within 90±30 seconds.

3. Results

The shear in bending strength of the test specimen shall be calculated from the formula:

$$f_{vm} = 0.75\ P_{max}/hb'\ (N/mm^2)$$

where f_{vm} is the shear in bending strength (BSS) (P/mm^2); F_{max} is the maximum load (N); h and b' are determined from the actual dimensions of the section (mm).

The shear strength in bending shall be calculated and recorded to three significant figures. The mode of fracture of each test specimen shall also be recorded.

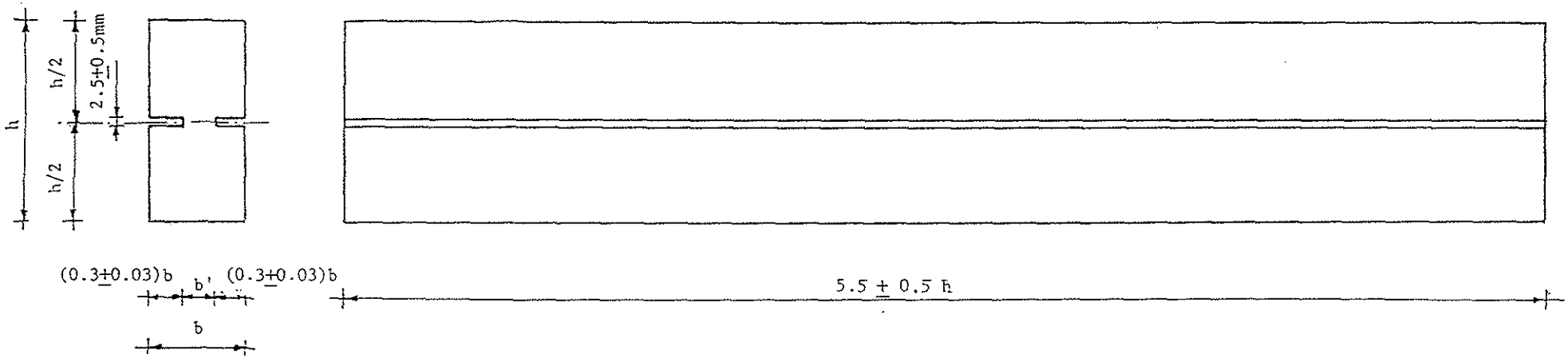

Fig 1 - Dimensions of shear strength in bending test specimen

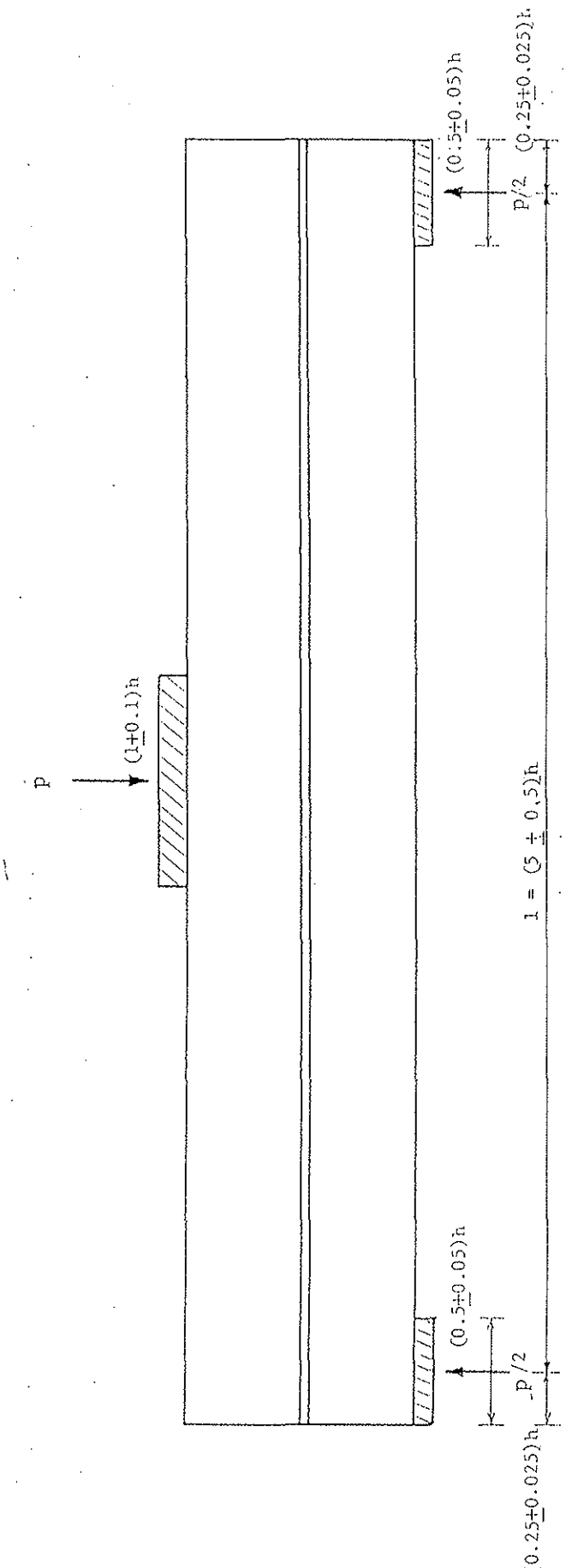

Fig 2 - Test arrangement for determining shear strength in bending

CIB-W18A/21-7-1

INTERNATIONAL COUNCIL FOR BUILDING RESEARCH STUDIES AND DOCUMENTATION

WORKING COMMISSION W18A - TIMBER STRUCTURES

NAILS UNDER LONG-TERM WITHDRAWAL LOADING

by

T Feldborg and M Johansen
Danish Building Research Institute
Denmark

MEETING TWENTY-ONE
PARKSVILLE, VANCOUVER ISLAND
CANADA
SEPTEMBER 1988

Nails under long-term withdrawal loading

Introduction

The axial withdrawal resistance depends on a large number of variables. Considerable research has been performed in order to be able to describe the mechanism of the holding power and to obtain basic data for the design.

In 1982, some ceilings of corrugated asbestos-cement sheets fixed with annularly threaded nails fell down. Variations in moisture content of the timber were suspected to have caused the failure, possibly as a consequence of progressive withdrawal. The withdrawal resistance of the nails after an extreme moisture change from wet to dry condition was determined at the laboratory of the Danish Building Research Institute (SBI), but the test results failed to provide an explanation.

It was therefore decided to study how the nail movement and the withdrawal resistance were affected by long-term load under constant and alternating relative humidity.

The load was about maximum service load, and the loading time was about two years. The climate was normal room temperature with the relative humidity varying between 50 and 85 per cent.

This paper gives the principles of the tests, the main results and the conclusions. Documentation, such as test programme, material properties, specimens, test arrangements and equipment, is given in (7).

The symbols used are in conformity with ISO 3898 (3). Special symbols are defined when used.

Test programme

Annularly threaded nails with shank diameter 4.4 mm and length 90 mm were used. The nails were driven perpendicular to the grain of the timber, with three different depths of penetration.

The nails were loaded in axial withdrawal with a constant load, corresponding to maximum service load, for a period of approximately two years. One group of nails was placed in a climate chamber with normal room temperature and with the relative humidity changed every sixth weeks either from 85 to 50 per cent or from 50 to 85 per cent, resulting in nine drying-out periods. Other groups of loaded nails were placed in climate chambers with constant relative humidity (85 and 65 per cent).

Reference groups with no-load nails with the same humidity histories as the loaded nails were included in the tests.

For all specimens, the distance between the timber surface and the head of the nail was measured before and after the two-year period of long-term loading, and for the no-load nails under alternating humidity, also during the test period.

After the two years, the withdrawal resistance of all the nails was measured in a short-term test (4).

The conditioning programme is outlined in figure 1; the detailed test programme is described in (7).

Series	Conditioned at room temperature and the following relative humidities:		
	Before the nail-driving	During the long-term loading	Before the short-term withdrawal
	RH per cent	RH per cent	RH per cent
1L and 1N	65	65	65
2L and 2N	85	85	85
3L and 3N	85	85	50
4L and 4N	85	85 alt. with 50	85
5L and 5N	85	85 " " 50	50

Figure 1 Conditioning programme for long-term loaded specimens (L) and no-load specimens (N).

Specimens

The test specimens are shown in figure 2.

Swedish spruce with a density in the range of 0.41 to 0.51 (mass and volume at moisture content $\omega \sim 0.15$) was used.

The timber members were cut from the timber material and distributed over the test series so as to have the same average density for all series in order to obtain a good basis for comparison of the test results. Furthermore, a specimen belonging to the reference group of no-load specimens was taken adjacent to a corresponding specimen for long-term testing.

The long-term load was 0.4 F_k, F_k being the characteristic value of the short-term withdrawal resistance determined on the basis of preliminary tests.

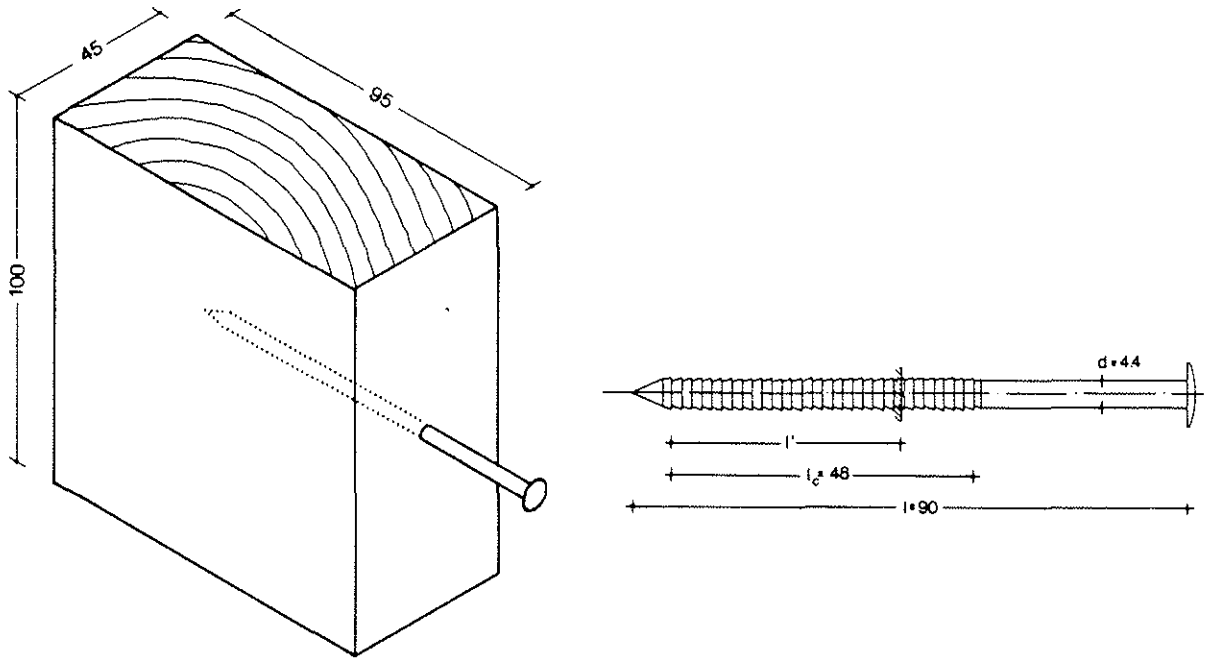

Figure 2 Specimen with nail for axial withdrawal loading. l' is the depth of penetration. Dimensions are in mm.

Test methods

Long-term loading

The long-term load was applied, in principle, as shown in figure 3. The specimens were arranged horizontally in a sort of chain, and a steel weight on a lever was used to apply the required withdrawal load to 10 nails.

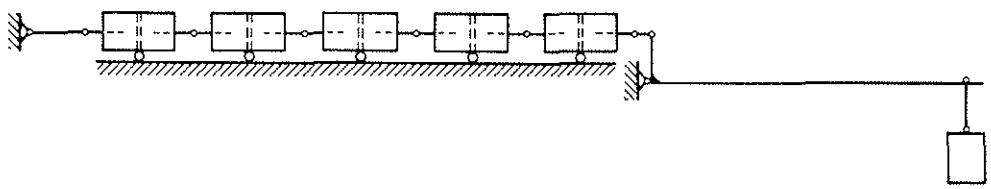

Figure 3 Principle of long-term withdrawal loading af nails.

Short-term testing

The withdrawal resistance was determined in accordance with Nordtest-method NT BUILD 134 (4) in a mechanical testing machine.

Measurement of nail height

The nail height, i.e. the distance between the top of the nail head and the timber surface, was measured by means of a displacement gauge.

Results

Test variables

The nails were annularly threaded nails 4.4 • 90 mm.

The following abbreviations are used for the test variables in the presentation of the results:

1': The depth of penetration, disregarding the nail point. The following depths were tested:

1' = 22 mm

1' = 48 mm (~ threaded length)

1' = 63 mm (~ threaded length + 15 mm)

L: Long-term loaded

N: No-load (reference groups).

5 series with different conditioning treatment at normal room temperature and relative humidity as shown in figure 4.

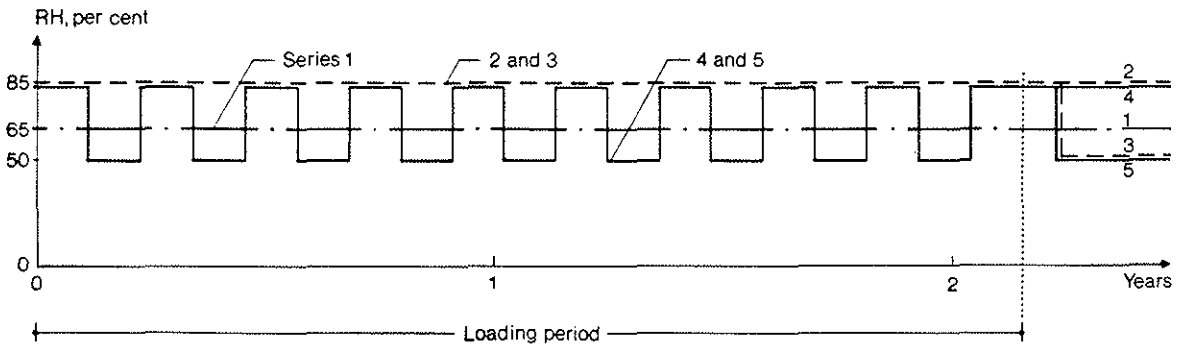

Figure 4 Conditioning history of test series 1 to 5.
Series 4 and 5 had 9 drying-out periods.

Nail movement during long-term loading

The axial movement of the nail in relation to the timber surface caused by alternating shrinking and swelling of the timber (nail popping) and - for the long-term loaded nail - also by the withdrawal load is shown in figure 5. The measurements were carried out just after driving and just after unloading, and for the no-load reference groups 4N and 5N, also during the long-term loading period. The results from series 4N are shown in figure 6.

The no-load nail (series N) backed out during a shrinkage of the wood and returned on the whole to its original position in the wood after a corresponding swelling, see figure 6. It will, in particular, be seen that the nail movement due to changing humidity was about 0.2 mm for series 4N 22 and about 0.4 mm for series 4N 48. Nail popping and its causes have previously been subjected to more thorough investigation, see reference (6), one conclusion of which was that properly threaded nails can minimize or eliminate nail popping.

The nail movement caused by long-term loading was moderate for the nails in constant relative humidity (series 1L and 2 + 3L).

After nine shrinking periods, the movements of the long-term loaded nails in the series 4L and 5L averaged 0.7 mm and 1.4 mm for nails with l' = 22 mm and 48 mm depth of penetration, respectively, see figure 5.

However, the results do not show whether the development of the movements has stopped, and the possibility of progressive withdrawal can not be eliminated.

In spite of the same level of long-term withdrawal load per mm depth of penetration, $0.4\ F_k/l' \sim 19$ N/mm, the nail movement for nails with l' = 48 mm (series L48) was, on average, about twice that for nails with l' = 22 mm (series L22).

To summarize: long-term loading combined with alternating humidity caused movements that were about three times bigger than movements due to alternating humidity alone and about seven times bigger than movements due to long-term load alone.

Series	Relative humidity	Sample size[1]	Long-term load	Nail movement for 1' = 22 mm	48 mm	63 mm[2]
	per cent		N	mm	mm	mm
1 N	65	10	0.0	0.0	0.0	0.0
1 L	65	10	0.4 F_k	0.1	0.2	
2 + 3 N	85	20	0.0	0.0	0.0	0.0
2 + 3 L	85	20	0.4 F_k	0.1	0.2	
4 + 5 N	85 alt. 50[3]	20	0.0	0.0[4]	0.1[5]	0.3
4 + 5 L	85 alt. 50[3]	20	0.4 F_k	0.7	1.4	

1) For each depth of penetration 1'.
2) Length of threaded shank ~ 48 mm.
3) Beginning and ending with 85 per cent RH.
4) 0.2 mm at the end of the last drying-out period.
5) 0.4 mm at the end of the last drying-out period.

Figure 5 Average movements of nails in timber under various humidity and load conditions. The measurements were taken just after driving (reference values) and just after unloading. The long-term load 0.4 F_k was 400 N for nails with 1' = 22 mm and 920 N for the others. The loading period was about 2 years.

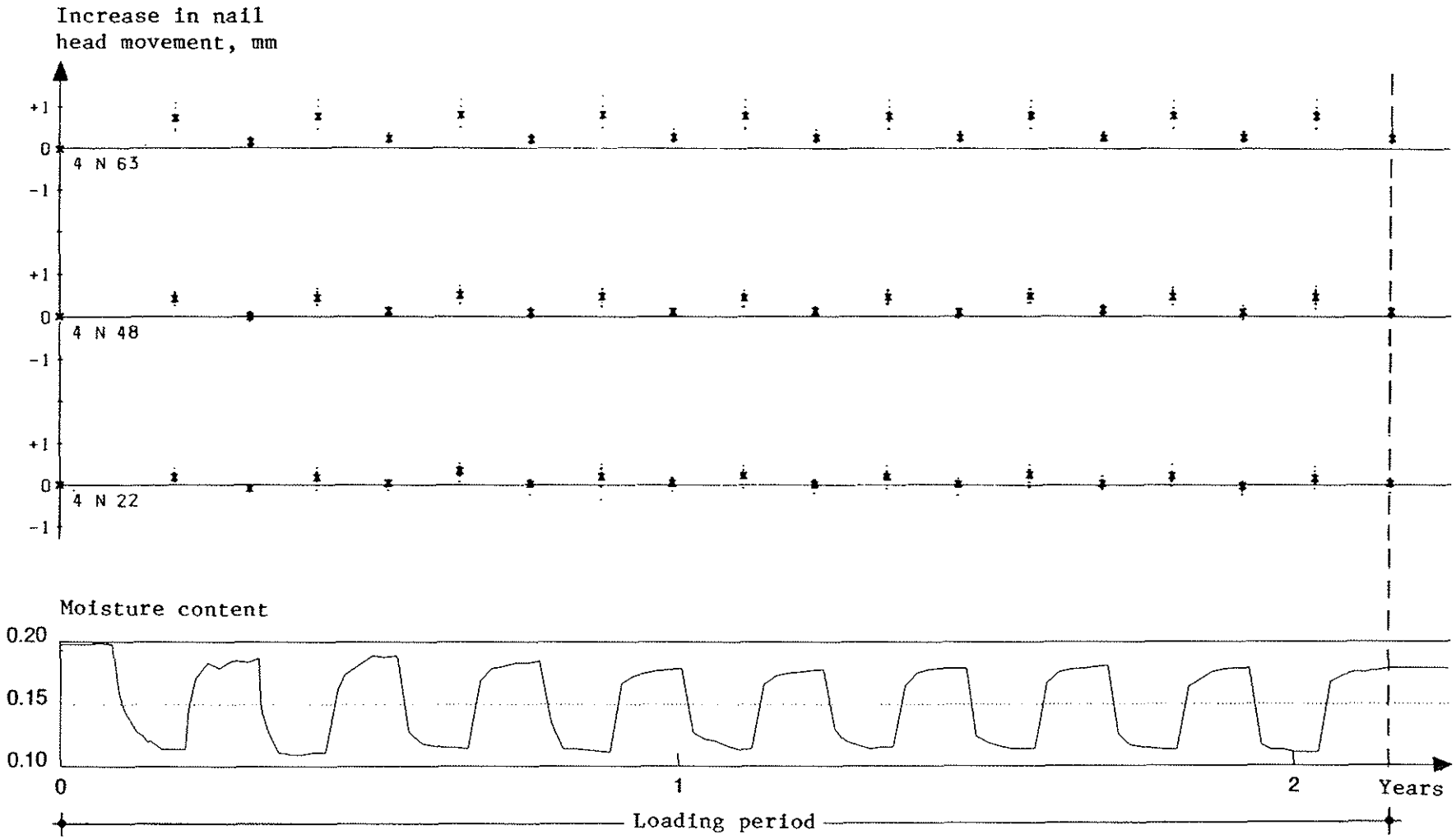

Figure 6 Average values of the increase in nail head movement caused by moisture-dependent dimensional changes of the timber. The reference value of the nail head movement, i.e. the distance between nail head and timber surface, was measured just after driving. There were 10 samples in each series.

Short-term withdrawal resistance

The results are shown in figure 8.

The typical load-displacement curve is shown in figure 7. The proportional limit F_p was seen as a more or less distinct change of inclination at the recorded curves. The lowest values measured and the applied long-term values are indicated in figure 8 at series L.

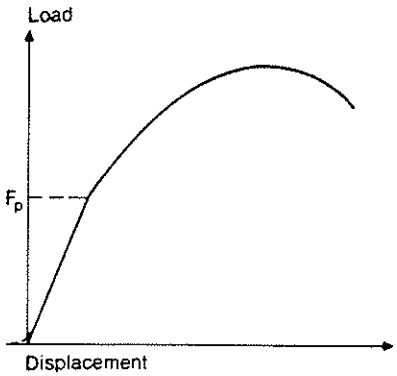

Figure 7 Typical load-displacement curve. F_p is the load at the proportional limit.

Several statistical analyses were performed on the withdrawal resistance of the 250 nails.

A 3-way analysis-of-variance on the test results for the depth of penetration 1' = 22 mm and 48 mm showed that the withdrawal resistance of no-load (N) and long-term loaded (L) nails did not differ significantly, whereas the 5 different humidity treatments caused a significant change in the withdrawal resistance (level of significance: 99.9 per cent).

The analysis also showed that the withdrawal resistance in N/mm was slightly higher for 1' = 22 mm than for 1' = 48 mm (level of significance: 95 per cent). Investigations referred in (1), including similar tests with 1' = 7d, 11d, and 14d, did not show such significant difference.

A 2-way analysis-of-variance on 1' = 63 mm (= 48 mm threaded length + 15 mm plain-shank) and 1' = 48 mm (= threaded length) again showed a significant influence on the withdrawal resistance from the 5 humidity treatments (level of significance: 95 per cent). The withdrawal resistance for 1' = 63 mm was, on average, about 12 per cent higher than for the nails with 1' = 48 mm (level of significance: 99.9 per cent). The difference is explained by ineffective wood fibres near the surface. If the withdrawal resistance of the nails with 1' = 48 mm were to be corrected for this ineffectiveness, the design depth of penetration would have to be reduced by 1.0d to 1.8d.

When the 5 different humidity treatments are not regarded as independent treatments as above, we find that the load condition (N or L) does interact with, for example, the moisture content. The estimates show that the long-term load tends to increase the strength, as can also be seen in figure 8.

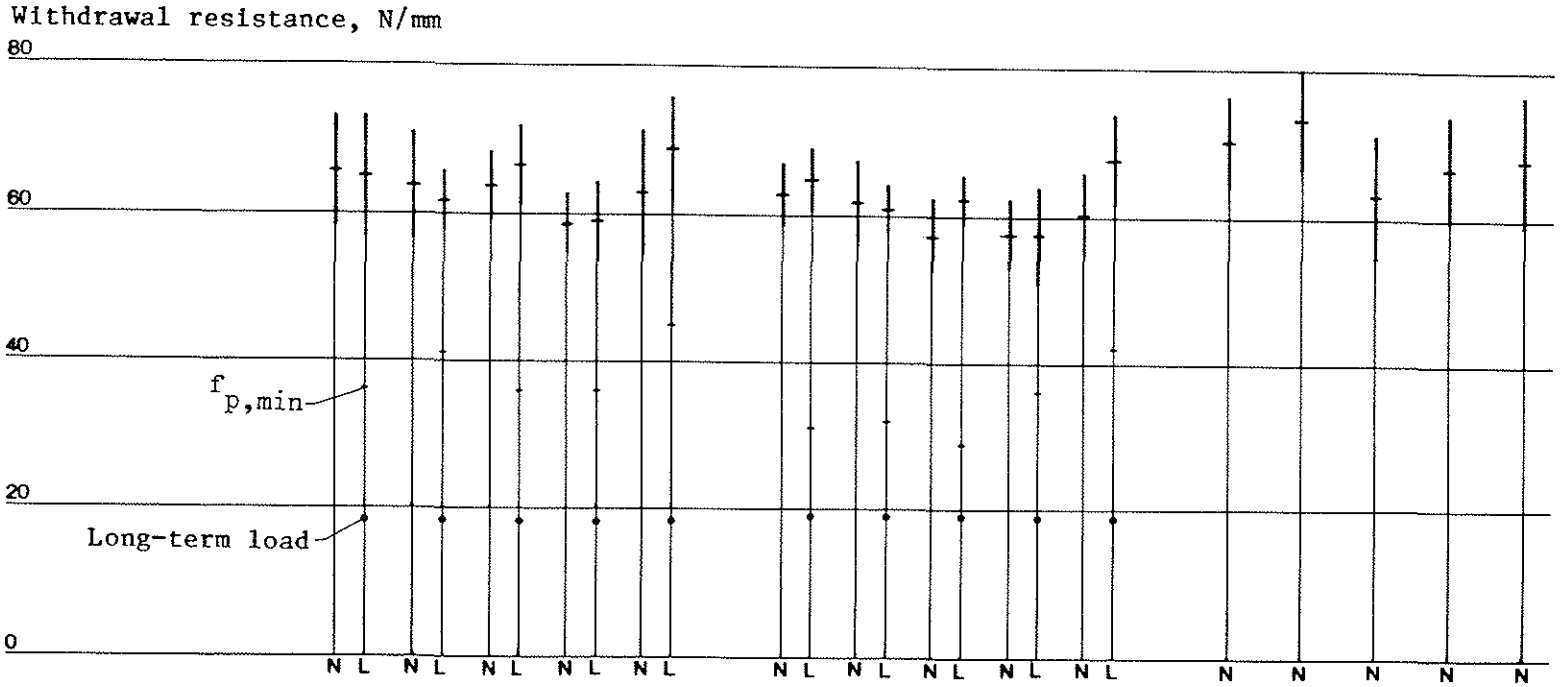

Series		1	2	3	4	5	1	2	3	4	5	1	2	3	4	5
Moist. at fabr.	%	14	21	21	21	21	14	21	21	21	21	14	21	21	21	21
Rel. hum.	%	65	85	85	85-50	85-50	65	85	85	85-50	85-50	65	85	85	85-50	85-50
Moist. at test	%	14	20	11	18	11	14	21	11	18	11	14	20	11	18	11
Depth of penetr.		1' = 22 mm					1' = 48 mm					1' = 63 mm (Threaded length + 15 mm)				

Figure 8 Withdrawal resistance of annularly threaded nails, d = 4.4 mm, l = 90 mm, from short-term testing of no-load nails (N) and long-term loaded nails (L). Average values from 10 specimens and 95 per cent confidence intervals. $f_{p,min}$ is the measured minimum value of the proportional limit.

Conclusions

The nail movement due to long-term axial withdrawal loading was moderate for nails in timber under constant relative humidity, but considerable under cyclically changing relative humidity. The residual movement increased with increasing depth of penetration.

For no-load nails under alternating relative humidity the nail movement (nail popping) was negligible.

Long-term loading, corresponding to maximum working load, for a period of approximately two years under constant and alternating relative humidity, did not reduce the short-term withdrawal resistance of the tested nails.

In practice, nails in withdrawal are used in the following conditions:

- short-term loading under constant humidity
- short-term loading after alternating humidity
- long-term loading under constant humidity
- long-term loading under alternating humidity.

The investigation indicates that the withdrawal resistance of nails of the type tested can be based on a generally accepted standard short-term test with a specified test climate (e.g.(4)).

The relatively large movements for long-term loaded nails under alternating humidity call for attention and indicate the possibility of progressive nail movement leading to withdrawal failure.

A further clarification of this problem requires recordings of the nail movements during long-term loading and alternating humidity. Aiming at design values, where long-term withdrawal loading is involved, more levels of load and alternating humidity must be considered. It seems possible, for instance, that the nail movements are stable at smaller loads than tested, but unstable at larger loads.

References

(1) Withdrawal resistance of nails. Th. Feldborg and Marius Johansen. SBI-report 84. Danish Building Research Institute. 1972. (In Danish with an English summary).

(2) DS 413. Code of practice for the structural use of timber. Translation edition. 1983.

(3) ISO 3898. Basis for design of structures. Notation. General symbols. 1976.

(4) NT BUILD 134 Nails in wood - Withdrawal strength. Nordtest-method. 1981.

(5) Nailed joints in wood structures. J. Ehlbeck. Bulletin No. 166. Virginia Polytechnic Institute. 1979.

(6) Nail popping, its causes and prevention. E. Georg Stern. Bulletin No. 24. Virginia Polytechnic Institute. 1956.

(7) Nails under long-term withdrawal loading. Documentation for CIB-W18 paper presented at meeting twenty-one, 1988.
ID 880205. Structural Division, Danish Building Research Institute. 1988.

(8) Varmforzinkede kamsøms udtræksmodstand. (Withdrawal resistance of galvanized annularly threaded nails. The withdrawal resistance influenced by variations in thread geometry). Th. Feldborg. Documentation for SBI-project F-513. ID 870412. Structural Division, Danish Building Research Institute. 1987. (In Danish).

CIB-W18A/21-7-2

INTERNATIONAL COUNCIL FOR BUILDING RESEARCH STUDIES AND DOCUMENTATION

WORKING COMMISSION W18A - TIMBER STRUCTURES

GLUED BOLTS IN GLULAM
- PROPOSALS FOR CIB CODE

by

H Riberholt
Technical University of Denmark
Denmark

MEETING TWENTY-ONE
PARKSVILLE, VANCOUVER ISLAND
CANADA
SEPTEMBER 1988

Preface

This paper presents partly a proposal for some sections in /CIB, 1983/ concerning glued-in steel bolts, partly the basis for the proposals. This basis is given in the comments to which there is referred by numbers followed by a bracket.

Proposal for some sections on glued-in steel bolts.

6.2.1 Glued bolts

1) Unless the adhesion between glue and steel is secured by special measures, the bolt must have a rough surface.

: Threaded rods are very suitable.

2) It is assumed that the position of the lateral force is known to be e from the wood surface, and that the axial force acts in the center of the bolt.

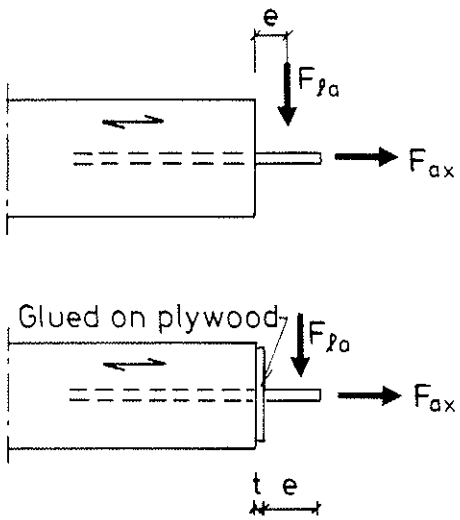

Figure 6.2.1.a Position of forces.

6.2.1.1 Laterally loaded bolts.

Glued bolts perpendicular to grain

1) The characteristic load-carrying capacity of bolts glued in perpendicular to grain may be calculated from (6.1.2.1.a) - (6.1.2.1.f) if the diameter d is substituted by the core diameter of the bolt, and α is put equal to 90°.

Glued bolts parallel to grain

The characteristic load-carrying capacity in N for a force acting a distance e from the wood surface is

2) $$F = \left(\sqrt{e^2 + \frac{2 M_y}{df_e}} - e\right) df_e \qquad (6.2.1.1.a)$$

where

M_y Characteristic yield moment of the bolt in Nmm

d $\max \begin{cases} \text{Hole diameter} \\ \text{Outer bolt diameter} \end{cases}$ in mm

f_e Embedding strength. For d in mm

$$f_e = (2.3 + 750\, d^{-1.5})\rho \qquad (6.2.1.1.b)$$

3) If a plywood sleeve is bonded to the end grain the characteristic load-carrying capacity in N for an eccentric force is

$$F = \left(\left(\sqrt{e^2 + k_s} - e - t\right) f_e + t f_{e,s}\right) d \qquad (6.2.1.1.c)$$

where the notation partly is given in context with (6.2.1.1.a) and partly signifies

$$k_s = \frac{2 M_y}{df_e} - t(2e + t)\left(\frac{f_{e,s}}{f_e} - 1\right) \qquad (6.2.1.1.d)$$

t Thickness of plywood sleeve

$f_{e,s}$ Embedding strength of the plywood sleeve.

4) Minimum distances are given in figure 6.2.1.1.a, and they depend on whether the glue may bond to the bolt.

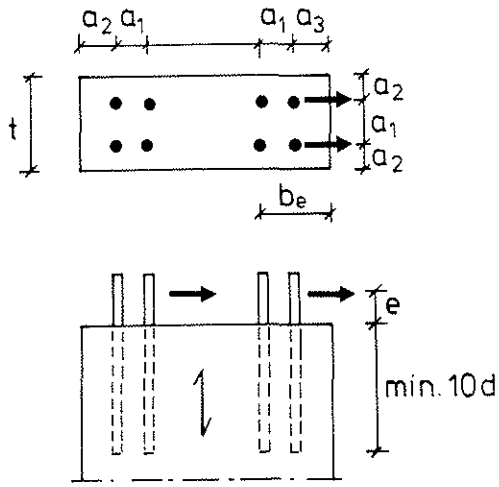

		Min. distance	
Glue bonds to bolt:		Yes	No
Without a plywood sleeve			
a_1	Mutual	2d	4d
a_2	Edge	2d	2.8d
a_3	Loaded edge	4d	4d
With a plywood sleeve			
a_1	Mutual	2d	2d
a_2	Edge	1.5d	2.5d
a_3	Loaded edge	3d	3d

Figure 6.2.1.1.a Minimum distances and glued-in length.

5) Splitting may be counteracted by a glued-on plywood sleeve. Otherwise it must be shown that

$$F \leq \frac{2}{3} b_e t f_v \qquad (6.2.1.1.d)$$

where F is the total lateral force on a separate group of bolts, b_e is the distance from the loaded edge to the furthest bolt, and t is the thickness of the member. See fig. 6.2.1.1.a.

If the plywood sleeve only covers a part of the beam end (6.2.1.1.d) still applies but with b_e as the distance from the loaded edge to the furthest end of the sleeve.

6.2.1.2 Axially loaded bolts.

1) Axially loaded bolts may be emploied in all structures in moisture class 1 and 2. In moisture class 3 they should only be used if they are parallel to the grain, or perpendicular on this with a glued-in length of max. 200 mm.

The characteristic withdrawal resistance in N is

2)
$$F = \begin{cases} f_{ws} \quad \rho \quad d \quad \sqrt{\ell_g} & \text{for} \quad \ell_g \geq 200 \text{ mm} \qquad (6.2.1.2.a) \\ f_{w\ell} \quad \rho \quad d \quad \ell_g & \text{for} \quad \ell_g < 200 \text{ mm} \qquad (6.2.1.2.b) \end{cases}$$

where

f_{ws} Withdrawal parameter for the square root case $N/mm^{1,5}$.

$f_{w\ell}$ Withdrawal parameter for the linear case N/mm^2.

d $\max \begin{cases} \text{Hole diameter} \\ \text{Outer bolt diameter} \end{cases}$ in mm

ℓ_g Glued-in length in mm.

: For brittle glues, such as Resorcinol and some Araldites, the withdrawal parameters have been determined to

: $f_{ws} = 520 \ N/mm^{1,5}$

: $f_{w\ell} = 37 \ N/mm^2$

: For non-brittle glues, e.g. 2-component Polyurethan glued into wood with a moisture content of max. 0.12, the values are

: $f_{ws} = 650 \ N/mm^{1,5}$

: $f_{w\ell} = 46 \ N/mm^2$

: For bolts in end grain the withdrawal parameters may be increased 15% if a plywood sleeve is glued to the end.

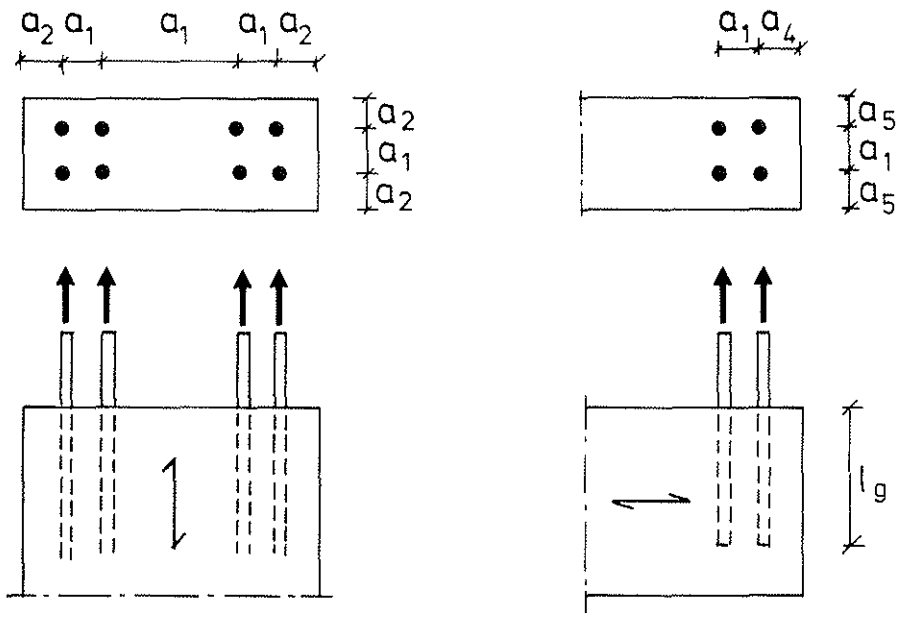

Glue bonds to bolt		Min distance Yes	No
a_1	Mutual	2d	4d
a_2	Edge	1.5d	2.5d
a_4	End grain	2d	4d
a_5	Side	2.5d	2d

3) Figure 6.2.1.2.a Minimum distances.

For bolts perpendicular to grain it should further be shown that the inequality (6.1.2.1.h) is valid for $b_e = \ell_g$, which is defined in fig. 6.2.1.2.a.

For bolts parallel to grain it should be shown that the total force F_{tot} in a group of bolts is less than the tension strength of the effective area A_{eff} behind the bolts. See fig. 6.2.1.2.b.

$$F_{tot} < A_{eff} f_{t,0} \qquad (6.2.1.2.c)$$

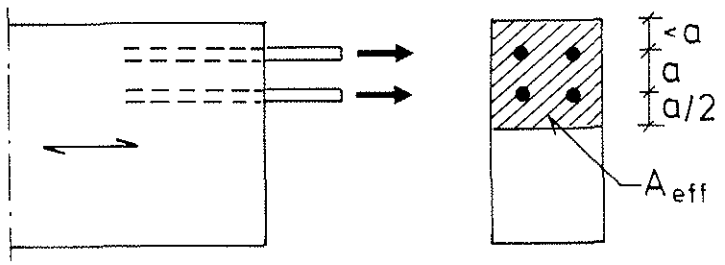

Figure 6.2.1.2.b Effective area behind bolts parallel to grain.

4) Due to stability failure in a compressed bolt the normal stress in it should be less than 400 MPa.

5) The withdrawal failure mode is rather brittle for a little glued - in length. So if the force distribution over a group of bolts is statically indeterminate the glued-in length should be at least d^2 mm, where d is the diameter of the bolts in mm.

Addition to chap. 8.3 Joints.

At the time of gluing the moisture content of the wood should maximum be 0.15.

1) Glued bolts loaded axially must be protected properly against corrosion. Unprotected bolts should not be used. It is recommended to employ threaded rods or bolts with a similar rough surface.

2) Glued bolts may be put in oversize holes if an adhesive capable of bonding to the bolt surface is used. If the adhesive does not bond to the bolt this must have a mechanical grip of the wood. A threaded rod with a longitudinal groove may be screwed into a hole with a diameter approximately equal to the mean of the outer and inner diameter of the thread.

3) For connections with groups of several glued bolts it is essential that the bolts are tightened identically.

Comments to chapter 6.2.1 Glued bolts.

1) Bonding of metal.

It has been experienced, that good and reliable bonding between glue and a smooth steel surface requires such measures, which hardly can be established in praxis every time.

2) Force assumptions.

Since the bolt frequently is connected to other types of material it is necessary to give the lateral load capacity either for a known eccentricity or for given material combinations and gaps between the material surfaces.

Comments to chapter 6.2.1.1 Laterally loaded bolts.

1) Bolts perpendicular to grain.

This simplification gives capacities on the safe side partly because d_{core} is less than d_{hole}, partly because the measured values of the embedding strength are larger than those assumed in /CIB 1983/. These are determined from

$$f_e = 70 \cdot \rho \, k_\alpha \quad \text{MPa} \qquad (1.1)$$

where

ρ is the relative density of the wood

k_α is the angle and diameter correction factor.

In /Möhler & Hemmer, 1981/ the embedding strength has been measured for this case (bolt perpendicular to grain) and for a relative density of 0.44. Table 1.1 gives the values.

Table 1.1 Embedding strengths, MPa. Measured mean values and characteristic values from /CIB 1983/.

Source		Diameter of bolt or threaded rod: 16 mm	30 mm
/CIB, 1983/, ρ = 0,44	α = 0	30.8	30.8
	α = 45	22.5	20.5
	α = 90	17.7	15.4
/Möhler & Hemmer, 1981/		31.7	19.0

2) Bolts parallel to grain.

The formula (6.2.1.1.a) has been emploied to calculate the embedding strength based on test results. From these it is suggested to employ the following empirical formula for the embedding strength f_e in MPa. The formula is similar to (5.13) in /Riberholt, 1986/.

$$f_e = (3.0 + 1000\ d^{-1,5})(2.1 - 0.009 \cdot \omega)\ \frac{\rho}{0.42} \qquad (1.2)$$

where

d is the outer diameter of the bolt or threaded rod, or the hole diameter.

ω is the moisture content in percent.

ρ is the relative density

This formula gives the expected/mean values of f_e and in table 1.2 these are compared with test results.

Table 1.2 Embedding strengths f_e from measurements and from formula (1.2)

Reference	Hole/bolt dia, mm	Moi.cont ω	Dens. ρ	f_e, MPa Measur.	(1.2)
Riberholt, 1986	13	12.3	0.40	24.3	23.0
"					
Mohler & Hemmer, 1981	16	11.2	0.44	17.8	21.3
Riberholt, 1977	16	11	0.45	21.8	22.2
Riberholt, 1986	21	12.6	0.41	13.8	12.6
"					
Mohler & Hemmer, 1981	30	11.2	0.44	9.1	10.4

The characteristic value of f_e is estimated to be 70% of the value of (1.2). This corresponds to a Log-Normal distribution with a coefficient of variation of 0.18.

According to /CIB, 1983/ moisture class 2 may result in $\omega = 18$ percent thus the characteristic value $f_{e,k}$ becomes

$$f_{e,k} = (2.3 + 750\ d^{-1.5})\rho \qquad (1.3)$$

It must be envisaged that this empirical formula is determined from tests with spruce specimens. It is likely to be valid for other coniferous softwoods.

The load-duration and moisture-class factors in table 5.1.0 of /CIB, 1983/ appear to be reasonable for the embedding strength given by (1.3). This has been reduced seriously by emploiing a moisture content $\omega = 0.18$ in formula (1.2), so $f_{e,k}$ from (1.3) should give a conservative load-carrying capacity, may be too conservative.

3) Reinforcement by glued on plywood sleeves.

By gluing plywood sleeves to the end grain and drill the hole through the sleeve the lateral load-carrying capacity of the bolt may be increased. From tests reported in /Riberholt, 1986/ it appears that the embedding strength the plywood is similar to its compression strength. So if the bonding to the end grain is

sufficient the lateral load carrying capacity may be calculated from formula (5.9) and (5.10) in /Riberholt, 1986/ which are repeated here..

$$F_{lat} = ((\sqrt{e^2 + k_s} - e - t)f_e + tf_{e,s})\, d \qquad (1.4)$$

where the notation partly is given previously partly signifies:

$$k_s = \frac{2\, M_y}{df_e} - t(2e + t)\left(\frac{f_{e,s}}{f_e} - 1\right) \qquad (1.5)$$

t Thickness of plywood sleeve

$f_{e,s}$ Embedding strength of the plywood sleeve.

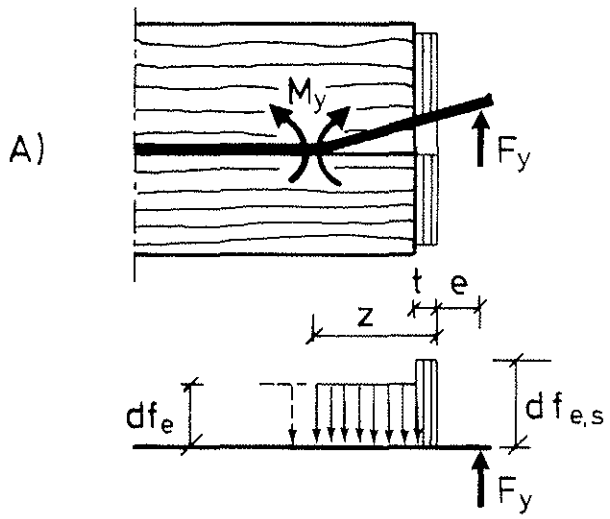

Figur 1.1 Stresses and forces on a laterally loaded glued bolt with a sleeve.

Further there is another advantage by sleeves, which is that the minimum distances to the edge may be reduced to only 1.5d.

It is suggested to incorporate sleeves in the CIB-Code, but it must be realized that the extent of tests supporting sleeve reinforcement is less than that of unreinforced bolts. May be the best argument is, that plywood sleeves have been utilized for the hub connection in the 20 m long wooden blades of the wind turbine in Nibe. The hub connection is designed with glued bolts and has now functioned 4 years without any problems.

4) Minimum distances for bolts parallel to grain.

The glued-in length must be at least 10d in order to secure the assumed failure mode with formation of a yielding-hinge in the bolt.

The minimum distances depend on whether the glue bonds to the bolt. If it bonds the tendency to splitting is reduced. For practical purposes it is important to have a close spacing between the bolts, in this way it is possible to obtain a capacity of the connection which is close to that of the glulam cross section.

5) Splitting.

The proposed rules are not supported by direct test results. But they are drived partly from full-scale tests with moment-stiff column connections, see /Riberholt, 1986/ chap. 6, partly from tensile tests with bolts glued-in perpendicular to grain, see /Riberholt, 1986/ chap. 9. More research is suggested.

Comments to chapter 6.2.1.2 Axially loaded bolts.

1) Limitation on bolts in moisture class 3.

For bolts parallel to grain tests have demonstrated that for outdoor climate the long term withdrawal capacity is approximately half the short term strength of dry specimens. See /Riberholt, 1986/. Apparently there is a threshold for damage caused by the moisture induced residual stresses.

But for bolts perpendicular to grain such a knowledge does not exist. It is thus a "guestimate" that (6.2.1.2.b) applies with the suggested parameter values.

2) Characteristic withdrawal resistance.

In /Riberholt, 1986/ it is reported that a regression analysis has resulted in the following estimate in N of the withdrawal resistance of bolts in oversize holes and glued with a brittle Araldit or a more soft or ductile 2-component Polyurethan glue.

$$F_{ax,estim} = \begin{cases} -9{,}400 + 834 \cdot d_h \sqrt{\ell_g}\ \rho & \text{Polyurethan} \quad (1.6) \\ 3{,}500 + 237 \cdot d_h \sqrt{\ell_g} & \text{Araldit} \quad (1.7) \end{cases}$$

Meanwhile for simplicity it is suggested to employ

$$F_{ax,estim} = f_{ws}\ d_h \sqrt{\ell_g}\ \rho \qquad \begin{matrix} f_{ws} = 784 \text{ for Polyurethan} \\ f_{ws} = 627 \text{ for Araldit} \end{matrix} \qquad (1.8)$$

This equation gives almost the same values as (1.6) and (1.7).

If the glued-in length ℓ_g is little the formulas tend to overestimate the withdrawal resistance. They are set up for a range of ℓ_g of 160-500 mm. So it is suggested that for ℓ_g less than 200 mm (1.8) is substituted by

$$F_{ax,estim} = f_{w\ell}\ d_h\ \ell_g\ \rho \qquad \begin{matrix} f_{w\ell} = 55.4 \quad \text{for Polyurethan} \\ f_{w\ell} = 44.3 \quad \text{for Araldit} \end{matrix} \qquad (1.9)$$

In this way the mean shear stress in the wood along the glue line is maximum 7.5 MPa.

Further it is suggested to employ Araldit-estimates for bolts glued with Resorcinol glue. This is approximately as brittle as Araldit so the failure in the surrounding wood should be similar.

Table 1.3 contains a comparison between measured and estimated withdrawal capacities from different test reports available. For bolts glued with Resorcinol it has been assumed that (1.9) applies.

Table 1.3 Comparison of withdrawal resistances.

Source	Glue	Bolt dia. d mm	Hole dia. d_h mm	Glue. ℓ_g mm	Rel.dens ρ	F-axial,kN F_{mea}	F_{est}	Ratio
Bolts parallel to grain								
Riberholt,	PU	20	21	190	0.39	85	86	0.99
1986	PU	20	21	296	0.44	123	125	0.98
	PU	20	21	294	0.43	119	121	0.98
	A	20	21	294	0.42	89	95	0.94
	PU	20	22	503	0.41	149	159	0.94
	PU	12	13	167	0.43	49	52	0.94
	A	12	13	172	0.42	44	42	1.05
Riberholt,	R	16	15	153	0.44	55	48	1.15
1977	R	16	15	317	0.41	78	73	1.07
	R	24	22	245	0.42	107	99	1.08
	R	24	22	479	0.41	179	135	1.33
Möhler &	R	16	14.7	160	0.44	43	50	0.85
Hemmer, 1981	R	16	14.7	160	0.44	40	50	0.80
	R	16	14.7	256	0.44	65	71	0.92
	R	30	27.8	300	0.44	94	143	0.66
Riberholt & Spøer, 1983	A	40	42	500	0.44	281	256	1.10
Ehlbeck &	R	16	15	150	0.44	36	47	0.77
Siebert,1987	R	20	18	300	0.44	99	96	1.03
Riberholt, 1988	PU	20	21	402	0.41	133	136	0.98
Bolts perpendicular to grain								
Riberholt	R	16	15	157	0.47	56	52	1.08
1977,compr.	R	16	15	321	0.43	77	77	1.00
Ehlbeck &	R	16	15	100	0.44	30	39	0.77
Siebert,1987	R	16	12-14	87	0.44	27	34	0.79
Tension	R	16	15	140	0.44	36	44	0.82
Values of	R	26.5	30	500	0.44	130	185	0.70
single tests	R	26.5	30	750	0.44	166	227	0.73
	R	26.5	30	1000	0.44	217	262	0.83
	R	32	36	750	0.44	230	272	0.85
	R	32	36	1000	0.44	319	314	1.02
	PU	26.5	30	850	0.44	317	302	1.05
	PU	26.5	30	1000	0.44	350	327	1.07
	PU	32	36	850	0.44	389	362	1.07

It should be noticed that the measured withdrawal resistance of bolts glued with Resorcinol in oversize holes always is less

than the estimated value. It is proposed that this production method is excluded, also in view of the initial hardening shrinkage of the Resorcinol glue.

Considering the variation of the ratio between measured and estimated withdrawal resistance it is found advisable to divide the estimated values with 1.2, 1/1.2 = 0.83. The withdrawal parameters given in the Code proposal has been derived in this way.

The characteristic value of the withdrawal resistance should be estimated by using a characteristic density in equation (6.2.1.2.a) and (6.2.1.2.b)

It appears from table 1.3 that the withdrawal resistance is the same for bolts parallel or perpendicular to grain.

The load duration and moisture content modification factor given in table 5.1.0 of /CIB, 1983/ are not inconsistent with measurements reported in /Riberholt, 1986/. So they should be applicable.

3) Minimum distances and splitting.

The minimum distances are in accordance with proposals in the references. But they are not large enough to secure against failure in the wood arround a group of bolts. But the proposed strength control methods should prevent that.

The method for bolts perpendicular to grain has been verified in /Riberholt, 1986/. The one for bolts parallel to grain has emerged from an engineering comprehension combined with a calibration of some frame corner tests reported in /Riberholt, 1986/ and /Riberholt, 1988/.

4) Stability failure of a compressed bolt.

This failure mode has been observed for a M16 threaded rod. See /Riberholt, 1977/.

5) Requirements to the ductility of the glued bolts.

From tests with frame corners and moment stiff column-foundation connections the proposed rule appears to be reasonable and necessary. Otherwise a zipper-failure may occur because small inaccurancies can result in, that one bolt takes a large part of the force, it fails and then the next bolt will be overloaded and fail. The zipper-failure may be counteracted by use of a ductile (a long glued-in length) bolt connection.

Comments to chapter 8.3. Construction of joints.

1) Corrosion protection

For glued bolts loaded axially it is essential that corrosion is prevented. Otherwise the rust will have to transfer the large shear stresses and the bonded connection may be destroied by the expansion of the rust.

Threaded rods with a zinc coating as reguired in chapter 4.7 of /CIB 1983/ should function properly. Further, it is not critical if the bonding of the zinc to the steel is of poor quality.

Some glues give to some extent a corrosion protection, but for bolts with a threaded surface it is suggested not to rely on that effect. But for bolts with a smooth surface it is questionable to use a zinc coating because it could be difficult to produce a sufficient reliable and strong adhesion between zinc and steel.

2) Production of a glued-in bolt connection

If the glue bonds to the bolt it appears to be reasonable to use an oversize hole. But in the other case oversize holes result in

a reduction of the withdrawal resistance, see table 1.3 with comments. Further the initial shrinkage of the Resorcinol glue may cause a less reliable strength.

It is essential to have a longitudinal groove in a threaded rod which is screwed into a hole. With no groove there will during the screwing be formed a hydrostatic pressure, which will split the wood.

3) Tightening of bolts.

The identical tightening of the bolts should secure against the previously described zipper-failure when the very glued bolt connection has a certain ductility.

References.

CIB, 1983. Structural Timber Design Code. Sixth edition.

Ehlbeck, Jürgen & Siebert, Wichard, 1987. Praktikable Einleimmethoden und Wirkungsweise von eingeleimten Gewindestangen unter Axialbelastung bei übertragung von grossen Kräften und bei aufnahme von Querzugkräften in Biegetragern. Teil 1. Uni. Fridericiana Karlsruhe.

Möhler, Karl & Hemmer, Klaus, 1981. Versuche mit eingeleimten Gewindestangen. Lehrstuhl für Ingenieurholzbau und Baukonstruktionen. Universität Karlsruhe.

Riberholt, Hilmer, 1977. Bolte indlimet i limtræ. Rapport R 83. Dept. of Struc.. Eng. Technical University of Denmark. (Report R 99 is a German translation).

Riberholt, Hilmer & Spøer, Peter 1983. Indlimede bolte til indfæstning af vingerne på Nibe-mølle B. Rapport R 167. Dept. of Struc. Eng. Technical University of Denmark.

Riberholt, Hilmer, 1986. Glued bolts in glulam. Report R 210. Dept. of Struc. Eng. Technical University of Denmark.

Riberholt, H., 1988. Glued bolts in glulam. Part 2. Report R 228. Dept. of Struc. Eng. Technical University of Denmark.

CIB-W18A/21-7-3

INTERNATIONAL COUNCIL FOR BUILDING RESEARCH STUDIES AND DOCUMENTATION

WORKING COMMISSION W18A - TIMBER STRUCTURES

NAIL PLATE JOINT UNDER SHEAR LOADING

by

T Poutanen
Tampere
Finland

MEETING TWENTY-ONE
PARKSVILLE, VANCOUVER ISLAND
CANADA
SEPTEMBER 1988

Nail Plate Joint under Shear Loading

by

T. Poutanen
M.Sc. (dipl.eng.), Director, Insinööritoimisto Tuomo Poutanen Ky, Omenapolku 3A, SF-33270 TAMPERE, FINLAND
Specialist lecturer, Tampere University of Technology

Abstract

Some (15) shear tests with nail plate joints were conducted. The new thing was that the stress distribution (i.e. the moment distribution) was measured. It was found that the joint behavior changes considerably if the plate has a plastic deformation. The present nail plate design and testing allows and utilizes steel plasticity: The characteristic values of the nail plate are defined after the steel plasticity limit and the design assumption for the stress distribution in the joint is assumed to be a plastic one. This brings some advantages e.g. the design values for shear are high and it is believed that the design is simple. But there are disadvantages too: the calculation actually becomes more complicated because the analysis model should take into consideration the degree of plasticity (or if plate plasticity is not considered the calculation is inaccurate and even unsafe); further the plasticity (at least in some common cases in practice) leads to an unfavorable stress distribution and to an excess timber volume.

The paper also considers two phenomena in a nail plate joint: lock action and gap constraint action and concludes that the lock action cannot be utilized in spite of its potential benefits and the gap constraint action is mainly harmful but in some cases it can be used for useful purposes.

In the author's opinion it is very obvious that linear joint behavior leads to a better total reliability, quality and economy than the present concept based on the strength criterion and plastic joints.

Contents

1. Introduction

1.1 Background

This paper is based on tests which are a part of a current Finnish research project (behavior of nail plate joint). This paper describes the effect of steel plasticity in a nail plate shear joint on the stress distribution which has not been measured before and its consequences have not been realized. Some further tests have been planned to measure the observed phenomena in full scale trusses. A summary report will be published later. This paper is presented because (in the author's opinion) the phenomena have many consequences in nail plates, nail plate testing and design.

1.2 Aim

The aim of the tests was to study steel plasticity, friction, lock action and gap constraint action in a nail plate shear joint.

1.3 Present tests

The present method to shear test nail plates is based on the two member test recommended by RILEM [1], fig. 1. Norén [2] applied the method in a modified form, fig. 2, and showed that the previous three member test, fig. 3, gives the same result with high accuracy. In Finland the RILEM-test has been applied in slightly simpler form, fig. 4, and the shear test, besides being used to test the shear strength of the plate (steel), is also used to test the lateral resistance strength as explained by Kangas [3].

At present the design shear value of the nail plate is based on the ultimate load; in some cases where the plate buckles the design value may be based on the displacement. The present tests do not pay any attention to steel plasticity.

Van der Put [8] and Lau [9] have made sophisticated studies of nail plate shear joints. These studies show that plasticity brings benefits in strength and ductility.

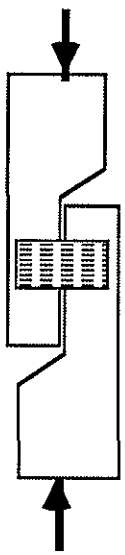

Fig. 1, The RILEM-test

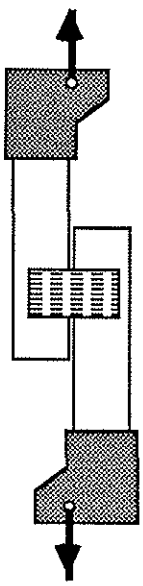

Fig. 2, The RILEM-test modified by Noren

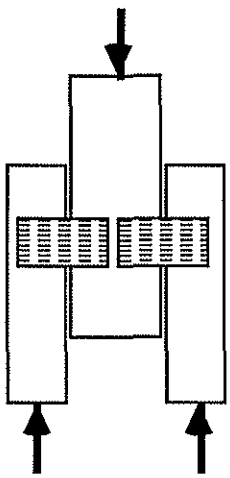

Fig. 3, The old test

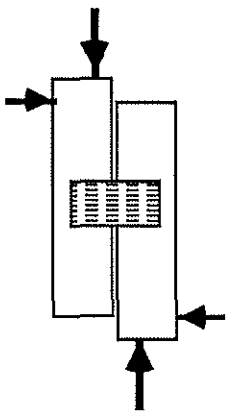

Fig. 4, The Finnish test

1.4 Contact, friction

There has been a lot of discussion whether the tests should be done with or without friction i.e. what should be the gap between the timber members during the assembly. The present RILEM recommendation prescribes a gap of 2 mm in the shear test. This means at least some contact and friction. Long plates having tension force in the main direction may have a big contact and friction which results in a high shear strength. As the contact occurs the results are (at least to some extent) diffuse both from the stiffness and the strength point of view because the plate and the contact have a different behavior e.g. in the slip and the eccentricity calculation. It is better (in the author's opinion) to conduct the tests without the contact i.e. the gap during the assembly should be at least ≈3 mm. If a contact still occurs an even bigger value should be applied. This may be needed in joint types with long narrow plates with tension force in the main direction and also some plates have wide spikes which swell the timber under the plate and reduce the intended gap.

In real structures gaps in the joints (consequently contact and friction, too) vary considerably due to many reasons e.g. a) production accuracy, b) moisture changes in timber and c) load combinations increasing or decreasing gaps. Contact and friction must be utilized carefully due to their diffuse behavior and it should happen explicitly in the design phase. The present procedure is not a good one. The nail plate approvals include an undefined amount of friction which is not a good basis for design. It is not possible to judge to what extent the friction can be utilized.

Due to the problems in friction and contact calculation it may be prescribed that the friction must not be utilized (in addition to the approvals). This restriction would obviously not have much effect in practice but it does not look elegant as the friction really exists in the structures because contact must be required. The present structures cannot be made (with the present nail plates) without contact. Joints with big compression force (e.g. top chord splice and apex) or big moment must have contact, and if not, completely new and more expensive nail plate types must be developed or the potential scope of trussed rafters is essentially reduced.

1.5 Concept of orthogonal strength

Bovim and Aasheim [4] have suggested that the steel strength of nail plates is derived from the basic six strength values in the main directions (p_{at}, p_{ac}, s_a, p_{bt}, p_{bc}, s_b). This method apparently works well if the steel is fully plasticized on the joint line. Different nail plates plasticize differently (mainly depending on the opening pattern) but (probably) all plates plasticize before failure if the plate is large enough not to have an anchorage failure. This new concept requires a full plasticity of steel. The author's studies of joint eccentricity [7] and the new phenomena explained here support the concept of not having any plasticity because steel plasticity (often) leads to an unfavorable stress distribution and increased timber volume. Further steel plasticity actually makes the calculation more complicated though the approximate analysis is a simple one. That is why the concept of orthogonal strength can (apparently) be applied only in simplified and approximate calculations.

2. Test assembly

The tests were conducted in the assembly shown in appendix 1. There were four timber beams to create two coupled symmetrical joints to eliminate the possible nonsymmetrical eccentricity stresses caused by the gripping mechanism. The moment was measured at the middle of the center beams by a method explained by the author [5] using direct computer registration. The computer was used to obtain a moment versus load graph. This moment defines the eccentricity of the end joints. There is a direct relation between the eccentricity and the moment and for the sake of simplicity the results are presented in unitized form: relative eccentricity (er), e.g. er=50% meaning eccentricity h/2 and moment F*h/2.

3. Results

The results have been presented in appendixes 2 and 3. The symbols used have been explained in appendix 3. The major result applies the eccentricity (er) and the increase in the eccentricity (D) at the failure load level compared to the medium and the low load levels. Fig. 5, applying test #1, shows a typical graph of load (F) versus eccentricity (er). In all cases the eccentricity increases considerably after a load level of appr. 60% of the ultimate. At lower load levels the eccentricity remained somewhat constant but very low load levels often had a little higher eccentricity than the medium ones.

Test #2 had originally the plate size 192*100 but before failure the plate was cut in the middle and the test was continued with two plates 96*100 as denoted by test #3. In this case the relative eccentricity should be ≈50% regardless of the plate plasticity and this case is not comparable to the other tests and tests #2, 3 have been excluded from the further considerations.

The major message of the tests lies in the increase in eccentricity at failure load compared to the low and medium load levels (denoted as D). The mean increase in eccentricity was 16% and the biggest increase was 28% (test #13). The smallest increase was 6% (test #6); in this case the reason for the small value clearly was the lock action.

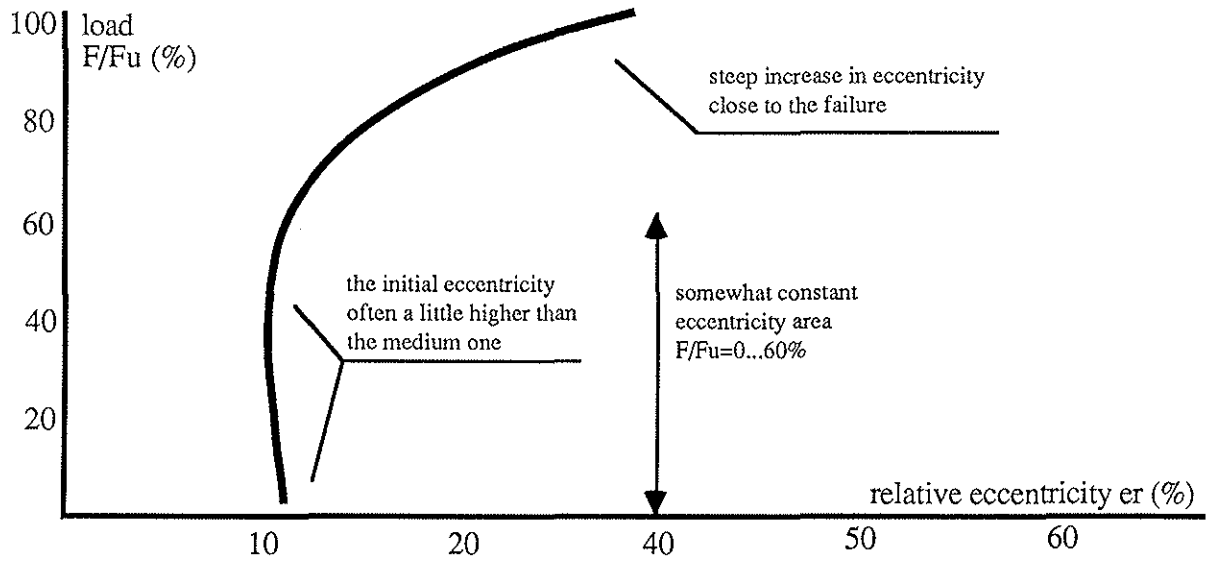

Fig. 5, Typical graph (applying appr. test #1) of relative eccentricity (er) versus load (F)

4. Discussion

4.1 Steel plasticity

The author has shown [7] that there are three eccentricities, timber, plate and contact eccentricity to be considered in joint analysis. If the plate has a plastic deformation the location of the force between the plate and the timber cannot be defined easily. At low load levels the plate acts on its full size and the plate force can be defined from the anchorage area with satisfactory accuracy, fig. 7. If the plate plasticizes only the joint line (and the plate close to it) is active and the location of the plate force must be defined differently. It would be quite complicated to calculate the "exact" location of this force but probably the joint line (or ≈20 mm away from it) might be a good approximation, fig. 8. But the plasticity would bring a more complicated problem: the steel plasticity opens a new dimension in the

joint. The forces acting on the plate are not controlled by the anchorage area only but also the degree of plasticity on the joint line. The degree of plasticity has a two-way effect: it limits the forces which the plate can transfer and it relocates the forces in the plate. The degree of plasticity defines the force location on the joint line and it may be called a "joint line eccentricity" i.e. a fourth eccentricity in a nail plate joint (in addition to three others: timber, plate and contact eccentricity). Thus plate plasticity raises joint modeling to a higher level of complexity. This eccentricity can be avoided by not allowing any plastic deformation in the plate.

One may try to avoid these complicated calculations and use simplified methods. If the nail plate may plasticize the present pin joint-edge eccentricity model comes to mind first, fig. 11. But as shown by the author [7] this is very approximate and it leads in some cases to an unsafe design and in some other cases to unrealistically high stresses and uneconomic structures. To get a satisfactory outcome the joint eccentricity and the moment bearing behavior must be considered. The author does not see this possible in practice other than assuming linear joint behavior i.e. steel plasticity should not be allowed.

There is one more consideration which has some importance: the moment can transmit over the joint via three paths: a) eccentric plate, b) eccentric contact and c) rotation difference between the timber and the plate. As the steel yielding happens the last path practically completely disappears and the plate eccentricity is further defined by the joint line and not by the whole plate size and the plate location. This means that a considerable part of the moment bearing potential is lost. The practical meaning is the following: as the load increases the normal force also increases linearly regardless of the joint type (in most structures) but due to the steel yielding the moment increase is far less than the linear one and the stresses are transferred from joints to timber. The consequence is higher stress in timber and an increased timber volume.

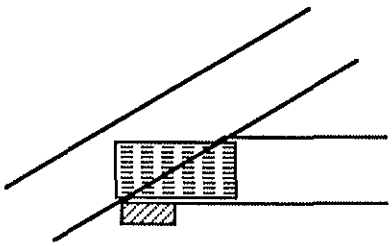

Fig. 6, A heel joint to demonstrate eccentricity

Fig. 7, If plasticity is not allowed the plate acts with its full size and the plate-timber force is located in the middle of the anchorage area

Fig. 8, If the plate plasticizes only the plate close to the joint line is active

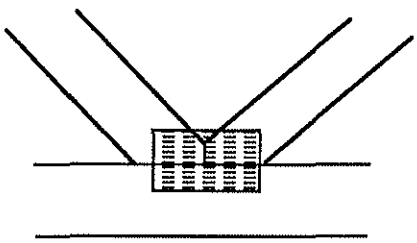

Fig. 9, K-joint to demonstrate the analysis model

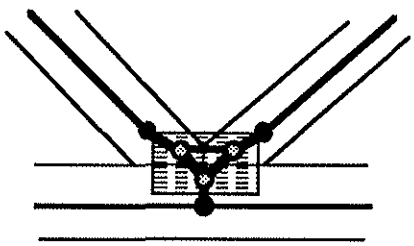

Fig. 10, The model if plasticity is not allowed

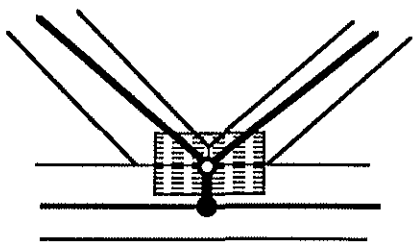

Fig. 11, The approximate model if plasticity is allowed

4.2 Lock action

Lock action occurs mainly in a tension shear joint with a long and narrow nail plate, fig. 12, but it may occur with a smaller effect in standard shear joints. In the lock action joint the plate presses the timber members to each other and due to friction the joint strength may be very high or even infinity (because with some plates the failure never occurs at the joint). After some initial slip the friction locks the timber members to each other and no slip (in the sense of a mechanical fastener) happens in the joint. This applies also to rotation and the joint is completely moment rigid. Rigid joints bring clear benefits in practical design and one may wonder if the lock action cannot be utilized. Some tests were conducted and the benefits could be recorded. The lock action can be seen in tests #11,12 and 13. These tests differed from each other only as to the gap 0, 2 and 4 mm. Test #11 with no gap had the biggest ultimate load, the least eccentricity, the least increase in eccentricity and the least slip. This means that a part of the load has been transferred via friction but the eccentricity has not increased, which is possible only if there occur simultaneously perpendicular forces i.e. compressive forces which compensate for the increased eccentricity due to friction. On the whole the joint behaves closer to a glued joint than the other ones. In this case lock action shows all its benefits: high ultimate load, small slip, small eccentricity. However, the tests have not been continued because other things have appeared to make lock action look less interesting: lock action requires an initial slip which is based on the steel plasticity of the plate or alternatively the gap must be very narrow.

A narrow gap is not possible in practice and (in the author's opinion) steel plasticity should not be allowed. In all cases the plate size and the load combination must be suitable to lock action so it occurs only in a few shear joints. Further lock action is largely subjected to the (mainly unfavorable) gap constraint action. Therefore lock action apparently cannot be utilized in standard trussed rafter design (or if the designer wants to utilize lock action the most benefits are gained by standard friction calculation).

The friction existing in the present nail plate approvals is mainly caused by lock action.

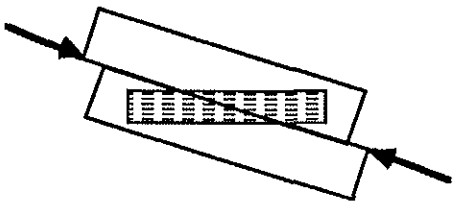

Fig. 12, A joint with lock action

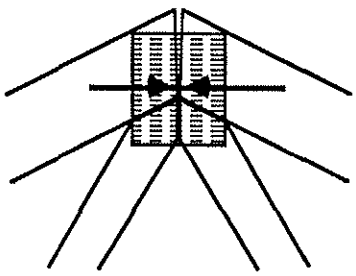

Fig. 13, A joint with gap constraint action due to (defined) compression force

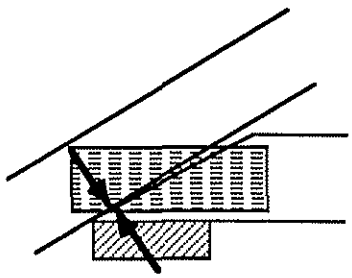

Fig. 14, A joint with gap constraint action due to (undefined) lock action

4.3 Gap constraint action

Cap constraint action may be defined as the action (mainly the eccentricity moment) created by the contact force in cases where the contact location is essentially caused by nonparallel contact surfaces. This force creates an excess

moment (compared to parallel contact surfaces) and it may vary greatly due to the contact force size and the location. The force may be created by the compression force in the timber, fig. 13 or by lock action, fig. 14. The first case can be calculated with reasonable effort during the design phase. The latter case occurs in shear joints and the author does not know a means of considering it in practical design. In both cases the action depends upon the gap size and form. As the author can see it, gap constraint action created by lock action is mostly harmful. It is by nature an excess load which can be avoided (practically completely) if steel plasticity is not allowed. This is one further disadvantage of steel plasticity.

If again the normal force creates the action it can be calculated in the design phase and used to improve the design aims in two cases: the joint can be formed in such a way that the contact occurs in a good location (i.e. bringing a benefit to the stress distribution). Another possibility is to form the joint by not allowing any contact at all or the contact is excluded in the bad location.

There were two test couples #8, 9 and #14, 15 which show the effect of gap constraint action in a shear joint. A negative gap, tests #8 and #14, shows smaller eccentricity.

4.4 Consequences in practice

It is quite clear that the problem is a complex one and to be able to draw definite conclusions full-scale tests and design would be needed. However the following study is presented to estimate the consequences in practice:

Steel plasticity changes the nail plate behavior considerably. According to the test conducted the average relative eccentricity changed 16%, the maximum change was 28%. The phenomenon applies to the failure load level. If the characteristic values of the plate have been made (according to the present practice) following the strength criterion the phenomenon is fully developed in a "tough" design.

As plasticity is not considered in the design it must be handled as excess load. The test indicates that this load is er≈16%. The timber members in rafters are stressed approximately equally by the normal force and the moment. The original dimensioning equation

$$\frac{N}{b*h*f} + \frac{M}{b*h^2/6*f} = 0.5 + 0.5 = 1.00 \qquad (1)$$

becomes after steel yielding

$$\frac{N}{b*h*f} + \frac{M}{b*h^2/6*f} + \frac{0.16*h*b*h*f*.5}{b*h^2/6*f} = 0.5 + 0.5 + 0.48 = 1.48 \qquad (2)$$

According to this the csi (compound stress index) increases by 48% (due to steel plasticity). The maximum increase in eccentricity was 28% and consequently the increase in csi is 84% i.e. practically the whole moment capacity of the timber is spent by the excess plasticity moment and the timber beam would not stand any other moment. If the beam were fully loaded by a normal force the eccentricity increase of 16% would increase the csi by 96% in the average case and 168% in the maximum one.

Now we have to judge whether the deduction is relevant in practice. There are (at least) three reasons why the deduction overestimates the consequences: a) The tests represent a completely unsymmetrical joint which has the biggest change due to steel plasticity. In a symmetrical joint (with symmetrical timber beams) the phenomenon explained here does not occur at all. Practical joints lie between symmetrical and unsymmetrical ones. b) The moment caused by steel plasticity and other moments do not necessarily coincide in their maximum value and in many cases a direct addition is not valid. c) The nail plate may be overdimensioned with reference to its shear value

and the phenomenon does not occur with its full effect. On the other hand there are (at least) three facts which indicate that the effect is even bigger in practice. d) The tests were done with simple moment-free shear joints. It may be deduced that load combinations which open up the gap show a still bigger effect. e) As the design procedure utilizes moment-bearing joints it may be deduced that steel plasticity has a far bigger effect, probably such an effect that moment-bearing joints are possible only in nonplastic joints (at least in most cases). f) As steel yielding happens the plate size and location loses most of its effect and at the same time the designer loses these tools to adjust the stress distribution.

5. Conclusions

1. Steel plasticity in the nail plate changes the joint behavior considerably and according to the test the eccentricity increased on average by 16%. This produces an excess load increasing the csi by appr. ...50%.
2. Lock action brings many benefits to the nail plate joint but it apparently cannot be utilized in practice due to the requirement of a small gap or a big initial slip.
3. Gap constraint action is mainly harmful in nail plate joints but it can be utilized in some cases.
4. If steel plasticity occurs in a nail plate joint the degree of plasticity should be taken into consideration and if not the calculation includes a considerable error.
5. Nail plate tests should be conducted measuring the steel plasticity limit and the characteristic values of the plate should be fixed to this limit.
6. Nail plate shear tests should be conducted without contact.

6. Acknowledgement

The tests were carried out by M.Sc. Kalevi Kantojärvi, Technical Research Centre of Finland and graduate student Jyrki Oksanen, Tampere University of Technology.

7. References

1. RILEM/CIB-3TT, Testing Method for Joints with Mechanical Fasteners in Load-Bearing Structures, Annex A, Punched Metal Plate Fasteners, CIB-W18/15-7-1, Karlsruhe, Germany, 1982
2. Norén B.: Shear Tests for Nail Plates, CIB-W18/19-7-8, Florence, Italy 1986
3. Kangas J.: , A Detailed Testing Method for Nail Plate Joints, CIB-W18/18-7-4, Beit Orein, Israel, 1985
4. Bovim N.I, Aasheim E.: The Strength of Nail Plates, CIB-W18/18-7-6, Beit Orein, Israel, 1985
5. Poutanen T.: A Method for Moment Measurement in Timber Cross-Section, IUFRO, Turku, Finland, 1988
6. Poutanen T.: Nail Plate Joint Eccentricity, CIB-W18/19-7-8, Florence, Italy 1986
7. Poutanen T.: Eccentricity in a Nail Plate Joint, 1988 Timber Engineering Conference, Seattle, U.S.A. 1988
8. Van der Put T.A.C.M.: Design of Nail Plate Connections, Pacific Timber Engineering Conference, New Zealand, 1984
9. Lau P.W.C.: Behavior of Truss Plate Joints under Shear Loading, FORINTEK, no 03-55-57-401, Ottawa, 1984

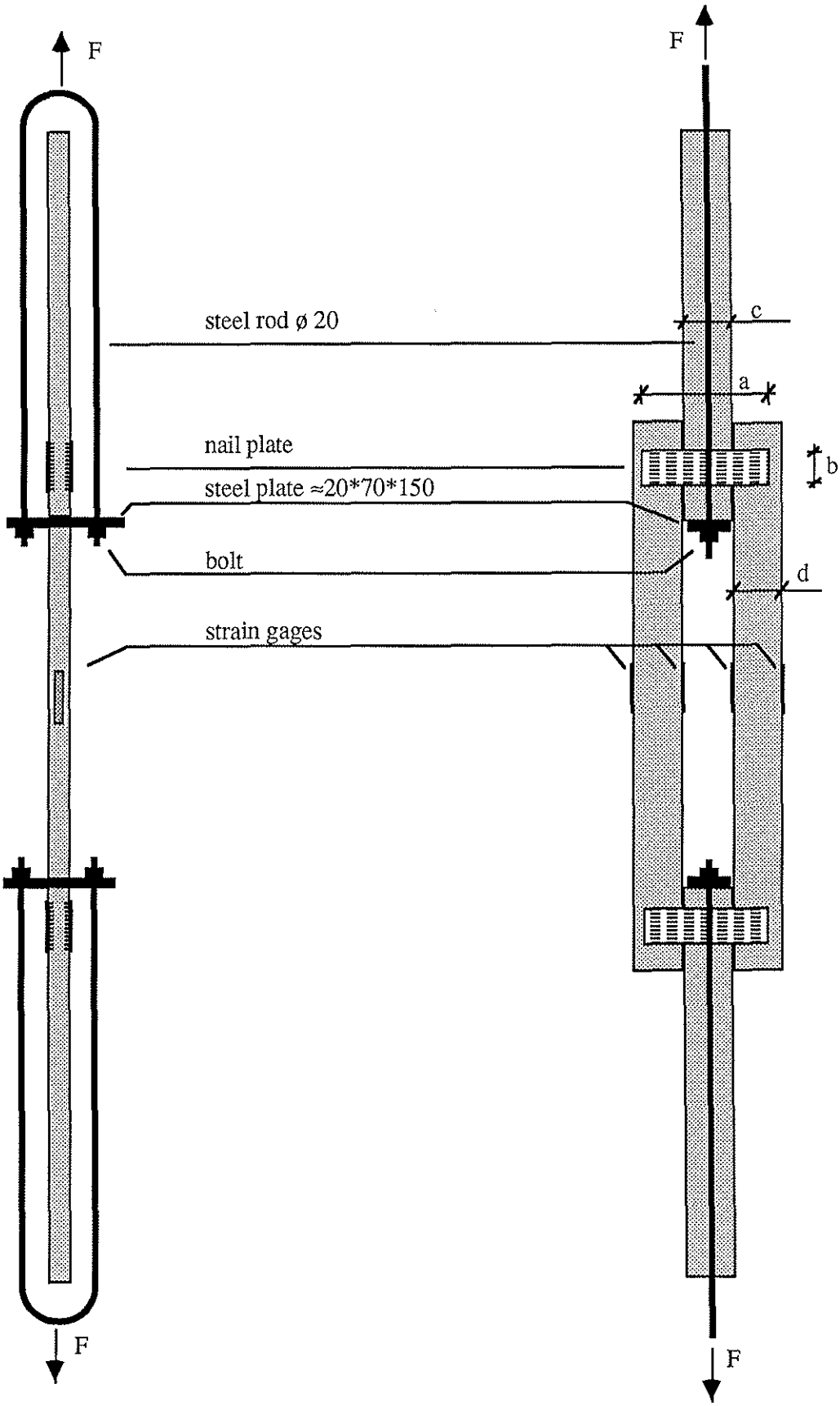
F
F
steel rod ø 20
c
a
nail plate
b
steel plate ≈20*70*150
bolt
d
strain gages
F
F

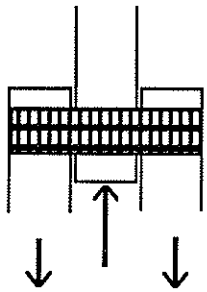

Test #1
P:W288*100
T:48*96+2*48*96,L:1840
E:12000, r:410, u:9.1
A:8800, d:100, g:3
Fu:46750, shear
t:2.65, s:233
er:12...13...38%
D:26%

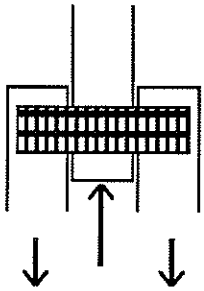

Test #2,3
P:W(192*100) 2*96*100
T:48*96+2*48*96,L:1530
E:12000, r:465, u:9.8
A:4000, d:100, g:3
Fu:43560, anchorage
t:5.45, s:218
er:35...41...51%

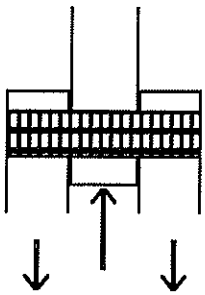

Test #4
P:W288*100
T:48*96+2*48*96,L:1200
E:12000, r:435, u:11
A:9100, d:100, g:0
Fu:57800, shear
t:3.17, s:289
er:15...14...29%
D:15%

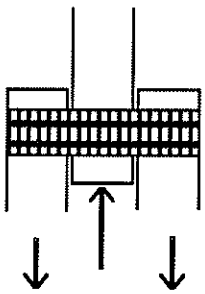

Test #5
P:W288*100
T:48*96+2*48*96,L:2000
E:12000, r:440, u:10.8
A:8800, d:100, g:3
Fu:52480, shear
t:2.98, s:262
er:11...11...30%
D:19%

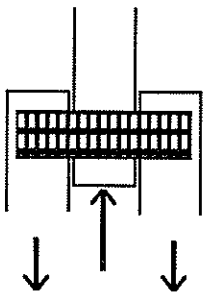

Test #6
P:TFB191*102
T:48*96+2*48*96,L:1690
E:12000, r:430, u:10.5
A:4000, d:100, g:3
Fu:46700, shear
t:5.83, s:234
er:20...21...32%
D:12%

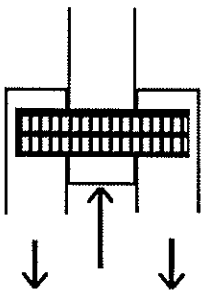

Test #7
P:W192*100
T:48*96+2*48*96,L:890
E:12000, r:445, u:10.5
A:4300, d:100, g:0
Fu:56960, shear, anchorage
t:6.62, s:285
er:23...22...34%
D:12%

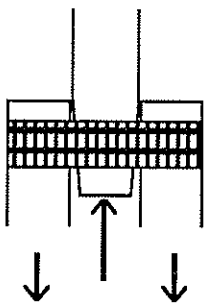

Test #8
P:W288*100
T:48*96+2*48*96,L:940
E:12000, r:445, u:10.5
A:9100, d:100, g:0...3
Fu:55840, shear
t:3.07, s:279
er:19...18...38%
D:18%

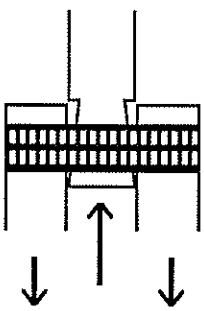

Test #9
P:W288*100
T:48*96+2*48*96,L:620
E:12000, r:410, u:9.5
A:9100, d:100, g:-3...0
Fu:57520, shear
t:3.16, s:288
er:25...23...38%
D:15%

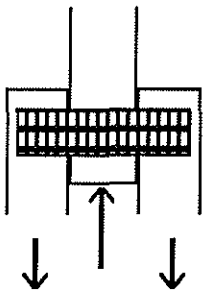

Test #10
P:TFB192*102
T:48*96+2*48*96, L:250
E:12000, r:410, u:9.5
A:4300, d:100, g:0
Fu:50930, shear, anchorage
t:5.92, s:255
er:31...33...47%
D:16%

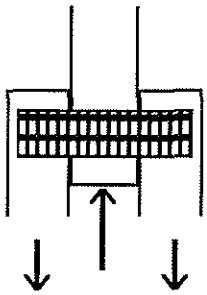

Test #11
P:TOP172*92
T:48*70+2*48*60,L:2000
E:≈12000, r:≈500, u:≈11
A:4186, d:92, g:0
Fu:47880, anchorage
t:5.72, s:260
er:8...7...13%
D:6%

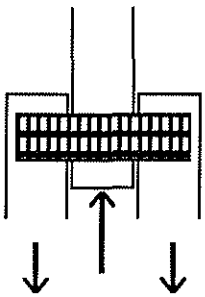

Test #12
P:TOP172*92
T:48*70+2*48*60,L:1700
E≈12000:, r:≈500, u:≈11
A:4002, d:92, g:2
Fu:41840, shear
t:5.23, s:227
er:9...8...21%
D:13%

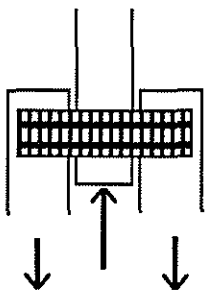

Test #13
P:TOP172*92
T:48*70+2*48*60,L:1410
E:≈12000, r:475, u:10.3
A:3818, d:92, g:4
Fu:42600, shear
t:5.57, s:232
er:11...11...39%
D:28%

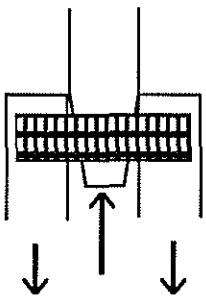

Test #14
P:TOP172*92
T:48*70+2*48*60, L:1100
E:≈12000, r:475:, u:10.3
A:4186, d:92, g:0...3
Fu:47180, shear
t:5.63, s:256
er:6...8...17%
D:11%

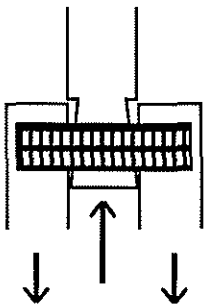

Test #15
P:TOP172*92
T:48*70+2*48*60,L:780
E:≈12000, r:≈450, u:≈10
A:4186, d:92, g:-3...0
Fu:47800, shear
t:5.71, s:260
er:13...13...24%
D:11%

Explanation of symbols:

Test #test number
P:plate type plate width (mm)*plate length (mm)
T:timber depth*width center +2*edges (mm*mm),L: (edge)timber length (mm)
E: MOE (MPa), r: density (kg/m3), u: moisture content (%)
A: eff. area of plate (mm*mm), d: eff. joint length (mm), g: gap (mm)
Fu: ultimate load (N), failure type
t: ultimate (anchorage) shear stress (MPa), s: ultimate shear stress in plate (N/mm)
er: relative eccentricity, low, medium and ultimate load level (%)
D: incease in relative eccentricity (%)

CIB-W18A/21-7-4

INTERNATIONAL COUNCIL FOR BUILDING RESEARCH STUDIES AND DOCUMENTATION

WORKING COMMISSION W18A - TIMBER STRUCTURES

DESIGN OF JOINTS WITH LATERALLY LOADED DOWELS. PROPOSALS FOR IMPROVING THE DESIGN RULES IN THE CIB-CODE AND THE DRAFT EUROCODE 5

by

J Ehlbeck and H Werner
University of Karlsruhe
Federal Republic of Germany

MEETING TWENTY-ONE
PARKSVILLE, VANCOUVER ISLAND
CANADA
SEPTEMBER 1988

Design of joints with laterally loaded dowels

Proposals for improving the design rules in the CIB-Code and the draft Eurocode 5

Jürgen Ehlbeck and Hartmut Werner
University of Karlsruhe, FRG

1 Introduction

During the 20th meeting of CIB-W18A in Dublin 1987 a proposal for the revision of the existing formulae in draft Eurocode 5 |1| was presented by Whale, Smith and Larsen |2|. This proposal was discussed during the meeting, and an additional comment and modifying proposals were announced, based on recent tests carried out with dowels (drift bolts) at the University of Karlsruhe (FRG). One of the reason of this research work |3| was to clear up the question if it is necessary to stagger the dowels in a joint with respect to the grain direction of the timber members.

A calculation model based on Johansen's and Moeller's theory (see |4|) was used for evaluating the test data. The results invited to present a new proposal to modify the formulae for calculating the characteristic load-carrying capacity of wood-to-wood joints as given in the draft Eurocode 5.

2 Tests

With a total of 149 test specimens as shown in Fig. 1 the load-carrying capacity and the load-deformation behaviour of double-shear dowel joints with a diameter up to 30 mm was investigated with taking into consideration several influencing parameters. All specimens were loaded in grain direction. The ratio of middle member thickness, t_2, to side member thickness, t_1, was constant, with $t_2/t_1 = 1.33$. The

joint configuration (see fig. 1) was chosen with the minimum spacing allowable according to the German timber design code DIN 1052. The pre-bored holes in the timber members were equal to the nominal diameter of the dowels. The main investigation was carried out with glulam made of European whitewood (picea abies). The mean density at a temperature of 20 °C and a relative humidity of 0.65 of all glulam members was 443 kg/m^3 with a standard deviation of 36 kg/m^3. Beyond that, solid timber joints made of whitewood (picea abies), European Douglas fir (pseudotsuga menziesii), beech (fagus sylvatica) Afzelia (afzelia bipindensis) and Bongossi/Azobé (lophira alata) were tested. The dowels were cold formed as well as hot forged. The test procedure used was in line with the ISO-Standard 6891 - "Timber structures - Joints made with mechanical fasteners - General principles for the determination of strength and deformation characteristics."

3 Test results

Detailed test results are given in |3| and are not stated in this paper by reason of extent. The main findings are, however, summarized as follows:

1. There was no significant difference in the load-carrying capacity parallel to grain for dowelled joints having staggered or non-staggered arrangement of the dowels in grain-direction.

2. The load-carrying capacity as well as the stiffness of the joints increased approximately linear with increasing density of the members. For linear regression equations the coefficients of correlation ranged between 0.77 and 0.94. There was, however, a better correlation for compression shear tests than for tension shear tests. This may be attributed to the more brittle failure behaviour of wood under tension compared to compression.

3. The load-carrying capacity of the joints tested in tension shear was significanty smaller than that of compression shear. A reduction of approximately 20 % was realized.

4. The embedding strength, f_h, calculated from the test data using the calculation model as mentioned before, depends on the dowel diameter, d. In Fig. 2 the relationship between embedding strength and dowel diameter is given for glulam (species: picea abies). The linear regression equation, related to the mean density of the wood, reads:

$$\begin{aligned} \bar{f}_h &= 31.95 \cdot (1 - 0.012\ d) \\ &= 0.072 \cdot (1 - 0.012\ d) \cdot \bar{\varrho} \end{aligned} \qquad (1)$$

with a correlation coefficient of r = 0.79.

In equ. (1) is: f_h in N/mm^2; d in mm
ϱ in kg/m^3.

A slight simplification of equ. (1) reads:

$$\bar{f}_h = 0.07 \cdot (1 - 0.01\ d) \cdot \bar{\varrho} \qquad (2)$$

It does not reveal a difference worth mentioning when the load-carrying capacity of the joint is calculated using this equ. (2).

Equ. (2) differs shightly from the proposal of Whale and Smith [5]:

$$\bar{f}_h = 0.082 \cdot (1 - 0.01\ d) \cdot \bar{\varrho} \qquad (2a)$$

This is primarily traceable to smaller spacings of the fasteners used in the tests in Karlsruhe (see also |6|). Thus, a modification factor may be introduced to take into consideration the spacing, a, of the dowels in grain direction and the end distance, a_1, from the square-cut end of the member.

Draft EUROCODE 5		DIN 1052	
a	= 7 d	a	= 5 d
$a_{1,t}$	= 7 d	$a_{1,t}$	= 6 d
$a_{1,c}$	= 4 d	$a_{1,c}$	= 3 d

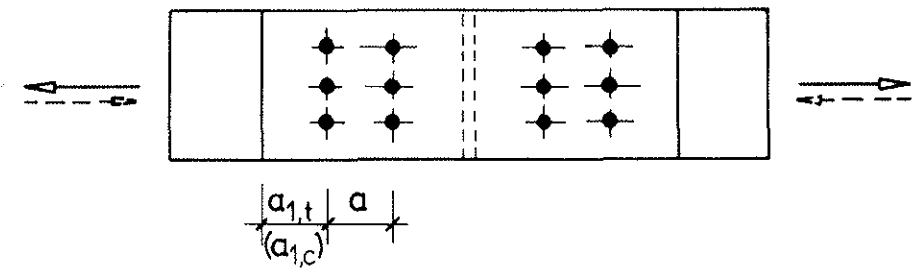

Minimum spacings of dowels

In draft Eurocode 5 the minimum spacings and end distances are:

$$a = 7\ d \quad \text{and} \quad a_1 = 7\ d \ \text{(tension)}, \ 4\ d \ \text{(compression)}$$

In this case equ. (2a) may be assumed to give reliable values for the embedding strength.

In the German design code DIN 1052 the corresponding values are:

$$a = 5\ d \quad \text{and} \quad a_1 = 6\ d \ \text{(tension)}, \ 3\ d \ \text{(compression)}$$

Then equ. (2) is appropriate.

Using

$$\bar{f}_h = k_a \cdot 0.082 \, (1 - 0.01 \, d) \, \bar{\varrho} \qquad (3)$$

it can be proposed to take $k_a = 1$ if the spacings according to draft Eurocode 5 are observed, whereas $k_a = 0.85$ for spacings according to DIN 1052.

If other spacings and end distances are chosen other k_a - values are appropriate.

5. The simplified formula for symmetrical 3-member joints, as proposed by Whale, Smith and Larsen (see |2|) reads:

$$\frac{R_u}{f_1 \cdot d^2} = 0{,}5 \cdot \sqrt{\frac{2}{3} \cdot \frac{f_2}{f_1 + f_2} \cdot \frac{f_y}{f_1}} + 0{,}2 \cdot \frac{t_1}{d} \qquad (4)$$

This equation is identical with equ. (5.3.5e) in draft Eurocode 5 for $f_1 = f_2 = f_b$ and $f_y = 240$ N/mm² with the force acting in direction of the grain. This formula is valid in case that the failure of the joint occurs with two yield points in the dowel. The evaluation of test data showed that this equation agrees better than the strong theory. This can be seen from Figs. 3 to 6 showing the load-carrying capacity per shear plane for a symmetrical 3-member joint in relation to the slenderness-ratio t_2/d for different dowel diameters.

6. The evaluation of the test data proved that it is more realistic to use a "fictive" yield strength being the arithmetic mean of the tensile strength and the yield strength of the dowel:

$$f_y^* = 0.5 \, (f_t + f_y) \qquad (5)$$

This is explicable with the fact that, especially hot forged steel, has a substantial strain hardening effect beyond a distinct yield point.

7. It was found that the embedding strength of Bongossi/Azobé (Lophira alata) was not significantly dependent on the dowel diameter. This effect may be attributed to hardwoods with low tendency to splitting and should be investigated in additional tests.

8. The slip modulus, C, per shear plane and dowel as defined in ISO 6891, is dependent of the dowel diameter as well (see Fig. 7). The mean value can be described as:

$$\bar{C} = (1.2\ d - 1.6) \cdot \bar{\rho} \qquad (6)$$

with $\bar{C}$ in N/mm ; d in mm; $\bar{\rho}$ in kg/m^3.

The slip modulus of the hardwoods tested was approximately 25 % higher. For simplification (see Fig. 7) it may be assumed

$$\bar{C} = d \cdot \bar{\rho} \qquad (7)$$

because a rather high variation was observed in one test series, and some influencing parameters - such as friction and steel quality - under serviceability loads are difficult to grasp.

4 Proposals

Based on the results described, the following proposals can be made to improve the design formulae given in the draft Eurocode 5 and the CIB-Timber design code:

4.1 Factor k_a

Different spacings influence the embedding strength of the individual dowel in a joint. This influence is, above all, depending on the spacing a (distance between dowels in a row parallel to the grain) and the end-distance $a_{1,t}$. This can be taken into account by a factor k_a as given in Table 1.

Table 1: Factor k_a

spacing a \ end distance $a_{1,t}$	4 d	5 d	6 d	7 d
5 d	0,50	0,70	0,85	0,88
6 d	0,55	0,72	0,87	0,92
7 d	0,60	0,75	0,90	1,00

Thus, the embedding strength for laterally loaded dowels, given in Equ. (5.3.6) in draft Eurocode 5, should be changed to

$$f_b = k_a \cdot 0.082 \cdot (1 - 0.01 \cdot d) \cdot \varrho_k \qquad (8)$$

With the minimum spacings and distances given in Fig. 5.3.5 of draft Eurocode 5, $k_a = 1.0$.

This formula also applies for bolts. Hence, it should also substitute Equ. (5.3.5 q) of draft Eurocode 5. There is basically no reason to use different embedding strength values for laterally loaded bolts and dowels.

4.2 Calculation value for the yield strength f_y

Instead of using the real yield strength of the fastener it is more realistic to use a "fictive" yield strength, which can be taken as the arethmetic mean of the real yield strength and the tensile strength of the fastener.

4.3 Influence of compressive shear effect

The formulae given in the draft Eurocode 5 for calculating the characteristic lateral load-carrying capacity of wood-to-wood joints loaded in grain direction are applicable for tension-shear joints. They may be increased by a factor of 1.25 for joints loaded in compression shear parallel to grain.

4.4 Joint slip u

The joint slip of a bolted or dowelled joint at a load level less than 40 % of the characteristic load can be estimated by using the following formula:

$$u = \frac{F}{C} \cdot k_{creep} + u_s \qquad (9)$$

with $$C = d \cdot \varrho_k \qquad (10)$$

(d in mm; ϱ_k in kg/m^3 and C in N/mm)

The slip modulus of hardwoods may be multiplied with a factor of 1,25. u_s is the joint settlement and can be taken as given in Table 2.

Table 2: Joint settlement u_s (mm)

type of joint	softwood	hardwood
laterally loaded bolts	1,2	1,1
laterally loaded dowels	0,2	0,1

This proposal is compared with the test values obtained from the glulam dowel-joints in Table 3. Using equ. (6) and (9) with the actual mean density of the test specimens, there is a good agreement. With a characteristic density of 400 kg/m^3 - as given as an example in Table A 2.2, Annex 2, of the draft Eurocode 5 for a density class of D 400 - slightly greater slip values follow from the lower density.

Table 3: Joint slip under load F; comparison of test results with design proposal

dowel diameter d [mm]	load F [1)] [kN]	slip u [mm] (test results) min.	mean	max.	calculated slip u [mm] (Eqs. 6 a. 9) $\bar{\varrho} = 443$ kg/m³	(Eqs. 9 a. 10) $\varrho_k = 400$ kg/m³
8	1,60	0,35	0,61	0,85	0,65	0,70
16	6,35	0,48	0,98	1,42	1,02	1,19
24	14,25	1,05	1,54	1,95	1,39	1,68
30	22,25	1,10	1,58	2,05	1,66	2,05

1) F : load per dowel and shear plane ($F \simeq 0.4 \cdot F_u$)

5 Remarks to the problem of joints under loads acting at an angle to grain

There are less values available for the embedding strength perpendicular to grain or under an angle to grain. However, Whale, Smith and Larsen proposed to use a factor of

$$\frac{f_{h,\alpha}}{f_{h,0}} = \frac{1}{2{,}3 \cdot \sin^2\alpha + \cos^2\alpha} \qquad (11)$$

α is the angle between force and the direction of the grain.
In the draft Eurocode 5, this influence is taken into account by using k_α -values:

$$k_\alpha = \frac{k_{90}}{k_{90} \cdot \cos^2\alpha + \sin^2\alpha} \qquad (12a)$$

$$k_{90} = 0.32 + 10\, d^{-1,5} \qquad (12b)$$

Equ. (11) corresponds to Equ. (12a, b) in case of d = 20 mm. It must be realized, however, that Whale et al. presume the embedding strength, $f_{h,0}$, to be dependent on the diameter d, whereas in the draft Eurocode 5 a diameter-independent embedding strength is assumed. It should be checked, if the k_α -values in draft Eurocode 5 are still realistic if the embedding strength values given in eqs. (2a) or (3) are used instead of eq. (5.3.5 q) in draft Eurocode 5.

Equ. (11), proposed by Whale et al. leads to significantly lower characteristic load-carrying capacities for $\alpha = 90°$. This may result from tests where in many cases not the embedding strength but the

Table 4: Test results of glulam joints with dowels d = 16 mm loaded perpendicular to grain (Möhler/Siebert 1980)

test No.	m / n[1)]	h [cm]	a_r [cm]	$\frac{a_r}{h}$	F_u [N]	$f_{h,90}$ [N/mm^2]	k_{90} [2)]	failure mode [3)]
V 2	3 / 2	120	30	0,25	7500	9,38	0,363	TPG
V 3	3 / 4	120	30	0,25	4667	5,83	0,226	TPG
V 4	2 / 2	120	30	0,25	8125	10,16	0,394	TPG
V 24	3 / 2	60	15	0,25	5792	7,24	0,281	TPG
V 27	3 / 2	60	15	0,25	5208	6,51	0,252	TPG
V 28	2 / 2	60	15	0,25	7000	8,75	0,339	TPG
V 9	3 / 6	120	60	0,50	4986	6,23	0,242	TPG
V 11	3 / 4	60	30	0,50	4583	5,73	0,222	TPG
V 25	3 / 2	60	30	0,50	6250	7,81	0,303	TPG
V 13	3 / 2	60	45	0,75	15000	18,75	0,727	ES
V 23	3 / 2	120	90	0,75	15833	19,72	0,767	ES
V 26	3 / 2	60	45	0,75	18333	20,48	0,794	YM

1) m : number of rows
n : number of dowels in line

2) $k_{90} = \frac{f_{h,90}}{f_{h,0}}$
$f_{h,0} = 25,8 \ N/mm^2$

3) TPG : tension – perpendicular – to – grain failure
ES : embedding strength in middle member was reached
YM : yield moment of dowel was reached

tensile strength of the member perpendicular to grain caused the failure of the joint. Möhler and Siebert |7| tested joints with glulam beams with loads acting perpendicular to grain (see Fig. 8). Some results of these tests are listed in Table 4.

It becomes obvious that the load-carrying capacity of such joints depends on the configuration of the joint, i.e. primarily the ratio of a_r/h. In all cases with a_r/h less than 0.7 there were tension-perp-to-grain failures, and the resulting "fictive" embedding strength, $f_{h,90}$, of the middle member was extremely low and the k_{90}-value, defined as

$$k_{90} = f_{h,90}/f_{h,o} \qquad (13)$$

was less than 0.4.
For $a_r/h > 0.7$, real embedding strength failures happend, and the k_{90}-value was between 0.7 and 0.8.

Consequently, it is of immense importance to check the danger of failure due to exceeding the tensile strength perpendicular to grain. This must be proved in cases where a_r/h is less than 0.7. It should be reconsidered to add an appropriate note in the draft Eurocode 5 or the CIB-Code, respectively. More research work in this field is suggested.

6 Notations

f_h	=	Embedding strength
$\bar{f}_h$	=	Mean embedding strength
$f_{h,1}$; f_1; $f_{h,0°}$	=	Side member embedding strength
$f_{h,2}$; f_2	=	Middle member embedding strength
$f_{h,k}$; f_b	=	characteristic embedding strength
$f_{h,90}$	=	Embedding strength perpendicular to grain
f_y	=	Yield strength of fastener
f_y^*	=	fictive yield strength
f_t	=	Tensile strength of fastener
F	=	Load
F_u	=	Load-carrying capacity (ultimate load)
R_k	=	Characteristic load-carrying capacity
C	=	Slip modulus
$\bar{C}$	=	Mean slip modulus
u	=	Joint slip
u_s	=	Joint settlement
a	=	Spacing
$a_{1,t}$; $a_{1,c}$	=	End distance
a_r	=	Distance of the upper row of fasteners (see Fig. 8)
h	=	Depth of beam
t_1	=	Side member thickness
t_2	=	Middle member thickness
d	=	fastener diameter
$\bar{\varrho}$	=	Mean density
ϱ_k	=	Characteristic density
k_{creep}	=	Creep factor
k_a	=	Factor, taking into consideration the influence of spacing and end distance
k_{90}	=	Factor, taking into consideration the influence of force perpendicular to grain

7 References

|1| Eurocode 5 (1987): Common unified rules for timber structures. Draft published by the Commission of the European Communities, Brussels/Belgium.

|2| Whale, L.R.J., I. Smith and H.J. Larsen (1987): Design of nailed and bolted joints-proposals for the revision of existing formulae in draft Eurocode 5 and the CIB Code. CIB-W18A/20-7-1. Proceedings of meeting twenty of CIB-W18A, Dublin/Ireland.

|3| Ehlbeck, J. and H. Werner (1988): Tragverhalten von Stabdübeln in Brettschichtholz und Vollholz verschiedener Holzarten bei unterschiedlichen Rißlinienanordnungen. Forschungsbericht der Versuchsanstalt für Stahl, Holz und Steine, Abt. Ingenieurholzbau, University of Karlsruhe/FRG.

|4| Larsen, H.J. (1979): Design of bolted joints. CIB-W18/12-7-2. Proceedings of meeting twelve of CIB-W18, Bordeaux/France.

|5| Whale, L.R.J. and I. Smith (1986): The derivation of design clauses for nailed and bolted joints in Eurocode 5. CIB-W18/19-7-6. Proceedings of meeting nineteen of CIB-W18, Florence/Italy.

|6| Yasumura, M., T. Murota and H. Sakai (1987): Ultimate properties of bolted joints in glued-laminated timber. CIB-W18A/20-7-3. Proceedings of meeting twenty of CIB-W18A, Dublin/Ireland.

|7| Möhler, K. and W. Siebert (1980): Ausbildung von Queranschlüssen bei angehängten Lasten an BSH-Träger oder Vollholzbalken. Forschungsbericht der Versuchsanstalt für Stahl, Holz und Steine, Abt. Ingenieurholzbau und Baukonstruktionen, Universität (TH) Karlsruhe.

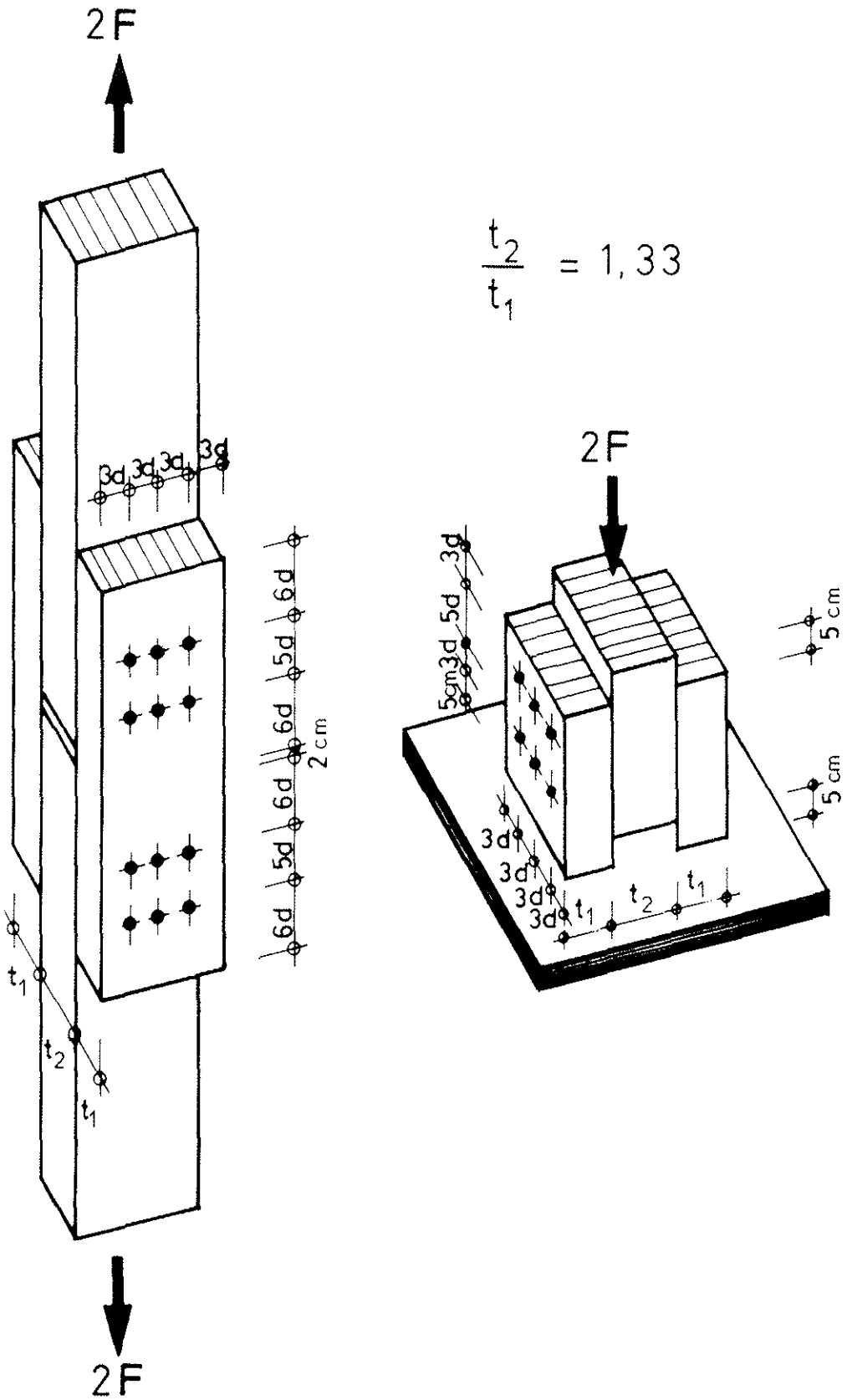

Fig. 1: Specimen for shear tests loaded in tension and compression

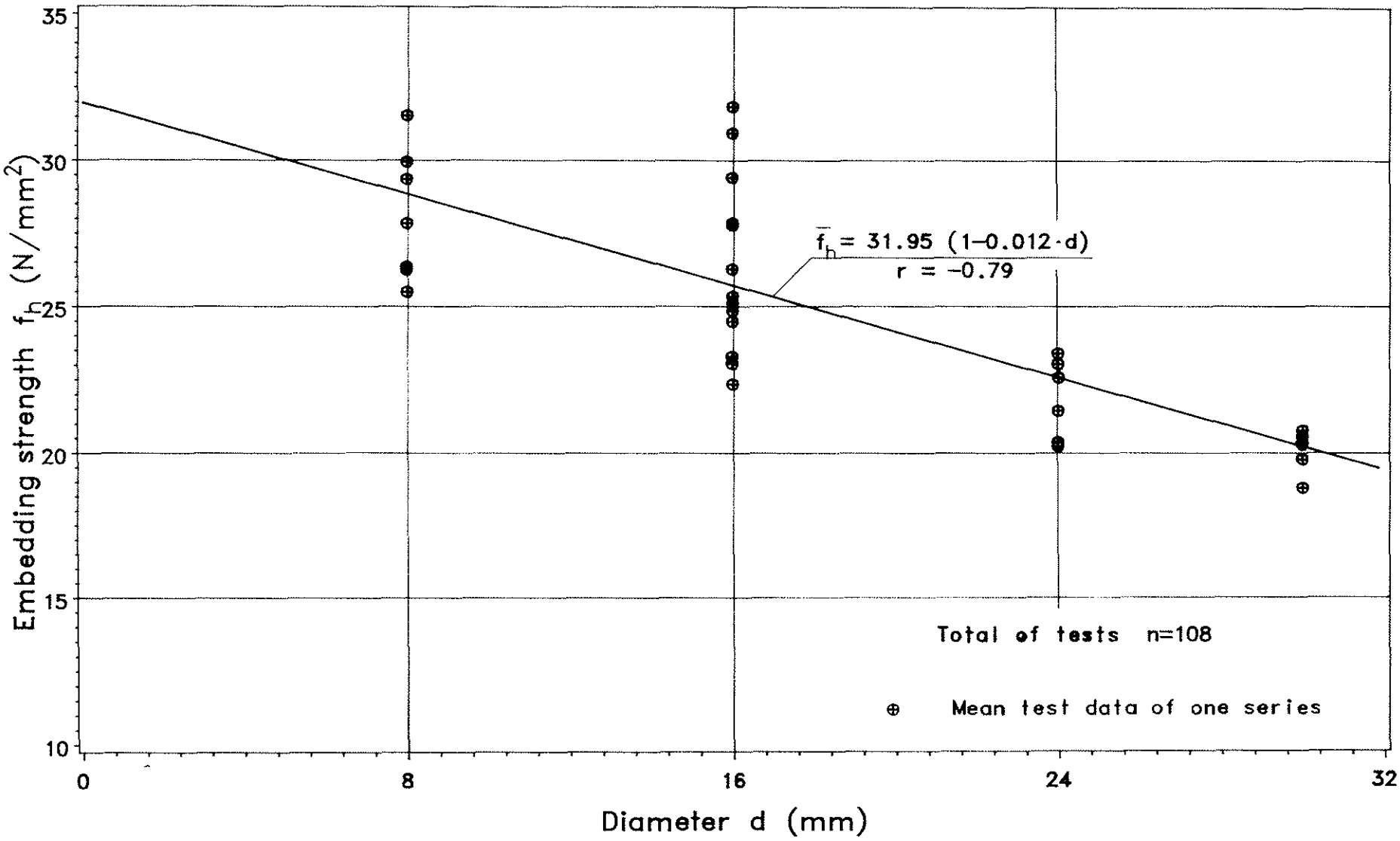

Fig. 2: Embedding strength, f_h, from tests with glued laminated timber over dowel diameter, d

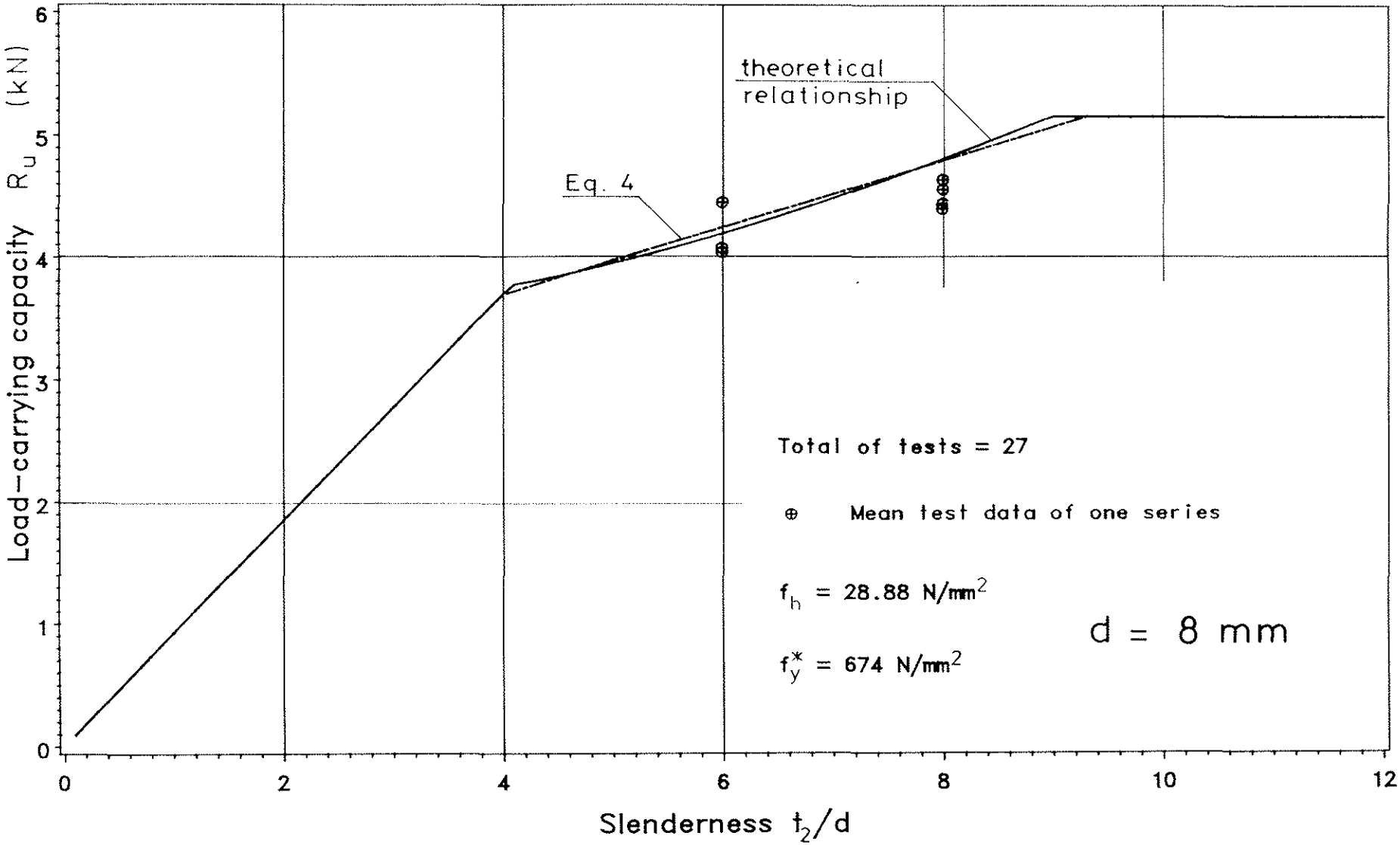

Fig. 3: Load-carrying capacity R_u per shear plane of a symmetrical joint over slenderness t_2/d for a dowel diameter of 8 mm

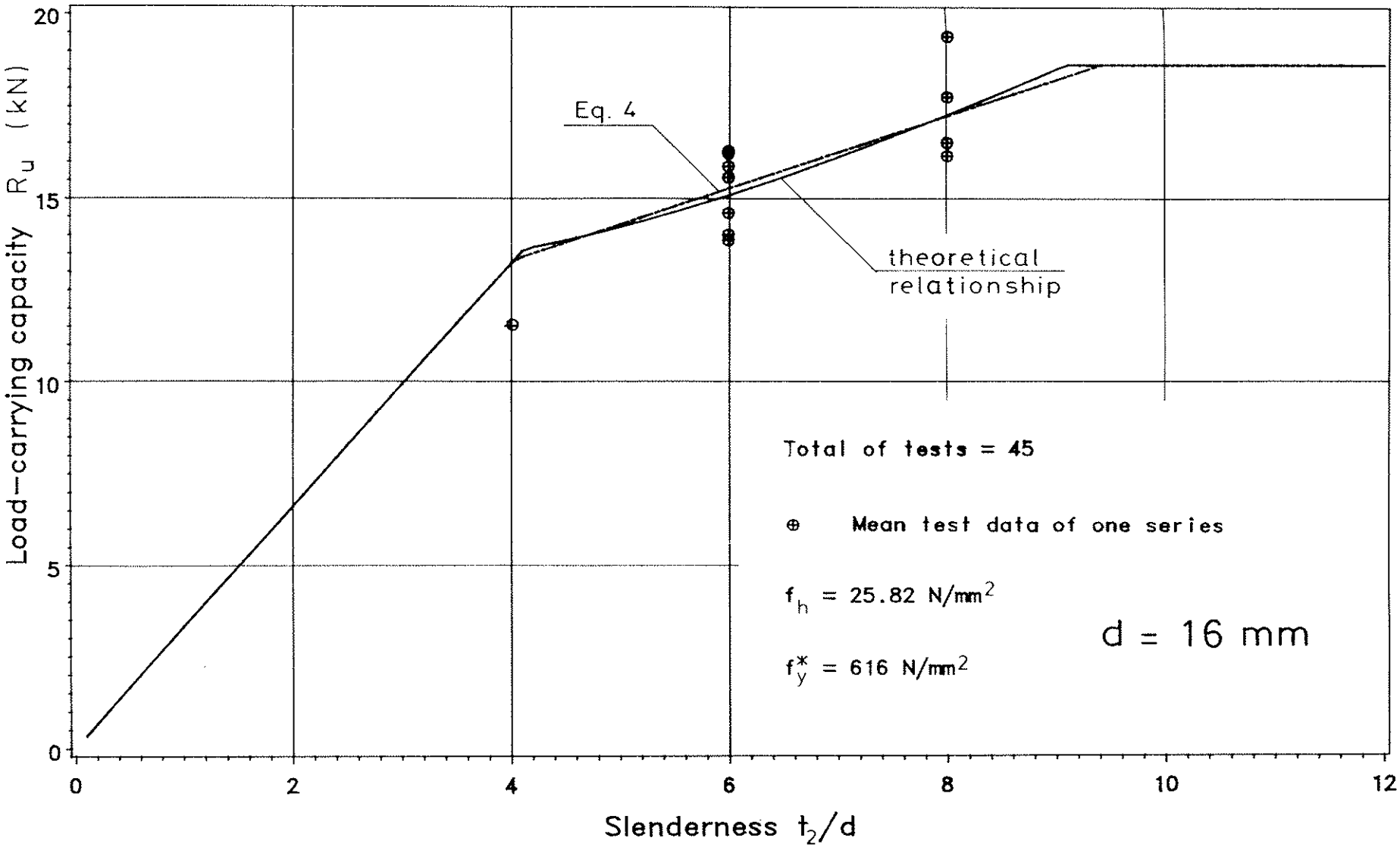

Fig. 4: Load-carrying capacity R_u per shear plane of a symmetrical three-member joint over slenderness t_2/d for a dowel diameter of 16 mm

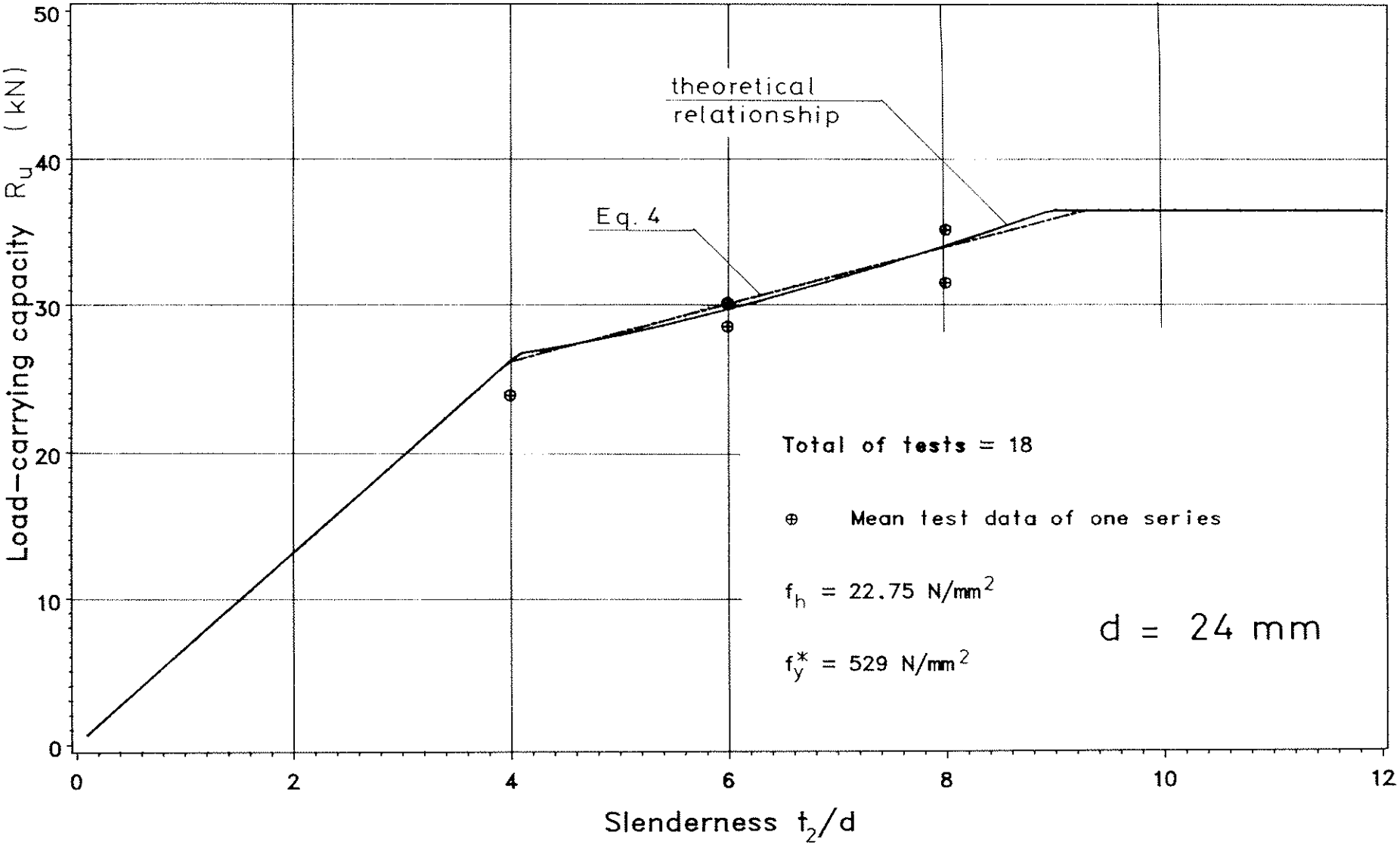

Fig. 5: Load-carrying R_u per shear plane of a symmetrical three-member joint over slenderness t_2/d for a dowel diameter of 24 mm

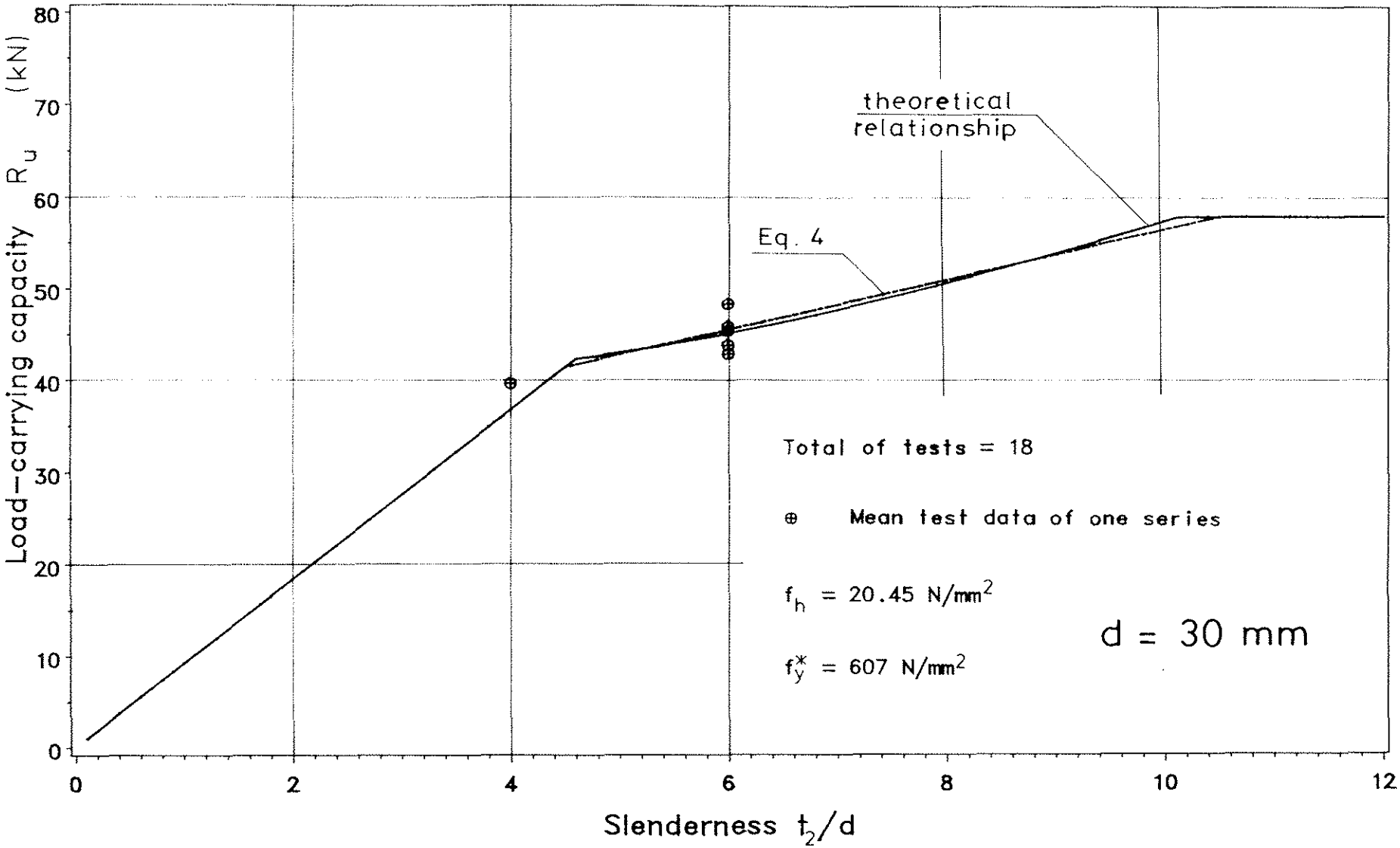

Fig. 6: Load-carrying capacity R_u per shear plane of a symmetrical three-member joint over slenderness t_2/d for a dowel diameter of 30 mm

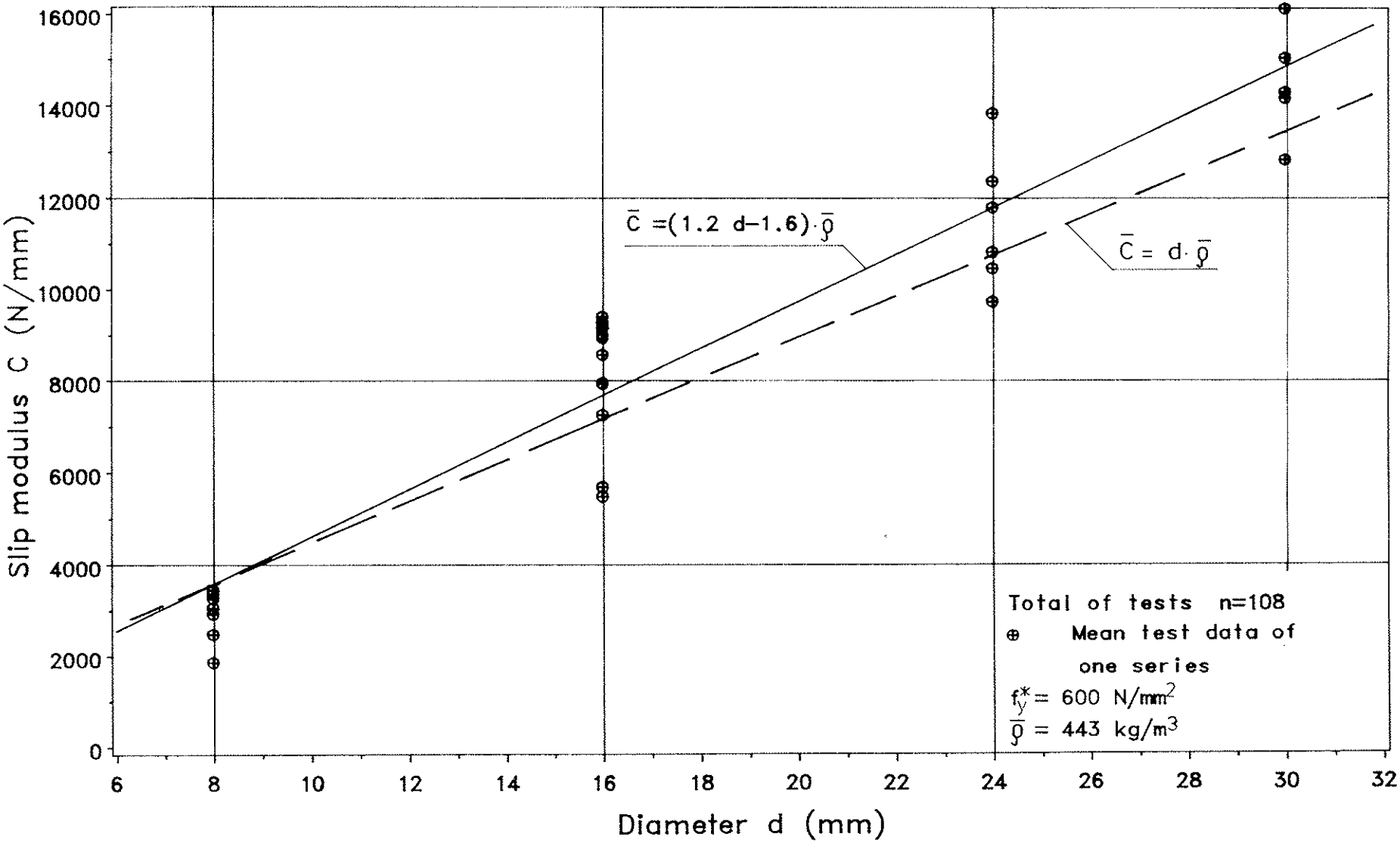

Fig. 7: Slip modulus C per shear plane and dowel of a symmetrical three-member joint over dowel diameter d

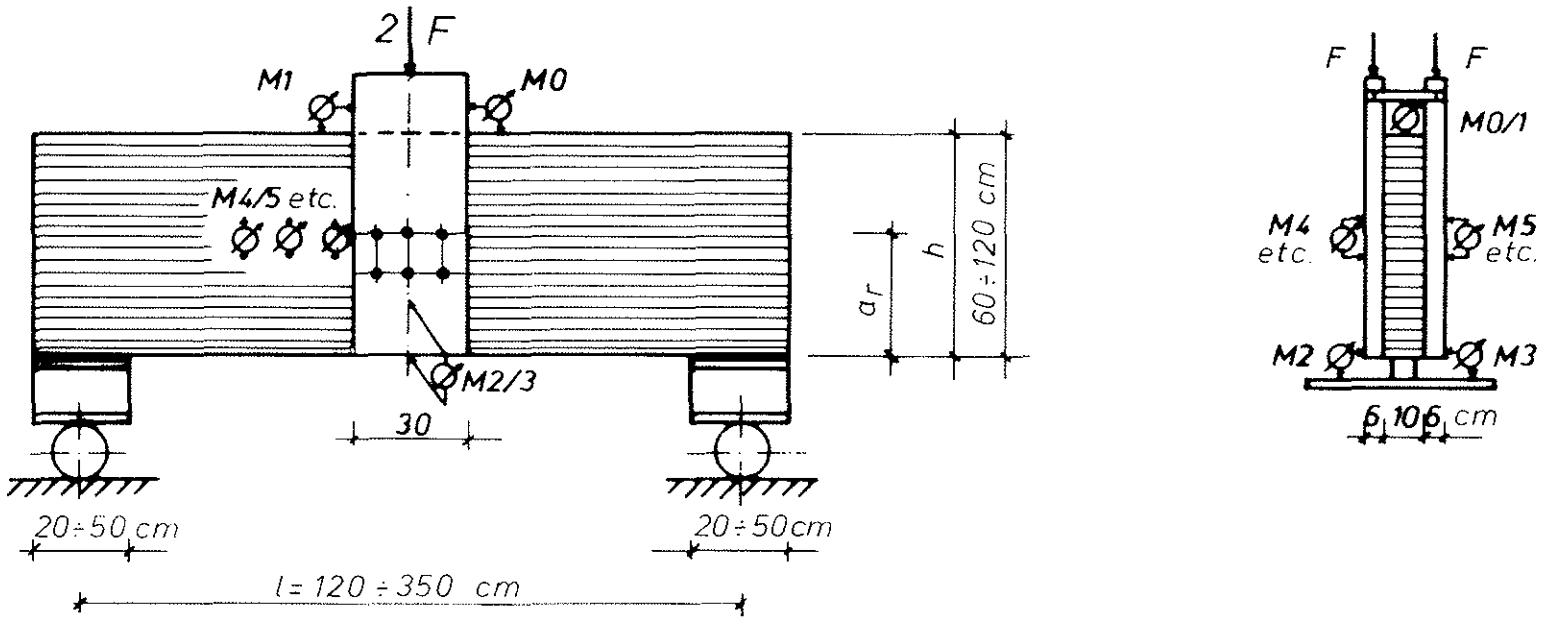

Fig. 8: Specimen and test set-up for joints loaded perpendicular to grain

CIB-W18A/21-7-5

INTERNATIONAL COUNCIL FOR BUILDING RESEARCH STUDIES AND DOCUMENTATION

WORKING COMMISSION W18A - TIMBER STRUCTURES

AXIALLY LOADED NAILS
- PROPOSALS FOR A SUPPLEMENT TO THE CIB-CODE -

by

J Ehlbeck and W Siebert
University of Karlsruhe
Federal Republic of Germany

MEETING TWENTY-ONE
PARKSVILLE, VANCOUVER ISLAND
CANADA
SEPTEMBER 1988

Axially loaded nails
- Proposals for a supplement to the CIB-Code -

Jürgen Ehlbeck and Wichard Siebert
University of Karlsruhe, FRG

1 Preface

The CIB Structural Timber Design Code (1983) includes a formula for the characteristic withdrawal resistance for all types of nails:

$$F = f_1 \cdot d \cdot \ell \qquad (1)$$

with d = nail diameter |mm|, ℓ = depth of penetration (mm) and F = characteristic withdrawal capacity (N). The factor f_1 depends on several influencing parameters, such as type of nail (smooth, threaded etc.), timber species and density. A proposal for ordinary round nails is given with $f_1 = 6 \cdot \rho^2$, but this value was checked and turned out to be of no use. In the draft Eurocode 5 (1987) a revised value was introduced as a proposal for ordinary round nails:

$$f_1 = 18 \cdot 10^{-6} \cdot \rho^2 \qquad (2)$$

with the characteristic density ρ in kg/m^3.

No values are given, however, in the CIB-Code and the draft Eurocode 5 for all types of threaded and ring-shank nails.

During the last two decades numerous tests were made at the University of Karlsruhe to obtain data on the withdrawal resistance of axially loaded nails; most tests were used as a basis for a national approval for special types of nails with profiled shanks. An attempt was made to obtain general data for the factor f_1 in Eq. (2), in order to complete the specification in the CIB-Code and the draft Eurocode 5.

2 Nails and wood

The tests mentioned were carried out with very different types of nails, from annularly threaded nails with different design details, such as double or single crest features, rounded thread roots etc., to helically threaded nails with small and large thread angles.

All tests were made with European whitewood (picea abies), but the wood density ranged from 350 to 550 kg/m^3.

It is well understood that it is not possible to evaluate these more than 3.800 single test data on a serious statistical basis because there are so many influencing parameters; but it was tried to find out a rough and conservative estimate of the f_1-value in relation to the wood density. Even this procedure has to be regarded as an estimate, because the individual density of each single test specimen - that is the density of the wood right next to the nail - was not available, but only the mean density of the wood stick under scrutiny.

Furthermore, the moisture content of the wood was not constant in all cases, although the wood was normally acclimatized at a 65 % relative humidity and a 20 °C temperature climate. Nevertheless, there may be slight differences in the moisture content at manufacturing and at testing the test specimens. On the other hand, it is well known from methodical tests that some percent difference in moisture content reveal marked difference in the withdrawal resistance of nails.

Thus, it was not surprising that during this attempt of evaluating all test data a great variability was found, and it was not easy to prove a tight relationship between the withdrawal resistance and the wood density or the square of the wood density, as it is proposed for ordinary round nails in the model codes.

3 Ordinary round nails

Ordinary round nails, i.e. nails with a smooth shank, have a relatively small withdrawal resistance changing with time and any changes of the moisture content of the wood. Therefore, smooth nails should never be used for long-term loads. Fig.1 demonstrates all tests performed with round wire nails of different nail diameters; all tests were carried out within some hours after nailing, mostly with a moisture content of the wood within the range of 12 to 18 %. These test data do not significantly prove a relationship between the withdrawal load and the square of the density, but the draft Eurocode 5 proposal may be acceptable and should be checked by systematic withdrawal tests using different wood species and a greater range of the wood density. In a small range, e.g. from 425 to 475 kg/m^3, f_1 could obviously also be described by a fix value, independent of density. For European whitewood, a constant value of $f_1 = 3$ is absolutely acceptable, but the given proposal in draft Eurocode 5 fits as well and may be infinitely good for all wood species with the understanding that different splitting tendencies of the wood species are of negligible signification.

4 Ring-shank nails

Fig. 2 presents test results with different ring-shank nails, such as for special steel-to-wood joints, for gypsumboard nailing or for general application in load-bearing timber joints. A relationship between density and nail withdrawal resistance is obvious. A regression curve using the formate

$$f_1 = a \cdot \rho^{b} \qquad (3)$$

was found for these 250 mean values as shown in Fig. 2:

$$f_1 \approx 2500 \cdot 10^{-6} \cdot \rho^{1.4} \qquad (4)$$

Assuming a coefficient of variation of approximately 22 to 25 %, the characteristic f_1-value can be described by

$$f_{1,k} = 1500 \cdot 10^{-6} \cdot \rho^{1.4} \qquad (5)$$

Eq. (5) is plotted in Fig. 2.

If a formate using ρ^2 is supposed to be more convenient, Eq. (5) can easily be changed to

$$f_{1,k} = 36 \cdot 10^{-6} \cdot \rho^{2} \qquad (6)$$

which is acceptable as well as long as the density ranges from 350 to 550 kg/m^3.

It should be stated, however, that the withdrawal resistance decreases slightly with increasing nail diameter as long as the feature of the nail shank does not change significantly. A decrease of appr. 20 % was observed with a nail diameter increase from 3 mm to 5 mm. This can be neglected, because a total coefficient of variation of 22 to 25 % was assumed for the estimation of the characteristic values given in Eq. (5) or (6), respectively, whereas the coefficient of variation decreases if only test data are evaluated which are obtained from tests with nails of similar shank feature.

5 Helically threaded nails

The available test data with helically threaded nails produced a tremendous variability, although most tests were carried out with softwood of a density between 420 and 460 kg/m^3. In this case the thread angle is among others, of significant influence. As long as there are not more test data systematicly analized, it can only be recommended to use the same f_1-value as proposed for ring-shank nails with the assumption that the thread angle is not greater than 60° for application in softwood timber.

For hardwoods larger thread angles are used in order to facilitate driving the nail into the wood. For the time being, no test data with hardwood are available in Germany. Hence, no proposals can be submitted for these special types of threaded nails.

6 Conclusion and proposals

Without doubt, the withdrawal resistance of nails is influenced by many parameters. One of them is the density of the wood. Another important paramter is the shank feature of annularly or helically threaded nails.

As long as the wood density remains in a relatively small range, e.g. between 350 and 550 kg/m^3 as given for most of the European softwoods, it is unimportant and insignificant to describe the characteristic withdrawal resistance in relationship of ρ or ρ^2 or $\rho^{1.5}$ or whatever.

Under this assumption, eq. (2), which is the present proposal in draft Eurocode 5, describes the characteristic withdrawal capacity of smooth, i.e. ordinary round nails in European softwoods in a satisfactory manner.

Based on a large number of tests with threaded nails of different features it can be stated that - on the safe side - for these nails the withdrawal resistance is at least twice that of ordinary round nails. In individual cases special nails have a distinctly higher withdrawal resistance, but this cannot be involved in a general application rule of a timber design code. If required, special approvals are necessary or the rules must be supplemented if more detailed data are submitted by the manufacturers of such special nails.

Thus, it is proposed to add in the CIB-Code and in the draft Eurocode 5 chapter 5.3.3:

"For annular ring-shank and helically threaded nails with a thread angle not more than 60° it may be assumed

$$f_1 = 36 \cdot 10^{-6} \cdot \rho^2$$

if no other data are proved by tests."

As an alternative (see Figs. 3 and 4), these application rules can also be accepted as follows:

"For ordinary round nails $f_1 = 400 \cdot 10^{-6} \cdot \rho^{1.5}$ and for annular ring-shank and helically threaded nails with a thread angle not more than 60° $f_1 = 800 \cdot 10^{-6} \cdot \rho^{1.5}$ may be assumed if no other data are proved by tests. ρ is the characteristic density in kg/m^3".

Both alternatives are useful, but comments will be appreciated, especially to the question, if the influence of density is better represented by ρ^2 or by $\rho^{1.5}$.

Beyond this recommendation some requirements with respect to the geometrical feature of the nail shanks must be laid down in the code.

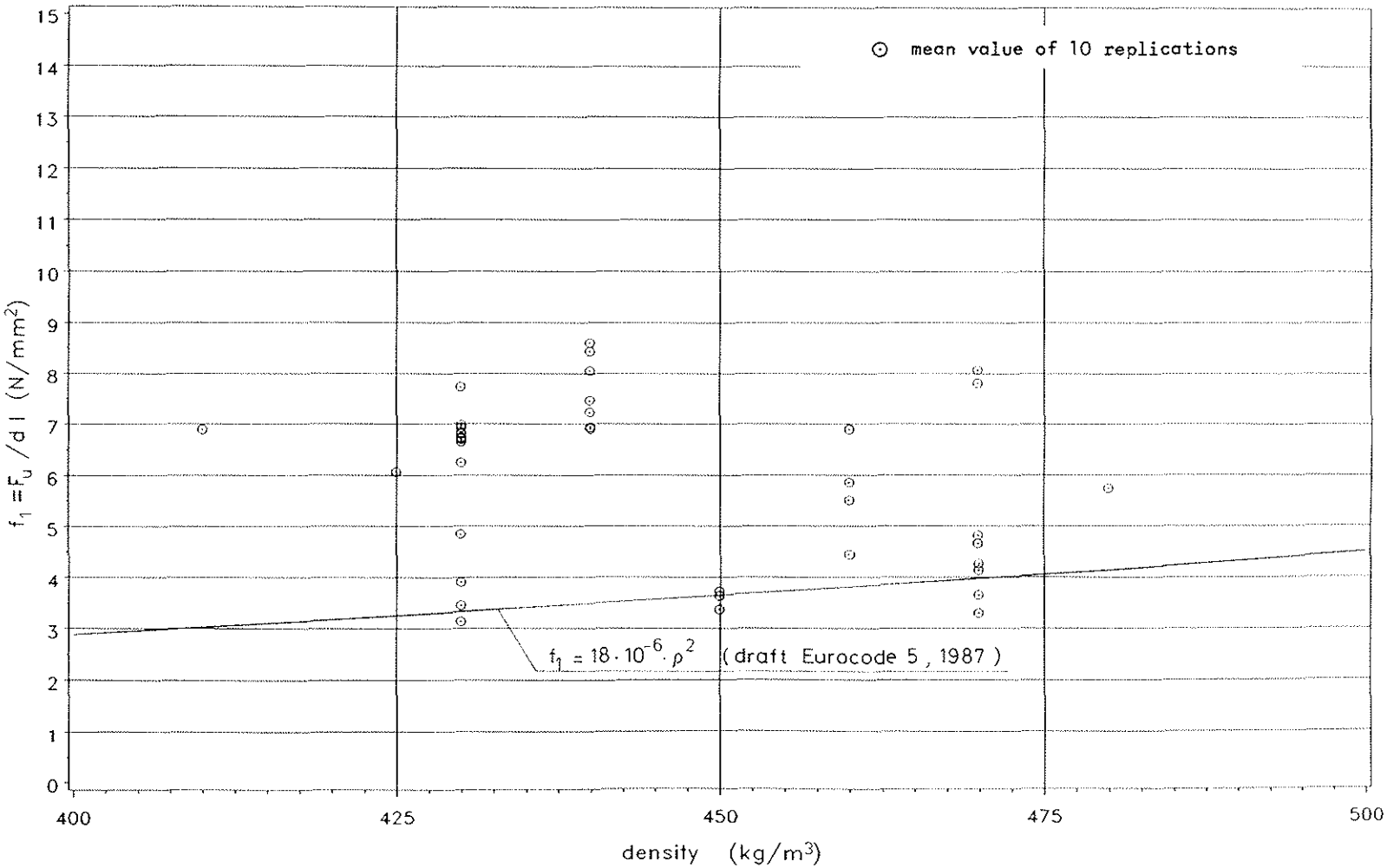

Fig. 1: Withdrawal resistance of ordinary round nails in European whitewood (picea abies)

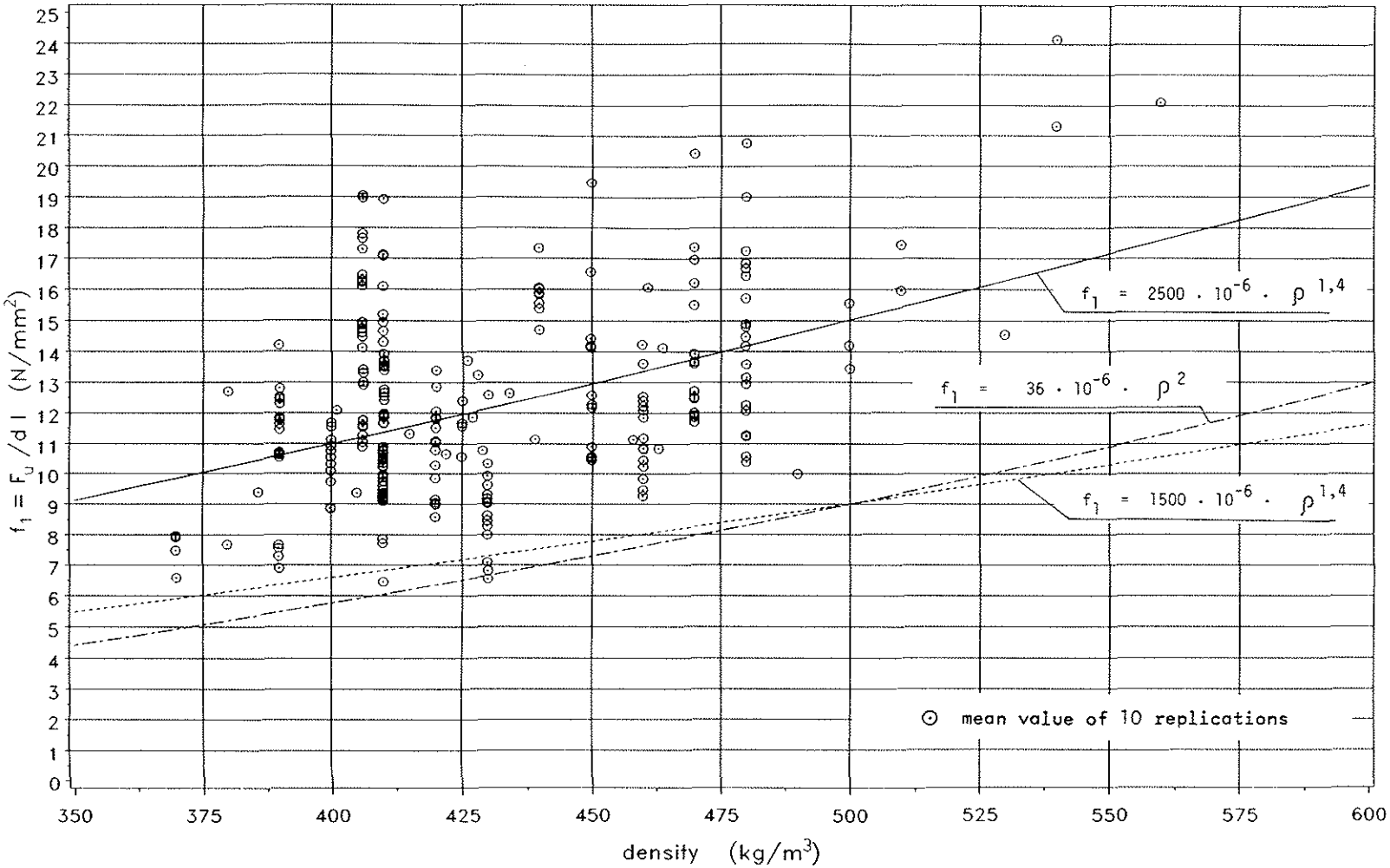

Fig. 2: Withdrawal resistance of ring-shank (annularly threaded) nails of diefferent features in European whitewood (picea abies)

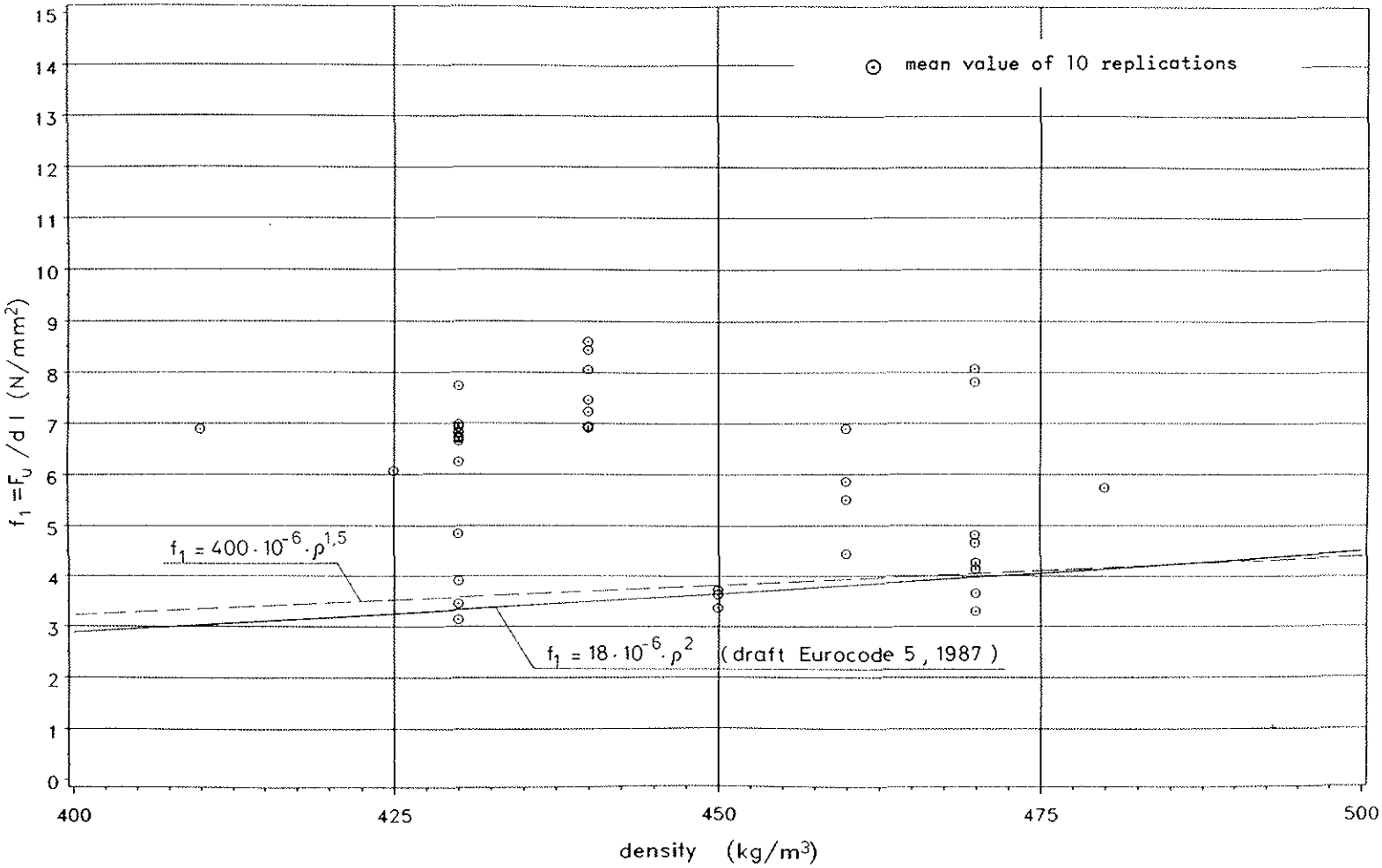

Fig. 3: Withdrawal resistance of ordinary round nails in European whitewood (picea abies)

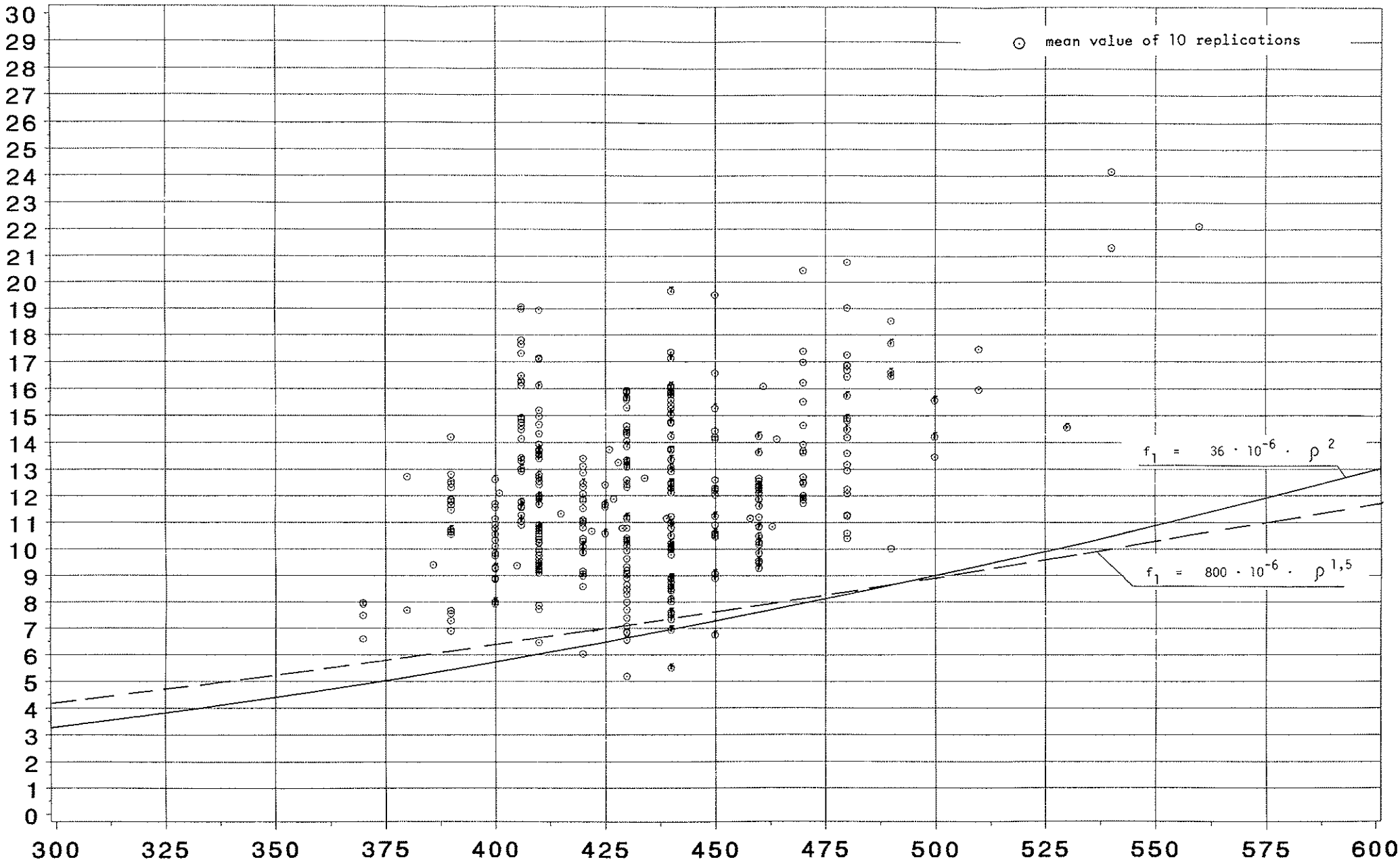

Fig. 4: Withdrawal resistance of annularly threaded and helically threaded nails in European whitewood (picea abies)

INTERNATIONAL COUNCIL FOR BUILDING RESEARCH STUDIES AND DOCUMENTATION

WORKING COMMISSION W18A - TIMBER STRUCTURES

AN ADDENDUM TO PAPER 20-8-1 - PROPOSED CODE REQUIREMENTS FOR VIBRATIONAL SERVICEABILITY OF TIMBER FLOORS

by

Y H Chui and I Smith
University of Mew Brunswick
Canada

MEETING TWENTY-ONE
PARKSVILLE, VANCOUVER ISLAND
CANADA
SEPTEMBER 1988

INTRODUCTION

At the 1987 CIB-W18A Meeting, the authors proposed a possible code approach (1) for designing against poor vibrational serviceability for light-weight wooden floors in the domestic setting. Suggestions by certain participants of the meeting have led to further work by the authors. This mainly involved additional discussion with others, who are investigating or have investigated related problems, and conducting a comparison between various design approaches.

Main differences between different design approaches are presented. Assessments of vibrational serviceability, using each approach, of a series of wooden floors covering a wide range of floor sizes, are presented.

In addition, possible extension of the proposed design equations in the previous paper (1) to include the stiffening effect due to a flooring with high bending stiffnesses is also discussed.

PROPOSAL SUMMARY

In the 1987 paper, it is proposed that for any wooden floor to have acceptable vibrational performance its fundamental natural frequency (f_n) and the frequency-weighted root-mean-square acceleration (A_r) of its response caused by a defined natural footfall impact should not be lower than 8 Hz and higher than 0.45 m/s^2 respectively. These human threshold limits are derived from the British Standard BS6472 "Evaluation of human exposure to vibration in buildings (1 Hz to 80 Hz)" (2), which is technically similar to the ISO Standard 2631 (3). Practical significance of these limits has been verified by measurements taken from in-situ floors (9). The authors would like to stress that these do not represent

new human perception threshold levels but are simply values interpreted from BS6472.

To assist designers in determining vibrational serviceability of a design the authors also derived and proposed the following equations for calculating f_n and A_r.

$$f_n = \frac{\pi}{2a^2}\sqrt{\frac{E_j I_j (n-1)}{\rho_s hb + \rho_j A (n-1)}} \quad \text{Hz} \qquad (1)$$

where:

a = floor span

E_j = MOE of joists

I_j = second moment of area of joists

n = number of joists

ρ_s = density of sheathing

h = thickness of sheathing

b = floor width

A = cross section area of joists

ρ_j = density of joists

$$A_r = \frac{2000\ K}{\pi f_o^2\ m} \quad m/s^2 \qquad (2)$$

where:

$$f_o = \frac{\pi}{2a^2}\sqrt{\frac{E_j I_j (n-1)}{\rho_s hb + \rho_j A (n-1) + \frac{280}{a}}} \quad \text{Hz}$$

$$m = \frac{a}{2}\left(\rho_s hb + \rho_j A (n-1) + \frac{280}{a}\right) \quad \text{kg}$$

K = a function of f_o, damping ratio and duration of impact producing the vibration.

The values of K are tabulated in Table 1 in reference number 1.

Equation 1 calculates the lowest natural frequency of an unloaded two-way wooden floor system. Equation 2 pre-supposes that the vibrational response caused by the footfall impact was dominated by the fundamental mode of vibration with negligible contributions from the higher modes. The assumption is only justifiable when the floor is not highly orthotropic. This requirement can be partially met by supporting edge joists and installing adequate stiffening material in the transverse direction. Such practices are beneficial and should be specified as standard construction practices.

COMPARISON WITH OTHER PROPOSALS

Communications with other researchers(4, 5) have led to the conclusion that there should be more reliable design guidelines than those available to designers in current national and international design codes. These guidelines should relate to dynamic response instead of static behaviour.

Commenting on the proposal in the previous section of this paper, Ohlsson (4) expressed his main concern over the fact that the design model shown in equation 2 ignores the contribution of the higher order modes. The authors were aware of this point when developing the design model. It was, however, thought that by including the effect of higher modes, the ultimate design equation would be too complex for normal design use. In addition it was found that there are usually large errors associated with practical predictions of higher modes. This then led to the development of a one degree-of-freedom design model (i.e. equation 2) and the previously mentioned accompanying construction requirements (i.e. support

of edge joists, and transverse stiffening). The use of single degree-of-freedom design models has also been suggested by Rainer (6) of the National Research Council of Canada. He reckons that since "vibration problems tend to be very complicated simplifying assumptions and empirical methods often have to be employed".

Ohlsson (7) and Onysko (8) have both proposed alternative methods of determining vibrational serviceability of wooden floors. Ohlsson's method (7) involves the calculations of fundamental natural frequency and initial peak velocity. Effects of natural frequencies up to 40 Hz are claimed to be included in an approximate manner. The prediction of natural frequencies requires, as inputs, the stiffnesses in the two orthogonal directions. Along joists stiffness can usually be predicted with a good degree of accuracy. There are, however, dfficulties in estimating across-joists stiffness of a wooden floor, and the validity of modelling assumptions differ from mode to mode. Accuracy of predicted natural frequencies could be seriously impaired by the errors in the determinations of floor stiffnesses. A performance rating chart is given for assessment of vibrational serviceability, (7). To cover a wide range of span to floor width ratios encountered in practice a large number of design charts are needed for the calculation of natural frequencies.

Based on results and survey of owners assessment from field studies, Onysko (8) proposes static deflection limits under a concentrated load of 100 kg as means of discriminating wooden floors. The limit is constant up to a certain span. Above this the limit is a function of the span. The main advantage of such a method is that it is simple to apply. But there are always some uncertainties over possible projections of likely human response to floor vibrations through static deflection checks.

Table 1 presents the results of assessment of a wide range of floors designed to Canadian Standard (9), based on each of the three methods discussed here. It is observed that none of the floors would be classified as acceptable according to Onysko's criteria. This may imply that the limits proposed are too stringent. Assessments based on Ohlsson's and the authors' both classify 5 floors as acceptable and 7 floors as unacceptable. Nearly all the acceptable floors according to Ohlsson are long span floors (5.78 m). It can be noticed that, out of the three methods, only the authors' has the capability of being sensitive to floor size as a variable. For a given span, the magnitude of response (A_r) decreases with increasing floor width. This is in agreement with results from the study conducted by the first author (10).

EFFECT OF HIGH BENDING STIFFNESSES OF SHEATHINGS

At the last CIB-W18A meeting it was suggested that the advantage of using stiff sheathing should be allowed for in the design equations. This is achieved by adding a term C to the numerator inside the square root sign of the expressions for calculating f_n and f_o in equations 1 and 2 respectively, such that:

$$C = bK_x + \frac{a^4}{b^3} K_y + \frac{2a^2}{b} K_\nu + \frac{4a^2}{b} K_G \qquad (3)$$

where:

$$K_x = \frac{E_x h^3}{12\ (1-\nu_{xy}\ \nu_{yx})}$$

$$K_y = \frac{E_y h^3}{12\ (1-\nu_{xy}\ \nu_{yx})}$$

$$K_\nu = \nu_{xy}\ K_x$$

$$K_G = G_{xy} \frac{h^3}{12}$$

E_x = MOE of sheathing in the span direction

E_y = MOE of sheathing in the transverse direction

ν_{xy}, ν_{yx} = Poisson's ratios

G_{xy} = modulus of rigidity in plane of sheathing

a, b and h are as denoted in equation 1

Thus the expressions for f_n and f_o become

$$f_n = \frac{\pi}{2a^2} \sqrt{\frac{E_j I_j (n-1) + C}{\rho_s hb + \rho_j A (n-1)}} \quad \text{Hz} \qquad (4)$$

$$f_o = \frac{\pi}{2a^2} \sqrt{\frac{E_j I_j (n-1) + C}{\rho_s hb + \rho_j A (n-1) + \frac{280}{a}}} \quad \text{Hz} \qquad (5)$$

The above refinement has already been discussed by the authors in another CIB-W18A paper, (11). For conventional flooring materials the term C need not be included as it is very small compared with the $E_j I_j (n-1)$ term.

CONCLUSION

The additional information supports the previous contention that the design method proposed by the authors should be accepted as suitable for inclusion in future editions of the CIB Code.

REFERENCES

1. CHUI, Y.H. and SMITH, I. Proposed code requirements for vibrational serviceability of timber floors. Paper No. 20-8-1. Proceedings of CIB-W18A Meeting, Dublin, 1987.
2. BRITISH STANDARDS INSTITUTION. Evaluation of human exposure to vibration in buildings (1 Hz to 80 Hz). British Standard BS6472. London, BSI. 1984.
3. INTERNATIONAL ORGANIZATION FOR STANDARDIZATION. Guide for the evaluation of human exposure to vibration. ISO Standard 2631. Geneva, IOS, 1978.
4. OHLSSON, S. Verbal communication. May 1988.
5. ONYSKO, D.M. Verbal communication. May 1988.
6. RAINER, J.H. An approach to a vibration standard for buildings. IRC Paper No. 1387. National Research Concil of Canada, Ottawa. 1986.
7. OHLSSON, S. Springiness and human induced floor vibration - A design guide. Document No. D12: 1988, Swedish Council for Building Research, Stockholm. 1988.
8. ONYSKO, D.M. Serviceability criteria for residential floors based on a field study of consumer response. Project No. 03-50-10-008. Forintek Canada Corporation, Ottawa, 1985.
9. CANADIAN STANDARDS ASSOCIATION. Engineering design in wood. CSA Standard CAN 3-086-M84. Rexdale, Ontario, CSA. 1984.
10. CHUI, Y.H. Vibrational performance of wooden floors in domestic dwelling. Ph.D. Thesis. Council for National Academic Awards, London. 1987.
11. SMITH, I. and CHUI, Y.H. Predicting the natural frequencies of light-weight wooden floors. Paper No. 19-8-1, Proceedings of CIB-W18A Meeting, Florence. 1986.

Table 1: Assessment of a series of floor designs using different proposed methods.

					Chui & Smith (1)			Ohlsson (8)			Onysko (9)	
Floor	Span (m)	Width (m)	Joist Spacing (mm)	Size (mm)	fn (Hz)	A_r (m/s^2)	Rating*	f_1 (Hz)	h max (mm/s/Ns)	Rating*	Y (mm)	Rating*
1	2.46	2.4	600	38 x 140	28.3	0.83	U	27.1	28	A	3.50	U
2	2.46	3.6	600	38 x 140	28.3	0.60	U	27.1	39	U	3.50	U
3	2.46	4.8	600	38 x 140	28.3	0.59	U	27.1	41	U	3.50	U
4	3.72	2.4	400	38 x 184	19.6	1.02	U	18.8	28	U	5.33	U
5	3.72	3.6	400	38 x 184	19.6	0.64	U	18.8	33	U	5.33	U
6	3.72	4.8	400	38 x 184	19.6	0.45	A	18.8	38	U	5.33	U
7	3.72	6.0	400	38 x 184	19.6	0.34	A	18.8	43	U	5.33	U
8	3.72	7.2	400	38 x 184	19.6	0.27	A	18.8	44	U	5.33	U
9	5.78	3.6	400	38 x 286	13.8	0.66	U	13.3	20	A	5.32	U
10	5.78	4.8	400	38 x 286	13.8	0.50	U	13.3	22	A	5.32	U
11	5.78	6.0	400	38 x 286	13.8	0.40	A	13.3	22	A	5.32	U
12	5.78	8.4	400	38 x 286	13.8	0.29	A	13.3	23	A	5.32	U

Floor data: $E_j = 10 \times 10^9$ N/m^2

$\rho_j = \rho_s = 500$ kg/m^3

$h = 15.5$ mm.

*A: Acceptable U: Unacceptable

CIB-W18A/21-8-2

INTERNATIONAL COUNCIL FOR BUILDING RESEARCH STUDIES AND DOCUMENTATION

WORKING COMMISSION W18A - TIMBER STRUCTURES

FLOOR VIBRATIONAL SERVICEABILITY AND THE CIB MODEL CODE

by

S V Ohlsson
Chalmers University of Technology
Sweden

MEETING TWENTY-ONE
PARKSVILLE, VANCOUVER ISLAND
CANADA
SEPTEMBER 1988

1. INTRODUCTION

The aim of this paper is twofold:

- To initiate a general discussion about to what extent and in which forms floor serviceability related design methods and criteria should be presented in international model codes.

- To comment upon a paper which was presented at the last meeting of CIB-W18A (Chui, Y.H. & Smith, I.: Proposed Code Requirements for Vibrational Serviceabitility of Timber Floors).

It has been a long time tradition in the structural design of houses and civil engineering structures to focus on the load-bearing capacity and to relate the design to different codes of practice. What to-day is known as the serviceability limit state is a rather modern concept in the construction area, relatively speaking. If we, for a moment, compare the situation with some other sector of engineering, we find that the corresponding words used often are "performance" and "comfort", etc. This is for instance the case in the automotive industry, where the "serviceability" of the product is of main importance to the design, but is normally not regulated by codes. The serviceability criteria used in this sector, on the other hand, do stimulate the technical development of the car design. As examples of such development we nowdays have cars with smaller unsprung wheel masses, individual suspensions, etc. This may not have been the case if the serviceability criteria in use had been of the same type as we use for the structural design of houses.

Research in the area of floor vibration and serviceability has been undertaken in several countries and is still going on. Reference (8) may serve as an orientation about the field. Reference (4) is a design guide, which also includes a proposed design method. It has been

in use among practicing engineers in Sweden and occasionally in Norway and Finland since 1984 and so far it seems to work reasonably well. Some general aspects on design with respect to floor vibrations and a short review of the proposed design method is included in Ref. (9). No further general information on the subject of floor vibration is included here due to limited space.

2. CRITERIA ON A PROPER DESIGN CRITERION/METHOD

A design method with respect to floor vibration should:

A. Reflect the degree of vibrational serviceability.
B. Be neutral with regard to construction material and structural configuration.
C. Only include such well defined quantities, that are possible both to calculate and to measure.
D. Be clearly understandable and enable the engineer to predict the effects of structural modifications.

The abovementioned four criteria may seem rather obvious, but some background will be presented for each of them.

The first one is maybe the most obvious. The reason for including it is that several existing proposals do actually not meet it. The background in most cases is that the problems have been "oversimplified" to such an extent that the resulting expressions or parameters simply miss the target. Two examples of such less good approaches ought to be mentioned. The first one concerns suggestions where purely *static* stiffness is to be limited as the only measure to guarantee a proper performance under *dynamic* loading. Different responses for floors of different weight will not be reflected by such methods. The second one relates to the case of transient loading of lightweight, strongly orthotropic floors, i.e. timber joist floors. When

this case is handled by a method assuming that the fundamental mode alone is governing the response it will heavily underestimate the response. This is unfortunately the case in the proposal (1). The simplification only to account for the lowest eigenfrequency is very common and justified in many cases. In the case of a strongly orthotropic plate under impulse loading it is, however, not a proper one.

The second criterion B. is founded on the assumption that the user of a building is not primarily interested in what constuction material or what design configuration that has been used, but rather in the performance as it can be experienced during normal use. This assumption justifies the need for *criteria* that is neutral to different construction materials. Also, a comment on design parameter values may be adequate, although it is strictly speaking outside the scope of this paper. Wood is commonly known as a construction material with relatively good damping properties. Since modal damping of floors is mainly governed by the method of construction including the use of partitions and other non-engineered components, this is unfortunately of minor importance. There is, for instance, no rational basis for assuming essentially higher damping in a floor in a traditional timber framed house compared to that of a floor with light-gage steel joists in a house built with the same technique, c.f. (6). The neutrality to design configuration is essential for good development and fair competition. It should in other words be possible to compare different alternatives such as joist structure - grillage structure - sandwich structure - stressed skin structure and simply supported design - design with continuous spans - framed design, etc. The design proposal (1) is neither neutral with respect to material nor to the type of structural design.

The third criterion C. is incorporated for educational purposes as well as for the purpose to enable engineers to use standard calculation procedures (hand or computer based) known from structural mechanics. There are frequent examples of design criteria which are presented by rather lengthy equations including numerous parameters raised to exponents with two or more decimals and where the origin of the values are unknown to almost everybody, except

to the author. This is obviously discouraging and should be avoided. Another type of failure to meet the criterion C. is to incorporate less well-defined quantities. An example in the actual field is the use of the so-called "heel impact load" as the prescribed load intended to be used for design calculations.

The last criterion D. is essential to stimulate a sound engineering development of commonly used floor designs, cf. the previous example from the automotive industry. The best way to fulfill the intentions of this criterion is to aim at general concepts formulated in a way that simplifies the application of sensitivity analysis. This is not easily achieved, but it is very valuable if such studies are enabled. The last section of Ref. (9) contains an attempt to such a sensitivity study related to the design method in (7). The result is reasonably clearifying, although the design method suffers a bit from the fact that it includes more than one design parameter.

3. INTERNATIONAL COORDINATION

Attempts to formulate design methods aiming at the design of floors with acceptable vibrational properties are made by scientists in different countries. Furthermore, the result from several of these efforts seem to be intended for publication by various international scientific organizations. As far as the CIB is concerned, the author took an initiative by writing a letter to some of the CIB coordinators interested in the matter (appended to this paper).

In line with the intentions of the letter a short informal meeting was arranged in Ottawa during the Symposium on Serviceability of buildings. Ten persons attended the meeting. Among them were representatives of CIB-W18, CIB-W56, CIB-W85, CEB, ASTM and ISO. No detailed discussion of technical matters were possible due to time constraints, but it was agreed that:

- An informal coordination of different proposals regrding the design for floor vibrational serviceability would be advantageous.

- The author should start this work by producing a list of different design proposals and related organizations/authors.

The task of international coordination and harmonization is not an easy one. Since the matter of vibrational serviceability is a rather new aspect on structural design, it seems somehow as a possibly fruitful subject for an attempt.

4. CONCLUDING WORDS AND SUGGESTIONS

Considering various aspects of the matter it is the authors opinion that a sound engineering development of floor structures will benefit if:

- The design proposal (1) is not accepted for inclusion in the CIB model timber code.

- The authors of the proposal (1) contribute together with other specialists in the field of floor vibration in the process of international coordination aiming at design criteria that are independent of construction material and configuration.

- Scientists and engineers with special knowlege in any specific construction material contribute in research and development aiming towards recommendations about which structural configurations should be preferred, which detail designs that are most suitable, etc. Such work could preferably be based on the result of the abovementioned international coordination.

5. REFERENCES

1. Chui. Y.H. & Smith, I. Proposed Code Requirements for Vibrational Serviceability of Timber Floors. Proc. of CIB-W18A meeting, Dublin 1987, paper No. 20-8-1.

2. ISO/DIS 2631-2.2 . Evaluation of Human Exposure to Whole-Body Vibration. Part 2: Human Exposure to Continuous and Shock-Induced Vibrations in Buildings 1-80 Hz. Draft International Standard, ISO 1987.

3. Ohlsson, S. Floor Vibration and Human Discomfort, Doctoral thesis, ISBN 91-7032-077-2, Chalmers Univ. of Techn., Div. of Steel & Timber Struct., Gothenburg 1982.

4. Ohlsson, S. Svikt, svängningar & styvhet hos bjälklag; Dimensioneringsmetoder. (In Swedish. Reference No. 7 is an English version) Swedish Council for Building Research, Publ. T20:1984, Stockholm 1984.

5. Ohlsson, S. A Note on Floor Vibration and Serviceability. Summary of a presentation at the CIB-W56 meeting, Stockholm 1986.

6. Ohlsson, S. Stiffness Criteria and Dynamic Serviceability of Light-Weight Steel Floors. Proc. of IABSE Coll. in Stockholm 1986, IABSE Rep. Vol. 49, pp. 427-433, Zürich 1986.

7. Ohlsson, S. Springiness & Human-Induced Floor Vibrations; A Design Guide. Document D12:1988, Swedish Council for Building Research, Stockholm 1988, ISBN 91-540-4901-6. (Translation of Ref. No 4). Marketed by Svensk Byggtjänst P.O. Box 7853, S-103 99Stockholm, Sweden.

8. Ohlsson, S. Ten Years of Floor Vibration Research - A Review of Aspects and some Results. The Symposium on Serviceability of Buildings, University of Ottawa, Canada May 1988.

9. Ohlsson, S. A Design Approach for Footstep-Induced Floor Vibration. Paper submitted for presentation at the 1988 Int. Conf. on Timber Engineering, Seattle, WA., Sept. 1988.

APPENDIX 1. COMMENTS ON THE PROPOSAL (1)

Some time after the proposal (1) was presented the author of this paper had the opportunity to meet with the authors of (1), Dr. Chui and Dr. Smith for an informal discussion on the subject. Although the discussion were fruitful, it still remains different opinions about the proposal. This section provides a summary of some properties of (1), which due to my opinion are less favourable. Very compact presentation is used in order to keep the section short.

a. Only fundamental mode response is assumed. This gives erraneous results and leads to a situation where the bending rigidity perpendicular to the joists doesn't influence the estimated response in a proper way.

b. Vibration *acceleration* is used as design parameter instaed of vibration *velocity* which is commonly accepted to give constant human disturbance in the actual frequency band cf. (2). In fact, the proposal uses a factor to compensate for this, but the result is less clear.

c. A weighted RMS-value A_r is used as representation of the response due to a transient force in the shape of a rectangular impulse load of 0.07s duration. It is unconventional to apply RMS-averageing to transient signals and the averaging time (1s) chosen is not motivated.

d. The suggested limit value for A_r seems rather high.

e. The reference to BS6472 indicates that the level of acceptability should have been laid down by other scientists already. This is, however, not the case since the load function is originally chosen in (1), The degree of representativity of this design load as related to expected service loads from people in motion is not discussed. Further more, the

background research to BS6472 and ISO 2631 has mainly been focused on vibrations generated by other sources than people in motion.

f. The suggested value for the relative modal damping $c/c_{cr} = 3\%$ is far too high to be used in design. It is probably higher than an expected mean value and damping is a parameter that shows very large scatter.

g. Only one of three different sources to possible human disturbance is included. The semi-static phenomenon included in the sensation of springiness is ignored as well as the case of steady vibration.

h. Long span gluelam floors will be prohibited via the demand on $f_1 > 8$ Hz. It was already pointed out in (3) that more severe conditions will result for floors with low fundamental frequencies, but to prohibit their use seems to be rather drastic.

i. The proposed design expressions seem to be unneccesary complicated, especially the peculiar parameter K in Eq. 5 in (1).

j. Last, but not least; the proposal is not able to meet most of the criteria discussed in section 2.

Appendix 2

CHALMERS UNIVERSITY OF TECHNOLOGY
DEPARTMENT OF STRUCTURAL ENGINEERING
DIVISION OF STEEL AND TIMBER STRUCTURES
Dr Sven Ohlsson
Member of CIB-W56

1987-11-02

Mailing list

On floor vibration and serviceability problems.
- CIB activities and the CIB model Code.

Dear Sirs,

The design of floors with respect to possibly annoying vibration due to dynamic loading, especially human footfall, has been a matter of increasing interest in later years. Some early research was conducted in Norway in the late 1950ies. During the 1970ies research was initiated mainly in Canada, in USA and in Sweden. In later years Great Britain and other countries have started research within the floor vibration field as well.

Recently, I got a letter from Mr Chui, TRADA, in Great Britain referring to a paper presented at the last meeting in Dublin of CIB W18A - Timber Structures. Mr Chui asks me to comment upon the paper, which in fact is a proposal to a design method for timber floor vibration, which the author suggested to be incorporated in the CIB model code for timber structures (CIB-W18). I have not yet studied the proposal from a technical point of view. However, independently of the technical qualities of the proposal I would like to suggest a coordination of the floor vibration topics within the body of CIB. The need for coordination is supported by the following aspects:

- Floor vibration serviceability is often governing the design and dimensions.
- Floor vibration problems are rather *independent of construction material*.
- National Codes or guidelines for floor vibration already exist in some countries, for instance in Canada and Sweden.
- At least two other working groups of CIB are involved in floor vibration and serviceability (CIB W56 - Lightweight construction and CIB W85 - Serviceability requirements for structural deformations.

Postal address
S-412 96 GOTEBORG
SWEDEN

Street address
Sven Hultins gata 8

Telephones
031 - ~~81 91 00~~
~~81 02 00~~
722027

As I am the coordinator of a subgroup of CIB-W56 with the responsibility to produce relevant papers on vibrational serviceability of light-weight floors I could act as an informal "collector" of views on this matter from different groups within the CIB until April 1988. Then a Symposium on Serviceability of Buildings will be held at the University of Ottawa in Canada. This symposium, I believe, will attract most researchers within the field of floor vibration and will hopefully be an event where also the formal coordination of the matter could be discussed with members of different CIB working groups.

Looking forward to receive your opinion,

Yours sincerely,

Sven Ohlsson

MAILING LIST

Professor Gy. Sebestyén
Secretary General CIB
P.O.Box 20704, Weena 704
3001 J A Rotterdam
Netherlands

Dr. C.K.A. Stieda
Chairman of CIB-W18A
Forintek Canada Corp.
6620 NW Marine Drive
Vancouver, BC
Canada, V6T 1X2

Professor J.M.Davies
Chairman of CIB-W56
Univ. of Salford
Dep. of Civil Engineering
Salford M5 4WT
Great Britain

Dr. D.E. Allen
Chairman of CIB-W85
Division of Building Research
National Research Council of Canada
Montreal Road, M-20
Ottawa
Canada, K1A OR6

19

CIB-W18A/21-10-1

INTERNATIONAL COUNCIL FOR BUILDING RESEARCH STUDIES AND DOCUMENTATION

WORKING COMMISSION W18A - TIMBER STRUCTURES

A STUDY OF STRENGTH OF NOTCHED BEAMS

by

P J Gustafsson
Lund Institute of Technology
Sweden

MEETING TWENTY-ONE
PARKSVILLE, VANCOUVER ISLAND
CANADA
SEPTEMBER 1988

A STUDY OF STRENGTH OF NOTCHED BEAMS

by

Per Johan Gustafsson
Division of Structural Mechanics
Lund Institute of Technology
Box 118, S–221 00 Lund, Sweden

1. INTRODUCTION

1.1 General

Short time strength of wooden beams with a rectangular end–notch on the tension side according to Figure 1 is studied. A simple closed–form equation for the strength is derived by means of fracture mechanics and test results are presented. Test results from literature are compiled.

The study is inspired by differences of principle between conventional formulas used for design and theoretical results obtained by fracture mechanics and finite elements. Influence of size on strength represents such a difference.

1.2 Design formulas in codes

Conventional design formulas for end–notched beams are not known to have any theoretical basis. These formulas are numerically different, but analogous, giving the strength of notched beams by reduction of allowable formal beam shear stress:

$$\frac{V_f}{b\,\alpha d} = \frac{2}{3}\, f_v\, f(\alpha) \qquad (1)$$

where the geometrical quantities b, α and d are defined in Figure 1. V_f is the shear force at fracture of the notch, f_v is the shear strength of wood and $f(\alpha)$ is a reduction factor which reflects influence of stress concentration due to the notch. Accordingly, V_f is made proportional to f_v and the reduction factor is made dependent only of the relative depth of the notch, often by $f(\alpha)=\alpha$.

The design equation in EUROCODE 5 (1987) for glued laminated timber is somewhat

different from equation 1. In this code Weibull–analysis is applied to the shear strength of un–notched glulam beams with a volume of more than 0.1 m^3, making the shear strength dependent of the volume of the beam. As in equation (1), the strength of a notched beam is then taken as an α–dependent fraction of the strength of the un–notched beam:

$$\frac{V_f}{b\,\alpha d} = \frac{2}{3} f_v\, f(\alpha)\, \left(\frac{0.1\,m^3}{V}\right)^{0.2} \frac{1}{1-2d/\ell} \qquad (2)$$

In addition to beam volume, V, notch strength is made dependent also of d/ℓ, reflecting increase in shear force capacity if the shear span is very short.

In the australian code AS1720–1975 a design equation different by principle from equations (1) and (2) is given. This equation is partly based on theoretical fracture mechanics analysis. In addition to α, $V_f/(b\alpha d)$ is made dependent also of the relative length of the notch, β, and the absolute depth of the beam, d, measured in mm. Properties of the material are considered as in the conventional formulas by V_f being proportional to f_v:

$$\frac{V_f}{b\,\alpha d} = \begin{cases} \dfrac{2 f_v}{\sqrt{d}\,(1+1.2\beta/\alpha)} & \text{for } \alpha \le 0.9 \\ \dfrac{2 f_v}{3\sqrt{(1-\alpha)d}\,(1+1.2\beta/\alpha)} & \text{for } \alpha > 0.9 \end{cases} \qquad (3)$$

In equation (1) and (2) $f(\alpha)=1.0$ for $\alpha=1.0$. This means that two different failure modes – crack development from the tip of the notch and shear failure of the net cross–section – are covered by one design formula. Equation (3) is valid only for notch failure. This type of failure can not develop when $\alpha=1.0$ and equation (3) gives $V_f \to \infty$ when $\alpha \to 1.0$.

In Figure 2 a comparison between various design formulas can be found. The figure shows $V_f/(b\alpha d)$ versus α for $f_v=10$ MPa (1450 psi). This is a typical value for the shear strength of Scots pine (Pinus sylvestris L.). Design values of f_v are much lower.

1.3 Theoretical analysis

Theoretical analysis by some maximum stress or strain criterion is difficult due to the strain singularity at the tip of a notch. Due to the singularity, neither Weibull–theory seems to give any meaningful information, see (Gustafsson and Enquist, 1988).

Theoretical analysis is however feasible by fracture mechanics. Leicester (1971) indicated by linear fracture mechanics a general and significant size–effect in $V_f/(bad)$. Later, numerical results have been obtained by linear fracture mechanics and finite elements: recent developments have been presented by Lum and Foschi (1988) and the paper of these authors also provide a brief summary of previous analyses. The linear elastic fracture mechanics analyses referred to relate V_f to properties of the wood in form of "new" material property parameters, i.e. a set of critical stress intensity factors special for a 90° reentrant corner.

By means of finite elements also a non–linear fracture mechanics model has been applied (Gustafsson, 1985). Though this model relates V_f to stress–strain and stress–deformation properties of the material, for beams of large and ordinary sizes, the size of the fracture process region being relatively small, essentially the same results as by linear fracture analysis were obtained.

Due to requirement of simplicity, finite element analysis is hardly suitable for calculation of strength of notched beams during ordinary design. Numerical theoretical analysis, e.g. by finite elements, may become laborious also if sensitivity to various parameters is to be studied for various material properties and beam geometries.

2. THEORETICAL ANALYSIS

2.1 Derivation of basic expression

An equation for the notch strength of a beam according to Figure 3 is obtained by energy balance consideration. The material is assumed to be orthotropic and linear elastic. At zero external load all stresses within the beam are assumed to be zero. The energy potential for the symmetric half of the system consisting of external load and beam is:

$$W_p = -\frac{1}{2} V\delta \tag{4}$$

where δ is the load point deflection of the beam.

If a crack of length Δx develops from the tip of the notch at constant shear force, V, the potential changes by ΔW_p due to increase $\Delta\delta$ in deflection:

$$\Delta W_p = -\frac{1}{2} V\Delta\delta = -\frac{1}{2} V^2\Delta(\delta/V) \tag{5}$$

The crack is assumed to have a distinct tip and crack development is assumed to occur at shear force $V=V_f$ when the loss of potential energy, $-\Delta W_p$, equals the energy required to form a crack. This fracture energy depends on properties of the material. Using notation G_c for fracture energy/crack area one obtains:

$$\frac{1}{2} V_f^2 \Delta(\delta/V) = G_c b \Delta x \tag{6}$$

The part of the beam below the crack is assumed to be inactive, giving no contribution to the stiffness of the beam. This means that the crack development Δx is equivalent to an increase in the length of the notch from βd to $\beta d+\Delta x$. Therefore the crack growth may be interpreted as a change $\Delta\beta$ of β:

$$\Delta x = d\Delta\beta \tag{7}$$

Using equation (7), for $\Delta x \to 0$ equation (6) yields:

$$\frac{V_f}{b\alpha d} = \sqrt{\frac{2G_c}{b\alpha^2 d} / \frac{\partial(\delta/V)}{\partial\beta}} \tag{8}$$

δ/V is the compliance of the symmetric half of the beam. To obtain V_f the variation with β in compliance or deflection of the beam must be calculated. Beam deflection may be separated into four terms:

$$\delta = \delta_l+\delta_v+\delta_r+\delta_b \tag{9}$$

δ_l corresponds to local deformation of the material at the points of loading and support. δ_l is assumed to be constant during variation of β and need therefore not be calculated.

δ_v corresponds to shear deflection of the beam. The shear modulus of the material is denoted by G_{xy} and for a beam with rectangular cross section the following linear variation in δ_v with β is obtained:

$$\delta_v = \frac{1.2V}{G_{xy}} \left[\frac{\beta d}{b\alpha d} + \frac{\ell/2-\beta d}{bd}\right] \tag{10}$$

δ_r corresponds to the effect of elastic clamping of the cantilever βd to the rest of the beam: as compared to the result of ordinary beam theory, for $\alpha<1$ additional curvature develops close to the abrupt change of beam depth. This additional curvature is because the bending rigidity of the unreduced beam depth is not fully activated close to the abrupt change of cross section. δ_r is assumed to be proportional to bending moment,

$V\beta d$, and length of cantilever, βd, giving variation in δ_r with β^2:

$$\delta_r = Vc\beta^2 d^2 \tag{11}$$

where c is the compliance of the moment spring that models elastic clamping. An apparently simple choice would be c=0. This choice would underestimate beam deflection. Another choice is made below.

δ_b corresponds to ordinary beam curvature due to bending. Conventional theory gives variation in δ with β^3:

$$\delta_b = \frac{V}{E_x b d^3/12}\left[\frac{\ell^3}{24} + \frac{(\beta d)^3}{3}\left(\frac{1}{\alpha^3} - 1\right)\right] \tag{12}$$

Making a certain choice of c:

$$c = \frac{12}{b(\alpha d)^2}\sqrt{\frac{(1-\alpha)(1-\alpha^3)}{10\ G_{xy}\ E_x}} \tag{13}$$

total beam deflection, equation (9), can be written in a simple form:

$$\delta = A(B+\beta d)^3 + \text{constant} \tag{14}$$

where the constant is constant with respect to variation of β,

$$A = \frac{V}{3E_x b d^3/12}\left(\frac{1}{\alpha^3} - 1\right) \tag{15}$$

and

$$B = d\sqrt{\frac{E_x}{10G_{xy}}\ \frac{(1/\alpha - 1)}{(1/\alpha^3 - 1)}} \tag{16}$$

Equation (14) is similar to the expression for deflection of a cantilever, $P\ell^3/(3EI)$. Length B may be interpreted as an equivalent increase in cantilever length, taking into account additional deflection beyond that caused by ordinary beam curvature, i.e. deflection due to shear and due to additional beam curvature close to the notch. For common values of E_x and G_{xy} length B is very roughly equal to αd.

Using equations (14)–(16), an explicit closed–form expression for notch strength is obtained by equation (8):

$$\frac{V_f}{b\,\alpha d} = \frac{\sqrt{G_c/d}}{\sqrt{0.6(\alpha-\alpha^2)/G_{xy}} + \beta\sqrt{6(1/\alpha-\alpha^2)/E_x}} \qquad (17)$$

This relation is obtained not only for the type of notch indicated in Figure 3, but also for various notches indicated in Figure 4. In the more general case it is convenient to replace β by M/Vd, M and V being bending moment and shear force, respectively, acting on the beam cross–section at the tip of the notch. With β=M/Vd, equation (17) may alternatively be written as a fracture criterion:

$$\tau\sqrt{8(\alpha-\alpha^2)/G_{xy}} + \sigma\sqrt{5(\alpha-\alpha^4)/E_x} \le \sqrt{30G_c/d} \qquad (18)$$

where τ and σ are formal shear stress and bending stress, respectively, according to conventional formulas:

$$\tau = \frac{3}{2}\frac{V}{b\,\alpha d} \qquad \text{and} \qquad \sigma = \frac{M}{b(\alpha d)^2/6}$$

Equation (18) implies V and M greater than or equal to zero, positive signs being defined in Figure 4.

G_c represents the material dependent fracture energy for splitting along the grain at the actual combined action of both shear stress and tension stress perpendicular to grain. For the sake of simplicity, for a notch on the tension side of a beam it may be reasonable to assume that the actual mixed mode fracture energy is equal to the fracture energy in pure tensile splitting perpendicular to grain:

$$G_c = G_{f,y} \qquad (19)$$

2.2 Influence of size of fracture region

In the above analysis it has been assumed that the tip of a crack is distinct, with zero size of the fracture process region. The assumption of zero or negligible size of the fracture region is consistent with linear fracture mechanics and may be appropriate for beams of large size, the size of the fracture region being comparatively small in such beams. To obtain more accurate results for beams of ordinary and small sizes, the non–zero length of the fracture region may have to be considered.

With the exception of extremely small "beams", according to non–linear fracture mechanics, (Gustafsson, 1985), the length of the fracture region is roughly o.25 $G_{f,y}\sqrt{E_x\,G_{xy}}/f_{t,y}^2$ at start of unstable crack development, $f_{t,y}$ being tensile strength

perpendicular to grain. For softwood this length is roughly about 10 mm (0.5 in). The non–zero length of the fracture zone is of significant matter for notch strength if the distance βd is just a few times 10 mm or less.

In equation (17) non–zero fracture zone length can be taken into account by assuming that the distinct tip of the crack is located a small distance, $\gamma G_{f,y}\sqrt{E_x G_{xy}}/f_{t,y}^2$, ahead of the tip of the notch. Applying equation (19) and taking into account non–zero length of the fracture zone, equation (17) yields:

$$\frac{V_f}{b\alpha d} = \frac{\sqrt{G_{f,y}\sqrt{E_x G_{xy}}/d}}{\sqrt{0.6(\alpha-\alpha^2)\sqrt{E_x/G_{xy}}} + (\beta+\gamma l_m/d)\sqrt{6(1/\alpha-\alpha^2)/\sqrt{E_x/G_{xy}}}} \qquad (20)$$

where l_m is short for $G_{f,y}\sqrt{E_x G_{xy}}/f_{t,y}^2$. Normalizing $V_f/(b\alpha d)$ with respect to tensile strength perpendicular to grain, $f_{t,y}$, equation (20) can alternatively be written:

$$\frac{V_f}{f_{t,y}b\alpha d} = \frac{\sqrt{l_m/d}}{\sqrt{0.6(\alpha-\alpha^2)\sqrt{E_x/G_{xy}}} + (\beta+\gamma l_m/d)\sqrt{6(1/\alpha-\alpha^2)/\sqrt{E_x/G_{xy}}}} \qquad (21)$$

for γ=0 and with G_c=$G_{f,y}$, equations (20) and (21) are identical to equation (17). On basis of numerical results regarding length of fracture zone, γ is made equal to 0.2 in following comparison to experimental results. Comparison for γ=0 is also made.

In equation (18), non–zero length of the fracture zone may be taken into account by applying beam shear force, V, and bending moment, M, for the beam cross section 0.2 l_m ahead of the notch.

2.3 Initial cracks and knots

During handling and construction cracks of various geometry may develop from the tip of a notch. Such cracks may develop due to large moisture and temperature gradients. For a crack with simple geometry, estimation of its notch strength reducing effect can be obtained in a simple manner.

According to the actual theory, a crack of length a along the beam and with the same width as the beam is equivalent to an increase of notch length, βd, by a.

A long crack, or a pair of long cracks, along the side, or sides, of the beam, not penetrating the entire width of the beam but reducing its effective width from b to b', may be studied by replacing b in equation (17), (18), (20) or (21) by the net width b'

and replacing the material stiffness parameters G_{xy} and E_x by the corresponding equivalent beam stiffnesses $(b/b')G_{xy}$ and $(b/b')E_x$, respectively. As an example, $b'=b/2$ yields a reduction in notch strength from V_f to $V_f/\sqrt{2}$.

Influence of knots of various geometry at the tip of a notch might be roughly estimated in a similar manner. Depending on type and orientation, the influence of a knot may be very different, but if regarded as equivalent to a crack one would expect estimations to be on the safe side.

3. TESTS

3.1 Present tests

In a rather thorough manner, a small number of notched beams, see Figure 1, were tested. Load versus deflection and load versus deformation close to the tip of the notch were recorded and various material property parameters were determined for specimens cut from the vicinity of the notch of each beam.

The test program included beams of three different sizes and for each size 7 nominally equal beams were tested. The beams were all rather small, beam depths being 192, 48 and 12 mm (7.56, 1.89 and 0.47 in). All in–plane dimensions of the beams were scaled in proportion to beam depth. Beam width was equal for all beams: b=44 mm (1.73 in).

The test material was cut from machine graded planks (T30, 44x196 mm^2) of Pinus sylvestris L., additionally graded visually so that the vicinity of the notch became free from knots. Before testing the material was stored for several months at constant relative humidity and temperature, 65 percent and 20°C (68°F), respectively. The rate of beam deflection was made proportional to beam depth, making the strain rate in beams of different size approximately equal. The time to notch fracture was roughly 5 minutes for all beams.

The material parameters determinal were: stiffness parameters E_x, E_y, G_{xy} and ν_{xy}, tensile strength perpendicular to grain, $f_{t,y}$, and at 45° angle to grain, $f_{t,45}$, fracture energy for tensile fracture perpendicular to grain, $G_{f,y}$, density, ρ (wet weight/wet volume), moisture content, M (weight of water/weight of oven–dry sample), shrinkage, ϵ_v (relative decrease in volume when dried from actual moisture content to M=0) and a mean value, $\overline{\varphi}$, of angel φ between tangential direction of timber and z–axis. The coordinate system used, see Figure 1, is orientated according to the geometry of the beams: x–direction corresponds to length–direction, y–direction corresponds to

depth–direction and z–direction corresponds to width–direction. Regardless of beam size, material property parameters were determined for specimens of equal size.

Fracture energy $G_{f,y}$ was determined according to Figure 5. The sample to be tested is glued to piece of wood forming a symmetric beam with a slit. This beam is loaded in three point bending, the entire load versus deflection response, P vs δ, being recorded. $G_{f,y}$ is then evaluated from the total work required for complete fracture of the net section, A_{net}, of the beam:

$$G_{f,y} = \frac{1}{A_{net}} \left[\int_0^{\delta_o} P(\delta) d\delta + mg\delta_o \right] \tag{22}$$

δ_o is the beam deflection when P becomes zero. At this instant the beam collapses due to its own weight, mg.

The tests used to determine other material parameters are described in (Gustafsson and Enquist, 1988).

3.2 Test results

In Table 1 test results are compiled. A significant size–effect in $V_f/(b\alpha d)$ is evident. This is consistent with theoretical results of fracture mechanics. E_y is lower then probable values of modulus of elasticity in the radial and tangential directions. E_y is, however, influenced by angle φ and the low values of E_y are probably due to the low stiffness of wood in rolling shear.

In Figures 6–9 average curves for deflection and deformations are shown. Normalized global stiffness of the smallest beams is found to be greater than for the larger beams. This is presumably due to the fact that the smallest beams were almost entirely free from knots. The other beams were free from knots only in the vicinity of the notch.

Figures 7 and 8 show an apparently plastic plateau in load versus deformation close to notch. This plateau may indicate stable growth of a fracture process zone before start of rapid crack development. Figure 10, showing typical examples of load versus elongation for samples of the actual material when loaded to failure in uniform tension perpendicular to grain and in 45° angle to grain, does not expose plastic properties of the wood but instead an almost linear elastic performance before peak stress.

3.3 Comparison test–theory

In Figure 11 $V_f/(f_{t,y}b\alpha d)$ versus $d/(G_{f,y}\sqrt{E_x G_{xy}}/f_{t,y}^2)$ is shown according to the present test results and according to the theory given in Section 2. The theoretical result, equation (20) and (21), is shown for $E_x/G_{xy}=30.5$. This value of ratio E_x/G_{xy} is the mean value obtained from the material property tests. $\gamma=0.0$ represents the assumption of zero size of the fracture process region and $\gamma=0.2$ represents a non–zero size according to the preceding discussion.

The theory appears to predict about the same size–effect as that obtained in the tests. For the smallest beams the length of the fracture region is of the same order of magnitude as the notch length, βd, which reduces the size–effect.

Absolute values of notch strength, V_f, seem to be overestimated by the theory by about 10 percent. Having in mind that equation (20) is simple and derived theoretically without use of any empirical adjustment factor, the deviation between tests and theory is surprisingly small.

Concerning the relative influence of various variables, additional comparisons between tests and theory are made in Section 3.4, using test results compiled from literature.

3.4 Test results from literature

To verify the present beam test results and the theoretical approach, Table 2 has been compiled. Table 2 comprises 36 different beam test series with 34 different combinations of geometry and material, divided among 9 different studies. References and available information about material properties are indicated in the table.

η indicates ratio between distance from support to point of loading and beam depth, d. Other geometry parameters are defined in Figures 1 and 3. n is the number of tests. In cases where η, η/α or $\eta-\beta$ is small, corresponding to a very short shear span, one may expect V_f to be greater than for normal beams. Therefore, a test result obtained for a small η/α, say less than about 2.5, is probably not representative for a normal beam.

With the exception of study i), all beams had a 90° notch extending all the way from support to x=βd. In study i), for the two test–series indicated by β=5.5 the notch extended from x=2.5d to x=5.5d and for the two series indicated by β=2.5 the notch was a slit at x=2.5d.

In Table 2 comparison is made with the results of three equations: equation (1) with $f(\alpha)=\alpha$, equation (17) and equation (20) with $\gamma=0.2$. During calculation of V_f according to these equations, the same material property parameters have been applied throughout, regardless of type and quality of wood tested. In equation (1) f_v is made equal to 10 MPa, representing a normal and typical value for the short time shear strength of Pinus sylvestris L. free from defects and with a moisture content of about M=12 percent. Material parameters applied in equations (17) and (20) are the mean values obtained in present material property tests: in equation (17) $(G_{f,y}\sqrt{E_x G_{xy}})^{0.5}$ = 0.855 MPa $\sqrt{m}$ (777 psi$\sqrt{in}$) and E_x/G_{xy} = 30.5, and in equation (20) it is additionally assumed that $f_{t,y}$=4.04 MPa (585 psi) and that γ=0.2.

A study of Table 2 shows that equation (20) gives reasonable predictions regarding influence of α, β and d. With the exception from results of studies f) and g), the agreement between tests and theory may even be regarded as very good. Results from studies f) and g) are somewhat contradictory with respect to influence of α: for an increase of α from 0.50 to 0.917, $V_f/(b\alpha d)$ increases by a factor 2.7 in study f), by a factor 1.5 in study g) and by a factor 2.1 according to theory, equation (20).

Equation (17) gives almost the same result as equation (20), a significant difference being apparent only for small beams with a very short distance, βd, between support and tip of notch.

Applying material property parameters valid for Pinus sylvestris L., theory gives absolute values of $V_f/(b\alpha d)$ in good agreement with test results for Pinus sylvestris L. and Pseudotsuga menziesii Franco (Douglas fir). Fracture toughness $(G_{f,y}\sqrt{E_x\ G_{xy}})^{0.5}$ for hardwood Eucalyptus obligua seems to be twice that of the actual softwoods.

Equation (1), applied with $f(\alpha)=\alpha$, seems to give un–conservative results, in particular for large beams, for intermediate values of α and for large values of β. By definition, equation (1) gives no prediction regarding influence of β and d. According to both test results and theory, these parameters have a significant influence on notch strength.

Figure 12 shows $V_f/(b\alpha d)$ versus α according to equation (20) for different values of β and d. Material parameter values adopted in this figure are those obtained in the present tests of Pinus sylvestris L. The theoretical result shown in Figure 12 may be compared with various design equations illustrated in Figure 2.

4. CONCLUDING REMARKS

4.1 Size–effect, discussion

In Figure 13 relative influence of beam size on notch strength is shown by means of various test results, indicated numerically in Table 2. The rest results unamimously show a significant size–effect in notch strength.

In general, a size–effect may have its explanation in large strain gradients, associated with fracture mechanics analysis, scatter in strength, often associated with Weibull theory, or "false" size effects caused by for instance different grading of timber of different size.

Although the Weibull concept is applied also to notch strength in EUROCODE 5, scatter in strength is hardly the prime basic reason for the actual size–effect. Notch failure develops at the tip of a notch and therefore the number of possible notch failure locations does not increase with the volume of the beam. Instead the size–effect predicted already by deterministic analysis may be of prime importance in the present case. The size–effect predicted by linear fracture mechanics is due to constant size of the fracture process region, the size of the fracture region not being proportional to beam size making this active region relatively small in large beams. Linear fracture mechanics is valid if the fracture region is small relative to other dimensions. For small beams the relative size of the fracture region is significant, making the size–effect less than predicted by linear fracture mechanics. Theoretically, for extremely small beams the size of the fracture region becomes proportional to beam size and then the size–effect is no longer at hand.

While fracture mechanics gives information about influence of in–plane dimensions of the beam, also beam thickness, b, might influence $V_f/(b\alpha d)$. According to the formula given in EUROCODE, $V_f/(b\alpha d)$ is proportional to $b^{-0.2}$ if length and depth of beam are kept constant. The test results from literature compiled in Table 2 provide no information regarding possible influence of beam thickness.

4.2 Size–effect according to various analyses

Different approaches for fracture mechanics analysis predict somewhat different size–effect. The present simple analysis gives, according to equation (17):

$$\frac{V_f}{b\alpha d} \sim \frac{1}{\sqrt{d}} \qquad (23)$$

Equation (20) gives:

$$\frac{V_f}{b\alpha d} \sim \frac{1}{\sqrt{d}(1+\text{constant}/d)} \tag{24}$$

Linear elastic fracture mechanics together with plane stress plate theory, (Leicester, 1971), gives

$$\frac{V_f}{b\alpha d} \sim \frac{1}{d^{\lambda}} \tag{25}$$

where λ is about 0.45 for a 90° notch in an orthotropic material such as wood.

A non–linear fracture mechanics analysis by finite elements, (Gustafsson, 1985), gave numerical results that accurately could be summarized by:

$$\frac{V_f}{b\alpha d} \sim \frac{1}{(\text{constant}+d)^{0.46}} \tag{26}$$

Compared with test results, the size–effect of equations (25) and (26) seems somewhat more accurate than that of equations (23) and (24). The difference is, however, slight. For small beams, equations (24) and (26) seem more accurate than equations (23) and (25), respectively. In most engineering applications, equation (23) may give a sufficiently accurate estimation of the size–effect for a 90° notch in a wooden beam.

4.3 Conclusions

Following conclusions relate to the strength of a 90° notch on the tension side of a wooden beam. By notch strength is meant $V_f/(b\alpha d)$.

1) Several test results unanimously demonstrate a significant size–effect in notch strength. Weibull theory can hardly be regarded to give a valid explanation to this size–effect.

2) Notch failure may be analysed theoretically by fracture mechanics and a closed–form expression for notch strength has been obtained. This expression seems to give results in good agreement with tests and may provide useful information during development of a design formula.

3) Material properties stiffness and fracture energy are found to be decisive for notch strength. Among stiffness parameters, shear modulus, G_{xy}, and modulus of elasticity in

grain direction , E_x, are of prime importance. For constant E_x/G_{xy} the notch strength is approximately proportional to $(G_{f,y}\sqrt{E_xG_{xy}})^{0.5}$, $G_{f,y}$ being the fracture energy in tension perpendicular to grain.

4) According to the theory, tensile strength perpendicular to grain is of minor importance for notch strength. Co–variation between tensile strength and other material properties may give an apparent influence of tensile strength. As for the present test results, however, no statistical correlation between notch strength and tensile strength perpendicular to grain could be found, see (Gustafsson and Enquist, 1988).

5) The distance βd from the support to the notch tip, which determines the bending moment at the notch tip, is of significant importance for notch strength.

6) During increase in notch depth, the notch strength decreases rapidly when $1.0>\alpha>0.7$. For smaller values of α, the influence of α is less. For $\alpha\rightarrow 1.0$ notch strength becomes theoretically infinite, reflecting that notch failure can not occur at the tip of a non–existing notch.

7) Applicability of linear elastic fracture mechanics depends on the length βd. Non–linear fracture mechanics is estimated to give good results also for small beams with a small β.

8) A conventional formula, such as $V_f/(b\alpha d) = (2/3)\alpha f_v$, may in some cases overestimate notch strength very much.

Table 1 Test results: material properties and notch strength. No 1–7: d=192 mm (7.56 in), No 8–14: d=48 mm (1.89 in), No 15–21: d=12 mm (0.47 in)

No –	E_x MPa	E_y Mpa	ν_{xy} MPa	G_{xy} MPa	$f_{t,y}$ MPa	$f_{t,45}$ MPa	$G_{f,y}$ N/m	ρ kg/m³	M %	ϵ_v %	$\bar{\varphi}$ o	$V_f/(b\alpha d)$ MPa
1	16400	198	.68	348	4.11	7.50	335	525	15.1	8.4	34	1.41
2	10000	184	.52	367	4.92	7.94	233	402	14.9	7.2	33	1.13
3	10000	189	.65	368	3.15	7.01	359	408	14.9	5.8	33	1.64
4	10400	171	.50	398	3.03	4.91	274	418	14.8	6.9	47	1.24
5	8870	185	.30	421	5.33	6.33	254	411	14.8	5.8	32	1.50
6	9570	152	.69	774	4.57	6.23	278	501	15.4	6.7	54	1.51
7	9110	94	.62	191	3.04	4.94	257	372	15.2	5.8	61	0.67
1–7	10620	167	.57	410	4.02	6.41	284	434	15.0	6.7	42	1.30
8	13900	168	.35	290	4.09	6.32	219	482	14.8	7.5	61	2.54
9	13500	158	.63	601	3.05	6.47	359	464	14.6	8.2	73	3.06
10	14500	148	.43	597	3.72	5.13	301	506	15.0	7.0	63	2.55
11	16400	147	.37	422	3.94	5.94	320	506	14.7	9.1	42	3.03
12	15400	164	.60	582	4.29	5.77	339	497	14.8	8.8	67	2.34
13	17000	149	.67	628	4.80	6.21	220	527	14.8	8.6	58	2.83
14	18500	152	.38	608	4.45	7.39	371	514	14.7	7.6	57	2.89
8–14	15600	155	.49	533	4.05	6.18	304	499	14.8	8.1	60	2.75
15	Same as No 8										50	3.23
16	Same as No 9										54	3.11
17	Same as No 10										54	3.17
18	Same as No 11										57	4.08
19	Same as No 12										63	3.64
20	Same as No 13										52	2.40
21	Same as No 14										58	3.61
15–21	Same as No 8–14										55	3.32
1–14												
Mean	13110	161	.53	471	4.04	6.29	294	467	14.9	7.4	51	–
St.d	3360	26	.14	161	0.76	0.94	54	53	0.2	1.1	14	–
Var.	26%	16%	26%	34%	19%	15%	18%	11%	1%	15%	27%	–

Table 2. Notch strength: list of various test results and comparison to computational results obtained for Pinus sylvestris L. $f(\alpha)=\alpha$ in eq. (1) and $\gamma=0.2$ in eq. (20).

d	α	β	η/α	b	n	$\frac{V_f}{b\alpha d}$	Coef. of var.	$V_{f,theory}/V_{f,test}$		
mm				mm		MPa		ekv. (1)	ekv. (17)	ekv. (20)
12	.75	.50	3.6	44	7	3.32	16%	1.5	1.9	1.2
48	–"–	–"–	–"–	–"–	–"–	2.75	10%	1.8	1.1	1.0
196	–"–	–"–	–"–	–"–	–"–	1.30	25%	3.9	1.2	1.2

a) Present test, Pinus sylvestris L., properties acc. to Table 1, time to failure about 5 min, M=14.9%, ρ=467 kg/m^3

50	.50	.50	10.0	45	2	2.00	16%	1.7	1.2	1.0
100	–"–	–"–	5.0	–"–	–"–	1.46	11%	2.3	1.2	1.1
200	–"–	–"–	2.5	–"–	–"–	1.18	6%	2.8	1.0	1.0

b) Carlsson, Shahabi and Sunding (1983), Pinus sylvestris L., short time loading, M≈12%

45	.50	.50	6.7	45	6	1.72	9%	1.9	1.5	1.2
195	–"–	–"–	6.2	–"–	–"–	0.93	17%	3.6	1.3	1.2

c) Students course tests 1985, Pinus sylvestris L., short time loading, M≈18%

45	.50	.50	6.7	45	4	1.92	9%	1.7	1.3	1.1
195	–"–	–"–	6.2	–"–	–"–	0.96	4%	3.5	1.3	1.2

d) Students course tests 1986, Pinus sylvestris L., short time loading, M≈18%

9.5	.50	1.92	9.3	38	4	3.90	–	0.9	0.6	0.5
19	–"–	–"–	–"–	–"–	4	3.08	–	1.1	0.6	0.5
37	–"–	–"–	–"–	–"–	≥2	1.90	–	1.8	0.7	0.6
58	–"–	–"–	–"–	–"–	4	1.77	–	1.9	0.6	0.5
154	–"–	–"–	–"–	–"–	4	1.07	–	3.1	0.6	0.5

e) Leicester (1973), (Eucalyptus obligua), "air dry", E_x=21900 MPa, E_y=1880 MPa G_{xy}=1430 MPa, ν_{xy}=0.42

600	.917	.417	2.2	100	5	2.00	13%	3.1	0.8	0.8
–"–	.833	–"–	2.4	–"–	4	1.61	28%	3.5	0.7	0.8
–"–	.750	–"–	2.7	–"–	–"–	0.88	12%	5.7	1.1	1.1
–"–	.667	–"–	3.0	–"–	–"–	0.86	16%	5.2	1.0	1.0
–"–	.500	–"–	4.0	–"–	–"–	0.75	7%	4.4	1.0	1.0

f) Möhler och Mistler (1978), glulam made of "Fichtenholz" (spruce), time to failure more than 1 min, $f_{c,x}$=41 MPa at M=15%, ρ=470 kg/m^3 at M=9.3%

g) Möhler och Mistler (1978), "Fichtenholz" (spruce), free from defects, time to failure more than 1 min, $f_{c,x}$=42.4 MPa at M=15%, ρ=510 kg/m^3 at M=10.8%, tests at M≈11–12%

120	.917	.250	3.4	32	6	2.36	11%	2.6	1.7	1.6
–"–	.833	–"–	3.8	–"–	27	1.93	15%	2.9	1.5	1.4
–"–	.750	–"–	4.2	–"–	43	1.68	19%	3.0	1.5	1.4
–"–	.667	–"–	4.7	–"–	14	1.52	18%	2.9	1.4	1.4
–"–	.583	–"–	5.4	–"–	10	1.50	18%	2.6	1.4	1.3
–"–	.500	–"–	6.3	–"–	49	1.59	18%	2.1	1.3	1.2
–"–	.333	–"–	9.5	–"–	10	1.48	16%	1.5	1.3	1.2

h) Kollmann (1951), "Red tulip oak".
*Only ratio (ultimate load with notch)/(ultimate load without notch) known. Absolute values of $V_f/(b\alpha d)$ have been calculated at the assumption $V_f=(2/3)bdf_v$ for beam without notch assuming f_v=10 MPa

100	.875	≈0.3	2.0	50	1	5.56*	–	1.0	0.6	0.6
–"–	.750	–"–	2.4	–"–	2	3.47*	–	1.4	0.7	0.7
–"–	.625	–"–	2.9	–"–	1	2.77*	–	1.5	0.8	0.7
–"–	.500	–"–	3.6	–"–	2	2.53*	–	1.3	0.8	0.7
–"–	.250	–"–	7.2	–"–	1	≈1.9*	–	≈0.9	≈1.0	≈0.9

i) Murphy (1986), glulam made of Douglas fir (Pseudotsuga menziesii Franco) free from defects, short time loading

305	.700	2.5	14.3	79	2	0.46	8%	10.1	1.0	1.0
–"–	–"–	5.5	–"–	–"–	2	0.24	2%	19.4	1.0	1.0
457	–"–	2.5	–"–	–"–	2	0.38	10%	12.3	1.0	1.0
–"–	–"–	5.5	–"–	–"–	1	0.16	–	29.2	1.2	1.2

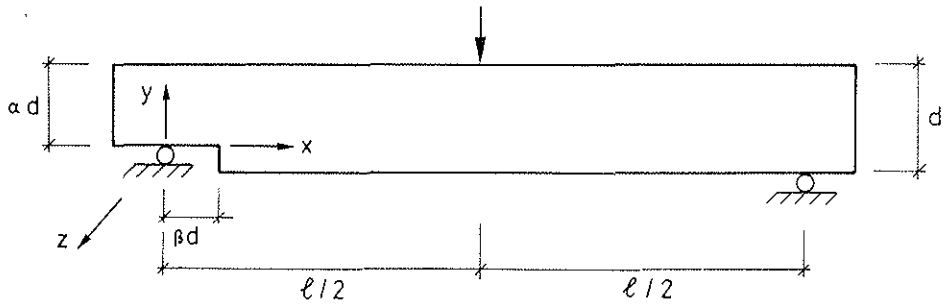

Figure 1. Beam with a rectangular end–notch. In present tests: α=0.75, β=0.5 and b=44 mm (1.73 in). b represents width of beam.

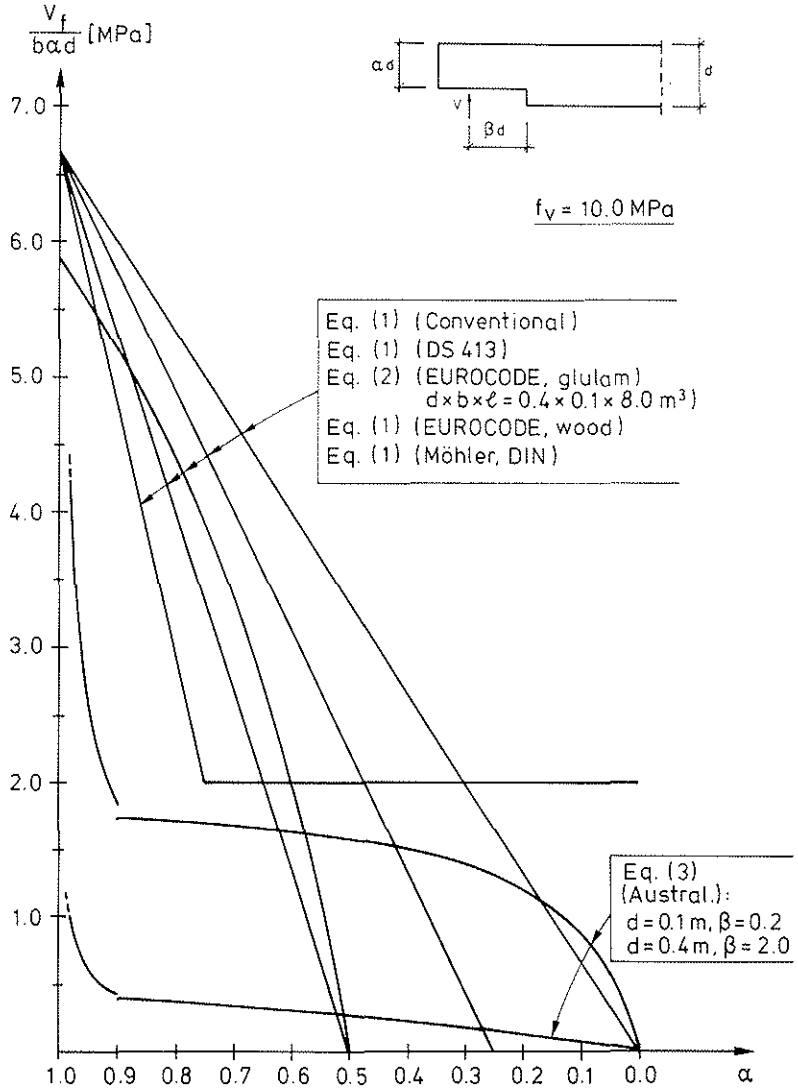

Figure 2. Comparison between code–formulas for notch strength. Design values of f_v given in codes are much less than 10 MPa.

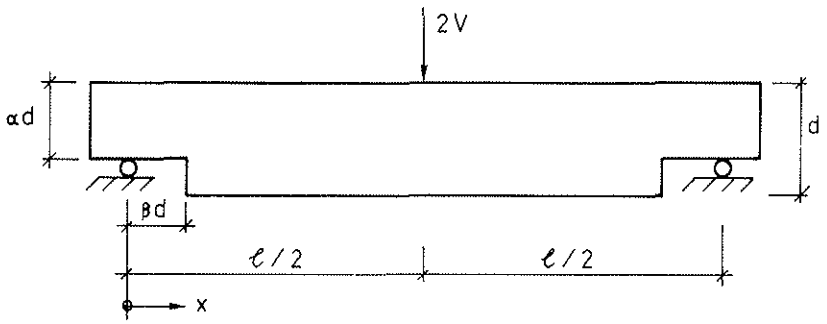

Figure 3. Beam studied in the theoretical analysis.

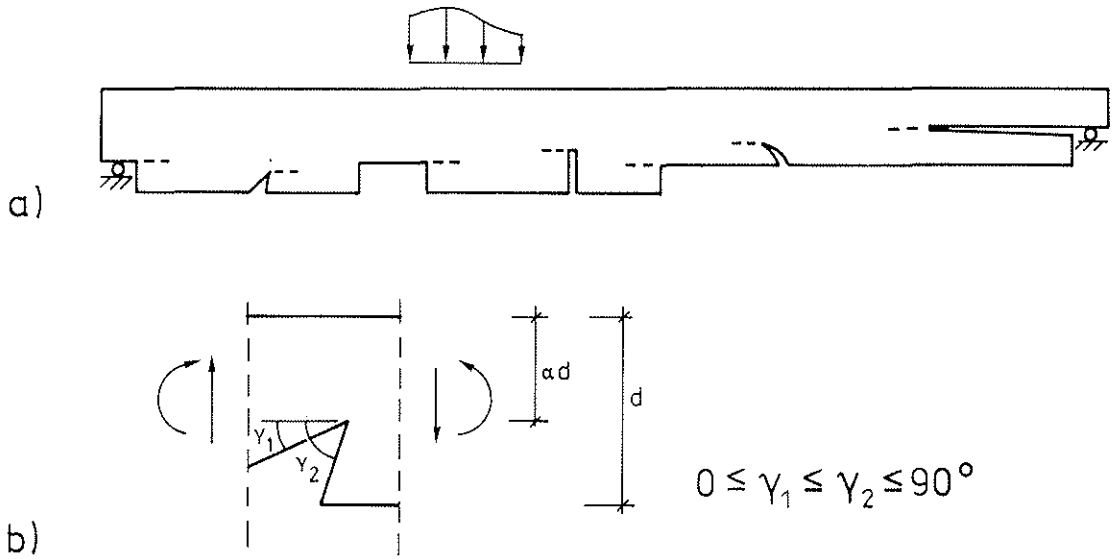

Figure 4. Various notches comprised by a theory.

Figure 5. Test set–up to determine fracture energy $G_{f,y}$.

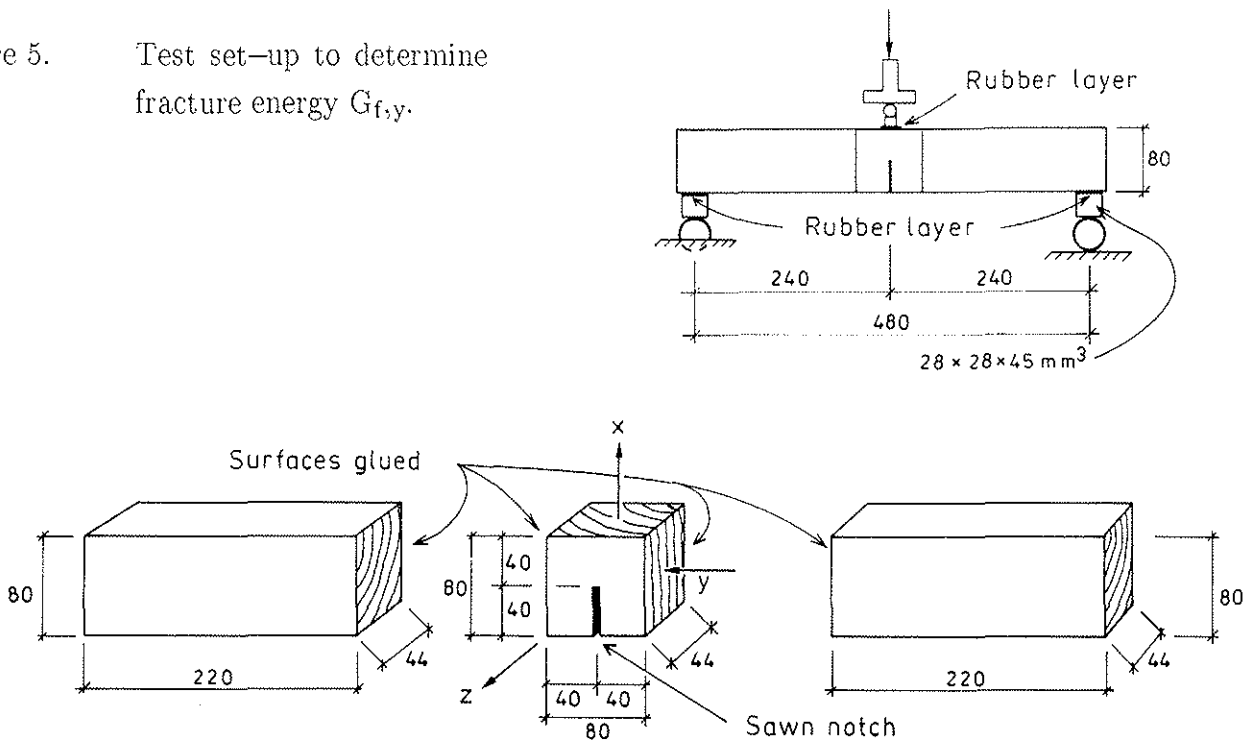

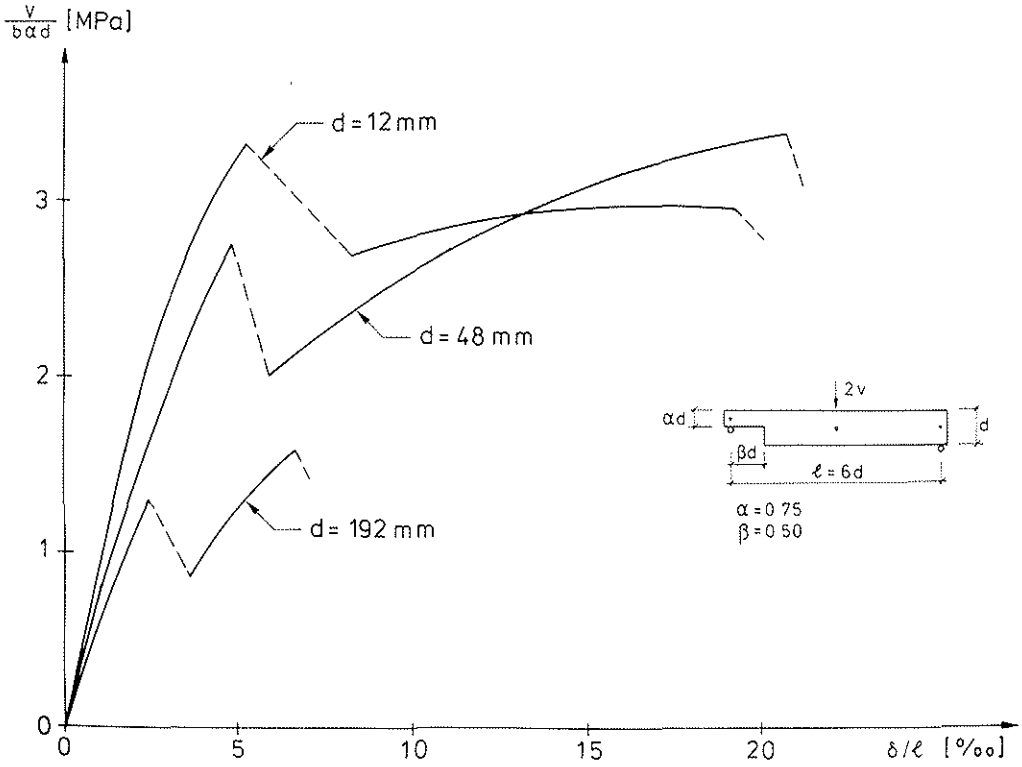

Figure 6. Test results: normalized load vs. normalized deflection for beams of various sizes.

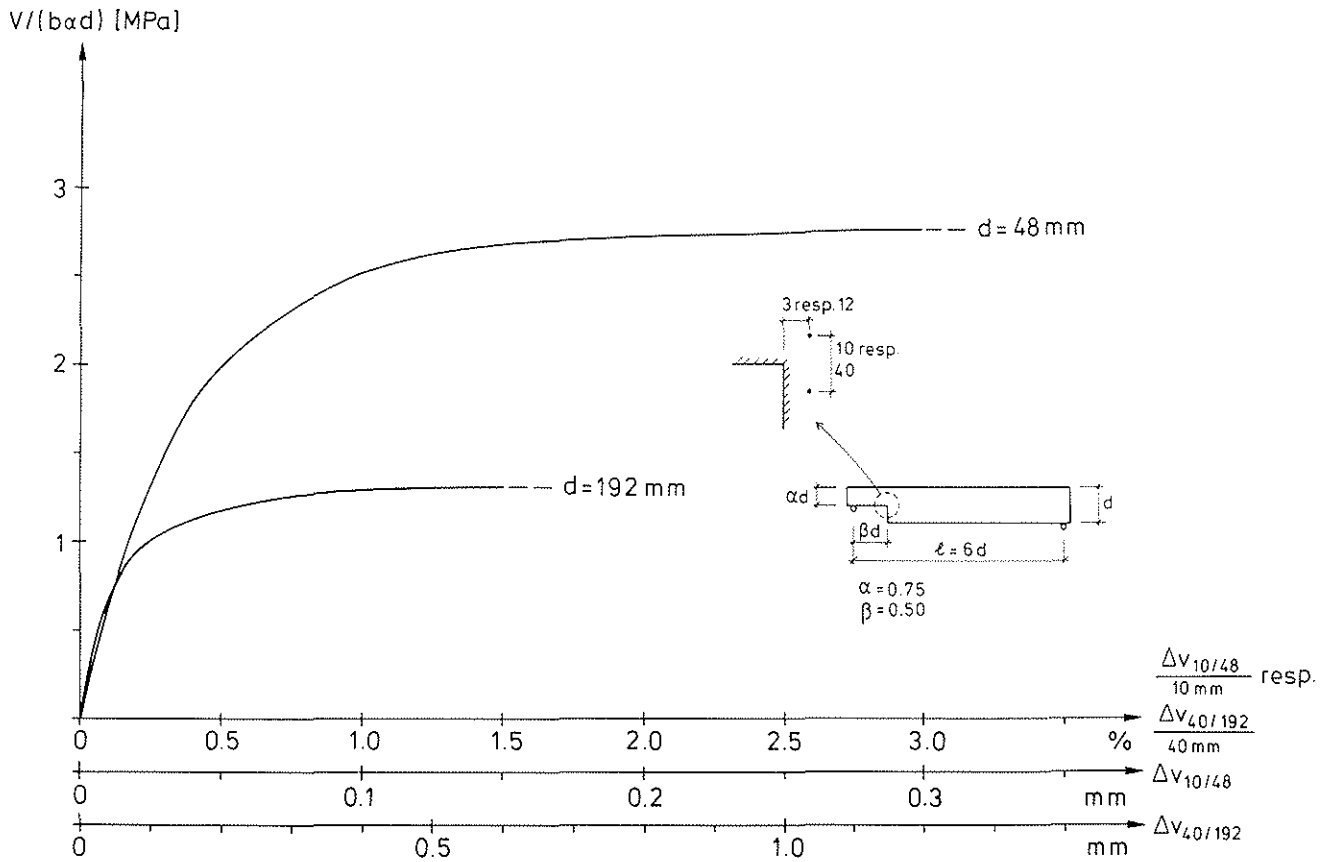

Figure 7. Test results: normalized load vs. vertical strain close to the notch tip.

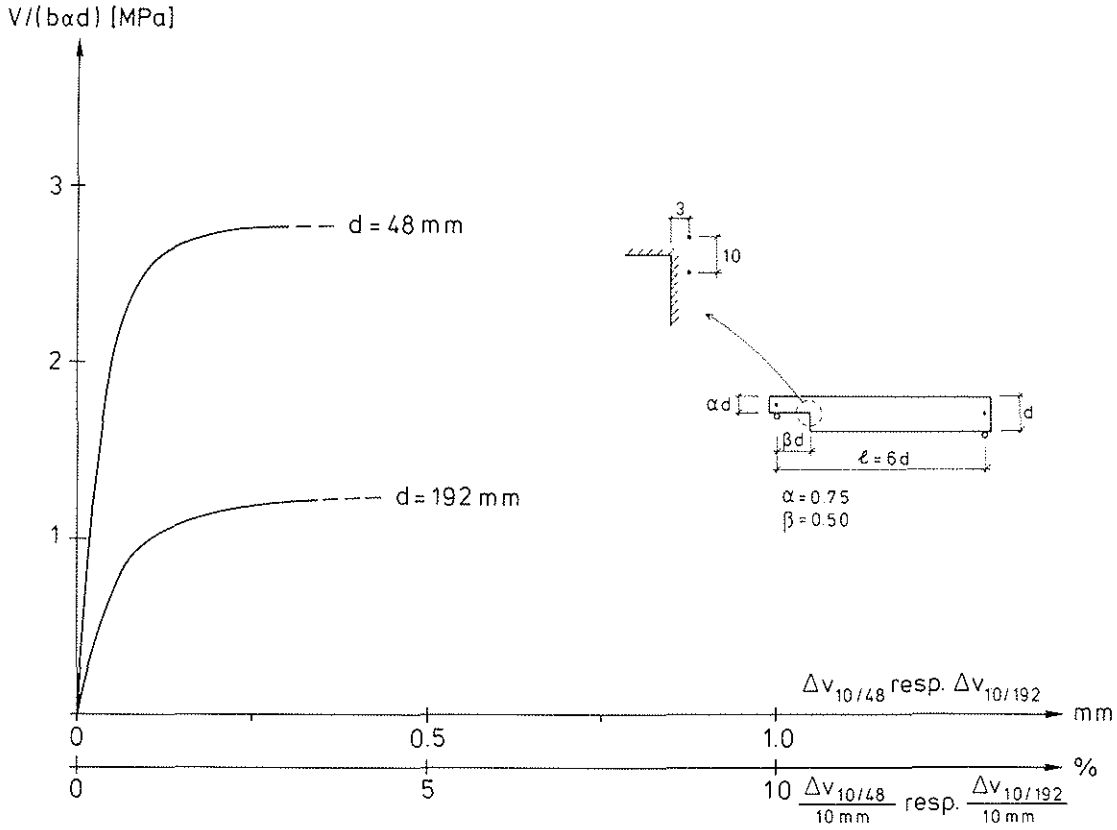

Figure 8. Test results: normalized load vs. vertical absolute deformation close to the notch tip.

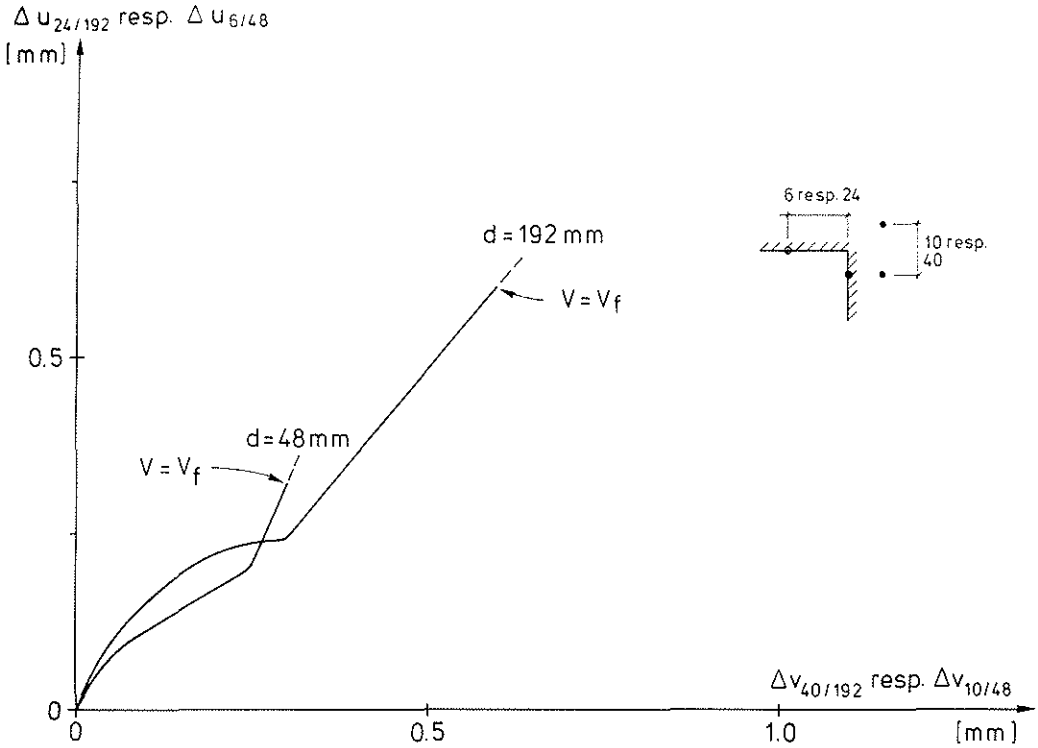

Figure 9. Test results: horisontal deformation vs. vertical deformation for beams of depths 48 mm and 192 mm.

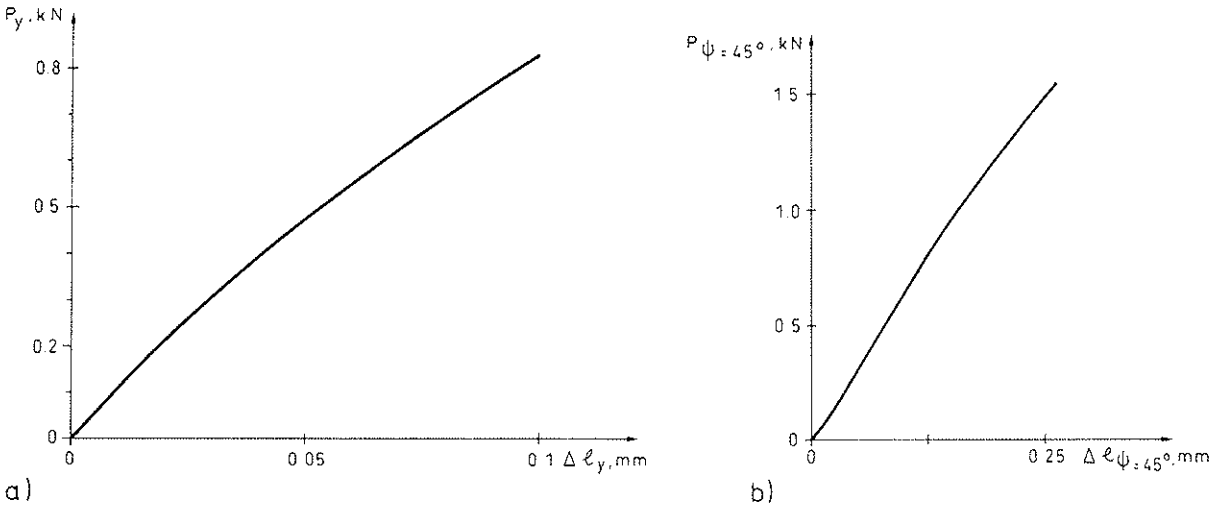

Figure 10. Load vs. elongation for samples loaded to failure in uniform tension perpendicular to grain, a), and in 45° angel to grain, b).

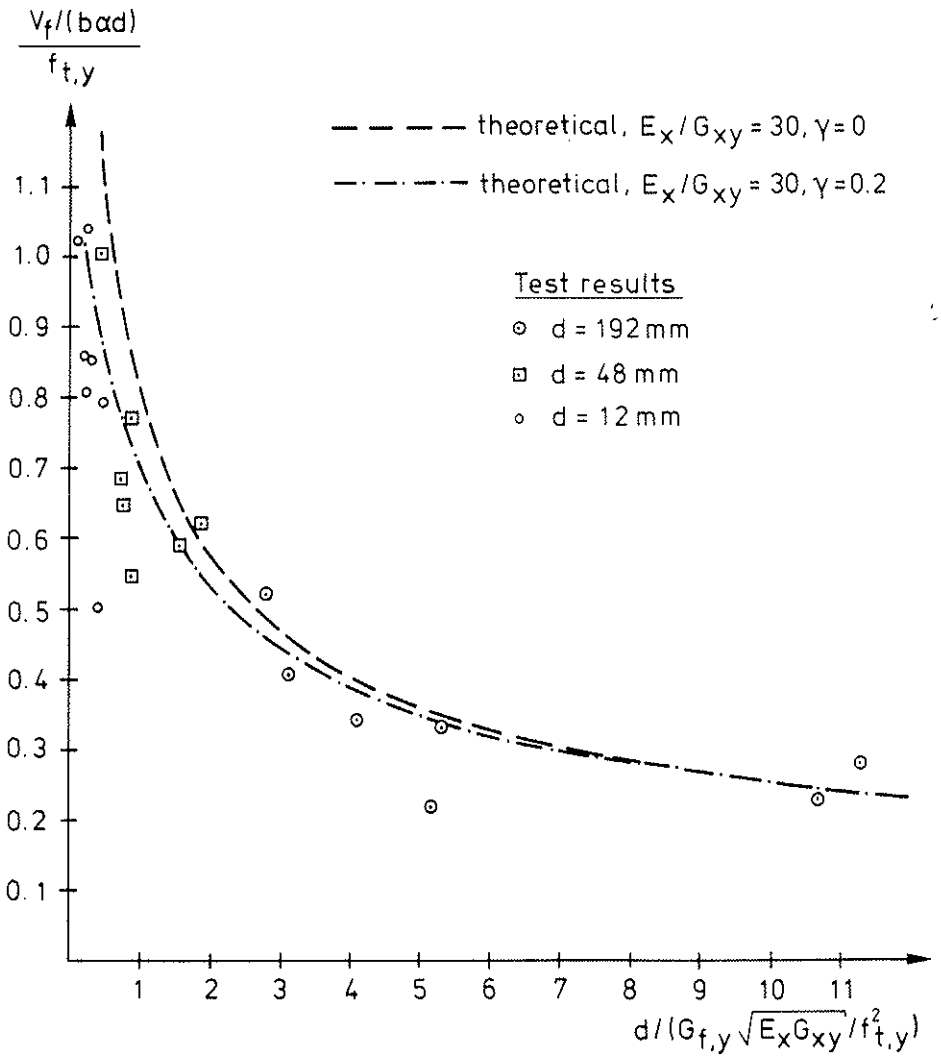

Figure 11. Normalized strength vs. normalized beam size according to tests and theory, equation (21). For γ=0 equation (21) is equivalent to equation (17).

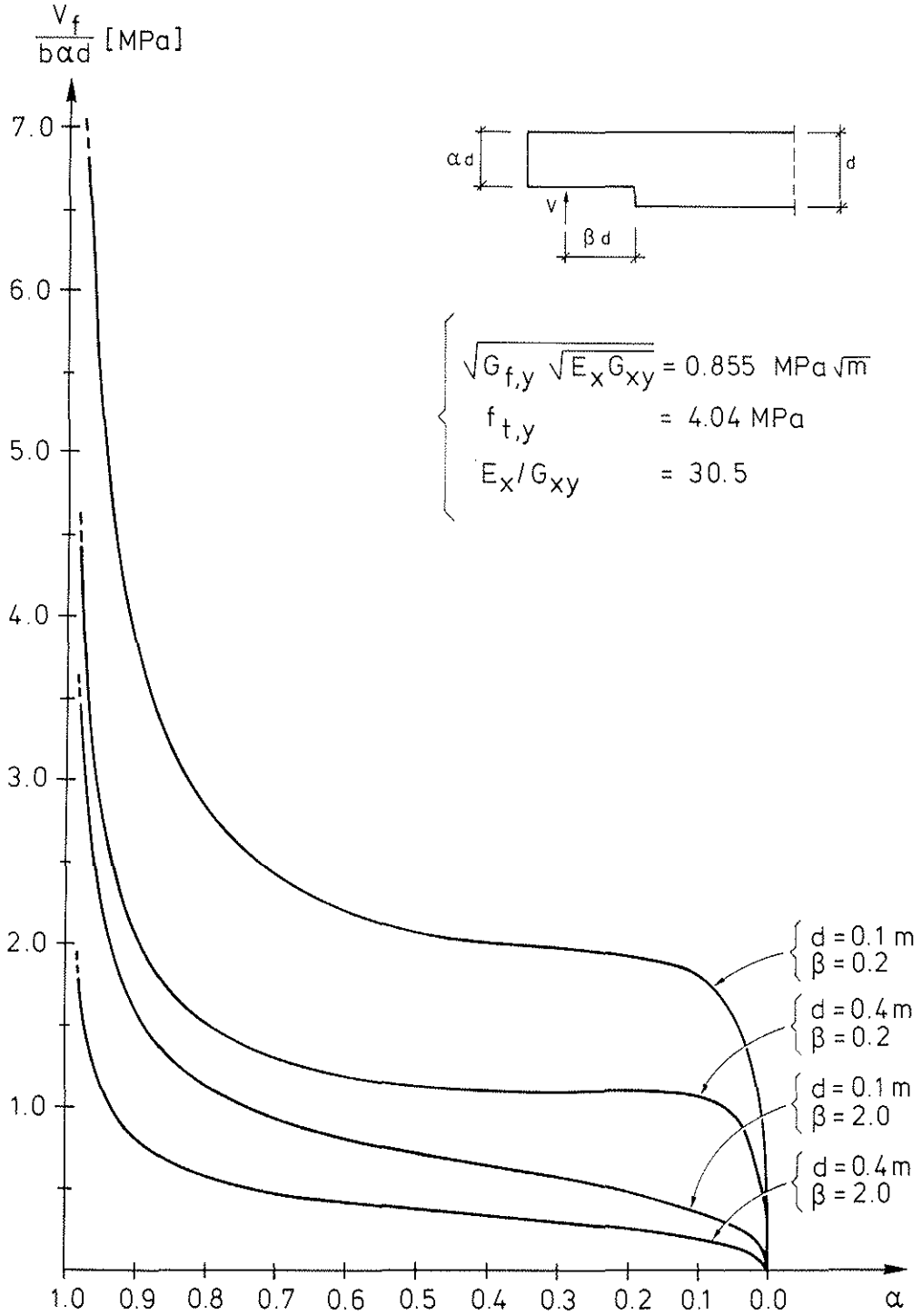

Figure 12. Notch strength vs. relative depth of notch according to theory for various beam sizes and relative lengths of notch. The material property parameters are obtained from testing of Pinus sylvestris L.

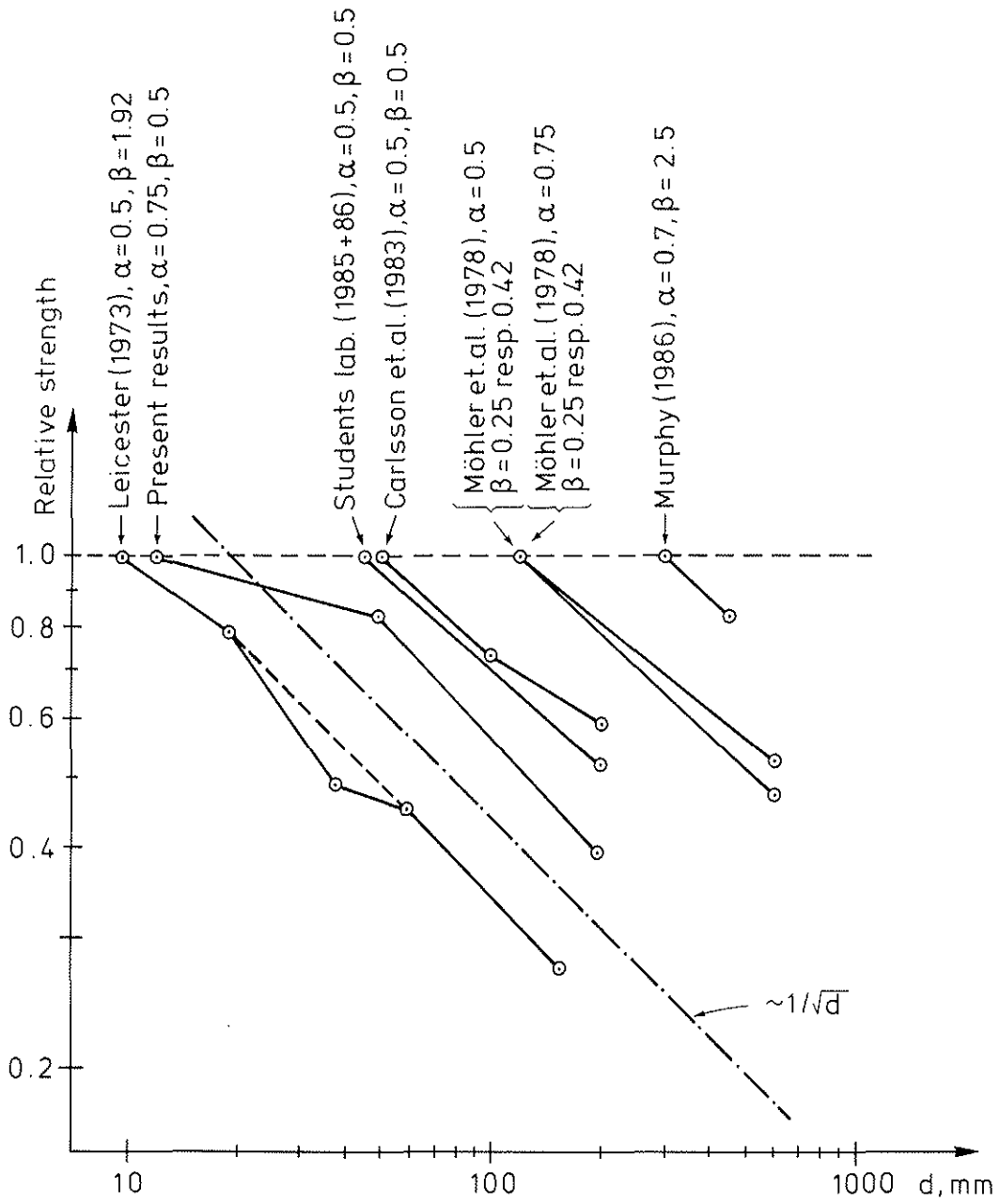

Figure 13. Influence of beam size on notch strength according to various test results.

REFERENCES

Carlsson, T., Shahabi, A. and Sunding, L. (1983) Träs brottbeteende (Fracture performance of wood), Seminar essay (in swedish), Div. of Build.Mat., Lund Inst. of Techn., Sweden.

EUROCODE 5 (1987), Common unified rules for timber structures, Report EUR 9887 EN, Commission of the European Communities.

Gustafsson, P.J. (1985), Fracture mechanics studies of non–yielding materials like concrete – modelling of tensile fracture and applied strength analyses. Report TVBM–1007, Div. of Build. Mat., Lund Inst. of Techn., Sweden.

Gustafsson, P.J. and Enquist, B. (1988), Träbalks hållfasthet vid rätvinklig urtagning (Strength of wooden beam at right angle notch), Report TVSM–7042 (in swedish), Div. of Struct. Mech., Lund Inst. of Techn., Sweden.

Kollmann, F. (1951), Technologie das Holzes und der Holzerkstoffe (Erster band), Springer–Verlag BRD.

Leicester, R.H. (1971), Some aspects of stress fields at sharp notches in orthotropic materials, Techn. Paper No. 57, Div. of Forest Products, CSIRO, Australia.

Leicester, R.H. (1973), Effect of size on the strength of structures, Techn. Paper No. 71, Forest Products Lab., Div. of Building Research, CSIRO, Australia.

Lum, C. and Foschi, R.O. (1988), Arbitrary V–notches in orthotropic plates, J. of Engineering Mech., Vol. 114, No. 4, pp. 638–655, ASCE.

Möhler, K. and Mistler, M.–L. (1978), Untersuchungen ueber den Einfluss von Ausklinkungen in Auflagerbereich von Holzbiegetraegern auf die Tragfestigheit, Rapport, Lehrstuhl für Ingenieurholzbau und Baukonstruktionen, Universität Karlsruhe (TH), BRD.

Murphy, J.F. (1986), Strength and stiffness reduction of large notched beams, J. of Struct. Eng., Vol. 112, No. 9, pp 1989–2000, ASCE.

CIB-W18A/21-11-1

INTERNATIONAL COUNCIL FOR BUILDING RESEARCH STUDIES AND DOCUMENTATION

WORKING COMMISSION W18A - TIMBER STRUCTURES

DURABILITY CLASSIFICATIONS: A PROPOSED FORMAT FOR ENGINEERING PURPOSES

by

R H Leicester and J E Barnacle
CSIRO
Australia

MEETING TWENTY-ONE
PARKSVILLE, VANCOUVER ISLAND
CANADA
SEPTEMBER 1988

DURABILITY CLASSIFICATIONS: A PROPOSED FORMAT FOR ENGINEERING PURPOSES

by

R.H. Leicester and J.E. Barnacle

(CSIRO, Melbourne, Australia)

1. INTRODUCTION

Recommendations for sizing timber members in protected structures are based on relatively sophisticated procedures which make use of extensive quantitative data related to material strength and stiffness, and to load characteristics. However if the structure is unprotected, the potential loss of strength due to decay and insect attact is not usually stated in quantified terms and the rationale on which conventional structural design is based disappears. Of course, this type of comment applies not only to timber but also to most other structural materials.

As a first step towards quantifying the structural effects of durability, it is proposed that structural durability be stated in terms of the performance criterion defined in Table 1.

It should be noted that to the structural engineer it is not the strength of the average structure that is of significance; rather the focus is on the weakest structures within a set. Similarly with respect to durability it is more important to focus attention on the performance of the most rapidly deteriorating specimens of timber rather than on the average ones.

The purpose of this paper is to suggest the type of format in which data may be used to predict durability performance ratings. Because of time limitations, the examples to be given are based on a rough assessment of Australian conditions. However no care has been taken to ensure the numerical accuracy of the data shown; hence the following disclaimer is made:

> Quantitiative data given in this paper are based only on very rough guesstimates: they are provided only for the purpose of illustrating a proposal for a format: they are not intended to be specific recommendations.

Finally it should be mentioned that the spirit of this proposal is to provide a first estimate of durability performance ratings in the absence of other information. It is not intended that procedures of this type will be used to provide completely reliable predictions of performance.

2. CLASSIFICATION PROCEDURE

2.1 Natural Durability

A first step in the classification is to define the 'natural durability' of the timber. For this purpose the CSIRO natural duability classes will be used. These classes will be denoted by Class (1), (2), (3) and (4), with Class (1) being the rating corresponding to greatest durability. The CSIRO durability classes are defined in Appendix A, and lists of species classed on this basis can be obtained from various publications (Standards Association of Australia 1979, 1980).

2.2 Basic Performance Ratings for Untreated Timbers

For the case of untreated timber, the natural durability class is used to obtain a natural durability rating in accordance with Table 2, the highest ratings giving the better performance. The performance rating is then obtained from Table 3 which makes use of durability ratings, structure situation, and hazard location. The hazard locations are defined in Figures 1-3.

2.3 Basic Performance Ratings for Treated Timber

For timber treated in accordance with the specifications of the Australian standard AS1604 (Standard Association of Australia; 1980) the performance ratings are obtained directly from Table 4. Note that in this context the performance ratings are applicable only to that part of the structural element that has been treated and not, for example, to any untreatable heartwood that may be present.

2.4 Modification Factors

The performance ratings for treated and untreated timber will require modification as follows,

(a) For joint strength;

- for unprotected joints with poor detail, reduce the performance rating by a factor of 0.5, and
- for unprotected joints facing west, reduce the performance rating by a factor of 0.5.

(b) For timber strength;

- for unprotected timber facing west, reduce the performance rating by a factor of 0.5, and
- for timber greater than 100 mm in thickness, increase the the performance rating to P_W given by

$$P_W = P_{100} \left[1 + \frac{W-100}{200} \right]$$

where P_{100} denotes the performance rating for 100 mm thick members (i.e. the normal rating) and W is the member thickness in mm.

3. COMMENTARY

3.1 Basis of the Tables

Comparison of Tables 1, 2 and 3 shows that the intent is to define performance in terms of the expected performance of the heartwood of the four durability classes when placed in ground contact in locations of

low hazard. Specifically the heartwoods of mature trees in this situation are expected to have a Performance Rating of 4.0, 3.0, 2.0 and 1.0 for durability Classes of (1), (2), (3) and (4) respectively. The other factors represent a variation from this performance. In rough terms the first two columns of Table 1 may be considered to relate to the time for 30% and 10% respectively of the timber members to be lost due to attack by various biological organisms. The third column represents the time for 5% of the surface of members to be destroyed to a depth of 5mm.

The performance classification of treated sapwood is based on the assumption that AS1604 is targeted at a Class 3 performance regardless of species and hazard. Appendix B summarises some of the treatment processes specified in AS1604.

The hazard classifications for above-ground and ground-contact situations shown in Figures 1 and 2 are based on considering the hazards due to decay, cryptotermes and termites as shown in Figures A1-A3.

The reasons for the modification factors suggested are fairly obvious and will not be discussed.

3.2 Assessment of the Proposal

The primary difficulty with setting up a durability specification in terms of structural performance is that there is very little suitable data in quantified terms that is available for calibration purposes. One set of relevant data is the study on rail-sleeper connectors by Tucker and Barnackle (1983). This gives data, in statistical terms, for a

connector system in a just-off-ground situation for several treated and untreated Australian species.

However, even if directly applicable data is not readily available, the structural performance classification system provides a useful framework for the discussion and assessment of durability studies for engineering purposes.

3.2 Further Modifications

The example given herein has deliberately been kept simple so as to facilitate illustration of the format. For practical purposes two further refinements would be needed.

The first is to refine the classification of hazards to include further subgroups; for example the termite hazard may be divided into two or more sets of species. The second modification would be to replace the use of hazard maps by the use of climate classes: in this way the durability estimates may be applied in countries where the biological hazards have not been mapped.

4. REFERENCES

1. Johnson, G.C., Thornton, J.D. and Saunders, I.W. (1986). An in-ground natural durability field test of Austrlaian timbers and exotic reference species. III. Results after approximately 15 years' exposure Material und Organismen, Vol. 21, No. 4, pp. 251-264.

2. Standard Association of Austrlaia (1979). Timber poles for overhead lines. Australian Standard 2209-1979, 19 pages.

3. Standards Association of Australia (1980). Preservative treatment for sawn timber, veneer and plywood. Australian Standard 1604-1980, 22 pages.

4. Tamblyn, N. (1966). Natural durability ratings. Forest Products Newsletter, No. 335, Nov., 1 page.

5. Thornton, J.D., Walters, N.E.M., and Saunders, I.W. (1983). An in-ground natural durability field test of Australian timbers and exotic reference species. I. Progress Report after more than 10 years' exposures. Material und Organismen, Vol. 18, No. 1, pp. 27-49.

6. Tucker, S.N. and Barnacle, J.E. (1983). Railway sleeper service life distributions in an Australian rail track and their likely effects on maintenance strategies. Proc. of 5th International Rail Track Conference. Newcastle, NSW, Australia, pp. 242-256.

APPENDIX A

NATURAL DURABILITY CLASSIFICATION

The CSIRO natural durability classifications defined by Tamblyn (1966) are shown in Table A1. These ratings, originally conceptual, have in recent years been studied in more formal and quantitative terms (Johnson *et al.*, 1986, Thornton *et al.*, 1983).

APPENDIX B

SPECIFIED TREATMENT FROM AS1604

The following is extracted from the Australian standard AS1604, and is quoted to show that the standard is targeted at providing a specific performance rating regardless of the hazard locations, i.e. the treatment varies with the hazard location.

Hazard	CCA treatment for softwoods* (kg/m^3)
Above ground, not exposed	0.0
Above ground, exposed and kept well painted:	
- moderate hazard location	5.6
- severe or tropical location	8.0
Above ground, unpainted:	
- moderate hazard location	8.0
- severe or tropical hazard location	12.0
Ground contact:	
- moderate hazard location	12.0
- severe or tropical hazard location	20.0
In sea:	
- below 20^oS	32.0
- above 20^oS	50.0**

* based on single treatment using Tanilith C
** an estimate, condition not specifically covered by AS1604.

TABLE 1 DEFINITION OF PERFORMANCE RATINGS

Performance rating	Time to failure for loaded structures (years)		
	For 50% of beams	For 5% of beams or 50% of joints	For 5% of joints
1	2	1	0.5
2	10	5	2
3	50	20	10
4	100+	80	50
5	100+	100+	100 +

100+ = greater than 100 years

TABLE 2 DURABILITY RATING FOR UNTREATED TIMBER

Natural durability class	Durability rating			
	Sapwood	Heartwood		Pith or inner heartwood
		Age of tree less than 70 years	Age of tree greater than 70 years	
(4)	1.0	1.0	1.0	1.0
(3)	1.0	2.0	2.0	1.0
(2)	1.0	2.5	3.0	1.0
(1)	1.0	3.0	4.0	1.0

TABLE 3 PERFORMANCE RATING FOR UNTREATED TIMBER

Situation	Performance rating							
	Low hazard location				High hazard location			
	DR= 1.0	DR= 2.0	DR= 3.0	DR= 4.0	DR= 1.0	DR= 2.0	DR= 3.0	DR= 4.0
Above ground, sheltered	5.0	5.0	5.0	5.0	1.5	2.0	2.5	4.0
Above ground, exposed	1.5	2.5	3.5	4.0	1.0	2.0	3.0	3.5
In water	1.5	2.5	3.0	4.0	1.0	1.5	2.5	3.0
In ground contact	1.0	2.0	3.0	4.0	0.5	1.0	2.0	2.5

DR = durability rating (see Table 2 for relationship to durability classification).

TABLE 4 PERFORMANCE RATING FOR TIMBER TREATED IN ACCORDANCE WITH AS1604

Natural durability class	Performance rating		
	Sapwood	Heartwood	Pith or inner heartwood
(4)	3.0	1.5	2.0
(3)	3.0	2.5	2.0
(2)	3.0	3.5	2.0
(1)	3.0	4.0	2.0

TABLE A1 DEFINITION OF DURABILITY CLASSIFICATIONS

Durability class	Representative Species*	Effective resistance to decay and termite attack**
Class (1)	Red ironbark (*Eucalyptus sideroxylon*)	25-50 years
Class (2)	Yellow stringybark (*Eucalyptus muellerana*)	15-25 years
Class (3)	Messmate (*Eucalyptus obliqua*)	8-15 years
Class (4)	Radiata pine (*Pinus radiata*)	1-8 years

* as classified in AS1604 and AS2209

** untreated heartwood in ground contact at a low hazard location.

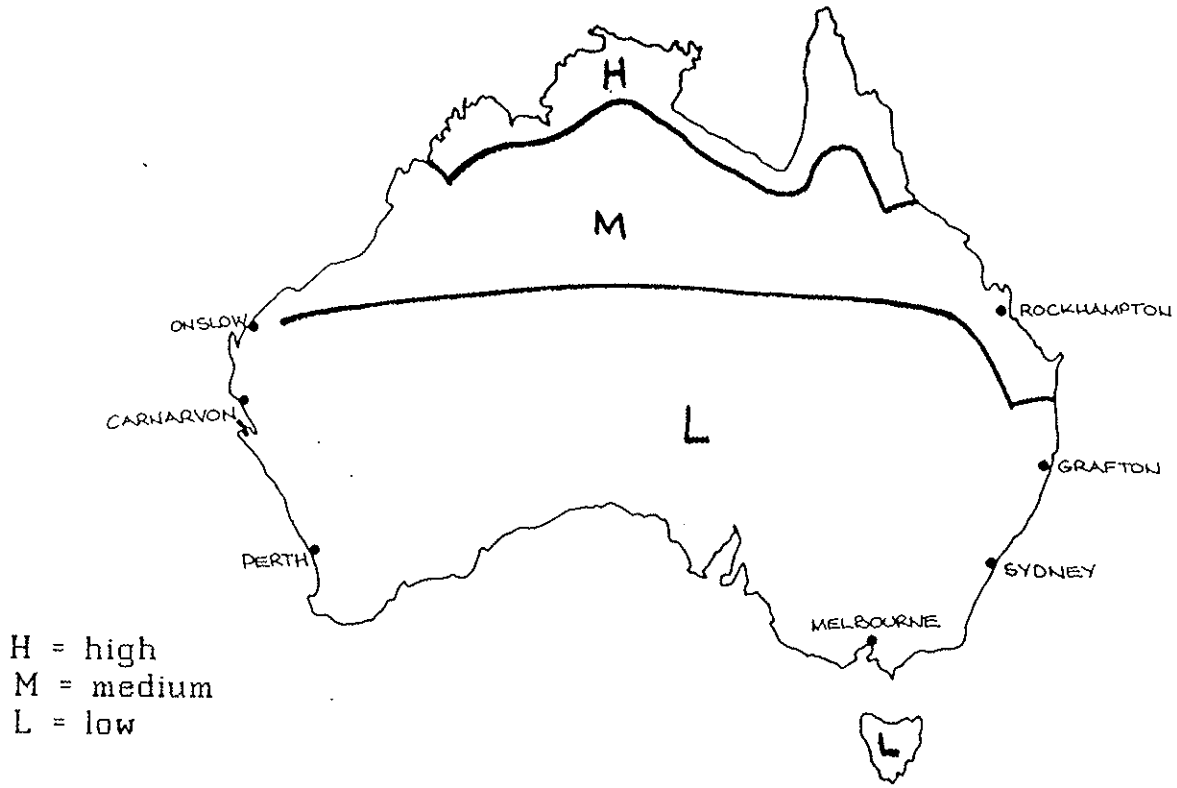

FIG.1 ABOVE GROUND HAZARD

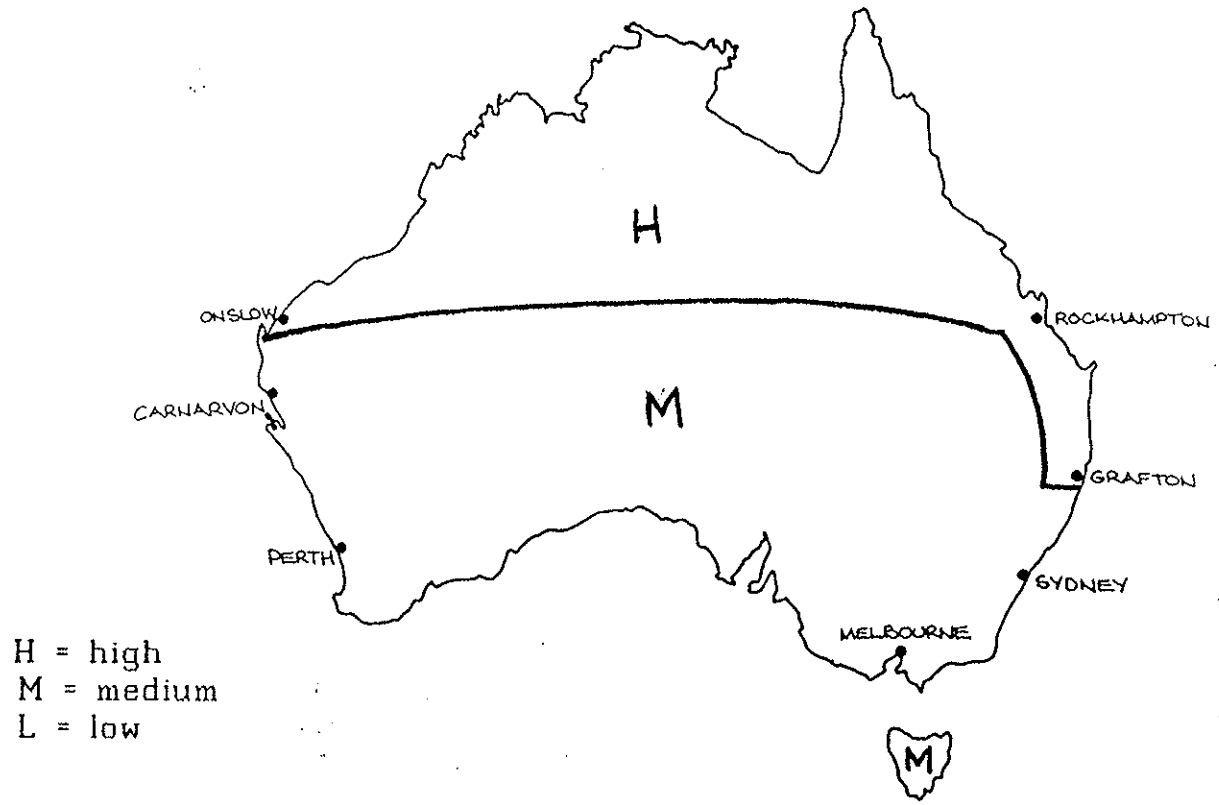

FIG. 2 GROUND-CONTACT HAZARD

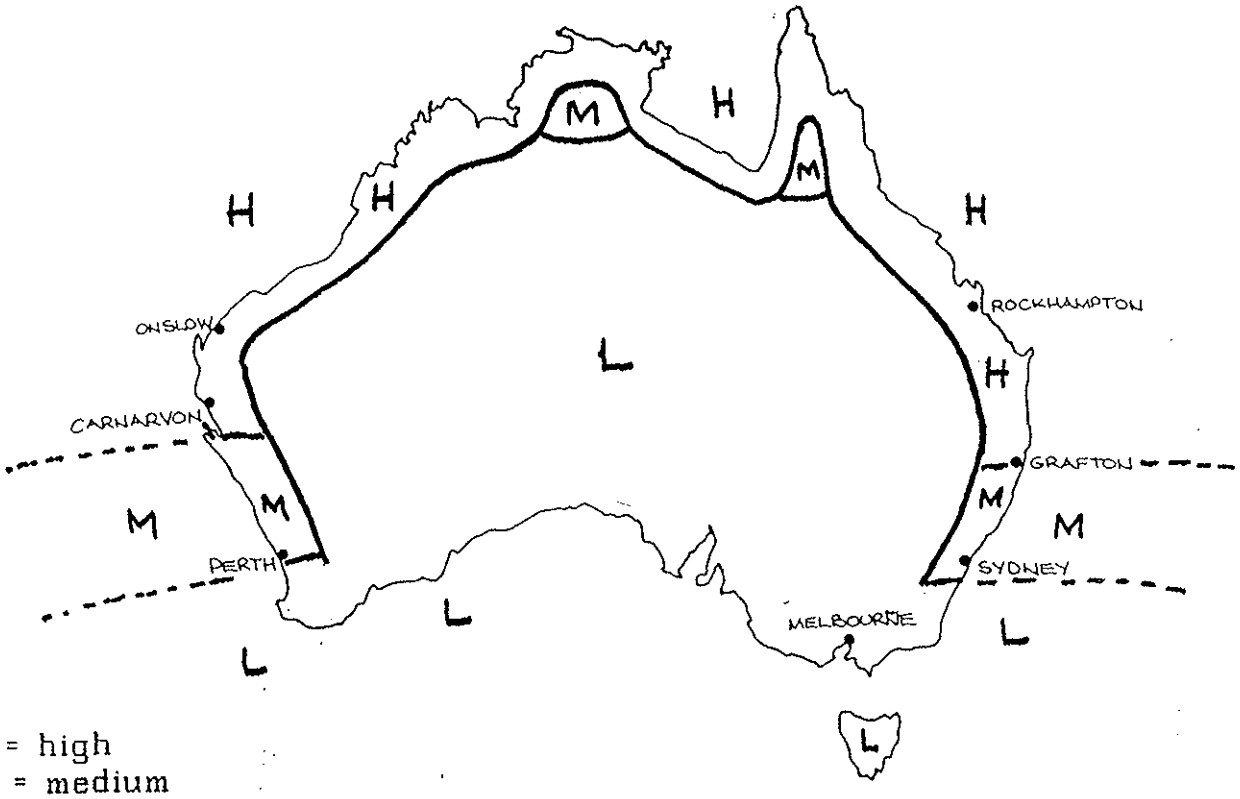

H = high
M = medium
L = low

FIG. 3 IN-WATER HAZARD

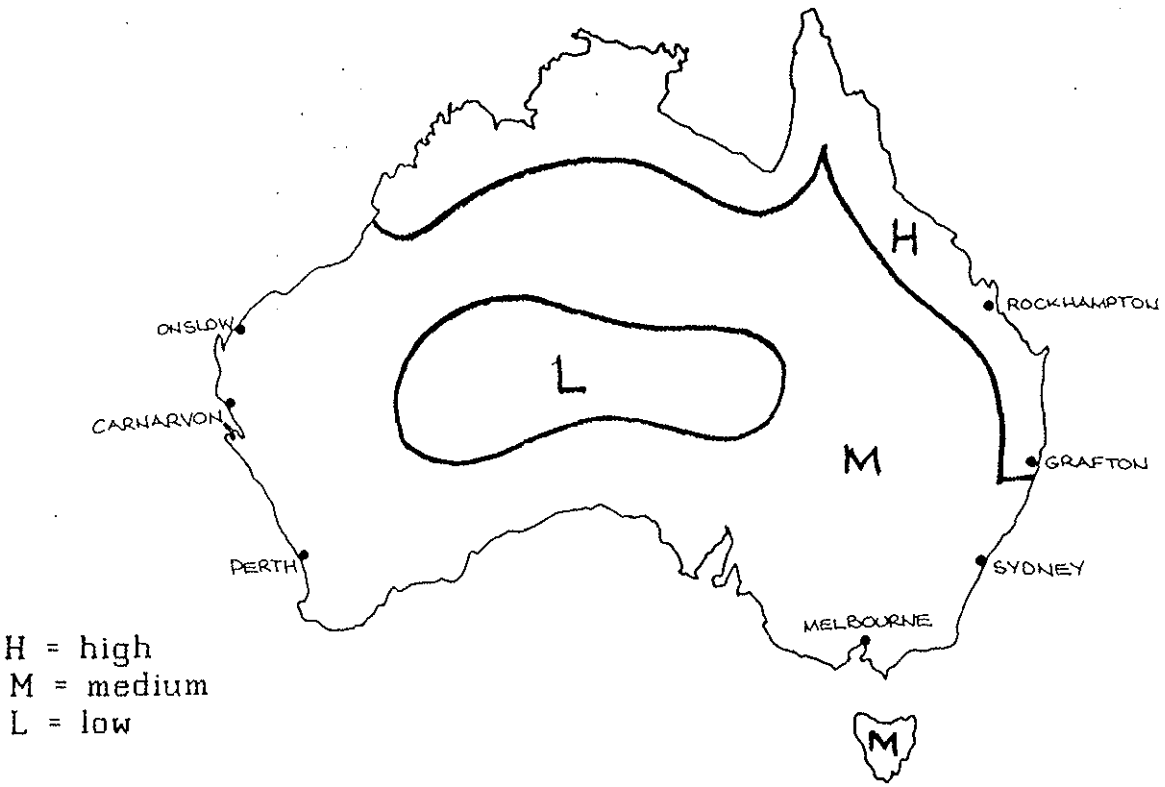

FIG. A1 DECAY HAZARD

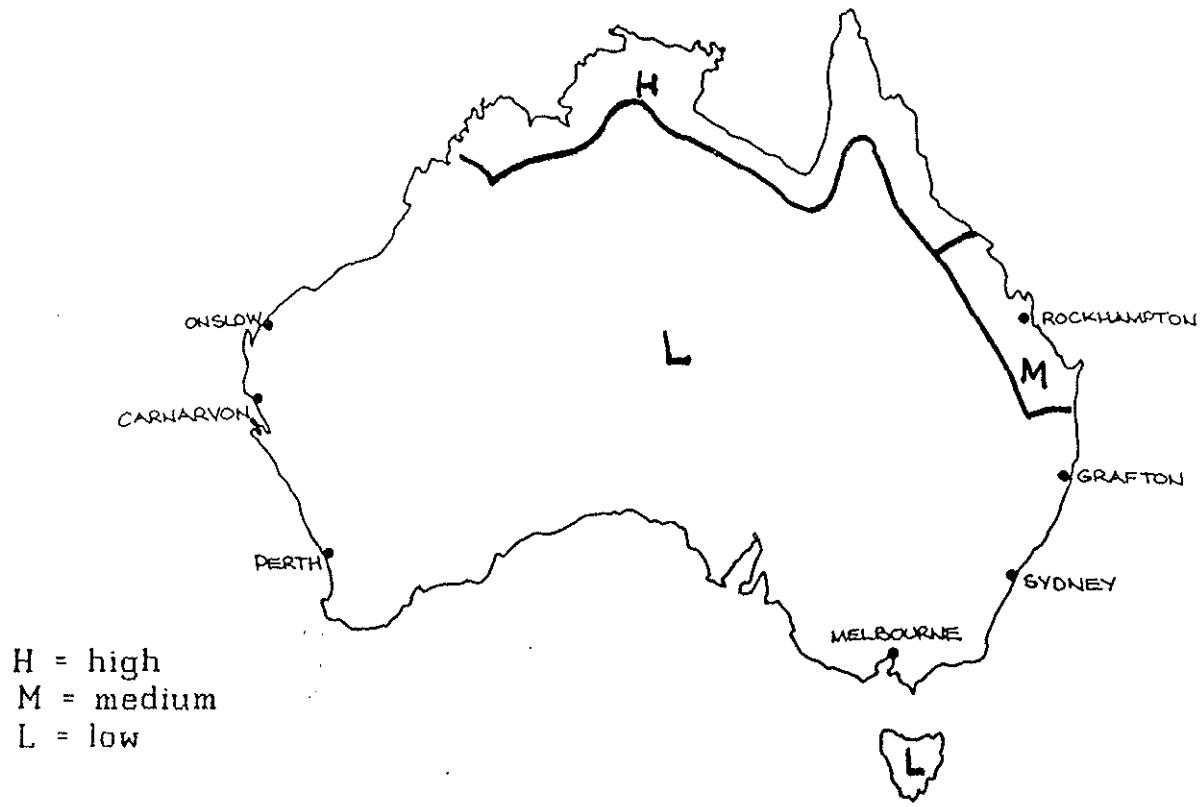

FIG. A2 CRYPTOTERMES DRYWOOD HAZARD

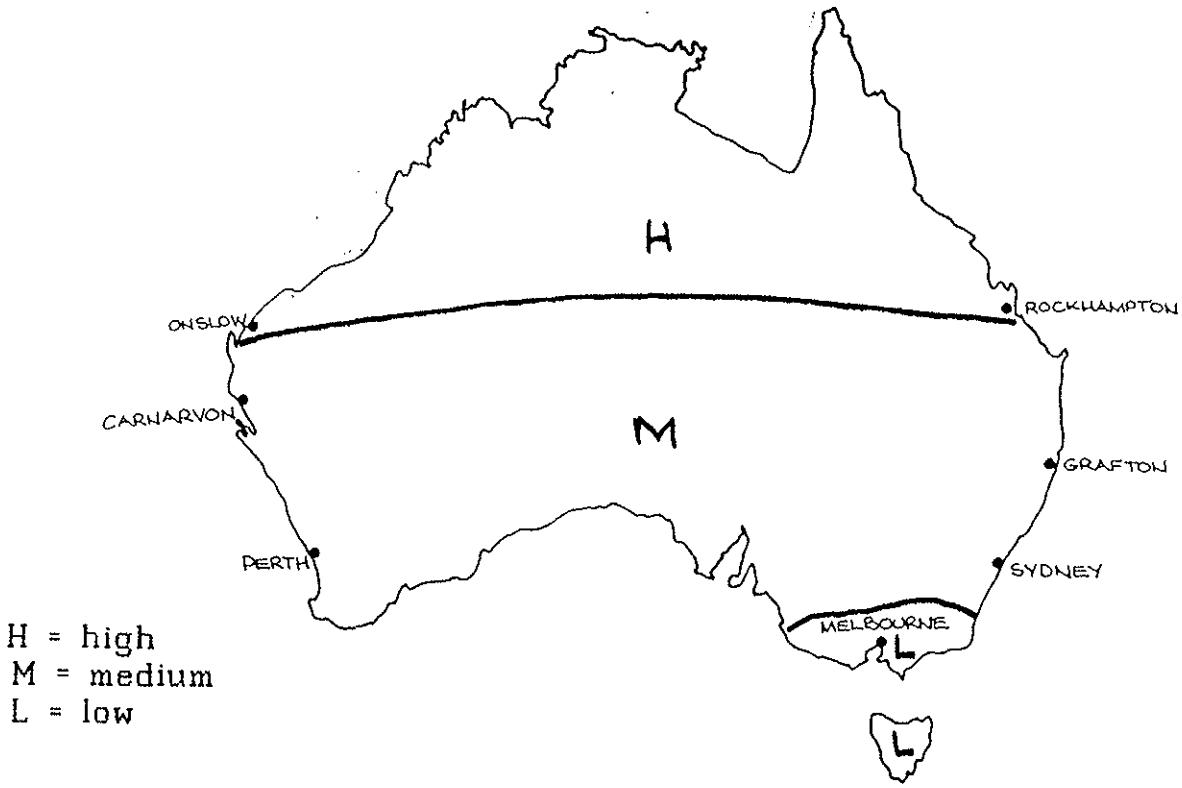

FIG. A3 SUBTERRANEAN TERMITE HAZARD

CIB-W18A/21-12-1

INTERNATIONAL COUNCIL FOR BUILDING RESEARCH STUDIES AND DOCUMENTATION

WORKING COMMISSION W18A - TIMBER STRUCTURES

MODULUS OF RUPTURE OF GLULAM BEAM COMPOSED OF ARBITRARY LAMINAE

by

K Komatsu and N Kawamoto
Forestry and Forest Products Research Institute
Japan

MEETING TWENTY-ONE
PARKSVILLE, VANCOUVER ISLAND
CANADA
SEPTEMBER 1988

[Paper for the Meeting of CIB-W18A, 24-27 September 1988]

MODULUS OF RUPTURE OF GLULAM BEAM COMPOSED OF ARBITRARY LAMINAE

BY

Kohei Komatsu Dr. Agr., Senior Research Scientist*

Norio Kawamoto B. Agr., Research Scientist*

ABSTRACT

An equation is derived for predicting the modulus of rupture(MOR) of glued laminated beam(glulam) composed of laminae with arbitrary grade, arbitrary size and arbitrary arrangement at the most critical section in the beam. Numerical experiments based on the Monte Carlo method is applied to compare the theory with the experimental results obtained on the full-size Douglas fir glulam beams. Comparisons between numerical experiments and full-size experiments indicate that the MORs of glulam beams can be predicted if the distributions of MTS(maximum tensile strength) and MOR of laminae as well as the co-relations between MTS and MOE(modulus of elasticity) and MOR and MOE of laminae are known. Size effect(depth effect) can be also explained well by the equation proposed in this study.

1. INTRODUCTION

The glued laminated beam (described as "glulam" hereafter) is a kind of multi-layered composite material composed of many laminae. The strength properties of such composite materials can, generally speaking, be easily predicted by knowing the mechanical properties of each lamina and its arrangement (location) at the most critical section.

In the analysis of the multi-layered composite beam with interlayer slips (e.g. Goodman[1]), stress acting in each layer is usually separated into two components, i.e. the axial force and the bending moment. It might be possible to use the same concept for the analysis of glulam beam providing that the interlayer slip is zero in this case.

An equation is derived on the basis of the idea mentioned above for predicting the MOR(modulus of rupture) of glulam beams composed of laminae with arbitrary mechanical properties, arbitrary size(thickness and width) and arbitrary arrangement in the most critical section. The equation derived is used for the numerical experiments based on the Mote Carlo method to evaluate the experimental results obtained on the full-size Douglas fir glulam beams.

---

* Forestry and Forest Products Research Institute
P.O. Box.16, Tsukuba Norin Kenkyu Danchi,
Ibaraki 305,
JAPAN

2. LIST OF SYMBOL

A_i = cross sectional area of i-th layer
b_i = width of i-th layer
E_i = modulus of elasticity of i-th layer
E_iI_i = flexural rigidity of i-th layer
$(EI)_e$ = flexural rigidity of glulam beam composed of arbitrary laminae
ε_{i-t} = strain due to bending moment
ε_{i-t} = strain due to axial force
f_{i-t} = maximum tensile strength of i-th layer
f_{i-b} = maximum flat-wise bending strength of i-th layer
F_i = axial force acting in i-th layer
g_i = distance from neutral axis of glulam beam to the centroid of i-th layer
h_i = sum of thickness t_i (refer to equation 5))
H = depth of glulam beam
n = number of lamination
M = moment acting on the glulam beam
M_i = moment acting in i-th layer
λ = distance from top surface to the neutral axis(N-N')
ρ = curvature of beam (= curvature of each layer)
r_i = ratio of MTS to MOR of i-th layer (f_{i-t}/f_{i-b})
t_i = depth or thickness of i-th layer
σ_{i-t} = stress due to axial force
σ_{i-b} = stress due to bending moment
Z_e = section modulus of glulam beam

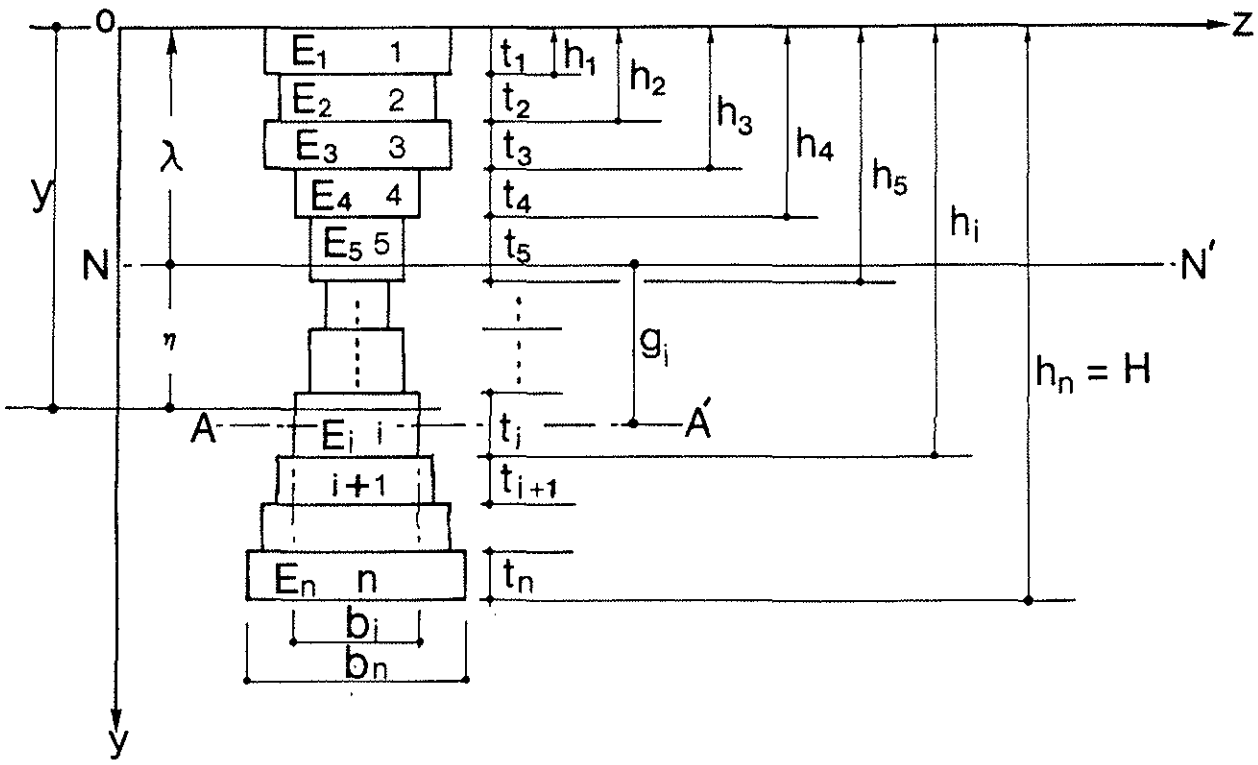

Figure 1 Definition of cross-section of glulam beam.

3. MODULUS OF RUPTURE

3.1 Flexural Rigitity

Figure 1 shows a definition of the cross-section of the glulam beam composed of arbitrary laminae. From the first equilibrium condition of the beam, the equivalent flexural rigidity of glulam beam with arbitrary lamination is given by:

$$(EI)_e = \sum_{i=1}^{n} E_i I_{i-NN} \qquad \text{.....1)}$$

$$I_{i-NN} = I_i + g_i^2 A_i = b_i t_i^3/12 + g_i^2 b_i t_i \qquad \text{.....2)}$$

$$g_i = \lambda + t_i/2 - h_i \qquad \text{.....3)}$$

$$\lambda = \frac{1/2 \sum E_i (h_i^2 - h_{i-1}^2)}{\sum E_i t_i} \qquad \text{.....4)}$$

$$h_i = \sum_{k=1}^{i} t_k \qquad \text{.....5)}$$

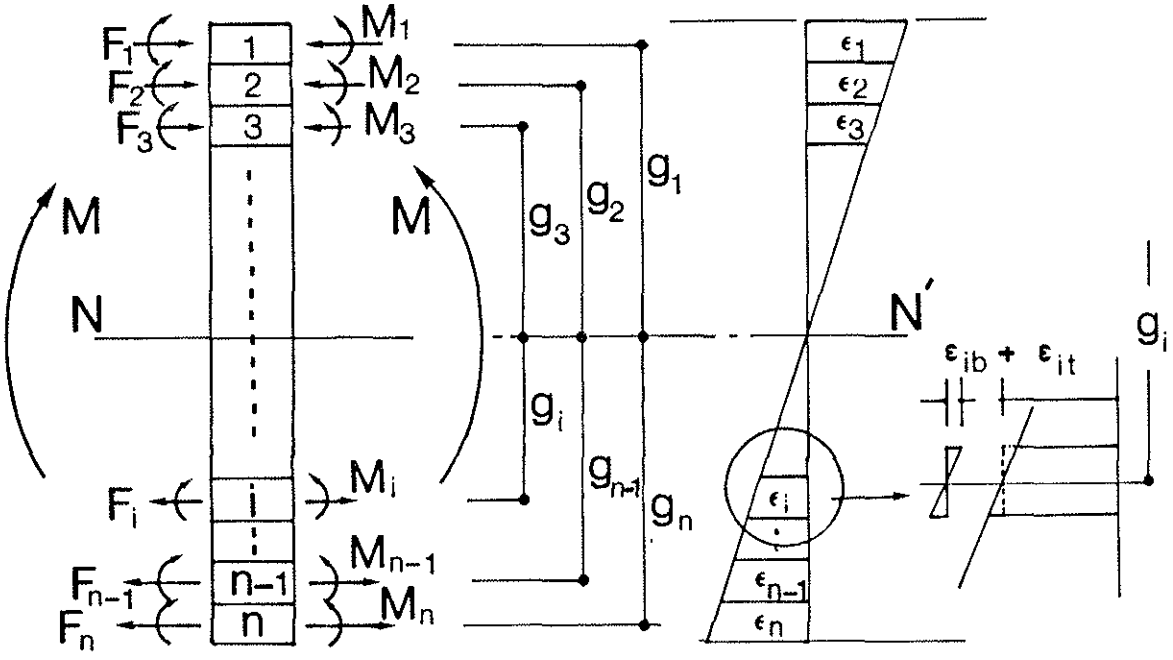

Figure 2. Assumption on stresses and strains in each layer

3.2 Stresses in i-th Layer

Strain ε_i of each lamina is assumed as a sum of the strain ε_{i-b} by bending moment and the ε_{i-t} by axial force as shown in Figure 2.

$$\varepsilon_i = \varepsilon_{i-t} + \varepsilon_{i-b} \qquad \text{.....6)}$$

Stress σ_{i-b} by the bending moment M_i of each layer is obtained by using the condition that the curvature of each layer coincides with that of glulam beam:

$$1/\rho = M/(EI)_e = M_i/E_iI_i \qquad M_i = \{E_iI_i/(EI)_e\}M$$
$$\sigma_{i-b} = M_i/Z_i = (t_i/2)\{E_i/(EI)_e\}M \qquad \text{..... 7)}$$

Stress σ_{i-t} by the axial force F_i of each layer is determined by using following relations (refer to Figure 2):

$$\varepsilon = (y-\lambda)/\rho,\ \varepsilon_b = 0 \text{ at } y-\lambda = g_i \text{ so, } \varepsilon_{i-t} = g_i/\rho = (F_i/A_i)/E_i$$
$$1/\rho = M/(EI)_e \qquad \sigma_{i-t} = F_i/A_i = g_i\{E_i/(EI)_e\}M \qquad \text{..... 8)}$$

3.3 Fracture Criterion

The fracture criterion of equation 9) which is used to the case of combined stresses condition is also applied in this analysis.

$$\frac{\sigma_{i-b}}{f_{i-b}} + \frac{\sigma_{i-t}}{f_{i-t}} = 1 \qquad \text{..... 9)}$$

Substituting equations 7) and 8) into equation 9), the maximum moment M_c acting at the most critical section can be expressed as:

$$M_c = \frac{(EI)_e}{E_i} \cdot \frac{2f_{i-t} \cdot f_{i-b}}{t_i f_{i-t} + 2g_i f_{i-b}} \qquad \text{..... 10)}$$

By introducing the relation of $M_c = MOR \times Z_e$, where MOR is modulus of rupture of glulam beam and Z_e is section modulus of the glulam beam, MOR of any glulam beam composed of arbitrary laminae might be predicted by the following equation.

$$MOR_i = \frac{(EI)_e}{E_iZ_e} \cdot \frac{f_{i-t}}{(t_i/2)r_i + g_i} \qquad \text{..... 11)}$$

$$r_i = f_{i-t}/f_{i-b} \quad \text{(ratio of MTS and MOR of i-th lamina)}$$

In equation 11), MOR_i means a value of MOR that the fracture occurs in the i-th layer. This also means that the weakest MOR_i, among all possible $\{MOR_1, MOR_2 \ldots MOR_k\}$ where $i=1,2,3,\ldots k$ are laminae number belonging to the tensile stress zone, gives the maximum load carrying capacity of the whole glulam beam.

3.4 Characteristics of Equation 11)

The qualitative characteristics of equation 11) are shown in Figure 3. In this example, parameters are assumed as $E_i = E$, $t_i = t$, $b_i = B$, $n = H/t$ (H: depth of beam, t: thickness of laminae) and $r_i = r = f_t/f_b = 0.4 \sim 1.0$ for simplicity.

Figure 3 demonstrates that the equation 11) gives MOR of lamina itself when number of lamination n is 1 and indicates decrease of MOR of glulam beam as the number of lamination n increases, and it finally gives MTS(maximum tensile strength) of lamina when the number of lamination n becomes large enough.

By employing equation 11), so-called size effect of glulam beam can be explained qualitatively by using such practical parameters as MOR and MTS(maximum tensile strength) of laminae. This is the most characteristic point of the equation 11).

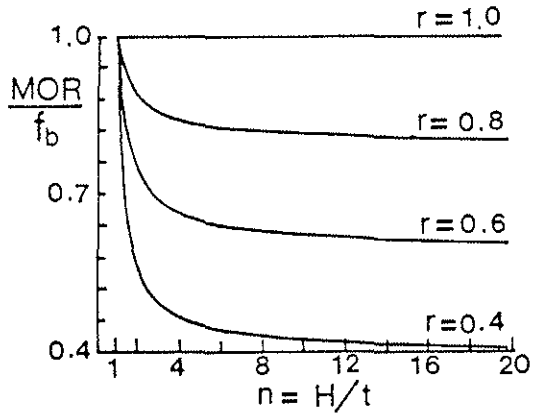

Figure 3. Qualitative characteristics of equation 11)

4. EXPERIMENT

4.1 Glulam Beam Specimens

Table 1 shows the configurations of specimen tested. Three replications in eight different configurations were prepared for the test. As a total, 24 specimens were tested in bending. All glulam beams were made in United State using Douglas fir laminae, and shipped to Japan. There were no information on the materials except stamps on the top surfaces certifying that some of the laminae were proof-loaded subjected to the AITC standard.

Table 1 Configuration of Test Specimen (Replication in each configuration = 3)

Specimen Code	Length of Beam L_o (m)	Depth of Beam H (cm)	Width of Beam B (cm)	Thickness of Laminae t (cm)	Number of Lamination n	Span L (cm)	Shear Span L_s (cm)
H91B17	12	91.0	17.2	3.5	26	1100	500
H76B17	12	76.2	17.2	3.5a	21+1a	1100	500
H76B13	12	76.0	13.0	3.8	20	1100	500
H62B17	11.7	61.0	17.2	3.5b	17+1b	1100	500
H62B13	11.7	60.8	13.0	3.8	16	1100	500
H57B08	10.8	57.0	7.9	3.8	15	1000	405
H46B17	8.4	45.5	17.2	3.5	13	840	380
H31B17	5.7	30.6	17.2	3.4	9	560	250

a:only top lamina = 2.7cm b:only top lamina=1.5cm

4.2 Bending Test Method for Glulam Beam

As the size of specimens were too big to destroy by the standard testing machine, large size specimens (H91B17 ~ H62B13, refer to Table 1 for the specimen code name) were tested to destroy using the special test arrangement set on the laboratory strong floor shown in Figure 4. and Photo.1 . The rest of specimens (H57B08 ~ H31B17) were tested by the standard full-size bending testing machine shown in Figure 5 and Photo.2.

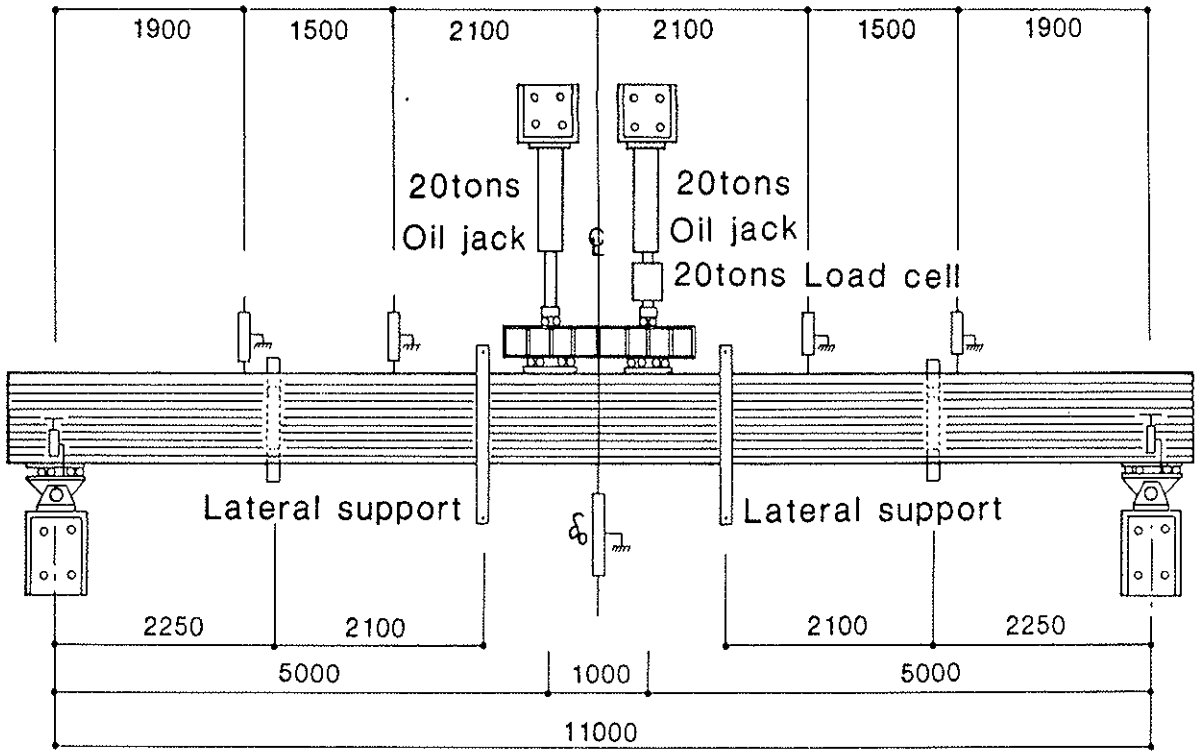

Figure 4 Bending test configuration for large size specimens.

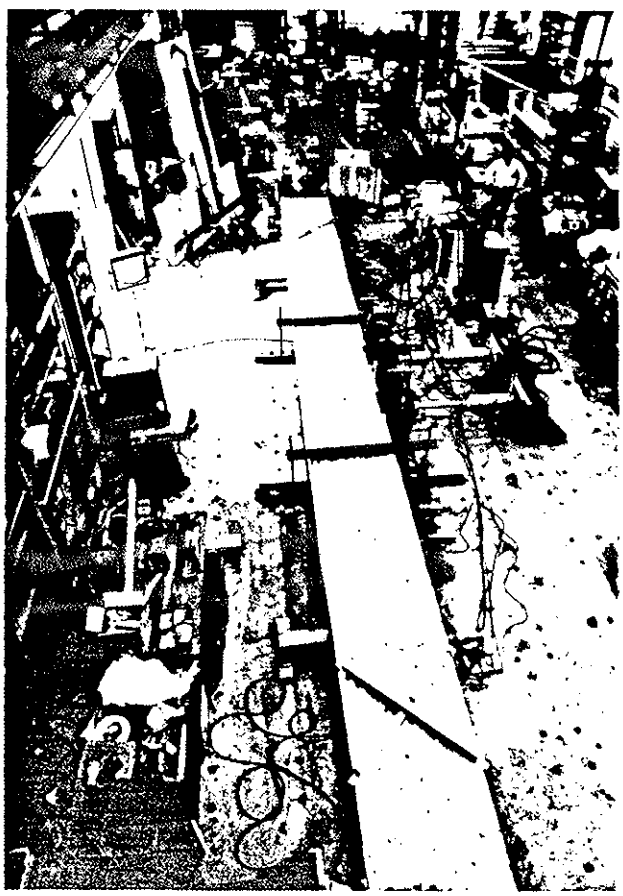

Photo.1 Test arrangement set on the laboratory's strong floor for large glulam beam

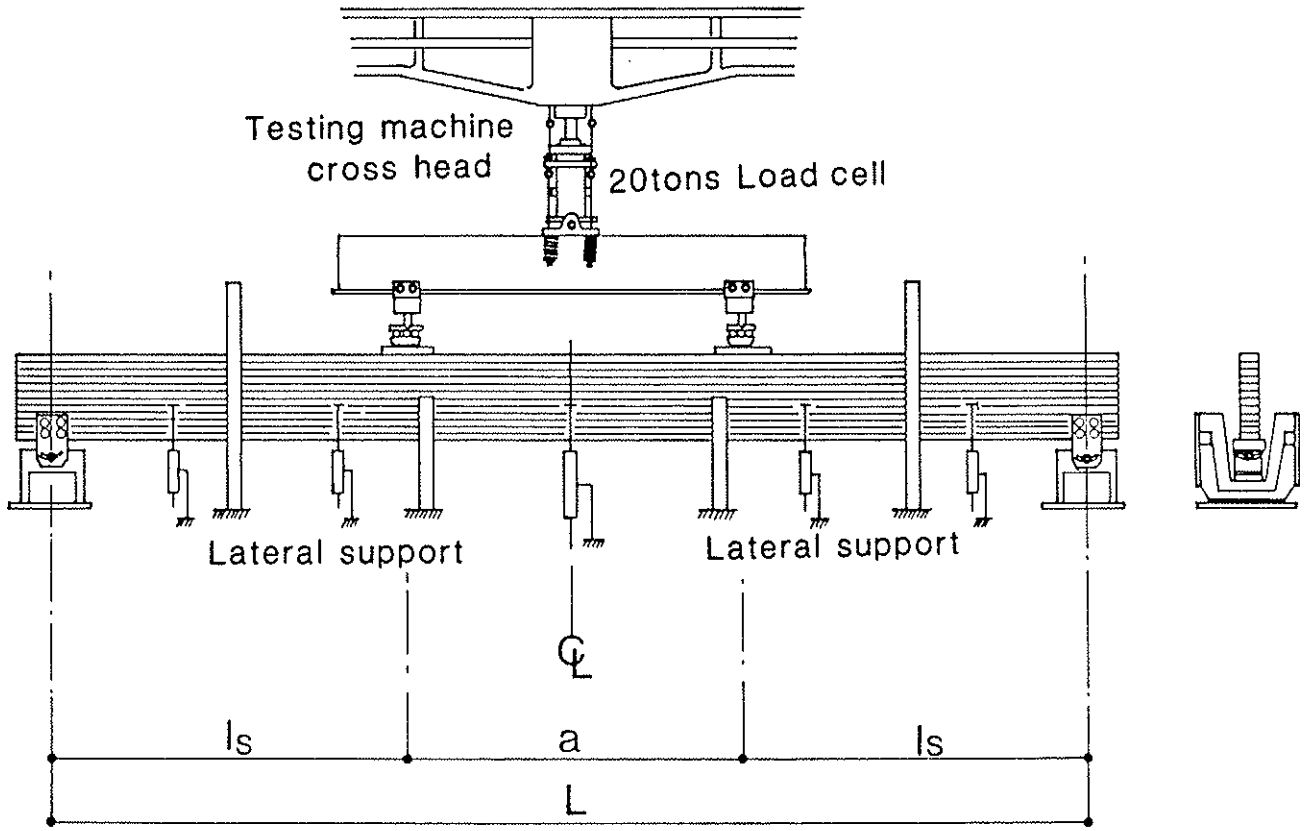

Figure 5 Bending test configuration for standard size specimens.

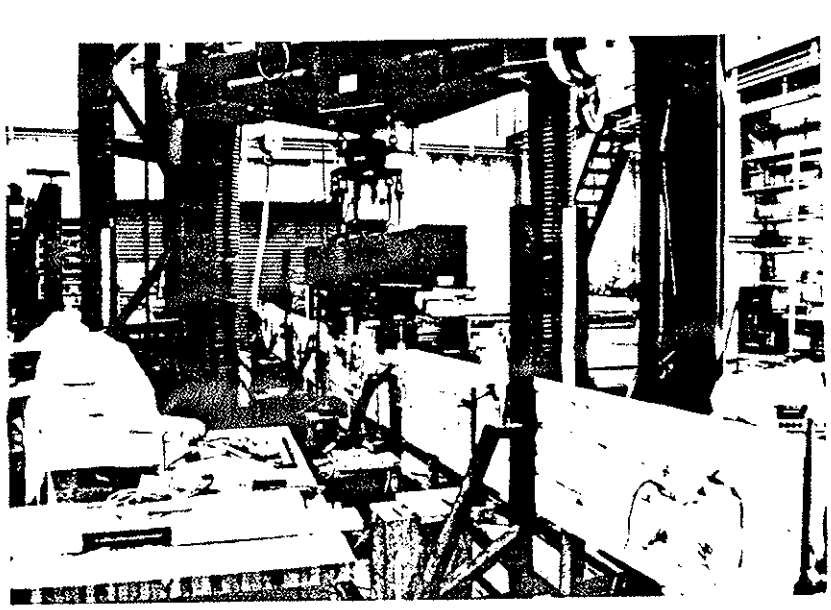

Photo.2 Test arrangement by the standard bending test machine.

4.3 Bending and Tension Tests for Laminae

After all bending tests on the full-size glulam beams were finished, several laminae were taken from undamaged tension zone of each broken glulam beams so as to keep the original lamina's size as possible. It was almost impossible to keep the length and thickness of all test specimens constant. Also, some of the specimens include finger joints, but some of them didn't. The three-points center loading bending test shown in Photo.3 was done on the half of test specimens sorted from the group with odd number. Span length for the bending test was 270cm.

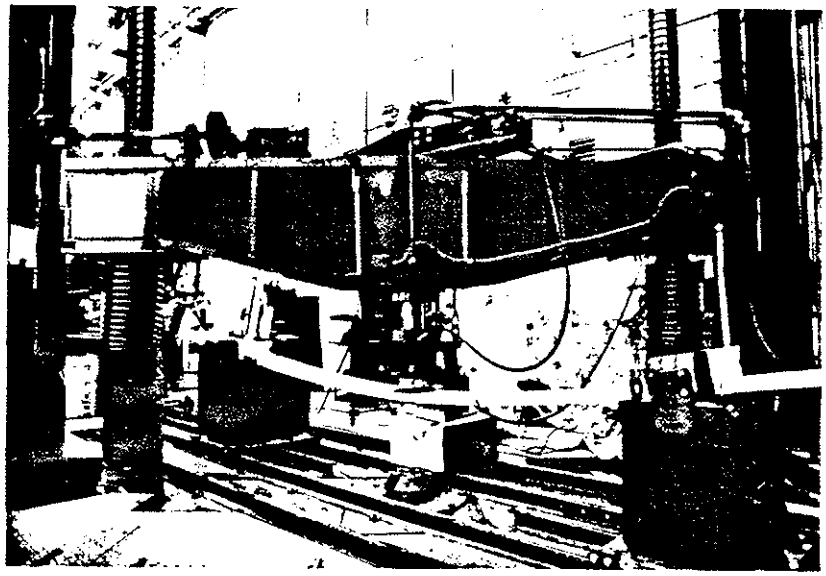

Photo.3 Three points center-loading bending test for laminae.

The specimens taken from the group with even number were tested to failure in tension using a tension proof-loading machine shown in Photo.4.

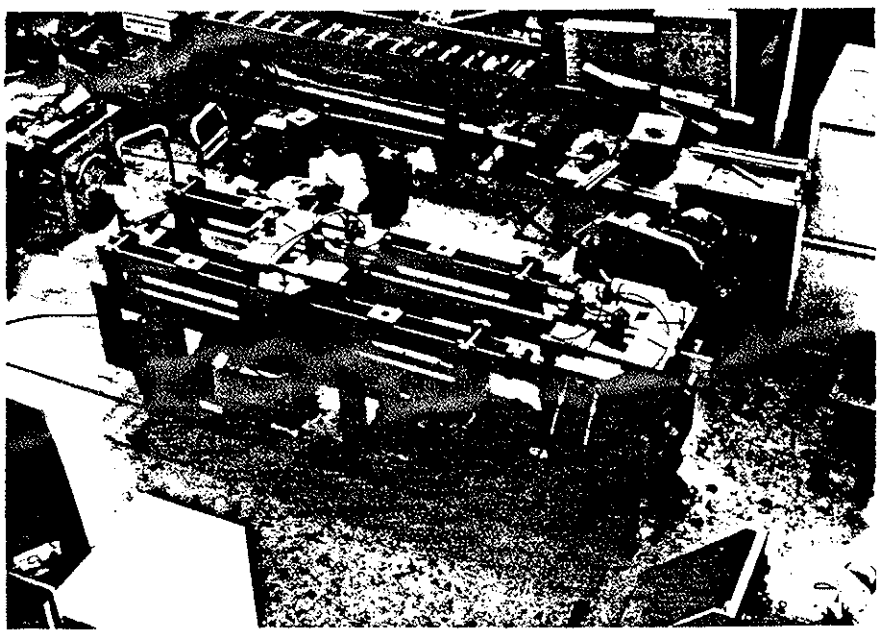

Photo. 4 Tension test by tension proof-loading machine.

5. Monte Carlo Method

Figure 6 shows a flow chart of the Monte Carlo method for predicting the MORs of glulam beams based on the equation 11).

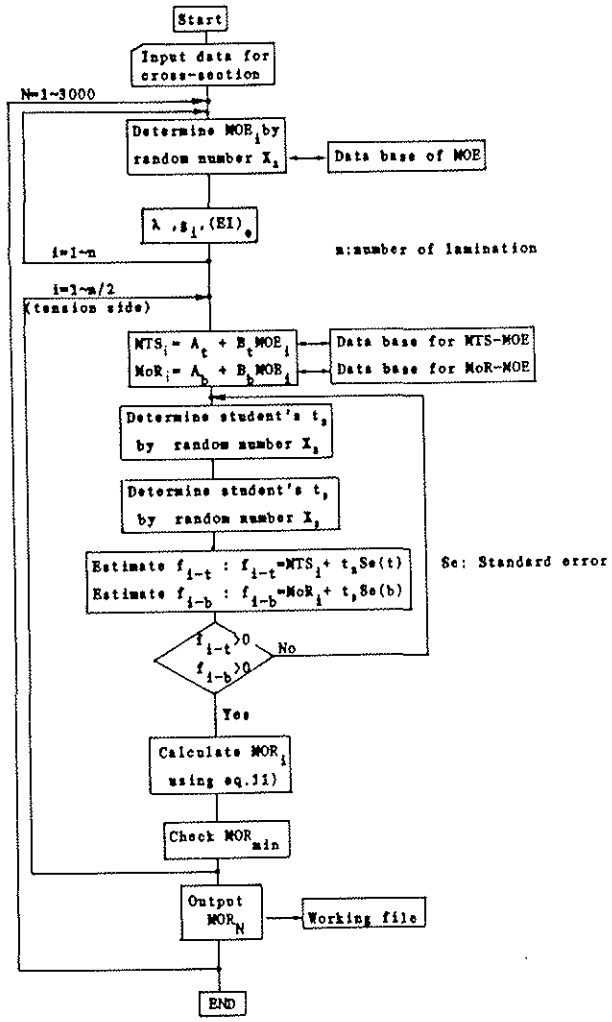

Figure 6 Flow chart of Monte Carlo method for predicting MORs of glulam beams based on equation 11).

The procedure of the Mote Carlo method used in this study is explained as follows with referring to the flow chart in Figure 6 and/or Figure 7 which visually explains actual procedure:

[1] Determine MOE_i of i-th layer using the random number X_1 from a diagram in which MOE distribution is expressed in the form of three parameters Weibull function as shown in Figure 7.

[2] Estimate f_{i-t} and f_{i-b} of each layer belonging to the tensile zone through the co-relations between MTS and MOE as well as MOR and MOE as follows:

$$f_{i-t} = MTS_i + Se(t) \cdot t_2 \quad \cdots\cdots\cdots 12)$$

$$f_{i-b} = MOR_i + Se(b) \cdot t_3 \quad \cdots\cdots\cdots 13)$$

where, MTS_i and MOR_i are estimated mean values through the regression equations using MOE_i. Se(t) and Se(b) are standard error arisen from the regression operation and assumed as the normal distribution. The Student's t_k (k=2,3) is determined by the random number X_2 and X_3 .

As a special option for the glulam made in U.S.A., we assumed that the outer 18% of laminations have strength value higher than 5%-ile value because laminae weaker than 5%-ile must have been rejected by proof loading test as in the case of Weyerhaeuser system(2). This assumption is confirmed by the fact that there were stamps on the top surfaces of glulam beams certifying the proof loading test.

[3] Calculate MOR_i using equation 11) for the laminations existing in the tension zone, then find the weakest MOR_i and let it MOR of the glulam beam.

[4] Repeat the process from [1] to [3] for 3000 cycles for each beam configurations. Distribution of MOR obtained by the Monte Carlo method is also fitted to the three parameters Weibull function and determine lower 5%-ile value of glulam beam MOR.

In this Monte Carlo method, the three parameter's Weibull equation of equation 14) was used to express discrete data set as a distribution function. The computer program used was originally developed by Iijima(3).

$$MOR\ ,\ MTS\ or\ MOE = \gamma + \theta[-\log_e(1-X)]^{1/m} \qquad \ldots\ldots\ 14)$$

where, γ : location parameter θ : scale parameter
m : shape parameter X : probability (random number)

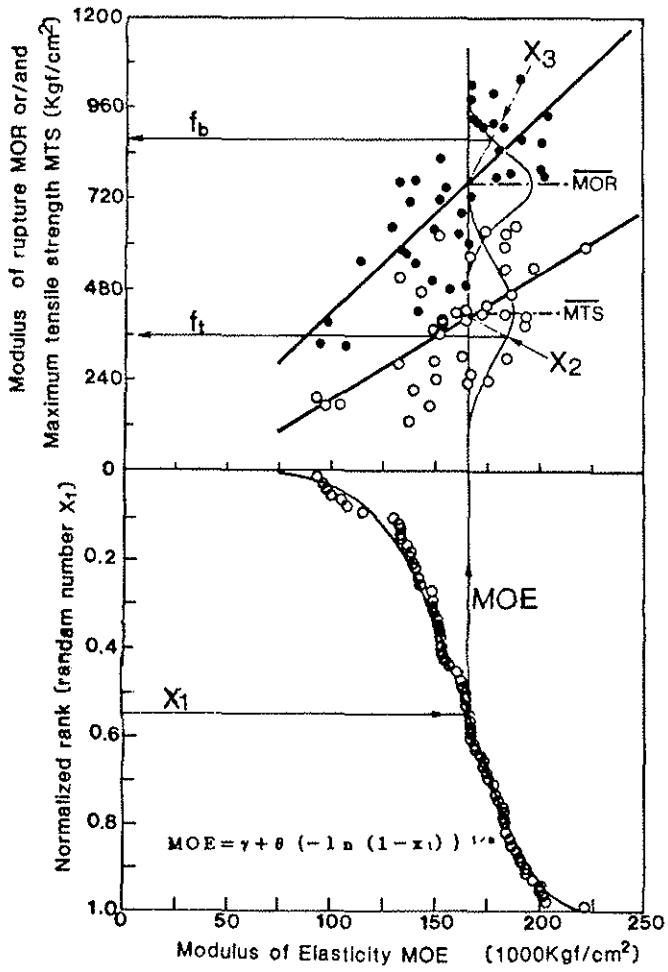

Figure 7 Figure for explaining the Monte Carlo simulation visually.

6.RESULTS AND DISCUSSION

6.1 MTS vs MOR of Laminae

Table 2 shows MOE, MTS and MOR distribution for laminae taken from glulam beam destroyed.

Table 2 Test results on laminae

	Flat-wise MOE ($X10^3$Kgf/cm)	Flat-wise MOR (Kgf/cm²)	Tensile Strength MTS (Kgf/cm²)
[Normal Distribution]			
N	77	40	38
Mean	160	727	395
S.D.	27	194	150
C.V.	17%	27%	38%
5%-ile value	115	400	141
[Weibull distribution]			
location γ	0	0	67.4
scale θ	172	806	374.5
shape m	6.41	3.82	2.06
5%-ile value	108	370	156

Time to failure in tension test of laminae was very short compared with 3-points bending test because a proof loading machine was used. Nevertheless, the ratio MTS/MOR (MTS = maximum tensile strength, MOR = modulus of rupture of laminae) was about 0.43 ~ 0.63 as shown in Figure 8. Here, MTS/MOR is defined as the ratio of two Weibull distribution functions tabulated in Table2.

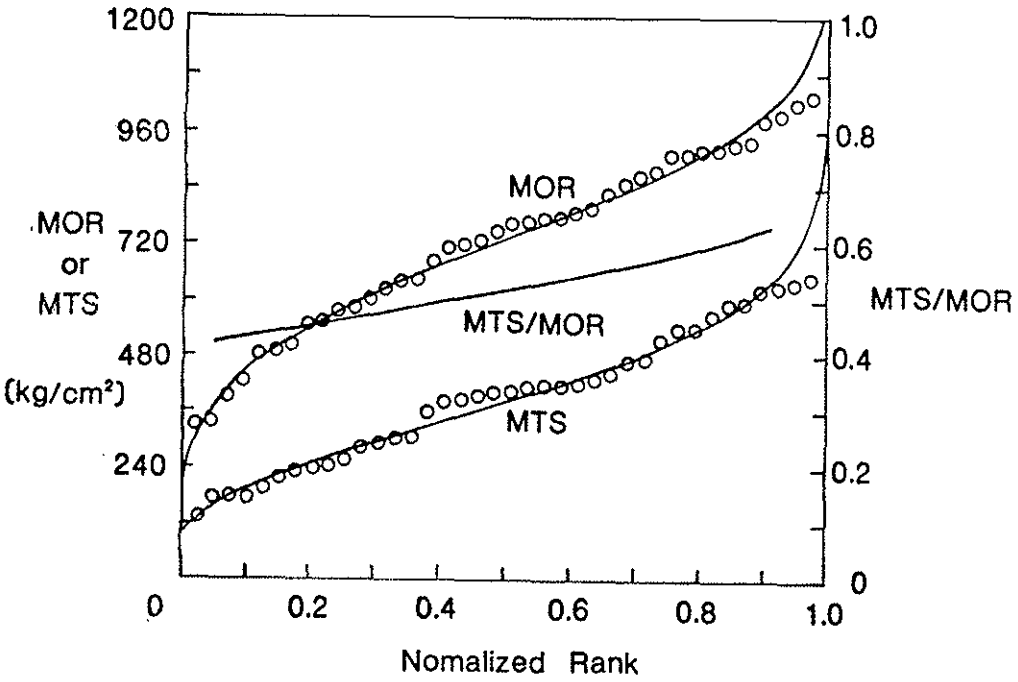

Figure 8 Distribution of lamina's MTS, MOR and MTS/MOR

The value 0.43 ~ 0.63 for MTS/MOR seems to be reasonable value compared with another examples [e.g. Walford(4)], so it was recognized that the effect of test speed on MTS was not so significant as the case of small clear specimens.

6.2 Bending Test Results on Glulam Beams

Table 3 shows individual results obtained from full-size experiments on the Douglas fir glulam beam specimens as well as those obtained from the Monte Carlo simulation done on the imaginary glulam beams having the same configurations as the corresponding actual beams.

Table 3 Individual result by full-size experiment and Monte Carlo simulation

Specimen Code	Full-Size Experiment MOE* ($X10^3$Kgf/cm²)	Full-Size Experiment MOR (Kgf/cm²)	Monte Carlo Simulation Weibull 3-parameter function for MOR location:γ (Kgf/cm²)	Scale:θ (Kgf/cm²)	Shape:m	5%-ile (Kgf/cm²)
(replication)	N1 N2 N3	N1 N2 N3				
H91B17	142,136,141	403,408,383	67.9	334.8	3.8042	221
H76B17	141,132,133	350,440,408	67.6	350.5	3.8026	228
H76B13	131,137,137	474,454,438	142.6	283.8	2.9348	246
H62B17	131,132,157	447,549,435	126.5	265.3	2.9704	224
H62B13	141,136,127	453,447,480	71.6	372.9	3.7321	240
H57B08	135,157,136	363,361,410	not done			
H46B17	108,152,167	595,443,489	54.3	412.5	4.0371	252
H31B17	156,136,142	381,233,400	44.5	449.9	4.1866	266
H18B17	not done		32.2	504.9	4.5274	294

* Modulus of elasticity of glulam beam was calculated by putting E/G=20. We actually determined the modulus of rigidity G of glulam beam for large specimens (H91B17~H76B13) by measuring the diagonal deformations near beam ends and confirmed as E/G=20 .

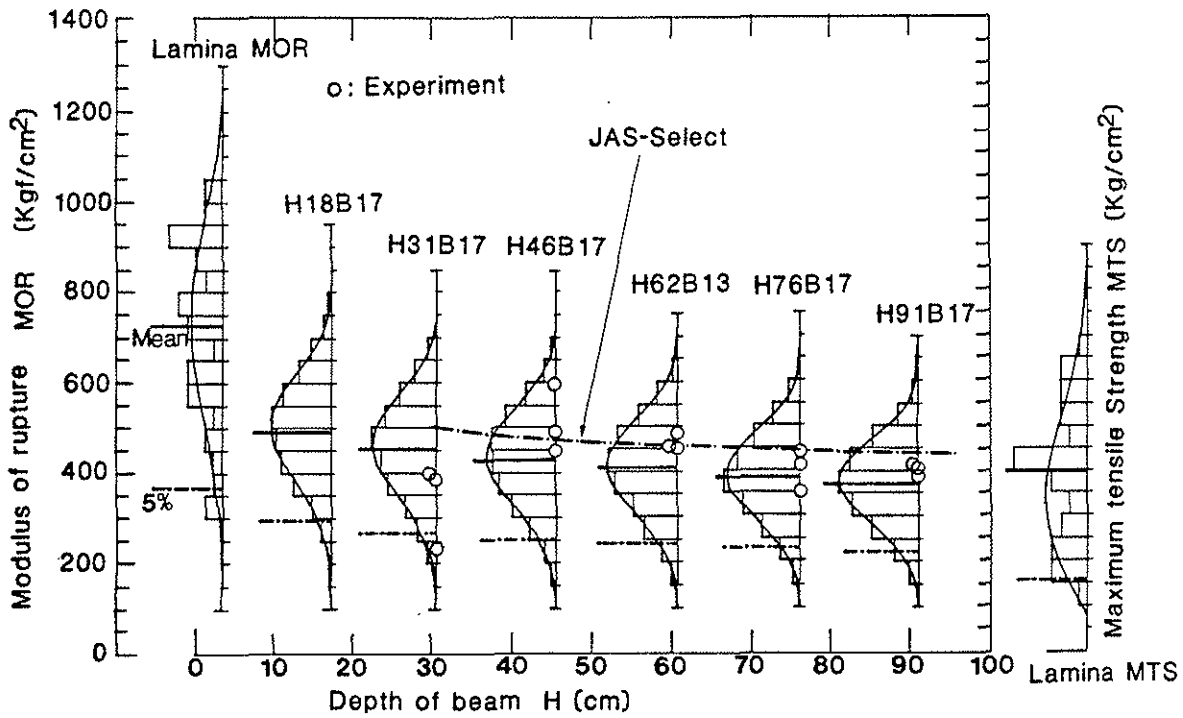

Figure 9 Depth effect on glulam beam MOR

Figure 9 demonstrates the depth effect on the MOR of glulam beams. In this figure, the term "Mean" indicates the arithmetical mean value, and the term "5%" indicates the Weibull 5%-ile value. And "JAS-Select" indicates the standard value assigned to the select grade glulam in the Japanese Agricultural Standard for Glued Laminated Timber(5). Most of experimental values except H31B17-N2 were higher than the 5%-ile level predicted by the Monte Carlo method. The only exceptional case is very rare indeed, but likely to be exist with less probability than 5% according to the Monte Carlo simulation done in this study.

From this figure, it can be clearly seen that the modulus of rupture of large glulam beams can be predicted if both distributions of MOR and MTS of laminae are known, and that the depth effect can be also explained well with equation 11) derived in this study without using the size effect factor .

7. CONCLUSION

Modulus of rupture (maximum bending moment of beam/ section modulus of beam) of any glulam beam will be able to be predicted by applying the multi-layer composite beam concept as described in this report, if the MTS(maximum tensile strength) and MOR(flat-wise maximum bending strength) of laminae and other information for cross section of the beam are known.

In order to complete this approach more in general, research involving the longitudinal variation of material properties would be required.

REFERENCES

(1) Goodman, J.R., Layered wood systems with interlayer slip , Wood Science, Vol.1, No.3, pp.148-158, 1969.
(2) Eby, E.R., Proofloading of finger-joints for glulam timber , Forest Products Journal, Vol.31,No.1,pp.37-41,1981.
(3) Iijima et al, Structural timber - Establishment of data base and its analysis - , partly distributed book ,Timber Engineering Working Group , Japan Wood Research Society,1988.
(4) Walford, G.B., Comparison of the tensile and bending strengths of 100x50mm radiata pine , FRI Bulletin, No.21, N.Z.Forest Service,1982.
(5) Japanese Agricultural Standard (JAS), Notification No.2054 of the Ministry of Agriculture, Forestry and Fisheries, 1986.

Acknowledgements

We wish to thank Messrs. Oguni (Kumamoto), Saito (Miyagi), Kamiya (Nagoya), Inamasu (Shizuoka), Ikeda (Shizuoka) and Nishikawa (Ishikawa), who were visiting staffs from each prefecture, for their help to the full-size beam experiments, and also Drs. Hatayama, Hirashima, Kanaya and Fujii for their valuable advice in carrying out this research.

CIB-W18A/21-12-2

INTERNATIONAL COUNCIL FOR BUILDING RESEARCH STUDIES AND DOCUMENTATION

WORKING COMMISSION W18A - TIMBER STRUCTURES

AN APPRAISAL OF THE YOUNG'S MODULUS VALUES SPECIFIED FOR GLULAM IN DRAFT EUROCODE 5

by

L R J Whale, B O Hilson and P D Rodd
Brighton Polytechnic
United Kingdom

MEETING TWENTY-ONE
PARKSVILLE, VANCOUVER ISLAND
CANADA
SEPTEMBER 1988

INTRODUCTION

In the CIB-Structural Timber Design Code (1983) no strength or stiffness parameters are published for glulam. It is stated that these parameters should be determined by standardised short-term tests in accordance with "RILEM/CIB-3TT-3 : Timber Structures - Timber in structural sizes - Determination of some physical and mechanical properties", combined with appropriate methods for determining the strength and stiffness of the glulam from the properties of the lamellae.

In the draft Eurocode 5 (1987), characteristic strength values and mean E-values are given for a number of glulam grades manufactured in accordance with specific production requirements. Ehlbeck and Colling (1986) explain the basis of the derivation of these values and state that for the modulus of elasticity, some account was taken of the overall mix of physical properties in different laminations when assigning the mean modulus values to each glulam grade.

This paper presents the results of an appraisal of the Young's modulus values specified for glulam in the draft Eurocode, using a computer simulation technique based upon the properties of the individual laminations.

MOTIVATION

In November 1986 a research project began at Brighton Polytechnic, aimed at studying areas which were of concern to the UK glulam industry. One such area was the magnitude of Young's modulus values specified in BS 5268 : Part 2 (1984), which from the experience of many practitioners and fabricators, were considered to be too low.

A background study of stock beam designs revealed that 86% of all light duty beams (66 x 315 to 115 x 495 mm) specified in the UK were likely to be deflection controlled. Heavier duty standard sections (90 x 450 to 215 x 1035 mm) were likely to be governed by deflection criteria in 75% of cases. If a 15% increase in the modulus of elasticity for glulam could be justified, then only about 50% of the beam designs would be controlled by deflection considerations, and laminations could be saved on approximately half of all beams produced. The resulting savings in material costs were estimated to be around £10,000 per 1000 m^3 of glulam produced. Given the magnitude of current and projected glulam consumption, the potential savings which could be gained from such refinements to glulam E-values provided ample justification for more detailed research in this area.

PREDICTIVE TECHNIQUES

The method used to evaluate E values for glulam beams was to develop analytical models which could mimic the behaviour of real beams. This would allow properties for beams made with existing or future grades to be established without recourse to extensive full-scale testing. Testing was restricted to that necessary to verify that the analytical models were providing sufficiently accurate predictions of real beam behaviour.

Two such models were developed, one using a two-dimensional grid of finite elements to model the variation of material properties along individual laminations, and the other using a transformed section approach which split the beam into a number of cross-sections, each with its own equivalent homogenized EI value.

The finite element model, based upon PAFEC (1984), is presently linear elastic and has the capability of modelling both the inhomogeneous, orthotropic nature of the timber lamellae and the homogeneous, isotropic properties of the interconnecting glue layers. The model makes use of 8-noded isoparametric elements and was developed primarily to investigate the sensitivity of glulam behaviour to the properties of the gluelines. The model can be extended to cater for nonlinearity and creep, but considerable computer run time would be envisaged.

The transformed section or finite interval model was developed by Pellicane and Hilson (1985) as a rapid numerical means of evaluating the deflected profile of beams with inhomogeneous laminations. The model is based upon a division of the beam into a number of segments along its length, the calculation of transformed sectional properties within each finite interval and the application of the Unit-Load-Theorem to calculate deflected shapes, as follows :

$$\Delta_A = \int_0^L \frac{M(x)\, m(x)}{EI(x)}\, dx + k \int_0^L \frac{V(x)\, v(x)}{GA(x)}\, dx \qquad \ldots\ldots (1)$$

where

Δ_A	=	total deflection at A (bending + shear)
M(x) and V(x)	=	bending moment and shear force at point x
m(x) and v(x)	=	bending moment and shear force at point x caused by unit load at A
EI(x) and GA(x)	=	bending stiffness and shear stiffness of the transformed section at x
K	=	form factor taken as 1.2 for rectangular sections
L	=	length of beam

Since the EI(x) and GA(x) terms are assumed constant within each of the longitudinal segments, the integrals in Equation 1 could be rewritten thus :

$$\Delta_A = \frac{1}{EI_1} \int_0^{L/n} M(x)\, m(x)\, dx + \frac{K}{AG_1} \int_0^{L/n} V(x)\, v(x)\, dx$$

$$+ \ldots \frac{1}{EI_n} \int_{(n-1)\frac{L}{n}}^{L} M(x)\, m(x)\, dx + \frac{K}{AG_n} \int_{(n-1)\frac{L}{n}}^{L} V(x)\, v(x)\, dx \quad \ldots\ldots (2)$$

where :

EI_i ($i = 1 \ldots\ldots n$) = homogenized EI value for each beam segment
GA_i ($i = 1 \ldots\ldots n$) = homogenized GA value for each beam segment

Each of the integrals in (2) were then numerically approximated over incremental distances Δx to yield the following equation for total deflection at point A :

$$\Delta_A = \sum_{i=1}^{n} \left[\frac{1}{EI_i} \sum_{j=a}^{b} M(x)_j\, m(x)_j\, \Delta x + \frac{K}{AG_i} \sum_{j=a}^{b} V(x)_j\, v(x)_j\, \Delta x \right] \quad \ldots\ldots (3)$$

Explicit equations expressing the variation of M(x), m(x), V(x) and v(x) over the beam length were developed for a number of load cases. The shear modulus, G, was taken as E/16 and hence Equation 3 provided a rapid means of establishing deflections in beams where the variation in elastic properties of the individual lamellae was known.

MODEL VERIFICATION

To test the accuracy of the analytical models, deflections and extreme fibre strains measured in a total of 18 miniature and full-scale beam tests were compared with predicted values. Data from 10 of these beams were obtained from tests carried out at Chalmers University by Johanssen (1975). Details of the validatory test beams are given in Table I.

TABLE I. -- TEST-BEAMS

Origin	Number of beams	Number of laminations	Laminate thickness mm	Beam Length mm	Loading pattern
Brighton Polytechnic (models)	7	10	5	950	3-point
Brighton Polytechnic	1	5	45 & 30	3000	3-point
Sweden (Chalmers University)	10	18	33	8000	4-point

In each case the section size and lengthwise variation in E-value along each lamella acted as the input to the analytical models. Previous sensitivity studies conducted using the models had indicated that the glueline properties have a negligible effect upon the composite modulus of glulam beams and so can be ignored. No attempt was made to model finger joint properties. In the beams tested at Brighton Polytechnic, plank E values were obtained from static bending tests using a span of 160 mm in the miniature beams and 500 mm in the larger beam. Those used for the Chalmers University beams were obtained from machine grading records over incremental distances of 150 mm. All E-values were corrected for shear.

In all the full-size beams, linear elastic behaviour was observed up to 80% of ultimate load. The average model accuracies at this level are shown in Table II, by expressing the differences from measured values as a percentage error.

No tendency was observed for the models to either consistently over-estimate or under-estimate beam deflections. From Table II, both the finite element (FE) and finite interval (FI) models are seen to give

reasonably accurate predictions of overall beam behaviour, based upon the properties of individual laminations. Those errors which do exist are felt to be largely attributable to approximations in the input data for E variations along planks, brought about by the need to use finite spans to establish local E values.

TABLE II. -- AVERAGE MODEL ACCURACIES

Beams	Deflection Errors		Strain Errors*	
	FE model	FI model	FE model	FI model
Model beams	4.1%	4.7%	Not measured	Not measured
Brighton Poly	1.4%	6.1%	8.0%	6.9%
Chalmers Univ	7.9%	6.8%	13.4%	14.2%

* strain at 80% ultimate load

GLULAM BEAM SIMULATIONS

Before the models could be used to predict deflections in real glulam beams, data concerning the variation in Young's modulus along planks were required. A data bank of this type was kindly supplied by the Princes Risborough Laboratory, based upon their Cook-Bolinder machine grading records for over 500 European whitewood planks, 47 x 97 in section. For each plank lengthwise bending E values were available at 100 mm centres, along with the corresponding knot area ratio information necessary to sort the planks into ECE grades S6, S8 and S10 (corresponding to EC5 grades C2, C4 and C6). Accordingly, 104 planks were assigned to S10 grade, with 335 planks graded S8 and 62 planks graded S6; 37 planks were rejected.

Planks from these hypothetical stocks of timber were then randomly selected and arranged to form 4, 7, 15 and 20 lamination beams in each of these three grades. Selective beam lay-ups were also constructed with S10 laminations occupying the outer sixths of the beam and S6 laminations occupying the inner two thirds (corresponding to EC5 glulam grade LC6/2). All beams possessed a span to depth ratio of 20 and randomly positioned end joints were incorporated in the beams, arranged so that no alignment occurred in adjacent laminations. The properties of these end joints and of the interconnecting glue layers were not modelled. Before being input into the model, all plank E values were corrected for shear. By virtue of the machine grading process, the E values relate to 900 mm bending spans, but are assigned to successive 100 mm cells occupying the central region of each span.

This simulation process was repeated until 1600 beams had been constructed in each of the glulam grades. On each occasion the finite interval model was used to determine the maximum deflection of the beams when simply supported and subjected to uniformly distributed load. From the values of maximum deflection produced by the model, equivalent shear free E values were calculated for the beams, assuming a homogeneous material. By repeating this process within the simulation procedure, a representative global mean E value became apparent for beams within each grade.

RESULTS AND DISCUSSION

The results of the glulam beam simulations are presented in Table III.

It can be seen that the mean moduli for each of the EC5 glulam grades LC2/2, LC4/4, LC6/2 and LC6/6 are predicted to be approximately 10200 N/mm^2, 11000 N/mm^2, 11000 N/mm^2 and 11500 N/mm^2 respectively. For the lower glulam grades the predicted moduli are higher than those currently specified in Eurocode 5, whereas in the

higher grades they are lower. (The current range specified in EC5 is 9000 N/mm^2 to 13000 N/mm^2). The modulus currently specified for LC4/4 glulam is upheld with this research. As is normally assumed, the mean modulus of glulam beams is seen to remain independent of the number of laminations used.

TABLE III - GLULAM BEAM SIMULATION RESULTS

Glulam Grade	Number of Laminations	Number of of beams	E_{mean} (N/mm^2)	Coeff. of Variation
LC 2/2	4	1600	10271	11.90
	7	1600	10152	10.85
	15	Insufficient planks		-
	20	in data-base		-
			10212	11.38
LC 4/4	4	1600	11066	9.98
	7	1600	11010	9.63
	15	1600	11015	10.47
	20	1600	10979	8.84
			11017	9.73
LC 6/2	12	1600	10959	11.37
	18	1600	10947	10.88
			10953	11.13
LC 6/6	4	1600	11543	9.88
	7	1600	11488	9.36
	15	1600	11486	10.26
	20	Insufficient planks in data base		
			11506	9.83

The reason for this tightening in the range of expected E values for glulam is felt to be the masking effect of the better quality timber surrounding the short sections of lower modulus material which determine the grade of each plank. The properties of this overwhelming majority of timber are all but independent of the grade of the plank, and have the effect of smoothing out differences between the E values associated with particular grades.

Since graded whitewood will not conveniently fall into strength class C1, glulam beams encompassing this grade could not be constructed. It is adjudged, however, that the modulus of LC2/1 glulam will be approximately the same as LC2/2 glulam, being 10200 N/mm^2. If LC4/1 glulam follows the indication given by LC6/2 glulam in being intermediate between the moduli derived for glulam composed of the upper and lower grades throughout, then its mean modulus is likely to be around 10700 N/mm^2. These values are felt to have a more rational basis than those currently specified in Table A2.5 of Eurocode 5, and are considered to be more accurate estimates of those which will exist in practice.

CONCLUSIONS

Simulation studies have suggested the range of E values currently specified for glulam in draft Eurocode 5 is too broad. More appropriate values are considered to be :

Grade LC2/1 - 10200 N/mm^2
Grade LC2/2 - 10200 N/mm^2
Grade LC4/1 - 10700 N/mm^2
Grade LC4/4 - 11000 N/mm^2
Grade LC6/2 - 11000 N/mm^2
Grade LC6/6 - 11500 N/mm^2

REFERENCES

CIB (1983) Structural Timber Design Code.
Publication 66. CIB-W18.

Commission of the European Communities (1987) - Eurocode 5 : Common unified rules for timber structures.
Report EUR 9887 EN.

J. Ehlbeck and F. Colling (1986) - Strength of glued laminated timber.
CIB-W18 Paper 19-12-1. Florence, Italy.

British Standards Institution (1984) - BS5268 : Part 2 : 1984.
Structural use of timber. Part 2. Code of practice for permissible stress design, materials and workmanship.
BSI, London.

PAFEC (1984) - Data preparation user manual. Level 5.1.
Pafec Ltd., Nottingham.

P.J. Pellicane and B.O. Hilson (1985) - A computer model to predict the elastic response of composite beams with inhomogeneous lamellae.
Brighton Polytechnic Report to the Timber Research and Development Association, UK.

C.J. Johanssen (1975) - Glued laminated beams with laminated tension laminations. Report 5 - Bending tests on 14 glued laminated beams.
Chalmers Tekniska Hogskola. Internal Report No. S75:1. Goteborg.

ACKNOWLEDGEMENTS

The authors wish to thank Mr. A.R. Fewell (Princes Risborough Laboratory), for supplying the plank property data used in this study, amd SERC and TRADA for financing the project.

CIB-W18A/21-12-4

INTERNATIONAL COUNCIL FOR BUILDING RESEARCH STUDIES AND DOCUMENTATION

WORKING COMMISSION W18A - TIMBER STRUCTURES

COMPARISON OF A SHEAR STRENGTH DESIGN METHOD IN EUROCODE 5 AND A MORE TRADITIONAL ONE

by

H Riberholt
Technical University of Denmark
Denmark

MEETING TWENTY-ONE
PARKSVILLE, VANCOUVER ISLAND
CANADA
SEPTEMBER 1988

Comparison of a shear strength design method in Euro Code 5 and a more traditional one.

H. Riberholt, Dept. Struc. Eng., Technical Univ. of Denmark

The failure criterion in Euro Code 5

$$Q_d \leq k_{vol,v}\, k_{dis,v}\, k_\ell\, (\tfrac{4}{3}\, bh\, f_{v,d}) \qquad \text{(EC)}$$

is compared with a more traditional one

$$\tau_d \leq k_{vol,v}\, K_{dis,v}\, k_\ell\, f_{v,d} \qquad \text{(Tra)}$$

The notation is the same as in Euro Code 5.

For a skew distributed load the criterion (EC) can result in a shear force which is almost twice the value according to (Tra). Of course there exists a limit to how skew the load can be distributed. But do experience or tests exist which support the validity of (EC) for skew loads?

The volume and the length factors $k_{vol,v}$ and k_ℓ are the same so

$$k_\ell = \frac{\ell}{\ell - 2h}$$

$$k_{vol,v} = \left(\frac{V_o}{V}\right)^{2/k_{Wei}}$$

But the distribution factors are different. The one in EC5 $k_{dis,v}$ is suggested substituted by

$$K_{dis,v} = 0.7 + \frac{0.3}{1 + \Sigma F_i / \Sigma(q_i \ell_i)}$$

where ΣF_i The total load from concentrated forces on a beam element.

$\Sigma(q_i \ell_i)$ The total load from distributed loads on a beam element.

A comparison of (EC) and (Tra) has been done by comparing the total loads which a beam can carry according to the two criteria. The loads have been normalized by division with the load carrying capacity of a simple supported beam with uniform load $q\ell$. The lengths and the volumes are identical.

So for (EC) the proportion between the load capacity of an arbitrary beam Q_{cap} and a simple supported beam $Q_{cap,SS,q}$ becomes

$$\frac{Q_{cap}}{Q_{cap,SS,q}} = \frac{k_{dis,v}}{k_{dis,v,SS,q}} = \frac{k_{dis,v}}{1.43}$$

The max shear force V_{max} which is used to determine τ_d in (Tra) is calculated from

$$V_{max} = \begin{cases} k_v \, q\ell & \text{for distributed load} \\ k_v \, F & \text{for concentrated load} \end{cases}$$

So for (Tra) the similar proportion is

$$\frac{Q_{cap}}{Q_{cap,SS,q}} = \frac{k_{v,SS,q} \, K_{dis,v}}{k_v K_{dis,v,SS,q}} = \frac{0.5 \quad K_{dis,v}}{k_v \quad 1.0}$$

Table 1 Comparison of max total loads normalized with the capacity of a simple supported beam with an uniform distributed load.

Beam and load	Failure criterion: (EC) $k_{dis,v}$	$\frac{Q_{cap}}{Q_{cap,SS,q}}$	k_v	(Tra) $k_{dis,v}$	$\frac{Q_{cap}}{Q_{cap,SS,q}}$
Distributed loads					
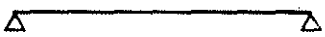	1.43	1.00	0.5	1.0	1.00
	1.62	1.13	0.45	1.0	1.11
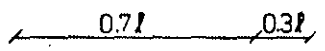	1.97	1.38	0.41	1.0	1.22
	1.87	1.31	0.4	1.0	1.25
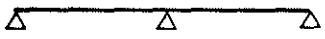	2.49	1.74	0.31	1.0	1.60
Concentrated load					
	1.00	0.70	0.5	0.7	0.70
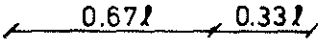	0.63	0.44	1.0	0.7	0.35
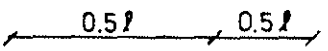	0.50	0.35	1.0	0.7	0.35
	1.11	0.39	1.0	0.7	0.35
	1.08	0.76	0.59	0.7	0.59

It is seen from table 1 that the two failure criteria result in almost the same load carrying capacities. The differences are small compared with the uncertainty in the estimation of the characteristic shear strength when drying cracks are considered.

CIB-W18A/21-13-1

INTERNATIONAL COUNCIL FOR BUILDING RESEARCH STUDIES AND DOCUMENTATION

WORKING COMMISSION W18A - TIMBER STRUCTURES

DESIGN VALUES FOR NAILED CHIPBOARD - TIMBER JOINTS

by

A R Abbott
Timber Research and Development Association
United Kingdom

MEETING TWENTY-ONE
PARKSVILLE, VANCOUVER ISLAND
CANADA
SEPTEMBER 1988

DESIGN VALUES FOR NAILED CHIPBOARD - TIMBER JOINTS

BACKGROUND

In recent years there has been increasing interest in the potential use of chipboard for structural applications. This has highlighted the need to derive and publish working stresses for the material to enable it to compete on a level basis with other sheet materials such as plywood, tempered hardboard and fibre building board, and also with conventional tongued and grooved boarding in all types of flooring.

It has long been considered in the UK that any design values for existing grades of chipboard would be too low to be competitive with other materials. Furthermore, a number of chipboards already exist with superior strength characteristics to those required of Type II and III boards in BS 5669: 1979 (1). These are therefore not being utilised to their full extent. In early 1982 it was proposed to the British Standards Institution (BSI) chipboard material committee (TIB/14) that if design stresses were to be derived for chipboard, then these should relate to a higher specification board than is covered in BS 5669 : 1979. This was subsequently agreed by the BSI Committee, and provision was made in the current revision of BS 5669 for the specification of a structural grade chipboard.

A joint project between the Timber Research and Development Association (TRADA) and the Princes Risborough Laboratory of the Building Research Establishment (PRL) was defined in 1982 to carry out the necessary research into test methods and to undertake the considerable amount of testing required to furnish data from which a material specification could be derived. This project commenced in April 1983 and was sponsored by TRADA, PRL, the United Kingdom Department of the Enviroment (DOE), the Chipboard Promotion Association (CPA) and the United Kingdom Particleboard Association (UKPA).

The original proposal to BSI recommended that the specification for a structural grade chipboard should generally possess higher property levels than those currently given in BS 5669 for existing board types. Initial mean values of around 3750 N/mm^2 for bending modulus of elasticity 22 N/mm^2 for bending modulus of rupture and 0.75 N/mm^2 for tensile strength perpendicular to the plane of the board were regarded as possible target values for a standard grade of board.

Whilst these figures are representative of the top of the range for the higher quality existing boards, two further requirements were to be satisfied before any particular brand of board could be chosen.
These were that:

1) The brand should have been in production for a considerable period of time and should have exhibited a consistently high level of performance during this period.

11) The brand should have a moisture-resistant adhesive of MUF or PF type, and should satisfy the V313 requirements set out in BS 5669.

Consideration of the likely end-uses of a structural grade board resulted in the following choices of thickness to be tested:

12mm Typically for use for webbed and box beams, and stressed skin panels.

18mm Mainly for use in office and industrial flooring and in industrial shelving.

22mm For uses similar to 18mm, where higher loadings are anticipated.

It was considered essential that the boards should be properly sampled on a statistical basis to enable both within-board and between-board variations to be quantified. It was decided that a realistic representative measure of between-board variation could be obtained by taking one sample board from each of six consecutive production shifts. However, in view of the large number of tests to be undertaken, the requisite number of test specimens could not be cut from six standard size boards, and consequently samples comprising two consecutive boards were obtained, making a total of twelve boards for each thickness of each board type.

After consideration of the vast number of tests that would have to be performed, it was decided that all three brands of board would be evaluated at 18mm and 22mm thickness, but that only one brand of board would be evaluated at 12mm thickness.

This project finished in late 1985. An extension of the work to cover boards up to 38mm in thickness was undertaken in 1986. The results from both programmes have since been analysed and a specification for a structural grade of chipboard has been produced for consideration by the BSI committee responsible for the re-drafting of BS 5669:1979 under the direction of the Timber Standards Committee.

Tentative design stresses and associated modification factors have also been produced relating to the new structural grade of chipboard (designated as type C5), and these are also currently being discussed by BSI for inclusion in a future amendment to BS 5268: Part 2 (2).

It was always recognised that information on the performance of fasteners, nails and screws with structural grade chipboard must accompany any design stresses if the boards are to be fully utilised in a structural manner. A further project to provide some of this information has recently been completed at TRADA, aimed at deriving design values for laterally loaded chipboard-to-timber joints.

INTRODUCTION

This paper outlines the derivation of design data for nailed chipboard-to-timber joints in which nails are laterally loaded in single shear. The data used in this derivation were obtained from tests conducted at TRADA, using chipboard selected on the same basis as that used in the test programme described above, from which the specification for Type C5 chipboard has been derived. It is therefore concluded that the joint values presented here will be applicable to Type C5 chipboard and may be used in design in conjunction with the dry grade stresses and modification factors already produced.

The approach adopted was similar to that used for the derivation of design values for nailed tempered hardboard-to-timber joints which are included in BS5268: Part 2, and centres around a large testing programme from which the joint characteristics may be ascertained.

It should be noted that this procedure has yet to be fully accepted by BSI; the values given in this paper should therefore be considered as tentative at this stage.

The basic test data were obtained from standard tests carried out on nailed joints. 20 replicate joints were tested for each of the following combinations, giving a total of 900 individual test specimens.

3 nail sizes (2.65 mm, 3.35 mm, 4.00mm diameter)
5 chipboard thickness (9 mm, 18 mm, 22 mm, 30 mm, 38 mm)
3 framing timber species (British Sitka spruce, imported redwood, keruing)

All specimens were conditioned to constant weight in an environment of 20° C and 85% RH before testing, which approximates to the upper limit of the dry exposure condition given in BS 5268. For each individual test specimen a graph of load vs. joint displacement was produced throughout the entire loading procedure. The load-displacement responses were observed to follow the same basic trends as seen previously for other types of laterally loaded joint (3), and therefore it was possible, with some confidence, to fit the same form of exponential curve through each individual load-embedment data set. This curve, which has been used by Foschi (4) and Smith (5) amongst others, is defined mathematically by the following equation:-

$$P = (k_2 + k_3\delta)\left(1 - \exp\left(\frac{-k_1\delta}{k_2}\right)\right) \quad - (1)$$

where P = load
δ = displacement
k_1 = initial tangent stiffness
k_2 = intercept of final tangent on load axis
k_3 = final tangent stiffness

DERIVATION PROCEDURE

The deriviation procedure requires that the following basic data be obtained from each batch of 20 joint specimens :-

i. Mean value of maximum load (Pmax) and corresponding coefficient of variation

ii. Mean value of maximum load at 0.4 mm deflection (P0.4) and corresponding coefficient of variation

iii. Mean values of density of the timber framing member

Design loads are calculated both from Pmax and P0.4, and the minimum value is selected as the appropriate safe design load for the particular chipboard thickness/nail size/timber strength class combination.

Values of Pmax were obtained directly from the load-displacement graph and values of P0.4 were obtained from the fitted envelope curve using the value of the initial stiffness tangent (k_1).

The calculation procedure used to derive the joint design values is described below. All calculations were performed using a computer spreadsheet programme. Since the procedure is basically the same for both sets of data, only the method using Pmax will be described, however, where differences do occur between the methods these will be highlighted.

i. Values of mean maximum load (Pmax), the corresponding coefficient of variation and the density of the timber framing members for each chipboard thickness/nail diameter/timber species provide the basic data for the calculations.

ii. For each thickness of chipboard and diameter of nail, values of Pmax were plotted against timber density for the three species of framing member. Best-fit lines through the origin were then defined, from which values of maximum load corresponding to the lowest mean density for timber in each of the four BS 5268 strength groups were calculated.

[In BS 5268 : Part 2, the four strength groups are SC1/2, SC3/4, SC5 and SC6/7/8/9, with corresponding lowest (1 percentile) mean densities of 340,380,470,and 550kg/m^3 respectively].

iii. A procedure identical to (ii) above was used to calculate values of coefficient of variation which correspond to the maximum load values.

iv. Design values (single shear lateral loads) were calculated from the following equation:-

$$\text{Design Load} = \frac{Pm(1-2.33c)}{2F}$$

Where Pm is the mean maximum load calculated in (iii) above
c is the coefficient of variation appropriate to Pm
2.33 is a statistical factor
F is a load factor

The value of 2 in the denominator takes account of the fact that the joint tests comprised 2 nails whereas the design values are for a single nail.

The load factor F includes allowance for workmanship and a safety factor, but principally modifies the strength determined from a short duration laboratory test to give a value appropriate for a long-term duration of loading.

- For all-timber nailed joints F = 3.0

- For tempered hardboard-to-timber joints, the value of 3.0 was factored by the ratio of the long-term load duration factor for solid timber (0.5625) to the long term load duration factor established for the strength properties of tempered hardboard (0.4250) (Reference 6). Hence, for tempered hardboard-to-timber joints:-

$$F = 3.0 \times \frac{0.5625}{0.4250} = 4.0$$

Using the same argument as above, the corresponding value of F for chipboard-to-timber-joints is :-

$$F = 3.0 \times \frac{0.5625}{29.8/100.2} = 5.67$$

For the design values determined on the basis of the load at 0.4 mm deflection, the equation is :

$$\text{Design load} = \frac{Ps\ (1-2.33c)}{2}$$

where Ps is the mean load at 0.4 mm deflection
c is the coefficient of variation corresponding to Ps

v. The revision of BS 5669 will include four thickness classes for Type C5 chipboard (12 - 19 mm, 20 - 25 mm, 26 - 32 mm and 33 to 40 mm). It is therefore necessary to calculate design values appropriate to these four thickness classes.

Taking each set of values calculated for a given timber Strength Class group and nail size, a graph of design load vs chipboard thickness was produced. A best-fit straight line was then fitted to the data points using a least square regression technique. It was observed that the design loads increase with increasing board thickness and therefore to give a conservative estimate, values of design load were taken at the lower end of each thickness class, and assumed to be applicable for the entire thickness range.

vi. Finally, the design values calculated from the maximum load and load at 0.4 mm displacement was compared, and the minimum value in each case was selected as suitable for code inclusion.

Table 1 contains the design values (corrected for thickness) obtained by each method, and gives the proposed design values for inclusion in the ammendment to BS 5268 Part 2.

The design loads calculated apply to fully embedded nailed of lengths not less than those used in the test viz:

40 mm for 2.65 mm diameter nails
45 mm for 3.35 mm diameter nails
60 mm for 4.00 mm diameter nails

These values are for long term loading and modification factors for other load durations are required. Using the expression $(1 + k_{12}/2)$ as given in clause 3.19.3 of CP 112: 1972 and the values of k_{12} as 1.8 for medium-term and 3.2 for short-term load, the modification factors for nailed chipboard to timber joints become 1.4 and 2.1 for medium term and short term loads respectively.

References

1. BRITISH STANDARDS INSTITUTION. Specification for wood chipboard and methods of test for particleboard. British Standard BS 5669. London BS5. 1979

2. BRITISH STANDARDS INSTITUTION. Structural use of Timber. Part 2. Code of Practice for permissible stress design, materials and workmanship. British Standard 5288:Part 2. London BSI. 1974.

3. WHALE L.R.J. and SMITH I. Mechanical timber joints. TRADA Research Report 18/86. Hughenden Valley, TRADA 1986.

4. FOSCHI R.O. Load-slip characteristics of nails. Wood science, July 1974, 7 (1) 69-76.

5. SMITH I. Interpretation and adjustment of results from short term lateral load tests on whitewood joint specimens with nails or bolts. TRADA Research Report 5/82. Hughenden Valley, TRADA. 1982

6. BROCK G. Design data for nailed joints of tempered hardboard to timber. CSB/32/7 - 79/3, BSI Committee paper 1979.

DESIGN VALUES (corrected for thickness) Calculated from MAXIMUM LOAD							DESIGN VALUES (corrected for thickness) Calculated from LOAD AT 0.4mm DEFLECTION						DESIGN VALUES (corrected for thickness) Minimum of previous two values						DESIGN VALUES (corrected for thickness) PROPOSED VALUES FOR CODE INCLUSION					
Thickness Class	Nail Diameter	Strength Class	Strength Class	Strength Class	Strength Class		Thickness Class	Nail Diameter	Strength Class	Strength Class	Strength Class	Strength Class	Thickness Class	Nail Diameter	Strength Class	Strength Class	Strength Class	Strength Class	Thickness Class	Nail Diameter	Strength Class	Strength Class	Strength Class	Strength Class
(mm)	(mm)	SC1/2	SC3/4	SC5	SC6/7/8/9		(mm)	(mm)	SC1/2	SC3/4	SC5	SC6/7/8/9	(mm)	(mm)	SC1/2	SC3/4	SC5	SC6/7/8/9	(mm)	(mm)	SC1/2	SC3/4	SC5	SC6/7/8/9
12-18	2.650	35.317	38.768	45.993	51.785		12-18	2.650	90.966	95.131	99.468	97.475	12-18	2.650	35.317	38.768	45.993	51.785	12-18	2.650	35	39	46	52
	3.350	44.527	48.942	58.245	65.777			3.350	134.807	142.987	155.481	159.715		3.350	44.527	48.942	58.245	65.777		3.350	45	49	58	66
	4.000	64.451	71.267	86.012	98.432			4.000	140.787	150.813	168.339	178.069		4.000	64.451	71.267	86.012	98.432		4.000	64	71	86	98
19-25	2.650	37.897	41.524	49.043	54.983		19-25	2.650	90.831	95.334	100.707	99.951	19-25	2.650	37.897	41.524	49.043	54.983	19-25	2.650	38	42	49	55
	3.350	51.874	56.997	67.768	76.466			3.350	128.810	136.208	146.882	149.430		3.350	51.874	56.997	67.768	76.466		3.350	52	57	68	76
	4.000	73.074	80.550	96.506	109.685			4.000	146.161	155.941	172.240	180.094		4.000	73.074	80.550	96.506	109.685		4.000	73	80	96	110
26-32	2.650	39.832	43.590	51.331	57.382		26-32	2.650	90.730	95.487	101.636	101.809	26-32	2.650	39.832	43.590	51.331	57.382	26-32	2.650	40	44	51	57
	3.350	57.384	63.037	74.911	84.483			3.350	124.312	131.123	140.433	141.717		3.350	57.384	63.037	74.911	84.483		3.350	57	63	75	84
	4.000	79.542	87.512	104.377	118.125			4.000	150.191	159.788	175.166	181.612		4.000	79.542	87.512	104.377	118.125		4.000	80	87	104	118
33-40	2.650	42.090	46.001	54.001	60.180		33-40	2.650	90.611	95.665	102.721	103.976	33-40	2.650	42.090	46.001	54.001	60.180	33-40	2.650	42	46	54	60
	3.350	63.813	70.085	83.244	93.835			3.350	119.065	125.191	132.909	132.717		3.350	63.813	70.085	83.244	93.835		3.350	64	70	83	94
	4.000	87.088	95.635	113.559	127.972			4.000	154.894	164.275	178.579	183.384		4.000	87.088	95.635	113.559	127.972		4.000	87	96	114	128

Table 1. Summary of design values for laterally loaded nailed chipboard-to-timber joints

CIB-W18A/21-15-1

INTERNATIONAL COUNCIL FOR BUILDING RESEARCH STUDIES AND DOCUMENTATION

WORKING COMMISSION W18A - TIMBER STRUCTURES

RECTANGULAR SECTION DEEP BEAM-COLUMNS WITH CONTINUOUS LATERAL RESTRAINT

by

H J Burgess
Timber Research and Development Association
United Kingdom

MEETING TWENTY-ONE
PARKSVILLE, VANCOUVER ISLAND
CANADA
SEPTEMBER 1988

This paper is abbreviated from TRADA internal reports arising from a project partly funded by the British government Department of the Environment, with the title `Bracing of timber and composite constructions`.

CONTENTS

RECTANGULAR SECTION DEEP BEAM-COLUMNS WITH CONTINUOUS LATERAL RESTRAINT

The basic bracing equations and solutions have been presented by Brüninghoff, who has also made proposals for the CIB Code (Brüninghoff 1983,1984,1985). The object of the following work is to introduce the type of initial imperfections which have been adopted in recent studies of lateral instability (Burgess, 1987) and then lead on to the consideration of multiple-mode buckling for columns with continuous elastic restraint.

A special case of the solution corresponds to a simple method that has been applied to estimate the remedial bracing requirements of initially unbraced or badly-braced trussed rafters which have deflected laterally to only a small extent (Burgess, 1982). The calculation in effect makes use of the well known formula for the design of columns with lateral load

$$1 = \frac{\sigma_c}{f_c} + \frac{\eta\sigma_c + \sigma_b}{f_b\left(1 - \frac{\sigma_c}{\sigma_{ew}}\right)}$$

when plotted beyond the region for column design as shown in Figure 1. The part of the curve below the horizontal axis caters for restraint loading which prevents further buckling. The same publication also considered the simple method given by Winter (1958) for estimating the bracing stiffness required and the corresponding brace strength. The following work provides a basis for a more extended study of Winter's method given in a separate paper. Related expressions have been developed to allow for torsional restraint in addition to lateral restraint at the centre line, but these will be reserved for a later study of multiple-mode buckling in beams.

ELASTIC LATERAL RESTRAINT AT CENTROID

From equation (5) of the 1987 report (paper 20-2-1)

$$EI\frac{d^4u_1}{dz^4} - \gamma M\frac{d^2}{dz^2}(\phi_1 + \phi_o) + P\frac{d^2}{dz^2}(u_1 + u_o) + ku_1 = 0 \qquad (1)$$

The term ku_1 has been added to represent the effect of a continuous elastic restraint load of modulus k N/mm^2 which is built up as the deflection u_1 increases. Timoshenko and Gere (1961) consider the case without end moments and with no initial imperfections, reaching the solution

$$\frac{P_{cr}}{P_e} = 1 + \frac{k}{EI}\frac{\ell^4}{\pi^4} \qquad (2)$$

for the first-mode buckling considered here. P_{cr} is the end load that causes lateral buckling of an `ideal` column with elastic lateral restraint. Equation (6) of the 1987 report is unchanged and leads to

$$\phi_1 = -\frac{M}{C\left(1 - \frac{P}{P_\phi}\right)}u_1 + \frac{\frac{P}{P_\phi}}{1 - \frac{P}{P_\phi}}\phi_o \sin\frac{\pi}{\ell}z - \frac{M}{C\left(1 - \frac{P}{P_\phi}\right)}u_o \sin\frac{\pi}{\ell}z \qquad (3)$$

Differentiating twice and inserting the result in (1) gives

$$EI\frac{d^4u_1}{dz^4}+\left\{\frac{\gamma M^2}{C\left(1-\frac{P}{P_\phi}\right)}+P\right\}\frac{d^2u_1}{dz^2}+ku_1 = \frac{\pi^2}{\ell^2}\left\{\frac{\gamma M^2}{C\left(1-\frac{P}{P_\phi}\right)}+P\right\}u_0\sin\frac{\pi}{\ell}z-\frac{\gamma M}{\left(1-\frac{P}{P_\phi}\right)}\frac{\pi^2}{\ell^2}\phi_0\sin\frac{\pi}{\ell}z$$

This is solved in the manner adopted previously, yielding the solution

$$u_1=\frac{\left\{\frac{M^2}{M_{cr}^2}+\frac{P}{P_e}\left(1-\frac{P}{P_\phi}\right)\right\}u_0-\frac{C}{M}\frac{M^2}{M_{cr}^2}\phi_0}{\left(1-\frac{P}{P_e}\right)\left(1-\frac{P}{P_\phi}\right)-\frac{M^2}{M_{cr}^2}+\frac{k}{EI}\frac{\ell^4}{\pi^4}\left(1-\frac{P}{P_\phi}\right)}\sin\frac{\pi}{\ell}z$$

or
$$u_1=\frac{\frac{M^2}{M_{cr}^2}+\frac{P}{P_e}\left(1-\frac{P}{P_\phi}\right)u_0-\frac{C}{M}\frac{M^2}{M_{cr}^2}\phi_0}{\left(\frac{P_{cr}}{P_e}-\frac{P}{P_e}\right)\left(1-\frac{P}{P_\phi}\right)-\frac{M^2}{M_{cr}^2}}\sin\frac{\pi}{\ell}z \qquad (4)$$

The total central deflection of the centre-line is

$$u=u_0+u_1=\frac{\frac{P_{cr}}{P_e}\left(1-\frac{P}{P_\phi}\right)u_0-\frac{C}{M}\frac{M^2}{M_{cr}^2}\phi_0}{\left(\frac{P_{cr}}{P_e}-\frac{P}{P_e}\right)\left(1-\frac{P}{P_\phi}\right)-\frac{M^2}{M_{cr}^2}} \qquad (5)$$

When M = 0, $u=\frac{u_0}{1-\frac{P}{P_{cr}}}$ for comparison with the previous report, but the term $\left(1-\frac{P}{P_\phi}\right)$ has been cancelled and this is sometimes invalid as shown later.

When P = 0,
$$u=\frac{\frac{P_{cr}}{P_e}u_0-\frac{C}{M}\frac{M^2}{M_{cr}^2}\phi_0}{\frac{P_{cr}}{P_e}-\frac{M^2}{M_{cr}^2}}$$

$\frac{P_{cr}}{P_e}$ is here used as an abbreviation from (2) although no end load is applied.

The solution for ϕ_1 may be found by inserting the expression for u_1 in equation (3) to give at the centre

$$\phi_1=\frac{-\frac{M}{C}\frac{P_{cr}}{P_e}u_0+\left\{\frac{M^2}{M_{cr}^2}+\frac{P}{P_\phi}\left(\frac{P_{cr}}{P_e}-\frac{P}{P_e}\right)\right\}\phi_0}{\left(\frac{P_{cr}}{P_e}-\frac{P}{P_e}\right)\left(1-\frac{P}{P_\phi}\right)-\frac{M^2}{M_{cr}^2}}$$

The total central twist is given by

$$\phi=\phi_0+\phi_1=\frac{-\frac{M}{C}\frac{P_{cr}}{P_e}u_0+\left(\frac{P_{cr}}{P_e}-\frac{P}{P_e}\right)\phi_0}{\left(\frac{P_{cr}}{P_e}-\frac{P}{P_e}\right)\left(1-\frac{P}{P_\phi}\right)-\frac{M^2}{M_{cr}^2}} \qquad (6)$$

When M = 0, $\phi=\frac{\phi_0}{1-\frac{P}{P_\phi}}$

as in the earler report, unaffected by the lateral restraint.

When P = 0,
$$\phi=\frac{\frac{P_{cr}}{P_e}\left(-\frac{M}{C}u_0+\phi_0\right)}{\frac{P_{cr}}{P_e}-\frac{M^2}{M_{cr}^2}}$$

Related initial twist and curvature

As discussed in the earlier report, the initial imperfections u_o and ϕ_o will now be related in the same way as the deflections u and ϕ in an ideal beam buckling under end moments only (Burgess, 1986).

Putting $\phi_o = -\frac{\pi}{\ell}\sqrt{\frac{EI}{C\gamma}}\, u_o$ in (5)

$$u = \frac{\frac{P_{cr}}{P_e}\left(1-\frac{P}{P_\phi}\right)+\frac{M}{M_{cr}}}{\left(\frac{P_{cr}}{P_e}-\frac{P}{P_e}\right)\left(1-\frac{P}{P_\phi}\right)-\frac{M^2}{M_{cr}^2}}\, u_o \qquad (7)$$

and putting $u_o = -\frac{\ell}{\pi}\sqrt{\frac{C\gamma}{EI}}\, \phi_o$ in (6)

$$\phi = \frac{\frac{M}{M_{cr}}\frac{P_{cr}}{P_e}+\left(\frac{P_{cr}}{P_e}-\frac{P}{P_e}\right)}{\left(\frac{P_{cr}}{P_e}-\frac{P}{P_e}\right)\left(1-\frac{P}{P_\phi}\right)-\frac{M^2}{M_{cr}^2}}\, \phi_o \qquad (8)$$

Similarly for u_1, from (4),

$$u_1 = \frac{\frac{M^2}{M_{cr}^2}+\frac{P}{P_e}\left(1-\frac{P}{P_\phi}\right)+\frac{M}{M_{cr}}}{\left(\frac{P_{cr}}{P_e}-\frac{P}{P_e}\right)\left(1-\frac{P}{P_\phi}\right)-\frac{M^2}{M_{cr}^2}}\, u_o \qquad (9)$$

From (1) integrated twice or adapting (5) of the earlier report,

$$EI\,\frac{d^2u_1}{dz^2} = \gamma M(\phi_1+\phi_o) - P(u_1+u_o) - k\frac{\ell^2}{\pi^2}u_1$$

As found in previous work the sign before P must be changed so that the effects of M and P are additive in the combined stress expression which will be reached using

$$\frac{d^2u_1}{dz^2} = \frac{\gamma M}{EI}\phi + \frac{P}{EI}u - \frac{k}{EI}\frac{\ell^2}{\pi^2}u_1 \qquad (10)$$

and $$\sigma_{max} = \frac{M}{Z} + \frac{P}{A} + \frac{Eb}{2}\frac{d^2u_1}{dz^2} \qquad (11)$$

To achieve simplicity the last term of (10) must be partitioned into two components when inserting it in (11). Writing β for the denominator of u_1 in (9) the term will be

$$\frac{Eb}{2}\frac{k}{EI}\frac{\ell^2}{\pi^2}u_1 = \frac{Eb}{2}\frac{k}{EI\beta}\frac{\ell^2}{\pi^2}\frac{M}{M_{cr}}\left(\frac{M}{M_{cr}}+1\right)u_o + \frac{Eb}{2}\frac{k}{EI\beta}\frac{\ell^2}{\pi^2}\frac{P}{P_e}\left(1-\frac{P}{P_\phi}\right)u_o$$

In the first term on the right, put

$$u_o = \frac{\ell}{\pi}\frac{C_x}{EI}\phi_o \qquad \text{to give}$$

$$\frac{Eb}{2}\frac{k}{EI}\frac{\ell^2}{\pi^2}u_1 = \frac{Eb}{2}\frac{k}{EI\beta}\frac{\ell^2}{\pi^2}M\frac{\ell}{\pi}\sqrt{\frac{\gamma}{CEI}}\frac{\ell}{\pi}\sqrt{\frac{EX}{EI}}\left(\frac{M}{M_{cr}}+1\right)\phi_o + \frac{Eb}{2}\frac{k}{EI\beta}\frac{\ell^2}{\pi^2}\frac{P\ell^2}{\pi^2 EI}\left(1-\frac{P}{P_\phi}\right)u_o$$

$$= \frac{b}{2}\frac{k}{EI\beta}\frac{\ell^4}{\pi^4}M\frac{\chi 12}{hb^3}\left(\frac{M}{M_{cr}}+1\right)\phi_o + \frac{b}{2}\frac{k}{EI\beta}\frac{\ell^4}{\pi^4}\frac{P12}{hb^3}\left(1-\frac{P}{P_\phi}\right)u_o$$

$$= \left(\frac{P_{cr}}{P_e}-1\right)\frac{M}{Z}\frac{k}{b}\frac{\chi\phi_o}{\beta}\left(\frac{M}{M_{cr}}+1\right) + \left(\frac{P_{cr}}{P_e}-1\right)\frac{6u_o}{b\beta}\frac{P}{kb}\left(1-\frac{P}{P_\phi}\right)$$

$$= \frac{M}{Z}\frac{\eta'}{\beta}\left(\frac{P_{cr}}{P_e}-1\right)\left(\frac{M}{M_{cr}}+1\right) + \frac{\eta}{\beta}\frac{P}{A}\left(\frac{P_{cr}}{P_e}-1\right)\left(1-\frac{P}{P_\phi}\right) \qquad (12)$$

Then inserting the expressions for ϕ, u and u_1 in (10) the whole combined stress expression becomes

$$1 = \frac{\sigma_m}{f_m} + \frac{\sigma_c}{f_c} + \frac{\frac{\sigma_m}{f_m}\eta'\left(1-\frac{P}{P_e}+\frac{M}{M_{cr}}\right) + \frac{\sigma_c}{f_c}\frac{f_c}{f_m}\eta\left(1-\frac{P}{P_\phi}+\frac{M}{M_{cr}}\right)}{\left(\frac{P_{cr}}{P_e}-\frac{P}{P_e}\right)\left(1-\frac{P}{P_\phi}\right)-\frac{M^2}{M_{cr}^2}}$$

or

$$1 = \frac{\sigma_m}{f_m} + \frac{\sigma_c}{f_c} + \frac{\frac{\sigma_m}{f_m}\eta'\left(1-\frac{\sigma_c}{\sigma_{eu}}+\frac{\sigma_m}{\sigma_{cr}}\right) + \frac{\sigma_c}{f_c}\frac{f_c}{f_m}\eta\left(1-\frac{\sigma_c}{\sigma_{tor}}+\frac{\sigma_m}{\sigma_{cr}}\right)}{\left(\frac{P_{cr}}{P_e}-\frac{\sigma_c}{\sigma_{eu}}\right)\left(1-\frac{\sigma_c}{\sigma_{tor}}\right)-\left(\frac{\sigma_m}{\sigma_{cr}}\right)^2} \qquad (13)$$

- to compare with (15) of the earlier report.

The only difference is the insertion of $\frac{P_{cr}}{P_e}$ replacing unity in the denominator.

When P = 0,

$$1 = \frac{\sigma_m}{f_m} + \frac{\frac{\sigma_m}{f_m}\eta'\left(\frac{\sigma_m}{\sigma_{cr}}+1\right)}{\frac{P_{cr}}{P_e}-\left(\frac{\sigma_m}{\sigma_{cr}}\right)^2} \qquad (14)$$

When M = 0,

$$1 = \frac{\sigma_c}{f_c} + \frac{\frac{\sigma_c}{f_c}\frac{f_c}{f_m}\eta}{\frac{P_{cr}}{P_e}-\frac{\sigma_c}{\sigma_{eu}}} \qquad (15)$$

if $1-\frac{\sigma_c}{\sigma_{tor}}$ is cancelled, which may not be permissible.

Plotted relationship with lateral restraint

As in previous work, equation (13) is plotted in Figure 2 by setting values of $\frac{\sigma_c}{f_c}$ then for each value incrementing $\frac{\sigma_m}{f_m}$ in fine steps until the right-hand side exceeds unity. Interpolation between the final and previous values of $\frac{\sigma_m}{f_m}$ gives the result to be plotted for the next point on the curve.

With this form of plotting it is important to establish correct start and finish values on the vertical and horizontal axes for each curve. If (15) is used for values of (13) on the horizontal axis, erratic results are obtained for high $\frac{\ell}{b}$ ratios. The reason is that $\frac{P}{P_\phi}$ becomes limiting rather than $\frac{P}{P_e}$, and as $1 - \frac{\sigma_e}{\sigma_{tor}}$ tends to zero, function (13) approaches a limit where $\frac{\sigma_e}{f_c} = \frac{\sigma_{tor}}{f_c}$ is smaller than the value given by (15). Thus for high $\frac{\ell}{b}$ ratios cancelling $1 - \frac{\sigma_e}{\sigma_{tor}}$ is invalid when putting $\sigma_m = 0$ in (13).

The problem is overcome by selecting the smaller of two finishing values, one calculated from (15) and the other as follows, bearing in mind that I_o is taken about the centre of rotation at a distance below the centroid of

$$R = \frac{u_o}{\phi_o} = \frac{\ell}{\pi}\sqrt{\frac{C\gamma}{EI}}$$

$$\sigma_{tor} = \frac{P_\phi}{A} = \frac{C}{I_o}$$

$$= \frac{C}{\frac{bh^3 + hb^3}{12} + bh\frac{\ell^2}{\pi^2}\frac{C\gamma}{EI}}$$

$$= \frac{1}{\frac{16\times 3(bh^3+hb^3)}{E\times 12\, hb^3\left(1-0.63\frac{b}{h}\right)} + \frac{\ell^2}{\pi^2}\frac{\gamma\cdot 12}{Eb^2}}$$

$$= \frac{E}{4\frac{\left(\frac{h}{b}\right)^2+1}{1-0.63\frac{b}{h}} + \frac{12\gamma}{\pi^2}\left(\frac{\ell}{b}\right)^2}$$

Finishing values of $\frac{\sigma_e}{f_c} = \frac{\sigma_{tor}}{f_c}$ when torsional buckling is critical are given by

$$\frac{\sigma_e}{f_c} = \frac{\frac{E}{f_c}}{4\frac{\left(\frac{h}{b}\right)^2+1}{1-0.63\frac{b}{h}} + \frac{12\gamma}{\pi^2}\left(\frac{\ell}{b}\right)^2} \qquad (16)$$

In Figure 2, which is plotted for $\frac{h}{b} = 8$ and $k = 0.0005$ N/mm^2, the changeover between the two limiting conditions occurs between $\frac{\ell}{b} = 120$ and $\frac{\ell}{b} = 130$. Higher values of k make it occur at lower $\frac{\ell}{b}$ ratios because if the column is more heavily restrained against lateral buckling there will be a greater tendency for torsion to become the limiting condition.

AGREEMENT WITH EXTENDED PERRY-ROBERTSON FORMULA

It is stated in the introduction that the solution found for M = 0 is the same as that produced using the formula for the design of columns with lateral load when taken to negative values for the applied bending stress σ_m. This will be demonstrated algebraically but is true only if torsion is not the governing factor. However it is valid for ordinary column applications where there is an initial curvature but no initial twist.

Algebraic demonstration

In the work leading to (13) the last term in (10) was partitioned into two components. If this is not done, the following more complicated combined stress expression is reached:

$$1 = \frac{\sigma_m}{f_m} + \frac{\sigma_c}{f_c} + \frac{\frac{\sigma_m}{f_m}\eta'\left(\frac{\sigma_m}{\sigma_{cr}}\frac{P_{cr}}{P_e} + \frac{P_{cr}}{P_e} - \frac{\sigma_c}{\sigma_{eu}}\right) + \frac{\sigma_c}{f_c}\frac{f_c}{f_m}\eta\left\{\frac{P_{cr}}{P_e}\left(1-\frac{\sigma_c}{\sigma_{tor}}\right) + \frac{\sigma_m}{\sigma_{cr}}\right\} + \frac{\sigma_r}{f_m}\left\{\left(\frac{\sigma_m}{\sigma_{cr}}\right)^2 + \frac{\sigma_c}{\sigma_{eu}}\left(1-\frac{\sigma_c}{\sigma_{tor}}\right) + \frac{\sigma_m}{\sigma_{cr}}\right\}}{\left(\frac{P_{cr}}{P_e} - \frac{\sigma_c}{\sigma_{eu}}\right)\left(1-\frac{\sigma_c}{\sigma_{tor}}\right) - \left(\frac{\sigma_m}{\sigma_{cr}}\right)^2}$$

When M = 0, if $(1-\frac{\sigma_c}{\sigma_{tor}})$ is cancelled

$$1 = \frac{\sigma_c}{f_c} + \frac{\frac{\sigma_c}{f_c}\frac{f_c}{f_m}\eta\frac{P_{cr}}{P_e} - \frac{\sigma_r}{f_m}\frac{\sigma_c}{\sigma_{eu}}}{\frac{P_{cr}}{P_e} - \frac{\sigma_c}{\sigma_{eu}}} \qquad (17)$$

In these expressions

$$\frac{\sigma_r}{f_m} = \frac{6k}{hb^2}\frac{\ell^2}{\pi^2}\frac{u_e}{f_m} \qquad (18)$$

where the portion $\frac{6k}{hb^2}\frac{\ell^2}{\pi^2}$ is the bending stress set up per unit of central deflection by the elastic lateral restraint.

Then $$\frac{\sigma_r}{f_m}\frac{\sigma_c}{\sigma_{eu}} = \frac{6k}{hb^2}\frac{\ell^2}{\pi^2}\frac{u_e}{f_m}\frac{P\ell^2}{\pi^2 E I} = \frac{k}{EI}\frac{\ell^4}{\pi^4}\frac{6}{b}\frac{P}{A}\frac{u_e}{f_m}$$

$$= \left(\frac{P_{cr}}{P_e} - 1\right)\frac{\sigma_c}{f_m}\eta \qquad (19)$$

The extended Perry-Robertson formula allowing for stress due to lateral load σ_m, when σ_m is inserted as negative to become a stress due to restraint load, has the basis

$$1 = \frac{\sigma_c}{f_c} + \frac{\frac{\sigma_c}{f_c}\frac{f_c}{f_m}\eta - \frac{\sigma_m}{f_m}}{1 - \frac{\sigma_c}{\sigma_{eu}}} \qquad (20)$$

From (17), the value of the restraint stress ratio built up under end load alone is

$$\frac{\sigma_m}{f_m} = \frac{\frac{\sigma_r}{f_m}\frac{\sigma_c}{\sigma_{eu}}}{\frac{P_{cr}}{P_e} - \frac{\sigma_c}{\sigma_{eu}}} \qquad (21)$$

Inserting this in (20) gives

$$1 = \frac{\sigma_c}{f_c} + \frac{\frac{\sigma_c}{f_m}\eta}{1-\frac{\sigma_c}{\sigma_{eu}}} - \frac{\frac{\sigma_r}{f_m}\frac{\sigma_c}{\sigma_{eu}}}{\left(1-\frac{\sigma_c}{\sigma_{eu}}\right)\left(\frac{P_{cr}}{P_e}-\frac{\sigma_c}{\sigma_{eu}}\right)}$$

$$= \frac{\sigma_c}{f_c} + \frac{\frac{\sigma_c}{f_m}\eta\left(\frac{P_{cr}}{P_e}-\frac{\sigma_c}{\sigma_{eu}}\right) - \frac{\sigma_r}{f_m}\frac{\sigma_c}{\sigma_{eu}}}{\left(1-\frac{\sigma_c}{\sigma_{eu}}\right)\left(\frac{P_{cr}}{P_e}-\frac{\sigma_c}{\sigma_{eu}}\right)}$$

Substituting for $\frac{\sigma_r}{f_m}\frac{\sigma_c}{\sigma_{eu}}$ from (19),

$$1 = \frac{\sigma_c}{f_c} + \frac{\frac{\sigma_c}{f_m}\eta\left(\frac{P_{cr}}{P_e}-\frac{\sigma_c}{\sigma_{eu}}\right) - \left(\frac{P_{cr}}{P_e}-1\right)\frac{\sigma_c}{f_m}\eta}{\left(1-\frac{\sigma_c}{\sigma_{eu}}\right)\left(\frac{P_{cr}}{P_e}-\frac{\sigma_c}{\sigma_{eu}}\right)}$$

giving

$$1 = \frac{\sigma_c}{f_c} + \frac{\frac{\sigma_c}{f_m}\eta}{\frac{P_{cr}}{P_e}-\frac{\sigma_c}{\sigma_{eu}}} \qquad (22)$$

which is the same as (15). Thus the Perry-Robertson formula when extended into the region where σ_m is negative, i.e. applied to the initially convex face of the column, does give the same result as the theory for beam-columns with lateral restraint when M = 0.

Design calculations

If σ_c is given, k may easily be found from (15) using (2).

If k is known (15) may be solved for σ_c to give

$$\frac{\sigma_m}{f_m} = \frac{1}{2} + \frac{1}{2}\left(\frac{P_{cr}}{P_e}+\frac{f_c}{f_m}\eta\right)\frac{\sigma_{eu}}{f_c} - \sqrt{\left\{\frac{1}{2}+\frac{1}{2}\left(\frac{P_{cr}}{P_e}+\frac{f_c}{f_m}\eta\right)\frac{\sigma_{eu}}{f_c}\right\}^2 - \frac{P_{cr}}{P_e}\frac{\sigma_{eu}}{f_c}} \qquad (23)$$

Equations (15) and (23) for limiting the stress ratio summation to unity are closely comparable with the well-known formulae for unrestrained columns. However they are of limited practical use because with high ℓ/b ratios and the very low restraint appropriate to first mode buckling, deflection rather than combined stress will be the limitation and the formulae in the earlier report (Burgess, 1982) will be needed.

Equations (15) and (23) may be applied for higher buckling modes but then behaviour in the unrestrained direction gains importance and a further term must be included in the stress ratio summation as shown in a separate paper (Burgess, 1988).

References

Brüninghoff, H.(1983) - Determination of bracing structures for compression members and beams. CIB-W18 paper No. 16-15-1, Lillehammer, May/June 1983.

Brüninghoff, H.(1984) - Proposal for Chapter 7.4, Bracing. CIB-W18 paper No. 17-15-1, Rapperswil, May 1984.

Brüninghoff, H.(1985) - Stabilizing bracings. CIB-W18 paper No. 18-15-2, Beit Oren, June 1985.

Burgess, H.J.(1982) - Bracing calculations for trussed rafter roofs. CIB-W18 paper No. 15-14-3, Karlsrühe, June 1982.

Burgess, H.J.(1987) - Lateral buckling theory for rectangular section deep beam-columns. CIB-W18A paper No. 20-2-1, Dublin, September 1987.

Burgess, H.J.(1988) - Buckling modes and permissible axial loads for continuously braced columns. CIB-W18A paper No. 21-15-2, Vancouver, September 1988.

Timoshenko, S.P. and Gere, J.M. (1961) - Theory of elastic stability, 2nd edition, McGraw-Hill, London 1961.

Winter, G (1958) - Lateral bracing of columns and beams. Jl. Struct. Div., ASCE, Paper 1561, March 1958.

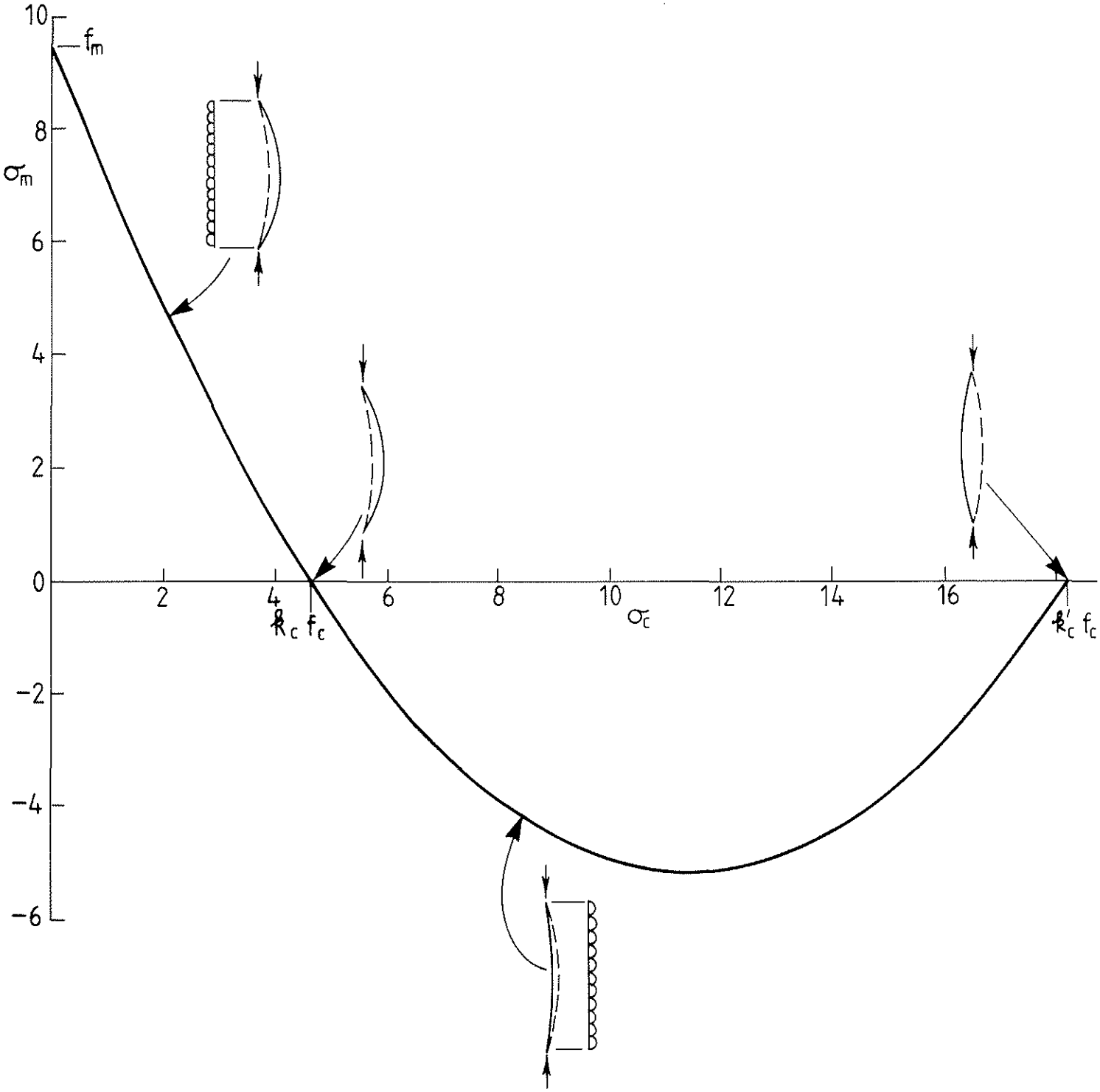

Fig. 1

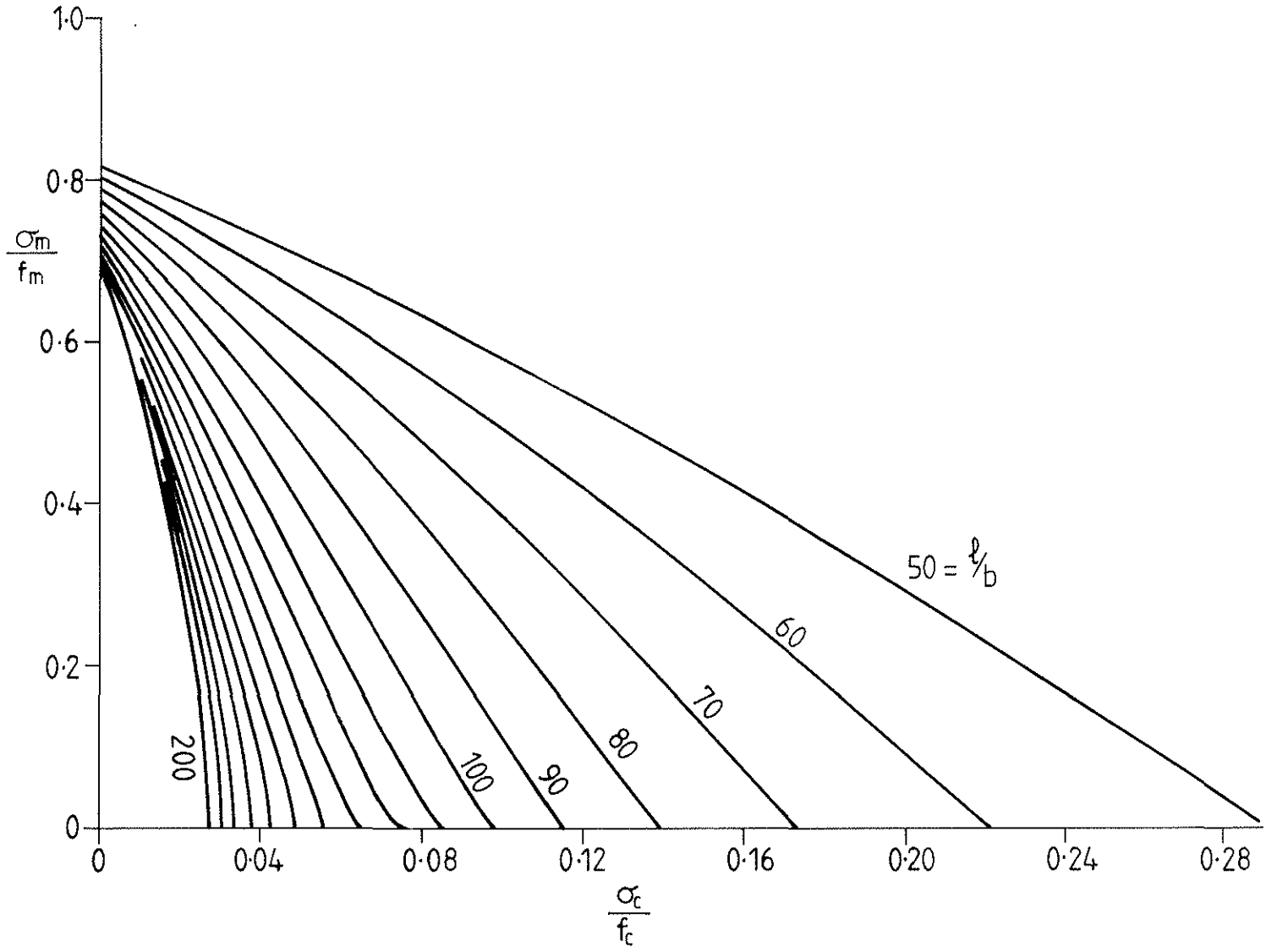
1·0
0·8
$\frac{\sigma_m}{f_m}$
0·6
0·4
0·2
0
0
0·04
0·08
0·12
0·16
0·20
0·24
0·28
$\frac{\sigma_c}{f_c}$
50 = $\frac{\ell}{b}$
60
70
80
90
100
200

Fig. 2

CIB-W18A/21-15-2

INTERNATIONAL COUNCIL FOR BUILDING RESEARCH STUDIES AND DOCUMENTATION

WORKING COMMISSION W18A - TIMBER STRUCTURES

BUCKLING MODES AND PERMISSIBLE AXIAL LOADS FOR CONTINUOUSLY BRACED COLUMNS

by

H J Burgess
Timber Research and Development Association
United Kingdom

MEETING TWENTY-ONE
PARKSVILLE, VANCOUVER ISLAND
CANADA
SEPTEMBER 1988

CONTENTS

BUCKLING MODES AND PERMISSIBLE AXIAL LOADS FOR CONTINUOUSLY BRACED COLUMNS

A separate report (Burgess, 1988) examines the limitation of combined stress in braced columns buckling in a single half-wave. When dealing with buckling modes higher than the first, it will be assumed that the initial shape of the column is sinusoidal in each half-wave but with the direction of curvature reversing in each successive half-wave. For example when considering the second mode the initial shape is taken as two half waves forming an S-shape.

When considering the restraint modulus at mode boundaries, the values relating to ideal columns are used, supporting the general approach adopted by Winter (1958) for initial imperfections of the type assumed. However when exploring methods of simplifying the design method it will be an advantage to know also the restraint modulus at which the maximum compressive stress becomes equal in adjacent modes, and the following work will calculate the appropriate figures.

LIMITATION OF COMBINED STRESS

Mode changeover values

Equation (15) of the separate report appears as follows except that $\frac{P_{cr}}{P_e}$ is here replaced by $\frac{\sigma_{cr}}{\sigma_{eu}}$ using σ_{cr} as the critical end stress for a braced ideal column*.

$$1 = \frac{\sigma_c}{f_c} + \frac{\frac{\sigma_c}{f_m}\eta}{\frac{\sigma_{cr}}{\sigma_{eu}} - \frac{\sigma_c}{\sigma_{eu}}} \qquad (1)$$

where σ_{cr}, σ_{eu} and η had appropriate values for the single half-wave. The calculations which follow will adopt the practice applied by Timoshenko & Gere (1961) for ideal columns, and these three symbols will have values based on the full length L of the column. Then equation (1) for n half-waves will become

$$1 = \frac{\sigma_c}{f_c} + \frac{\frac{\sigma_c}{f_m}\frac{\eta}{n}}{\frac{\sigma_{cr}}{n^2\sigma_{eu}} - \frac{\sigma_c}{n^2\sigma_{eu}}}$$

or

$$1 = \frac{\sigma_c}{f_c} + \frac{\frac{\sigma_c}{f_m}\frac{\eta}{n}}{1 + \frac{k}{EI}\frac{L^4}{n^4\pi^4} - \frac{\sigma_c}{n^2\sigma_{eu}}} \qquad (2)$$

The number of half-waves is expressed by n for the calculations relating to stress limitation but m will be used in expressions for `ideal` columns and the limitation of deflection. The reason for this will become clear later.

---

*NOTE: In a previous report (Burgess, 1987) the symbol σ_{cr} was used for the critical bending stress of an ideal deep beam loaded by equal end moments. In the present paper the only critical stress values are σ_{eu} for an unbraced ideal column and σ_{cr} for a continuously braced ideal column.

If the restraint modulus is increased in a given mode it will reach a value where the maximum compressive stress is the same as that calculated for the next higher mode, using the same modulus. To calculate the changeover value of the restraint modulus k, the value of σ_c will first be found by eliminating k from (2) and from the corresponding equation for mode (n+1), and then k may be found from (2) using the calculated value of σ_c.

From (2),

$$k = \left(\frac{n\pi}{L}\right)^4 EI \left[\frac{\frac{\sigma_c}{f_m}\frac{\eta}{n}}{1-\frac{\sigma_c}{f_c}} + \frac{1}{n^2}\frac{\sigma_c}{\sigma_{eu}} - 1 \right] \qquad (3)$$

For mode (n+1), replacing n by (n+1) in (2) and again solving for k gives

$$k = \left\{\frac{(n+1)\pi}{L}\right\}^4 EI \left[\frac{\frac{\sigma_c}{f_m}\frac{\eta}{(n+1)}}{1-\frac{\sigma_c}{f_c}} + \frac{1}{(n+1)^2}\frac{\sigma_c}{\sigma_{eu}} - 1 \right] \qquad (4)$$

Equating (3) and (4) gives

$$\frac{\sigma_c}{f_c} = T \pm \sqrt{T^2 - (2n^2+2n+1)\frac{\sigma_{eu}}{f_c}} \qquad (5)$$

in which $$T = \frac{1}{2}\left\{\frac{3n^2+3n+1}{2n+1}\frac{\sigma_{eu}}{f_m}\eta + 1 + (2n^2+2n+1)\frac{\sigma_{eu}}{f_c}\right\}$$

Inserting the values of σ_{eu} and η and taking the negative root,

for n = 1, $\frac{\sigma_c}{f_c}$ = 0.1327 for change from 1st to 2nd mode

and for n = 2, $\frac{\sigma_c}{f_c}$ = 0.2856 for change from 2nd to 3rd mode

Similarly the value of $\frac{\sigma_c}{f_c}$ for the changeover from any mode n to mode n+1 may be found by inserting the appropriate value for n in (5).

The corresponding value of k is then found from (3), giving

for n = 1, k = 0.002202 compared with 0.0025975 for the ideal column

for n = 2, k = 0.01780 compared with 0.02338 for the ideal column

For higher modes, $\frac{\sigma_c}{f_c}$ is shown plotted against $\frac{k}{\sigma_{eu}}$ in the lower curve of Figure 1. The higher curve is for ideal columns, considered later.

For plotting, equation (3) is expressed in the form

$$\frac{k}{\sigma_{eu}} = n^4\pi^2\frac{h}{b}\left(\frac{b}{L}\right)^2 \left[\frac{\frac{\sigma_c}{f_m}\frac{\eta}{n}}{1-\frac{\sigma_c}{f_c}} + \frac{1}{n^2}\frac{\sigma_c}{\sigma_{eu}} - 1 \right] \qquad (6)$$

Intermediate values

Values of $\frac{\sigma_c}{f_c}$ as k varies within a given mode may be found from (2) by inserting values for k which are intermediate between those at the upper and lower ends of the mode concerned.

Writing $$\frac{\sigma_{cr}}{n^2\sigma_{eu}} = 1 + \frac{k}{EI}\frac{L^4}{n^4\pi^4} \tag{7}$$

in (2) gives

$$1 = \frac{\sigma_c}{f_c} + \frac{\frac{\sigma_c}{f_m}\frac{\eta}{n}}{\frac{\sigma_{cr}}{n^2\sigma_{eu}} - \frac{\sigma_c}{n^2\sigma_{eu}}} \tag{8}$$

Solving for $\frac{\sigma_c}{f_c}$,

$$\frac{\sigma_c}{f_c} = \tfrac{1}{2}\left(1 + \frac{\sigma_{cr}}{f_c} + n\frac{\sigma_{eu}}{f_m}\eta\right) \pm \sqrt{\left\{\tfrac{1}{2}\left(1 + \frac{\sigma_{cr}}{f_c} + n\frac{\sigma_{eu}}{f_m}\eta\right)\right\}^2 - \frac{\sigma_{cr}}{f_c}} \tag{9}$$

For insertion in this expression for a given value of L/b and h/b, $\frac{\sigma_{cr}}{f_c}$ is found as follows.

$$\frac{\sigma_{cr}}{n^2\sigma_{eu}} = 1 + \frac{k}{EI}\left(\frac{L}{n\pi}\right)^4$$

$$= 1 + \frac{k}{\sigma_{eu}}\frac{(L/b)^2}{n^4\pi^2}\left(\frac{b}{h}\right) \tag{10}$$

$$\text{Then } \frac{\sigma_{cr}}{f_c} = \frac{\sigma_{cr}}{\sigma_{eu}}\frac{\sigma_{eu}}{f_c} = n^2\left\{1 + \frac{k}{\sigma_{eu}}\frac{(L/b)^2}{n^4\pi^2}\left(\frac{b}{h}\right)\right\}\frac{\sigma_{eu}}{f_c}$$

and for plotting in Figure 1 the appropriate value of $\frac{k}{\sigma_{eu}}$ is used rather than k.

The curved lines plotted for a given mode diverge very little from a straight line joining the mode changeover points at each end of the mode. For this particular L/b ratio (L/b = 8), $\frac{\sigma_c}{f_c}$ may be approximated very closely and on the conservative side by linear interpolation between the end points.

Graph without initial imperfections

The upper graph in Figure 1 gives the results of similar calculations for the ideal column, showing the large differences that occur at higher modes.

As given by Timoshenko & Gere (1961), for mode m

$$P = \frac{\pi^2 EI}{L^2}\left(m^2 + \frac{kL^4}{m^2\pi^4 EI}\right) \tag{11}$$

giving $$k = \frac{m^2\pi^4 EI}{L^4}\left(\frac{PL^2}{\pi^2 EI} - m^2\right) \tag{12}$$

and for mode (m+1)

$$P = \frac{\pi^2 EI}{L^2}\left\{(m+1)^2 + \frac{k L^4}{(m+1)^2 \pi^4 EI}\right\} \tag{13}$$

giving

$$k = \frac{(m+1)^2 \pi^4 EI}{L^4}\left\{\frac{PL^2}{\pi^2 EI} - (m+1)^2\right\} \tag{14}$$

Equating the two values of k leads to

$$P = \left(2m^2 + 2m + 1\right)\frac{\pi^2 EI}{L^2}$$

or

$$\frac{\sigma_c}{f_c} = \left(2m^2 + 2m + 1\right)\frac{\sigma_{eu}}{f_c} \tag{15}$$

for the changeover points, and k may be found by inserting in (12) the value of $\frac{\sigma_c}{f_c}$ found from (15) to give

$$\frac{k}{\sigma_{eu}} = m^2(m+1)^2 \frac{k}{b}\frac{\pi^2}{(h/b)^2} \tag{16}$$

Intermediate results

Putting $\eta = 0$ in (9) gives after some manipulation

$$\frac{\sigma_c}{f_c} = \frac{1}{2}\left(1 + \frac{\sigma_{cr}}{f_c}\right) \pm \sqrt{\frac{1}{4}\left(1 - \frac{\sigma_{cr}}{f_c}\right)^2} \tag{17}$$

$$= \frac{1}{2}\left(1 + \frac{\sigma_{cr}}{f_c}\right) \pm \frac{1}{2}\left(1 - \frac{\sigma_{cr}}{f_c}\right) \tag{18}$$

$$= 1 \quad \text{or} \quad \frac{\sigma_{cr}}{f_c} \tag{19}$$

where

$$\frac{\sigma_{cr}}{f_c} = m^2\left(1 + \frac{k L^4}{m^4 \pi^4 EI}\right)\frac{\sigma_{eu}}{f_c}$$

Alternatively from (11)

$$P = \frac{\pi^2 EI}{L^2} m^2\left(1 + \frac{k L^4}{m^4 \pi^4 EI}\right) = \frac{\pi^2 EI}{L^2}\frac{\sigma_{cr}}{\sigma_{eu}}$$

$$\sigma_c = \sigma_{eu}\frac{\sigma_{cr}}{\sigma_{eu}}$$

$$\frac{\sigma_c}{f_c} = \frac{\sigma_{cr}}{f_c} \tag{20}$$

(7) shows that $\frac{\sigma_{cr}}{\sigma_{eu}}$ varies linearly with k for a given mode, so from (20)

$$\frac{\sigma_c}{f_c} = \frac{\sigma_{cr}}{f_c} = \frac{\sigma_{cr}}{\sigma_{eu}}\frac{\sigma_{eu}}{f_c} \tag{21}$$

also varies linearly.

LIMITATION OF DEFLECTION

The above development considered only the limitation of combined stress, disregarding the possibility of excessive deflection. To consider deflection in isolation, without reference to combined stress, use will be made of equation (9) of the previous report (Burgess, 1988) which gave the additional central deflection u_1 of a column under end load P as

$$u_1 = \frac{\frac{P}{P_e}}{\frac{P_{cr}}{P_e} - \frac{P}{P_e}} \, u_o \qquad (23)$$

If u_1 is limited to a fraction t of the mode length ℓ, for example if $t = 0.003\ell$, then from (23)

$$t = \frac{u_o}{\ell} \times \frac{\frac{\sigma_c}{\sigma_{eu}}}{\frac{\sigma_{cr}}{\sigma_{eu}} - \frac{\sigma_c}{\sigma_{eu}}} \qquad (24)$$

or transposing

$$\frac{\sigma_c}{\sigma_{eu}} = \frac{\frac{t\ell}{u_o}\frac{\sigma_{cr}}{\sigma_{eu}}}{1 + \frac{t\ell}{u_o}} \qquad (25)$$

The values σ_{cr} and σ_{eu} were based on the mode length. If these symbols are changed to refer to the full length L, and taking

$$\frac{u_o}{\ell} = \frac{0.005}{\sqrt{3}} = 0.002887$$

as in the previous report, then (25) becomes

$$\frac{\sigma_c}{m^2\sigma_{eu}} = 0.5096\left\{1 + \frac{k}{EI}\left(\frac{L}{m\pi}\right)^4\right\} \qquad (26)$$

$$\text{or} \quad \frac{\sigma_c}{f_c} = \frac{\sigma_c}{\sigma_{eu}}\frac{\sigma_{eu}}{f_c} = 0.5096\left\{1 + \frac{k}{EI}\left(\frac{L}{m\pi}\right)^4\right\} m^2\frac{\sigma_{eu}}{f_c} \qquad (27)$$

for mode m, where σ_{eu} refers to the full length L.

From (27)

$$k = \left(\frac{\frac{\sigma_c}{f_c}}{0.5096\, m^2 \frac{\sigma_{eu}}{f_c}} - 1\right) EI\left(\frac{m\pi}{L}\right)^4 \qquad (28)$$

A similar expression is obtained by replacing m by m+1 and equating the two expressions for k gives

$$\frac{\sigma_c}{f_c} = 0.5096\left(2m^2 + 2m + 1\right)\frac{\sigma_{eu}}{f_c} \qquad (29)$$

Comparing this with (15) for the ideal column it is seen that the deflection-governed values of $\frac{\sigma_c}{f_c}$ are 0.5096 times those for the ideal column.

Putting $\frac{\sigma_c}{f_c}$ from (29) into (28) gives

$$k = m^2(m+1)^2 E I \frac{\pi^4}{L^4}$$

$$\text{or} \quad k = m^2(m+1)^2 E \frac{h}{b} \frac{\pi^4}{12} \left(\frac{b}{L}\right)^4$$

$$\text{i.e.} \quad \frac{k}{\sigma_{eu}} = m^2(m+1)^2 \frac{h}{b} \frac{\pi^2}{(L/b)^2} \qquad (30)$$

Alternatively k may be found directly by equating the two σ_c values from (27) as it stands and from (27) with m replaced by m+1.

The expression for $\frac{k}{\sigma_{eu}}$ is identical with equation (16) giving the boundary values for a column with no initial imperfections, and again it is clear that the graph for $\frac{\sigma_c}{f_c}$ against $\frac{k}{\sigma_{eu}}$ may be derived from the top graph in Figure 1 by multiplying its ordinates by 0.5096.

Figure 2 shows the graphs for the strength and deflection limitations for a column with initial sinusoidal curvature as defined earlier, taking $u_o = 0.002887\ell$ in each mode together with a deflection limitation $t = 0.003\ell$ in each mode.

BUCKLING IN STIFF DIRECTION

As mentioned in the companion report (Burgess, 1988) bracing against deflection in the less-stiff direction makes it necessary to allow for the stress set up by stiff-direction bending (see Figure 3). To include this in the strength plot of Figure 2, equation (2) is modified to

$$1 = \frac{\sigma_c}{f_c} + \frac{\frac{\sigma_c}{f_m}\eta''}{1 - \frac{1{\cdot}5\,\sigma_c}{\sigma_{eu,x}}} + \frac{\frac{\sigma_c}{f_m}\eta_r}{\frac{\sigma_{cr}}{n^2\sigma_{eu}} - \frac{\sigma_c}{n^2\sigma_{eu}}} \qquad (32)$$

The figure 1.5 has been inserted so that the solution with full restraint against lateral buckling will be the same as in ordinary design calculations. The plotting program also makes allowance for a term $\frac{f_c}{f_m}$ deriving from

$$\frac{\sigma_c}{f_m}\eta'' = \frac{\sigma_c}{f_c}\frac{f_c}{f_m}\eta''$$

This is so that the plotted results will be exactly comparable with a design calculation ignoring the effect of distortion in the less-stiff direction. The design calculation is based on the equation.

$$1 = \frac{\sigma_c}{f_c} + \frac{\frac{\sigma_c}{f_c}\frac{f_c}{f_m}\eta''}{1 - \frac{1{\cdot}5\,\sigma_c}{\sigma_{eu,x}}}$$

The solution of this equation given as a Perry-Robertson formula in Appendix C of BS 5268 : Part 2 takes $\frac{f_c}{f_m}$ as unity.

The strength curve in Figure 2 for $\frac{h}{b} = 8$ is shown in Figure 4 with lower curves showing the drop in permissible $\frac{\sigma_c}{f_c}$ values when equation (32) is applied. The mode limits for $\frac{k}{\sigma_{eu}}$ are taken as the same as for Figure 2 although this is not strictly correct. Figure 4 shows that the effect of stiff direction buckling is negligible in the first and second modes but becomes very severe in higher modes. The diagram is really valid only for the odd modes 1,3,5..... because the maximum stress due to single mode buckling is added to the maximum due to lateral buckling as though both occurred at the same cross-section, which is only true for odd mode lateral buckling such as the fifth mode shown in Figure 3.

Figure 4 also includes the results for $\frac{h}{b} = 4$. The mode boundary values for $\frac{\sigma_c}{f_c}$ are the same as for $\frac{h}{b} = 8$, as may be seen from equation (5), but equation (6) shows that the mode boundary values for $\frac{k}{\sigma_{eu}}$ are proportional to $\frac{h}{b}$. Thus the plotted boundary values of $\frac{k}{\sigma_{eu}}$ for $\frac{h}{b} = 4$ are halved compared with those for $\frac{h}{b} = 8$ in Figure 4.

The upper lines for $\frac{h}{b} = 4$ and 8 may be brought into coincidence by plotting against $\frac{k}{\sigma_{eu}}\frac{b}{h}$ instead of $\frac{k}{\sigma_{eu}}$. This is done in Figure 5 showing a range of curves for $\frac{h}{b} = 2,4,6$ and 8, together with the top strength curve showing mode boundaries when stiff-direction buckling is disregarded. The interruptions in the four curves taking account of stiff-direction buckling show that the mode boundaries are somewhat different with this effect included, but the interrupted curves are adequate for present purposes.

The curve for lateral deflection limitation is also shown, and at the right of each strength curve a short horizontal line is added to indicate the value of $\frac{\sigma_e}{f_c}$ that would be found in an ordinary design calculation for stiff-direction buckling. For $\frac{h}{b}$ = 6 and 8, lateral buckling causes a severe drop in the permissible axial load for modes up to the sixth. For $\frac{h}{b}$ = 4 the reduction is only small and for $\frac{h}{b}$ = 2 it is not detectable.

For $\frac{h}{b}$ = 6 and 8, the lateral deflection limitation would require bracing to mode 4. For $\frac{h}{b}$ = 4, mode 3 would be required. The position is not clear for $\frac{h}{b}$ = 2, which will require plotting to a larger scale, but evidently the necessary restraint modulus is very low.

Variation of L/b

The graphs in Figure 5 for L/b = 180 and h/b = 8 are repeated in Figure 6 together with similar lines for L/b = 108 and h/b = 8.

The value 108 is chosen as three-fifths of 180 so that it may be taken as applying to the central three half-waves in Figure 3. The third mode of the `length` 108 should behave in the same way as the fifth mode of `length` 180 if the end load and restraint modulus are the same for both. That is, the central half-wave of either should be governed by the same limitations of combined stress and deflection, and it should be possible to plot end stress against restraint modulus in such a way that coincidence is obtained between the third mode of the plot for L/b = 108 and the fifth mode of that for L/b = 180.

This is not achieved in Figure 6 because the base values $\frac{h}{\sigma_{eu}}\frac{b}{f_h}$ incorporate σ_{eu} which varies for different L/b values. To obtain the desired coincidence, the same graphs are plotted in Figure 7 on a base showing $\frac{h}{f_e}\frac{b}{f_h}$. The `180` graph with intersection points shown by crosses coincides in its fifth mode with the third mode of the `108` graph marked by circles for the intersection points.

At the same time, the dropped lines allowing for stiff direction buckling are brought into near-coincidence by using h/b = 8 for L/b = 180 and h/b = 4.8 for L/b = 108 so that L/h = 22.5 in both cases and the short horizontal line for the standard stiff-direction buckling calculation is applicable to both.

Deflection graphs have been added in Figure 8, which is otherwise the same as Figure 7, and the desired coincidence is obtained for deflection also.

Figure 5 for L/b = 180 showed graphs allowing for stiff-direction buckling for h/b = 8,6,4 and 2. In Figures 7 and 8 the only dropped graphs shown are for h/b = 8 when L/b = 180 or h/b = 4.8 when L/b = 108.

Figure 9 is an enlarged plot for h/b = 4,3 and 2 when L/b = 180 or three-fifths (0.6) of these values when L/b = 108. This shows that for the most commonly-used sections the curves for L/b = 180 and 108 can be taken as concurrent if the bracing stiffness is such that lateral deflection is limited to 0.003 times the mode length, and the permissible value of $\frac{\sigma_e}{f_c}$ even for h/b = 4 (with L/b = 180) is only slightly below that shown by the short horizontal line for stiff-direction buckling as calculated by the conventional method. This has been mentioned in connection with Figure 5, which shows that for still deeper sections lateral buckling causes a severe drop in the permissible end stress as calculated conventionally unless the restraint modulus is very high.

For timber sections of the common size range, Figure 9 gives a basis allowing design aids to be developed which could make provision for the quite small reductions caused by lateral buckling. This is indicated in Figure 10 showing intermediate h/b values for the two L/b ratios considered. Since lines for these widely different ratios are found to coincide for practical purposes it may be supposed that the same will apply to other ratios within the range.

In Figure 10 the discontinuities at mode boundaries which appear in Figure 5 have been eliminated. The formula limiting combined stress is given by (32). A similar formula but with n replaced by (n+1) will apply to mode (n+1), and subtracting the two leads to

$$\frac{\sigma_c}{f_c} = \left(\frac{k}{f_c}\frac{b}{h}\right)\left(\frac{L/b}{\pi}\right)^2 \left\{\frac{3n^2+3n+1}{n^2(n+1)^2}\right\} - n(n+1)\frac{\sigma_{eu}}{f_c} \qquad (33)$$

When plotting $\frac{\sigma_c}{f_c}$ on a base of $\frac{k}{f_c}\frac{b}{h}$ from (32) for mode n, plotting continues for increments of $\frac{k}{f_c}\frac{b}{h}$ until $\frac{\sigma_c}{f_c}$ is found to have a value less than the right-hand side of (33). For the next (higher) mode, plotting is started at a value of $\frac{k}{f_c}\frac{b}{h}$ one increment less than the terminating value for the previous mode.

WINTER'S METHOD

The study of columns by Winter (1958) starts with an analysis of discretely braced columns, finding the expression

$$k_{req} = k_{id}\left(\frac{d_o}{d} + 1\right) \tag{34}$$

for the required stiffness of the brace. d_o is the initial central deflection and d is the acceptable further deflection under load. k_{id} takes the value for ideal columns given by

No. of braces	1	2	3	4
k_{id}	$\frac{2P_e}{L}$	$\frac{3P_e}{L}$	$\frac{3.41P_e}{L}$	$\frac{3.63P_e}{L}$

where P_e is the Euler load for the free length between braces.

For the columns with continuous elastic restraint considered above, Winter assumes without proof that the similar relation

$$\beta_{req} = \beta_{id}\left(\frac{d_o}{d} + 1\right)$$

will apply. β_{req} is the particular value of the restraint modulus k which is required to support buckling in the mode corresponding to β_{id} for the ideal column, without d exceeding the additional deflection which is allowed.

The expression is reminiscent of equation (25) above for limiting deflection. If $t\ell$ is replaced by d and u_o is replaced by d_o, this becomes

$$\frac{\sigma_c}{\sigma_{cr}} = \frac{\frac{\sigma_{cr}}{\sigma_{cr}}}{\frac{d_o}{d} + 1}$$

but this is a relationship showing the limitation of σ_c as a proportion of σ_{cr} if the additional deflection d is not to be exceeded, and is not a relation between restraint moduli for columns with and without initial imperfections.

Restraint values achieving the object of limiting the deflection without consideration of combined stress may be found from a pair of curves such as the upper curve of Figure 1 (for the ideal column) and the upper curve of Figure 2 (for a column with initial imperfections in the same form as the buckled shape). Curves of this kind, which are actually formed from straight-line segments, are shown in Figure 11. The object will be to find the restraint modulus from the upper curve for a given value of $\frac{\sigma_c}{f_c}$, then the modulus required to obtain the same value of $\frac{\sigma_c}{f_c}$ for the lower curve. The ratio of the two moduli gives the figure by which the restraint modulus for the ideal column must be multiplied in order to restrain the column with imperfections under the same end load.

The necessary calculation is made in the computer program associated with Figure 11, for values of $\frac{k}{f_c}\frac{b}{h}$ which are incremented in steps. At each step the corresponding value of $\frac{\sigma_c}{f_c}$ is first found from the upper curve using equations (10) and (20). Equation (10) gives

$$\frac{\sigma_{cr}}{f_c} = \frac{\sigma_{cr}}{\sigma_{eu}}\frac{\sigma_{eu}}{f_c} = m^2\left\{\frac{\sigma_{eu}}{f_c} + \left(\frac{k}{f_c}\frac{b}{h}\right)\frac{(l/b)^2}{m^4\pi^4}\right\}$$

and from equation (20)

$$\frac{\sigma_c}{f_c} = \frac{\sigma_{cr}}{f_c}$$

The appropriate value of m is established by using the mode limits calculated for $\frac{k}{f_c}\frac{b}{h}$ when plotting the crosses shown in the diagram.

Using this value of $\frac{\sigma_c}{f_c}$, the corresponding value of $\frac{k'}{f_c}\frac{b}{h}$ on the lower curve, generally in a higher mode, is found from (27) which is

$$\frac{\sigma_c}{f_c} = 0.5096\left\{1+\frac{k'}{EI}\left(\frac{l}{m\pi}\right)^4\right\}m^2\frac{\sigma_{eu}}{f_c}$$

$$= 0.5096\,\frac{\sigma_{cr}}{m^2\sigma_{eu}}\,m^2\frac{\sigma_{eu}}{f_c}$$

so $$\frac{\sigma_{cr}}{f_c} = \frac{\sigma_c}{f_c}\times\frac{1}{0.5096}$$

Having found $\frac{\sigma_{cr}}{m^2 f_c} = \frac{\sigma_{eu}}{f_c} + \frac{k'}{EI}\frac{l^4}{m^4\pi^4}\frac{\sigma_{eu}}{f_c} = \frac{\sigma_{eu}}{f_c} + \left(\frac{k'}{f_c}\frac{b}{h}\right)\left(\frac{l}{b}\right)^2\frac{1}{m^4\pi^4}$

then $$\frac{k'}{f_c}\frac{b}{h} = \frac{\left(\frac{\sigma_{cr}}{m^2 f_c} - \frac{\sigma_{eu}}{f_c}\right)m^4\pi^2}{\left(\frac{l}{b}\right)^2}$$

and $\frac{k'}{f_c}\frac{b}{h}$ is divided by the original set value of $\frac{k}{f_c}\frac{b}{h}$ to establish the required ratio.

The ratio is plotted in Figure 11, appearing roughly constant with a value of about 4. Its value shown in a computer print-out accompanying Figure 11 is about 3.86.

Equal values for initial and additional deflections

In specimen calculations, Winter accepts an additional deflection equal to the initial central deviation from straightness, i.e. $d = d_o$ or $(\frac{d}{d}o+1) = 2$. The value 0.5096 used in the calculations above for Figure 11 came from equation (25) with a deflection limit of $t = 0.003$ times the span and $u_o = 0.005\,\ell/i = 0.002887$ times the span. Winter's practice will correspond to changing 0.5096 to 0.5; the values printed out for higher modes are very close to 4.0, which is double the ratio used by Winter in equation (39) when d is given the same value as d_o.

Algebraic Solution

The figures 3.86 (corresponding to 0.5096) and 4.0 (for 0.5) were reached by the computer method described above. An approximate solution in symbols is also possible by taking the two curves of Figure 11 as smooth curves through the crosses marking mode boundaries.

From (15) $$\frac{\sigma_c}{f_c} = \left\{ 2\,(m^2 + m) + 1 \right\} \frac{\sigma_{cu}}{f_c} \qquad (35)$$

From (16) $$\frac{k}{\sigma_{cu}} = m^2\,(m+1)^2\,\frac{h}{b}\,\frac{\pi^2}{(L/b)^2}$$

giving $$m^2 + m = \frac{L/b}{\pi}\,K\,\frac{f_c}{\sigma_{cu}} \qquad (36)$$

where $K = \frac{k}{f_c}\frac{b}{h}$, and putting this in (35),

$$\frac{\sigma_c}{f_c} = \left\{ 2\,\frac{L/b}{\pi}\,K\,\frac{f_c}{\sigma_{cu}} + 1 \right\} \frac{\sigma_{cu}}{f_c} \qquad (37)$$

This is the required smooth relationship for the upper curve. For the lower curve with imperfections, if the same value of $\frac{\sigma_c}{f_c}$ is obtained with $\frac{k}{f_c}\frac{b}{h} = K'$

then $$m^2 + m = \frac{L/b}{\pi}\,K'\,\frac{f_c}{\sigma_{cu}}$$

and from (29) $$\frac{\sigma_c}{f_c} = 0.5096 \left\{ 2(m^2 + m) + 1 \right\} \frac{\sigma_{cu}}{f_c}$$

$$= 0.5096 \left\{ 2\,\frac{L/b}{\pi}\,K'\,\frac{f_c}{\sigma_{cu}} + 1 \right\} \frac{\sigma_{cu}}{f_c} \qquad (38)$$

giving a smooth relationship for the lower curve.

Transposing (37) for K gives

$$K = \frac{\pi^2}{4(L/b)^2}\,\frac{\sigma_{cu}}{f_c}\left(\frac{\sigma_c}{\sigma_{cu}} - 1\right)^2$$

and transposing (38),

$$K' = \frac{\pi^2}{4(L/b)^2}\,\frac{\sigma_{cu}}{f_c}\left(\frac{1}{0.5096}\,\frac{\sigma_c}{\sigma_{cu}} - 1\right)^2$$

This gives the value of $\frac{k}{f_c}\frac{b}{h}$ needed to obtain the same value of $\frac{\sigma_c}{f_c}$ as for the higher curve.

Then $$\frac{K'}{K} = \left(\frac{\frac{1}{0.5096}\,\frac{\sigma_c}{\sigma_{cu}} - 1}{\frac{\sigma_c}{\sigma_{cu}} - 1} \right)^2 \qquad (39)$$

For the higher modes $\frac{\sigma_c}{\sigma_{cu}}$ is large compared with `1` giving the close approximation

$$\frac{K'}{K} = \frac{1}{(0.5096)^2} = 3.85$$

or for the practice in Winter's examples with $d = d_o$

$$\frac{K'}{K} = \frac{1}{(0.5)^2} = 4.0$$

Permissible end load for given restraint modulus

The above work has considered the restraint modulus required for a given end load. If the restraint modulus is given, the critical end load for an ideal column may be found from (37), and the end load that may be applied to an imperfect column without exceeding the permissible deflection is given by (38).

The following work finds equivalent results more directly and in a manner more clearly identifiable with the equations in Timoshenko & Gere (1961) which are taken as the starting point.

From (11) and (13) for the ideal column,

$$\frac{P_{cr}}{P_e} = m^2 + \frac{k L^4}{m^2 \pi^4 E I} \qquad \text{for mode m} \qquad (40)$$

and

$$\frac{P_{cr}}{P_e} = (m+1)^2 + \frac{k L^4}{(m+1)^2 \pi^4 E I} \qquad \text{for mode (m+1)} \qquad (41)$$

At the intersection of the straight lines for the two modes, k is such that the expressions on the right hand side of each equation have the same value, and equating them gives

$$\frac{k L^4}{\pi^4 E I} = m^2 (m+1)^2 \qquad (42)$$

allowing the buckling mode to be found easily from the value m (m+1) for a given k .

Writing the first m^2 of (40) as

$$m^2 = \frac{k L^4}{\pi^4 E I (m+1)^2} \qquad \text{from (42)}$$

gives

$$\frac{P_{cr}}{P_e} = \frac{k L^4}{\pi^4 E I} \left\{ \frac{1}{(m+1)^2} + \frac{1}{m^2} \right\} = \frac{k L^4}{\pi^4 E I} \left\{ \frac{2m(m+1)+1}{m^2 (m+1)^2} \right\}$$

Using (42) to replace the expressions in m in both numerator and denominator gives

$$\frac{P_{cr}}{P_e} = 2 \frac{L^2}{\pi^2} \sqrt{\frac{k}{E I}} + 1 \qquad (43)$$

as the smooth curve passing through the intersection crosses.

At an intersection the result is exact and may also be written as

$$\frac{P_{cr}}{P_e} = 2m(m+1) + 1 \qquad (44)$$

$$= m^2 + (m+1)^2$$

The smooth curve (43) through the intersection crosses gives a good approximation to the exact line formed from straight-line segments. As a further approximation, the `1` may be dropped from (43) to give

$$\frac{P_{cr}}{P_e} = 2 \frac{L^2}{\pi^2} \sqrt{\frac{k}{E I}} \qquad (45)$$

Curves from (43) and (45) are plotted in the upper curves of Figure 12, showing that both approximations are very good, sandwiching the exact straight line between them as made clear in Figure 13 which is an enlargement of the bottom left corner of Figure (12). It is seen that the approximation (45) is tangential to each straight line drawn between intersection crosses, while (43) of course passes exactly through the crosses.

The lower curves of Figure 12 apply to columns with initial curvature as defined earlier. The smooth curve through the crosses may be derived from (38) or simply by multiplying (43) by 0.5096 to give

$$\frac{P}{P_e} = 0.5096\,\frac{P_{cr}}{P_e} \qquad (46)$$

and then $$\frac{\sigma_c}{f_c} = \frac{\sigma_c}{\sigma_{eu}}\,\frac{\sigma_{eu}}{f_c} = \frac{P}{P_e}\,\frac{\sigma_{eu}}{f_c}$$

The tangential curve corresponding to (45) is

$$\frac{P}{P_e} = 0.5096 \times 2\,\frac{L^2}{\pi^2}\sqrt{\frac{k}{EI}} \qquad (47)$$

and both curves again appear as very good approximations.

Also appearing in Figure 12 are three lines showing values for the ratio $\frac{K'}{K}$ plotted on the same horizontal and vertical scales. The irregular line is the same as in Figure 11, plotted by the computer method described above. The smooth curved line is calculated from equations (37) and (39), i.e. using the smooth curves through intersection crosses for the ideal and imperfect columns. The straight horizontal line takes $\frac{K'}{K} = \frac{1}{(0.5096)} = 3.85$. The curves are included in Figure 13 to an enlarged scale, showing that either (39) or $\frac{K'}{K} = 3.85$ will give satisfactory values for modes higher than the second. For Winter's method, 4.0 would be appropriate rather than 3.85.

Tangential approximation

The approximation (47) has the extremely useful property that it is tangential to all the deflection mode lines for all values of L/b. The fact that it is independent of L/b is easily shown by manipulating (47) into the form

$$\frac{\sigma_c}{f_c} = 0.5096\sqrt{\frac{E}{3 f_c}\left(\frac{k}{f_c}\frac{b}{h}\right)} \qquad (48)$$

The point of tangency may be found as follows. From (27) the graph of the mode line is

$$\frac{\sigma_c}{f_c} = 0.5096\left\{1 + \frac{k}{EI}\left(\frac{L}{m\pi}\right)^4\right\} m^2\,\frac{\sigma_{eu}}{f_c}$$

$$= 0.5096\left\{\frac{\sigma_{eu}}{f_c} + \frac{1}{m^4\pi^2}\left(\frac{k}{f_c}\frac{b}{h}\right)\left(\frac{L}{b}\right)^2\right\} m^2 \qquad (49)$$

Differentiating (48) and (49) and equating the results since the slopes are equal at the point of tangency gives

$$\frac{k}{f_c}\frac{b}{h} = m^4\pi^2\left(\frac{b}{L}\right)^2\frac{\sigma_{eu}}{f_c} \qquad (50)$$

and putting this in (47),

$$\frac{\sigma_c}{f_c} = \frac{0.5096}{6}\, m^2 \pi^2 \left(\frac{b}{L}\right)^2 \frac{E}{f_c} \qquad (51)$$

which may also be written as

$$\frac{\sigma_c}{f_c} = 0.5096\ m^2 \times 2\, \frac{\sigma_{eu}}{f_c} \qquad (52)$$

(50) and (52) give the coordinates of the tangent point. The slope at the point of tangency for both the straight line and the tangential curve is found by inserting (50) in the differentiated version of (48) or simply as the differentiated version of (49), i.e.

$$\text{slope} = \frac{0.5096}{m^2 \pi^2}\left(\frac{L}{b}\right)^2$$

SMOOTH CURVE FOR STRESS INTERSECTIONS

A formula (38) has been found for the smooth curve through the intersections of the deflection mode lines. A method of plotting such a curve for the stress intersections would also be advantageous for use in simplified design aids as mentioned at the beginning of this report.

In the stress ratio summation, equation (32), the denominator of the last term may be written as

$$1 + \frac{k}{EI}\frac{L^4}{n^4\pi^4} - \frac{\sigma_c}{n^2\sigma_{eu}} = 1 + \frac{1}{n^4}\left(\frac{k}{f_c}\frac{b}{h}\right)\left(\frac{L/b}{\pi}\right)^2 \frac{f_c}{\sigma_{eu}} - \frac{\sigma_c}{n^2\sigma_{eu}} \qquad (53)$$

Equation (33) was obtained by subtracting (32) and its counterpart with (n + 1) replacing n, so transposing (33) for $\frac{k}{f_c}\frac{b}{h}$ and inserting in (53) will give an expression relating to the mode intersection points.

Transposing (33),

$$\frac{k}{f_c}\frac{b}{h}\left(\frac{L/b}{\pi}\right)^2 = \frac{n^2(n+1)^2}{3n(n+1)+1}\left\{\frac{\sigma_c}{f_c} + n(n+1)\frac{\sigma_{eu}}{f_c}\right\} \qquad (54)$$

and inserting this in (53) leads to the result

$$1 = \frac{\sigma_c}{f_c} + \frac{\frac{\sigma_c}{f_m}\eta''}{1 - \frac{1{\cdot}5\,\sigma_c}{\sigma_{eu,x}}} + \frac{\frac{\sigma_c}{f_m}\frac{\eta_b}{n}}{\frac{2n+1}{3n(n+1)+1}\left(2n^2+2n+1-\frac{\sigma_c}{\sigma_{eu}}\right)} \qquad (55)$$

If n could be eliminated from (54) and (55), an equation giving $\frac{\sigma_c}{f_c}$ in terms of $\frac{k}{f_c}\frac{b}{h}$ would be obtained as the required smooth curve. As the elimination cannot be achieved conveniently, the smooth curve may be obtained alternatively by means of a `parametric plot` of the pair of equations (54) and (55).

The plot is performed for Figure 14 by incrementing values of n in (55) to work out values of $\frac{\sigma_c}{f_c}$ which are then inserted in (54) together with the corresponding n values to obtain $\frac{k}{f_c}\frac{b}{h}$. Then the $\frac{\sigma_c}{f_c}$ values are plotted against $\frac{k}{f_c}\frac{b}{h}$.

A parametric plot may also be obtained for the smooth curve through the intersections of the deflection mode lines, by plotting the pair

$$\frac{k}{f_c}\frac{b}{h} = m^2 (m+1)^2 \left(\frac{\pi}{L/b}\right)^2 \frac{\sigma_{cu}}{f_c} \qquad (56)$$

and

$$\frac{\sigma_c}{f_c} = \left\{ 2m (m+1) + 1 \right\} \frac{\sigma_{cu}}{f_c} \times 0.5096 \qquad (57)$$

However it should be noted that `m` does not have the same value in this pair of equations as n has in the pair (54) and (55).

If (54) and (55) are transformed horizontally by plotting the pair (55) and (56) instead, m will have the same value for both deflection and stress at a given value of $\frac{k}{f_c}\frac{b}{h}$. Attempts have been made to find means of determining in which mode the true or smooth curves for stress and deflection will intersect, but without finding results simple enough for practical use other than by computer plotting.

The problem with the `true` curves is illustrated in Figure 15 for L/b = 180, where `dropped strength` curves are plotted for h/b = 8, 6, 4 and 2. For h/b = 6 there is an intersection with mode 3 of the deflection curve. To determine the restraint modulus needed to limit the lateral deflection to 0.003 times the length and the value of $\frac{\sigma_c}{f_c}$ that will then be permissible, some way is needed for predicting the mode in which deflection ceases to be a governing factor. This may involve predicting the mode containing an intersection such as the one marked in Figure 15. However because of the discontinuity between the dropped strength curves for adjacent modes there are also cases where there is no intersection but deflection governs throughout one mode but not at all in the next higher one.

Intersections at ends of deflection mode line

Helpful results are found by considering the intersections of the stress limiting equation (32) with the ends of the deflection mode line (49) where values of $\frac{\sigma_c}{f_c}$ and $\frac{k}{f_c}\frac{b}{h}$ are known from equations (29) and (30).

Transposing (32) with the denominator of the last term written as in (53) gives

$$1 - \frac{\sigma_c}{f_c} - \frac{\frac{\sigma_c}{f_m}\frac{\eta}{n}}{1 + \left(\frac{k}{f_c}\frac{b}{h}\right)\frac{1}{n^4}\left(\frac{L/b}{\pi}\right)^2 \frac{f_c}{\sigma_{cu}} - \frac{\sigma_c}{n^2\sigma_{cu}}} = \frac{\frac{\sigma_c}{f_m}\eta''}{1 - 1{\cdot}5\frac{\sigma_c}{\sigma_{cu,x}}} \qquad (58)$$

The left hand side may be evaluated from the known values of $\frac{\sigma_c}{f_c}$ and $\frac{k}{f_c}\frac{b}{h}$. Calling it α and taking $\eta = 0.005\frac{L}{t} = 0.01732\frac{L}{h}$,

$$\alpha = \frac{\frac{\sigma_c}{f_m} \times 0{\cdot}01732\frac{L}{h}}{1 - 1{\cdot}5\frac{\sigma_c}{\pi^2 E_{min}} \cdot 12\left(\frac{L}{h}\right)^2} \qquad (59)$$

or

$$\left(\frac{L}{h}\right)^2 + \frac{0.009497}{\alpha}\frac{E_{min}}{f_m}\left(\frac{L}{h}\right) - 0.5483\frac{E_{min}}{\sigma_c} = 0 \qquad (60)$$

After solving (60) for $\frac{L}{h}$, then $\frac{h}{b} = \frac{h}{L} \times \frac{L}{b}$ and for a particular $\frac{L}{b}$ value a line showing $\frac{\sigma_c}{f_c}$ as limited by combined stress may be plotted for the upper and lower limits of each mode. This is done in Figure 16 for $\frac{L}{b} = 180$, showing $\frac{h}{b}$ limits for the top and bottom of modes 2 and 3 and for the lower-end $\frac{\sigma_c}{f_c}$ and $\frac{k}{f_c}\frac{b}{h}$ values of mode 4. An upper $\frac{h}{b}$ line cannot be drawn for mode 4 as its upper limit lies above the `strength` line disregarding stiff-direction buckling and α is found to be negative when the upper-end values are inserted in (59).

If ready- computed solutions of this kind are available for mode boundaries, the approximate position of an intersection such as that marked in Figure 15 may be found by rough interpolation, giving a value of $\frac{\sigma_c}{f_c}$ and the corresponding value of $\frac{k}{f_c}\frac{b}{h}$. If in a practical example $\frac{k}{f_c}\frac{b}{h}$ is less than this, then $\frac{\sigma_c}{f_c}$ will be lower and governed by deflection. If $\frac{k}{f_c}\frac{b}{h}$ is greater, the permissible value of $\frac{\sigma_c}{f_c}$ will be higher than that at the intersection (but not for small $\frac{h}{b}$ ratios) and governed by combined stress.

Stress lines for constant L/h values

Figure 16 is plotted for $\frac{L}{b} = 180$ only. If lines for $\frac{L}{b} = 108$ are added, to achieve the near-coincidence mentioned under the heading `Variation of L/b` (page 8) in connection with Figure 7 a constant value of $\frac{L}{h}$ should be applied for both $\frac{L}{b}$ ratios, and this suggests plotting Figure 16 in the different way shown in Figure 17 where separate graphs for $\frac{L}{b} = 180$ and $\frac{L}{b} = 108$ are shown.

In Figure 17 the $\frac{L}{h}$ values 38.720 and 36.383 are at similar heights and therefore have similar values but they differ because their height is governed by node positions which do not have the same $\frac{\sigma_c}{f_c}$ value. In Figure 10 the near coincidence of lines for $\frac{L}{b} = 180$ and 108 is achieved because their position is not influenced by deflection mode boundaries.

MODE-FREE PLOT FOR STRENGTH LINES

A method of plotting $\frac{L}{h}$ lines in a manner independent of the deflection mode boundaries for particular $\frac{L}{b}$ ratios is suggested by overlaying Figure 12 for L/b = 180 on Figure 18 which is the same diagram for L/b = 108. The two sets of curves almost coincide. Referring to the lower curves of each diagram, the internal tangential curve is the same for each and the outer curve differs only slightly. The actual vertical difference may be found from the non-approximated version of (48) which is

$$\frac{\sigma_c}{f_c} = 0.5096 \sqrt{\frac{E}{3 f_c} \frac{f_k}{f_c} \frac{b}{h}} + 0.5096 \frac{\sigma_{eu}}{f_c} \qquad (61)$$

and $\frac{\sigma_{eu}}{f_c}$ with σ_{eu} calculated for the full first-mode length is quite small.

If only the tangential curve (48) is used as a conservative approximation, then this will be the same for any L/b ratio and can be used to establish starting values for $\frac{L}{h}$ lines without reference to the intersections of deflection mode lines. At any point on the tangential curve, values for $\frac{\sigma_c}{f_c}$ and $\frac{f_k}{f_c}\frac{b}{h}$ can be found for inserting in the left-hand side of (58) to yield α. Then α is inserted in (60) to find $\frac{L}{h}$.

To plot lines for particular values of $\frac{L}{h}$ with convenient increments, the process just described must be performed for incremented values of $\frac{f_k}{f_c}\frac{b}{h}$ in the tangential deflection curve (48) until the pair $\frac{\sigma_c}{f_c}$ and $\frac{f_k}{f_c}\frac{b}{h}$ give a solution of (60) which matches a pre-set $\frac{L}{h}$ value. The results of a computer plot with this basis are shown in Figure 19 for L/h = 90 and 30 and for the two L/b values, 180 and 108. The broken curve for L/b = 180 is the same as that for h/b = 6 in Figure 15, and the corresponding broken line for L/b = 108 is close to that for L/b = 180, coinciding completely for the fifth mode of L/b = 180 and the third mode of L/b = 108.

As in Figure 15, coincidence is approached more quickly for lower values of h/b (higher values of L/h) until when h/b = 2 or L/h = 90 the lines for different L/b values cannot be distinguished.

Parametric plot for strength

Figure 19 is only a step towards a mode-free plot. To draw the L/h lines for strength using (60), the mode number n has to be known for evaluating the left-hand side of (58), called α in (59). At each increment along the deflection line when seeking a match for a preset L/h value, the mode number has to be found using mode limits for $\frac{f_k}{f_c}\frac{b}{h}$ established in an earlier stage of the computer program.

To obtain a plot which removes reference to mode numbers, use may be made of the smooth curve through stress intersections obtained by parametric plotting of (54) and (55) as done in Figure 14. Again the procedure involves incrementing values along the deflection line until a preset L/h solution is reached, and the result is shown in Figure 20.

The incrementing procedure is needed only to establish the starting values for the strength curve where it meets the deflection line. For each pair of values $\frac{\sigma_c}{f_c}$ and $\frac{k}{f_c}\frac{b}{h}$ obtained from the deflection curve, a value for n is first obtained by incrementing it until its insertion in (55) and then (54) yields a result for $\frac{k}{f_c}\frac{b}{h}$ which just exceeds the deflection curve value. If the corresponding $\frac{\sigma_c}{f_c}$ for the strength curve exceeds that for deflection, the calculation proceeds for a higher point on the deflection line and the procedure is repeated until $\frac{\sigma_c}{f_c}$ for strength equals that for deflection and the intersection of the two curves is found.

Adapting the method that used (58), (59) and (60) for Figure 16, the expression for α from (55) will be

$$\alpha = 1 - \frac{\sigma_c}{f_c} - \frac{\frac{\sigma_c}{f_{tm}}\eta}{\frac{2n+1}{3n(n+1)+1}\left\{2n(n+1)+1-\frac{\sigma_c}{\sigma_{cu}}\right\}} \qquad (62)$$

and this is inserted in (60) to give a result for L/h at the position reached on the deflection line. This result is compared with the set value of L/h and iteration along the deflection line continues until the set value is reached and starting values for $\frac{k}{f_c}\frac{b}{h}$ and $\frac{\sigma_c}{f_c}$ are obtained. The strength curve is then plotted using the incremental procedure described in previous reports and used for example in plotting Figure 5.

An alternative is to use this same incremental procedure at each step along the deflection line until the required L/h value is reached. Both methods involve multiple nested iterative processes, and a quicker approximate method is found in the next section. The approximation also provides results which are useful as design formulae for manual calculations.

Approximate method for starting values

As mentioned in connection with equations (56) and (57), attempts have been made to find algebraically the intersection between the stress and deflection lines, but these have required the solution of at least cubic equations except when limited to the intersections of deflection mode lines when a quadratic solution can be obtained for (60).

With the mode-free type of plot such points are not available unless the plot is specialised for a particular L/b ratio, which is not desirable when the object of the plot is to provide for all L/b values. The method applied for determining starting values in Figure 20 indicates a means of overcoming the difficulty.

From (54), the equation used in determining the horizontal co-ordinate of the strength curve by the parametric plotting method is

$$\frac{k}{f_c}\frac{b}{h} = \left(\frac{\pi}{L/b}\right)^2 \frac{n^2(n+1)^2}{3n(n+1)+1}\left\{\frac{\sigma_c}{f_c} + n(n+1)\frac{\sigma_{cu}}{f_c}\right\} \qquad (63)$$

From (48) the equation plotted for the tangential deflection curve is

$$\frac{k}{f_c}\frac{b}{h} = \left(\frac{\sigma_c}{f_c} \times \frac{1}{0.5096}\right)^2 \frac{3f_c}{E} \qquad (64)$$

At an intersection between the deflection and strength curves, the two are equal and $\frac{\sigma_c}{f_c}$ has the same value in both. Equating them and solving for $\alpha = n(n+1)$ leads to a cubic equation in α. However if '+1' is omitted in the denominator of the right-hand side of (63) it becomes

$$\frac{k}{f_c}\frac{b}{h} = \frac{n(n+1)}{3}\left\{\frac{\sigma_c}{f_c} + n(n+1)\frac{\sigma_{cu}}{f_c}\right\}\left(\frac{\pi}{L/b}\right)^2 \qquad (65)$$

and the solution found is

$$n(n+1) = 1.27145 \frac{\sigma_c}{\sigma_{eu}} \tag{66}$$

Inserting this in (65) leads of course to (64), i.e.

$$\frac{k}{f_c}\frac{b}{h} = \frac{3}{(0.5096)^2}\frac{\sigma_c^2}{E f_c} = 11.552 \frac{\sigma_c^2}{E f_c} \tag{67}$$

From (66) the positive solution for n is

$$n = \frac{1}{2}\left(\sqrt{1+5.0858\frac{\sigma_c}{\sigma_{eu}}} - 1\right) \tag{68}$$

To find starting values along the deflection line for a diagram such as Figure 20, the deflection coordinates are incremented as before and n for insertion in (63) is found from (68). Then L/h is found from (60) and the process is continued until L/h equals the preset value. This greatly reduces the amount of iteration required. A plot using the approximate method is shown in Figure 21 for L/b = 180 and L/h = 90, 45, 30 and 22.5, the lowest value being shown by the top curve. The plotted curves are exact, as the approximation is used only to find starting values.

h/L lines

As illustrated in Figure 10 for part of the range, the depth ratios 8, 6, 4, 2 for L/b = 180 or 4.8, 3.6, 2.4 and 1.2 for L/b = 108 correspond to L/h ratios of 22.5, 30, 45 and 90 respectively. The reciprocals of the last four figures are the corresponding h/L ratios, i.e. 0.0444, 0.0333, 0.0222 and 0.0111. As these have uniform intervals and gave a more-or-less uniform spacing for the stress lines in Figure 10, it may be preferable to base the mode-free plot on uniform intervals for h/L as shown in Figure 22 for h/L values ranging from 0.01 to 0.04 in 0.001 steps. The raised portions at the right-hand end of each line show the permissible $\frac{\sigma_c}{f_c}$ value that would be found by the routine buckling calculation for the stiff direction, disregarding the effect of lateral buckling. Only lines for L/b = 180 are shown, providing also for L/b = 108 with only slight conservatism.

FURTHER POSSIBILITIES OF TANGENTIAL DEFLECTION CURVE

A point not fully brought out on page 15 but deducible from (52) is that for a tangent point on the deflection curve for the 'ideal' column, i.e. without the factor 0.5096

$$\frac{\sigma_{cr}}{m^2 \sigma_{eu}} = 2 \qquad (69)$$

At any point of tangency on the deflection curve for the column with imperfections, as given by (52)

$$\frac{\sigma_c}{f_c} = 0.5096 \times 2 m^2 \frac{\sigma_{eu}}{f_c}$$

$$= \frac{0.5096}{6} \left(\frac{m}{L/b}\right)^2 \pi^2 \frac{E}{f_c} \qquad (70)$$

and from (50)

$$\frac{h}{f_c} \frac{b}{h} = m^4 \pi^2 \left(\frac{b}{L}\right)^2 \frac{\sigma_{eu}}{f_c}$$

$$= \left(\frac{m}{L/b}\right)^4 \frac{\pi^4 E}{12 f_c} \qquad (71)$$

It will be realised that every point on the tangential deflection curve is in fact a point of tangency. A particular point will be a point of tangency for mode m of a certain L/b ratio. For example the point where $\frac{L/b}{m} = 62.5$ may relate to

mode 1 for L/b = 62.5
or mode 2 for L/b = 125
or mode 3 for L/b = 187.5

and so on.

An alternative is to consider $\frac{m}{L/b}$ simply as a parameter of the tangential deflection curve, without reference to modes or L/b values until the resulting plot is applied to practical numerical problems.

To find the intersection of the deflection curve with a strength line such as one of the four drawn in Figure 21 for different L/h ratios, putting $\frac{h}{f_c}\frac{b}{h}$ from (50) and $\frac{\sigma_c}{f_c}$ from (52) into the left-hand side of (58) gives

$$\alpha' = 1 - 0.5096 \times 2 m^2 \frac{\sigma_{eu}}{f_c} \left\{ 1 + 1.0196 \frac{f_c}{f_m} \frac{\eta}{m} \right\} \qquad (72)$$

$\frac{\sigma_c}{f_c}$ from (52) may also be inserted on the right-hand side to give

$$\alpha' = \frac{0.5096 \times 2 m^2 \frac{\sigma_{eu}}{f_c} \frac{f_c}{f_m} \times 0.01732 \frac{L}{h}}{1 - 1.5 \times \frac{0.5096}{\pi^2 E_{min}} \times 2 m^2 \frac{\sigma_{eu}}{f_c} f_c 12 \left(\frac{L}{h}\right)^2}$$

and solving for $\frac{L}{h}$ gives

$$\left(\frac{L}{h}\right)^2 + \frac{0.009497}{\alpha'} \frac{E_{min}}{f_m} \left(\frac{L}{h}\right) - \frac{0.5483}{0.5096 \times 2m^2} \frac{E_{min}}{\sigma_{eu}} = 0 \qquad (73)$$

- similar to (60) but with σ_c replaced by $0.5096 \times 2m^2 \sigma_{eu}$.

To solve for L/h at any point of the deflection curve without specifying L/b and m separately, $\frac{m}{L/b}$ for a particular value of $\frac{\sigma_e}{f_c}$ may be found from (70) which gives

$$\frac{m}{L/b} = 1.09222 \frac{f_c}{E} \frac{\sigma_e}{f_c}$$

Inserting this in (72) gives

$$\alpha' = 1 - 0.8383 \frac{E}{f_c} \left(\frac{m}{L/b}\right)^2 - 0.014803 \frac{E}{f_c} \frac{f_c}{f_m} \left(\frac{m}{L/b}\right)$$

and insertion in (73) gives

$$\left(\frac{L}{h}\right)^2 + \frac{0.009497}{\alpha'} \frac{E_{min}}{f_m} \left(\frac{L}{h}\right) - 0.65409 \frac{E_{min}}{E} \left(\frac{L/b}{m}\right)^2 = 0$$

To plot lines for a range of L/h values, $\frac{\sigma_e}{f_c}$ must be incremented until a set value of L/h is reached, as in the program which produced Figure 21. After getting a starting value for a pre-set L/h, the task is to plot (58) by incrementing $\frac{\sigma_e}{f_c}$ for intervals in $\frac{f_c}{f_c} \frac{b}{h}$.

If $\frac{L/b}{m}$ is maintained at its starting value, the last term on the left-hand side of (58) becomes

$$\frac{\frac{\sigma_e}{f_c} \frac{f_c}{f_m} \times 0.01732 \left(\frac{L/b}{m}\right)}{1 + \frac{f_c}{f_c} \frac{b}{h} \frac{12}{\pi^4} \frac{f_c}{E} \left(\frac{L/b}{m}\right)^4 - \frac{12}{\pi^2} \frac{\sigma_e}{f_c} \frac{f_c}{E} \left(\frac{L/b}{m}\right)^2} \qquad (74)$$

A plot performed with this basis is shown in Figure 23. The higher strength curves show permissible $\frac{\sigma_e}{f_c}$ values greater than in Figure 21 but may nevertheless be found useful, either by applying a reduction factor or because a lateral restraint system can be expected to apply some restraint also in the unbraced direction.

DEFLECTION IN STIFF DIRECTION

All the previous work has ignored the possibility of excessive deflection in the unbraced direction with bending in a single half-wave. With a limitation of 0.003 times the height, the maximum permissible value of $\frac{\sigma_c}{f_c}$ will be

$$\frac{\sigma_c}{f_c} = 0.5096 \frac{\sigma_{cu,x}}{f_c} \qquad (75)$$

For a plot such as Figure 22, the necessary cut-off may be found by inserting (75) in (55) to give a cubic expression in n only for a given L/h value. This may be solved by iteration and the resulting value of n is inserted in (54) together with $\frac{\sigma_c}{f_c}$ from (75) to find $\frac{k_c}{f_c}\frac{b}{h}$ for the deflection cut-off curve relating to the stiff direction.

The cut-off line is added to Figure 22 in Figure 24 and can be seen to make a large difference, all lines below the cut-off being invalid if the stiff-direction deflection may not exceed 0.003 times the column height. In Figure 25 the invalid lines are omitted.

PREFERRED FORM OF PLOT

In Figure 25 it will be noticed that the curves climb very slowly and $\frac{\sigma_c}{f_c}$ values for high restraint stiffness may be off the graph or difficult to measure because of the flatness of the curves. A plot dividing the horizontal scale by 20 and the vertical scale by 2 still leaves the same problems because the curves advance towards the values shown by the steps at their right-hand end, which are only reached at $\frac{k_c}{f_c}\frac{b}{h} = \infty$.

The difficulty is overcome by the well-known method of plotting the same $\frac{\sigma_c}{f_c}$ values against the reciprocal of $\frac{k_c}{f_c}\frac{b}{h}$ as shown in Figure 26. This plot shows the same information as Figure 25, with the same cut-off curves for deflection in the restrained and unrestrained directions, and will provide a basis for a design chart for a single grade and type of timber.

Figure 26 is composed of the accurate strength curves defined by equations (54) and (55). A similar plotting method may be applied with the basis adopted for Figure 23, using (58) with one term modified as shown by (74). As mentioned already, this procedure gives curves which are unconservative compared with Figure 26 but may nevertheless be found acceptable. The graphs adopting this basis are shown in Figure 27, where it is seen that the upward tilt of the curves at the left-hand end of Figure 26 has been eliminated. In fact the curves in Figure 27 are very close to straight lines over much of their range and for practical design purposes it would be reasonable to take them throughout as straight lines joining their ends.

To write a formula representing a curve of Figure 27 as a straight line, the subscript w (standing for Winter, see page 10 and references) will be used for its intersection with the deflection line. The values of $\frac{\sigma_c}{f_c}$ and $\frac{k_c}{f_c}\frac{b}{h}$ at the intersection will be taken as $\frac{\sigma_w}{f_c}$ and $\frac{k_w}{f_c}\frac{b}{h}$ and the formula derived is

$$\sigma_c = k_c f_c - \frac{k_w}{k}\left(k_c f_c - \sigma_w\right) \qquad (76)$$

giving $\sigma_c = k_c f_c$ when $k = \infty$ and $\sigma_c = \sigma_w$ at the intersection.

NOTE: k_c is the column buckling factor in the CIB Code, and is not a restraint modulus.

References

Brüninghoff, H. (1983) - Determination of bracing structures for compression members and beams. CIB-W18 paper No. 16-15-1, Lillehammer, May/June 1983.

Burgess, H.J. (1987) - Lateral buckling theory for rectangular section deep beam-columns. CIB-W18A paper No. 20-2-1, Dublin, September 1987.

Burgess, H.J. (1988) - Rectangular section deep beam-columns with continuous lateral restraint. CIB-W18A paper No. 21-15-1, Vancouver, September 1988.

Timoshenko, S.P. & J.M. Gere (1961) - Theory of elastic stability. 2nd edition, McGraw - Hill, London 1961.

Winter, G. (1958) - Lateral bracing of columns and beams. Jl. Struct. Div. ASCE, Paper 1561, March 1958.

Figure 1

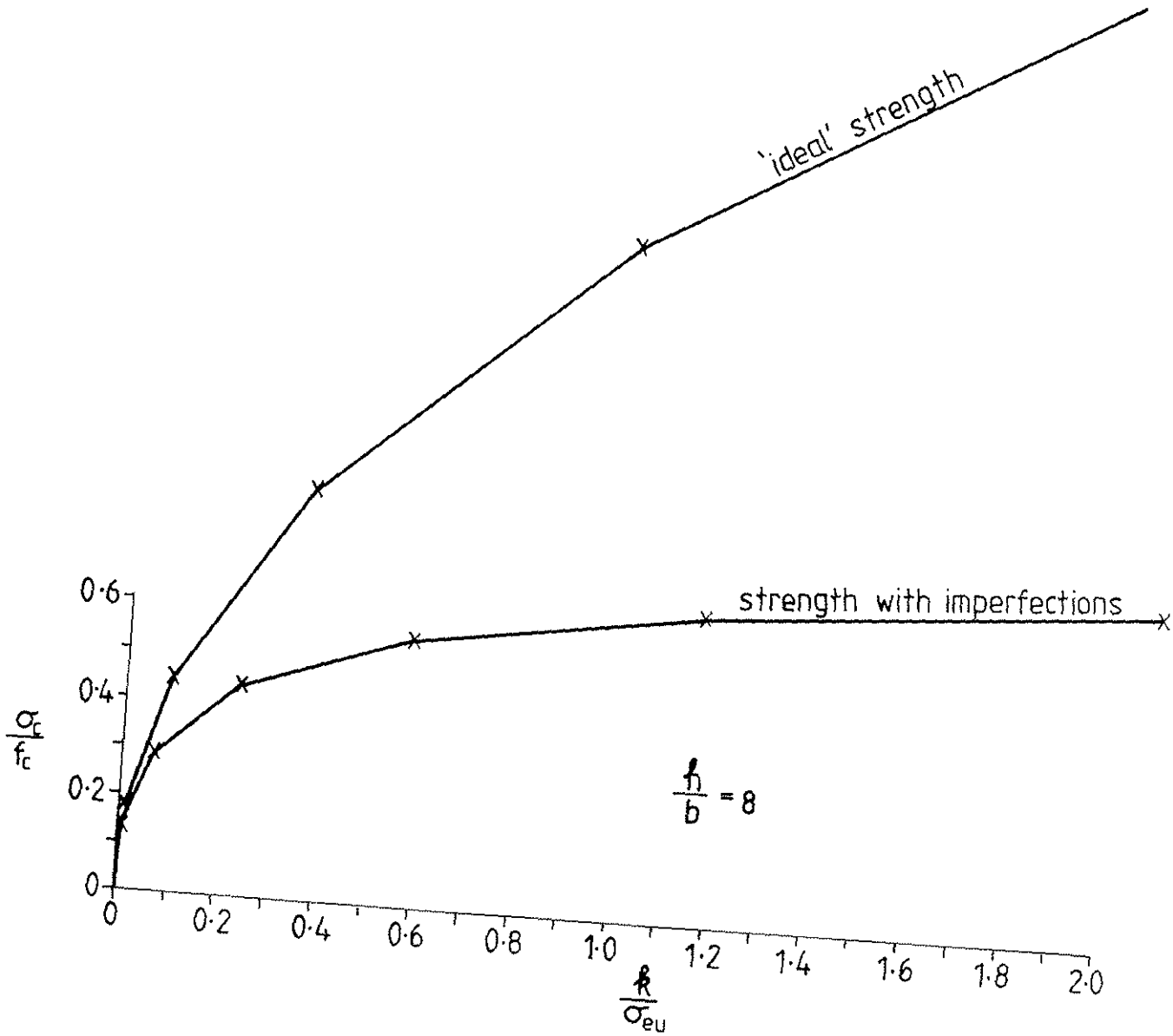
'ideal' strength
strength with imperfections
$\frac{\sigma_c}{f_c}$
0·6
0·4
0·2
0
0
0·2
0·4
0·6
0·8
1·0
1·2
1·4
1·6
1·8
2·0
$\frac{\ell}{\sigma_{eu}}$
$\frac{\ell}{b} = 8$

Figure 2

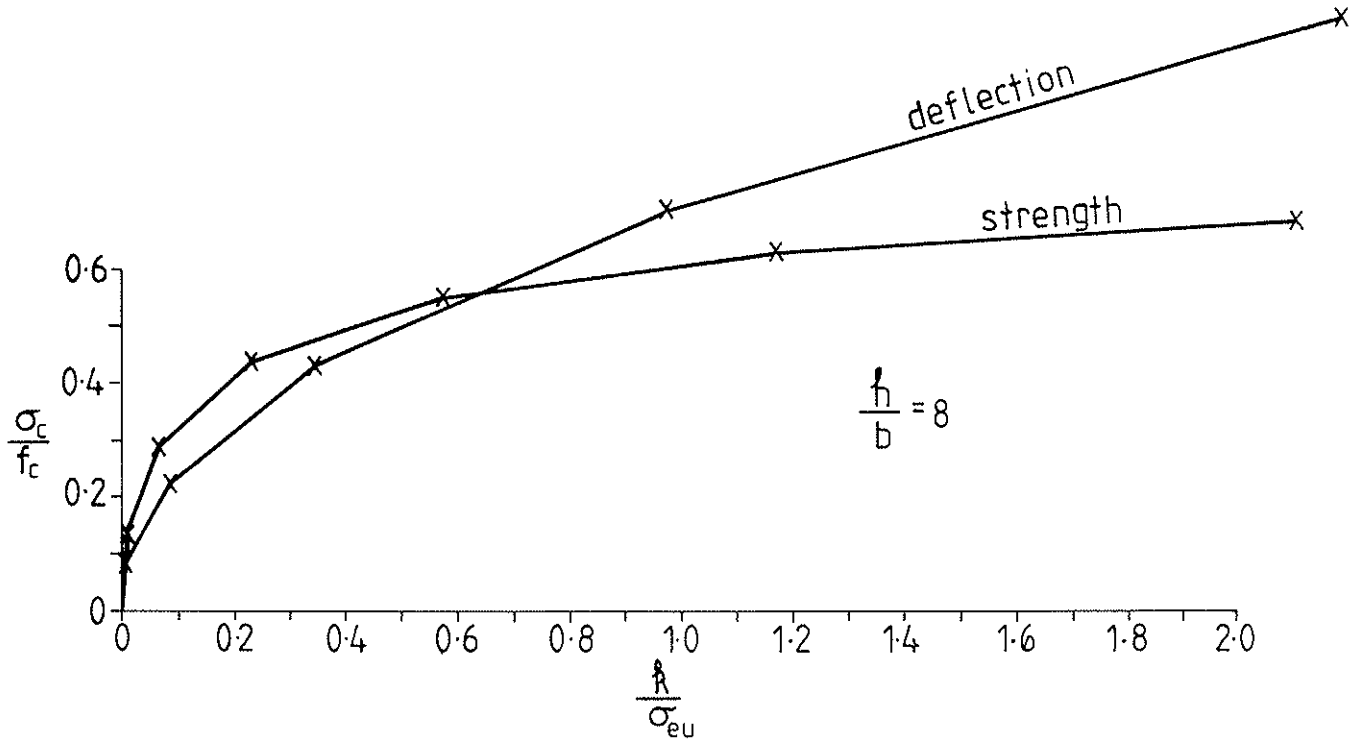

Figure 3

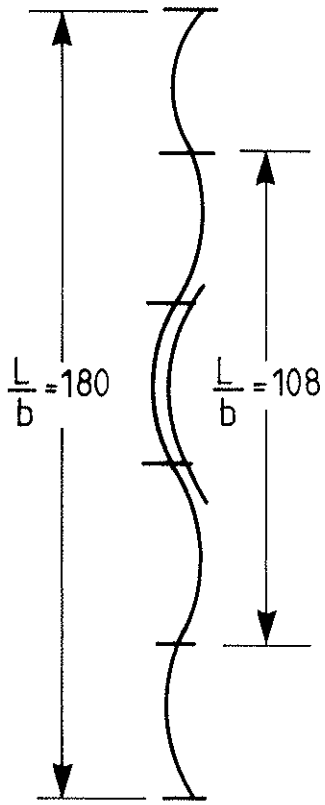

Figure 4

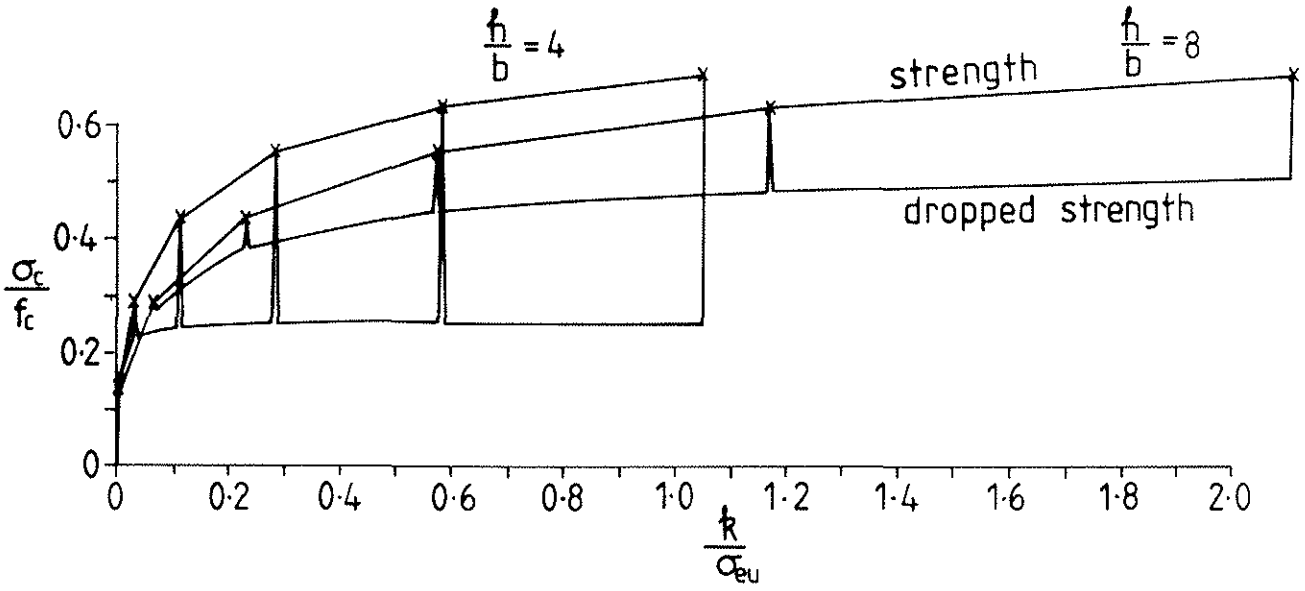

Figure 5

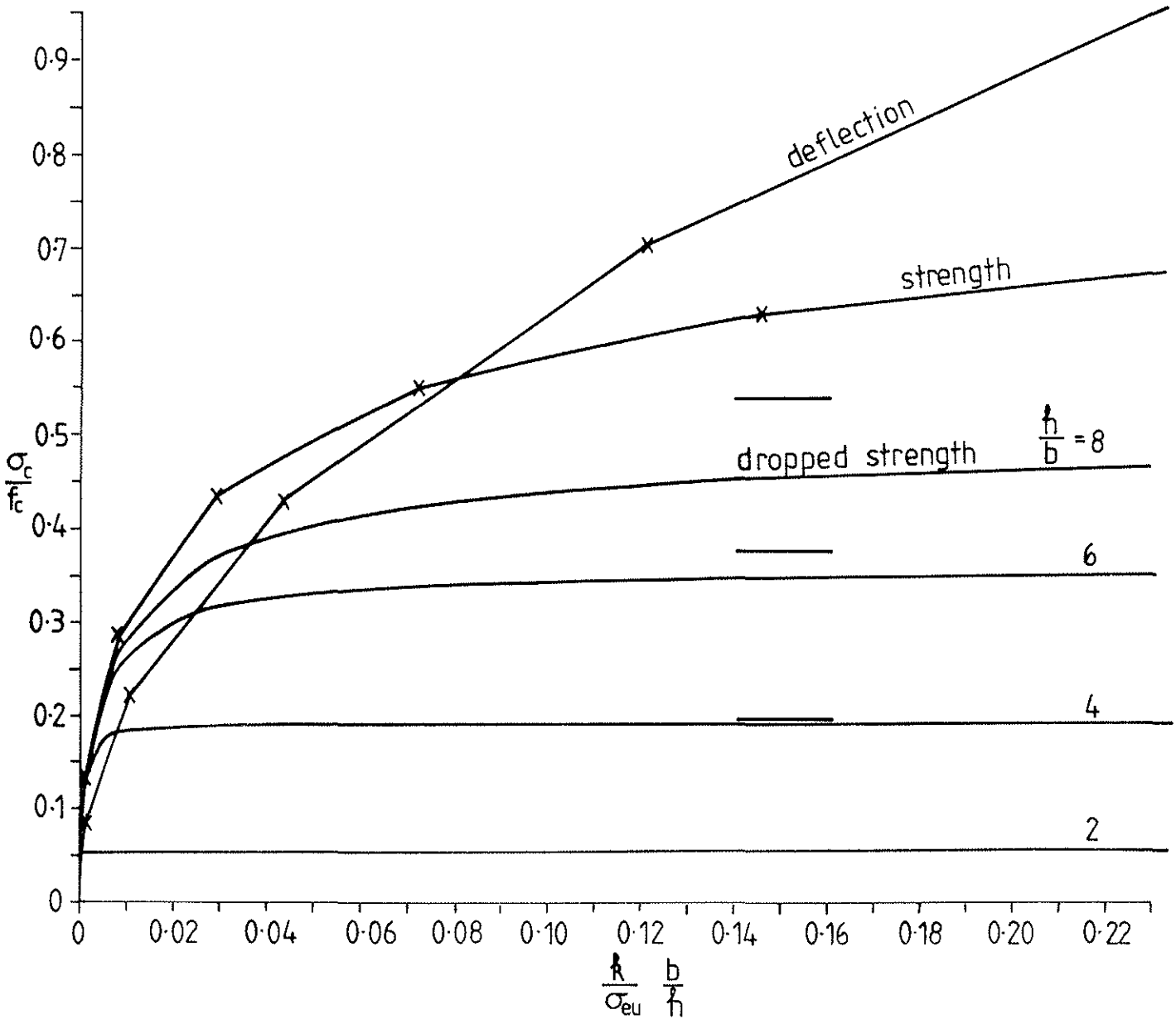

Figure 6

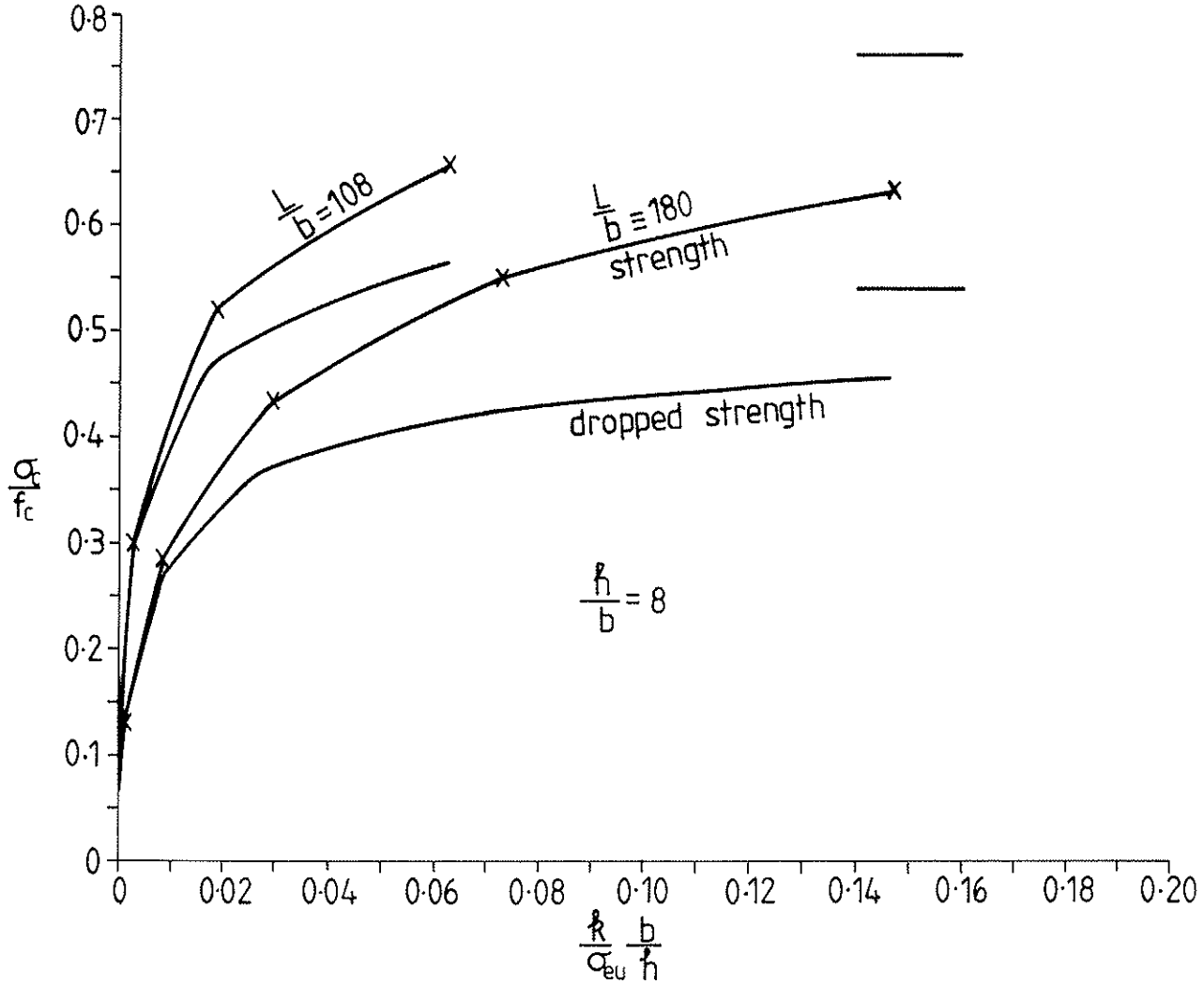

Figure 7

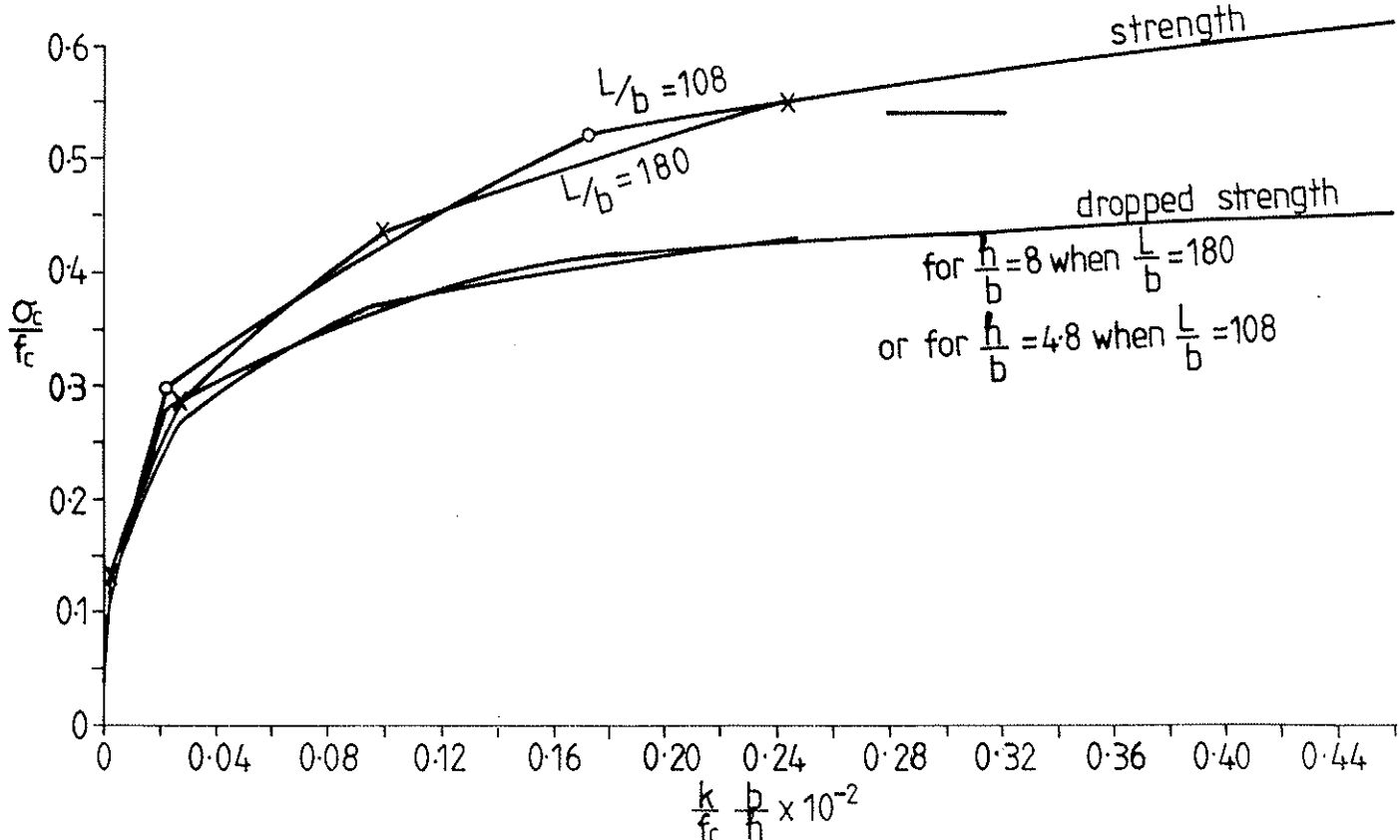

Figure 8

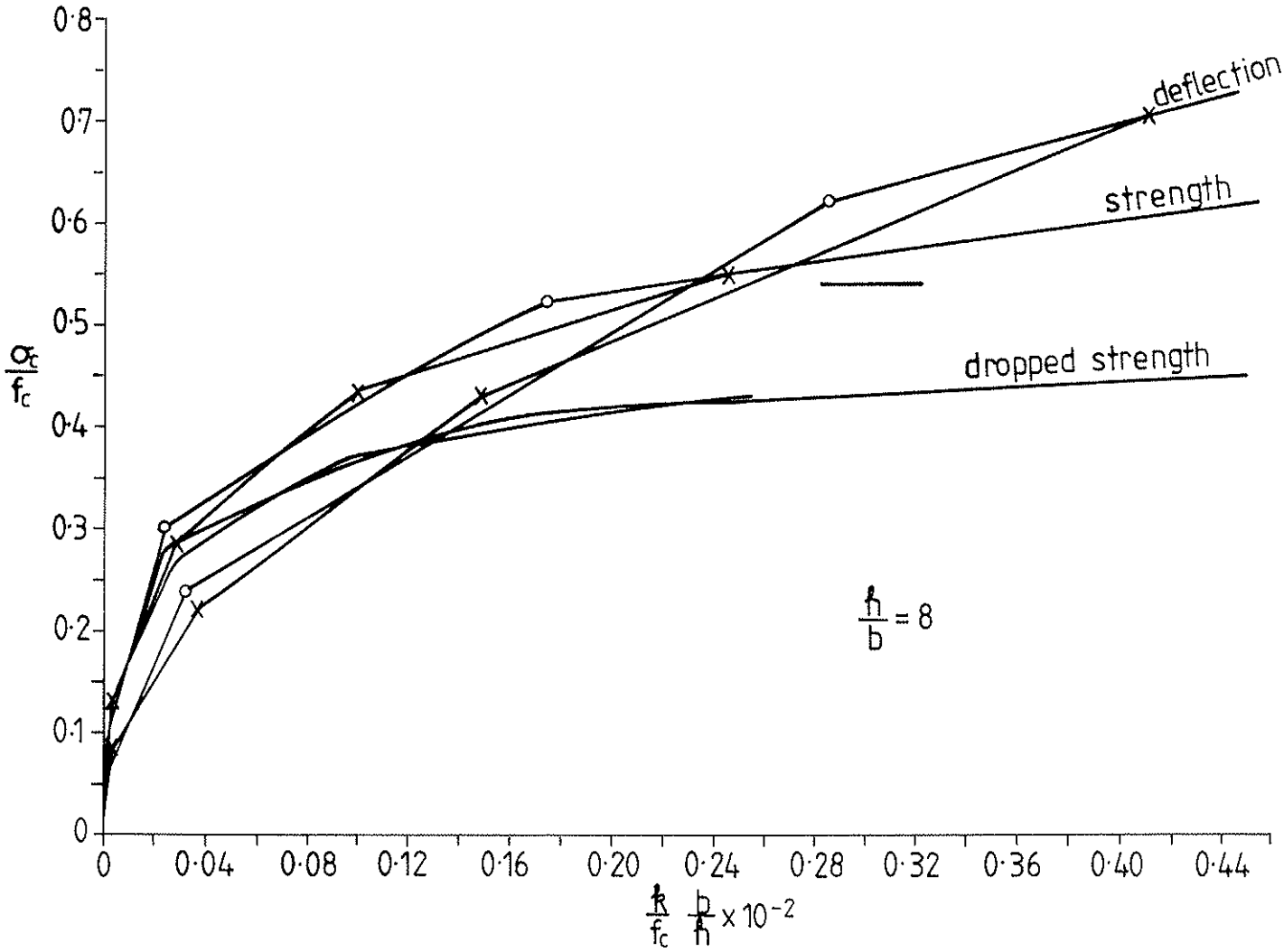

Figure 9

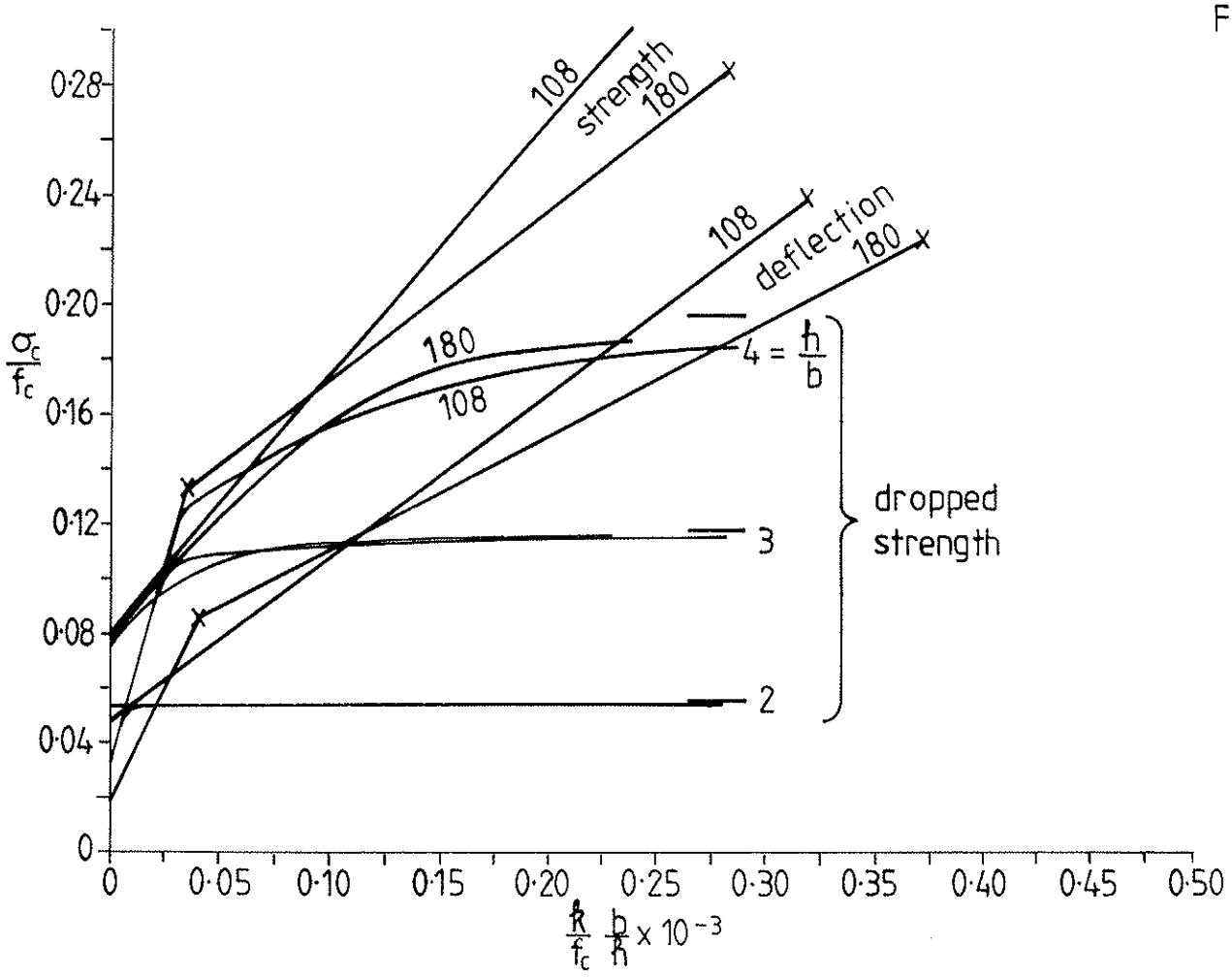

Figure 10

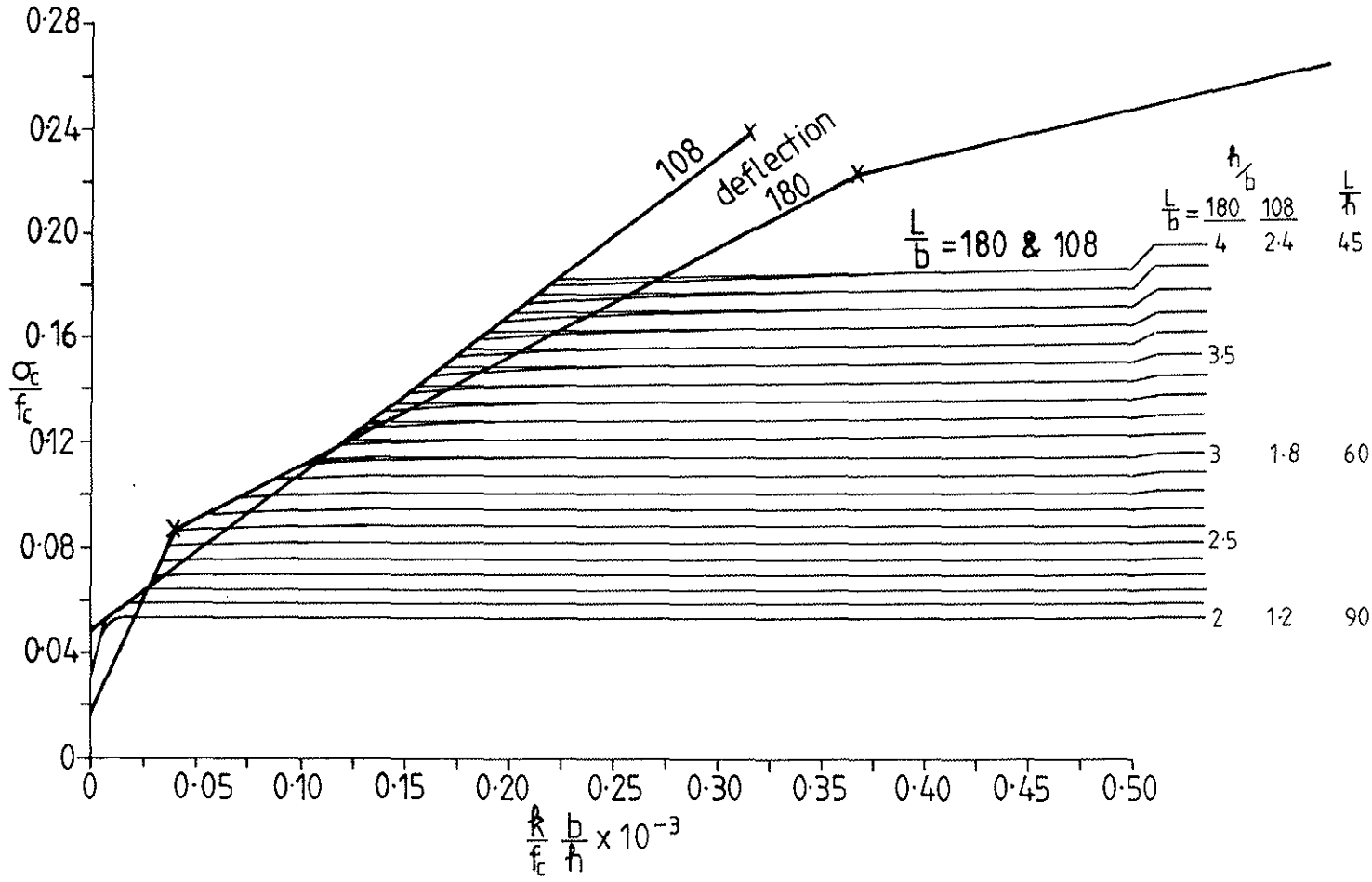

Figure 11

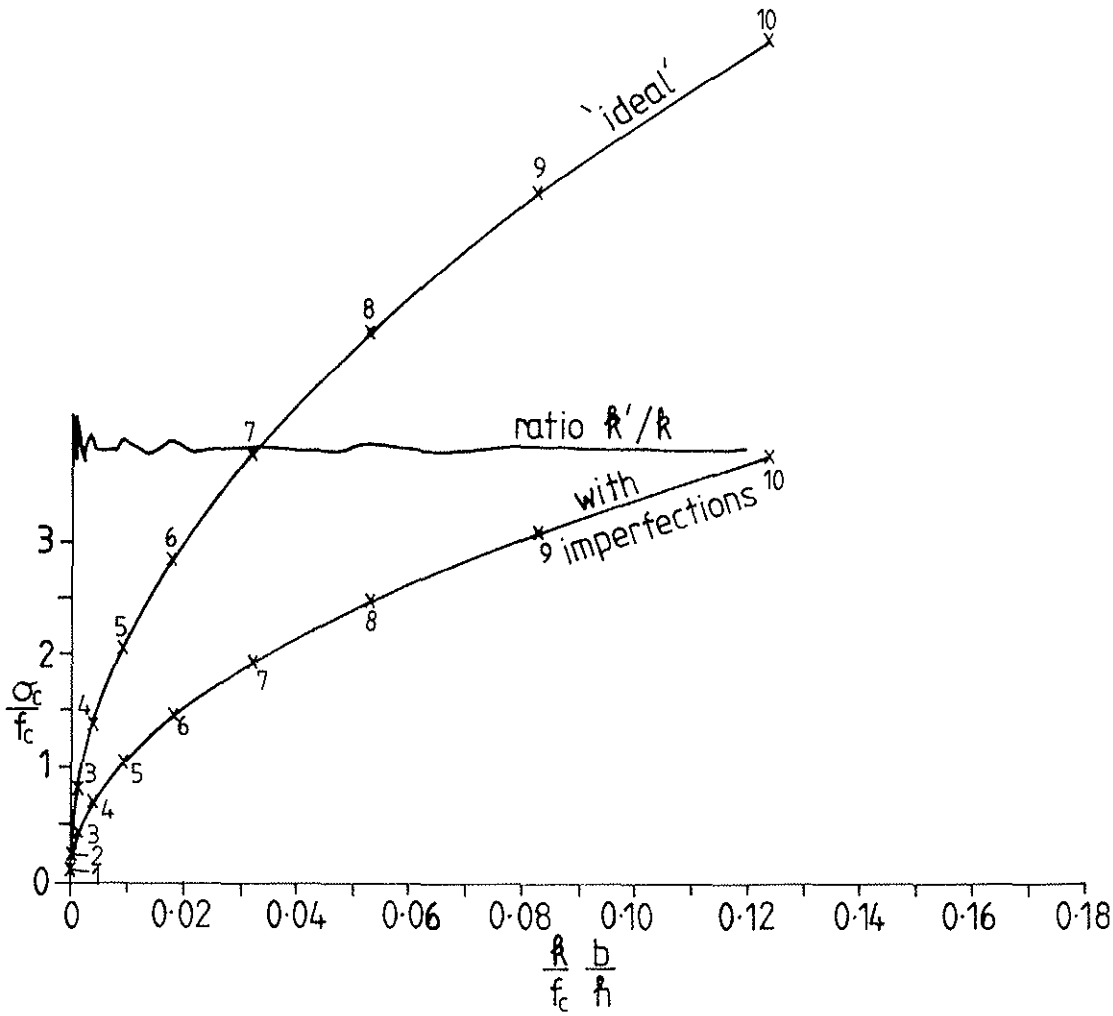

Figure 12

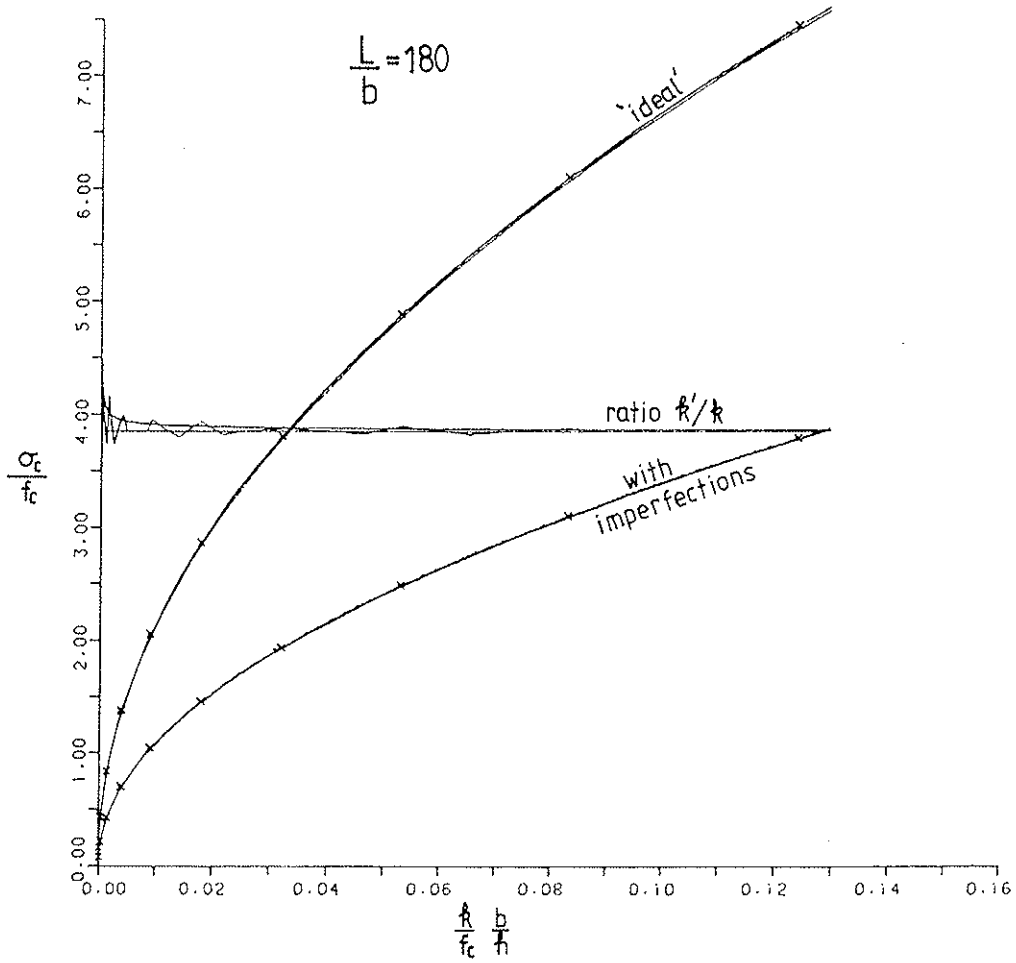

Figure 13

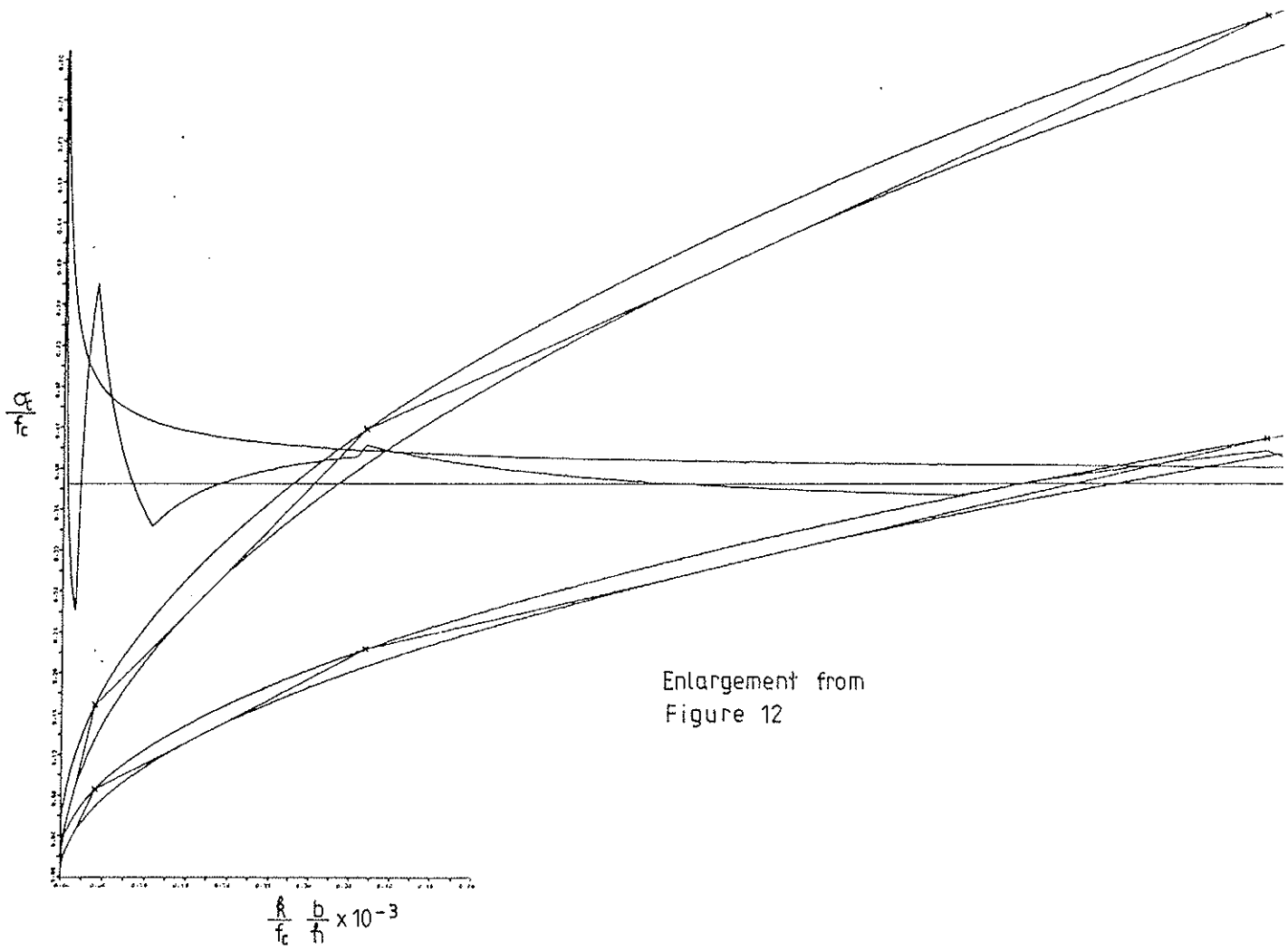

Enlargement from Figure 12

Figure 14

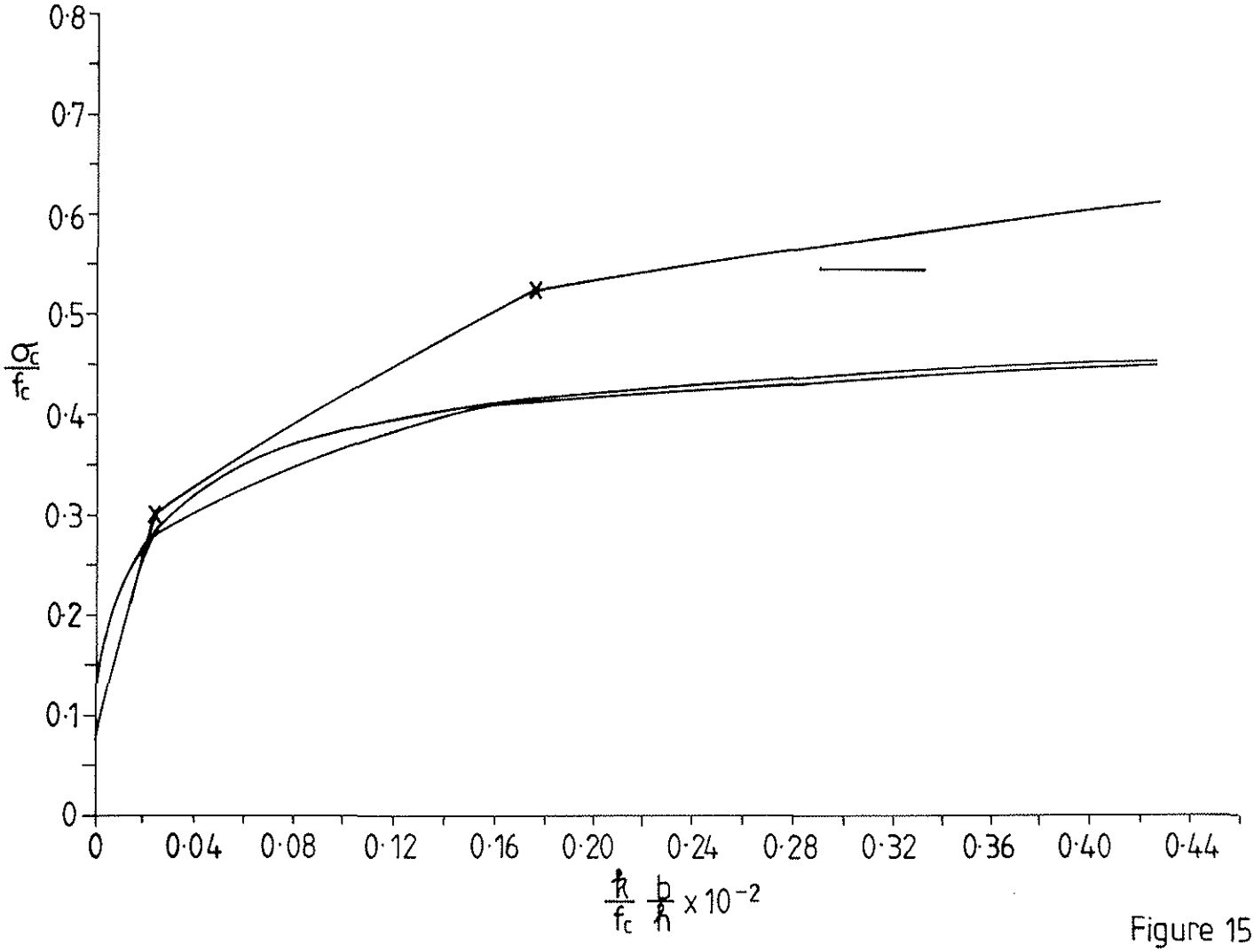

Figure 15

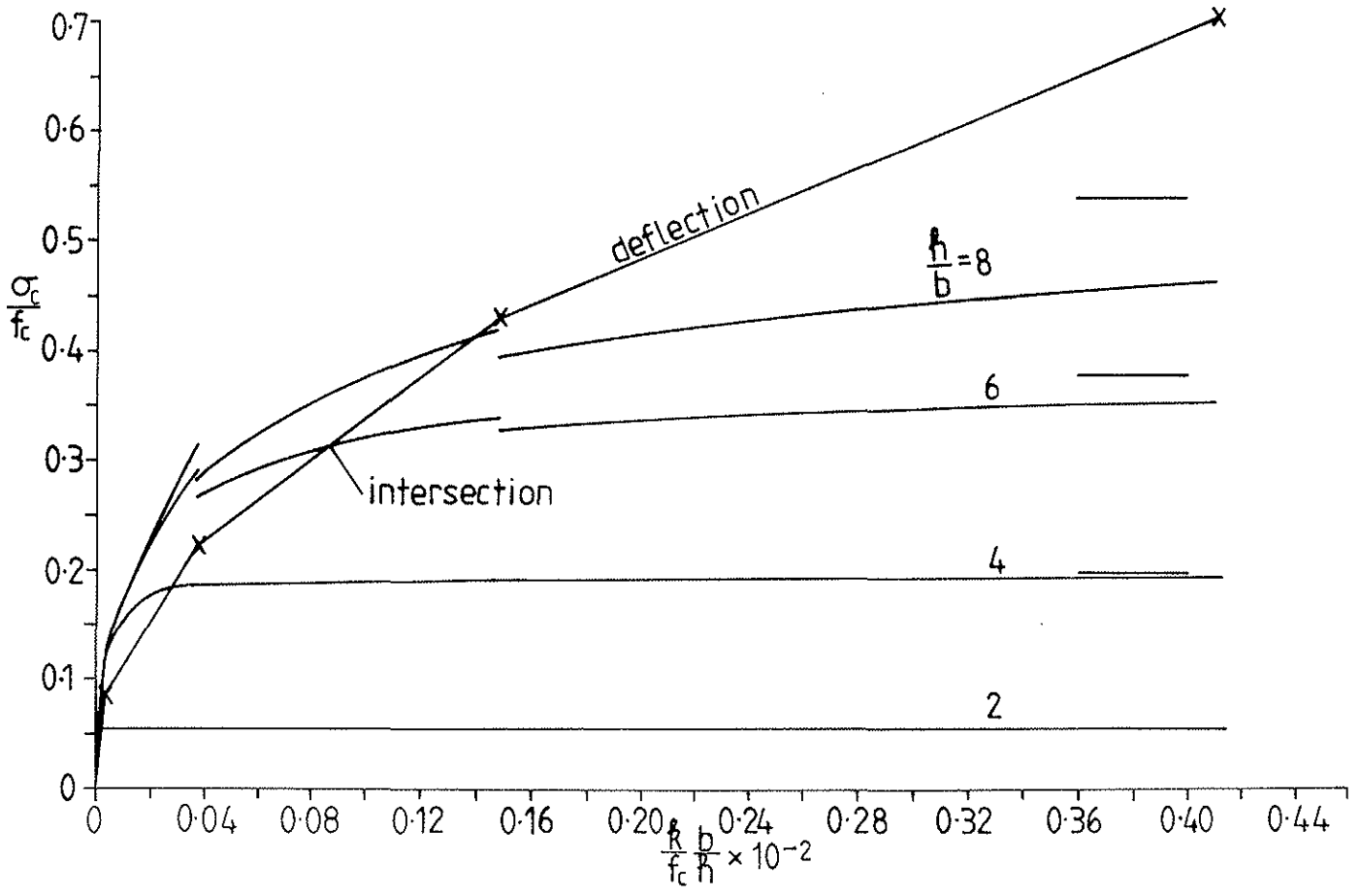

Figure 16

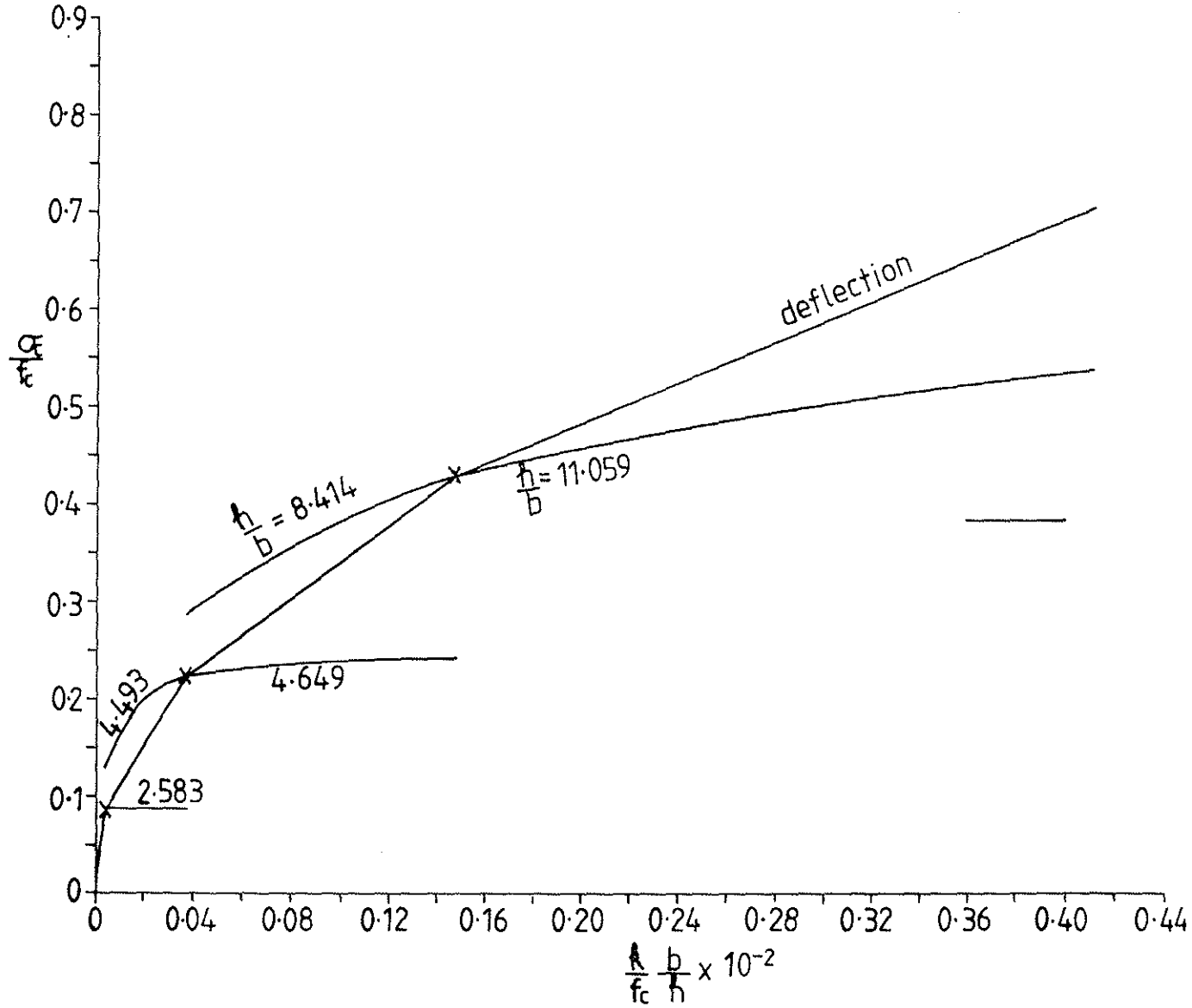
0·9
0·8
0·7
0·6
0·5
0·4
0·3
0·2
0·1
0
0
0·04
0·08
0·12
0·16
0·20
0·24
0·28
0·32
0·36
0·40
0·44
$\frac{Q}{f_c}$
$\frac{h}{f_c}\frac{b}{h} \times 10^{-2}$
deflection
$\frac{h}{b}$ = 8·414
$\frac{h}{b}$ = 11·059
4·493
4·649
2·583

Figure 17

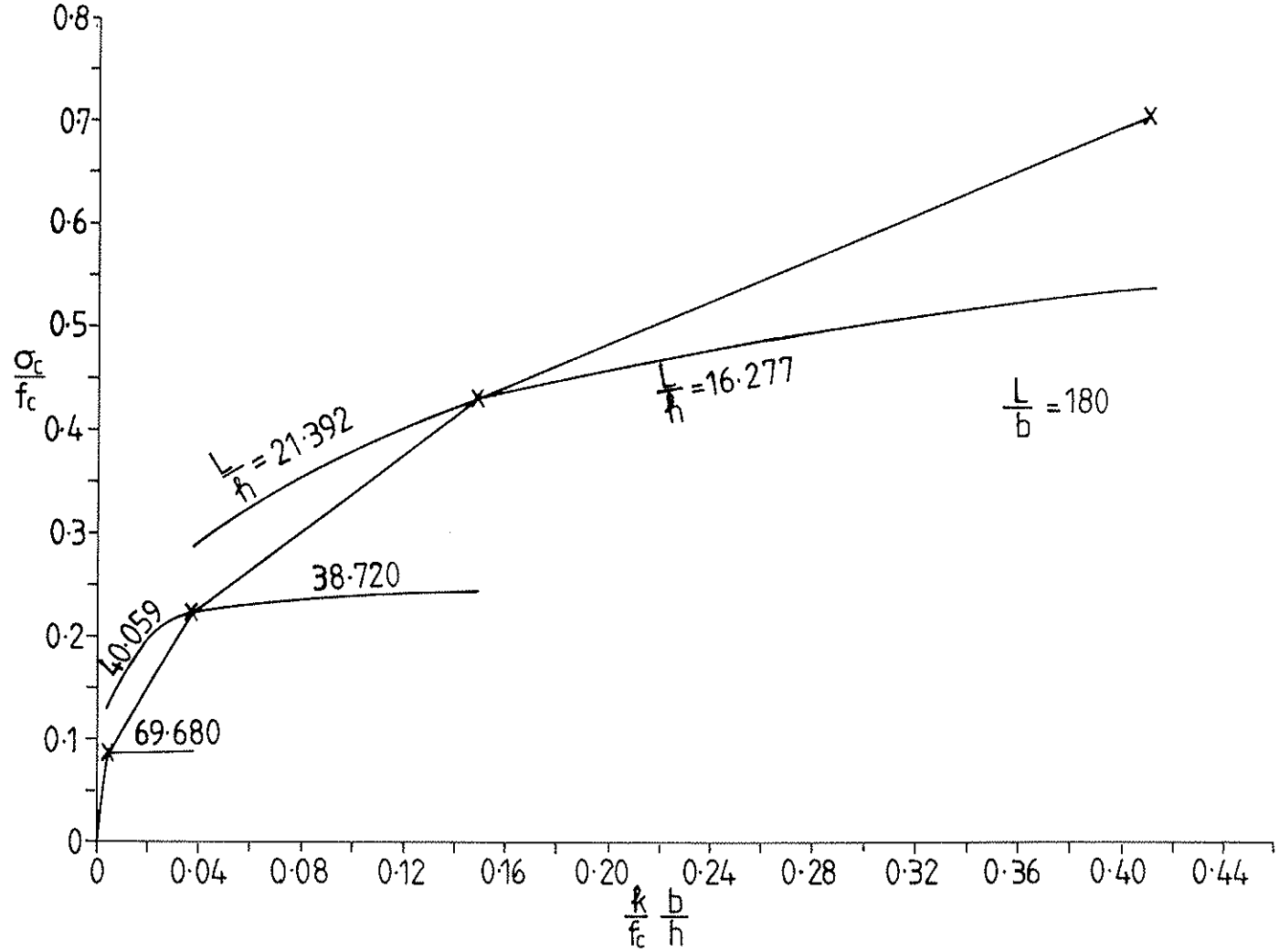
0·8
0·7
0·6
0·5
0·4
0·3
0·2
0·1
0
σc/fc
L/h = 21·392
L/h = 16·277
L/b = 180
38·720
40·059
69·680
0
0·04
0·08
0·12
0·16
0·20
0·24
0·28
0·32
0·36
0·40
0·44
f/fc b/h

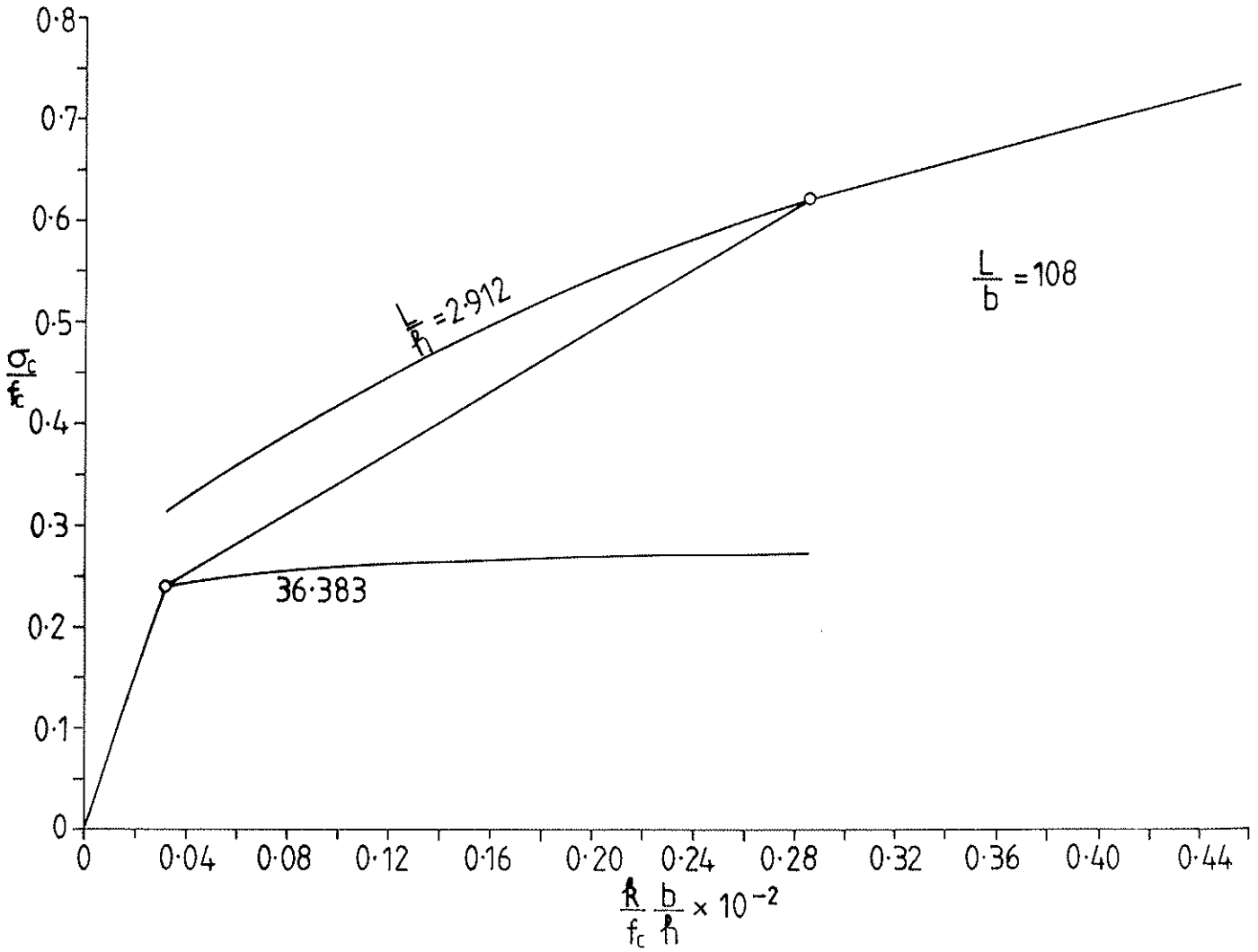
0·8
0·7
0·6
0·5
0·4
0·3
0·2
0·1
0
σc/fc
L/h = 2·912
L/b = 108
36·383
0
0·04
0·08
0·12
0·16
0·20
0·24
0·28
0·32
0·36
0·40
0·44
f/fc b/h × 10⁻²

Figure 18

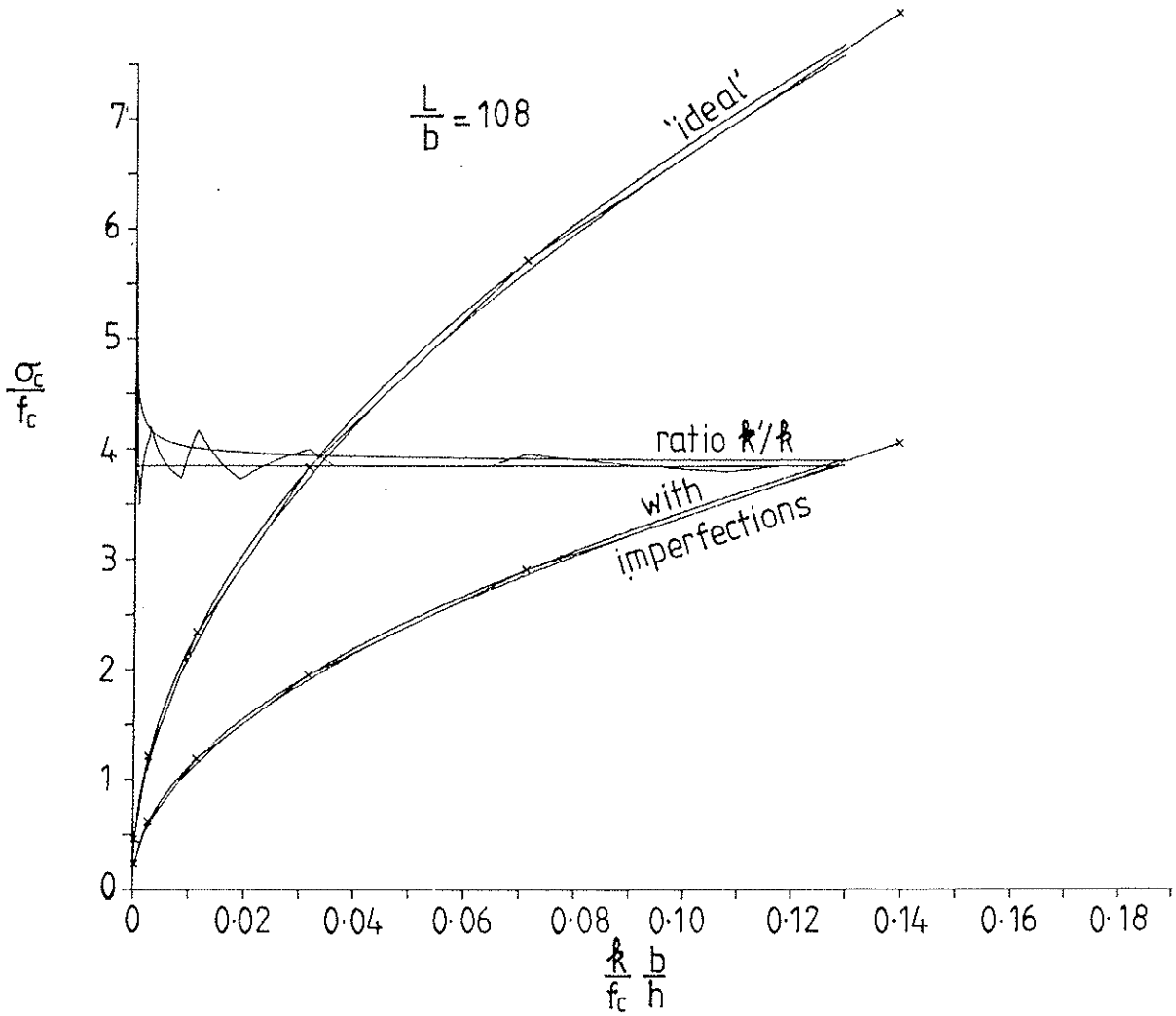

Figure 19

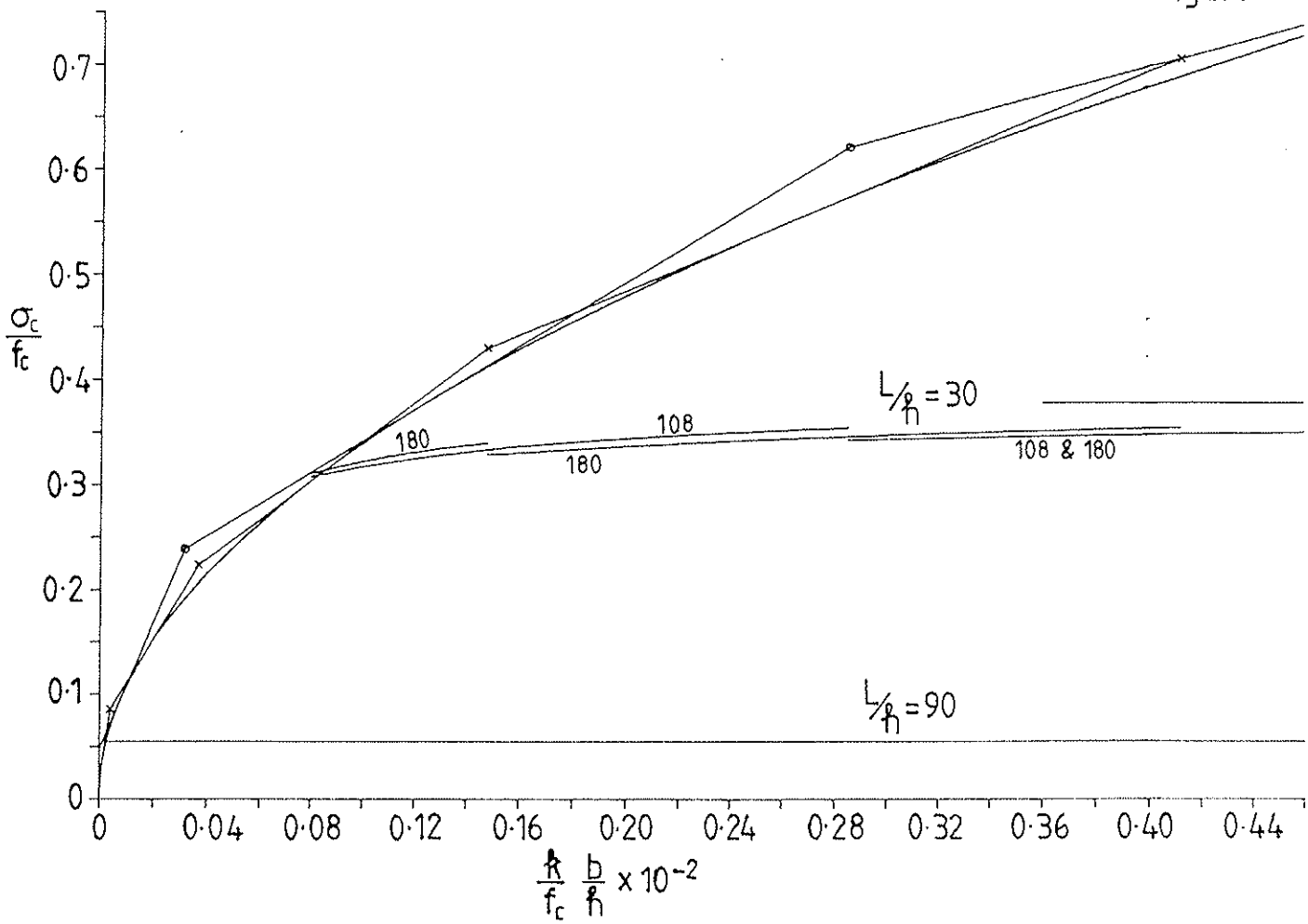

Figure 20

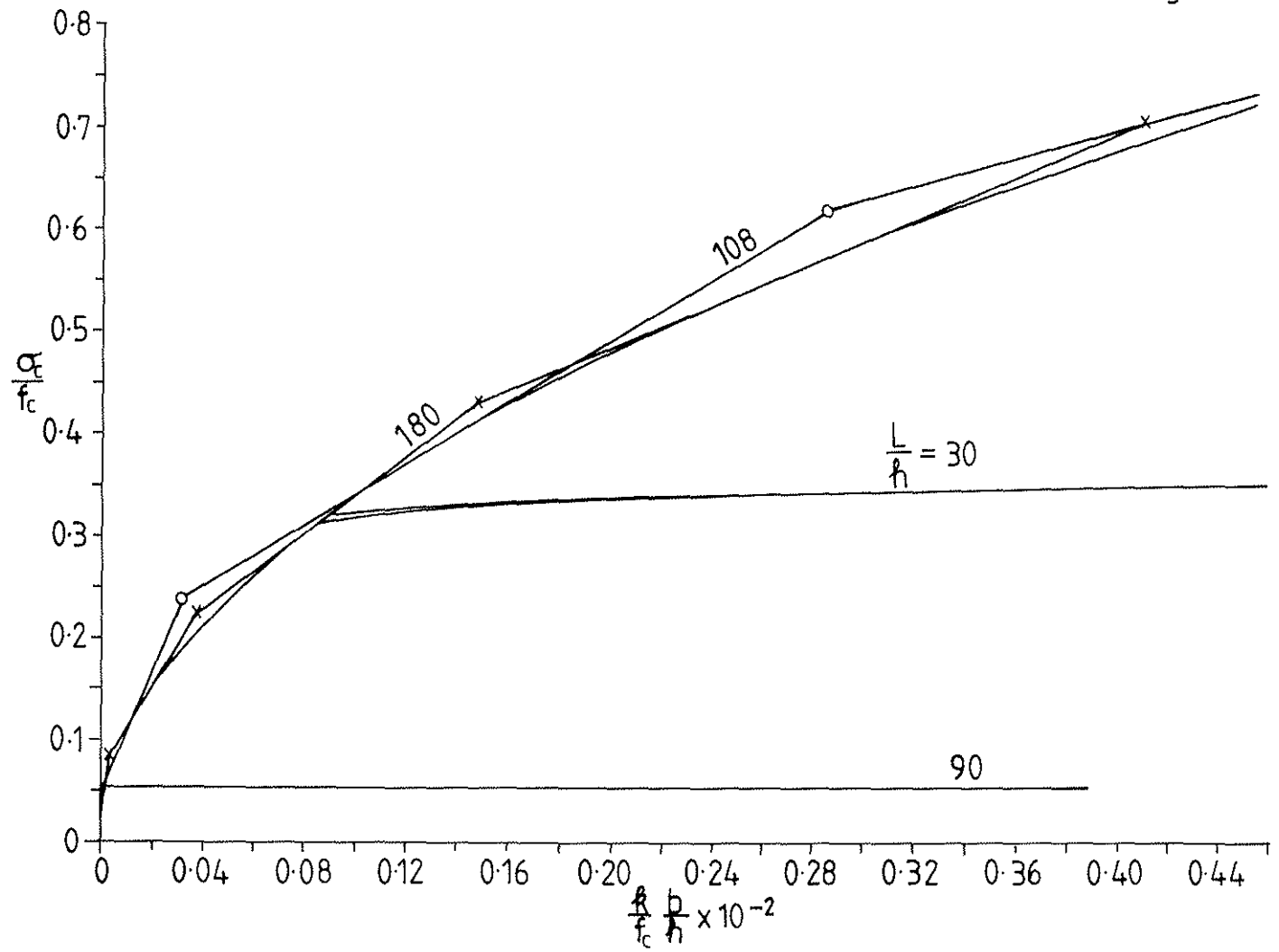

Figure 21

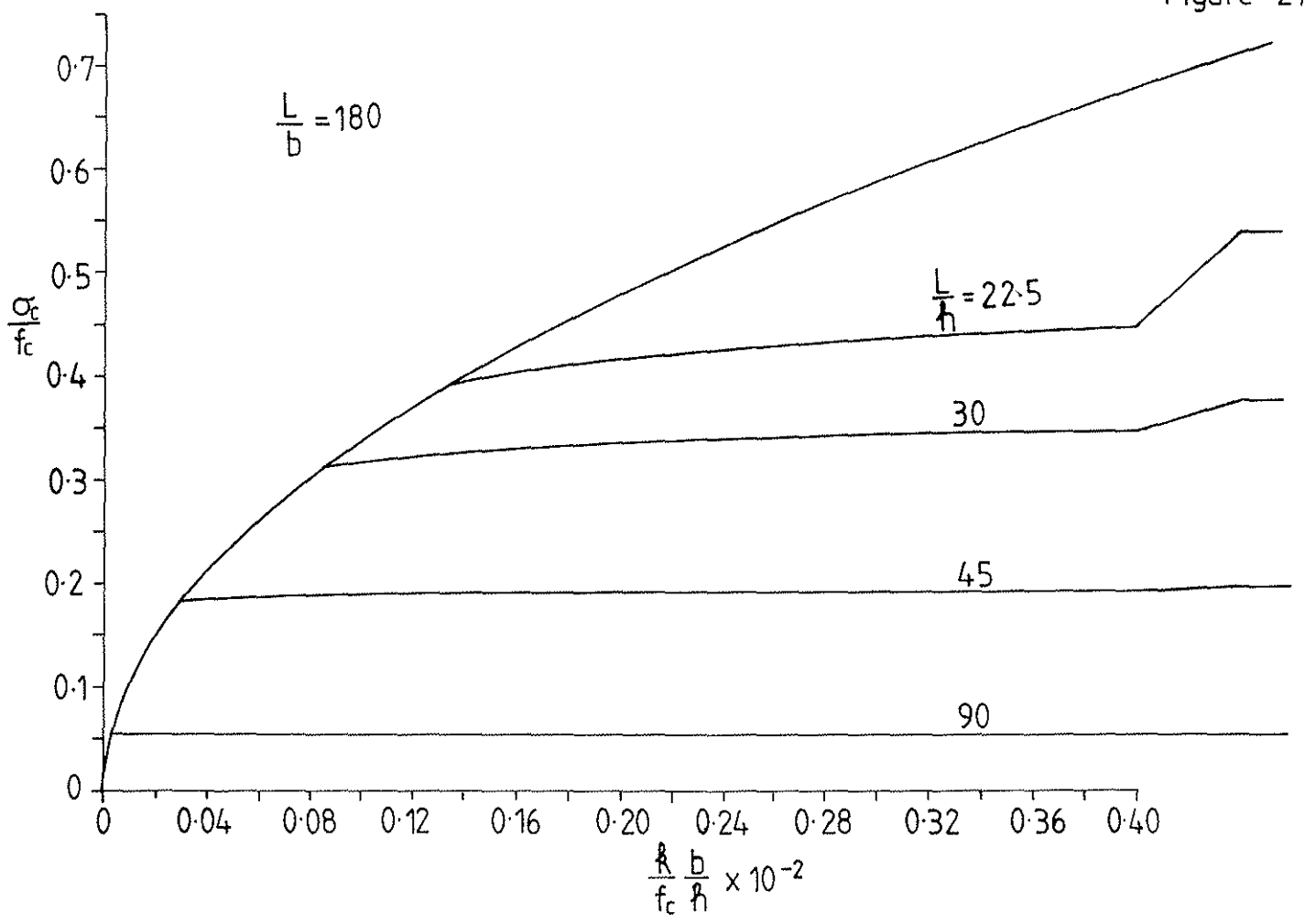

Figure 22

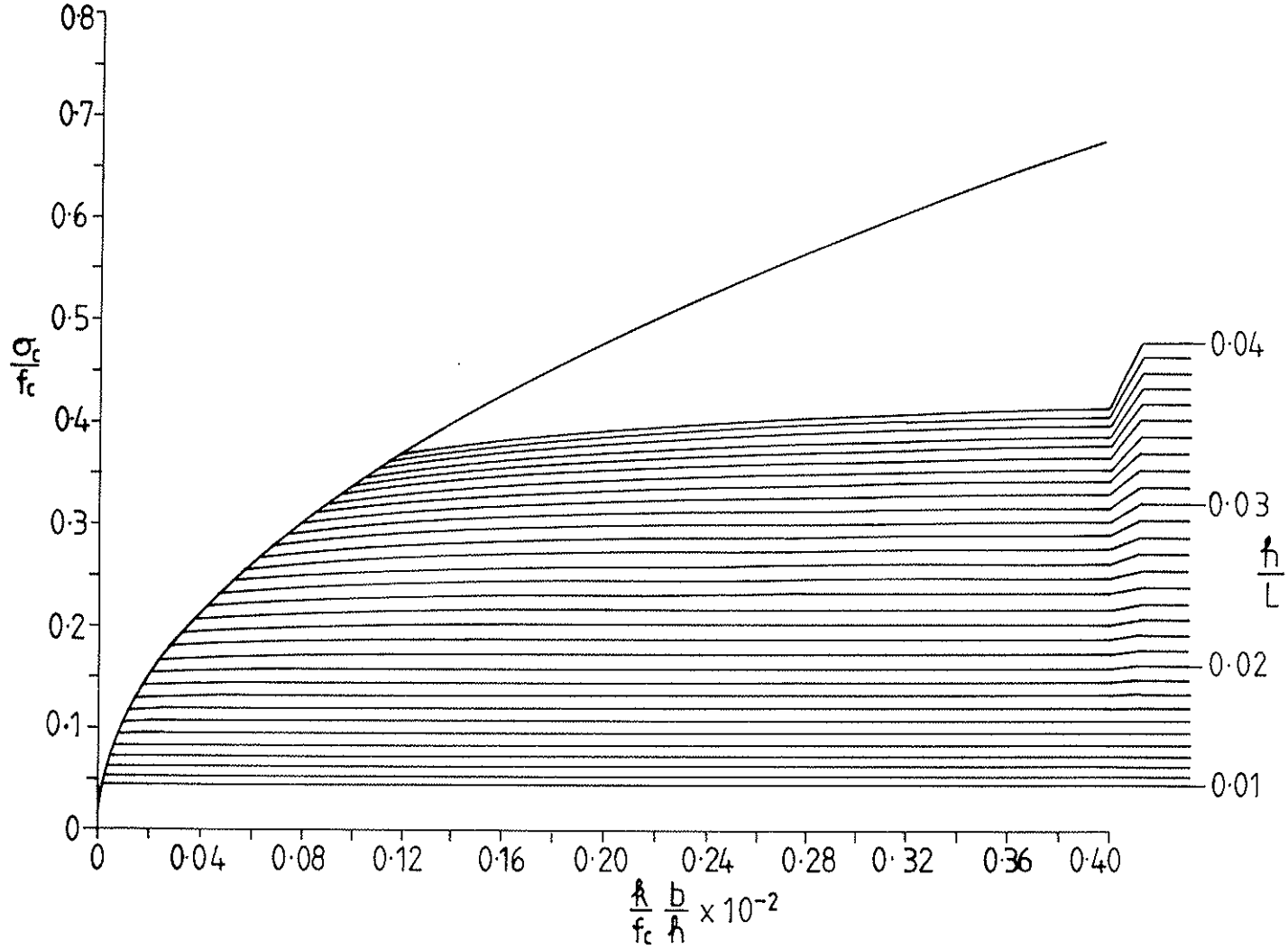

Figure 23

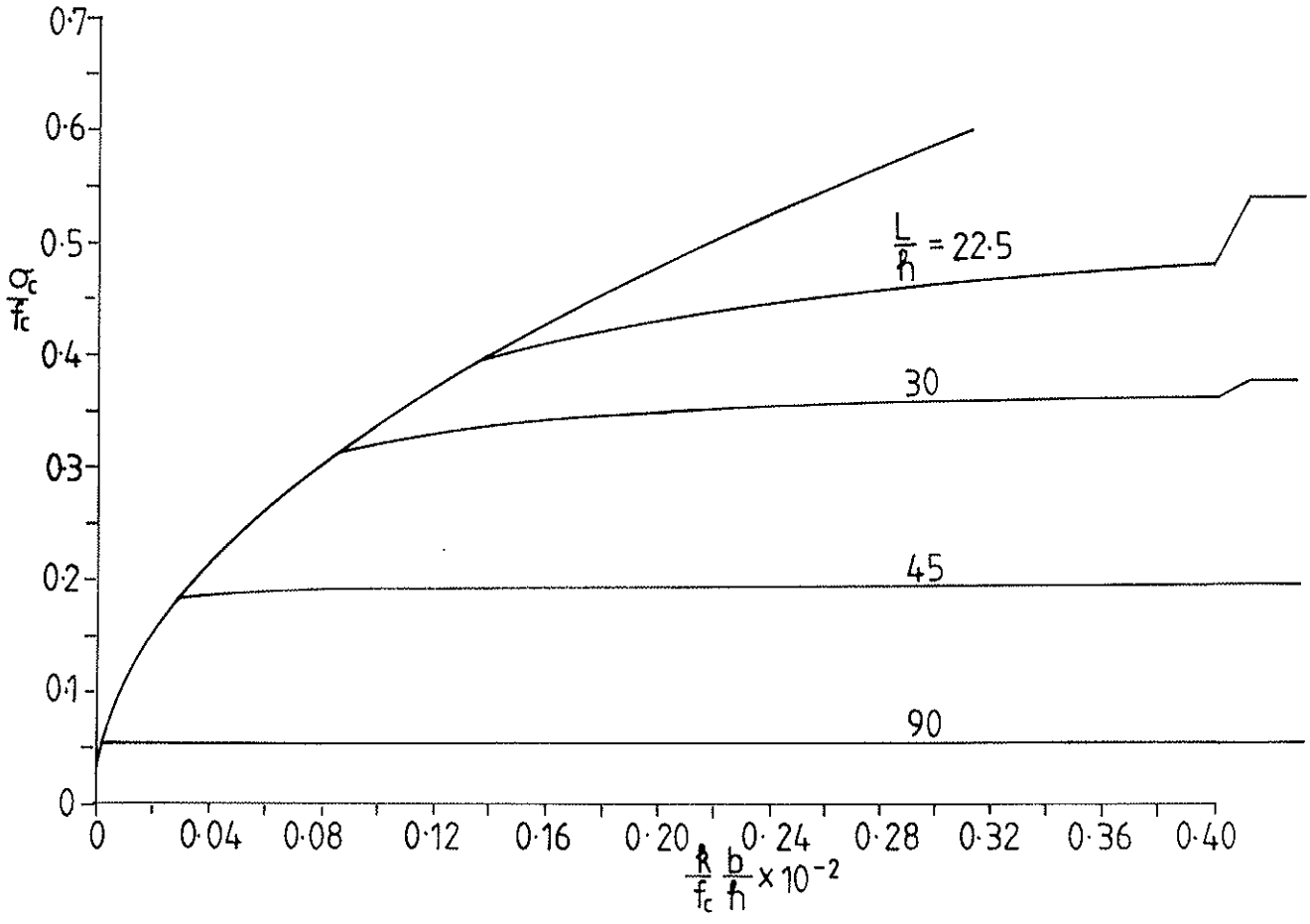

Figure 24

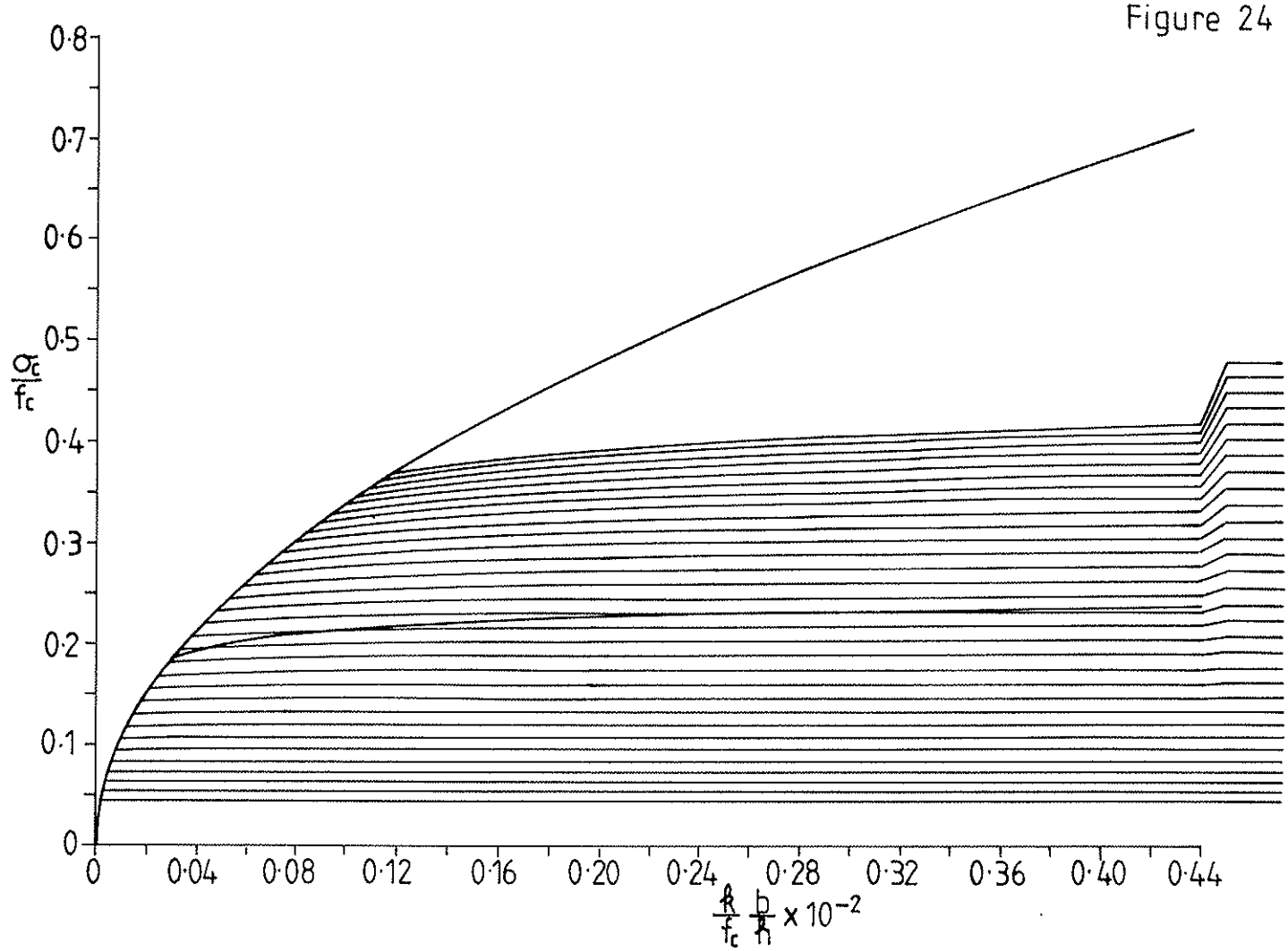

Figure 25

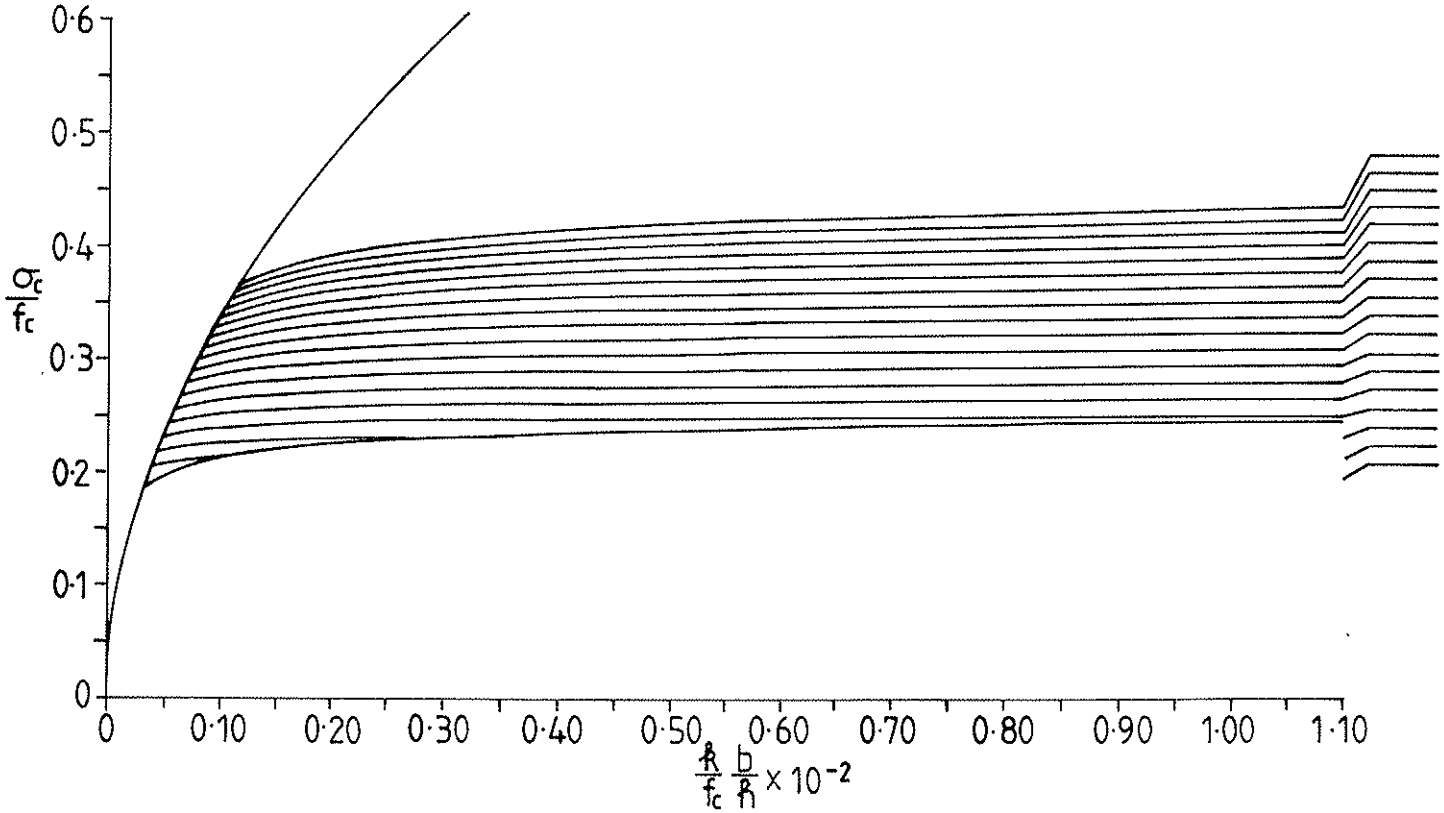

Figure 26

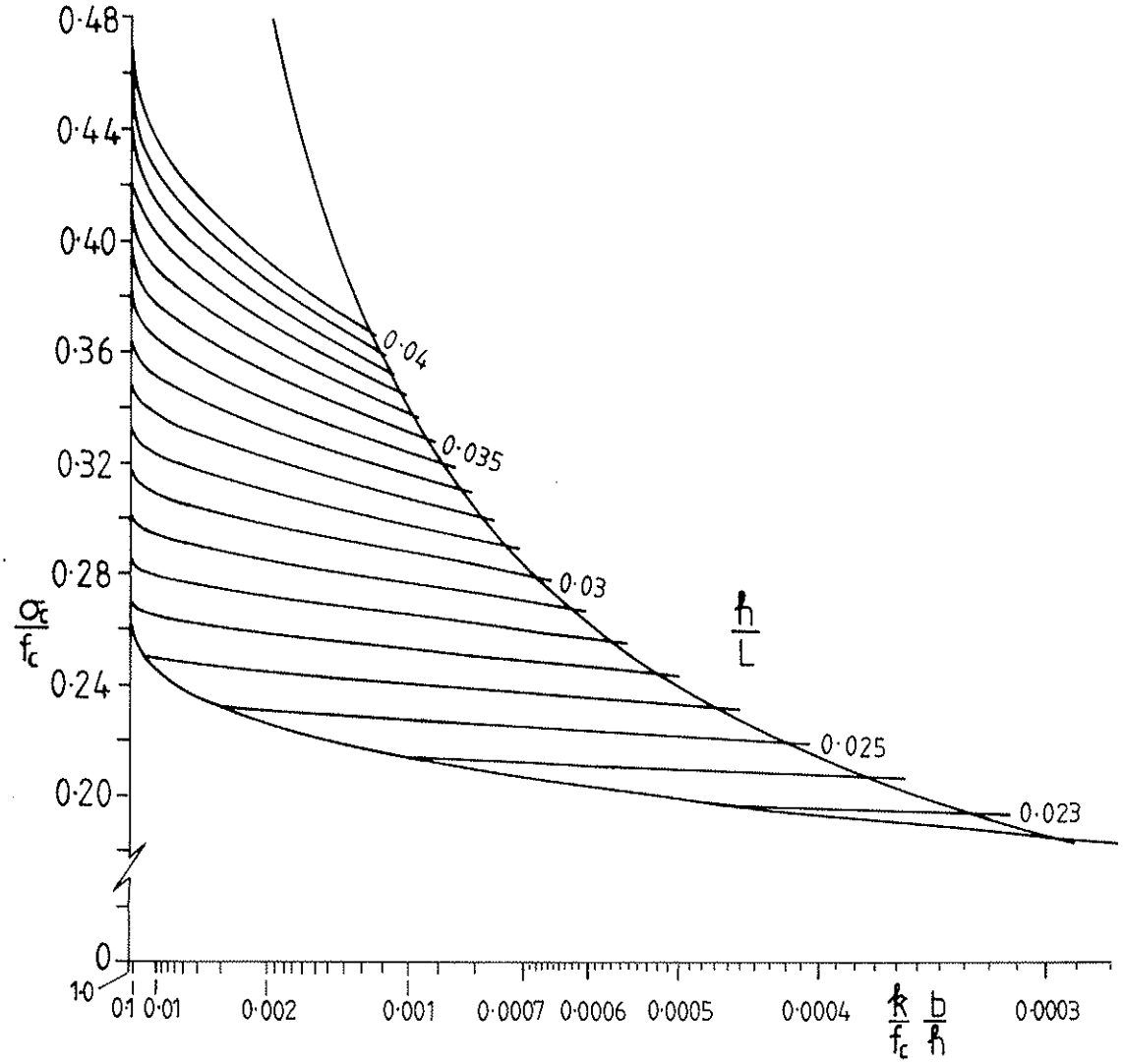

Figure 27

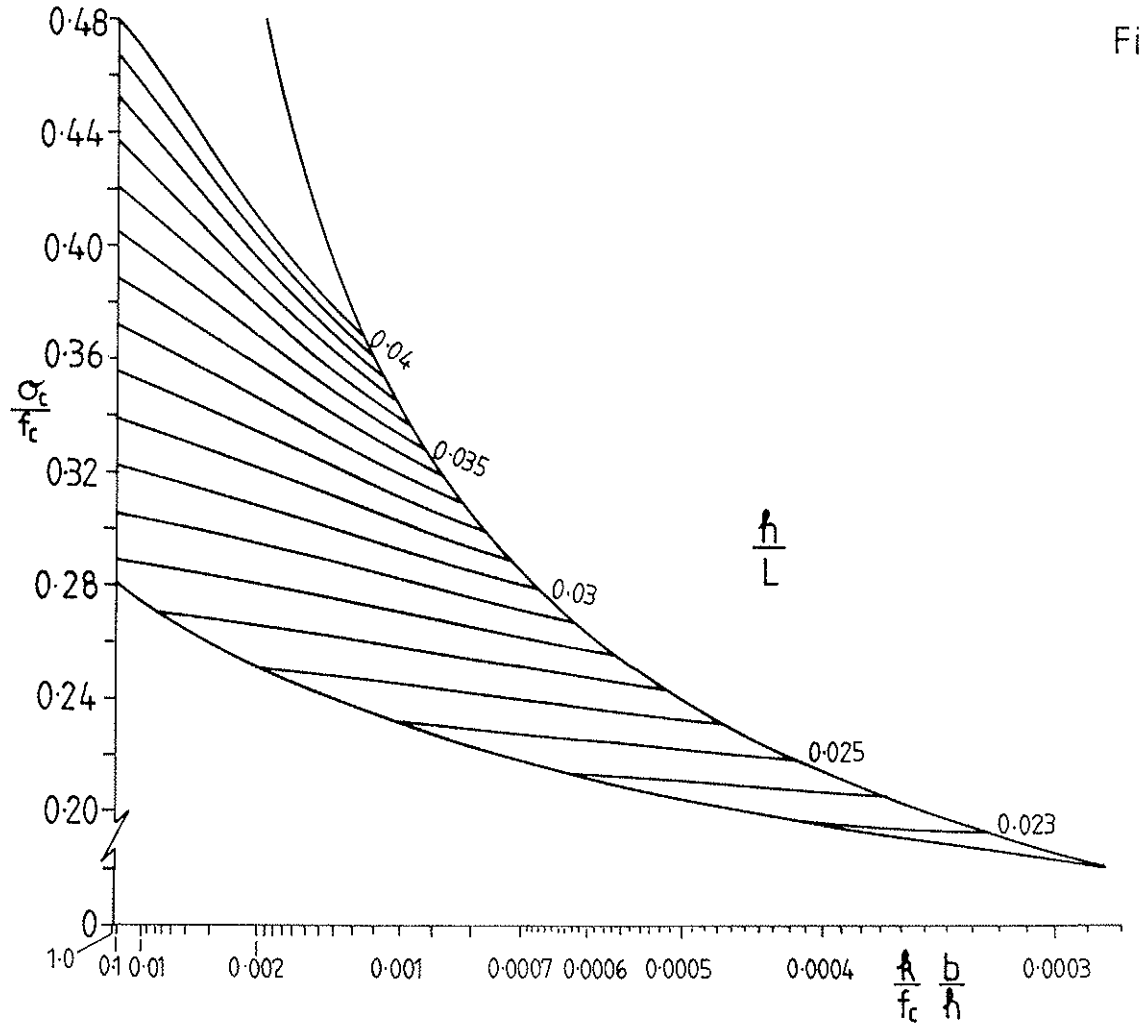

INTERNATIONAL COUNCIL FOR BUILDING RESEARCH STUDIES AND DOCUMENTATION

WORKING COMMISSION W18A - TIMBER STRUCTURES

SIMPLE APPROACHES FOR COLUMN BRACING CALCULATIONS

by

H J Burgess
Timber Research and Development Association
United Kingdom

MEETING TWENTY-ONE
PARKSVILLE, VANCOUVER ISLAND
CANADA
SEPTEMBER 1988

SIMPLE APPROACHES FOR COLUMN BRACING CALCULATIONS

The following work examines a formula for bracing given in DIN 1052 but is restricted to the simple case of column buckling. A more general approach by Brüninghoff (1983) extends also to beam-columns. The object of the present paper is to calculate the degree of approximation applied in the DIN 1052 formula, and to point out the importance of considering buckling modes higher than the first. Only sinusoidal loading is considered; the solution reached is then exact for the mathematical model involved and its adaptation for uniform load is shown by Brüninghoff.

Column with lateral load

It is rigorously proved (Timoshenko & Gere, 1961) and universally accepted that the effect of a sinusoidal lateral load on a column with initial sinusoidal curvature may be found by a special form of superposition, leading to the column formulae adopted in the CIB Code. Appendix 1 of an accompanying report (Burgess,1988a) shows that the same method is applicable to the case with elastic lateral restraint. The report does not include lateral load in addition to the restraint load acting in the opposite direction, so this case will be a further application of the method.

The deflection found from the approach leading to an extended Perry-Robertson formula is

$$u = a + u_1 = \frac{a + \frac{M}{P_e}}{1 - \frac{P}{P_e}}$$

where a is the initial deviation from straightness. This is derived in a number of papers, and corresponds to the combined stress formula which is shown by Appendix 1 to be applicable to a column with lateral restraint.

If there is both lateral (wind) load and lateral restraint the final loading on the column after deflection has taken place is a nett sinusoidal lateral load and the same theory is applicable, giving the total deflection as

$$u = \frac{a + \frac{M - M_r}{P_e}}{1 - \frac{P}{P_e}} \qquad (1)$$

where M = central value of the moment due to wind loading, taken as sinusoidal

M_r = central value of the moment due to lateral restraint, also sinusoidal

M_r generally exceeds M because the restraint loading provides for the effect of end load as well as wind load, so the lateral load is inserted as negative.

To derive a stress-limitation formula, the method proceeds by finding the central bending moment as

$$Pu + (M - M_r) = \frac{Pa}{1-\frac{P}{P_e}} + \frac{P(M-M_r)}{P_e\left(1-\frac{P}{P_e}\right)} + (M-M_r)$$

$$= \frac{Pa + (M-M_r)}{1-\frac{P}{P_e}} \qquad (2)$$

and the maximum compressive stress is

$$\frac{P}{A} + \frac{Pa}{1-\frac{P}{P_e}} \frac{h'}{Ai^2} + \frac{(M-M_r)}{1-\frac{P}{P_e}} \frac{h'}{Ai^2}$$

leading to

$$1 = \frac{\sigma_c}{f_c} + \frac{\eta\sigma_c + (\sigma_m - \sigma_r)}{f_m\left(1-\frac{\sigma_c}{\sigma_{eu}}\right)}$$

Derivation from differential equation

Equation (1) is the only formula needed to reach a comparison with the DIN 1052 formula as shown below. The same result may be derived from the single simple differential equation

$$EI\frac{d^2u_1}{dz^2} + P(u_1 + a) + M - k\frac{\ell^2}{\pi^2}u_1 = 0$$

u_1 is the additional deflection caused by the end load but resisted by the restraint. Thus the second term represents the bending moment applied by the end load P.

The last term is the moment due to the restraint stiffness of modulus k in N/mm per mm displacement. It is generated by the deflection u_1 due to wind and end loads, excluding the initial deflection, a.

The terms as written have the appearance of central values; it will be appreciated that in fact a represents $a\sin\frac{\pi}{\ell}z$, u_1 is really $u_1 \sin\frac{\pi}{\ell}z$ and $\frac{M}{P_e}$ is short for $\frac{M}{P_e}\sin\frac{\pi}{\ell}z$ where z is the distance along the braced column.

The equation to be solved for u_1 is then

$$\frac{d^2u_1}{dz^2} + \frac{P}{EI}u_1 - \frac{k}{EI}\frac{\ell^2}{\pi^2}u_1 = -\frac{P}{EI}a\sin\frac{\pi}{\ell}z - \frac{M}{EI}\sin\frac{\pi}{\ell}z$$

This is an ordinary linear differential equation with constant coefficients. The particular integral may be found exactly by the substitution

$$u_1 = B\sin\frac{\pi}{\ell}z$$

and with the end conditions $u_1 = 0$ at $x = 0$ and $x = \ell$ the sine and cosine terms of the complementary function disappear to give the complete solution with the central value

$$u_1 = \frac{\frac{P}{P_e}a + \frac{M}{P_e}}{\frac{P_{cr}}{P_e} - \frac{P}{P_e}}$$

where $$\frac{P_{cr}}{P_e} = 1 + \frac{k}{EI}\frac{\ell^4}{\pi^4}$$

Then the total central deflection is given by

$$u = u_1 + a$$

$$= \frac{a\frac{P_{cr}}{P_e} + \frac{M}{P_e}}{\frac{P_{cr}}{P_e} - \frac{P}{P_e}} \qquad (3)$$

The calculation need go no further since (3) is exactly the same as (1) and is all that is needed to derive the required bracing formula. Before showing the two expressions are identical, the work will be continued to obtain the combined stress expression and show that it is the same as the counterpart expression from the theory leading to (1).

The central bending moment is

$$Pu + M - k\frac{\ell^2}{\pi^2}u_1 = \frac{P\left(a\frac{P_{cr}}{P_e} + \frac{M}{P_e}\right) + M\frac{P_{cr}}{P_e} - M\frac{P}{P_e} - k\frac{\ell^2}{\pi^2}\left(\frac{P}{P_e}a + \frac{M}{P_e}\right)}{\frac{P_{cr}}{P_e} - \frac{P}{P_e}}$$

$$= \frac{Pa\frac{P_{cr}}{P_e} + M\frac{P_{cr}}{P_e} - k\frac{\ell^2}{\pi^2}\frac{\ell^2}{\pi^2 EI}(Pa + M)}{\frac{P_{cr}}{P_e} - \frac{P}{P_e}}$$

$$= \frac{Pa + M\left\{\frac{P_{cr}}{P_e} - \left(\frac{P_{cr}}{P_e} - 1\right)\right\}}{\frac{P_{cr}}{P_e} - \frac{P}{P_e}}$$

$$= \frac{Pa + M}{\frac{P_{cr}}{P_e} - \frac{P}{P_e}} \qquad (4)$$

and the maximum compressive stress is

$$\frac{P}{A} + \frac{Pa}{\left(\frac{P_{cr}}{P_e} - \frac{P}{P_e}\right)}\frac{h'}{Ai^2} + \frac{M}{\left(\frac{P_{cr}}{P_e} - \frac{P}{P_e}\right)}\frac{h'}{Ai^2}$$

$$= \sigma_c + \frac{\eta\sigma_c + \sigma_m}{\frac{P_{cr}}{P_e} - \frac{P}{P_e}}$$

leading to

$$1 = \frac{\sigma_c}{f_c} + \frac{\eta\sigma_c + \sigma_m}{f_m\left(\frac{\sigma_{cr}}{\sigma_{cu}} - \frac{\sigma_c}{\sigma_{cu}}\right)}$$

To show that the same result may be obtained from (1), the contribution of the restraint to the central bending moment above is

$$M_r = \frac{k\frac{\ell^2}{\pi^2}\left(\frac{P}{P_e}a + \frac{M}{P_e}\right)}{\frac{P_{cr}}{P_e} - \frac{P}{P_e}} = \frac{\left(\frac{P_{cr}}{P_e} - 1\right)\left(Pa + M\right)}{\frac{P_{cr}}{P_e} - \frac{P}{P_e}} \qquad (5)$$

and putting this in (2) gives

$$\frac{Pa+M}{1-\frac{P}{P_e}} - \frac{\left(\frac{P_{cr}}{P_e} - 1\right)\left(Pa+M\right)}{\left(1-\frac{P}{P_e}\right)\left(\frac{P_{cr}}{P_e} - \frac{P}{P_e}\right)}$$

$$= \frac{Pa+M}{\frac{P_{cr}}{P_e} - \frac{P}{P_e}}$$ which is the same as (4) and will lead to the same stress ratio summation.

Equivalence of deflection expressions

To show that (1) is the same as (3), inserting the value of M_r from (5) into (1) gives

$$u = \frac{a + \frac{M}{P_e} - \frac{k\ell^2}{\pi^2}\left(\frac{\frac{P}{P_e}a + \frac{M}{P_e}}{\frac{P_{cr}}{P_e} - \frac{P}{P_e}}\right)\frac{\ell^2}{\pi^2 EI}}{1-\frac{P}{P_e}}$$

$$= \frac{a + \frac{M}{P_e}}{1-\frac{P}{P_e}} - \frac{\left(\frac{P_{cr}}{P_e} - 1\right)\left(\frac{P}{P_e}a + \frac{M}{P_e}\right)}{\left(1-\frac{P}{P_e}\right)\left(\frac{P_{cr}}{P_e} - \frac{P}{P_e}\right)}$$

giving

$$u = \frac{a\frac{P_{cr}}{P_e} + \frac{M}{P_e}}{\frac{P_{cr}}{P_e} - \frac{P}{P_e}}$$, the same as (3).

Derivation of $\frac{P_{cr}}{P_e}$ form from equation (1)

Equation (3) was derived from the differential equation incorporating the restraint modulus k. Alternatively it may be produced directly from equation (1) manipulated to the form

$$M_r - M_w = P(a+u_1) - P_e u_1$$

where the subscript 'w' has been inserted for the wind moment. Multiplying by $\frac{\pi^2}{\ell^2}$

$$\frac{\pi^2}{\ell^2}M_r - \frac{\pi^2}{\ell^2}M_w = \frac{\pi^2}{\ell^2}P(a+u_1) - \frac{\pi^2}{\ell^2}P_e u_1 \qquad (6)$$

The first term $\frac{\pi^2}{\ell^2}M_r = q_r$ is the central value of the sinusoidal

restraint load, which equals the central deflection u_1 multiplied by the restraint modulus k, ie.

$$\frac{\pi^2}{\ell^2} M_r = k u_1$$

so $$k u_1 - \frac{\pi^2}{\ell^2} M_w = \frac{\pi^2}{\ell^2} P(a+u_1) - \frac{\pi^2}{\ell^2} P_e u_1$$

and multiplying through by $\frac{\ell^4}{\pi^4 EI}$ gives

$$\frac{k}{EI}\frac{\ell^4}{\pi^4} u_1 - \frac{M_w}{P_e} = \frac{P}{P_e}(a+u_1) - u_1 \qquad (7)$$

$$u_1\left(1+\frac{k\ell^4}{EI\pi^4}\right) = \frac{P}{P_e}(a+u_1) + \frac{M_w}{P_e}$$

$$u_1 = \frac{\frac{P}{P_e}a + \frac{M_w}{P_e}}{\frac{P_{cr}}{P_e} - \frac{P}{P_e}}$$

giving (3) when a is added.

Derivation of DIN 1052 formula

Equation (6) may be written as

$$q_{vs} = q_r - q_{vw} = \frac{\pi^2}{\ell^2} P(a+u_1) - \frac{\pi^2}{\ell^2} P_e u_1 \qquad (8)$$

Without the last term, this expression leads to a formula corresponding to the DIN 1052 formula as explained in (Bruninghoff 1983) and its source reference, where the derivation appears as

$$q_{vs} = \frac{\pi^2}{\ell^2} P(\bar{v} + f)$$

with $\bar{v} = \ell/\beta_v$ and $f = \ell/\beta_f$ so that

$$q_{vs} = \frac{P}{\ell \cdot \frac{1}{\pi^2\left(\frac{1}{\beta_v}+\frac{1}{\beta_f}\right)}} = \frac{P}{\ell k_n}$$

With $\beta_v = 400$ and $\beta_f = 1000$, $k_n \simeq 30$ giving

$$q_{vs} = \frac{P}{30\ell} \qquad (9)$$

as in DIN 1052.

Thus the DIN 1052 formula may be regarded as an approximation obtained by omitting the last term in equation (8). Looking back at equation (7) this corresponds to leaving out the '1' in the expression

$$\frac{P_{cr}}{P_e} = 1 + \frac{k}{EI}\frac{\ell^4}{\pi^4}$$

To plot (8) with and without its last term in the style of a related report (Burgess, 1986b) and retaining the values $a = 0.002887\ell$ and $u_1 = 0.003\ell$, the expression derived from (8) is

$$\frac{\sigma_c}{f_c} = 0.5096\left[\frac{\sigma_{cu}}{f_c} + \left(\frac{k}{f_c}\frac{b}{h}\right)\left(\frac{\ell/b}{\pi}\right)^2\right] \qquad (10)$$

and the same but excluding $\frac{\sigma_{cu}}{f_c}$.

The effect of the approximation is shown in Figure 1 for the values L/b =180 and 108 used previously. The lower of the two parallel lines in each diagram is drawn excluding $\frac{\sigma_{cu}}{f_c}$, giving a reasonable approximation for first mode behaviour.

For higher values of $\frac{k}{f_c}\frac{b}{h}$ the first mode expression will lead to values much greater than those corresponding to multiple-mode behaviour.

Both (8) and (9) are derived by limiting the maximum deflection. The related paper indicates that a combined stress limitation will become more restrictive if the graphs are taken to higher levels of $\frac{\sigma_c}{f_c}$ and $\frac{k}{f_c}\frac{b}{h}$.

REFERENCES

1. Brüninghoff, H. (1983) - Determination of bracing structures for compression members and beams. CIB-W18 paper no. 16-15-1, Lillehammer, May/June 1983. Also see Bemessung von aussteifungsverbänden fur druckstäbe und für biegeträger, in Ingenieurholzbau in Forschung und Praxis, ed. Ehlbeck, J., Steck, G. & Mohler, K., Bruderverlag, Karlsrühe 1982.

2. Burgess, H.J.(1988a) - Rectangular section deep beam-columns with continuous lateral restraint. CIB-W18 paper no. 21-15-1, Vancouver, 1988.

3. Burgess, H.J. (1988b) - Buckling modes and permissible axial loads for continuously braced columns. CIB-W18 paper no. 21-15-2, Vancouver, Sept. 1988.

4. Timoshenko, S.P. & Gere, J.M. (1961) - Theory of elastic stability, 2nd edition, Mc Graw - Hill, London 1961.

Figure 1

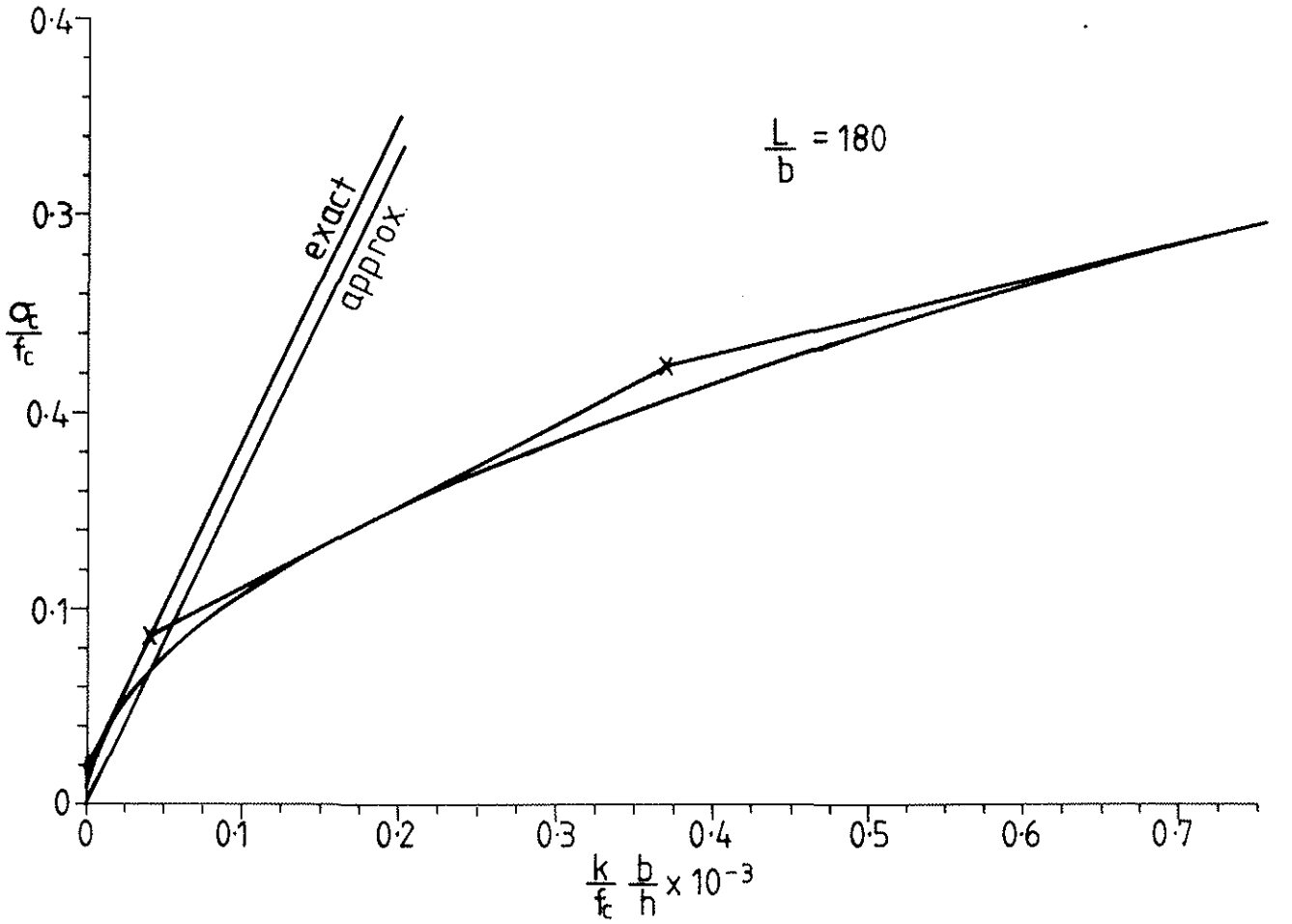
0·4
0·3
0·4
0·1
0
$\frac{\sigma_t}{f_c}$
$\frac{L}{b}$ = 180
exact
approx.
0
0·1
0·2
0·3
0·4
0·5
0·6
0·7
$\frac{k}{f_c}\frac{b}{h} \times 10^{-3}$

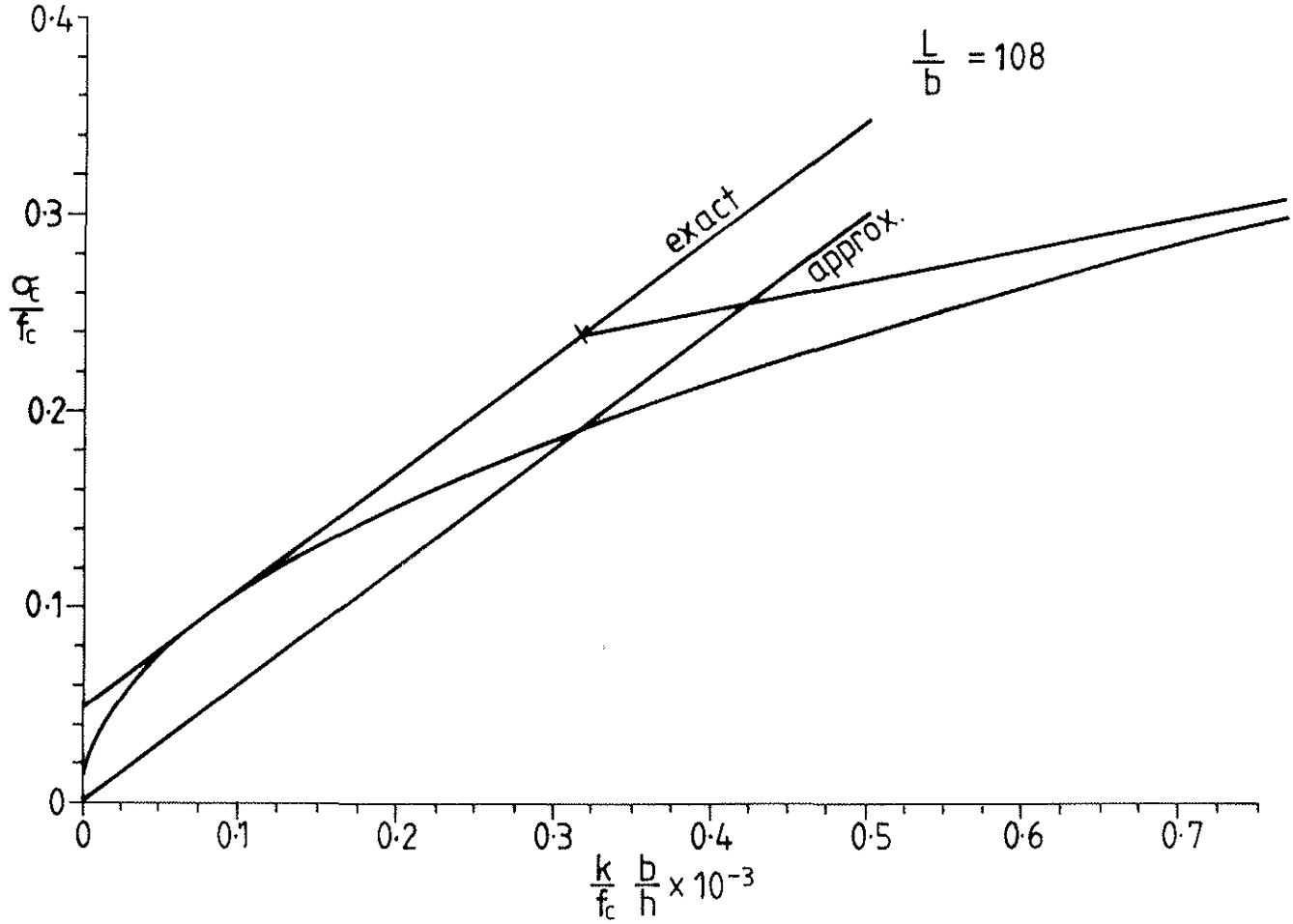
0·4
0·3
0·2
0·1
0
$\frac{\sigma_t}{f_c}$
$\frac{L}{b}$ = 108
exact
approx.
0
0·1
0·2
0·3
0·4
0·5
0·6
0·7
$\frac{k}{f_c}\frac{b}{h} \times 10^{-3}$

CIB-W18A/21-15-4

INTERNATIONAL COUNCIL FOR BUILDING RESEARCH STUDIES AND DOCUMENTATION

WORKING COMMISSION W18A - TIMBER STRUCTURES

CALCULATIONS FOR DISCRETE COLUMN RESTRAINTS

by

H J Burgess
Timber Research and Development Association
United Kingdom

MEETING TWENTY-ONE
PARKSVILLE, VANCOUVER ISLAND
CANADA
SEPTEMBER 1988

CALCULATIONS FOR DISCRETE COLUMN RESTRAINTS

A method of calculating the required stiffness and strength of column braces at discrete intervals may be derived from a recent study (Burgess, 1988) although it dealt with continuously restrained columns. The approach is suggested by that of Brüninghoff (1983) but takes account of buckling in modes higher than the first. The object will be to limit deflection to a certain fraction of the mode length, here taken as 0.003, on the assumption that separate calculations provide for limiting the maximum stress in the unsupported length if this is a more restrictive condition.

The previous study developed a formula for the permissible end stress in a continuously braced column as

$$\frac{\sigma_c}{f_c} = 0.5096\sqrt{\frac{E}{3f_c}\left(\frac{k}{f_c}\frac{b}{h}\right)} \qquad (1)$$

This is a curve tangential to the straight-line segments showing the permissible end stress for each buckling mode of a member of given slenderness L/b. The expression is independent of L/b and gives a conservative approximation for every slenderness ratio, to limit the deflection as desired for all buckling modes. The figure 0.5096 is based on an initial deviation from straightness of 0.002887ℓ equivalent to a value of η of 0.005 together with the deflection limit of 0.003 times the mode length, and is retained here for easy recognition in comparison with related reports.

From (1) $$\sigma_c^2 = (0.5096)^2 \frac{E}{3} k \frac{b}{h}$$

Multiplying by b^2 h^2 , the load limited by deflection is P in

$$P^2 = (0.5096)^2 \times 4EIk$$

From equation (25) of the previous report the origin of the figure 0.5096 may be traced as

$$\frac{u_1}{u_o+u_1} = \frac{0.003\ell}{(0.002887+0.003)\ell} = 0.5096$$

so $$P^2 = \left(\frac{u_1}{u_o+u_1}\right)^2 \times 4EIk$$

giving $$k = \left(\frac{u_o+u_1}{u_1}\right)^2 \frac{P^2}{4EI}$$

The calculation will later be related to a column of length L with a brace spacing of ℓ, having braces stiff enough to force a mode m with a half-wave length equal to the brace spacing so that $\ell = \frac{L}{m}$ as shown in Figure 1. If the continuously restrained column has a k value high enough to force this mode, the maximum displacement of the continuous restraint will occur at the centre of each mode length with the value u_1 .

The required restraint strength is therefore ku_1 at any point. That is, the resisting structure must be strong enough to exert a reaction of ku_1 without becoming overloaded.

The required maximum strength of the continuous restraint may alternatively be defined by considering the first mode shape of the column although the value of k is such that it actually buckles in mode m and never in the first mode. This is done so that when the continuous restraint is replaced by a row of discrete braces, the stiffness 'gathered' into each brace can be seen as $K = k\ell = k\ \frac{L}{m}$ and the maximum 'gathered strength' is $Q = k\ell \times u_1$, remembering that the maximum displacement is $u_1 = 0.003\ell$ in the actual buckled shape of mode m. This calculation allows for uniform load although the loading in the diagram is actually sinusoidal.

Still keeping to the continuously-restrained condition but bearing in mind that the restraint may be applied by a row of discrete braces, the maximum gathered strength in a brace will be

$$Q = k\ell \times u_1 = \left(\frac{u_0 + u_1}{u_1}\right)^2 \frac{P^2}{4EI}\ \frac{L}{m}\ u_1$$

$$= \frac{(0.002887 + 0.003)^2\ \ell^2}{0.003\ \ell}\ \frac{P^2}{4EI}\ \frac{L}{m}$$

$$= 0.01155\ \frac{P^2}{4EI}\ \frac{L^2}{m^2}$$

or $$\frac{Q}{P} = 0.001155\ \frac{P}{m^2 P_e}\ \frac{\pi^2}{4}$$

$$\frac{Q}{P} = 0.0285\ \frac{P}{m^2 P_e} \qquad (2)$$

- where $P_e = \frac{\pi^2 EI}{L^2}$ is the Euler load for the full length L.

Discrete bracing

When the continuous restraint is replaced by a row of braces which is still stiff enough to force mode m, an important change is that the mode length ℓ then has no lateral restraint. If the object is still to limit its deflection to 0.003ℓ, the permissible end force P will be reduced to a value which may be found from equation (23) of the previous report by writing $\frac{P_{cr}}{P'_e} = 1$ for zero restraint to give

$$u_1 = \frac{\frac{P}{P'_e}}{1 - \frac{P}{P'_e}}\ u_0$$

from which $$\frac{P}{P'_e} = \frac{u_1}{u_0 + u_1} = 0.5096$$

where P'_e is the Euler load for the mode length , i.e. $P'_e = m^2 P_e$ giving

$$\frac{P}{m^2 P_e} = 0.5096 \qquad (3)$$

Inserting this in (2) gives

$$\frac{Q}{P} = 0.0285 \times 0.5096$$

$$\frac{Q}{P} = 0.01452$$

This result stating that the necessary strength of each brace is about 1½ percent of the force in the column has a form very familar to users of certain design codes. In the British code for steelwork design it appears as 2½ percent and in an earlier version of DIN 1052 the figure used was 1 percent.

Different writers have indicated that the origin of the `2½ per cent rule` (for example) is obscure. A possible source has recently been suggested (Steer, 1988) but the 1931 text-book referenced gives an obviously incorrect reasoning; it is mentioned only because it shows that the 2½% and 1% figures were established before 1931, in advance of the 1933 paper described below.

From the development above it is evident that the important feature of the brace is its stiffness rather than its strength, since it is the stiffness modulus k which forces the desired mode when the restraint is continuous, and this is substituted by the gathered stiffness K when the continuous restraint is approximated by a series of equally spaced braces. However a required stiffness accompanied by the deflection limitation which is the object of the work does lead to a strength requirement as emphasised by Winter (1952).

The `gathered strength` $Q = k\ell \times u_1$ used above corresponds to uniform loading. If instead the load on each half-wave is taken as $\frac{2\ell}{\pi}\ ku_1$ for a sinusoidal distribution the result reached is $\frac{Q}{P} = 0.01452 \times \frac{2}{\pi} = 0.00924$, within the 1% formerly used in DIN 1052.

Direct approach for discrete bracing

Another approach leading to rather similar conclusions is given by Timoshenko and Gere (1961), making reference to work by Klemperer and Gibbons (1933). Before giving their results without repeating the derivation, the type of approach above will be shown to reach an expression of similar form when applied to the `ideal` columns considered by Klemperer and Gibbons. This is surprising since the work above follows an entirely different method starting with an idealised approximate curve independent of mode numbers.

The tangential curve for the ideal column in equation (45) of the previous report was

$$\frac{P_{cr}}{P_e} = 2\frac{L^2}{\pi^2}\sqrt{\frac{k}{EI}}$$

Leaving out the subscript `cr`, this corresponds to

$$\frac{\sigma_c}{f_c} = \sqrt{\frac{E}{3f_c}\left(\frac{k}{f_c}\frac{b}{h}\right)}$$

or $P^2 = 4EIk$ c.f. above

$$k = \frac{P^2}{4EI}$$

Gathered stiffness $K = \frac{P^2}{4EI}\frac{L}{m}$

$$= \frac{P^2}{4P_e}\frac{\pi^2}{Lm}$$

But the limit on P is $m^2 P_e$ where P_e refers to the full length, so

$$K = \alpha = \frac{\pi^2}{4}\frac{m^3 P_e}{L} \qquad (4)$$

$$\alpha = \frac{m^3 P_e}{\gamma L}$$

with $\gamma = \frac{4}{\pi^2} = 0.405$

α is the symbol corresponding to K in the reference quoted, which reaches the same formula but gives a table of γ values for different modes.

The result as stated by Timoshenko and Gere is

$$\alpha = \frac{mP}{\gamma L}$$

where $P = m^2 \pi^2 EI/L^2$ is the critical load for a single half-wave,

i.e. $\alpha = \frac{m^3 P_e}{\gamma L}$ if P_e refers to the full length. The table of γ values is as follows

Table 2-3. Values of the Factor in Eq. (2-30)

m	2	3	4	5	6	7	9	11
γ	0.500	0.333	0.293	0.276	0.268	0.263	0.258	0.255

Taking m = 3 as an example and using K instead of α for the required brace stiffness gives

$$K = 81\frac{P_e}{L}$$

To force mode 4, $K = 218.4\frac{P_e}{L}$

so mode 3 is appropriate for K ranging between these two values.

As in previous work, the same stiffness limits will be assumed for the case in which each mode length has an initial sinusoidal curvature. With no within-mode restraint, the permissible end load P may be found from (3) for each mode.

Taking a 37.5 x 300 mm column with length 6750 mm,

$$P_e = \frac{\pi^2 EI}{L^2} = 2998 \text{ N}$$

and the value of P applicable throughout the stiffness range of mode 3 will be

$$P = 0.5096 \times 9 \times 2998 = 13750 \text{ N}.$$

Figure 2 shows P plotted for each mode, calculated using the tabulated γ values.

Comparison with 1½ percent rule

To compare the results by Klemperer and Gibbons (1933) with the `1½ per cent` rule developed above, another graph similar to Figure 2 is needed. The stiffness limits are given by (4) and the permissible end load P is again obtained from (3), leading to the graph shown in Figure 3. This rises more steeply than Figure 2, indicating that the 1½ per cent rule underestimates the necessary bracing stiffness compared with that found by Klemperer and Gibbons. The stiffnesses calculated by the two methods are given in the following table, with their ratio shown in the bottom line.

m	2	3	4	5	6	7	9	11
K	7.10	36.00	97.00	201.13	357.13	579.19	1254.84	2318.03
$K_{1½}$	8.77	29.60	70.14	137.00	236.70	375.93	798.98	1458.70
$K/K_{1½}$	0.81	1.22	1.38	1.47	1.51	1.54	1.57	1.59

The ratio is fairly constant for higher modes. Using its maximum value of 1.59 to multiply the value $\frac{Q}{P} = 0.01452$ which gave the `1½ percent rule` above, this becomes

$$\frac{Q}{P} = 0.01452 \times 1.59$$

$$\frac{Q}{P} = 0.0231$$

The `2½ percent rule` of the British steel code thus seems very appropriate in relation to the work by Klemperer and Gibbons when it is adapted to limit within-mode deflection for members with initial curvature of the type adopted for the calculations above.

Direct derivation of 2½% rule

This `rule` was derived very roughly by comparing the results of calculations for discrete and continuous bracing. It may also be derived directly from the work quoted by Timoshenko & Gere as follows.

The minimum brace stiffness for mode m is obtained from the theory for ideal columns as

$$K = \frac{m^3 P}{\gamma L} e \qquad (5)$$

The permissible end load limited by deflection is

$$P = 0.5096\ m^2\ P_e$$

and substituting for P_e in (5) gives

$$K = \frac{mP}{0.5096\gamma L}$$

In the work on continuous bracing, gathered stiffness was converted to gathered strength by multiplying by $u_1 = 0.003\ \frac{L}{m}$, assuming this as the maximum permissible deformation of the continuous restraint. Adopting a similar limitation for the discrete bracing, i.e. the displacement of the brace may not exceed $0.003\frac{L}{m}$, the required restraint force is

$$Q = Ku_1 = 0.003\frac{L}{m} \times \frac{mP}{0.5096\gamma L}$$

$$\frac{Q}{P} = \frac{0.003}{0.5096\gamma} = \frac{0.005887}{\gamma}$$

As the number of braces increases, γ tends to the value 0.250, so the maximum required brace strength is

$$\frac{Q}{P} = \frac{0.005887}{0.250} = 0.0235$$

for which a `2½ per cent rule` is seen to be appropriate.

The figure 0.005887 is recognizable as the sum of the coefficients of $0.003\frac{L}{m}$ for the deflection limitation u_1, and $0.002887\frac{L}{m}$ for the initial deviation from straightness corresponding to $\eta = 0.005\ell/i$. The corresponding results for the η values in EC5 would be

$$\text{solid members, } \eta = 0.006, \qquad \frac{Q}{P} = 0.0258$$

$$\text{glulam members, } \eta = 0.004, \qquad \frac{Q}{P} = 0.0212$$

A $2\frac{1}{2}\%$ rule would cater for up to 9 braces for solid members or any number for glulam.

Brief derivation

Accepting the results by Klemperer and Gibbons including their γ values, the briefest derivation is obtained without discussing stiffness limits using expression (v) of Art. 2.6 in Timoshenko and Gere. Writing $Q = \alpha\delta$ where δ is the maximum permissible deflection of the support, (v) with amendments to suit the symbol usage $L = m\ell$ becomes

$$\frac{Q}{\delta} = \frac{P'_e}{\gamma\ell}$$

and using $P = 0.5096P'_e$,

$$P = 0.5096\frac{Q\ell\gamma}{\delta}$$

With $\delta = 0.003\ell$,

$$P = \frac{0.5096}{0.003} Q\gamma$$

$$\frac{Q}{P} = \frac{0.003}{0.5096\gamma} = 0.0235 \text{ as before.}$$

Writing $\delta = 0.003\ell$ cannot be justified properly without a deeper study of the work.

Comparison of uniform and discrete restraint

It may be wondered why a 2½% rule is obtained for the direct approach using Klemperer and Gibbons, compared with the 1½% rule derived by considering 'gathered stiffness' in the case of continuous restraint.

This is because the two approaches are not really compatible. It is not possible to approach continuous restraint by raising the number of discrete braces because within-mode restraint is still lacking in the small distance between closely-spaced braces.

Both approaches limit within-mode deflection to 0.003 x mode length. With discrete bracing the permissible end load is then $0.5096m^2 P_e$, but with continuous bracing equation (44) of the previous paper gives

$$\frac{P_{cr}}{P_e} = m^2 + (m+1)^2$$

which approaches 2 for large values of m, so the permissible end load is $0.5096 \times 2m^2 P_e$. After equation (5) above, if 2 x 0.5096 is inserted instead of 0.5096, the value of $\frac{Q}{P}$ will be halved. This is not a precise mathematical argument, but gives some indication of why the two approaches differ.

References

1. Brüninghoff, H. (1983) - Determination of bracing structures for compression members and beams. CIB-W18 paper no. 16-15-1, Lillehammer, May/June 1983.

2. Burgess, H.J. (1988) - Buckling modes and permissible axial loads for continuously braced columns. CIB-W18 paper no. 21-15-2, Vancouver, September 1988.

3. Klemperer, W.B. & H.B. Gibbons (1933) - Über die Knickfestigkeit eines auf elastischen Zwischenstützen gelagerten Balkens. Z. angew. Math. u. Mech., vol.13, p.251,1933.

4. Steer, P.J. (1988) - Stability: a general overview and non-standard solutions. UK Timber Engineering Group symposium on trussed rafters, London, March 1988.

5. Timoshenko,S.P. & J.M. Gere (1961) - Theory of elastic stability. 2nd edition, McGraw-Hill, London 1961.

6. Winter,G. (1958) - Lateral bracing of columns and beams. Jl. Struct. Div. ASCE, paper 1561, March 1958.

Figure 1

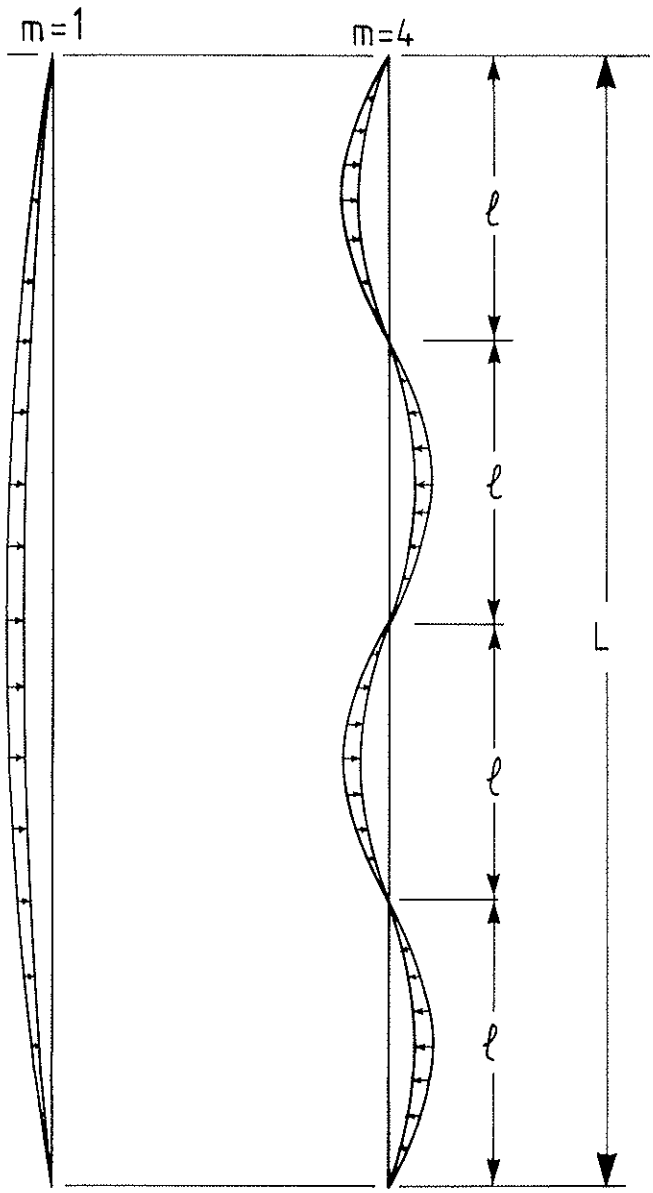

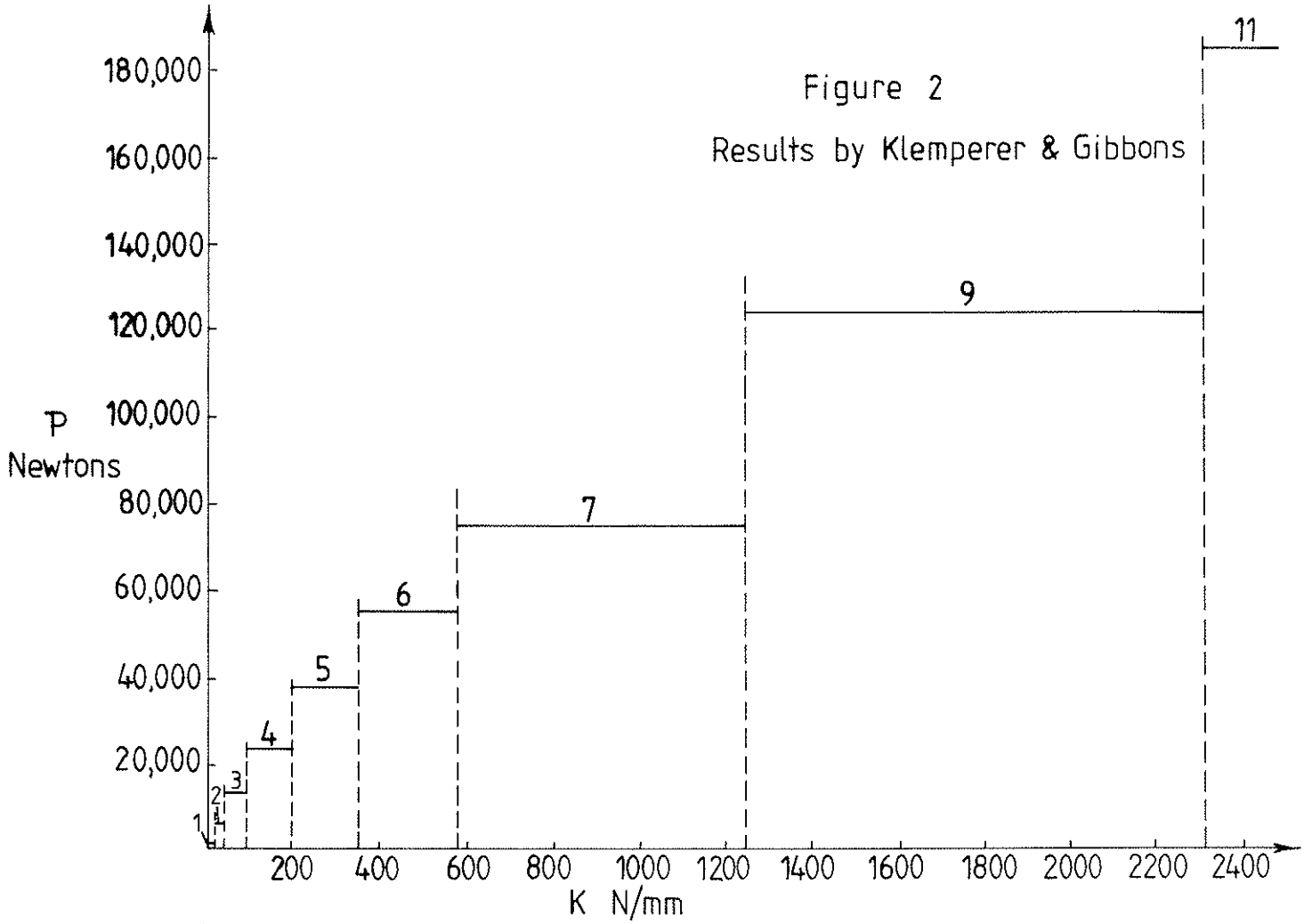

Figure 2

Results by Klemperer & Gibbons

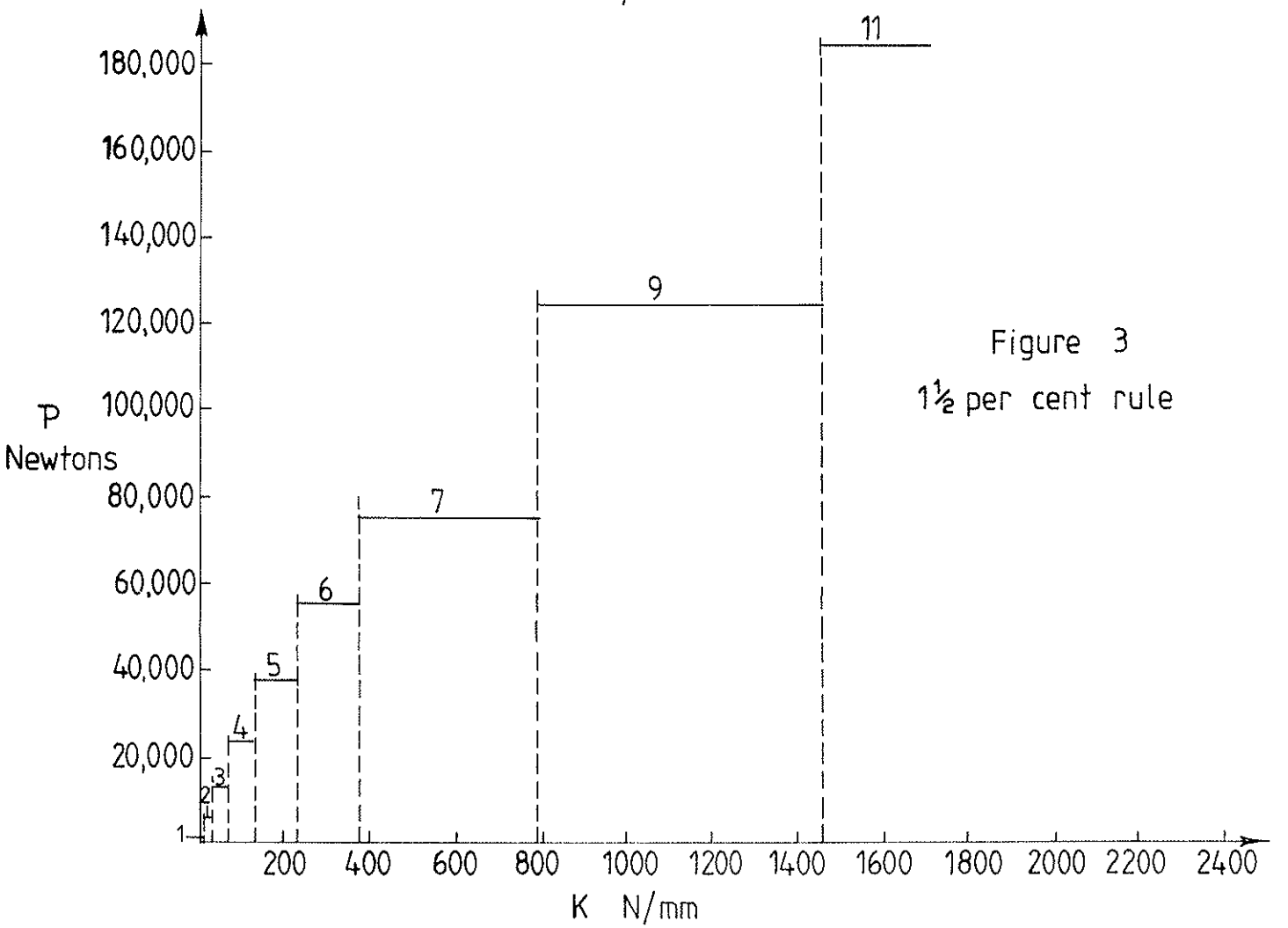

Figure 3

1½ per cent rule

CIB-W18A/21-15-5

INTERNATIONAL COUNCIL FOR BUILDING RESEARCH STUDIES AND DOCUMENTATION

WORKING COMMISSION W18A - TIMBER STRUCTURES

BEHAVIOUR FACTOR OF TIMBER STRUCTURES IN SEISMIC ZONES (PART TWO)

by

A Ceccotti
University of Trento
Italy

A Vignoli
University of Florence
Italy

MEETING TWENTY-ONE
PARKSVILLE, VANCOUVER ISLAND
CANADA
SEPTEMBER 1988

BEHAVIOUR FACTOR OF TIMBER STRUCTURES IN SEISMIC ZONES

(PART TWO)

Ario Ceccotti and Andrea Vignoli
University of Trento University of Florence

This report deals with some recent developments about theoric studies on behaviour coefficient q as mentioned in the paper "Behaviour factor of timber structures in seismic zones", presented at the Dublin meeting last year.

As suggested in chapter 5 "Conclusions and suggestion for further research" of the above mentioned paper, a more realistic behavioural model for semi-rigid joints under cyclic loading has been assumed by authors.

The new cycle with slip-joint is shown in figure 1 b. In the same figure the bilinear cycle without slip is reported as well (fig. 1 a).

The case of base restrained portal frame with four semi-rigid connections (which showed lower q values in comparison with two-hinged portal), has been reexaminated.

In fig. 2 are reported the plotted cycles for the same structure under Tolmezzo N-S earthquake.

In figure 3, the q values obtained respectively for the bilinear clycle and slip-cycle are reported.

"Ceteris paribus" a generalised decrement of q values occurred, but the minimum value still remains above q = 3 value.

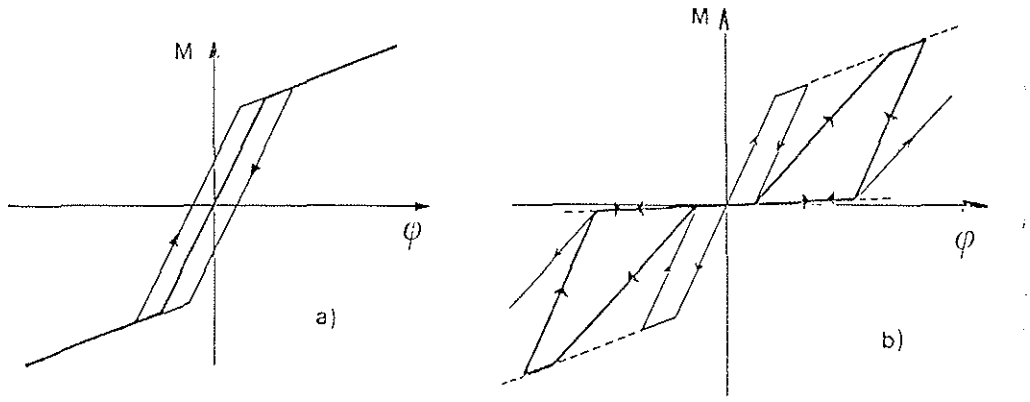
M
φ
a)
M
φ
b)

fig.1

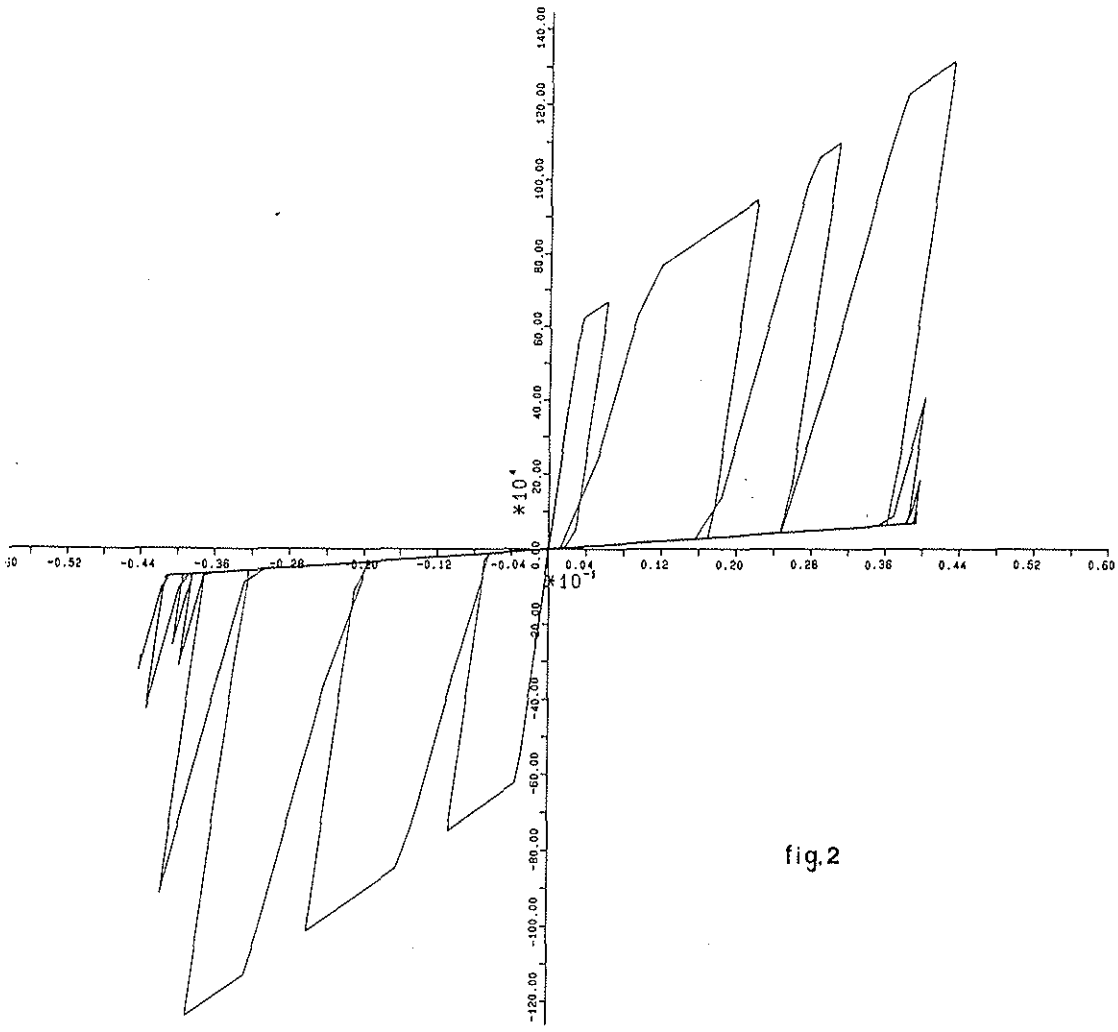
*10⁴
*10⁻⁵
-0.52
-0.44
-0.36
-0.28
-0.20
-0.12
-0.04
0.04
0.12
0.20
0.28
0.36
0.44
0.52
0.60
140.00
120.00
100.00
80.00
60.00
40.00
20.00
-20.00
-40.00
-60.00
-80.00
-100.00
-120.00

fig.2

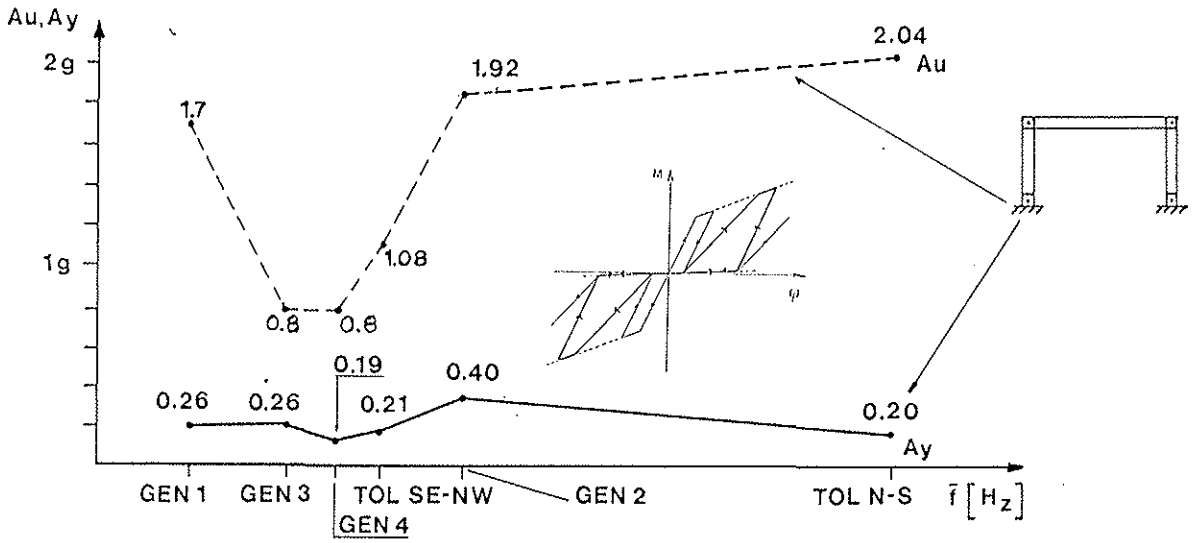
Au, Ay
2g
1g
1.7
0.8
0.8
1.08
1.92
2.04
Au
0.26
0.26
0.19
0.21
0.40
0.20
Ay
GEN 1
GEN 3
TOL SE-NW
GEN 4
GEN 2
TOL N-S
f [Hz]

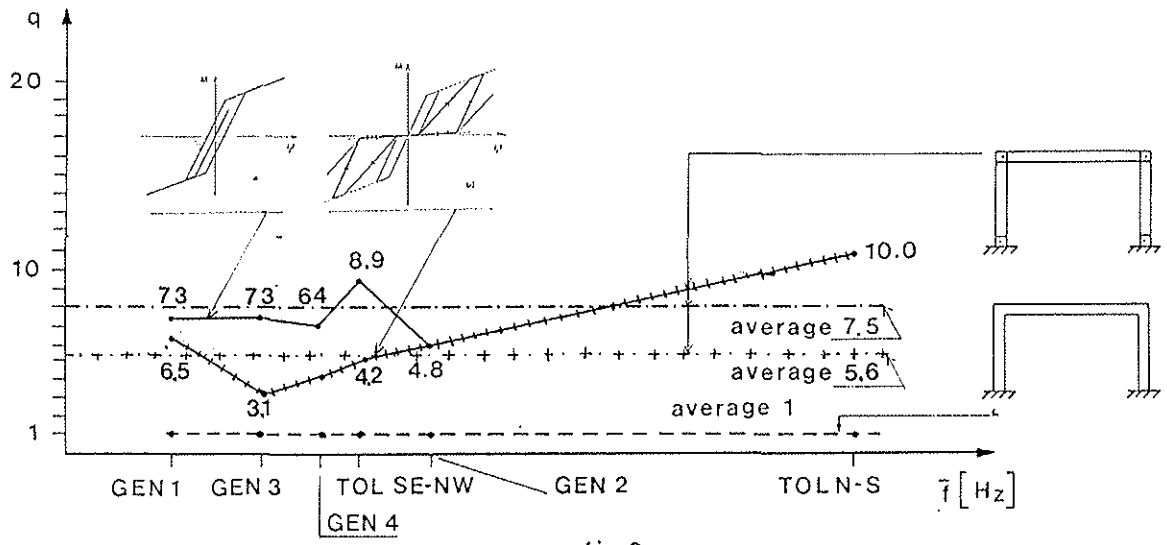
q
20
10
1
7.3
7.3
6.4
8.9
10.0
6.5
3.1
4.2
4.8
average 7.5
average 5.6
average 1
GEN 1
GEN 3
TOL SE-NW
GEN 4
GEN 2
TOL N-S
f [Hz]

fig.3

CIB-W18A/21-100-1

INTERNATIONAL COUNCIL FOR BUILDING RESEARCH STUDIES AND DOCUMENTATION

WORKING COMMISSION W18A - TIMBER STRUCTURES

CIB STRUCTURAL TIMBER DESIGN CODE
PROPOSED CHANGES OF SECTIONS ON LATERAL INSTABILITY, COLUMNS AND NAILS

by

H J Larsen
Danish Building Research Institute
Denmark

MEETING TWENTY-ONE
PARKSVILLE, VANCOUVER ISLAND
CANADA
SEPTEMBER 1988

0. INTRODUCTION

In the following are given proposals of changes to the sections on lateral instability, compression and bending without or with instability effects (columns) and nails in CIB Structural Timber Design Code (CIB Report, Publication 66, 1983) together with some background information and comments.

The proposals are based on the discussion at the Dublin meeting in September 1987.

1. LATERAL INSTABILITY

1.1 Background

The basis for the proposal is especially papers CIB-W18/20-2-1: Lateral Buckling Theory for Rectangular Section Deep Beam-columns and CIB-W18/20-10-1: Draft clause for the CIB Code for Beams with Initial Imperfections, both by H.J. Burgess, and discussions with H.J. Burgess.

1.2 Proposal

Replace 5.1.3 by

> 5.1.3 Bending
>
> The effective span of flexural members shall be taken as the distance between the centres of areas of bearing. With members extending further than is necessary over bearings the span may be measured between the centres of bearings of a length which would be adequate according to this code; attention should be paid to the eccentricity on the supporting structures.

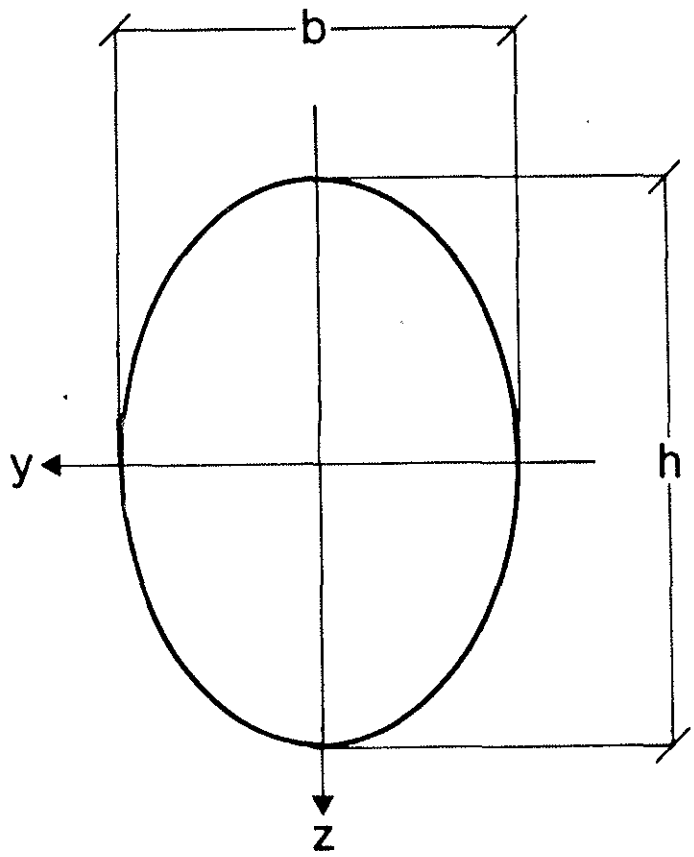

Figure 5.1.3a. Cross-section

For a beam

- free to deflect about both major axes (in figure 5.1.3a denoted y and z) except at the ends where it is assumed that the beam is held in position, and
- loaded in bending about the y-axis ($I_y > I_z$)

the bending stresses should satisfy the following condition

$$\sigma_{m,d} \leq k_{inst}\, f_{m,d} \qquad (5.1.3a)$$

where k_{inst} is a factor (≤ 1) taking into account the reduced strength due to failure by lateral instability (lateral buckling).

k_{inst} should be so determined that the total bending stresses, taking into account the effect of initial curvature, eccentricities and the deformations developed, do not exceed f_m.

$k_{inst} = 1$ may be assumed for beams where lateral displacement of the compression side is prevented throughout its length and where torsion is prevented at the ends.

k_{inst} may be determined from

$$k_{inst} = \frac{0.5}{\lambda^2_{m,rel}} \left[(1+\eta)(1+\lambda^2_{m,rel}) - \sqrt{((1+\eta)(1+\lambda^2_{m,rel}))^2 - 4(1+\eta)\lambda^2_{m,rel}} \right] \qquad (5.1.3b)$$

$\lambda_{m,rel}$ is the relative slenderness ratio in bending and η is a parameter depending on the initial curvature and eccentricities.

$$\lambda_{m,rel} = \sqrt{f_m/\sigma_{m,crit}} \qquad (5.1.3c)$$

where $\sigma_{m,crit}$ is the critical bending stress for a straight beam calculated according to the elastic theory of elasticity.

$$\eta = \pi \frac{b}{h} \frac{I_y}{I_z} \sqrt{1 - \frac{I_z}{I_y}} \sqrt{\frac{EI_z}{GI_v}} \eta_o \qquad (5.1.3d)$$

where

I_v is the torsional second moment of area

η_o the ratio between the maximum deviation from straightness e measured at midspan and the length (e/l).

For solid timber η_o=0,003 and for glued laminated timber η_o = 0,002 may be assumed.

For beams with rectangular cross-section

$$\lambda^2_{m,rel} = \frac{1}{\pi} \frac{l_e}{b} \frac{h}{b} \frac{f_{m,d}}{E_{o,d}} \sqrt{\frac{E_{o,mean}}{G_{mean}}} \sqrt{\frac{1-(/b/h)^2}{1-0.63b/h}} \qquad (5.1.3e)$$

and k_{inst} can be taken from figure 5.1.3b.

l_e is the effective length of the beam. For a number of structures and load combinations l_e is given in table 5.1.3 in relation to the free beam length l.

The free length is determined as follows:

a) When lateral support to prevent rotation is provided at points of bearing and no other support to prevent rotation or lateral displacement is provided throughout the length of a beam, the unsupported length shall be the distance between points of

bearing, or the length of a cantilever.

b) When beams are provided with lateral support to prevent both rotation and lateral displacement at intermediate points as well as at the ends, the unsupported length may be the distance between such points of intermediate lateral support. If lateral displacement is not prevented at points of intermediate support, the unsupported length shall be the distance between points of bearing.

Table 5.1.3 Relative Effective Beam Length l_e/l

Type of Beam and Load	l_e/l
Simply supported, uniform load or equal end moment	1,00
Simply supported, concentrated load at centre	0,85
Cantilever, uniform load	0,60
Cantilever, concentrated end load	0,85
Cantilever, end moment	1,00

The values apply to loads acting in the gravity axis. For downwards acting loads l_e is increased by 2 h for loads applied to the top and reduced by 0,5 h for loads applied to the bottom.

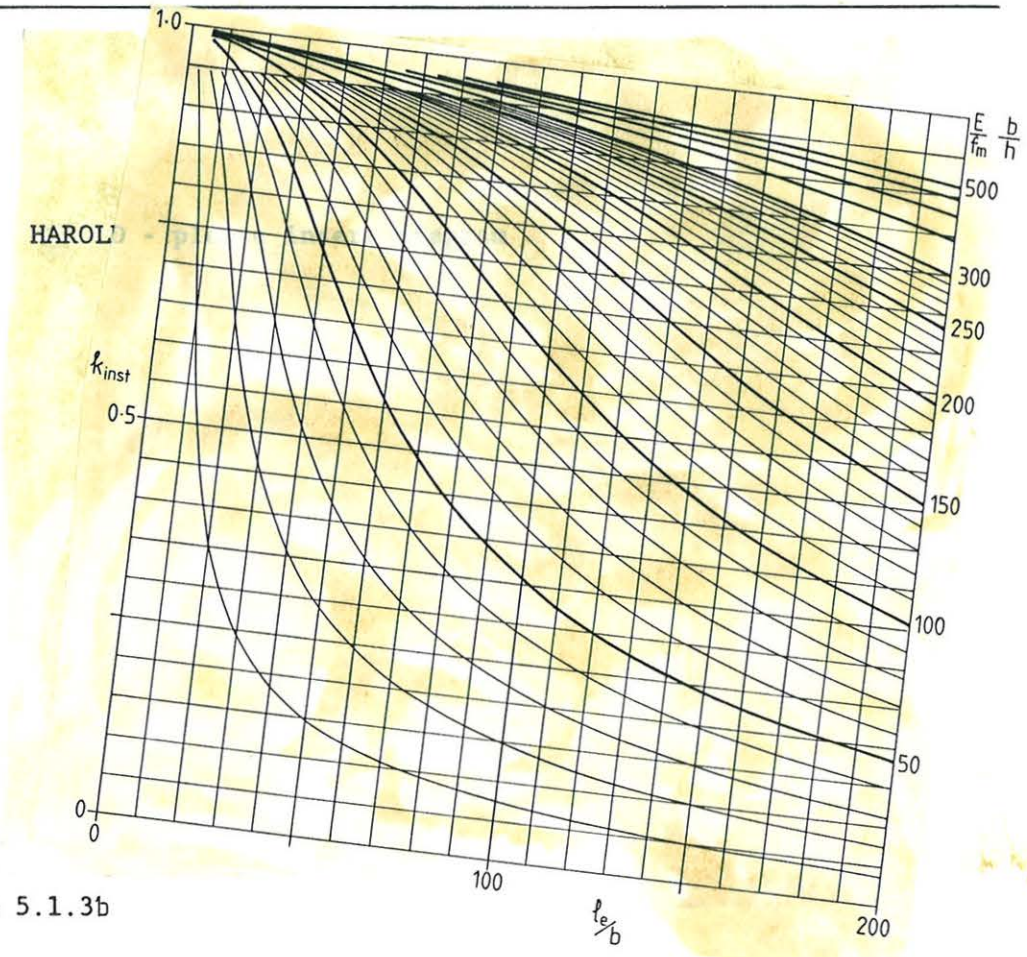

Figure 5.1.3b

1.3 Comments

Instead of the parameter k_M used in paper CIB-W18/20-10-1 the parameter $\lambda_{m,rel}$ is used to bring this section in line with that on columns. The same parameter is generally used for columns in other materials.

$$\lambda^2_{m,rel} = 1/k_M$$

The proposal is compared to the present CIB clause in figure 1. The difference is not important.

An advantage of the proposal is that it rests on a more sound theoretical basis.

A disadvantage is that k_{inst} is less than unity for all beams, and not only for beams with a slenderness ratio greater than a minimum value, corresponding to the test-beams used for determining f_m. This minimum value corresponds for $Eb((f_m h) = 50$ to l_e/b about 40.

A solution corresponding to the one proposed for columns in paper CIB W18/19-102-2 (Eurocode 5 and CIB Structural Timber Design Code - H.J. Larsen) could be used, but will complicate the formulae considerably. A simple solution - on the unsafe side for slender beams - would be to use a factor of about 1.1 on (5.1.3b).

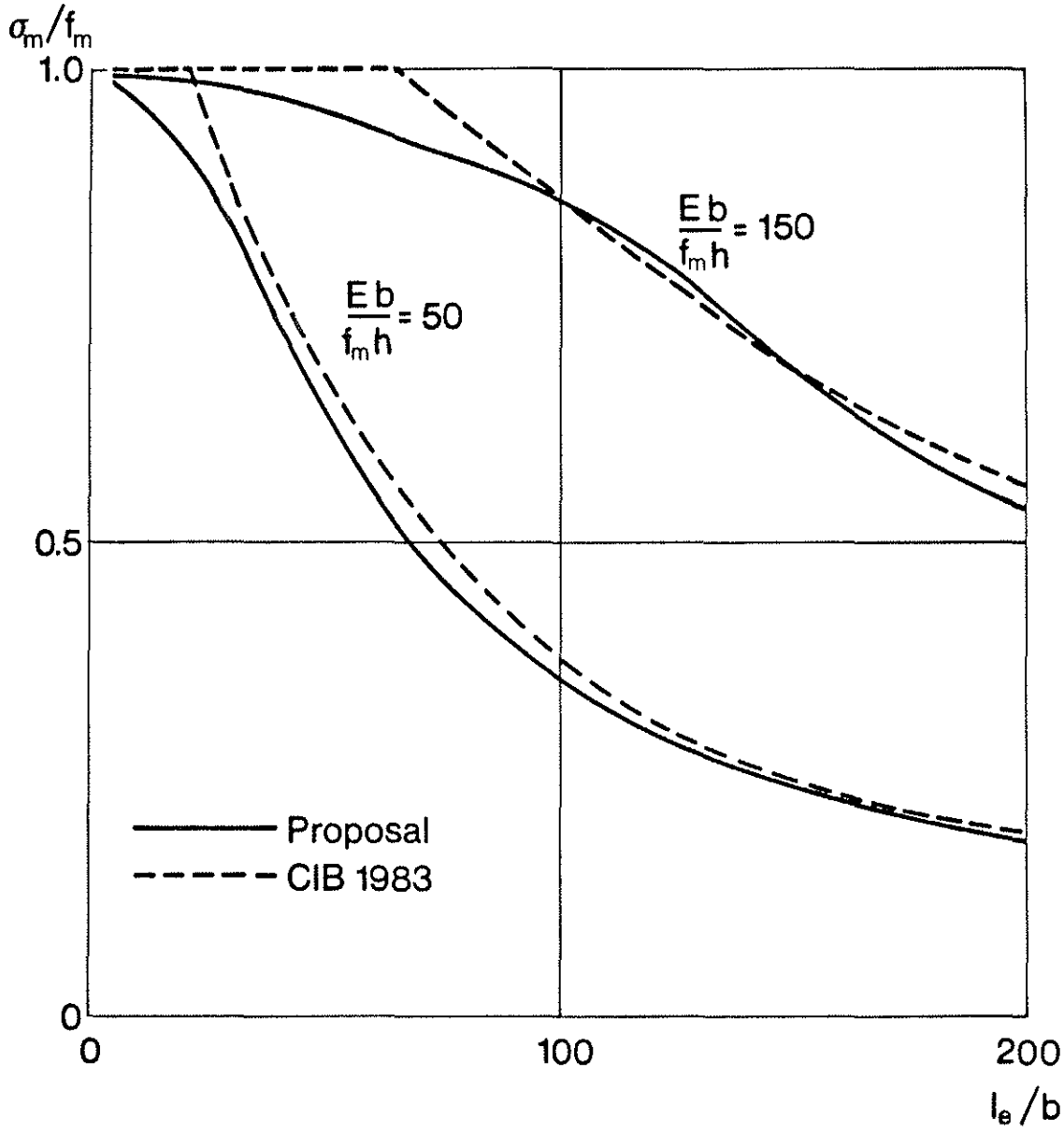

Figur 1

2. COMPRESSION AND BENDING

2.1 Background

The basis for the proposal is paper CIB-W18/20-2-1: Design of Timber Columns by H.J. Blass, and supplementary written comments from H.J. Blass.

2.2 Proposal

Replace 5.1.6.3 and 5.1.7 by

5.1.6.3 Compression and Bending with Instability Effects

The stresses should satisfy the following condition

$$\left(\frac{\sigma_{c,o,d}}{f_{c,o,d}}\right)^2 + \frac{\sigma_{m,d}}{f_{m,d}} \leq 1 \qquad (5.1.6.3a)$$

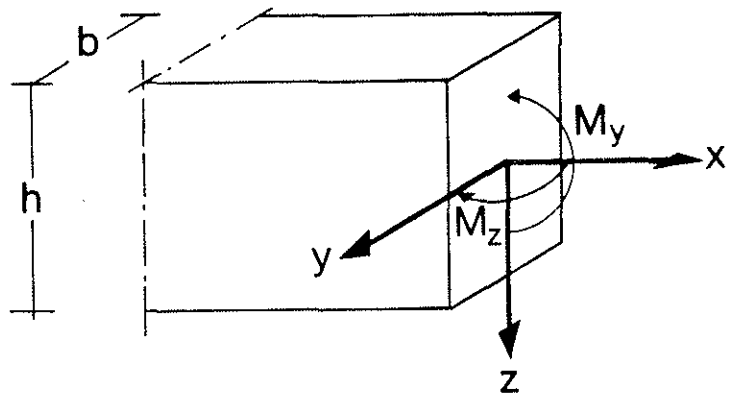

Figure 5.1.6.3 Rectangular Cross-section with Bending about two Axes. M_y giving $\sigma_{my} = 6M/(bh^2)$. M_z giving $\sigma_{mz} = 6M_z/b^2h)$.

For a rectangular cross-section $\sigma_{m,d}$ may be taken as

$$\sigma_{m,d} = \max \begin{cases} \sigma_{my,d} + 0.5\sigma_{mz,d} & (5.1.6.3b) \\ 0.5\sigma_{my,d} + \sigma_{mz,d} & (5.1.6.3c) \end{cases}$$

For other cross sections with bending about two axes giving in a point of the cross-section bending stresses $\sigma_{my,d}$ and $\sigma_{mz,d}$, $\sigma_{m,d}$ should be taken as

$$\sigma_{m,d} = \sigma_{my,d} + \sigma_{mz,d} \qquad (5.1.6.3d)$$

5.1.7 Columns

Axial Load alone

For a centrally loaded column the axial compressive stress should satisfy the following condition:

$$\sigma_{c,o,d} \leq k_c f_{c,o,d} \qquad (5.1.7a)$$

where

$$k_c = \begin{cases} 1 & \text{for } \lambda_{rel} \leq \lambda_o \qquad (5.1.7b) \\ \dfrac{1}{k + \sqrt{k^2 - \lambda_{rel}^2}} & \text{for } \lambda_{rel} > \lambda_o \qquad (5.1.7c) \end{cases}$$

λ_{rel} is the relative slenderness ratio

$$\lambda_{rel} = \frac{l_c}{i} \frac{1}{\pi} \sqrt{\frac{f_{c,o,k}}{E_{o,k}}} \qquad (5.1.7d)$$

and

$$k = 0.5 \left(1 + \beta_c(\lambda_{rel} - \lambda_o) + \lambda_{rel}^2\right) \qquad (5.1.7e)$$

The parameters β_c and λ_o depends on the grade of the column material and, especially, the intial curvature.

For columns of structural timber or glued laminated timber the values in table 5.1.7a may be used provided the maximum deviation from straightness e measured at midspan is less than the values stated.

Table 5.1.7a Parameters β_c and λ_o for Column Design and Corresponding maximum Deviation from Straightness e. l_c is the free column length.

	β_c	λ_o	maximum e
Structural timber	0.2	0.5	$l_c/300$
Glued laminated timber	0.1	0.5	$l_c/450$

Axial Load and Bending Moments

For $\lambda_{rel} \leq \lambda_o$ 5.1.6.3 applies.

For $\lambda_{rel} > \lambda_o$ the stresses should satisfy the following condition:

$$\frac{\sigma_{c,o,d}}{k_c f_{c,o,d}} + \frac{\sigma_{m,d}}{f_{m,d}} \leq 1 \qquad (5.1.7f)$$

For a rectangular cross-section two cases should be investigated, see figure 5.1.6.3:

- k_c corresponding to deflection in the y-direction with
$$\sigma_{m,d} = 0,5\ \sigma_{my,d} + \sigma_{mz,d} \qquad (5.1.7g)$$

- k_c corresponding to deflection in the z-direction with
$$\sigma_{m,d} = \sigma_{my,d} + 0,5\ \sigma_{mz,d} \qquad (5.1.7h)$$

For other cross-sections (5.1.6.3d) applies with k_c corresponding to the largest value of λ_{rel}.

The bending stresses are calculated without regard to deflection and initial curvature.

3. NAILS

3.1 Background

The basis for the proposal is especially paper CIB-W18/20-7-1: Design of Nailed and Bolted Joints - Proposals for the revision of existing formulae in Draft Eurocode 5 and the CIB Code, by L.R.J. Whale, I. Smith and H.J. Larsen, and supplementary written comments from Whale and Smith.

The presentation of the minimum spacings and distances are based on a proposal by Jürgen König from the Swedish Institute for Wood Technology Research.

3.2 Proposal

Replace 6.1.1 by

6.1.1 Nails and staples

6.1.1.1 Laterally loaded nails, wood-to-wood joints

The characteristic lateral load-carrying capacity per shear plane of a round nail may be determined by

$$F_k = d^2 \sqrt{f_{y,k}\, f_{h,k}/3} \qquad (6.1.1.1a)$$

provided the thickness of the thinnest member is not less than

$$l_{min} = d\left(\sqrt{f_{y,k}/f_{h,k}} + 1\right) \qquad (6.1.1.1b)$$

and provided the penetration lengths satisfy the following conditions, see figure 6.1.1.1a.

Nails in double shear driven
alternately from either side $l_1 \geq l_{min}$

Other cases
smooth nails $l_2 \geq 1.5\, l_{min}$
annular ringed shank and helically threaded nails $l_2 \geq l_{min}$

d is the diameter
$f_{y,k}$ is the characteristic tensile strength of the nail
$f_{h,k}$ is the characteristic embedding strength determined according to ISO xxxx.

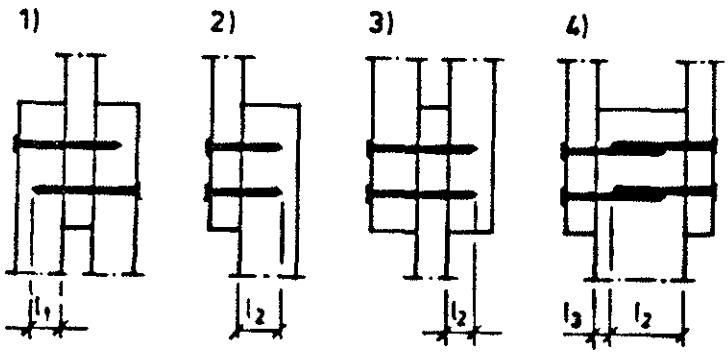

Figure 6.1.1.1*a* Penetration lengths. Case 3 should not be used for smooth nails.

For smaller thicknesses and penetration lengths the load-carrying capacity should be reduced in proportion to the thickness or length respectively. For smooth nails the penetration length l_2 should at least be 6d. For annular ringed shank and helically threaded nails the penetration length should at least be 4d.

It is assumed

- that the nails are driven in perpendicular to the grain,
- that holes are predrilled for wood with a characteristic density of more than 500 kg/m^3 (corresponding to a mean value of about 600 kg/m^3),
- that smooth nails in double shear are driven alternately from either side,
- that the thinnest member has a thickness of not less than 7d for $d \leq 5$ mm and (13 d - 30 mm) for $d > 5$ mm.

If l_3 is greater than 0,5 l_{min} (see figure 6.1.1.1a), nails from the two sides may overlap in the middle member.
There should normally be at least 2 nails in a joint.

Nails in the end grain should normally not be considered capable of transmitting force. Where nails in end grain are used in secondary structures - e.g. for fascia boards nailed to rafters - the characteristic value should be taken as 1/3 of the values for normal nailing.

For more than 10 nails in line the load-carrying capacity of the extra nails should be reduced by 1/3, i.e. for n nails the effective number n_{ef} is

$$n_{ef} = 10 + \frac{2}{3}(n - 10) \qquad (6.1.1.1c)$$

Minimum spacings (a_1 and a_2 in figure 6.1.1.1b) and minimum distances to end (a_3 in figure 6.1.1.1c) and edge (a_4 in figure 6.1.1.1d) are given in table 6.1.1.1.

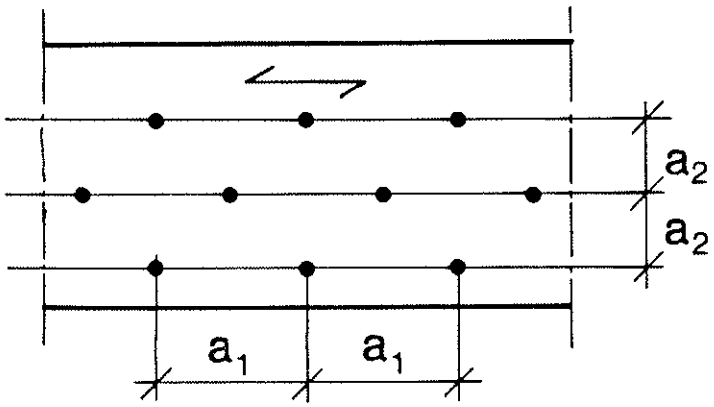

Figure 6.1.1.1b Spacings a_1 and a_2

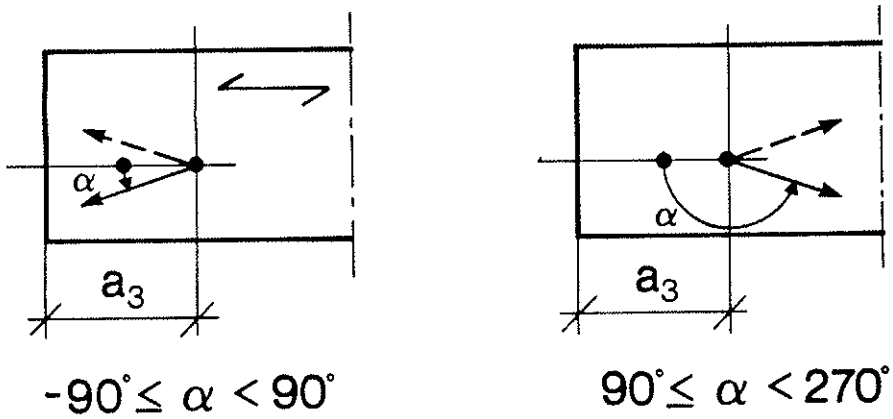

Figure 6.1.1.1c End distance a_3

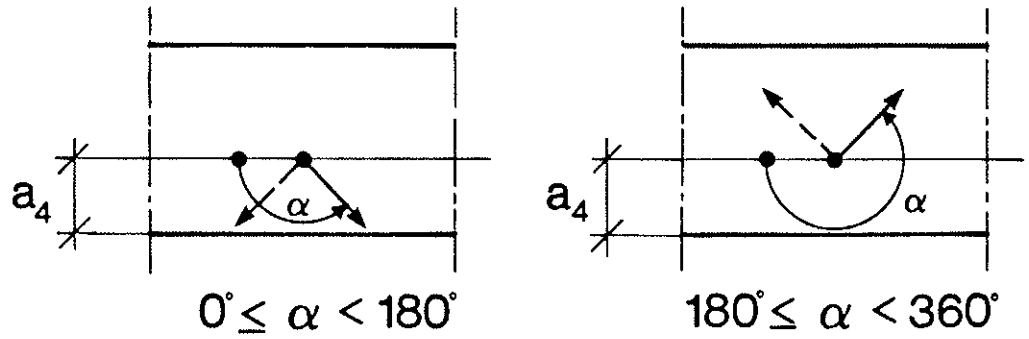

Figure 6.1.1.1d Edge distance a_4

Table 6.1.1.1 Minimum Spacings and End and Edge Distances in the Wood

	wood-to-wood joints in conifers with a characteristic density of 500 kg/m^3 and less with predrilling steel-to-wood joints board-to-wood joints	wood-to-wood joints in conifers with a characteristic density of 500 kg/m^3 and less without predrilling wood-to-wood joints in conifers with n density of more than 500 kg/m^3 and in non-conifers*
a_1	7d	10d
a_2	4d	5d
a_3		
$-90 \leq \alpha < 90$	10d	$(10 + 5 \cos\alpha)$d
$90 \leq \alpha < 270$	$(10 + 5 \cos\alpha)$d	10d
a_4		
$30 \leq \alpha \leq 150$	$10 \sin\alpha$ d	$10 \sin\alpha$ d
other α-values	5d	5d

* For a characteristic density of more than 500 kg/m^3 predrilling is required.

The characteristic embedding strength in MPa for round nails without predrilling may be taken as

$$f_{h,k} = 0.09 \rho_k d^{-0.36} \qquad (6.1.1.1d)$$

and 40 per cent higher with predrilling.

d is the diameter in mm and ρ_k the characteristic density in kg/m^3. For round nails with a diameter up to 6 mm and with a characteristic tensile strength in MPa of at least

$$f_{y,k} = 50(16 - d) \qquad (6.1.1.1e)$$

and with minimum thicknesses and penetration lengths corresponding to

$$l_{min} = 7d \qquad (6.1.1.1f)$$

(6.1.1.1a) may be replaced by

$$F_k = kd^{\beta} \text{ (in N)} \qquad (6.1.1.1g)$$

with $\beta = 1.6$ and

$$k = 5.7 \sqrt{\rho_k} \text{ without predrilling} \qquad (6.1.1.1h)$$

$$k = 6.8 \sqrt{\rho_k} \text{ with predrilling} \qquad (6.1.1.1i)$$

F_k is in N and ρ_k in kg/m^3.

The slip u for a load $F \leq F_k/3$ may be taken as

$$u = 0.5 \; d \; k_{creep} \; (F/F_k)^{1.5} \qquad (6.1.1.1j)$$

6.1.1.2 Laterally loaded nails, steel-to-wood joints

The relevant parts of 6.1.1.1 apply. The load-carrying capacity may, however, be taken 25 per cent higher than for the corresponding wood-to-wood joint.

Adequate strength of the steel plates is assumed.

Minimum spacings in the wood are given in table 6.1.1.1.

6.1.1.3 Laterally loaded nails, board material-to-wood joints

The relevant parts of 6.1.1.1 apply with (6.1.1.1a) replaced by

$$F_k = d^2 \sqrt{\frac{2 f_{y,k} \, f_{h,k,wood} \, f_{h,k,panel}}{3(f_{h,k,wood} + f_{h,k,panel})}} \qquad (6.1.1.3a)$$

provided the panel thickness is not less than

$$l_{min} = d \sqrt{f_{y,k}/f_{h,k,panel}} \qquad (6.1.1.3b)$$

For the wood (6.1.1.1b) apply.

$f_{h,k,wood}$ and $f_{h,k,panel}$ are the characteristic embedding strengths of the wood and the panel material respectively determined according to ISO xxxx.

For smaller thicknesses the load carrying capacity should be reduced proportionally to the thickness.

It is assumed that the diameter of the head of the nail is about 2d. For nails with smaller head diameters the load-carrying capacity should be reduced. For pins and oval headed nails, for example, the load carrying capacity in particle boards and fibre boards should be reduced by half.

Minimum nail spacings are given in table 6.1.1.1b. For particle boards the panel strength may require bigger spacings.

3.3 Comments

An alternative to (6.1.1.3a) is the following:

The load-carrying capacity for nails with heads with a diameter of at least 2d may be determined by formula (6.1.1.1e), provided the panel thicknesses are not less than

3d	for plywood of birch, beech, and similar hardwoods,
3,5d	for plywood with plies of alternating hardwood and softwood,
5d	for plywood of softwood,
3d	for hard or oil-tempered structural fibre board,
7d	for particle board.

For smaller thicknesses the load-carrying capacity should be reduced proportional to the thickness.

CIB-W18A/21-103-1

INTERNATIONAL COUNCIL FOR BUILDING RESEARCH STUDIES AND DOCUMENTATION

WORKING COMMISSION W18A - TIMBER STRUCTURES

CONCEPT OF A COMPLETE SET OF STANDARDS

by

R H Leicester
CSIRO
Australia

MEETING TWENTY-ONE
PARKSVILLE, VANCOUVER ISLAND
CANADA
SEPTEMBER 1988

CONCEPT OF A COMPLETE SET OF STANDARDS

R.H. Leicester
(CSIRO, Melbourne, Australia)

In the use of building Standards, particularly in developing countries, repeated difficulties arise because these Standards do not form a complete set. When the formal set of Standards is incomplete, the gaps must be filled in some de facto manner by the building industry. For example, if there are no formal Standards for the continuous verification of the quality of stress-graded timber, then eventually some informal mechanism such as customer reaction, will determine the acceptable limit to drift in quality.

It is helpful to make use of the concept of a complete set of Standards for use as a framework within which the existing or proposed new Standards of a country may be critically examined and if necessary, modified. An example of a complete set is shown schematically in Figure 1. The set comprises a hierarchy of Standards of five types of building elements as follows,

- materials and components,
- composite materials,
- single structural elements,
- composite structural elements, and
- total structures.

In essence, each type of building element is formed from those in a lower level of the hierarchy. Thus, for each type of building element there should be Standards for the associated process control and quality assurance. These Standards are illustrated schematically in Figure 2. The quality assurance should include acceptance criteria, together with continuous verification checks on product quality. The acceptance criteria may comprise any or all of the criteria based on engineering computation, product description, or performance testing. Some excellent models for process control and quality assurance are to be found in several industry Standards for plywood (1,2).

Table 1 shows, in schematic form, the relationships between the various types of quality assurance Standards discussed, together with one Australian example related to each type. The Table looks deceptively complete, but in fact many of the Standards required are missing. For example, in Australia there is no formal Standard for the continuous verification of visually stress-graded timber, an omission that causes frequent friction between suppliers and customers in the structural use of sawn timber.

The three types of acceptance Standards mentioned in Table 1 function in different ways, and if possible all three should be available.

Performance Standards are not product specific and hence they are particularly useful for facilitating trade or for the introduction of new products. For example, with the use of performance Standards particleboard may be used to replace plywood in flooring solely on the basis of material testing; no structural design need be involved.

However, to implement performance Standards requires access to extensive financial and technological resources. For countries with limited resources, the preferred option will be specification by product description. The third option for acceptance, that based on engineering computation, is the most flexible of the three; once building materials have been classified with respect to their structural properties, the process of engineering computation may be used as an acceptance criterion for all types of building elements and all types of structures. However it should be appreciated that a prerequisite for applying engineering computation is the drafting of Standards on timber engineering, structural loadings and design performance criteria, all of which are relatively sophisticated undertakings. Furthermore, they cannot be used directly by builders.

Table 1. – A COMPLETE SET OF STANDARDS FOR QUALITY ASSURANCE

Building element	Examples of building elements	Examples of Australian Quality Assurance Standards*			
		Acceptance criteria			Continuous verification
		Engineering computation	Product description	Performance test	
Material and components	Structural sawn timber, connector	None	AS 2082 (3) *VSG hardwood*	AS 1649(4) *metal connectors*	AS 1749 (5) *MSG softwood*
Composite materials	Plywood, particle-board, glulam	None	AS 2269 (6) *plywood*	PAA (2) *plywood*	PAA (2) *plywood*
Simple structural elements	Beam, column, joint	AS 1720 (7) *all simple elements*	Pham & Hawkins (8) *joints*	AS 1720 (7) *all simple elements*	None
Composite structural elements	Wall bracing panels floor system, roof truss	AS 1720 (7) *all composite elements*	PAA (9) *bracing walls*	Reardon (10) *bracingwalls*	None
Total structures	House, industrial building	AS 1720 (7) *all structures*	DLG (11) *houses*	Reardon (12) *houses*	None

*Notation
AS = Code of Practice by Standards Association of Australia.
AS 1720 = Timber Engineering Code.
DLG = Dept of Local Government, Queensland.
MSG = mechanically stress graded
PAA = Plywood Association of Australia.
VSG = visually stress graded
( ) = Reference number, see References.

References

1. American Plywood Association. 1986. Performance standards and policies for structural-use panels. APA PRP-108, Tacoma, USA, 72p.

2. Plywood Association of Australia. 1987. Quality control policy. Brisbane, Australia, 25p.

3. Standards Association of Australia. 1977. AS 2082 – Visually stress-graded hardwood for structural purposes. Sydney, Australia, 32p.

4. Standards Association of Australia. 1974. AS 1649 – Determination of basic working loads for metal fasteners for timber. Sydney, Australia.

5. Standards Association of Australia. 1978. AS 1749 – Rules for mechanical stress grading of timber Sydney, Australia, 11p.

6. Standards Association of Australia. 1979. AS 2269 – Structural plywood. Sydney, Australia, 23p.

7. Standards Association of Australia. 1982. AS 1720 – SAA Timber Engineering Code. Sydney, Australia, 150p.

8. Pham, L. and Hawkins, B.T. 1982. Fasteners for domestic construction to resist wind uplifting forces in non-cyclonic areas. Low-rise domestic and similar framed structures, Part 6. Special Report, CSIRO Division of Building Research, Melbourne, Australia, 66p.

9. Plywood Association of Australia. Undated. Structural plywood wall bracing – Design manual. Brisbane, Australia, 12p.

10. Reardon, G.F. 1980. Recommendations for the testing of roofs and walls to resist high wind forces. Technical Report No. 5, Cyclone Structural Testing Station, James Cook University of North Queensland, Townsville, Australia, June, 44p.

11. Department of Local Government. 1984. Home building code, Queensland – Appendix 4 to the standard building by-laws. Queensland Government Printer, Brisbane, Australia, May.

12. Reardon, G.F. 1987. The structural response of a brick veneer house to simulated cyclone wind loads. Proceedings of First National Structural Engineering Conference, Institution of Engineers, Melbourne, Australia, Aug., Vol. 2, 478-482.

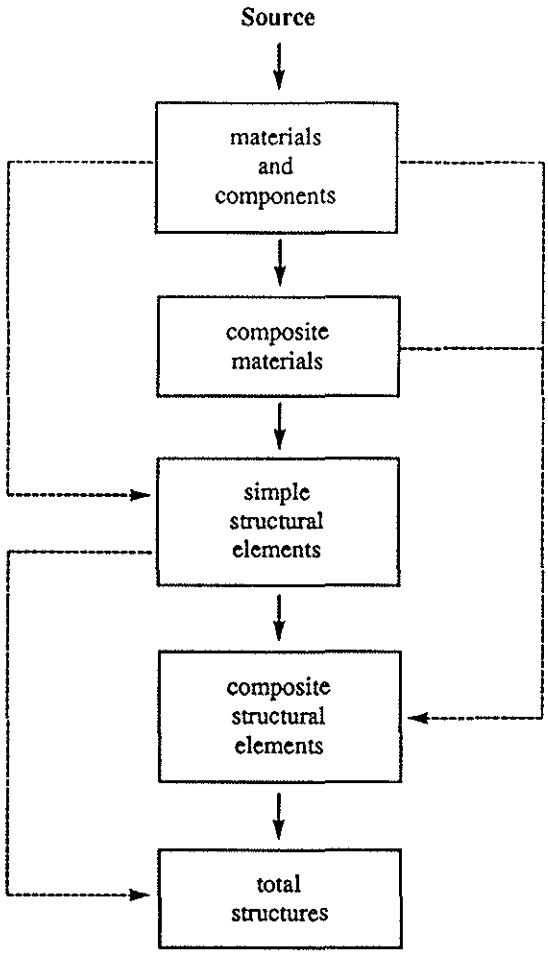

Figure 1. Hierarchy of Standards.

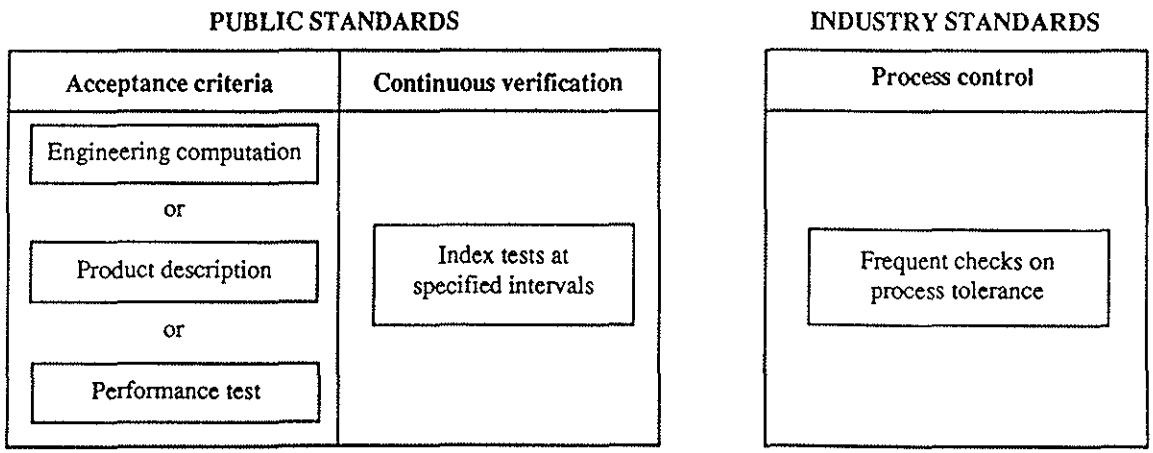

Figure 2. Standards for quality control.

CIB-W18A/21-105-1

INTERNATIONAL COUNCIL FOR BUILDING RESEARCH STUDIES AND DOCUMENTATION

WORKING COMMISSION W18A - TIMBER STRUCTURES

FIRST CONFERENCE

of

CIB-W18B

TROPICAL AND HARDWOOD TIMBER STRUCTURES

SINGAPORE
26 - 28 OCTOBER, 1987

by

R H Leicester
CSIRO
Australia

MEETING TWENTY-ONE
PARKSVILLE, VANCOUVER ISLAND
CANADA
SEPTEMBER 1988

PREFACE

In late 1986, CIB (International Council for Building Research and Documentation) decided to set up a Working Commission W18B that was to be devoted to matters related to tropical and hardwood timber structures. The four topics that are of concern to CIB-W18B are the following:

- technology,
- international standards,
- technology transfer to developing countries, and
- trade.

In the above, Documentation will be focused on those aspects in which hardwood and tropical timbers differ from softwoods. The interest in developing countries arises from the fact that much of world's hardwoods and tropical timbers are grown in industrially developing or recently developed countries. Finally, the topic of trade has been included because for the case of structural timber, both technology and Standards have been found to have a significant impact in assisting or blocking trade.

The first conference of CIB-W18B was held on 26-28 October at the Shangri-La Hotel in Singapore. It was intended to use the Conference to determine the course of CIB-W18B. Some 27 participants from 11 countries attended the Conference. More than 40 papers were submitted for the Conference, and 39 of these were presented and discussed during the Conference.

This set of proceedings gives the 39 papers presented together with one of the late papers (paper No. 40). In addition there is a list of participants to the Conference (Appendix I) a list of CIB-W18B members (Appendix II), the Conference Agenda, (Appendix III), a Conference Report, (Appendix IV), and a set of Project Proposals (Appendix V). Because of the difficulties associated with contacting participants from some countries, it was decided that all papers would be reproduced through photocopying the original unedited versions.

Finally, grateful acknowledgment must be made of the following sponsors for the Conference:

- ADAB (Australian Development Assistance Bureau) for fully funding the travel and participation costs of Dr Augustus Addae-Mensah from Ghana and Dr Ekasit Limsuwan from Thailand.

- CSIRO, Australia, for secretarial work and publishing the proceedings, and

- Gangnail-Australia, for organising the logistical support in Singapore.

R.H. Leicester
(Coordinator, CIB-W18B)

APPENDIX IV CONFERENCE REPORT

A4.1 PROGRAM

In order to encourage discussion, the Conference was run partly in a workshop mode. The program sequence was as follows:

- two days for presentation and discussion of papers
- half day for discussion on future activities of CIB-W18B
- half day for visits to view aspects of the timber industry in Singapore.

Live computer demonstrations were given in conjunction with Paper No. 11 (to demonstrate the Gangnail design package) and Paper No. 25 (to demonstrate a timber design Expert System).

Personel involved in the running of the Conference were as follows:

Conference Secretary: Dr R.H. Leicester

Session Chairmen: Dr Wong Wing Chong
Mr R.M. Hallett
Dr J. Johnson
Dr Surjono Sujokusmo
Dr R.H. Leicester

Rapporteurs: Mr C. Kondrup
Dr Ekasit Limsuwan

Singapore Organiser: Mr Yong Keng Hin

The discussion of the papers is given in Section A4.2 of this report; the project proposals arising from the half day discussion on the future of CIB-W18B are given in Appendix A5.

Probably because of the country origins of the participants, most emphasis on the Conference papers and discussions was placed on the topic of technology transfer to developing countries.

The industry visits were made to Sungei Kadut, the timber industry centre of Singapore, and to one building site. At Sungei Kadut the following organisations were visited;

- Econ Wood Products
- Fowseng Furniture and Construction
- Timber Ring

At the conclusion of the Conference awards were presented to Yong Keng Hin for his assistance in organisational matters, and to Janssen and Surjono Sujokusumo for the most interesting presentation from developed and tropical countries respectively. A vote of thanks was given to Leicester for organising the Conference.

The following is a summary of the discussion during the Conference.

A4.2 CONFERENCE DISCUSSION

A4.2.1 Introduction

Leicester, CIB-W18B coordinator, introduced the conference and explained the role of Working Commission. The CIB interest in timber structures was probably due to the fact that this field of research was not properly covered by either building research or forestry research organisations; it required input from both these types of organisations. This had led to the formation of CIB-W18 (now CIB-W18A) some fifteen years ago. The Working Commission CIB-W18 had been very active in the development of international standards.

The formation of a new additional Working Commission CIB-W18B had probably been motivated by the fact that most of the expertise within CIB-W18 was associated with researchers from countries with softwood economies and temperate climates. It was also a fact that currently no tropical country is represented as a participating member on ISO TC/165, the technical committee of ISO changed with the development of international standards related to timber structures.

Following discussions between the CIB Secretary and the nominated coordinator of CIB-W18B (Leicester), it was decided that a suitable role for CIB-W18B would be to concern itself with the following aspects of tropical and hardwood timber structures

- technology,
- international standards,
- technology transfer to developing countries, and
- trade.

Leicester suggested to the Conference that the focus of CIB-W18B activities should be on timber engineering, but certain aspects of other related fields could be considered where these had a direct effect on timber engineering. Examples of such related fields are durability/preservation, adhesives and possibly seasoning. Consideration should be given as to whether CIB-W18B should be concerned with single structural elements, total structure systems or complete houses and buildings.

The Working Commission CIB-W18B should develop specific areas of expertise that may not be adequately covered by other groups at the moment. Such areas could include the following:

- hardwood technology
- technology for mixed and multiple species timbers
- simplified design procedures
- effect of durability on structural design in tropical countries

Finally there are two important matters which CIB-W18B must also consider. The first is the potential interaction between CIB-W18B and other related organisations. Examples of such organisations are the following:

- Working Commission CIB-W18A
- IUFRO Division 5 (Forest Products Division, International Union of Forest Research Organisation)
- ISO TC/165 (Technical Committee on Timber Engineering, International Standards Organisation)
- UNIDO (United Nations Industrial Development Organisation)
- ITTO (International Tropical Timber Organisation)
- ATTC (Asean Timber Technology Centre)

- JUNAC (Junta del Acuerdo de Cartagena, the Andean Pact Group)
- PASC (Pacific Area Standards Congress)

The second matter is that of funding. Because the tropic of tropical and hardwood timber structures is of primary concern to developing countries, there will always be difficulties in securing the participation of researchers form tropical countries to attend Conferences, even if the meetings are all held within tropical countries. For most potential delegates travel costs are prohibitive. Enquiries with various development aid agencies has indicated that participation at Conferences was not a favoured activity for funding: however there would be reasonable chances of obtaining funds for work on specific projects.

A4.2.2 Technology

Discussion of the paper by Walford indicated that coconut wood, the stems of old coconut trees, was now used in some countries, such as the Phillipines, as an acceptable building timber. The relevant technology was available. Killman noted that there were now more than 500 publications on the use of coconut wood for building purposes. A difficult feature of coconut wood is the extreme range of density that occurs, even within a single stem. Two forms of stress grading are feasible: one is based on dry density and the other is based on the measurement of modulus of elasticity of the green timber. Grading through stiffness is easily achieved by noting the deflection of a sawn board under its own weight, because the density of green coconut wood is approximately 1000 kg/m|3|, regardless of its dry density.

Discussion on papers by Janssen, Abang Abdul Rahim and Boughton indicated that bamboo was widely used for construction in the rural areas of some countries. For example 70 per cent of houses in Indonesia use bamboo in some form. Although over 1000 species of bamboo are available, stress grading based on density is a feasible technique. Attack from insects creates a major durability problem and there was considerable discussion on potential preservation techniques. Connections using nails leads to splitting. Tied connections, preferably using nylon twine, were very effective.

Rubber wood is now an acceptable timber for furniture and hence should also be acceptable as timber for structural purposes.

Campbell stated that for durability purposes species identification was essential; species identification was required both for assessing the natural durability of heartwood and the penetrability of sapwood. Conventional pressure treatment processes were not suitable for many hardwoods; other techniques, such as double diffusion, should be developed to cope with these timbers.

The large number of potentially useful species grown in tropical countries was noted by several participants. Methods for coping with this situation were mentioned several times. For example Indonesia grows more than 4000 species of trees that could be used for structural purposes; Surjouro Sujokusomo discussed the use of mechanical stress grading (specifically the measurement of modulus of elasticity on flat over a span of 2440 mm) to grade an unidentified mixture of hardwood species.

Leicester described proof grading, a method of grading through proof testing. This method of grading was now in use in Australia and was particularly suitable for application to either multiple species timber or to mills in low technology environments.

Tropical environmental effects (such as high temperatures and humidity) were noted to influence both structural and durability properties in an interactive fashion. One paper by Jumaat addressed some aspects of this matter.

Commenting on the paper on nailed and bolted joints by Whale, Leicester noted that this was only a part of a very extensive connector study reported at a CIB-W18A meeting in 1986. However this study was limited to consideration of only one type of failure mode, i.e. failure through bearing on wood; for practical applications, other important modes such as failure through transverse splitting must also be considered.

A4.2.3 Engineering

Yong Keng Hin described the use of a high technology system, namely the Gangnail system of computerised roof stress design, in developing countries. He stated that the transfer of the design technology itself, via the computer, created no difficulty, although it was necessary to use thicker gauges plates and wider truss spacings to suit the timbers and building systems in use in some tropical countries. However there were difficulties associated with the selection of design standards, because many developing countries did not have complete documentation in this regard. For example, design loads for plate connector systems were often missing. The use of an overseas standard for design data on missing items created difficulties in matching the overseas standard with the local standard.

Two papers by Boughton on cyclone resistant housing in developing countries highlighted the extensive use of bamboo, the observed weakness of connector systems used, the significant effect of decay on connector systems and the difficulty of incorporating engineering principle into rural housing in economically depressed areas.

A4.2.4 Standards

The paper by Larsen on the draft ISO code drew a considerable amount of interest and discussion. In particular the notion of internationally accepted systems of strength group and stress grade classifications was seen as a very useful first step in the development of a technology to handle the timber of multiple species forests; these classifications were also useful as an aid to transfer technology to developing countries. Surjono Sujokusumo commented that the upper (high strength) end of the ISO classifications did not go high enough to cover all the useful timber species of Indonesia.

Campbell stated that the ISO stress grades were based primarily on strength, combined with a conservative estimate of stiffness. Because of the importance of stiffness in sizing many structural members, there could be a case for using stiffness as the primary criterion coupled with a conservative estimate of strength. This would be useful for coping with multiple species timbers, particularly when these are graded according to stiffness as outlined in an earlier paper by Surjono Sujokusmo.

Haryanto Nurhadi, Ekasit Limsuwan and Addae-Mensah commented on the difficulty of drafting standing standards in developing countries. Many of these countries do not have their own official standards. Some use overseas standards. Others modify overseas standards to suit their own particular needs. The Indonesian standards are derivatives of Codes from Germany, Sweden, United States, Norway, USA, Japan, Australia and Finland!

Simplified Codes would be appreciated for interim use by many developing countries. As examples, reference was made to the paper by Leicester and Walford and also to a 'Simplified Procedures' section of a draft Australian wind engineering standard.

Lapish described the Fijian Pine Code which was based on a New Zealand standard. The technology transfer appeared to be very effectively achieved through the use of numerous illustrations. Sharpe suggested that this approach could be enhanced through the use of Expert Systems, particularly systems developed for an educational function.

A4.2.5 Tropical Countries

Papers by several authors and the related discussion indicated that there were technical, social and legislative difficluties in the structural use of timber. Technical problems were assoiciated with the utilisation of multiple species forests, the loss of high quality species of timber, and the increasing pressure to use plantation timbers. The lack of standardisation in timber sizes was a continuing source of marketing difficulties. The social stigma (e.g. the use of timber in shanty towns) and technological stigma (such as that arising from the combustibility of timber) often led to unwarranted legislation prohibiting the use of timber.

Campbell commented on the lack of suitable and affordable texts in developing countries and suggested use of a desk top publishing facility to produce texts that could be suitably modified to suit each country as the need arose.

Boughton suggested that the mode of technology transfer to developing countries should vary depending on whether it was concerned with public buildings (direct transfer of developed technology), housing (based on the use of engineering principles to modify indigenous housing) or building materials (concerned with production and marketing technology).

A4.2.6 Trade

Three papers presented earlier at the Third International Symposium on World Trade in Forest Products in Seattle, USA, were used as a basis of discussion. The marketing of lesser known species and the use of standards as a barrier to international trade in structural timber were highlighted.

A4.2.7 Interactions

Papers and discussions were given on the interaction between CIB-W18B and other related organisations, these included organisations with related technical activities (such as CIB-W18A, ISO TC/165, IUFRO, JUNAC, ATTC) and organisations that could be in a position to fund CIB- W18B activities (such as UNIDO, IDRC, ATTC, ESCAP). For the technical interactions it is important not to duplicate work undertaken elsewhere.

The Asean Timber Technology Centre is scheduled to run Master of Science courses in Forest Products Technology for Foresters and engineers, plus other training and workshop courses. It will also set up a data base on wood technology and a data bank of experts.

In the paper by Kauman and related discussion, the point was made that the most cost-effective approaches to technology transfer in South American countries was through upgrading the local technology infrastructure.

The International Tropical Timber Organisation (ITTO) was set up primarily to promote trade in tropical timber, but does also fund related research projects. Of interest to CIB-W18B is the fact that ITTO has an interest in research on the utilisation of timber from multiple-species forests.

Hallett discussed in some detail the various methods for obtaining funding through UNIDO. At the simplest level UNIDO can provide seed money to organise workshops. At the| national| level it can act as an executing agency for projects requested by a country. UNIDO can also solicit funds from aid agencies (such as ADAB) for projects. At a| regional| level UNIDO can circulate project proposals among a region; if three countries back the proposals, then it could be possible to obtain UNDP funding for them. There was also the possiblity of obtaining funds for projects of| inter-regional| or global interest, such as the development of technology to handle lesser-known species. UNIDO is also well set up to publish documentation and to provide interpreters and translators for meetings.

In response to a question from Addae-Mensah, Hallett replied that UNIDO would initially execute a demonstration project in a developing country by using external consultants, but that once this was done the project control would be handed over to local consultants.

Adams commented that it was feasible for the Asean Timber Technology Centre to fund projects of regional interest.

A4.3 CONCLUSION

At the conclusion of the Conference a discussion was held on future activities of CIB-W18B. A set of feasible projects were proposed, and these are listed in Appendix A5. Janssen also proposed the setting up of a joint CIB-IUFRO umbrella group to study and document the topic of building with bamboo.

Funding for participants from developing countries to attend future Conferences was seen as a source of continuing difficulty, and as a result it was decided to hold the next CIB-W18B Conference in association with the International Conference on Timber Engineering; this Conference is scheduled to be held in Seattle in September 1988. In this way it could be possible for members attending the Conference to extend their stay to include the CIB-W18B meeting. A CIB-W18A meeting is scheduled to follow the Conference and it is planned to arrange for some interaction between CIB-W18A and CIB-W18B during this meeting.

Consideration should be given to the possibility of regionalising the activities of CIB-W18B in order to assist the active particpation of members.

Leicester proposed that 1991 be scheduled as a suitable date for a major conference on tropical and hardwood timber structures. It would be appropriate to use that conference as a target date for the completion of CIB-W18B project proposals.

To sum up the mood of the Conference, one would have to conclude that an over-riding concern was the topic of technology transfer to developing countries. This may have been due to the country of origin of the participants; however it may also indicate a real potential for a contribution by CIB-W18B. Certainly there was little doubt about the enthusiasm for timber engineering on the part of the participants from tropical countries.

APPENDIX V PROJECT PROPOSALS

A5.1 PROJECT No. 1 INTERNATIONAL STANDARDS

Purpose is to provide technical input for international standards. Areas of concern could include matters related to hardwoods and tropical timbers, timber from multiple species forests, the effects of tropical climates, and technology for developing countries. Examples of organisations to whom technical information is transmitted could include ISO TC/165 and the CIB-W18A code drafting committee.

A5.2 PROJECT No. 2 TRADE RELATED MATTERS

Purpose is to study trade related matters and, where suitable, take appropriate action to facilitate international trade in structural timber from tropical and hardwood timber producing countries. Initially the project will probably be concerned solely with the documentation of information.

Example of suitable topics for documentation are the following:

- comparison of national standards
- strength group systems in use
- standard timber sizes in use
- technical barriers to trade
- quality control and quality assurance systems.

A5.3 PROJECT No. 3 STRUCTURAL UTILIZATION OF MIXED SPECIES

Some of the aspects to be studied could include the following:

- stress grading
- connector systems
- adhesives
- durability/preservation
- seasoning
- structural systems.

A5.4 PROJECT No. 4 DESIGN WITH MONOCOTYLEDONS

Purpose is to draft procedures for the design of structures using monocotyledon species such as bamboo, coconut stem wood and palm wood. Initial work will be focussed on strength group classifications, design stresses, connectors and structural systems.

A5.5 PROJECT No. 5 MANUAL ON TECHNOLOGY FOR TROPICAL AND HARDWOOD TIMBER STRUCTURES

This will be a state-of-the-art documentation of research findings, written primarily for information to timber technologists. Focus will be on structural engineering with summary sections on topics such as adhesives, durability and seasoning.

A5.6 PROJECT No. 6 INTRODUCTION TO TECHNOLOGY FOR TROPICAL AND HARDWOOD TIMBER STRUCTURES

This manual will be of an introductory nature and targeted primarily at educators and design engineers.

A5.7 PROJECT No. 7 ENGINEERING PROPERTIES OF PLANTATION TIMBER FROM TROPICAL COUNTRIES

With the increasing development of hardwood and softwood plantations in tropical countries, timber from plantations has become increasingly significant as a source of structural material. For local use and for trade purposes, documentation is required on the engineering properties of these timbers. The variation of these properties with location, crop rotations and semicultural practices is of interest.

A5.8 PROJECT No. 8 SIMPLIFIED TIMBER ENGINEERING DESIGN CODES

This will be a complete suite of very simple codes that can be used to classify timber into structural grades and to design building structures therewith. The use of these codes will be either for educational purposes or for interim design purposes in countries that have no suitable standards.

A5.9 PROJECT No. 9 REGIONAL CODES

This project will be regionally based. The aim will be to pool the expertise within a region to assist in the drafting of timber engineering standards of all countries within that region.

A5.10 PROJECT No. 10 DESIGN CRITERIA

The aim will be to collate and document structural design criteria for specific types of buildings. Typical examples are housing and other non-domestic low rise buildings (such as industrial, agricultural, school and hospital buildings).

A5.11 PROJECT No. 11 POLE BUILDINGS

The project will be a documentation on all aspects involved in the design of pole frame buildings. The format used will be suitable for developing countries.

A5.12 PROJECT No. 12 BUILDING TO RESIST NATURAL HAZARDS

The documentation will be aimed at providing advice for building to resist natural hazards (such as typhoons and earthquakes) in the rural areas of developing countries. The documentation will be concerned with basic principles and detailing of connections: the presentation will be in the form of educational illustrative material, including cartoons. References to more sophisticated documentation and design standards will be included.

CIB-W18A/21-102-1

INTERNATIONAL COUNCIL FOR BUILDING RESEARCH STUDIES AND DOCUMENTATION

WORKING COMMISSION W18A - TIMBER STRUCTURES

RESEARCH ACTIVITIES TOWARDS A NEW GDR TIMBER DESIGN CODE BASED ON LIMIT STATES DESIGN

by

W Rug and M Badstube
Institute for Industrial Buildings
Academy of Building of the GDR
German Democratic Republic

MEETING TWENTY-ONE
PARKSVILLE, VANCOUVER ISLAND
CANADA
SEPTEMBER 1988

Research Activities Towards A New GDR Timber Design Code Based On Limit States Design

By W. Rug and M. Badstube
Academy of Building of the GDR,
Institute for Industrial Buildings

Berlin, 1988

Table of Contents

1. Status of research work

Recent basic research activities have resulted in further deepening the hitherto available state of knowledge, know-how and information included in the bibliographical references /1/, /2/ and /3/ as listed at the end of this paper.

In 1987, investigations have been accomplished in the GDR concerning the adaptation factors /4/, as to checking the load-bearing capacity of connecting means (timber fasteners) /8/, for acquiring basic values with nailed connections /17/, as to designing (dimensioning) compressed members /9/, /14/, /22/, concerning the compressive strength of structural timber /15/, as to the creep behaviour of structural timber /16/, and concerning the adaptation factors as to "aggressive media" /11/, /13/.

Furthermore, the latest publications were reviewed and evaluated and investigations into the material factor, into the standard values of the flexural strength of glued laminated timber, into the influence of the key-dovetail skew notch on the flexural strength of glued laminated timber, and into the tensile strength of key-dovetailed layers of timber boards have been performed. The results and findings of said investigations including a summary of all other results and findings are provided in reference /5/.

The hitherto existing draft code /1/ has been further improved.

A comparison of the improved draft code with the international trend shows that it complies widely with the ISO draft specification /23/ concerning the designations, the grades of moisture, the grades of load duration and with regard to the conditions prevailing for the experimental determination of the strength parameters of structural timber, glued laminated timber and connections (fasteners).

The great number of tests and experiments performed with a view to scientifically establishing and consolidating the new timber design code was effected in accordance with the standard recommendations as prepared by RILEM/CIB concerning the testing of structural timber and connections.

With the standard values of the design strength and of the magnitude of the material factor, in the main the Eurocode /25/ was followed. The adaptation factor as to "long-term behaviour" has been determined in accordance with the factors applied by the ISO Code and the Eurocode /25/, with the influence of the moisture on the strength as included in said factor being derived from the results of our own tests and experiments performed with beams when subjected to bending /2/.

The adaptation factors as to "cross-sectional height" and "curvature of timber" were obtained in accordance with the Swiss Code. In spite of the fact that the results and findings of our own tests and experiments performed with glued laminated timber beams with depths ranging between 192 mm and 900 mm - as related to the 5 % quantile - did not show any decrease in strength /3/, for the time being the proposed adaptation factor for the cross-sectional height will not be changed.

The adaptation factor for aggressive media considers mainly results and findings obtained from comprehensive investigations performed in the GDR.

In addition, investigations have been initiated with a view to preparing a special standard specification (code) concerning the analysis of the structural state of repair, the calculation (design) and restoration of historical timber structures /6/. Essential fundamentals for such a code are included in the papers as mentioned under /11/ to /13/ and /18/ to /21/.

2. Draft code

2.1. Basic values of the design strength and of the moduli of elasticity

The basic values of the design strength and of the moduli of elasticity are being obtained from the 5 % quantiles according to the formulae (1) and (2) as follows :-

$$R^{o} = \frac{R_{5\%} \cdot k_t}{\gamma_{m,o}} \qquad (1)$$

$$E^{o} = \frac{E_{5\%} \cdot k_t}{\gamma_{m,o}} \qquad (2)$$

k_t = time factor = 0.75 with tension across the grain, shear stress in the limit state of the load-bearing capacity for structural timber and glued laminated timber

k_t = time factor = 0.85 with bending and compressive stress and strain (across and parallel to the grain), tensile stress and strain parallel to the grain in the limit state of the loadbearing capacity for structural timber and glued laminated timber

$\gamma_{m,o}$ = 1.3 with bending and tensile stress and strain (across and parallel to the grain, shear stress and strain for structural timber and glued laminated timber

$\gamma_{m,o}$ = 1.1 with compressive stress and strain parallel to and across the strain in the limit state of the loadbearing capacity for structural timber and glued laminated timber

Since our own investigations into the influence of the load duration on the strength of structural timber and glued laminated timber are not yet completed, the time factor k_t was determined in accordance with the reviewed and evaluated international status. In this connection, mainly the standard recommendations included in /23/ and /24/ have been followed.

The material factor was obtained from a comparison with the method of permissible stresses and in accordance with the reviewed international publications. Additional investigations to be performed on a probabilistic basis are planned.

The calculated basic values as included in table 1 are based on the standard values as indicated in /2/.

2.2. Adaptation factor as to "long-term behaviour" $\gamma_{m,1}$

$\gamma_{m,1}$ covers the influence of the magnitude of loading, duration of loading, moisture of timber and temperature. As compared with /1/, the number of time grades has been increased from 3 to 4 (with time grade D applying to instantaneous load action - see table 2 b). The grouping into time grades subject

to the possible load combinations is represented in table 2 c. The tables 2 d and 2 e are indicating the values of $\gamma_{m,1}$ for the limit state of the loadbearing capacity and for the limit state of the usability.

2.3. Adaptation factor as to "cross-sectional height" $\gamma_{m,2}$

$\gamma_{m,2}$ is included in table 3 which has not been changed as compared with /1/.

2.4. Adaptation factor as to "curvature of timber" $\gamma_{m,3}$

$\gamma_{m,3}$ is included in table 4 which has not been changed as compared with /1/.

2.5. Adaptation factor as to "aggressive media" $\gamma_{m,4}$

Investigations recently performed by Erler as indicated in /11/ and /13/ resulted in an improvement of the recommendation included in /1/. $\gamma_{m,4}$ is given in the tables 5a to 5e subject to 3 stress degrees and to the cross-sectional size. The stress degrees are obtained from the grouping of available aggressive media (gases, solutions and solids) into ranges of aggressivity. With gases and solids, the grade of moisture must be considered when grouping them.

3. Results and findings of special investigations

3.1. Strength of key-dovetailed connections

When producing glued laminated timber, individual uniformly distributed layers of timber boards have been sampled from which test specimens subjected to tensile stress and strain (sized 10 by 70 by 550 mm - see figure 1) with and without key-dovetailing were manufactured.

With mechanically sorted layers of timber boards, 6 tests have been performed covering 20 to 68 specimens each (see tables 6a to 6d). Visually sorted layers of boards representing the quality grades I to III according to /26/ were sub-

jected to 3 tests covering 21 to 96 specimens each (see tables 7a and 7b).

The tests have been accomolished in the standard condition as follows :-

- temperature of 20°C,
- moisture of timber from 8 to 13 %,
- test duration from 3 to 5 minutes.

The standard values are the 5 % quantiles of the three-parametric Weibull distribution according to /27/. The results and findings are shown in the tables 6a, 6c and 7a.

To an extent of 78 % of the test specimens with key-dovetailing, the failure occurred within the zone of the key-dovetailed connection whereas the specimens without key-dovetailing failed in the cross sections with large knot areas.

Layers of timber boards without key-dovetailing have a tensile strength being in part very much higher than that of key-dovetailed layers of boards. In addition, the tensile strength of mechanically sorted layers of boards (without key-dovetailing)considerably exceeds the values obtained for visually sorted layers of timber boards. Analogous results are achieved with regard to the moduli of elasticity of layers of boards without any key-dovetailing. The values for the tensile strength of key-dovetailed layers of boards correspond to international values stated by Larsen /28/, Ehlbeck and others /29/.

3.2. Influence of the key-dovetailed connection on the flexural strength of glued laminated timber

Girders of glued laminated timber (hereinafter sometimes referred to as GLT in English or as BSH when abbreviated in German within figures and/or tables) are being produced the layers of boards of which were sorted mechanically (see figure 2). The GLT (or BSH, respectively) cross sections correspond to those included as BSH 4 and BSH 6 in table 8. The bottom layer within the test zone - abbreviated in German as PB (see figure 3, layer 1) - was provided both with and without key-dovetailing (abbreviated in German as KZ). The key-dovetail skew notching (abbreviated in German as KZV) between the first

and second layer amounts to 250 mm whereas with all other layers it is at choice. The key-dovetail length (abbreviated in German as KZL) amounts to 50 mm with these connections. With a view to providing a zone being free from transverse forces, a four-point loading has been selected for the test design and arrangement of the GLT girders. In order to avoid shear (diagonal tension) failures, an analysis of investigations performed by means of structural timber results in obtaining a ratio of 22 concerning the bending stress to shear stress, and in obtaining a ratio of 15 concerning the effective span to test-specimen height for a shear influence of about 6 per cent. Thus, the length of the test zone is obtained as 4 h (see figure 3).

By comparing the tests accomplished with and without key-dovetailing in layer 1, statements can be made concerning the effect of the key-dovetailing on the flexural strength of glued laminated timber (see table 9; comparison of test B1 with B2 and B3 with B4). Among other data, average values, 5 % quantile values and 1 % quantile minimum values of the flexural strength and of the modulus of elasticity in bending for the GLT girders are being indicated. The values are derived from three-parametric Weibull distributions. The results and findings one can state are as follows :-

1. As to their magnitude, the minimum values of the flexural strength and of the modulus of elasticity in bending correspond to the 5 % quantiles (see table 9; comparison of $R_{m,min}$ with $R_{m,5\%}$ and of $E_{m,min}$ with $E_{m,5\%}$).

2. Flexural strength and modulus of elasticity in bending are increasing with an improving quality of glued laminated timber (see table 9: B4 compared with B2; B3 compared with B1). Thus, the amounts of the increase in strength for the standard value of $R_m^n = R_{m,5\%}$ are with: BSH 6 (test B4) as compared with BSH 4 (test B2) equal to 43 %; BSH 6 (test B3) as compared with BSH 4 (test B1) equal to 42 %. The amounts of the increase in the modulus of elasticity in bending for the standard value of $E_m^n = \bar{E}_m$ are with: BSH 6 (B4) as compared with BSH 4 (B2) equal to 16 %; BSH 6 (B3) as compared

with BSH 4 (B1) equal to 16 %. One can see that the amounts of the increase in flexural strength and modulus of elasticity in bending with an improving quality of GLT in case of the girders without any key-dovetailing (tests B4 and B2) are nearly equal to those prevailing in case of the girders with key-dovetailing (tests B3 and B1).

3. The tests performed by means of BSH 4 without key-dovetailing in layer 1 of the test zone (see table 9: test B2) result in increased strength values being higher by 12 % for $R_{m,5\%}$ as compared with those tests accomplished by means of GLT with key-dovetailing (see table 9: test B1). The tests performed by means of BSH 6 without key-dovetailing (table 9: B4) result in increased strength values being higher by 11 % for $R_{m,5\%}$ as compared with those tests accomplished by means of GLT with key-dovetailing (table 9: B3). Thus, the key-dovetailing has adverse effects on the flexural strength of GLT (BSH) girders.

4. The failure of the GLT girders is initiated by the rupture of the first layer in the key-dovetailing area to an extent of about 80 % and in the layer cross section with large knots to an extent of about 20 % only.

3.3. Influence of the key-dovetail skew notch on the flexural strength of glued laminated timber

14 GLT girders have been selected the key-dovetail skew notching of which between the first and second layer (when counted from the bottom) amounted to 0 up to 800 mm; during the tests, the failure occurred always in the key-dovetailing of the first layer. The influence of the key-dovetail skew notch on the flexural strength R_m should be determined by means of a regression analysis. The regression analysis yields the regression equations with the appropriate correlation coefficients as indicated in table 10. The highest correlation coefficient amounting to $r = 0.473$ is provided by equation 4. However, the connection is weak (see reference /31/, page 85). The reason for this must be sought in the fact that the scattering or deviation due to the effect of

influencing factors other than key-dovetail skew notching is considerable.

With r = 0,473, R_m is equal to 32.71 (KZV)$^{0.0066}$ $(\frac{N}{mm^2})$. Measured values and functional values of the equation 4 are plotted in figure 4. As for a deviation of 1 % of the flexural strength with KZV = 800 mm, the result will be a minimum key-dovetail skew notch (min.KZV) between the first and second layer amounting to 150 mm.

3.4. Influence of the key-dovetail length

(a) Influence of the key-dovetail length on the flexural strength of glued laminated timber girders

GLT girders of the production A having a key-dovetail length (abbreviated in German as KZL) of 50 mm the failure of which during the tests occurred always in the key-dovetailing (abbreviated in German as KZ) are being selected and compared with GLT girders of the production B having a key-dovetail length of 20 mm.

The GLT girders consist of visually sorted layers of timber boards of grade II coniferous sawn timber (abbreviated in German as NSH II). The results of the tests are indicated in table 11 from Weibull distributions. When comparing the 5 % quantiles of the flexural strength, one will find out that glued laminated timber having a key-dovetail length of 20 mm (KZL 20) has an increased strength being by 23 % higher than that of glued laminated timber having a key-dovetail length of 50 mm (KZL 50).

The reasons for the increased strength values may be not only the key-dovetail lengths but also the different level of wear and tear (deterioration) of the technologies concerned (see table 11). Thus, for instance, the key-dovetailing press employed in case of production A is obsolete as compared with that employed in case of production B.

(b) Influence of the key-dovetail length on the tensile strength of key-dovetailed layers of timber boards

The tensile strengths obtained as a result of tests performed by means of visually sorted key-dovetailed layers of

timber boards (see table 7a) are being indicated in table 12. The test specimens are sampled from the productions A and B. When comparing the 5 % quantiles of the tensile strength (see table 12), one will find out that glued laminated timber of production B having a key-dovetail length of 20 mm (KZL 20) has an increased tensile strength being by 24 % higher than that of glued laminated timber of production A having a key-dovetail length of 50 mm (KZL 50). However, production B is also provided with a technology being better than that of production A. When comparing the 5 % quantiles of the flexural strength with those of the tensile strength (i.e. a comparison of table 11 with table 12), one will find out that the value of the flexural strength amounts to 1.7 times the value of the tensile strength in case of both the productions A and B.

4. Summary - Problems to be solved in future

The hitherto available draft code /1/ was further improved by making use of the latest knowledge, know-how and information. Changes and modifications occurred concerning the grades of load duration and with regard to the adaptation factor as to "aggressive media". The basic values of the design strength for structural timber and glued laminated timber were defined. A comparison of the tensile strength of key-dovetailed layers of timber boards with that of layers of boards without any key-dovetailing results in determining a decrease in strength by 38 % for key-dovetailed layers of timber boards.

The tensile strength of mechanically sorted layers of timber boards without any key-dovetailing is considerably higher than that of visually sorted layers. Glued laminated timber girders without any key-dovetailing have an increased flexural strength (being higher by 11 to 16 %) - when related to the 5 % quantile - as compared with girders with key-dovetailing in the test zone.

The research activities to be performed in future shall be orientated towards investigations into the following problems :-

1. The possibility of increasing the strength of glued laminated timber girders.

2. The loadbearing capacity of glued laminated timber girders subjected to a long-term loading (stress and strain).

3. Fundamentals required for the restoration of historical timber structures.

4. Fundamentals required for preparing a separate code applying to timber-based engineering material structures.

5. Fundamentals required for improving the methods and procedures of sorting.

5. Bibliographical references

(Note: The references marked (x) are indicating publications or papers in German!)

/1/ Rug, W.; Badstube, M.
New Developments of Limit States Design for the New GDR Timber Design Code
Academy of Building of the GDR, CIB-W18-Paper 19-102-4, Florence, 1986.

/2/ Rug, W.; Badstube, M.
Development of a GDR Limit States Design Code for Timber Structures
Academy of Building of the GDR, Institute for Industrial Buildings. CIB-W18-Paper 20-102-1; Dublin, 1987.

/3/ Badstube, M.; Rug, W. (x)
Forschungsarbeiten auf dem Gebiet der Bemessung nach Grenzzuständen in Vorbereitung auf den neuen DDR-Standard Holzbau (Research activities in the field of limit states design in preparing the new GDR Timber Design Code).
Published in: Holztechnologie, Leipzig 22 (1986):281-336; Bauforschung-Baupraxis Heft 205, Berlin 1988

/4/ Zimmer, K.-H. (x)
Anpassungsfaktoren für die Bemessung nach Grenzzuständen im Holzbau (Adaptation factors for limit states design in timber construction).
Published in: Bauforschung-Baupraxis Heft 205, Berlin 1988

/5/ Badstube, M.; Rug, W. (x)
Berechnung nach Grenzzuständen im Holzbau, Teilthema: Grundlagen, Berechnung und Konstruktion von Holzkonstruktionen (Limit states design in timber construction; Partial theme: Fundamentals, design and construction of timber structures). Academy of Building of the GDR, Institute for Industrial Buildings; Research report; Berlin, 1987.

/6/ Rug, W. (x)
Berechnung nach Grenzzuständen im Holzbau, Teilthema: Grundlagen, Berechnung und Instandsetzung von historischen Holzkonstruktionen (Limit states design in timber construction; Partial theme: Fundamentals, design and repair of historical timber structures).
Academy of Building of the GDR, Institute for Industrial Buildings; Research report; Berlin, 1987.

/7/ Rug, W. (x)
Internationaler Trend in der Normung
Mitteilung 1/88 des Fachausschusses Ingenieurholzbau und des Instituts für Industriebau, Berlin 1988 (in Vorbereitung).
(International trend in standardization - Information 1/88 of the Special Committee on Engineering Timber Construction and of the Institute for Industrial Buildings; Berlin, 1988 (under preparation)).

/8/ Zimmer, K.-H.; Lißner, K. (x)
Zum Nachweis der Tragfähigkeit von Verbindungsmitteln nach Grenzzuständen im Holzbau.
Mitteilung 1/88 ... Berlin 1988 (in Vorbereitung).
(On the check of the loadbearing capacity of Fasteners by adopting limit states in timber construction - Information 1/88 ...as above...Berlin, 1988 (under preparation)).

/9/ Kaiser, K. (x)
Zur Bemessung schlanker Holzdruckstäbe nach Theorie II. Ordnung - Mitteilung 1/88 ... Berlin 1988 (in Vorbereitung).
(On the design of slender compressed timber members by adopting the second-order theory - Information 1/88 ... as above...Berlin, 1988 (under preparation)).

/10/ Badstube, M. (x)
Rechenbeispiele zum 3. Entwurf des DDR-Fachbereichsstandards "Holzbau / Tragwerke / Teil 1". - Mitteilung 1/88 ... Berlin 1988 (in Vorbereitung).
(Calculation examples for the 3rd draft of the Special GDR Branch Code "Timber construction / Loadbearing systems / Part 1". - Information 1/88 ...as above...Berlin, 1988 (under preparation)).

/11/ Erler, K. (x)
Bauzustandsanalyse und Beurteilung der Tragfähigkeit von Holzkonstruktionen unter besonderer Berücksichtigung der Korrosion des Holzes (Analysis of the structural state of repair and evaluation of the loadbearing capacity of timber structures with particular consideration of the corrosion of timber).
Dissertation B (thesis); Wismar Engineering College, 1988.

/12/ Kothe, E. (x)
Grundlagen für die Berechnung und Instandsetzung alter Holztragwerke; Teilthema: Methode zur Bestimmung der Festigkeit von alten Holzkonstruktionen (Fundamentals for the design and repair of old timber loadbearing members; Partial theme: Method for determining the strength

of old timber structures).
Dresden University of Technology, Construction Engineering Department; Research report; Dresden, 1987

/13/ Erler, K. (x)
Berechnung nach Grenzzuständen im Holzbau
Teilthema: Anpassungsfaktor "Aggressive Medien" von Bau- und Brettschichtholz (Limit states design in timber construction - Partial theme: Adaptation factor as to "aggressive media" for structural timber and glued laminated timber).
Wismar Engineering College, Dept. for Technology in Construction; Research report; Wismar, 1987.

/14/ Kaiser, K. (x)
Berechnung nach Grenzzuständen im Holzbau
Teilthema: Beitrag zur Bemessung knickgefährdeter Holzbauteile nach der Methode der Grenzzustände (Limit states design in timber construction - Partial theme: Contribution to the dimensioning of timber components subjected to a risk of buckling by adopting the limit states method). Wismar Eng. Coll.; Research report; Wismar, 1987.

/15/ Kiesel, . (x)
Berechnung nach Grenzzuständen im Holzbau
Teilthema: Beitrag zur Ermittlung der Verteilungsfunktion der Festigkeitseigenschaften des Bauholzes unter besonderer Berücksichtigung des Festigkeitsverhaltens bei der Druckbeanspruchung für eine Bemessung nach der Methode der Grenzzustände (Limit states design in timber construction - Partial theme: Contribution to the determination of the distribution function of the strength properties of structural timber with particular consideration of the strength behaviour under compressive stress for a dimensioning by adopting the limit states method).
Wismar Eng. Coll.; Research report; Wismar, 1987.

/16/ Karstadt, M. (x)
Bemessung nach Grenzzuständen im Holzbau
Teilthema: Vorschlag für Anpassungsfaktoren zum Langzeitverhalten biegebeanspruchter Vollholzquerschnitte
(Limit states design in timber construction - Partial theme: Proposal for adaptation factors as to long-term behaviour of solid timber cross sections subjected to bending stress).
Wismar Eng. Coll.; Research report; Wismar, 1987.

/17/ Lißner, K. (x)
Bemessung nach Grenzzuständen im Holzbau
Teilthema: Experimentelle Ermittlung der Rechengrundwerte der Tragfähigkeit von Nagelverbindungen
(Limit states design in timber construction - Partial theme: Experimental determination of the basic design values of the loadbearing capacity of nailed connections)
Dresden University of Technology; Construction Engineering Dept.; Research report; Dresden, 1987.

/18/ Erler, K. (x)
Grundlagen zur Rekonstruktion von Holzkonstruktionen
(Fundamentals for the restoration of timber structures).
Wismar Eng. Coll.; Research report (not published);
Wismar, 1984.

/19/ Erler, K. (x)
Bauzustandsanalyse, Instandsetzung und Rekonstruktion
von Holzkonstruktionen
Entwurf einer Richtlinie; Mitteilung 1/85 des Fachausschusses Ingenieurholzbau und des Instituts für Industriebau, Berlin 1986
(Analysis of the structural state of repair, repair and restoration of timber structures; - Draft guideline specification - Information No. 1/85 of the Special Committee on Engineering Timber Construction and of the Institute for Industrial Buildings; Berlin, 1986).

/20/ Seemann, A. (x)
Durchführung von Versuchen zur Feststellung der Tragfähigkeit von eingebautem (alten) Bauholz und Auswertung der dazu vorhandenen Literatur
(Implementation of tests for determining the loadbearing capacity of built-in (old) structural timber and review of the available publications).
Weimar College of Architecture and Construction; University graduation paper; Weimar, 1988.

/21/ Mönck, W. (x)
Schäden an Holzkonstruktionen - Analyse und Behebung
(Damages done to timber structures - Analysis and repair).
1st edition; Berlin, 1987.

/22/ Duy, W. (x)
Ebenes Spannungsproblem im Holzbau, Berechnungsgrundlage
(Plane stress problem in timber construction; Design basis)
Published in: Bauforschung-Baupraxis, Heft 210; Berlin, 1987.

/23/ ISO-TC-165-N, 1983-05-11
Timber Structures, Design, First Working Draft; June, 1983; ISO, Technical Committee 165.

/24/ CIB-W18-Code
CIB - Structural Timber Design Code, Sixth Draft; January, 1983; CIB Report 1983, Publication G6, Working group W18, Timber Structures.

/25/ Larsen, H.-J.
Eurocode 5, Timber Structures
CIB-W18-Paper 18-1-2, Orew 1980.

/26/ DDR-Norm: (x)
TGL 117-0767, 1963. Bauschnittholz, Gütebedingungen
(GDR Code ... Sawn Timber - Quality Conditions).

/27/ RGW-Norm: (x)
ST-RGW 877-78; DDR-Norm TGL 38791/03
Angewandte Statistik, Bestimmung der Schätzwerte und Konfidenzgrenzen für Parameter der Weibull-Verteilungen (CMEA Code ... ; GDR Code ... - Applied Statistics; Determination of Estimated Values and Confidence Limits for Parameters of the Weibull Distributions).

/28/ Larsen, H.-J. (x)
Die Festigkeit von Brettschichtholz
In: Ingenieurholzbau in Forschung und Praxis
(The Strength of Glued Laminated Timber - Published in: ...as above...)
Karlsruhe, 1982.

/29/ Ehlbeck, J.; Colling, F.; Görlacher, R. (x)
Einfluß der Keilzinkenlamellen auf die Biegefestigkeit von Brettschichtholzträgern (Influence of the key-dovetailed lamellae on the flexural strength of glued laminated timber girders).
In (published in): Holz als Roh- und Werkstoff 43 (1985): 333-337; 43 (1985):369-373; 43 (1985):439-442.

/30/ Apitz, R. (x)
"Ermittlung von Festigkeitswerten für Vollholz bei der Beanspruchungsart Biegung durch Versuche"
(Determination of strength values for solid timber subjected to the bending type of stress and strain by means of tests)
Wismar Engineering College; Research report; Wismar, 1982.

/31/ Schindowski, Schürz (x)
"Statistische Qualitätskontrolle"
(Statistical Quality Control).
7th edition; Publishers: VEB Verlag Technik, Berlin.

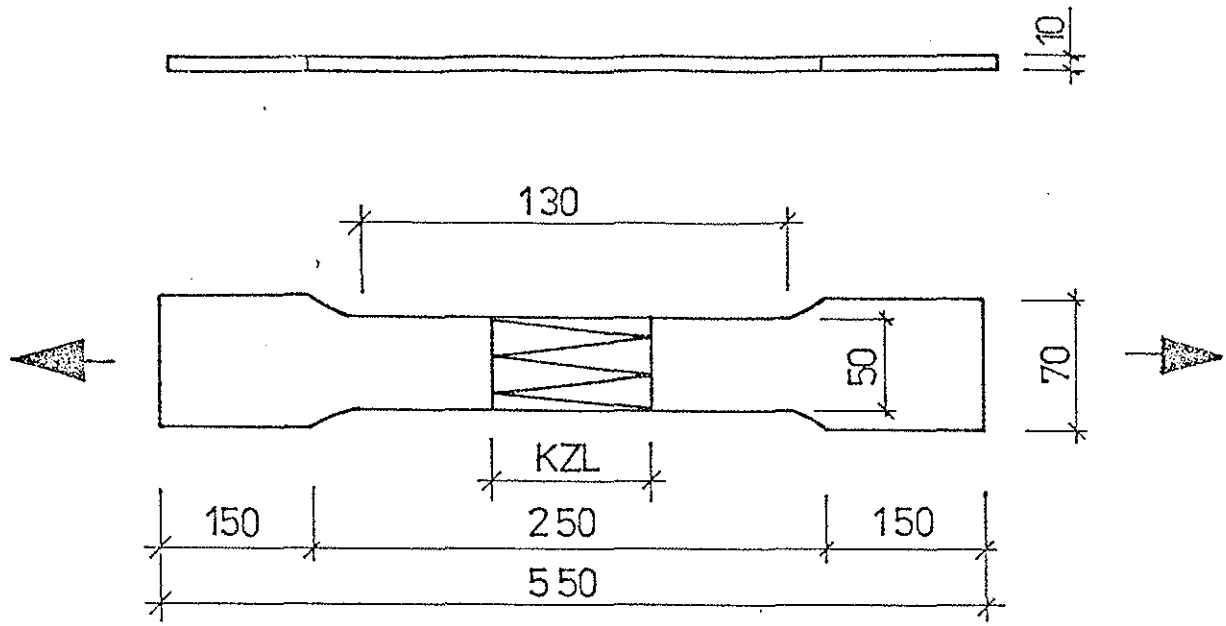

quality grade II sawn coniferous timber

key-dovetail length of 50mm with production A
key-dovetail length of 20mm with production B

Figure 1:Tensile test with key-dovetailing

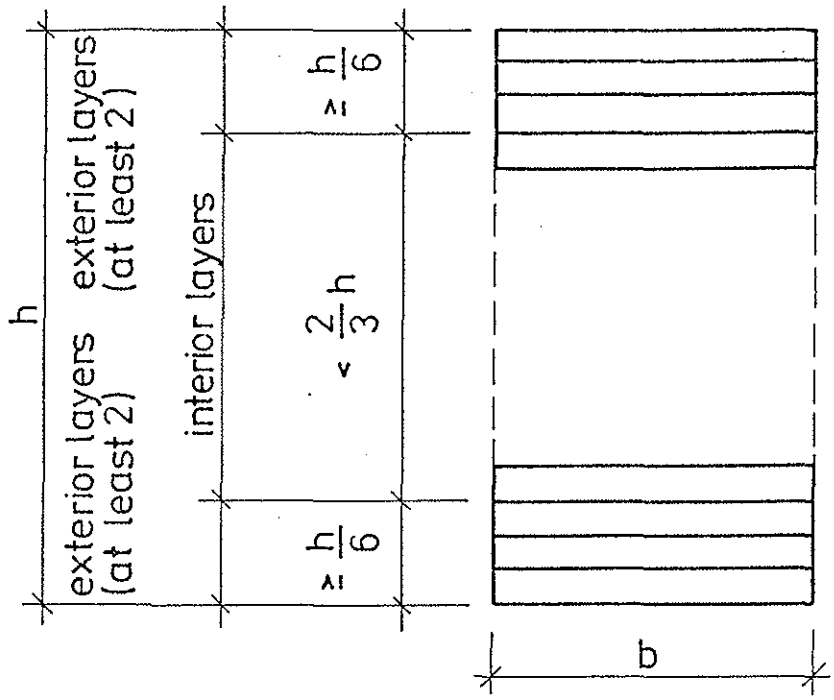

Figure 2: Design of glued laminated timber

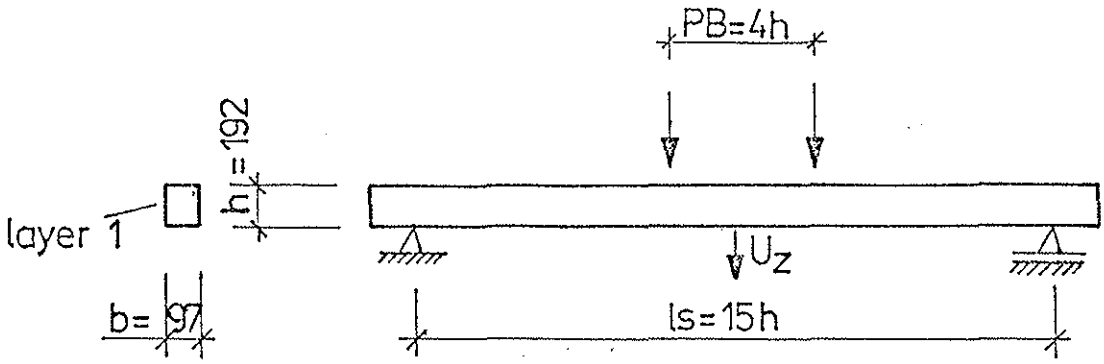

12 test specimens for each test

Designations:

PB = test zone
BSH = glued laminated timber
F = strength grade
KZ = key-dovetailing

Figure 3: Test arrangement

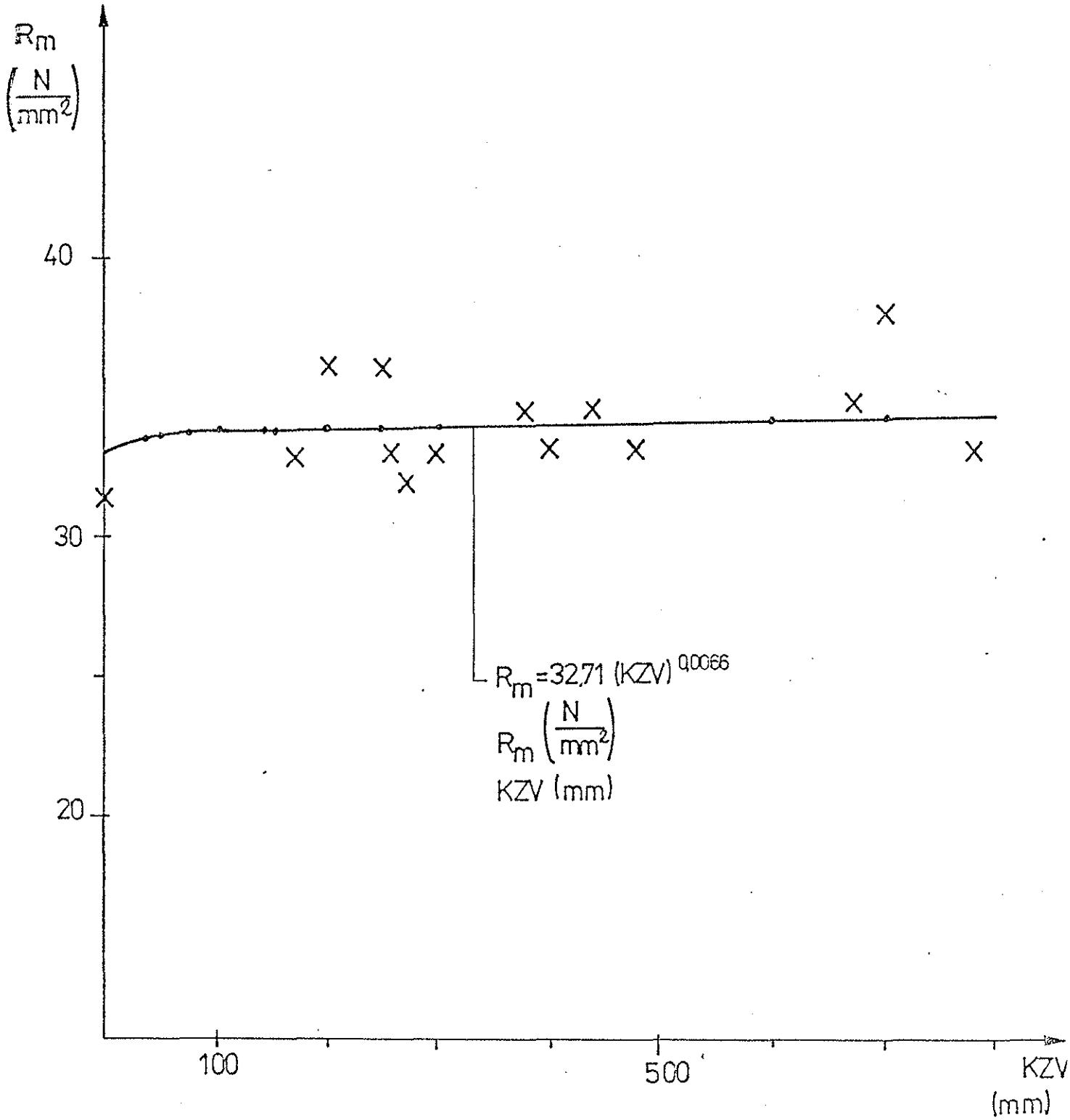

Figure 4: Behaviour of R_m(KZV)

KZV=key-dovetail skew notching

Table 1: Basic values of the design strength, standard and basic values of the elastic moduli (E) and shearing moduli (G), in $\frac{N}{mm^2}$

		softwood													hard-wood
		sawn timber						glued laminated timber						round timber	
		quality grade			strength grade			grade							
		I	II	III	I	II	III	1	2	3	4	5	6		
bending	R°_{m}	18,6	15,7	14,1	24,9	18,6	14,1	18,6	15,7	14,1	19,6	18,6	15,7	15,7	19,6
tension	$R^{\circ}_{t,o}$	11,8	8,5	4,9	15,7	11,8	7,2	8,5	6,2	8,5	9,5	10,1	8,8	8,5	13,1
	$R^{\circ}_{t,90}$	0,3	0,25	0,1	0,35	0,3	0,15	0,25	0,2	0,25	0,25	0,3	0,25	0,25	0,3
compres-sion	$R^{\circ}_{c,o}$	20,1	16,2	14,7	23,2	20,1	14,7	16,2	15,1	16,2	13,5	20,1	13,5	16,2	20,1
	$R^{\circ}_{c,90}$	6,2	5,8	5,4	8,5	6,2	5,4	5,8	5,4	5,8	5,8	6,2	5,8	5,8	6,2
shearing-off ll to the grain	$R^{\circ}_{v,o}$	1,3	1,2	1	1,7	1,3	1	1,3	1,2	1	1,4	1,3	1,2	1,2	1,7
shear from transv. force	R°_{v}	1,7	1,6	1,4	2,2	1,7	1,4	1,7	1,6	1,4	1,8	1,7	1,5	1,6	1,7
moduli	E^{n}_{o}	12 000	11 000	10 000	13 500	12 000	10 000	12 000	11000	10 000	12 500	12 000	11 000	11 000	12 500
	E^{n}_{90}	400	350	300	450	400	300	400	350	300	400	400	350	350	400
	G^{n}_{90}	750	700	600	850	750	600	750	700	600	800	750	700	700	800
	E°_{o}	5600	4900	4600	6200	5600	4600	5600	4900	4600	5900	5600	4900	4900	5900
	E°_{90}	170	140	120	190	170	120	170	140	120	170	170	140	140	170
	G°	310	290	250	350	310	250	310	290	250	330	310	290	290	330

Table 2 a: Moisture grades

Moisture grade (FK)	Relative air humidity φ (%)	Moisture of timber u (%)	Case of application / Category of structure
FK 1	< 65	≤ 18	Enclosed buildings/structures with and without heating; enclosed and ventilated animal shelter buildings without heating; open and partially open roofed-over buildings
FK 2	$65 \leq \varphi \leq 85$	>18 to 24	Free-standing loadbearing systems/members without any protection against climatic influences; industrial buildings with corresponding technologies; wet rooms
FK 3	> 85	> 24	Structures subjected to the immediate influence of water

Table 2 b: Time grades

Time grade	Duration of the load action
A	Permanently and/or for a long period (e.g. dead load, live load)
B	For a short period (e.g. live load, snow)
C	For a very short period (e.g. wind)
D	Suddenly (e.g. impact, earthquake)

Table 2 c: Load combinations; grouping into time grades

Load combination	Time grade			
	A	B	C	D
A + B	LA $\geq$ 85%	LA $<$ 85%	-	-
A + C	LA $\geq$ 85%	-	LA $<$ 85%	-
A + B + C	LA $\geq$ 85%	LC $\leq$ 15%	LC $<$ 15%	-
A + B + C + D	LA $\geq$ 85%	LD $\leq$ 15% LA $\leq$ 85%	- -	LD $>$ 15 % -

LA (etc.) means load percentage of time grade A (etc.) of the total load

e.g. $LA = \frac{A}{A+B}$

Table 2 d: Adaptation factor $\gamma_{m,1}$ as to "long-term behaviour" for the limit state of the loadbearing capacity (GZT)

Time grade	Moisture grade (FK) FK 1		FK 2		FK 3	
	BH	BSH	BH	BSH	BH	BSH
A	0.85	0.8	0.75	0.66	0.65	0.4
B	1	1	0.85	0.83	0.75	0.5
C	1.2	1.2	1	1	0.9	0.6
D	1,3	1.3	1.2	1.16	1.05	0.7

BH means structural timber; BSH means glued laminated timber
For air temperatures of $40^{\circ}C \leq T \leq 70^{\circ}C$ and FK 1, $\gamma_{m,1}$ shall be multiplied by 0.85.

Table 2 e: Adaptation factor $\gamma_{m,1}$ as to "long-term behaviour" for the limit state of the usability (GZN)

Time grade	Moisture grade (FK) FK 1		FK 2		FK 3	
	BH	BSH	BH	BSH	BH	BSH
A	0.65	0.8	0.4	0.5	-	-
B	0.75	0.85	0.5	0.6	-	-

Table 3: Adaptation factor $\gamma_{m,2}$ as to "cross-sectional height" for the GZT limit state

Cross-sectional height h (mm)	Structural timber	Glued laminated timber
≤ 200	1	1.00
$200 \leq h < 300$	0.95	1.00
$300 \leq h < 500$	-	0.95
$500 \leq h < 800$	-	0.9
$800 \leq h < 1500$	-	0.85
≥ 1500	-	0.8

Table 4: Adaptation factor $\gamma_{m,3}$ as to "curvature of timber" for the GZT limit state						
$\frac{t}{r}$	0	$2 \cdot 10^{-3}$	$4 \cdot 10^{-3}$	$6 \cdot 10^{-3}$	$8 \cdot 10^{-3}$	10^{-2}
$\gamma_{m,3}$	1	0.92	0.83	0.76	0.68	0.6

r is the radius of curvature of the curved timber.

t is the thickness of the curved timber or - with glued laminated timber - the thickness of one curved layer.

Table 5: Adaptation factor $\gamma_{m,4}$ as to "aggressive media" for the GZT and GZN limit states for BH and BSH	
The kind of the media is grouped into gases, solutions and solids. By considering the criteria as to concentration of the medium concerned and the grade of moisture, the stress degrees (BG) I, II, III are obtained:	
Stress degree (BG)	Explanation
BG I	Not or slightly aggressive
BG II	Moderately aggressive
BG III	Heavily aggressive

Upon grouping the medium concerned into a specific range of aggressivity, the stress degree (BG) can be determined by means of the tables following hereinafter. Depending on the cross-sectional size of the timber components concerned, the adaptation factor $\gamma_{m,4}$ for aggressive media can be drawn from table 5e with the stress degree concerned.

Ranges of aggressivity and stress degrees for gases

Table 5 a: Ranges of aggressivity for gases			
	Gas group with a concentration (mg/m^3) of:		
Gas, increasing aggressivity	A 1	A 2	A 3
1. CH_2O (formaldehyde)	1 ... 200	-	-
2. NH_3 (ammonia)	0.5... 20	-	-
3. SO_2 (sulphur dioxide)	0.2... 10	10...200	-
4. NO_2 (nitric oxide)	0.1... 5	5... 25	above 25
5. HCl (hydrogen chloride)	0.05... 1	1... 10	above 10
6. Cl_2 (chlorine)	0.02... 1	1... 5	above 5

Table 5 b: Stress degrees for gases

Range of aggressivity	Moisture grade FK 1	FK 2	FK 3
A 1	I	I	I
A 2	I	II	II
A 3	II	II	II

Table 5 c: Stress degrees for solutions

Group	Solution	pH-value	Concentration of the solution	Degree of dissociation	Stress degree
Acids	nitric acid HNO_3	below 2	up to 5 above 5	high	III III
	hydrochloric acid HCl		up to 5 above 5	high	III III
	sulphuric acid H_2SO_4		up to 5 above 5 / above 15	medium	I II/III
	acetic acid $C_2H_4O_2$	4	above 15	low	I
Bases	soda lye NaOH	above 13	up to 2 above 2	high	II III
	potash lye KOH		up to 2 above 2	high	II III
	ammonium hydroxide NH_4OH		up to 5 above 5	low	I II
Salt solutions	chlorid solutions KCl, NaCl	7	up to 10 above 10	medium	I II
	sulphate solutions: Na_2SO_4 (Glauber's salt)		up to 10 above 10	medium	I II
	$(NH_4)\ SO_4$ (ammonium sulphate)	5	up to 40		I
(Organic compound)	urea $CO\ (NH_2)_2$	2	up to 40		II

Table 5 d: Stress degrees for solid media

Solid medium	pH-value	Solubility in water	Hygroscopicity	Stress degree (BG) with FK1	FK2	FK3
potash fertilizer	8	good (up to 20 %)	good	I	II	II
urea	9	good (up to 40 %)	high	I	II	II
superphosphate	3	(up to 5%)	good	I	I	II
sodium chloride	7	good	good	I	I	II
ammonium sulphate	5	good (up to 40 %)	low	I	I	I

Table 5 e: Adaptation factors $\kappa_{m,4}$ for aggressive media subject to the timber cross-sectional size

Note: Minimum dimension of the timber component with stress degrees BG II and BG III: 40 mm
Minimum cross-sectional area: 4000 mm^2

Stress degree (BG)	Cross-sectional size (10^3 mm^2)	Factor $\kappa_{m,4}$
BG I		1.0
BG II	< 9	0.75
	< 30	0.85
	≥ 30	0.95
BG III	< 9	0.65
	< 30	0.75
	≥ 30	0.85

Table 6a: Tensile strengths of mechanically sorted layers of boards (values of tests after 3 to 5 minutes; Weibull distributions, production A, KZL 50)

test	sample	n (-)	$\bar{\rho}$ ($\frac{kg}{m^3}$)	$\bar{u}$ (%)	$\bar{R}t$ ($\frac{N}{mm^2}$)	V_R (%)	Rt 5% ($\frac{N}{mm^2}$)	Rt 1% ($\frac{N}{mm^2}$)	Rt min ($\frac{N}{mm^2}$)
Z 1	FI without KZ	35	582	6,0	67,4	23,8	41,6	33,9	29,7
Z 2	FI with KZ	20	548	5,4	32,1	26,1	18,5	14,1	15
Z 3	FII without KZ	38	537	5,8	52,5	31,9	25,5	17,4	18,8
Z 4	FII with KZ	39	538	5,6	27,4	26,3	15,7	12,1	10,8
Z 5	FIII without KZ	68	461	5,6	34,1	40,0	11,3	3,3	7,7
Z 6	FIII with KZ	37	459	5,6	21,0	26,1	12,6	10,7	12,1

F = strength grade
KZ = key-dovetailing
KZL 50 = key-dovetail length of 50mm

Table 6b: Moduli of elasticity in tension for mechanically sorted layers of boards (values of tests after 3 to 5 minutes; Weibull distributions; production A, KZL 50)

test	sample	n (-)	ρ $\frac{kg}{m^3}$	u (%)	E_t $\frac{N}{mm^2}$	V_E (%)	$E_{t,5\%}$ $\frac{N}{mm^2}$	$E_{t,1\%}$ $\frac{N}{mm^2}$	$E_{t,min}$ $\frac{N}{mm^2}$
Z 1	F I without KZ	7	536	9,0	14 071	14	12 252	12 181	12 470
Z 2	F I with KZ	—	—	—	—	—	—	—	—
Z 3	F II without KZ	17	499	9,0	11 475	12,1	9 569	9 249	9 590
Z 4	F II with KZ	—	—	—	—	—	—	—	—
Z 5	F III without KZ	23	476	9,0	8 949	19,1	6 533	6 077	6 490
Z 6	F III with KZ	21	481	—	5 408	20,7	3 691	3 257	3 560

F = strength grade
KZ = key-dovetailing
KZL50 = key-dovetail length of 50 mm

Table 6c: Tensile strengths of mechanically sorted layers of boards (values of tests after 3 to 5 minutes; Weibull distributions, production B, KZL 20)

test	sample	n (-)	$\bar{\rho}$ kg/m³	$\bar{u}$ (%)	$\bar{R}_t$ N/mm²	v_R (%)	$R_{t,5\%}$ N/mm²	$R_{t,1\%}$ N/mm²	$R_{t,min}$ N/mm²
Z 1	FI without KZ	16	456	8,7	56,8	15,7	41,1	34,7	42,3
Z 2	FI with KZ	—	—	—	—	—	—	—	—
Z 3	FII without KZ	40	441	6,6	45,6	25,6	249	15,7	16,2
Z 4	FII with KZ	7	434	—	28,4	18,7	19,8	15,2	19,2
Z 5	F III without KZ	13,7	413	9,1	30,4	38,7	11,8	6,6	6,1
Z 6	F III with KZ	93	420	—	26	28,3	15,2	13,0	11,0

F = strength grade
KZ = key-dovetailing
KZL50 = key-dovetail length of 50 mm

Table 6d: Moduli of elasticity in tension for mechanically sorted layers of boards (values of tests after 3 to 5 minutes; Weibull distributions, production B, KZL 20)

test	sample	n (-)	ρ $\frac{kg}{m^3}$	u (%)	E_t $\frac{N}{mm^2}$	V_E (%)	$E_{t,5\%}$ $\frac{N}{mm^2}$	$E_{t,1\%}$ $\frac{N}{mm^2}$	$E_{t,min}$ $\frac{N}{mm^2}$
Z 1	F I without KZ	12	448	9,0	13963	10,9	11778	11343	12030
Z 2	F I with KZ	—	—	—	—	—	—	—	—
Z 3	F II without KZ	20	428	8,7	11394	10,8	9407	8800	6570
Z 4	F II with KZ	—	—	—	—	—	—	—	—
Z 5	F III without KZ	15	416	9,0	9072	28,1	7001	6952	6950
Z 6	F III with KZ	31	435	—	6101	23,6	3740	2973	3340

F = strength grade
KZ = key-dovetailing
KZ 20 = key-dovetail length of 20 mm

Table 7a: Tensile strengths of visually sorted layers of boards (values of tests after 3 to 5 minutes; Weibull distributions, production A, KZL 50)

test	sample	n (-)	$\bar{\varrho}$ $\frac{kg}{m^3}$	$\bar{u}$ (%)	$\bar{R}_t$ $\frac{N}{mm^2}$	V_R (%)	$R_{t\,5\%}$ $\frac{N}{mm^2}$	$R_{t,1\%}$ $\frac{N}{mm^2}$	$R_{t,min}$ $\frac{N}{mm^2}$
Z 7	GK I without KZ	96	523	5,7	54	36,3	22,7	13,4	7,7
Z 8	GK II without KZ	23	512	5,8	39,2	39,6	13,1	3,0	11,2
Z 9	GK III without KZ	21	497	5,8	27,2	45,5	7,5	1,8	7,7

GK = quality grade
KZ = key-dovetailing
KZL 50 = key-dovetail length of 50 mm

test	sample	n (-)	$\bar{\varrho}$ kg/m³	u (%)	E_t N/mm²	V_E (%)	$E_{t,5\%}$ N/mm²	$E_{t,1\%}$ N/mm²	$E_{t,min}$ N/mm²
Z 7	GK I without KZ	17	514	8,9	11 760	21,9	8 317	7 791	8 390
Z 8	GK II without KZ	12	438	8,9	11 236	18,6	7 441	5 433	6 960
Z 9	GK II without KZ	18	478	9,1	9 148	20,3	6 327	5 638	6 490

GK = quality grade
KZ = key-dovetailing
KZL 50 = key-dovetail length of 50 mm

Table 7b: Moduli of elasticity in tension for visually sorted layers of boards (values of tests after 3 to 5 minutes; Weibull distributions, production A, KZL 50)

Table 8: Design of the grades of glued laminated timber

BSH - grade		BSH 1	BSH 2	BSH 3	BSH 4	BSH 5	BSH 6
sorting of the layers		visually	visually	visually	mechani-cally	mechani-cally	mechani-cally
exterior layers	kind of timber	NSH GkIII	NSH GkIII	NSH GkIII	NSH F I	NSH F II	NSH F II
	KZV (mm)	≥ 250	≥ 250	≥ 0	≥ 250	≥ 250	≥ 250
interior layers	kind of timber	NSH GkII	NSH GkIII	NSH GkII	NSH F III	NSH F II	NSH F III
	KZV (mm)	≥ 250	≥ 0	≥ 0	≥ 0	≥ 0	≥ 0

Designations:
BSH = glued laminated timber
NSH = sawn coniferous timber
KZV = key - dovetail skew notching
GK = quality grade acc. to /10/
F = strength grade acc. to /1/

Table 9: Results of the bending tests concerning mechanically sorted glued laminated timber

test	test specimen	ϱ $\left(\frac{kg}{m^3}\right)$	$\bar{u}$ (%)	$\bar{R}_m$ $\left(\frac{N}{mm^2}\right)$	s_R $\left(\frac{N}{mm^2}\right)$	$v_R = \frac{s_R}{R_m}$ (%)	$R_{m5\%}$ $\left(\frac{N}{mm^2}\right)$	$R_{m1\%}$ $\left(\frac{N}{mm^2}\right)$	$R_{m,min}$ $\left(\frac{N}{mm^2}\right)$	E_m $\left(\frac{N}{mm^2}\right)$	s_E $\left(\frac{N}{mm^2}\right)$	$v_E = \frac{s_E}{E_m}$ (%)	$E_{m5\%}$ $\left(\frac{N}{mm^2}\right)$	$E_{m1\%}$ $\left(\frac{N}{mm^2}\right)$	$E_{m,min}$ $\left(\frac{N}{mm^2}\right)$
B 1	BSH 4 + KZ 1)	502	10,8	40,4	4,0	9,8	36,1	35,8	35,9	12646	904	7,2	11155	10661	11050
B 2	BSH 4 o. KZ 2)	525	11,1	54,6	7,9	14,5	40,6	34,2	38,3	13818	1054	7,6	11879	10752	12040
B 3	BSH 6 + KZ	504	11,2	33,3	5,3	15,8	25,5	23,9	25,1	10909	968	8,9	9563	9320	9700
B 4	BSH 6 o. KZ	515	10,2	45,1	9,4	20,8	28,3	20,2	30,3	11876	1228	10,3	9915	9342	10054

Designations: ϱ = density; u = moisture of timber; R_m = flexural strength; E_m = modulus of elasticity in bending; s = standard deviation; v = variation coeffizient

1) BSH + KZ = glued laminated timber with key-dovetailing
2) BSH o. KZ = glued laminated timber without key-dovetailing

Table 10: Regression analysis of R_m (KZV)

	R_m $\left(\frac{N}{mm^2}\right)$	r (-)	r (-)
1	$32{,}87 + 0{,}003\ (KZV)$ KZV in mm	0,123	0,351
2	$32{,}47 + 0{,}2648\ \ln(KZV)$	0,212	0,460
3	$32{,}8 \cdot 0^{7{,}729 \cdot 10^{-5}\ (KZV)}$	0,128	0,358
4	$32{,}71\,(KZV)^{0{,}0066}$	0,224	0,473
5	$32{,}04 + 0{,}008\ (KZV) - 0{,}457 \cdot 10^{-6}\ (KZV)^2$	0,165	0,41

14 glued laminated timber girders; b=97mm, h=288, l_s=4 320 mm
layers sorted visually, at least grade II sawn coniferous timber
key-dovetailing (KZ) in the test zone (PB)
key-dovetail length (KZL) of 20 mm
moisture of timber u=8,1 to 11.7%
failure in the key-dovetailing, 1st layer
KZV=key-dovetail skew notching

Table 11: Flexural strengths of visually sorted glued laminated timber with key-dovetail skew notching of 50 and 20 mm

KZL=key-dovetail length (mm)	50	20
production	A	B
technology	planing of the glued laminated timber immediately after the curing of the glue	planing of the glued laminated timber immediately after the pressing
glued laminated timber girders	b=97 ; h=288 l_s=4450 mm	b=97 ; h=288 l_s=4450 mm
sawn coniferous timber layers	at least quality grade II	at least quality grade II
sorting	visually	visually
failure	in key-dovetailing, test zone, layer 1	in key-dovetailing, test zone, layer 1
moisture of timber u	6 -11,6 %	7,4 - 13,9%
key-dovetail skew notching layers 1-2	≥ 250 mm	≥ 250 mm
number of griders n	16	19
$R_m \left(\frac{N}{mm^2}\right)$	35	34,3
V_R (%)	17,1	9,4
$R_{m,5\%} \left(\frac{N}{mm^2}\right)$	24,7	30,5
$R_{m,1\%} \left(\frac{N}{mm^2}\right)$	20,7	30,1
$R_{m,min} \left(\frac{N}{mm^2}\right)$	24,9	30

Table 12: Tensile strengths of visually sorted key-dovetailed layers of timber boards with key-dovetail skew notching of 20 and 50mm (values of tests after 3 to 5 minutes; Weibull distribution)

KZL=key-dovetail length (mm)	50	20
production	A	B
technology	planing of the glued laminated timber after the curing of the glue at 20 °C	planing of the glued laminated timber immediately after the pressing
R_t $\left(\frac{N}{mm^2}\right)$	27,8	31,2
V_R (%)	28,6	26,9
$R_{t,5\%}$ $\left(\frac{N}{mm^2}\right)$	14,4	17,8
$R_{t,1\%}$ $\left(\frac{N}{mm^2}\right)$	9,5	13,9
$R_{t,min}$ $\left(\frac{N}{mm^2}\right)$	9,0	14,4

90 specimens each, made of quality grade II sawn coniferous timber u= 6 to 12%, failure in the key-dovetailing